Environmental Aspects of Oil and Gas Production

Scrivener Publishing
100 Cummings Center, Suite 541J
Beverly, MA 01915-6106

Publishers at Scrivener
Martin Scrivener (martin@scrivenerpublishing.com)
Phillip Carmical (pcarmical@scrivenerpublishing.com)

Environmental Aspects of Oil and Gas Production

John O. Robertson and George V. Chilingar

Contributors:

Moayed bin Yousef Al-Bassam, PhD – Corrosion

Michael D. Holloway, PhD – Fracturing

WILEY

This edition first published 2017 by John Wiley & Sons, Inc., 111 River Street, Hoboken, NJ 07030, USA and Scrivener Publishing LLC, 100 Cummings Center, Suite 541J, Beverly, MA 01915, USA
© 2017 Scrivener Publishing LLC
For more information about Scrivener publications please visit www.scrivenerpublishing.com.

All rights reserved. No part of this publication may be reproduced, stored in a retrieval system, or transmitted, in any form or by any means, electronic, mechanical, photocopying, recording, or otherwise, except as permitted by law. Advice on how to obtain permission to reuse material from this title is available at http://www.wiley.com/go/permissions.

Wiley Global Headquarters
111 River Street, Hoboken, NJ 07030, USA

For details of our global editorial offices, customer services, and more information about Wiley products visit us at www.wiley.com.

Limit of Liability/Disclaimer of Warranty
While the publisher and authors have used their best efforts in preparing this work, they make no representations or warranties with respect to the accuracy or completeness of the contents of this work and specifically disclaim all warranties, including without limitation any implied warranties of merchantability or fitness for a particular purpose. No warranty may be created or extended by sales representatives, written sales materials, or promotional statements for this work. The fact that an organization, website, or product is referred to in this work as a citation and/or potential source of further information does not mean that the publisher and authors endorse the information or services the organization, website, or product may provide or recommendations it may make. This work is sold with the understanding that the publisher is not engaged in rendering professional services. The advice and strategies contained herein may not be suitable for your situation. You should consult with a specialist where appropriate. Neither the publisher nor authors shall be liable for any loss of profit or any other commercial damages, including but not limited to special, incidental, consequential, or other damages. Further, readers should be aware that websites listed in this work may have changed or disappeared between when this work was written and when it is read.

Library of Congress Cataloging-in-Publication Data
ISBN 978-1-119-11737-7

Cover image: Provided by John O. Roberston and George V. Chilingar
Cover design by Kris Hackerott

Set in size of 11pt and Minion Pro by Exeter Premedia Services Private Ltd., Chennai, India

Printed in

10 9 8 7 6 5 4 3 2 1

This book is dedicated to the custodian of the Two Holy Mosques, His Majesty King ***Salman bin Abdul-Aziz Al Saud*** *in recognition of his support of all branches of Engineering and Sciences in order to improve the well-being of humankind.*

This book is also dedicated to the following:

Professor S, W. Golomb,

hailed as the father of modern digital communications – from deep space communications -- to the internet –- to cell phones. A man known for his recreational and discrete mathematics – and for his support of the University of Southern California.

Dr. John Mork,

president of "The Energy Corporation of America" for his support of the University of Southern California and his outstanding contributions to the Petroleum Industry.

Nina and Henry Chuang,

for their continuous support of graduate students at the University of Southern California and for Dr. Chuang's outstanding contributions to the petroleum Industry.

Contents

Acknowledgments **xvii**

1 Environmental Concerns **1**
1.1 Introduction 1
1.2 Evaluation Approach 3
1.3 Gas Migration 3
1.3.1 Paths of Migration for Gas 4
1.3.2 Monitoring of Migrating Gases 4
1.3.3 Identification of Biological vs. Thermogenic Gases 6
1.4 Underground Gas Storage Facilities 7
1.5 Subsidence 9
1.6 Emissions of Carbon Dioxide and Methane 10
1.7 Hydraulic Fracturing 11
1.7.1 Orientation of the Fracture 12
1.8 Oil Shale 13
1.9 Corrosion 14
1.10 Scaling 14
1.11 Conclusion 15
References and Bibliography 15

2 Migration of Hydrocarbon Gases **17**
2.1 Introduction 17
2.2 Geochemical Exploration for Petroleum 20
2.3 Primary and Secondary Migration of Hydrocarbons 20
2.3.1 Primary Gas Migration 21
2.3.2 Secondary Gas Migration 22
2.3.3 Gas Entrapment 22
2.4 Origin of Migrating Hydrocarbon Gases 23
2.4.1 Biogenic vs. Thermogenic Gas 24
2.4.1.1 Sources of Migrating Gases 24
2.4.1.2 Biogenic Methane 24
2.4.1.3 Thermogenic Methane Gas 26
2.4.2 Isotopic Values of Gases 27
2.4.3 Nonhydrocarbon Gases 30
2.4.4 Mixing of Gases 31
2.4.5 Surface Gas Sampling 32
2.4.6 Summary 33

2.5 Driving Force of Gas Movement 34
2.5.1 Density of a Hydrocarbon Gas under Pressure 34
2.5.2 Sample Problem (Courtesy of Gulf Publishing Company) 35
2.5.3 Other Methods of Computing Natural Gas Compressibility 38
2.5.4 Density of Water 40
2.5.5 Petrophysical Parameters Affecting Gas Migration 41
2.5.6 Porosity, Void Ratio, and Density 42
2.5.7 Permeability 46
2.5.8 Free and Dissolved Gas in Fluid 48
2.5.9 Quantity of Dissolved Gas in Water 48
2.6 Types of Gas Migration 49
2.6.1 Molecular Diffusion Mechanism 49
2.6.2 Discontinuous-Phase Migration of Gas 52
2.6.3 Minimum Height of Gas Column Necessary to Initiate Upward Gas Movement 54
2.6.4 Buoyant Flow 54
2.6.5 Sample Problem (Courtesy of Gulf Publishing Company) 56
2.6.6 Gas Columns 56
2.6.7 Sample Problem 2.2 (Courtesy of Gulf Publishing Company) 58
2.6.8 Continuous-Phase Gas Migration 59
2.7 Paths of Gas Migration Associated with Oilwells 61
2.7.1 Natural Paths of Gas Migration 63
2.7.2 Man-Made Paths of Gas Migration (boreholes) 64
2.7.2.1 Producing Wells 65
2.7.2.2 Abandoned Wells 66
2.7.2.3 Repressured Wells 66
2.7.3 Creation of Induced Fractures during Drilling 66
2.8 Wells Leaking Due to Cementing Failure 69
2.8.1 Breakdown of Cement 69
2.8.2 Cement Isolation Breakdown (Shrinkage—Circumferential Fractures) 70
2.8.3 Improper Placement of Cement 71
2.9 Environmental Hazards of Gas Migration 74
2.9.1 Explosive Nature of Gas 74
2.9.2 Toxicity of Hydrocarbon Gas 75
2.10 Migration of Gas from Petroleum Wellbores 78
2.10.1 Effect of Seismic Activity 78
2.11 Case Histories of Gas Migration Problems 79
2.11.1 Inglewood Oilfield, CA 80
2.11.2 Los Angeles City Oilfield, CA 81
2.11.2.1 Belmont High School Construction 81
2.11.3 Montebello Oilfield, CA 83
2.11.3.1 Montebello Underground Gas Storage 84
2.11.4 Playa Del Rey Oilfield, CA 84
2.11.4.1 Playa del Rey underground Gas Storage 84
2.11.5 Salt Lake Oilfield, CA 86
2.11.5.1 Ross Dress for Less Department Store Explosion/Fire, Los Angeles, CA 87

2.11.5.2 Gilmore Bank 88
2.11.5.3 South Salt Lake Oilfield Gas Seeps from Gas Injection Project 89
2.11.5.4 Wilshire and Curson Gas Seep, Los Angeles, CA, 1999 89
2.11.6 Santa Fe Springs Oilfield, CA 89
2.11.7 El Segundo Oilfield, CA 91
2.11.8 Honor Rancho and Tapia Oilfields, CA 91
2.11.9 Sylmar, CA — Tunnel Explosion 91
2.11.10 Hutchinson, KS — Explosion and Fires 91
2.11.11 Huntsman Gas Storage, NE 93
2.11.12 Mont Belvieu Gas Storage Field, TX 95
2.11.13 Leroy Gas Storage Facility, WY 95
2.12 Conclusions 97
References and Bibliography 98

3 Subsidence as a Result of Gas/Oil/Water Production 105
3.1 Introduction 105
3.2 Theoretical Compaction Models 108
3.3 Theoretical Modeling of Compaction 111
3.3.1 Terzaghi's Compaction Model 112
3.3.2 Athy's Compaction Model 115
3.3.3 Hedberg's Compaction Model 115
3.3.4 Weller's Compaction Model 116
3.3.5 Teodorovich and Chernov's Compaction Model 117
3.3.6 Beall's Compaction Model 118
3.3.7 Katz and Ibrahim Compaction Model 118
3.4 Subsidence Over Oilfields 119
3.4.1 Rate of Subsidence 121
3.4.2 Effect of Earthquakes on Subsidence 122
3.4.3 Stress and Strain Distribution in Subsiding Areas 122
3.4.4 Calculation of Subsidence in Oilfields 125
3.4.5 Permeability Seals for Confined Aquifers 128
3.4.6 Fissures Caused by Subsidence 128
3.5 Case Studies of Subsidence over Hydrocarbon Reservoirs 130
3.5.1 Los Angeles Basin, CA, Oilfields, Inglewood Oilfield, CA 130
3.5.1.1 Baldwin Hills Dam Failure 131
3.5.1.2 Proposed Housing Development 134
3.5.2 Los Angeles City Oilfield, CA 134
3.5.2.1 Belmont High School Construction 134
3.5.3 Playa Del Rey Oilfield, CA 136
3.5.3.1 Playa Del Rey Marina Subsidence 137
3.5.4 Torrance Oilfield, CA 138
3.5.5 Redondo Beach Marina Area, CA 138
3.5.6 Salt Lake Oilfield, CA 139
3.5.7 Santa Fe Springs Oilfield, CA 140

3.5.8 Wilmington Oilfield, Long Beach, CA 141
3.5.9 North Stavropol Oilfield, Russia 152
3.5.10 Subsidence over Venezuelan Oilfields 157
3.5.10.1 Subsidence in the Bolivar Coastal Oilfields of Venezuela 158
3.5.10.2 Subsidence of Facilities 160
3.5.11 Po-Veneto Plain, Italy 166
3.5.11.1 Po Delta 167
3.5.12 Subsidence Over the North Sea Ekofisk Oilfield 173
3.5.12.1 Production 174
3.5.12.2 Ekofisk Field Description 175
3.5.12.3 Enhanced Oil Recovery Projects 177
3.5.13 Platform Sinking 177
3.6 Concluding Remarks 178
References and Bibliography 179

4 Effect of Emission of CO_2 and CH_4 into the Atmosphere 187
4.1 Introduction 187
4.2 Historic Geologic Evidence 189
4.2.1 Historic Record of Earth's Global Temperature 189
4.2.2 Effect of Atmospheric Carbon Content on Global Temperature 191
4.2.3 Sources of CO_2 194
4.3 Adiabatic Theory 197
4.3.1 Modeling the Planet Earth 197
4.3.2 Modeling the Planet Venus 198
4.3.3 Anthropogenic Carbon Effect on the Earth's Global Temperature 203
4.3.4 Methane Gas Emissions 204
4.3.5 Monitoring of Methane Gas Emissions 206
References 207

5 Fracking 211
5.1 Introduction 211
5.2 Studies Supporting Hydraulic Fracturing 211
5.3 Studies Opposing Hydraulic Fracturing 212
5.4 The Fracking Debate 213
5.5 Production 214
5.5.1 Conventional Reservoirs 214
5.5.2 Unconventional Reservoirs 214
5.6 Fractures: Their Orientation and Length 217
5.6.1 Fracture Orientation 217
5.6.2 Fracture Length/Height 218
5.7 Casing and Cementing 218
5.8 Blowouts 219
5.8.1 Surface Blowouts 219
5.8.2 Subsurface Blowouts 219

5.9 Horizontal Drilling 220
5.10 Fracturing and the Groundwater Contamination 220
5.11 Pre-Drill Assessment 220
5.12 Basis of Design 222
5.13 Well Construction 222
5.13.1 Drilling 222
5.13.2 Completion 225
5.13.3 Well Operations 225
5.13.4 Well Plug and Abandonment P&A 226
5.14 Summary 227
5.15 Failure and Contamination Reduction 227
5.15.1 Conduct Environmental Sampling Before and During Operations 227
5.15.2 Disclose the Chemicals Used in Fracking Operations 227
5.15.3 Ensure that Wellbore Casings are Properly Designed and Constructed 228
5.15.4 Eliminate Venting and Work toward Green Completions 228
5.15.5 Prevent Flowback Spillage/Leaks 228
5.15.6 Dispose/Recycle Flowback Properly 228
5.15.7 Minimize Noise and Dust 229
5.15.8 Protect Workers and Drivers 229
5.15.9 Communicate and Engage 229
5.15.10 Record and Document 230
5.16 Frack Fluids 230
5.17 Common Fracturing Additives 231
5.18 Typical Percentages of Commonly Used Additives 232
5.19 Chemicals Used in Fracking 233
5.20 Proppants 235
5.20.1 Silica Sand 236
5.20.2 Resin-Coated Proppant 237
5.20.3 Manufactured Ceramics Proppants 238
5.20.4 Other Types of Proppants 238
5.21 Slickwater 238
5.22 Direction of Flow of Frack Fluids 239
5.23 Subsurface Contamination of Groundwater 239
5.23.1 Water Analysis 240
5.23.2 Possible Sources of Methane in Water Wells 242
5.24 Spills 242
5.24.1 Documentation 243
5.25 Other Surface Impacts 243
5.26 Land Use Permits 243
5.27 Water Usage and Management 244
5.27.1 Flowback Water 245
5.27.2 Produced Water 245
5.27.3 Flowback and Produced Water Management 245
5.28 Earthquakes 246
5.29 Induced Seismic Event 246

5.30 Wastewater Disposal Wells 247
5.31 Site Remediation 247
5.31.1 Regulatory Oversight 247
5.31.2 Federal Level Oversight 248
5.31.3 State Level Oversight 248
5.31.4 Municipal Level Oversight 248
5.32 Examples of Legislation and Regulations 248
5.33 Frack Fluid Makeup Reporting 249
5.33.1 FracFocus 250
5.34 Atmospheric Emissions 250
5.35 Air Emissions Controls 252
5.35.1 Common Sources of Air Emissions 253
5.35.2 Fugitive Air Emissions 253
5.36 Silica Dust 254
5.36.1 Stationary Sources 254
5.37 The Clean Air Act 255
5.38 Regulated Pollutants 255
5.38.1 NAAQS Criteria Pollutants 256
5.39 Attainment versus Non-attainment 257
5.40 Types of Federal Regulations 257
5.41 MACT/NESHAP 257
5.42 NSPS Regulations: 40 CFR Part 60 258
5.42.1 NSPS Subpart OOOO 258
5.42.2 Facilities/Activities Affected by NSPS OOOO 258
5.43 Construction and Operating New Source Review Permits 260
5.44 Title V Permits 260
5.45 Chemicals and Products on Locations 260
5.46 Material Safety Data Sheets (MSDS) 263
5.47 Contents of an MSDS 263
5.48 Conclusion 264
State Agency Web Addresses 264
References 265
Bibliography 266

6 Corrosion 269
6.1 Introduction 269
6.2 Definitions 270
6.2.1 Corrosion 270
6.2.2 Electrochemistry 270
6.2.3 Electric Potential 271
6.2.4 Electric Current 271
6.2.5 Resistance 271
6.2.6 Electric Charge 271
6.2.7 Electrical Energy 271
6.2.8 Electric Power 272
6.2.9 Corrosion Agents 272

6.3 Electrochemical Corrosion 273
6.3.1 Components of Electrochemical Corrosion 277
6.3.1.1 Electromotive Force Series 277
6.3.1.2 Actual Electrode Potentials 279
6.4 Galvanic Series 280
6.4.1 Cathode/anode Area Ratio 280
6.4.2 Polarization 280
6.4.3 Corrosion of Iron 280
6.4.4 Gaseous Corrodents 283
6.4.4.1 Oxygen 283
6.4.4.2 Hydrogen Sulfide 284
6.4.4.3 Carbon Dioxide 286
6.4.5 Alkalinity of Environment 286
6.4.6 The influence of pH on the Rate of Corrosion 287
6.4.7 Sulfate-Reducing Bacteria 287
6.4.8 Corrosion in Gas-Condensate Wells 288
6.5 Types of Corrosion 289
6.5.1 Sweet Corrosion 290
6.5.2 Sour Corrosion 292
6.6 Classes of Corrosion 293
6.6.1 Uniform Attack 293
6.6.2 Crevice Corrosion 294
6.6.3 Pitting Corrosion 294
6.6.4 Intergranular Corrosion 294
6.6.5 Galvanic or Two-metal Corrosion 294
6.6.6 Selective Leaching 294
6.6.7 Cavitation Corrosion 294
6.6.8 Erosion-corrosion 295
6.6.9 Corrosion Due to Variation in Fluid Flow 295
6.6.10 Stress Corrosion 295
6.7 Stress-Induced Corrosion 295
6.7.1 Cracking in Drilling and Producing Environments 296
6.7.1.1 Hydrogen Embrittlement (Sulfide Cracking) 297
6.7.1.2 Corrosion Fatigue 297
6.8 Microbial Corrosion 298
6.8.1 Microbes Associated with Oilfield Corrosion 302
6.8.2 Microbial Interaction with Produced Oil 303
6.8.3 Microorganisms in Corrosion 303
6.8.3.1 Prokaryotes 303
6.8.3.2 Eukaryotes 305
6.8.4 Different Mechanisms of Microbial Corrosion 305
6.8.5 Corrosion Inhibition by Bacteria 305
6.8.6 Microbial Corrosion Control 306
6.9 Corrosion Related to Oilfield Production 307
6.9.1 Corrosion of Pipelines and Casing 307
6.9.2 Casing Corrosion Inspection Tools 308
6.9.3 Electromagnetic Corrosion Detection 309

6.9.4 Methods of Corrosion Measurement 309
6.9.5 Acoustic Tool 309
6.9.6 Potential Profile Curves 310
6.9.7 Protection of Casing and Pipelines 310
6.9.8 Casing Leaks 312
6.9.9 Cathodic Protection 312
6.9.10 Structure Potential Measurement 315
6.9.11 Soil Resistivity Measurements 315
6.9.12 Interaction between an Old and a New Pipeline 317
6.9.13 Corrosion of Offshore Structures 318
6.9.14 Galvanic vs. Imposed Direct Electrical Current 320
6.10 Economics and Preventitive Methods 321
6.11 Corrosion Rate Measurement Units 322
References and Bibliography 322

7 Scaling 329
7.1 Introduction 329
7.2 Sources of Scale 330
7.3 Formation of Scale 332
7.4 Hardness and Alkalinity 334
7.5 Common Oilfield Scale Scenarios 334
7.5.1 Formation of a Scale 334
7.5.2 Calcium Carbonate Scale Formation 336
7.5.3 Sulfate Scale Formation 338
7.6 Prediction of Scale Formation 339
7.6.1 Prediction of $CaSO_4$ Deposition 341
7.6.2 Prediction of $CaCO_3$ Deposition 342
7.7 Solubility of Calcite, Dolomite, Magnesite and Their Mixtures 345
7.8 Scale Removal 345
7.9 Scale Inhibition 347
7.10 Conclusions 348
References and Bibliography 348

Appendix A 351

About the Authors 377

Author Index 379

Subject Index 387

Acknowledgments

The present book is the result of the work of many contributors whose research has enabled the writers to build on their work. The authors have attempted to give credit for the many ideas and research of many previous investigators. Without their ideas, this book would have been impossible. Science is an accumulation of ideas that slowly grows over time. Understanding of the present is only accomplished by understanding the past. Tomorrow, additional knowledge will modify our thoughts of today.

The writers owe a special thanks to the publisher, Phil Carmical, and his staff who made everything presented a little – and sometimes at lot – better.

Academician John O. Robertson owes a special thanks to the fellow staff and professors at **ITT-Tech**, National City, CA, for their support. Especial acknowledgment goes to his wife, Karen Marie Robertson, for her support and the hours she spent helping proof this text; and also his son Jerry John Robertson, for his important contributions.

Professor, Academician George V. Chilingar acknowledges the moral support and encouragement given by his wife Yelba Maria Chilingar, and his children Eleanor Elizabeth, Modesto George and Mark Steven.

Environmental Aspects of Oil and Gas Production.
John O. Robertson and George V. Chilingar.
© 2017 Scrivener Publishing LLC. Published 2017 by John Wiley & Sons, Inc.

1

Environmental Concerns

1.1 Introduction

This book is a systematic evaluation of surface and subsurface environmental hazards that can occur due to the production of hydrocarbons and how these problems can be avoided. The importance of such a study is dramatized by recent examples that have occurred within the Los Angeles Basin, CA:

1. ***In the early 1960s***, a portion of the Montebello Oilfield developed in the 1920s was converted to the Montebello Gas Storage Project, under the City of Montebello (a city within Los Angeles County). A minimal amount of work was done on the older wells to prepare the wells for repressurization. In the early 1980s, significant gas seepages were discovered alongside and under homes from several prior abandoned wells. Homes were torn down to allow a drilling rig to reabandon the leaking wellbores which were endangering the community with migrating gas. These home sites were then converted to mini-parks so that future casing leaks could be resealed if necessary. These problems led to the abandonment of the gas storage project in 2000.
2. ***On December 14, 1963***, water burst through the foundation of the earthen dam of the Baldwin Hills Reservoir, CA, a hilltop water storage facility which had been weakened by differential subsidence. This facility was located in a square-mile of metropolitan Los Angeles, CA, consisting of a large number of homes, of which 277 were damaged by moving water and inundated with mud and debris, or destroyed.

Hamilton and Meehan (1971) noted that differential subsidence was a result of fluid withdrawal from the Inglewood Oilfield and the subsequent reinjection of water into the producing formation (for secondary oil recovery and waste water disposal). This resulted in the differential subsidence that was responsible for the ultimate demise of the earthen dam (see Chapter 3).

3. ***On March 24, 1985***, migrating subsurface gas filled the Ross Dress for Less department store in the Fairfax area of Los Angeles. There was an explosion followed by a fire, due to a spark in the basement of the store. Over 23 people were injured and an entire shopping center was destroyed. The area around this center had to be closed down as migrating gas continued to flow into the area, burning for several days through cracks in sidewalks and around the foundations. This site was located directly over a producing oilfield containing many abandoned and improperly completed wells (see Chapter 2).
4. ***On October 23, 2015,*** massive volumes of escaping methane gas from a well (SS-25) in the Aliso Canyon Underground Storage facility reservoir flowed out and spread over the surrounding community of Porter Ranch, Los Angeles County, CA (Curwen, 2016). Engineers suspected that the escaping gas was coming from a hole in the 7-in casing about 500 ft below the surface. Therolf *et al*. (2016) reported the concerns of California Regulators to delay plans to capture and burn the leaking gas that had sickened and displaced thousands of Porter Ranch residents. The Aliso Oilfield was developed in the late 1930s and a portion of this oilfield was converted to a gas storage reservoir. The oilfield had previous fires from leaking wellbores that were put out by Paul "Red" Adair in 1968 and 1975 (Curwen, 2016). The escaping gas flowed into the nearby community for over 3 months, endangering the residents with health, fire and possible explosion hazards. At the time of writing of this book, the well has not been repaired.

Unfortunately, many oilfields located in urban settings similar to that of the Los Angeles Basin, CA, have been managed by catastrophe rather than through preventative management.

The objective of this book is to identify the environmental problems associated with the handling of hydrocarbons and suggest procedures and standards for safer operation of oilfields in urban environments.

This book is intended to help evaluate hydrocarbon production operations by looking at specific environmental problems, such as migrating gas and subsidence. The writers recommend a systems analysis approach that is supported by a monitoring program. Today there are many wells over 50 years of age and some over 100 years. The capability of these older wells to isolate and contain hydrocarbons decreases with time as the cement sheath deteriorates and the well casing corrodes. Chapter 3 describes the breakdown process of the cement in the wellbore with respect to time, resulting in the decrease of the ability for cement to isolate the reservoir fluids. Chapter 6 reviews the corrosion that can result in gas leaking holes in the casing. Thus, increased pressure by water injection, at a later date in the life of an oilfield, can create an environmental

hazard in areas that contain wells with weakened cement and corroded steel casing, or inadequately abandoned coreholes and oilwells.

The intent of the writers is also to identify and establish procedures and standards for safer drilling and production of oilfields within the urban community. A necessary adjunct to these procedures is the establishment of a monitoring program that permits detection of environmental problems before occurrence of serious property damage or personal injury. This includes the following:

1. Monitoring of wells for surface seepage of gas.
2. Monitoring for surface subsidence.
3. Recognition of the oilfield geologic characteristics, including fault planes and potential areas and zones for gas migration to the surface.
4. Establishing procedures for the systematic evaluation of the integrity of both producing and abandoned oilwells and coreholes.
5. Monitoring of distribution pipelines and frequent testing for corrosion leaks.

1.2 Evaluation Approach

This evaluation approach requires development of a functional model for each oilfield operation. This approach should identify the basic hydrocarbon drive mechanism that is responsible for the movement of hydrocarbons in the reservoir. Particular attention should be given to faults and the caprock of the reservoirs.

Emphasis should be placed on the individual well production history, i.e., gas/oil ratio, water production and pressure history. Frequent surface soil gas tests should be made for all wells 50 years of age and older.

In gravity drainage pools, oil moves downdip and gas moves updip. As the gas/oil ratio of updip wells increases, these wells are shut-in. Most of the production occurs at practically zero pressure in gravity drainage pools. Freed gas, which accumulates at the top of the structure and is no longer held in solution becomes available for migration. If there is a pathway for its migration toward the surface or if such an avenue is created, it will migrate to adjacent areas of lower pressure working its way to the surface. The freeing of solution gas substantially increases the volume of gas available for migration.

If this migrating gas encounters a fault (natural path) or a wellbore (man-made path), it can then move toward the surface. As also pointed out in Chapter 2, as the wells age the casing corrodes and the cement fractures enlarge. The reason that cement ages and develops fractures with time is hydration of the cement. The cement does not have the same capability to isolate the hydrocarbons that it did when first put in place. This is contrary to a mistaken belief by many, that the risk of gas seepage is reduced over time as the reservoir pressure declines through fluid production. There are many older wells, drilled and completed 50 to 100 years ago within urban settings that leak.

1.3 Gas Migration

The existence of oil and gas seeps in oil-producing regions of the world has been recognized for a long time. For example, Link (1952), then the Chief Geologist of Standard

Oil Company (NJ), wrote a comprehensive article on the significance of oil and gas seeps in oil exploration. In this publication, he documented oil and gas seeps located throughout the world. Although the primary purpose of Link's paper was to identify the importance of surface oil and gas seeps in the exploration and location of oil and gas, it is of no less importance in identifying the hazards associated with the seepage or migration of hydrocarbons to the surface.

Various state agencies have published maps identifying seepage of oil and gas. For example, the Division of Oil and Gas of the State of California has published a detailed listing of seepages located throughout the state of California (Hodgson, 1987).

Many of these seeps are located in or near the immediate vicinity of producing or abandoned oilfields. As pressure drops, gas comes out of solution, allowing the freed gas to migrate toward the surface.

About 90% of all oil and gas seeps in the world are associated with faults, which provide natural pathways for migration of gas. Man-made pathways (wellbores) may be also present.

1.3.1 Paths of Migration for Gas

Fault planes and wellbores can serve as conduits for migration of gas from the oil/gas reservoirs to the surface (see Chapman, 1983; Doligez, 1987). Consensus of opinion, up to the mid-1960s, was that faults generally act as barriers to petroleum or water migration. Obviously faults acted as traps for oil/gas accumulations. The authors believe that, at best, faults are "leaky" barriers and that at a minimal differential pressure of 100–300 psi there is a flow of fluids across the fault planes. Thus, evaluation of fluid flow along (and across) fault planes is an important consideration, especially when monitoring for surface seepage.

The identification of potential paths of migration (fault planes and/or wellbores) within the geologic setting of any oil or gas field is essential in establishing the surface locations where seepage monitoring stations ought to be established. Also of importance are those locations where subsurface fault planes intersect water aquifers. Jones and Drozd (1983) pointed out that there is little doubt that faults can provide permeable avenues for hydrocarbon migration.

It is important to establish sampling intervals for a gas seepage monitoring program. When the flow of fluids is variable, a continuous monitoring system is required to obtain valid results. If only isolated samples are sporadically collected, the result may be a failure to detect a hazardous condition.

Usually, fluid movement along the faults increases their permeability. Following the San Fernando, CA, earthquake of February 9, 1971, it was recognized that seismic activity could not only damage wells, but also "*trigger*" the migration of oil and gas to the surface (Clifton *et al.*, 1971). In conclusion, the mapping of surface faults is essential.

1.3.2 Monitoring of Migrating Gases

Measurement instrumentation and gas sampling procedures need to be considered for the reliable determination of gas seepage hazards. The objectives to be achieved

are: (1) gas identification and source determination, (2) seepage pattern characterization, and (3) long-term gas sensing for detection and warning.

That distinction is important because the instrumentation and measurement techniques are different for each of the above functional areas. Natural gas found in an oilfield environment contains primarily methane and small amounts of ethane, propane, isobutene and other higher-molecular-weight hydrocarbons. The mere presence of these higher-MW hydrocarbons establishes that the gas is of a thermo- or petrogenic origin rather than a biogenic, or decomposition origin. Additionally, the relative percentages of the respective higher-MW hydrocarbons are sometimes used to identify the origin of the gas. If the gas has migrated through thousands of feet of geologic strata in reaching the surface (where the sample has been gathered), substantial changes often occur in the relative percentages of the gas constituents due to selective absorption of various hydrocarbons and mixing of the thermogenic gases with biogenic gases that occur near the surface (Khilyuk *et al*., 2000).

Use of subsurface depth probes and the selection of the depth from which the samples are collected are important in obtaining credible results. In general, the gas sample must have a sufficiently high concentration of natural gas, and must have been collected from a sufficient depth, i.e., below the near-surface clay caprocks, in order to prevent misinterpretation of the results (Khilyuk *et al*., 2000).

Relatively inexpensive portable or semi-portable gas detectors allow determination of the percent composition in air of explosive gases, such as methane. These gas detectors can be used to efficiently characterize gas seepage patterns, and identify localized concentrations of explosive gases. They can also be utilized in monitoring soil gases near wellbores. Portable gas detectors can also be used for obtaining gas samples for isotopic analysis.

Continuous gas sensing and detection systems are often utilized throughout the basement and/or first floor areas of a building to detect the accumulation of natural gas. In this situation, a low-level alarm system can be established safely below any possible explosion level. Also, exhaust fans can be automatically activated by the system to purge accumulated gas from the building until the gas levels return to a safe level. A central control panel can be used to activate exhaust fans as well as to transmit a signal to an outside, central, 24-hr sentry station. This can be tied into the burglar alarm, fire protection, or other sentry systems to alert central control, especially if higher levels of explosive gas develop (high-level alarm). Although this type of system is practical for installation in new commercial construction or in retrofitting existing commercial structures, it is generally cost prohibitive for use in residential homes and small apartment houses.

Most U.S. states, for example, have established a regulatory agency to oversee the oil and gas production activities within the state, including certain safety aspects. However, none of these agencies have developed a systematic or comprehensive program for dealing with the hazards associated with oil and gas seepage, monitoring older wells (50 years or older) for gas seepage and land subsidence.

Clearly, there is a great need for a nationwide uniform set of procedures and guidelines to be established for the monitoring of dangerous levels of gas seepage and land subsidence, especially in urban areas where the surface dwellers usually have no idea of the hazard that underlies them (e.g., Porter Ranch, CA, gas well blowout).

1.3.3 Identification of Biological vs. Thermogenic Gases

One of the most important aspects of gas migration is proper identification of the source of the gas. Gas fingerprinting allows identification of the gas source (Coleman, 1987).

Identification involves the use of a variety of chemical and isotopic analyses for distinguishing gases from different sources (Coleman *et al*., 1977, 1990). In Chapter 2, Table 2.1 lists most of the chemical compounds and the percent composition typically found in natural gas that is associated with oil and gas production. For example, the presence of significant quantities of ethane, propane, butane, etc., in a migrating gas indicates that the source of the gas is of thermogenic origin rather than a biological one. Thermogenic gases (petrogenic gases) are formed by thermal decomposition of buried organic material made up of the remains of plants and animals that lived millions of years ago, and buried to depths of many thousands of feet.

In contrast, microbial gases (biogenic gases) are formed by the bacterial decomposition of organic material in the near-surface subsoil. These gases are usually composed of almost pure methane.

Actually, the thermogenic gas samples collected at or near the surface have undergone compositional transformation as a result of migration through thick sections of geologic strata. During migration, the gas composition can become primarily methane as the heavier hydrocarbons are stripped out of the migrating gas, giving the appearance of microbial or biogenic gas. In addition, they could be mixed with the biogenic gases near the surface. (A detailed discussion of this is presented in Chapter 2.)

Schoell *et al*. (1993) studied the mixing of gases. Their isotopic analysis is based upon the following fundamental concepts: Isotopes are different forms of the same element, varying only in the number of neutrons within their nuclei and thus their mass. Carbon, for example, has three naturally occurring isotopes: carbon-12, carbon-13 and carbon-14. The two stable (nonradioactive) isotopes of carbon, carbon-12 and carbon-13, are present in all organic materials and have average abundances of 98.9% and 1.1%, respectively. These two isotopes of carbon undergo the same chemical reactions. Once methane is formed, its carbon isotopic composition is relatively unaffected by most natural processes.

The third naturally occurring isotope of carbon, carbon-14, is a radioactive isotope formed in the upper atmosphere by cosmic rays and has a natural abundance in atmospheric carbon dioxide of about 0.1%. Carbon-14, is the basis for the radiocarbon dating method and is present in all living things.

Hydrocarbon gases which are formed from the decomposition of organic materials have a carbon-14 concentration equivalent to that of the organic material from which they were formed. Biogenic or microbial gases formed from organic material that is less than 50,000 years old contain measurable quantities of carbon-14. Thermogenic (petroleum related) gases, on the other hand, are generally formed from materials that are millions of years old and thus contain no carbon-14. Thus, the presence of carbon-14 can be used to distinguish between thermogenic (petrogenic) and microbial (biogenic) gas.

Hydrogen also has two naturally occurring stable isotopes: (1) protium, more commonly referred to as hydrogen (H) and (2) deuterium (D). The hydrogen isotopic ratio

D/H is used as a fundamental gas distinguishing parameter. The hydrogen isotope analysis of methane can be used to elucidate the microbial pathway by which the gas was formed (Khilyuk *et al.*, 2000).

In summary, the isotopic analysis permits distinguishing between the various sources of gases:

1. **Producing or abandoned oil or gas wells**: If the seepage evaluation is made in the vicinity of a producing or an abandoned well, leakage from the producing wells, or from abandoned wells that have been improperly plugged, can result in near-surface accumulations of gas. Also, near-surface gas accumulations are frequently observed as a result of upward seepage of gas along faults or fissures in the rocks.
2. **Natural gas pipelines**: If the seepage problem is located in an area where buried gas lines exist, leakage from these pipelines can result in subsurface accumulations of gas.
3. **Underground gas storage reservoirs**: In many parts of the country, natural gas is stored underground, under pressure, in abandoned oilfields. If gas leaks from one of these reservoirs (through fractured caprocks, for example), it can migrate sometimes several miles along faults or through aquifers before it appears at the surface, e.g., Hutchinson, KS.
4. **Landfill gas**: Landfills containing decomposing organic material generate a substantial quantity of methane gas. Significant lateral migration of methane (for up to several miles) from landfills has been documented.
5. **Sewer gas**: Gas also originates within a sewer system. Sewage decomposes through microbial action and can result in the production of significant quantities of methane. Sewer gas can migrate over large distances from the sewer and then move along subsurface cracks and fissures.
6. **Coal beds**: Coal beds are also a potential source of natural gas, as coal beds contain coal gas, which is typically high in methane.

The isotopic analysis procedure detailed in Chapter 2 is a necessary element of any successful identification of migrating gas study effort.

1.4 Underground Gas Storage Facilities

The use of underground storage of natural gas is a well-developed technology widely used in many parts of the world. This method of storage is popular as the costs to contain the gas are far less than the cost of constructing surface facilities storing similar volumes of gas. As indicated in examples #1 and #4 at the beginning of the chapter, these gas storage reservoirs can present a major hazard to an urban community if not properly monitored.

The primary concern of the presence of a gas reservoir in an urban area is that most underground storage facilities were once oilfields containing abandoned wells and coreholes (man-made pathways for gas migration). Unfortunately, wells within the project are not always properly evaluated to determine if all wells and coreholes within

the project were properly abandoned or capable of handling cycling of gas at higher pressures. The cost of properly reabandoning and recompleting the wells and coreholes within the project to today's standards are high and often not considered as a part of the project. Frequent problems resulting from gas migration and "leaking" gas from these storage facilities are often related to the failure of wells to contain the repressured gas at higher pressures.

Common failures of these storage facilities usually are: (1) existence of faults passing through the reservoir and caprock; (2) improperly abandoned coreholes, e.g., coreholes that were abandoned by filling with drilling fluids and not cement; and (3) active and abandoned wells incapable of handling the cycling of pressure stresses caused by increased/decreased pressure. Tek (1987) has shown that the typical life of a gas storage project is around 50 years; however, many such projects have a much shorter life due to geological and wellbore problems. If the gas storage project is located within an urban area, leaking gas may lead to health, fire and explosion problems. Thus, a much more careful evaluation and continuous monitoring must be made.

In October 1980, a serious gas leak developed in a storage field located in Mont Belvieu, Texas, a suburb of the greater Houston area. This migration of gas was first detected when an explosion ripped through the kitchen of a house when a dishwasher was started. More than 50 families were evacuated from their homes as a result of this gas leak. In this case, gas identification was important. For example, inasmuch as the gases were primarily a mixture of ethane and propane, it was possible to identify the gas coming from a nearby gas storage field. Again, this emphasizes the importance of monitoring gas storage fields on a continuous basis near urban areas.

The evaluation of the migration characteristics of the gas is also of considerable importance to the concerns herein, in that a primary objective is to establish appropriate monitoring procedures for locating seeping gas. For example, in the above instance, after the explosion, high concentrations of the gas were found around the foundations of the homes in the area.

Example No. 4 at the beginning of the chapter illustrates a recent serious problem occurring with the Aliso Canyon Gas Storage Project, which lies within the Los Angeles Basin, CA (Curwen, 2016). Gas containment of an older well broke down, exposing thousands of nearby residents to exposure of natural gas. Although the primary complaint of the residents was the odor of the gas, many residents also complained of health problems, e.g., nausea and bleeding noses. Because this gas storage project is in close contact with hundreds of homes, a primary objective must be the continuous monitoring of gas to insure that any leaking of gas may be quickly detected and stopped. This project demonstrates the unknown danger that gas storage reservoirs can present to a large number of people within an urban area.

In the Fairfax Explosion and then fire (Example No. 3 and discussed further in Chapter 2), after the initial explosion, high concentrations of the gas were found around the foundations of commercial and residential homes in the area. Migrating gas was also detected throughout the sewer lines, which acted as conduits for the gas. Again, no monitoring was made to detect migrating gas which could have alerted the residents of the potential danger.

1.5 Subsidence

Numerous studies have addressed the subject of surface subsidence due to fluid production (e.g., Poland, 1972; Chilingarian and Wolf, 1975, 1976). Classic oilfield subsidence cases are Wilmington, CA; Goose Creek, TX; and Lake Maracaibo, Venezuela. These studies focused primarily on developing procedures to arrest or ameliorate oilfield subsidence. This was largely accomplished by maintaining or replenishing underground pressure usually through water injection (waterflooding) [e.g., California Public Resources Code, Article 5.5. Subsidence, Section 3315(c) and Section 3316.4, Repressuring Operations Defined]. These studies, however, fail to address the increased hazards of displacing large volumes of freed gas in the reservoir resulting from the water injection. Typically, the water injection significantly increases pressures in the reservoir causing the freed gas (under higher pressures) from the reservoir to migrate toward the surface along paths of least resistance. This includes faults, fractures, abandoned wells, and producing and/or idle wells lacking mechanical integrity to hold the increased pressures.

The surface subsidence is usually caused by the production of fluid from the reservoir. This reduces the pore pressure supporting the layers of rock (strata) above the reservoir and increases effective (grain-to-grain) stress. Subsidence causes the formation of new fissures and faults and movement along preexisting faults. As a result of the decrease in pore pressure, some of dissolved (solution) gas is released as free gas, which is then free to migrate toward areas of lower pressure.

The problem of subsidence would be less severe if the settling of the surface were uniform; however, due to the heterogeneity of the rocks, the surface settles differentially, some areas settling greater distances than others. This results in the creation of cracks in roads, sidewalks and paved areas. Foundations of buildings when stressed by differential subsidence fail.

The differential subsidence caused the failure of the earthen Baldwin Hills Dam, Los Angeles, CA (see Chapter 3 and example No. 2 at beginning of this chapter). On December 14, 1963, water burst through the foundation of the earth dam of the Baldwin Hills Reservoir, a hilltop water-storage facility located in metropolitan Los Angeles. The contents of the reservoir, some 250 million gallons of water, emptied within hours onto the urban communities below the dam, damaging or destroying 277 homes (Hamilton and Meehan, 1971). A detailed study of this disaster established that it was caused by fluids being withdrawn from the underlying Inglewood Oilfield. This was aggravated by water injection under high pressure into the highly faulted and subsidence-stressed subsurface, which triggered differential subsidence under the dam. Hamilton and Meehan (1971) concluded that "fault activation was a near-surface manifestation of stress-relief faulting triggered by fluid injection"(see Chapter 3 for additional details).

Monitoring programs related to waste water disposal (where waste water produced from oil production is routinely reinjected into the geological strata) need to be established. Waste water disposal can create special problems of distributing the natural pressure equilibrium existing in the area of water injection, usually causing gas to migrate from the area into lower-pressured areas in the upper geologic strata, increasing the hazard of surface seepage of gas.

Great care is required during acidizing of these disposal wells. Acidizing is frequently used to "*clear out*" or increase the pore space in the geologic strata where the water is being disposed. The acidizing process reduces the pressure requirements for water-disposal. Problems can arise when the acid is injected under high pressure and not only enlarges the pores around the wellbore but also causes fracturing of the rocks. This may create new avenues for the migration of gas.

A common practice in older oilfields is to utilize waterflooding for the purposes of enhancing oil recovery. By initiating a waterflood, one can literally double the quantity of oil produced from a dissolved-gas drive type reservoir. Waterflooding can also be used to decrease subsidence due to production of fluids. This technique, although often effective, frequently ignores the problems associated with gas migration. Crossflow often occurs between subzones, and cracks (fractures) formed during the waterflooding can form additional avenues for gas migration. Additional fractures may be formed by the rebound of the ground if large water-injection pressures are used during waterflooding in the subsiding areas.

Additionally, special precautions must be taken in areas where abandoned wells and older coreholes are located. The mechanical integrity (casing and the cement sheath) of all of the wells penetrating the reservoir must be assured.

Injection of fluids into the ground under high pressure for waste water disposal is also known to trigger faulting. A classic example of this was the Rangely Oilfield, in western Colorado. High pressure water injection was responsible for the 1962–1965 Denver earthquakes at the Rocky Mountain Arsenal and for generation of smaller earthquakes.

Problems of subsidence are compounded in areas that are subject to seismic activity, such as Southern California. Initially, the subsidence sets up stresses as a result of depletion of reservoir pressure (reduction in reservoir pressure due to fluid withdrawal), which can precipitate the movement along pre-existing faults and formation of new faults allowing gas to migrate to the surface.

The identification of the hazards associated with subsidence resulting from fluid withdrawal must be carefully evaluated as part of any prudent oilfield operation. This is best accomplished by establishing a systematic measurement of surface subsidence and gas seepage.

1.6 Emissions of Carbon Dioxide and Methane

It has been assumed by some that the content of carbon in the atmosphere (carbon dioxide and methane) affects global temperature. This concept was first attributed to a Swedish scientist, Syante Arrhenius, in 1898, who stated that global warming was driven by the carbon dioxide content in the atmosphere. It should be noted that he had no factual data to support his idea that methane and carbon dioxide (fossil fuel combustion) had any effect on the global warming of the atmosphere. Unfortunately, this unsupported concept has driven political and some scientific thought for the past few years.

In Chapter 4, a review of the historic cyclic earth temperatures shows a 100,000-year cyclic relationship between temperature versus time for the past 800,000 years. Also

discussed in Chapter 4, the carbon content of the atmosphere is driven by temperature, but the carbon content does not affect the global temperature. In fact, several investigators found a 400-year to 1,000-year lag between the global temperature increase and increase in the carbon content of the atmosphere. This lag may be partially due to the time it takes the CO_2 to be driven out of the ocean water as the global temperature increases. There is no scientific support for the idea that higher concentrations of CO_2 in the atmosphere raise global temperatures, as some believe; in fact, scientific evidence show the opposite is true. It is a rise in temperature that can decrease CO_2 content in the ocean waters. The peaks in the sun's irradiation precede the peaks in CO_2 concentration in the atmosphere.

Chapter 4 investigates the greenhouse effect using an adiabatic model, relating the global temperature to the atmospheric pressure and solar radiation. This model allows one to analyze the global temperature changes due to variation in the release of carbon dioxide and methane into the atmosphere. The release of anthropogenic gases does not change the average parameters of the Earth's heat regime and has no essential effect on the Earth's climate. Moreover, based upon the adiabatic model of heat transfer, the additional releases of carbon dioxide and methane lead to cooling (and not to warming as the proponents of conventional theory of global warming state) of the Earth's atmosphere. Petroleum production and other anthropogenic activities resulting in accumulation of additional amounts of methane and carbon dioxide in the atmosphere have practically no effect on the Earth's climate.

1.7 Hydraulic Fracturing

The term hydraulic fracturing of hydrocarbon-bearing formations elicits emotions of fear in many people. The writers would suggest this is in part due to an ignorance of what fracturing is. Many in the public misunderstand the use and purpose of fracturing. ***Can fracturing cause environmental problems by creating pathways for gas to migrate into fresh water aquifers and escape to the surface?*** The answer is "yes" if we are careless and misuse the high pressure used in orientating the direction of fractures in the formations. Improper procedures can result in vertical fractures which can break down the containment of the hydrocarbons, e.g., fracturing the caprock and/or the cement sheath surrounding the wellbore. But the answer is "no" if we carefully design fracturing treatments and do not fracture the containment of the reservoir.

Fracturing the reservoir dramatically increases the surface area of drainage for the reservoir. For an unfractured wellbore, the drainage area is restricted to the inside surface area of the wellbore. In addition, this internal surface area has been reduced as a result of damage by plugging the reservoir pores by silt, bacteria, etc., resulting in reduced fluid production rates. By creating fractures that extend beyond this damaged area about the wellbore, the drainage surface area of the well is greatly expanded by the additional surface area of the fractures. This increase in drainage area for the well can be over 20 times greater than in the original unfractured well.

It is not always recognized that fracturing is one of the most regulated and controlled processes of petroleum operations with regard to the environment. Chapter 5, prepared by M. Holloway, a recognized expert on fracturing, presents the basic operations

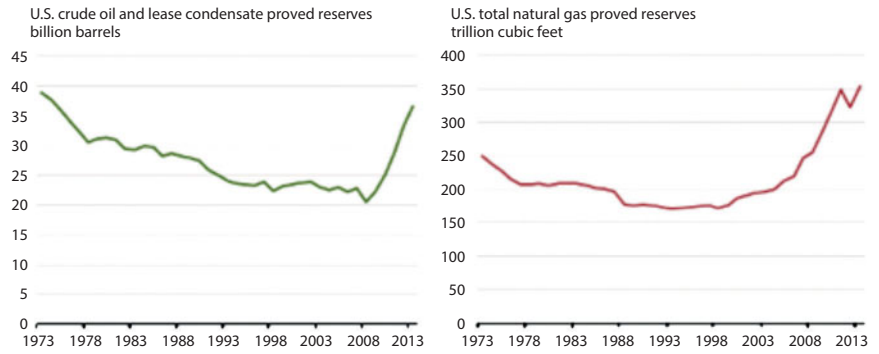

Figure 1.1 U.S. oil and natural gas proved reserves, 1973–2013. (After EIA, U.S.A., 2014, Figure 2.)

common to fracturing. A large body of literature has been published on the safety of the environmental aspects of hydraulic fracturing of oil wells. With the technological development in drilling operations, material selection and subsurface monitoring, the uncertainties associated with hydraulic fracturing have decreased.

Hydraulic fracturing has played a major role in increasing oil and gas reserves. Many wells in the United States are hydraulically fractured. The U.S. Energy Information Agency (EIA) (2014) noted that oil and natural gas reserves have increased by almost 10% in 2013, due to hydraulic fracturing (Figure 1.1). In 2013, proved reserves of crude oil and condensates increased by 3.1 billion bbls. As a direct result of this technology, oil prices reached their lowest level in 4 years in 2015.

1.7.1 Orientation of the Fracture

The orientation of a fracture depends upon the ratio of fracture pressure to the strength of the rock in a particular direction. In the case of hydraulic fracturing, fluid is injected into the formation in increasing pressure until the fluid pressure exceeds the strength of the rock, overcoming the stresses inherent in the rock to split apart (rupture), forming a fracture. Fracturing fluid must be pumped into the fracture rapidly enough to hold the new fracture open and allow a propping agent (e.g., sand) carried by the fluid to enter and fill the fracture. Fracturing creates new and larger flow channels through any damaged region surrounding the wellbore and also create additional surface area drainage for the well.

An excellent treatment of the mechanical behavior of rocks was presented by Haliburton Co. (1976). Competent rock behaves as an elastic and brittle material over certain ranges of conditions. The ratio of stress to strain, often referred to as Young's Modulus, E, is a fundamental property of a solid. Average values of E for rocks range from 0.5×10^6 (lightly consolidated sandstones) to 13×10^6 (denser limestone or dolomite). Rocks behave elastically up to some limiting value, then rupture or fail in tensile or shear failure depending upon the direction of the stress. The plane of shear failure depends upon the direction of stress and is located at an angle to the axis of stress. Because of lithological variations, stresses can vary in magnitude and/or direction from point-to-point in the rock. In general, fractures initiate and extend in a plane perpendicular to the least principle stress when the pressure exceeds the strength of rock (see Figure 1.2).

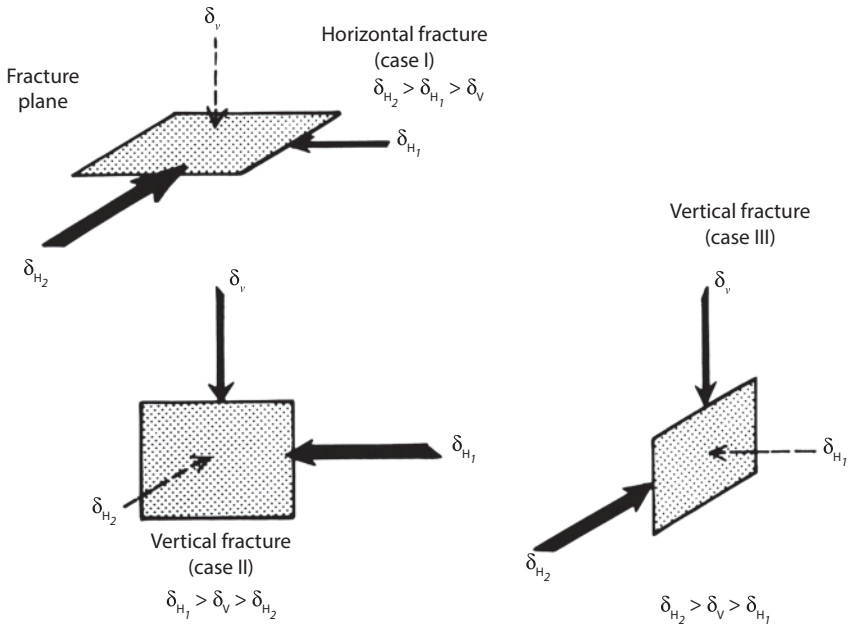

Figure 1.2 Effect of relative magnitude of principal stresses on fracture orientation. (After Fertl and Chilingarian, 1978, Figure A0-4, p. 301.).

Although hydraulic pressures pose little problems in destroying the containment of hydrocarbons within the reservoir when good engineering practice is followed, vertical fractures that extend through the containment zone (e.g., caprock, sheath of cement about the well casing, etc.) can create vertical gas migration pathways and in some cases pathways to overlying water aquifers.

Recently, some localized or statewide efforts attempted putting an end to the use of hydraulic fracturing regardless of its increased production benefits. For example, the residents of the City of Denton, TX, voted to ban all hydraulic fracturing in a referendum that was overwhelmingly passed on November 4, 2014 (Meshkati *et al.*, 2014). The Texas State Legislature in May 2015 passed House Bill #40 rendering the Denton hydraulic fracturing ban unenforceable and limiting the ability of any Texas city to regulate the oil and gas industry within the state (Bernd, 2015). New York State also banned the use of hydraulic fracturing of the Marcellus Shale in 2015; however, production from other parts of the Marcellus Shale in states such as Pennsylvania is continuing.

It is incumbent on the operating companies to be transparent with the public and communicate with local residents of the fracturing communities about all the scientific facts and risks of hydraulic fracturing.

In the opinion of the authors, fracturing can be done safely and be environmentally responsible as long as safe engineering practices are followed.

1.8 Oil Shale

In their classical contribution entitled "America's Unconventional Energy Opportunity," Porter *et al.* (2015), defined the unconventional gas/oil resources as well as those tight

oil/gas resources which are accessed and extracted primarily through the process of hydraulic fracturing. According to these authors, oil and gas from unconventional energy opportunities added more than 450 billion to the annual GDP of the United States, supporting more than 2.7 million American jobs that pay twice the median U.S. salary. To date, the commercial development of oil shale resources in other parts of the globe outside of the United States has not been initiated. A joint study by the United States Geological Survey (USGS) and the EIA has determined that there is technically recoverable shale oil and gas in 41 countries outside of the United States. Russia, China, Argentina, and Australia were identified as holders of the largest shale resources. Many countries possessing oil shale are facing high population growth rates and consequently higher energy demand in future years. The United States serves as a model in developing the shale's resources for these countries to meet their future energy requirements.

1.9 Corrosion

The corrosion of metals in an oilfield (see Chapter 6) affects the environment by breaking down the containment of hydrocarbons and allowing the escape of gas and fluids. The corrosion of pipelines and equipment damages their ability to contain hydrocarbons. In considering the economic cost, apart from the cost of repair, one must include the cost of cleaning up the environment due to these leaks. Methods of preventing corrosion, such as cathodic protection, sacrificial anodes, etc., are discussed in Chapter 6.

1.10 Scaling

Scaling is one of the biggest problems faced by many oil and gas producers. Minerals can be deposited in pipelines, formations, and/or surface facilities, often seriously impacting production. Scale inhibitors, chemicals that prevent or delay mineral deposition, along with innovative placement methods have been developed to control the deposition of scale. This depositional material may be deposited along water paths from injection wells, though the reservoir to production wells and surface equipment. Oilfield scale is a combination of deposits (e.g., inorganic minerals, sand and organic materials) that coat surface and subsurface tubing valves, perforations and the downhole formations. Most scale in the oilfield forms either by direct precipitation from water (e.g., due to a change in pressure or temperature) or as a result of produced water becoming oversaturated with scale components when two incompatible waters are mixed (Macay, 2008).

Water flowing through pipelines and/or formations often deposit inorganic scales. When the saturation of the ions dissolved in water exceeds the limit of solubility of that particular inorganic mineral, precipitation will occur coating: (1) perforations, (2) downhole completion equipment, e.g., safety equipment and gas mandrels and (3) the interior of pipelines, tubing and casing. Scale can form on the surface of almost any object or sometimes precipitate as particles that are suspended in the water (Oilfield Water Services, 2015). Methods of predicting the formation of scale are presented in Chapter 7.

1.11 Conclusion

As a final conclusion, the authors would like to quote the editorial of Professor George V. Chilingar, founder of *Journal of Petroleum Science and Engineering* and managing editor for many years (*J. Petrol. Sci. Eng*., 2005, 9:237): "... Underground gas storage and oil and gas production can be conducted safely if proper procedures are followed. After recognition of the existing problems, proper safe operating procedures can be developed."

References and Bibliography

Bernd, C., 2015, June 3. Exhausting Legal Options, Residents of Texas Town Take Direct Action to Enforce Fracking Ban. Truthout. http://www.truth-out.org/news/item/31,32-exhausting-legal-options-of-texas-town-take-direct-action-to-enforce-fracking-ban#

Chapman, R. E., 1983. *Petroleum Geology*, Elsevier, Amsterdam, pp. 245–251.

Chilingarian, G. V. and Wolf, K. H., 1975. *Compaction of Coarse-Grained Sediments I, Developments in Sedimentology* 18A, Elsevier, Amsterdam, 552 pp.

Chilingarian, G. V. and Wolf, K. H., 1976. *Compaction of Coarse-Grained Sediments II, Developments in Sedimentology* 18B. Elsevier, Amsterdam, 808 pp.

Chilingarian, G. V., Robertson, J. 0., Jr., and Kumar, S., 1987. *Surface Operations in Petroleum Production, I, Developments in Petroleum Science*, 19A. Elsevier. Amsterdam, 821 pp.

Chilingarian, G. V., Robertson, J. 0., Jr. and Kumar, S. 1989. *Surface Operations in Petroleum Production., II, Developments in Petroleum Science*. Elsevier, Amsterdam, 562 pp.

Clifton, H. E., Greene, H. G., Moore, G. W. and Phillips, R. L., 1971. Methane seep off Malibu Point following the San Fernando earthquakes. *U S Geol. Surv. Prof. Pap*. 733:112–116.

Coleman, D. D, Benson. L.J. and Hutchinson, P. J., 1990. The use of isotopic analysis for identification of landfill gas in the subsurface. In: *13th Annu. Int. Landfill Gas Symp.*, Lincolnshire, IL.

Coleman, D. D., 1987. Gas identification by geochemical fingerprinting. Trans. Am. Gas Assoc. Distribution/ Transmission Conf., Las Vegas, NV.

Coleman, D. D., Meents, W.F., Liv, C.L., and Keogh, R.A., 1977. Isotopic identification of leakage gas from underground storage reservoirs - a progress report 111. *State Geol. Surv. Pap.* 111:10 pp.

Curwen, T., 2016. *Los Angeles Times*, CA, Jan 3.

Doligez, B. (Editor), 1987. *Migration of Hydrocarbons in Sedimentary Basin*, 2nd 1FP Explor. Res. Conf., Carcans, France, Gulf Publ. Co., Houston, TX.

EIA, US, 2013. *Technically Recoverable Shale Oil and Shale Gas Resources: An Assessment of 37 Shale Formations in 41 Countries Outside the United States.* US Department of Energy/EIA, Washington, DC.

Endres, B., Chilingarian, G. V. and Yen, T. F., 1991. Environmental hazards of Urban Oilfield Operations. *J. Petrol. Sci. Engr.*, 6:95–106.

Fertl, W. H. and Chilingarian, G. V., 1978. Fracturing; in: G. V. Chilingarian and T. F. Yen (editors); *Bitumens, Asphalts and Tar Sands*. Elsevier, Amsterdam, pp. 269–306.

Hamilton, D. H. and Meehan, R. L., 1971. Ground rupture in the Baldwin Hills. *Science*, 72(3981): 333–344.

Heineke, J., Jabbari, N. and Meshkati, N., 2014. The role of human factors considerations and safety culture in the safety of hydraulic (fracking). *J. Sustainable Energy Engr.*, 2(2):130–151.

Hodgson, S.F. 1987. *Onshore Oil and Gas seeps in California*, Calif. Dep. Conser., Div. Oil Gas, Publ. TR26.

Jabbari, N., Ashayeri, C. and Meshkati, N., 2015. Leading Safety, Health, and Environmental Indicators in Hydraulic Fracturing. Paper presented at the SPE Western Regional Meeting held in Garden Grove, CA, 27–30 April, SPE-174059- MS. https://www.onepetro.org/download/conference-paper/SPE-174059-MS?id=conferencepaper%2FSPE-174059-MS.

Jenden, P. D. and Kaplan. 1. R., 1989. Analysis of gases in the Earth's crust. *Gas Res. Inst. Final Rep.* (March), Appendix A 6, A134–A157.

Jones, V. T. and Drozd. R. I., 1983. Predictions of oil or gas potential by near-surface geochemistry. *Am. Assoc. Pet. Geol. Bull.*, 67(6): 932–952.

Khilyuk, L. F., Chilingar, G. V., Robertson Jr., J. O. and Endres, B., 2000. *Gas Migration, Events Preceding Earthquakes*. Gulf Publishing Co., Houston TX, 386 pp.

Link. W. K., 1952. Significance of oil and gas seeps in world oil exploration. *Am. Assoc. Pet. Geol. Bull.*, 36(8):1505–1540.

Mackay, E. J., 2008. Oilfield scale. www.spe.org/dl/docs/2008/Mackay.pdf.

Meshkati, N., Jabbari, N. and Ashayeri, C., 2014. On Denton's upcoming referendum for a fracking ban. *Huffington Post*, http://www.huffingtonpost.com/najme. In meshkati/dentons-upcoming-referend_b_6072908.html.

Porter, M. E., Gee, D. S. and Pope, G. J., 2015. *America's Unconventional Energy Opportunity*. Harvard Business School/The Boston Consulting Group, 68 pp.

Schoell, M., 1983. Genetic characterization of natural gases. *Am. Assoc. Pet._Geol. Bull.*, 56(12):2225–2238.

Tek, M.R., 1987. Underground storage of natural gas. In: *Petroleum Geology and Engineering* (editor: G. V. Chilingar), Gulf Publ. Co., Houston, TX, pp. 321–323.

Therolf, G., Barboza, T. and Dolan, J., 2016. *Los Angeles Times*, CA, Jan. 17.

Yen, T. F. and Chilingarian, G. V., 1976. *Oil Shale*, Dev. Petrol. Sci., 5. Elsevier, Amsterdam, 292 pp.

Environmental Aspects of Oil and Gas Production.
John O. Robertson and George V. Chilingar.
© 2017 Scrivener Publishing LLC. Published 2017 by John Wiley & Sons, Inc.

2

Migration of Hydrocarbon Gases

2.1 Introduction

Seepage of methane and other hydrocarbons along faults, fissures, fractures, and outcrops from hydrocarbon-bearing formations is prevalent throughout the globe. The major composition of hydrocarbons in a natural gas migrating from a hydrocarbon reservoir (see Tables 2.1 and 2.2) is methane (typical range of 80% to 90%). Figure 2.1 shows that methane can be derived from several sources: (1) biogenic (shallow bacterial decomposition of organic matter) and (2) thermogenic (hydrocarbon deposits formed by deep burial). Methane is found in great abundance in association with oil and gas fields. Nikonov (1971) demonstrated the abundance of methane in many types of hydrocarbon gas sources (Figure 2.2).

Methane is the simplest hydrocarbon and occurs in significant quantities in many areas migrating through the Earth in a gaseous form. As a gas it is light (about half the density of air), flammable, colorless and odorless. If the concentration of methane in the air ranges from 5% to 15%, in the presence of a spark, this mixture is explosive. The consequences of undetected methane gas migrating through the soil under structures can be disastrous due to the explosive and flammable capabilities of the gas itself. It is encountered dissolved in fluids (oil/water) or as a gas.

The principal hydrocarbons present (generally greater than 90% by volume) in natural gas are methane (CH_4), followed by ethane (C_2H_6), propane (C_3H_8), butanes (C_4H_{10}), and heavier components. The heavier hydrocarbons are present in a natural gas in decreasing proportions because of their high molecular weights. Upon migration, heavier hydrocarbons are preferentially adsorbed on rock minerals, mainly clays.

Table 2.1 Typical composition of natural gases expressed in mole % (or volume %). (In: Chilingar *et al*., 1969, table 1, p.89.)

	Type of gas field					
				Separation Pressures[4]		
Component	Dry Gas[1] (mole %)	Sour Gas[2] (mole %)	Gas Condensate[3] (mole %)	400 psi (mole %)	50 psi (mole %)	Vapor (mole %)
Hydrogen sulfide	0	3.3	0	0	0	0
Carbon dioxide	0	6.7	0.68	0.3	0.68	0.81
Nitrogen and air	0.8	0	0	0		2.16
Methane	98.8	84.0	74.55	89.57	81.81	69.08
Ethane	2.9	3.6	8.28	4.56	5.84	5.07
Propane	0.4	1.0	4.74	3.60	6.46	8.76
Isobutane	0.1	0.3	0.89	0.52	6.46	2.14
n-Butane	Trace	0.4	1.93	0.90	2.26	5.02
Isopentane	0		0.75	0.19	0.50	1.42
n-Pentane	0		0.63	0.12	0.48	1.41
Hexane	0	0.7	1.25			
Heptane	0			0.15	1.05	4.13
Octane	0		6.3			
Nonane	0					
Total percent	100.0	100.0	100.0	100.0	100.0	100.0

[1]Gas from Los Medanos, CA; [2]Gas from Jumping Pound, Canada; [3]Gas from Poloma, CA; [4]Gas from Ventura, CA (oil and gas separators).

Table 2.2 Physical constants of light hydrocarbons and other components associated with natural gas. (Data abstracted from Natural Gas Processors Suppliers Association, 1981.)

Physical constants of selected light hydrocarbons								
Compound	Formula	Molecular weight	Boiling point @ 1 atm. (°F)	Vapor pressure @ 100 °F (psia)	Critical temperature (°F)	Critical pressure (psia)	Liquid specific gravity[1]	Gas specific gravity[2]
Hydrocarbons:								
Methane	CH_4	6.04	−258.68		−116.5	673.1		0.5555
Ethane	C_2H_6	30.07	−127.53		90.09	708.3	0.375	1.046
Propane	C_3H_8	44.09	−43.73	190	206.26	617.4	0.5077	1.547
n-Butane	C_4H_{10}	58.12	10.89	51.6	305.62	550.7	0.5841	2.071
Isobutane	C_4H_{10}	58.12	31.10	72.2	274.96	529.1	0.5631	2.067
Isopentane	C_5H_{12}	72.15	82.1	20.44	370.0	483	0.62476	2.4906
n-Pentane	C_5H_{12}	72.15	96.933	15.57	385.92	489.5	0.63116	2.4906
n-Hexane	C_6H_{14}	86.17	155.736	4.956	454.5	439.7	0.66405	2.9749
n-Heptane	C_7H_{16}	100.20	209.169	1.6199	512.62	396.9	0.68819	3.4591
n-Octane	C_8H_{18}	114.22	258.197	0.537	565.2	362.1	0.7077	3.*4432
n-Nonane	C_9H_{20}	128.25	303.436	0.179	(613)	(345)	0.72171	4.4275
n-Decane	$C_{10}H_{22}$	142.28	345.2	0.073	(655)	(320)	0.73413	4.9118
Nonhydrocabons:								
Nitrogen	N_2	28.02	−320.4		−232.8	92		0.9672
Oxygen	O_2	32.00	−297.4		−181.8	730		1.1047
Hydrogen	H_2	2.016	−422.9		−199.8	188		0.0696
Air	N_2 & O_2	28.97	−317.7		−221.3	547		1.0000
Carbon Dioxide	CO_2	44.01	−109.3		88.0	1073	0.8159	1.5194
Hydrogen Sulfide	H_2S	34.08	−76.5	554.6	212.7	1306	0.790	1.1764
Water	H_2O	18.02	212.0	0.9492	705.4	3206	1.000	0.6220

[1]all measurements made with respect to water Specific Gravity = 1.0
[2]all measurements made with respect to air Specific Gravity = 1.0

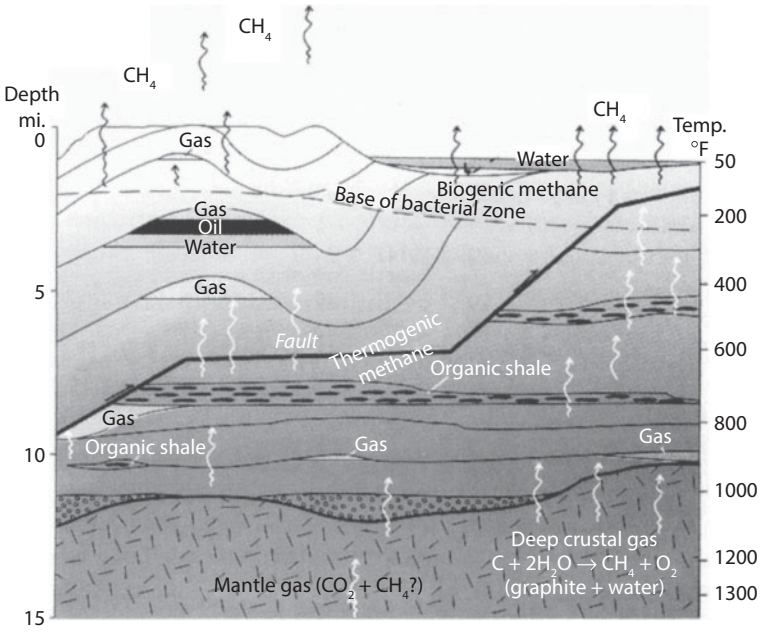

Figure 2.1 Three processes can generate methane (CH_4), the main component in natural gas. Biogenic methane is produced by microorganisms during metabolism. Thermogenic methane forms when heat and pressure decompose deeply-buried organic matter. Chemical reactions deep inside the Earth can also generate methane. (Modified after Howell *et al*., 1993; in: Khilyuk *et al*., 2000, p. 46, figure 3.2.)

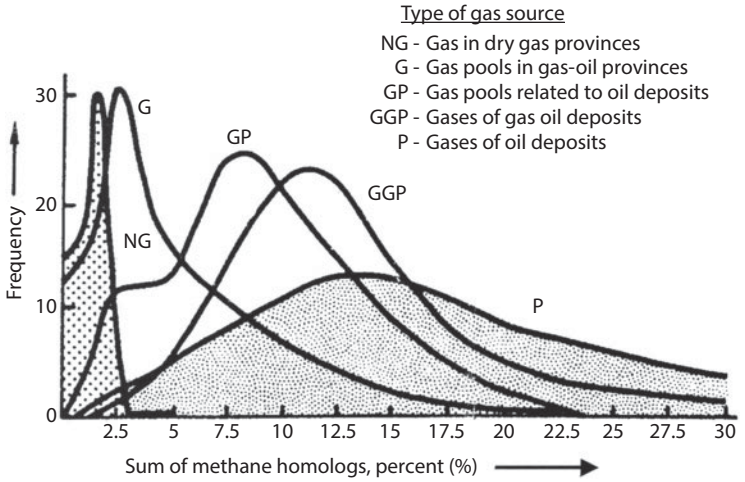

Figure 2.2 Frequency distribution of sum of methane gas homologs in different types of deposits. Figure based upon analysis and classification of 3500 worldwide reservoir gases. (Modified after Nikonov, 1971; in: Khilyuk *et al*., 2000, p. 47, figure 3.3.)

The composition of hydrocarbons in natural gases produced from an oil reservoir will vary with various operating oil/gas separator pressures. The example in Table 2.1 illustrates this variation of different components at various oil/gas separation pressures for the same produced gas.

2.2 Geochemical Exploration for Petroleum

The presence of methane in soil gas has long been used to identify the potential presence of petroleum. Based upon the potential migration of this hydrocarbon gas from a petroleum source, geochemical exploration for oil/gas is often conducted by sampling the air in surface samples of soil for the presence of hydrocarbons and then subjecting this gas to chromatographic analysis to detect the presence of methane and other hydrocarbons. This near-surface soil gas exploration for petroleum is based on the detection and interpretation of a great variety of natural phenomena occurring at or near the land surface or seafloor and attributed, directly or indirectly, to hydrocarbons migrating upward from "*leaky*" reservoirs (Sundberg, 1992).

Development of surface geochemical exploration was conducted in the early 1930s, with the chemical analysis of gaseous hydrocarbons found in the air above the surface and/or air within the pores of soil itself. Geochemical exploration presumes that all oil or gas reservoirs leak some hydrocarbons to the surface, and that these migrating hydrocarbons, if the volume of hydrocarbons is sufficient to be detected, can be related to possible subsurface oil/gas reservoirs. As an exploration technique, surface geochemistry assumes that (1) most reservoirs leak sufficient hydrocarbons to the surface to be recognized geochemically and (2) geochemical anomalies could be associated with commercial reservoirs. It also assumes that detected surface seepage of hydrocarbons is useful in determination of the presence of hydrocarbons of potential subsurface traps (reservoirs). This type of analysis of migrating hydrocarbon gas in the soil can be used to evaluate potential oil/gas reservoirs (Sundberg, 1994).

Sundberg (1994) pointed out that in hydrocarbon exploration the use of seeps for identifying the presence of a petroleum source is widely accepted and practiced throughout the petroleum industry. All companies use a variety of techniques aimed at seep detection and hydrocarbon characterization. Particular methods may vary, but the general objectives of the various surveyors are about the same (Sundberg, 1994):

1. locate hydrocarbon seeps,
2. map the seeps to relate them to subsurface prospects,
3. characterize the petroleum type hydrocarbons in a seep,
4. refine economic evaluations before drilling deeper wells, and
5. aid exploration departments in making lease relinquishments.

2.3 Primary and Secondary Migration of Hydrocarbons

Organic material is transformed first into kerogen and then into hydrocarbons as it decomposes and is subjected to pressure and temperature. Due to their lighter density (buoyancy) compared to that of water at the same depth, these hydrocarbons migrate from their source rock, where they were formed, to the reservoir rock, where they are currently found, and then to the surface.

2.3.1 Primary Gas Migration

Primary migration refers to the initial movement of hydrocarbons from the source rock to the reservoir. According to Chilingar *et al.* (2014), under the influence of increasing overburden pressure and geothermal temperature, kerogen in argillaceous sediments will generate petroleum hydrocarbons by thermal decomposition. The chemical process of generation of oil has become well established (Welte, 1972). The mechanism of petroleum migration out of source rocks, however, is still poorly understood. Many geologists believe that carrier water is necessary for the primary migration of oil (Hedberg, 1964). They consider that carrier water and oil migrate in the form of solution and/or emulsion. Interlayer water of montmorillonite released by transformation to illite during the late stage of diagenesis was considered to be essential for petroleum migration (Powers, 1964; Burst, 1969; Perry and Hower, 1972). On the other hand, Aoyagi and Asakawa (1980) concluded that both the interlayer and interstitial water expelled during the middle stage of diagenesis were responsible for oil migration.

Based on extensive observations, shales composed of non-expandable clays such as kaolinite and illite did not act as source rocks, because of the absence of water necessary to push out the oil (Chilingar, 1960; Aoyagi *et al.*, 1985). Also, many undercompacted (overpressed) shales did not act as source rocks, because compaction mechanisms were not operative to squeeze a sufficient amount of oil into the reservoir rocks.

On the other hand, McAuliffe (1966) has objected to these opinions on the basis that oil is only very slightly soluble in water. Also, some geologists have favored the migration theories based on the movement of oil and gas due to the capillary phenomena, buoyancy effect and gas expansion, which are generally independent of the movement of water (Dickey, 1975). Some migration of oil could also occur in a gaseous form (Chilingar and Adamson, 1964).

It is necessary to establish what conditions existed during the primary migration of oil (from source rocks to reservoir rocks) compared to those during the secondary migration of oil (during production) to make the former so much more efficient. Several possible explanations were presented by Chilingar *et al.* (2015): intense electrokinetics, Earth-tides, compaction, migration in a gaseous form, and seismic activity (earthquakes).

Schowalter (1999) pointed out that the mechanisms of primary hydrocarbon migration and the timing of hydrocarbon expulsion have been debated by petroleum geologists since the beginning of the science. His discussion of several proposed primary hydrocarbon migrations includes: solution in water, diffusion through water, dispersed droplets, soap micelles, and continuous-phase migration through the water-saturated pores. Some early workers generally favored early expulsion of hydrocarbons with the water phase of compacting sediments. Schowalter (1999) further noted that Cordell (1972) has suggested that oil is formed at depths where the petroleum source rocks have lost most of their pore fluids by compaction. On the basis of these conclusions, Dickey (1975) suggested a case for primary migration of oil as a continuous-phase globule through the pores of the source rock. Roof and Rutherford (1958) suggested that continuous-phase oil migration from source rock to reservoir is required to explain the chemistry of known oil accumulations.

Gas accumulations, however, can be explained by either continuous-phase primary migration or by discontinuous molecular-scale movement of gas dissolved in water. Price (1976) offered still another expulsion concept. He postulated molecular solution at high temperature, upward movement with compaction fluids, and exsolution at shallower depths in low-temperature saline waters.

In order to investigate some problems involved in primary migration of oil (Aoyagi *et al.*, 1985) compacted Na-montmorillonite clay mixed with seawater and crude oil for 25 days under a pressure of 1000 kg /cm^2 and a temperature of 60 °C. The proportion of oil in the expelled liquid increased with time. The porosity of the compacted sample decreased from 81% to ≈26%. These authors concluded that the primary migration of oil from source rocks to reservoir rocks occurred chiefly during the late compaction stage (ϕ = 10–30%). Considering the fact that tectonic activity during the primary migration of oil was intense, the oil was simply squeezed out (expelled) from the source rock.

2.3.2 Secondary Gas Migration

Secondary migration refers to the subsequent movement of hydrocarbons from the original reservoir toward the surface. This migration occurs while the hydrocarbons are clearly identifiable as crude oil and or gas, although the migrating gas can be found in either a (1) free form or (2) dissolved in fluids, e.g., oil and/or water. The density of most hydrocarbons is less than that of water; therefore, buoyancy of the hydrocarbons becomes a primary driving force moving the hydrocarbons due to differences in densities between water and hydrocarbons and also in response to differential pressures within the reservoir itself.

2.3.3 Gas Entrapment

Hydrocarbons (oil, gas and gas-dissolved-in-water) migrate along various pathways, moving from areas of higher pressure to lower pressure, pushed by buoyancy forces as they work their way toward the surface of the Earth. The reason for accumulation of hydrocarbons in a trapping area (reservoir) is that the hydrocarbons escape from this trapping area (reservoir) at a rate slower or equal to those entering the area. All hydrocarbon reservoirs leak over geologic time and, eventually, all hydrocarbons will escape from one trapping area to another, as they migrate toward the Earth's surface. The primary hydrocarbon trapping area is the primary reservoir, and the subsequent traps as the hydrocarbons migrate to the surface are secondary reservoirs.

The hydrocarbon reservoir could be viewed as a temporary holding tank, which leaks at a very slow rate as the petroleum migrates from one reservoir (trap) to another. The time period that any reservoir holds hydrocarbons can be on the order of thousands to millions of years, depending upon the type of migrating hydrocarbon, volume, chemical composition, and the reservoir properties (permeability, porosity, pressure, temperature, etc.) at that time. During this migration period, the hydrocarbon molecules under pressure and temperature are slowly breaking into smaller and lighter hydrocarbon molecules, evolving toward simpler molecules of hydrocarbon (e.g., methane) and, finally, carbon-dioxide. While the migration of larger hydrocarbon molecules can

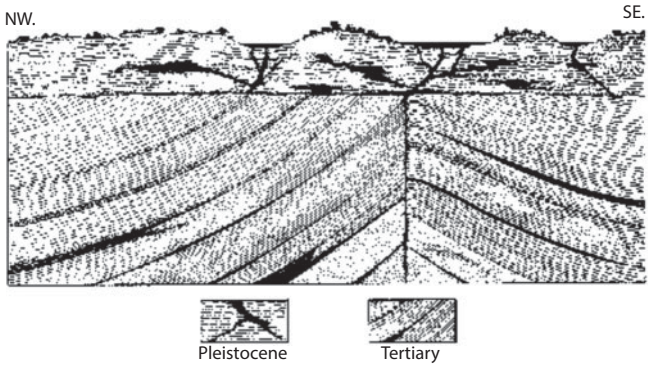

Figure 2.3 1907 U. S. Geological Survey drawing shows how oil from underground rock layers migrates upward to fill the La Brea pits. (Drawing from "Rancho La Brea, A Record of Pleistocene Life in California".)

be impeded by smaller migratory pathways of pore and fracture spaces, over time the breakdown of larger into smaller hydrocarbons results in the smaller hydrocarbon molecules having an easier task of passing through the finer pores and fractures (Khilyuk *et al*., 2000).

Migration of hydrocarbons, gas and oil (sometimes tar or heavy oil) has been long observed in petroleum seeps that breach the surface, e.g., La Brea Tar Pits, CA. In this case, oil and gas have naturally migrated along faults to the surface as shown in Figure 2.3. Khilyuk *et al*. (2000) noted that the primary migration of hydrocarbons occurred along the 3rd and 6th Street faults to the surface forming the La Brea Tar Pits. Additional secondary migration of gas occurred along paths that were man-made (abandoned wellbores), which resulted in migration of gas below several structures, giving rise to explosion and fire.

2.4 Origin of Migrating Hydrocarbon Gases

Stray natural gas migration refers to movement of natural gas (primarily methane) through rock formations and soil. This gas can originate from leakage of a variety of natural sources, including petroleum reservoirs, coal seams, landfill, or any source of decomposing organic material. It can also originate from man-made installations, e.g., from leaking pipelines and any wellbore (gas, oil, and/or water) leaking hydrocarbons to the water sands above, surface, etc. Freshly drilled and completed or abandoned oilwells (some many years ago) can leak hydrocarbons, liquids, and gas to the surrounding formations if the cement has not totally isolated the well fluids in the reservoir from the wellbore. When a well is drilled, a new man-made pathway for the potential migration of gas is created. This is partly due to the induced fracturing of the formation during the drilling percussion process as the drillbit cuts the formation. Particular care must be taken in completing the well to be sure that potential paths of migrating fluids are properly plugged to block the potential migration of fluids (gas and liquids).

The migration of stray gas is common, particularly, in areas that are underlain by deposits of petroleum, coal or decomposing organic materials.

2.4.1 Biogenic vs. Thermogenic Gas

Knowing whether a *natural gas show* is biogenic gas or thermogenic gas is critical to understanding the source of migrating hydrocarbons and if they are related to a petroleum deposit. Geochemical analyses can be utilized to reveal the origin of gas in a gas show or seep, and indicate the presence of petroleum deposit versus a natural (bacterial) source of gas (methane).

2.4.1.1 Sources of Migrating Gases

Natural gases, a mixture of light-hydrocarbon and non-hydrocarbon gases migrating from petroleum reservoirs, vary in chemical and isotopic composition depending on their origin and migration history. Here, natural gas refers to a gas present in petroleum reservoirs. Crustal degassing and thermogenic or biogenic decomposition of organic matter can generate methane, the major constituent of gases. Common sources of natural gases include low-temperature bacterial fermentation (Rice and Claypool, 1981), thermogenic breakdown of deeply buried sedimentary organic matter (Schoell, 1983), and the mantle (Gold and Soter, 1980, 1982). The thermogenic decomposition of organic material is a large source of methane. Methane gas is the major component of natural gases associated with petroleum deposits. The non-hydrocarbon gases often present in migrating gases are the "acid" and "inert gases." Carbon dioxide and hydrogen sulfide are referred to as "acid gases" as they can form acids on contact with water. Nitrogen and helium are referred to as "inert gases." Normally, gases are partially or completely saturated with water vapor. The source of sulfur found in hydrogen sulfide and mercaptans is from the organic material from which they were derived. Unless sulfur is present, gases are colorless and odorless.

2.4.1.2 Biogenic Methane

Methane is the primary component of gases resulting from the biogenic decomposition of organic material under low temperature and pressure. For biogenic and thermogenic decomposition of organic materials, almost all of the hydrocarbon gases are composed of methane with very few heavier hydrocarbons (i.e., ethane, propane, etc.) (Figure 2.4). Figure 2.5 is a schematic diagram for the conversion of organic matter to methane and carbon dioxide. Biogenic decomposition only occurs in shallow sediments where organic matter is exposed to low pressure and temperature without oxygen.

Kaplan (1994) noted that the landfill environment was ideal for the biogenic generation of methane and hydrogen sulfide. Methanogenic bacteria (*Archaeobacteria*) are responsible for producing methane (Woese and Wolfe, 1985). Ward *et al.* (1978) stated that biogenic methane involves a consortium of microorganisms. The first step in the process involves the enzymatic hydrolysis of complex biochemicals discharged into the environment. When some oxygen is present in the decompositional environment (i.e., in water) aerobic respiration may rapidly convert the organic material into carbon dioxide. If oxygen is excluded during rapid burial, metabolic degradation proceeds by fermentation. The methanogenic bacteria can disproportionate the acids into methane (see Table 2.3).

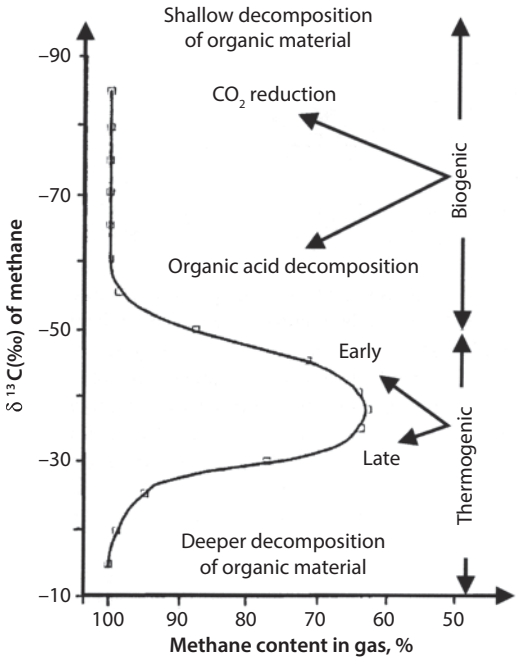

Figure 2.4 Relationship between the carbon isotope ratio and methane content $[C_1/(C_1\text{-}C_2)]$ in gas. (Modified after Kaplan, 1994, p. 305, figure 13.)

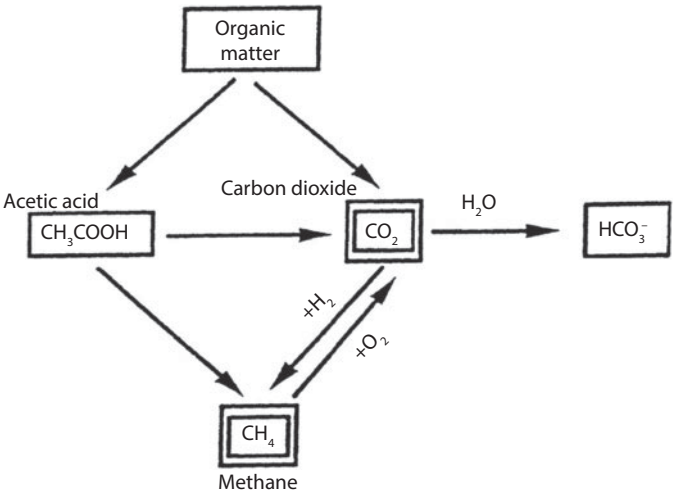

Figure 2.5 Schematic diagram for the conversion of organic matter to methane and carbon dioxide. (Modified after Kaplan, 1994, p. 298, figure 2.)

In biogenic systems, the type of environment influences the method of methane formation. Mah and Sussman (1967) noted that primarily methane forms through fermentation of sewage sludge. Claypool and Kaplan (1974) suggested that in marine environments (Figure 2.6), methane forms by reduction of CO_2. In fresh-water environments (i.e., swamps, lakes, or rice paddy fields) the process is that of fermentation.

Table 2.3 Types of chemical reaction leading to methane formation. (Modified after Kaplan, 1004, figure 1, p. 298.)

Acetic acid fermentation:	$CH_3COOH \rightarrow CH_4 + CO_2$
CO_2 reduction:	$CO_2 + 4H_2 \rightarrow CH_4 + H_2O$
Mixed reactions:	
(a) $CH_3(CH_2)(n-1)COOH + nH_2O \rightarrow CH_3(n-1)COOH + CO_2 + (n+1)H_2$	
(b) $nCO_2 + 4nH_2 \rightarrow nCH_4 + 2nH_2O$	

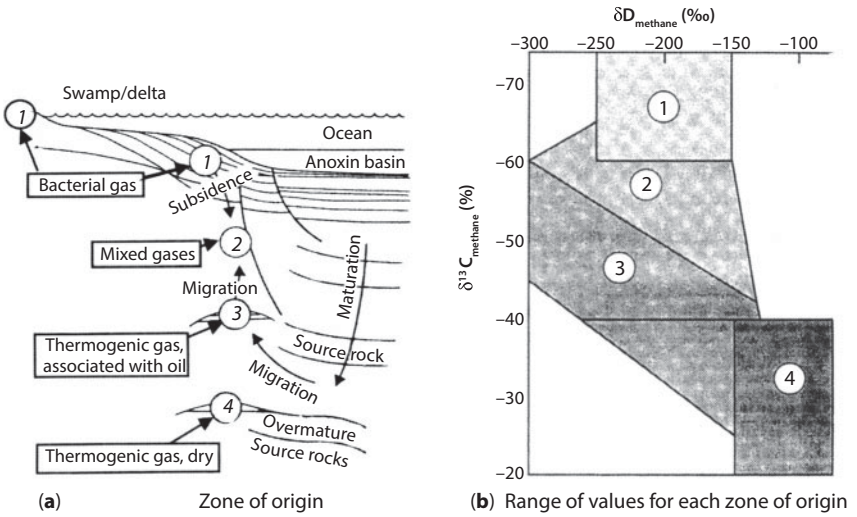

Figure 2.6 The isotopic composition of gas as related to its origin. The left panel depicts the geologic context of the gas origin (e.g., shallow bacterial, thermogenic, etc.) The right panel shows the range of anticipated values for carbon (y-axis) and hydrogen (x-axis) isotopic composition of methane in different genetic types of gases. Inasmuch as the PDB and SNOW are enriched in the13C and D in comparison to natural gases, the latter have negative $\delta^{13}C$ and δD values. (Modified after Schoell *et al.*, 1963, p. 338, figure 1.)

In saline environments and ruminating of herbivores, methane is produced by respiratory oxidation of hydrogen with CO_2. Mah *et al.* (1977) have suggested that methane forms by a combination of two metabolic processes (Figure 2.5).

Kaplan (1994) described the microbiological successions in an aqueous environment, such as a lake, swamp, or estuary (Figure 2.7), and suggested that the same microbiological succession can also apply to the rice paddy field or landfill site in an environment with high rainfall. In this case, the methane will form at a depth where the respiratory organisms, which can derive the maximum energy, are no longer able to compete. Methanogenesis by reduction of CO_2, is more efficient than methanogenesis by fermentation.

2.4.1.3 Thermogenic Methane Gas

Thermogenic decomposition of organic material may give rise to oil and gas under high temperature and pressure. As shown in Figure 2.4, this type of decomposition

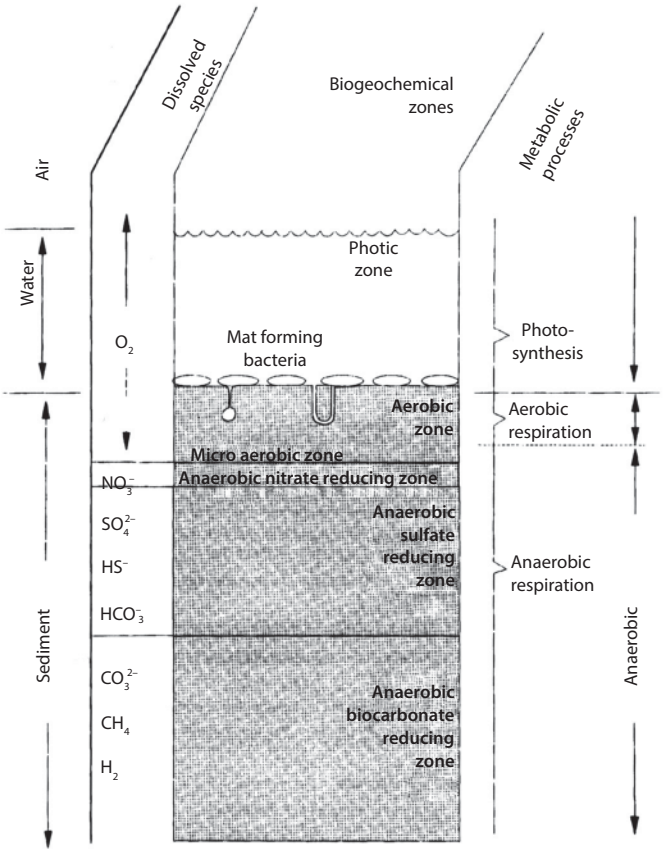

Figure 2.7 Biogeochemical process in a marsh. An idealized cross-setion of a deltaic organic-rich (reducing) sedimentary environment. The biogeochemical zones are a consequence of ecological succession. (After Claypool and Kaplan, 1994, p. 299, figure 4.)

creates not only methane, but also other light hydrocarbons. The methane content in the hydrocarbon portion of the gas is directly related to the temperature and pressure histories to which the organic material has been subjected. In order to differentiate the biogenic gases from thermogenic, it is necessary to know the ranges of isotopes of thermogenic and biogenic methane (Table 2.4). In fact, the isotopic values indicate the highest thermogenic pressure and temperature that the gas was exposed to. Examples of ranges for isotope ratios of carbon and hydrogen for various living and biologically derived materials, biological and nonbiological minerals, and gases are presented in Figures 2.8 and 2.9.

2.4.2 Isotopic Values of Gases

The origins of biogenic and thermogenic gases can be determined by isotopic gas analysis (the isotopic ratios of carbon and hydrogen). As shown in Figure 2.10, the isotope ratio of carbon ($^{13}C/^{12}C$) can be plotted versus the isotope ratio of hydrogen ($^{2}H/^{1}H$ or D/H). Clustering of data indicates the type of process in which the methane was formed. The heavy isotopes of ^{13}C and D (deuterium) are the rare species and constitute

Table 2.4 Ranges of carbon and deuterium isotope ratios for methane derived from different origins. (After Kaplan, 1994, table 2, p. 301.)

		$\delta^{13}C$	$\delta^{2}D$
Biogenic:	CO_2 reduction	−100 to −60	−250 to −150
	Organic acid decomposition	−60 to −45	−350 to −250
Thermogenic:	Immature (low temperature)	−50 to −40	−250 to −220
	Optimum maturity	−40 to −30	−220 to −160
	Highly mature (high temperature)	−30 to −15	−160 to −90

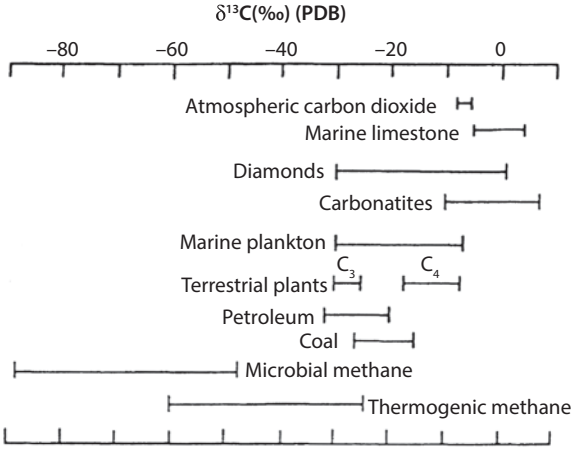

Figure 2.8 $\delta^{13}C$ values of selected materials. (Modified after Kaplan, 1994, p. 301, figure 5.)

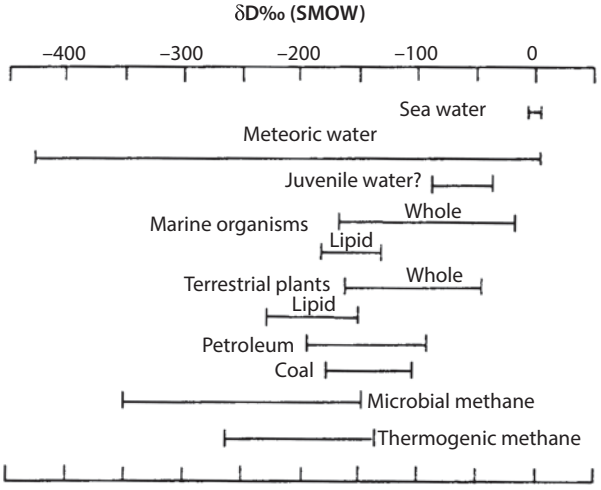

Figure 2.9 The δD values of selected materials. (Modified after Kaplan, 1994, p. 301, figure 5.)

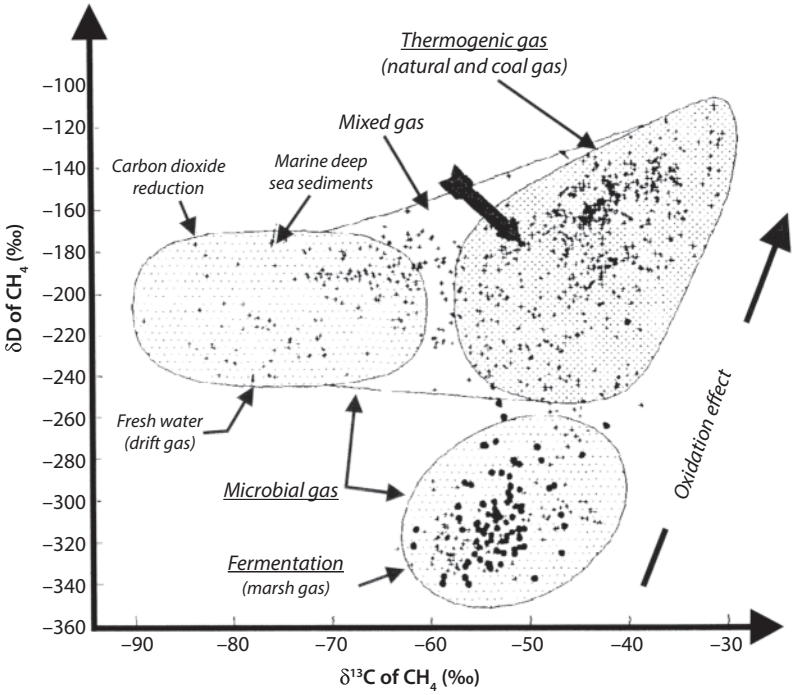

Figure 2.10 Carbon and hydrogen isotopic compositions of methane from various sources. The heavy arrow points to a specific thermogenic gas sample. (After Schoell, 1980, Figure 3.)

1% of all carbon and 150 ppm of all hydrogen, respectively. Small variations in $^{13}C/^{12}C$ and $D/^{1}H$ ratios can be measured very accurately with modern mass spectrometers. For convenience, ratios are expressed in δ-notation as part-per-thousand (‰) variations relative to the PDB (Peedee Belemnite; carbon) and SMOW (hydrogen) isotope standards as follows:

$$\delta^{13}C(‰) = \left[\frac{[^{13}C/^{12}C]_{sample}}{[^{13}C/^{12}C]_{PDB}} - 1 \right] \times 1000 \tag{2.1}$$

and

$$\delta^{13}D(‰) = \left[\frac{[D/^{1}H]_{sample}}{[D/^{1}H]_{SMOW}} - 1 \right] \times 1000 \tag{2.2}$$

$\delta^{13}C$ and δD values for a gas may vary widely depending on the origin of the gas (Figure 2.6). Biogenic gases are grouped by the isotope ratios in one portion of the graph, whereas the thermogenic gases are grouped in another area. These ratios do not change significantly with repressurization, solution, dissolution, or other physical processes that take place during the gas migration to the surface. Those ratios, which reflect the origin of gases, are stable and independent of reservoir and sampling conditions. Consequently, the ratios are useful as tracers of origin and detection of gas movement from one part of a petroleum reservoir to another. As shown in Figure 2.4,

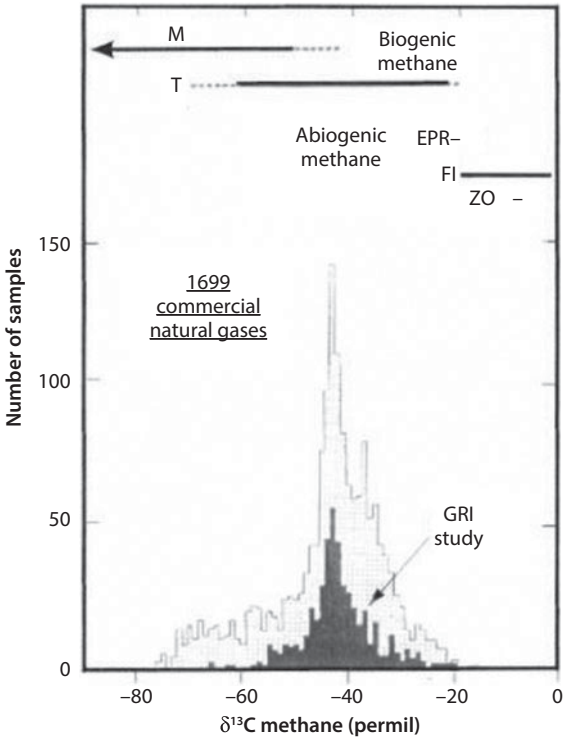

Figure 2.11 Number of commercial natural gas samples versus δ^{13}C of methane. (After Jenden and Kaplan, 1989, Figure 1 and Jenden *et al.*, 1993, p. 37, figure 1.)

the product of biogenic decomposition is almost all methane. Only small amounts of ethane and heavier hydrocarbons are generated. Although thermogenic decomposition does produce heavier hydrocarbons such as ethane in the earlier stages, in the later stages (higher pressures and temperatures) it also primarily produces methane.

According to Price and Schoell (1995), as natural gas migrates from its site of origin to the reservoir traps above, it may fractionate, becoming much richer in methane. Table 2.4 lists typical ranges of isotopes for the biogenic and thermogenic decomposition of organic material. Isotopic ratio yields information on the past history. The composition and the isotope ratios of a gas may help determine the source of the gas.

Isotope compositions of light hydrocarbon gases can help identify the origin of surface gas seeps. Gases formed by bacterial alteration of shallow-buried sediments, peats, and organic-rich shales are composed almost entirely of methane. These gases (methane $\delta^{13}C < -60‰$) are isotopically light (Table 2.4). Carbon and hydrogen compositions of methane from various sources is presented in Figure 2.10. Jenden and Kaplan (1989) and Jenden *et al.* (1993) presented a valuable distribution graph of δ^{13}C of methane versus number of commercial natural gases (Figure 2.11).

2.4.3 Nonhydrocarbon Gases

Poreda *et al.* (1988) stated that at least two mechanisms are responsible for the origin of CO_2 in the subduction gases. Decarbonation or oxidation reactions produce a

high-CO_2, low-$^3He/^4He$ gases, whereas high-$^3He/^4He$, CO_2-rich gas may originate from the mantle. He isotope ratios provide information on the input of magmatic gases into crustal systems. The magmatic He component has a $^3He/^4He$ ratio (R) ranging from 0.5 to 3.8 times the atmospheric value (R_A); also it has high $^3He/^4He$ ($R_A = 0.6 - 3.9$) and low $CH_4/^3He$ ($<10^6$) ratios. The crustal He component has low $^3He/^4He$ (0.01 R_A) and high $CH_4/^3He$ ratios (for details see Poreda *et al*., 1988).

The nitrogen-rich gases in the California Great Valley may originate from mixing (1) hydrocarbon-rich gas with $^3He/^4He \leq 0.1\ R_A$ (derived from microbial and thermogenic alteration of sedimentary organic matter), (2) hydrocarbon-rich gas having $^3He/^4He \geq 2.75\ R_A$ (derived from the localized pyrolysis of sediments by magmatic volatiles), and (3) nitrogen-rich gas with $^3He/^4He \approx 1\ R_A$. The nitrogen-rich component is characterized by methane $\delta^{13}C < -25‰$ and N_2/Ar ratios as high as 22,000 (for details see Jenden *et al*., 1988).

In most soil-gas samples, the presence of nitrogen, along with oxygen, would indicate contamination of the sample with air. In general, nitrogen is an inert trace component and is likely derived from the thermal alteration of sedimentary organic matter. Dry thermogenic gases produced in the Sacramento and northern San Joaquin basins of California contain up to 87% nitrogen (Jenden *et al*., 1988). Investigation indicates that this nitrogen has a complex origin involving mixing from multiple sources. It appears that a portion of the nitrogen is derived from the igneous intrusives and subducted metamorphic rocks. The methane $\delta^{13}C$ values as heavy as −15‰ indicate that this gas, high in nitrogen, originates from the deep-crustal, meta-sedimentary rocks.

Helium isotope ratios may identify the gas as being a product of mantle degradation. Poreda *et al*. (1988) noted that magmatic He appears to be a common constituent of gases from tectonically active areas. The associations of mantle He and volcanism suggests that the heat supplied by the igneous intrusions could have played a role in producing the methane by thermal alteration of organic sediments. There is no evidence to invoke a mantle origin for methane.

2.4.4 Mixing of Gases

Schoell *et al*. (1993) prepared cross-plots of the isotopic ratios for methane versus percentage of nitrogen for mixtures of injected (B) and native (A) gases. The straight line is called the "*mixing line*" and represents a mixture of gases A and B (Figure 2.12). The triangles represent the composition of the gas that is moving into the domain of the native gas, whereas the circles represent the native gas that is present in the pores. The squares represent mixtures of the two gases. Isotopic analysis provides an excellent method of identifying and quantifying the degree of mixing. The precision to which one can quantify mixtures of two different gases is dependent on the precision of the analysis and on the consistency of composition of native and migrating gases. Composition of the sample from observation well (d), which plots directly on the mixing line, contains approximately 40% injection gas and 60% native gas.

In the case of gas storage, the native or reservoir gas has a relatively constant composition, whereas those of the injected gas can vary with time, depending on the source. Figure 2.13 is an example presented by Schoell *et al*. (1993) showing how the isotopic ratios of carbon and hydrogen can be plotted to determine the composition or mixing

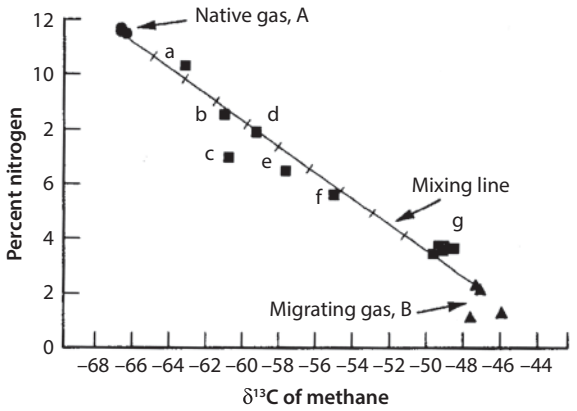

Figure 2.12 Nitrogen concentration plotted versus carbon isotope ratio for samples from a gas storage field. (After Schoell *et al*., 1993, p. 342.)

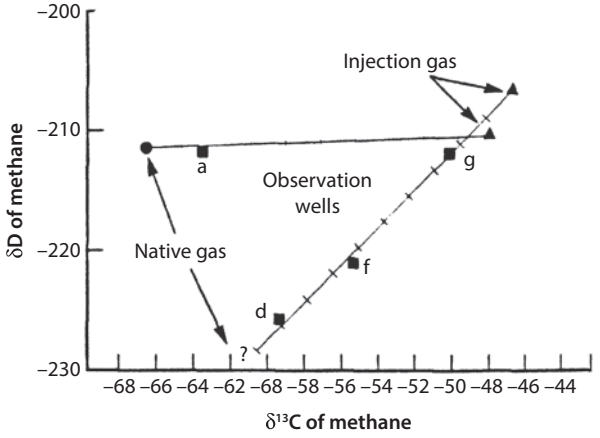

Figure 2.13 Carbon and hydrogen isotopic compositions of gas samples from a gas storage field. The question mark is located where 6D is that of a native gas of different vintage (no measurement of this gas was available). (After Schoell *et al*., 1993, p. 342, figure 7.)

ratio of the native and injected gases. In this case, the isotopic ratios show that there are two different native gases. This is not unusual in reservoirs that are divided into fault blocks. The data in Figure 2.13 would indicate that there is no communication within the reservoir between the well (a) and the other three wells (d, f, and g) as shown by isotopic ratios.

2.4.5 Surface Gas Sampling

The typical gas sampled at the surface is a mixture of biogenic gases (native) generated at the surface and thermogenic gases (migrating) that have migrated up from greater depths. A common problem is the determination of the origin of gas present at the surface: did it migrate from greater depths or is it simply the product of biological reactions at the surface? This is particularly important if one is attempting to determine whether

gas is migrating from a petroleum reservoir or not. A cross-plot, such as the one shown in Figure 2.10, helps determine if the mixed gas is of thermogenic or biogenic origin. As the thermogenic (migrating) gas is mixed with the surface biogenic (native) gas, the isotope ratios will occupy a certain area of the diagram. The effect of oxidation of the gases is also shown in this figure. If the isotopic ratios of the native and migrating gas are known, the proportions of gases in a mixture can be directly calculated using a linear relationship (e.g., see Figures 2.12 and 2.13). For greater detail, refer to the classical works of M. Schoell, I. R. Kaplan, P. D. Jenden, A. W. A. Jeffrey, R. J. Poreda, G. E. Claypool, and D. D. Coleman.

2.4.6 Summary

In summary, there are two processes that produce hydrocarbon (methane) gas: (1) biogenic and (2) thermogenic degradation of organic matter. Biogenic gas is formed at shallow depths and low temperatures by anaerobic bacterial decomposition of sedimentary organic matter. In contrast, thermogenic gas is formed at deeper depths by: (1) thermal cracking of sedimentary organic matter into hydrocarbon liquids and gas (this gas is co-genetic with oil, and is called "primary" thermogenic gas), and (2) thermal cracking of oil at high temperatures into gas ("secondary" thermogenic gas) and pyrobitumen. Each process leaves the gas with distinctive characteristics.

Biogenic gas tends to be very dry as it consists almost entirely of methane. In contrast, thermogenic gas can be either dry, or can contain significant concentrations of "*wet gases,*" e.g., ethane, propane, butanes, condensate (C_{5+} hydrocarbons), benzene etc.

Figure 2.10 illustrates the use of gas geochemistry in revealing whether the source of a gas is biogenic or thermogenic. Weatherford Laboratories (2011) point out that the composition of a thermogenic gas also reveals the thermal maturity of the source rock that generated the gas.

Biogenic gas is unrelated to the processes that form oil at higher temperatures. As a result, if a gas seep or show is bacterial in origin, then the presence of this gas says nothing about the likelihood of an effective petroleum system existing in the region (Weatherford Laboratories, 2011). Hydrocarbon liquids could be present in the area, however, because the concentrations of thermogenic methane are too low to be detected. As noted, sampled surface gases are often a mixture of biogenic and thermogenic gases. When the values are plotted on Figure 2.10, they fall in the region of a mixed gas where there is dilution of the bacterial gases with the gas coming from a thermogenic source.

In contrast, if a gas show is found to be thermogenic in origin, then it is likely that the gas is derived from a petroleum source. This gas can then be further evaluated examining specific aspects of the composition of the thermogenic gas. Specifically, Weatherford Laboratories (2011) offer the following information on sources of a gas:

1. Biogenic methane, on average, contains isotopically lighter carbon (i.e., is more depleted in ^{13}C) than thermogenic methane. Biogenic gas is also drier than many thermogenic gases. Ranges of gas composition corresponding to (1) bacterial gas, (2) thermogenic, oil-associated gas, (3) dry, post-mature thermogenic gas, and (4) gas of mixed biogenic/thermogenic origin must be defined, facilitating the interpretation of

gas compositional data (e.g., see Schoell, 1983, 1988; Faber *et al.*, 1992; Whittaker, 1994). In cases where gas seeps may be derived from biogenic decomposition of anthropogenic wastes ("landfill" gases), other tracers, such as ^{14}C and tritium, can be used to distinguish landfill gases from older biogenic gases unassociated with anthropogenic waste (Coleman, 1995).

2. Thermogenic gas components (methane, ethane, propane) generated at a given thermal maturity contain, on average, isotopically heavier carbon than do the corresponding gas components generated at a lower thermal maturity. Relationships between gas isotopic compositions and source maturity have been calibrated, allowing the reflectance equivalent of the gas source to be estimated from the gas geochemistry (Faber, 1987; Berner and Faber, 1988; Berner, 1989).

2.5 Driving Force of Gas Movement

The primary force moving stray gas through the Earth is the difference in densities between the surrounding saline water and the hydrocarbon gas, commonly referred to as buoyancy. As the gas migrates toward the surface, the pressure on the gas lessens and its density decreases as the gas expands. The change in water density at various depths is far lower than that of the gas since the water is incompressible; however, the water density will slightly change due to salinity and temperature changes. In as much as the change in density for water is much lower than that for the gas, the buoyancy force between the water and the gas increases as it approaches the surface. The exact values for the density force between the liquid and gas may be calculated at any depth as discussed below.

2.5.1 Density of a Hydrocarbon Gas under Pressure

There are several techniques to calculate a hydrocarbon's gas density. In working with gases at low pressures (below 300 psia), the Ideal Gas Law will generally give a satisfactory answer; however, with higher pressures the use of this law may lead to errors as great as 500% as compared to 2% to 3% at atmospheric pressures (NGSMA, 1957). This is due to the fact that, for this equation, the size and forces between the atoms at higher temperatures and pressures have a greater effect on the real volume of the gas. A simple method of compensating for such errors is the introduction of compressibility factor, z.

Assuming 1 lb of gas,

$$\gamma_g = \frac{1}{v} = \frac{p}{nRT} = \frac{M}{RT} \tag{2.3}$$

where p = pressure, psia; v = specific volume, ft^3/lb; n = number of pound-moles; R = universal gas constant, 10.73 psi-ft^3/lb-mol °R; T = absolute temperature, °R = °F + 460; γ_g = specific weight, lb/ft^3; and M = molecular weight of gas. Thus:

$$Pv = znRT \tag{2.4}$$

$$\gamma_g = \frac{Mp}{zRT} \tag{2.5}$$

The composition, temperature and pressure of the gas determine the "*compressibility factor, z*." For a single compound, z is a function of reduced temperature, T_r:

$$T_r = \frac{T}{T_c} \tag{2.6}$$

and reduced pressure, p_r:

$$P_r = \frac{P}{P_c} \tag{2.7}$$

where T = absolute temperature of gas in degrees Rankine, °R; T_c = critical temperature of the compound, °R; p = pressure of gas, psia; and p_c = critical pressure of the compound, psia (see Table 2.2). The "compressibility factor," z, can be obtained from Figure 2.14, if T_r and p_r are known.

If the gas represents a mixture of gases, the compressibility factor z_n may be computed by first calculating the pseudo-reduced temperatures, T_{pr}, and the pseudo-reduced pressures, p_{pr}, for gases in the mixture and then obtaining an average value:

$$T_{pr} = \frac{T}{T_{pc}} = \frac{T}{\sum_1^n y_i T_{ci}} \tag{2.8}$$

$$P_{pr} = \frac{P}{P_{pc}} = \frac{P}{\sum_1^n y_i P_{ci}} \tag{2.9}$$

where y_i = mole fraction of individual gas in a mixture.

The pseudo-critical temperature and pressure of a mixture of gases may be calculated as the molecular average critical temperature and/or pressure of the components (volume % is equal to mole % for gases), as shown below.

2.5.2 Sample Problem (Courtesy of Gulf Publishing Company)

Calculate the density of a gas mixture containing 90% methane, 8% ethane, and 2% propane at 55 °F and 1,100 psig.

Composition	Mole fraction, y	Molecular weight, M	yM	Critical temperature, °R	yT_c	Critical pressure psia	yp_c
Methane	0.90	16		343		668	
Ethane	0.08	30		550		708	
Propane	0.02	44		666		616	
	1.00		17.7		366		670

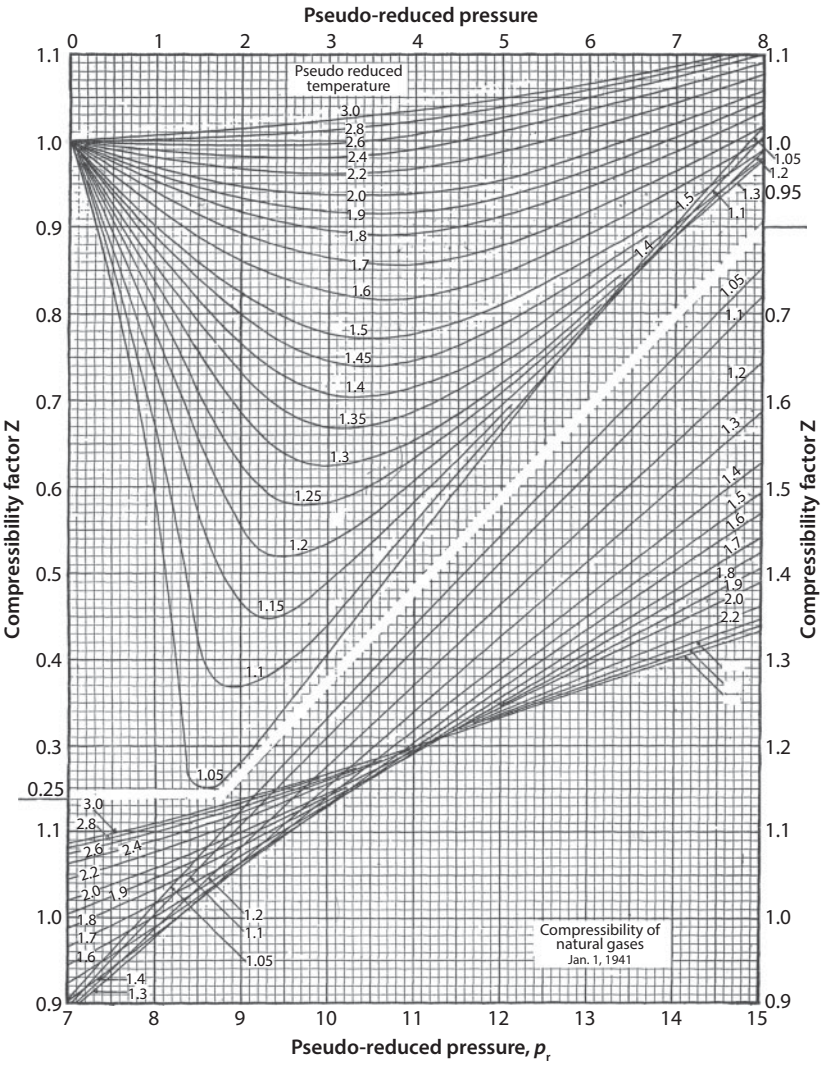

Figure 2.14 Compressibility factors for natural gases. (Modified from Brown *et al*., 1941; in: Natural Gasoline Supply Men's Association, 1957, and Natural Gas Processors Suppliers Association, 1981, figure 16.3, p. 16.8.)

Solving for T_{pr} by using Eq. 2.8:

$$T_{pr} = \frac{(55+460)}{366} = 1.41$$

Solving for p_{pr} by using Eq. 2.9:

$$p_{pr} = \frac{(1100+14.7)}{670} = 1.66$$

From Figure 2.14: $z = 0.81$.

Using Eq. 2.5:

$$\gamma_g = \frac{Mp}{zRT} = \frac{(17.7)(1100+14.7)}{(0.81)(10.73)(55+460)} = 4.4 \text{ lb/ft}^3$$

The molecular weight of a natural gas can be determined from its composition. Assuming the following analysis of the natural gas:

Component	**Composition, %**
Methane (CH_4)	92.16
Ethane (C_2H_6)	4.88
Propane (C_3H_8)	1.85
i-Butane (C_4H_{10})	0.39
n-Butane (C_4H_{10})	0.55
i-Pentane (C_5H_{12})	0.17

The molecular weight can be calculated as follows:

Component	**Mole fraction, *y***	**Molecular weight, *M***	***y* × *M***
Methane	0.9216	16.03	14.80
Ethane	0.0488	30.05	1.47
Propane	0.0185	44.06	0.815
i-Butane	0.0039	58.08	0.227
n-Butane	0.0055	58.08	0.319
i-Pentane	0.0017	72.09	0.123
Average molecular weight			17.754

The specific gravity of gas (SG), with respect to air, can be calculated as follows:

$$SG = \frac{\text{Molecular weight of gas}}{\text{Molecular weight of air}} = \frac{\text{Molecular weight of gas}}{28.966} = \frac{17.754}{28.966} = 0.612 \quad (2.10)$$

The specific weight (lb/ft^3) of gas is equal to:

$$\frac{\text{Molecular weight of gas}}{379.498 \text{ ft}^3/\text{lb-mole}} = \frac{17.754}{397.498} = 0.0468 \text{ lb/ft}^3$$

2.5.3 Other Methods of Computing Natural Gas Compressibility

The value of compressibility, *z*, is defined as the ratio of the real gas volume to the ideal gas volume. To determine the value of *z*, for a real gas, the real and ideal gas volumes must be determined at the same temperature, pressure and gas composition. The real gas volume is the measured volume of a given mass of gas at an equilibrium temperature and pressure. The ideal gas volume is a calculated volume at the same temperature, pressure and gas composition as the measured volume. The real gas compressibility factor corrects the volume relative to the assumptions in the ideal gas equation. A real gas that behaves as an ideal gas has a compressibility factor value of 1, which is generally the case at low pressures and high temperatures (see Savidge, 2000).

Savidge (2000) presented Figure 2.15, which illustrates the variation in compressibility factors at various pressures and temperatures for pure methane. Each curve in the figure is at constant temperature. The temperature range illustrates the behavior of methane's compressibility factor at conditions for liquefied natural gas, gas processing, surface exposed pipeline conditions, transmission lines, and well conditions. As the methane is compressed, the volume occupied by the real gas relative to the ideal gas volume is reduced, i.e., the real to ideal volume ratio becomes less than 1. Thus, the compressibility factors are less than 1 for methane.

The amount of compressibility in a volume of hydrocarbon gas depends on the average MW of that gas at a particular temperature and pressure. As pressure is increased, repulsive forces between molecules in the real gas begin to affect the compressibility of the gas. This leads to a reversal in the compressibility factor value and results in an increase in the real to ideal volume ratio as pressure is further increased. Savidge (2000) also noted that most chemical components found in natural gas mixtures follow the general behavior of methane as shown in Figure 2.15. Figure 2.16 focuses on the lower pressures of methane covered by Figure 2.15, showing in greater detail the values of compressibility factors for pure methane with constant temperature curves at various pressures up to 2000 psia. The constant temperature curves in this figure between 0 °F and 100 °F cover most gas phase measurement conditions.

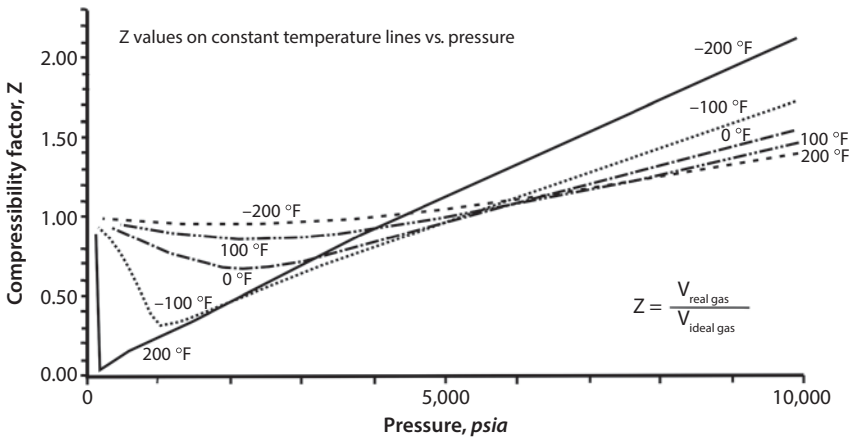

Figure 2.15 Methane compressibility factor, *Z*, at low to high pressures. (Modified after Savidge, 2000, figure 1.)

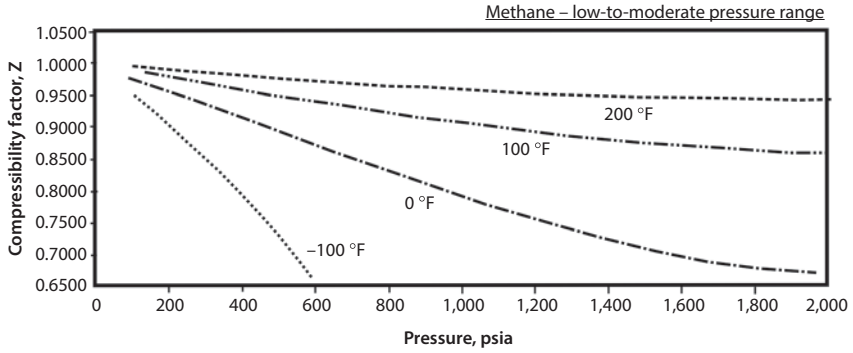

Figure 2.16 Methane compressibility behavior example factors, *Z,* on constant temperature lines vs. low to moderate pressures. (Modified after Savidge, 2000, figure 3.)

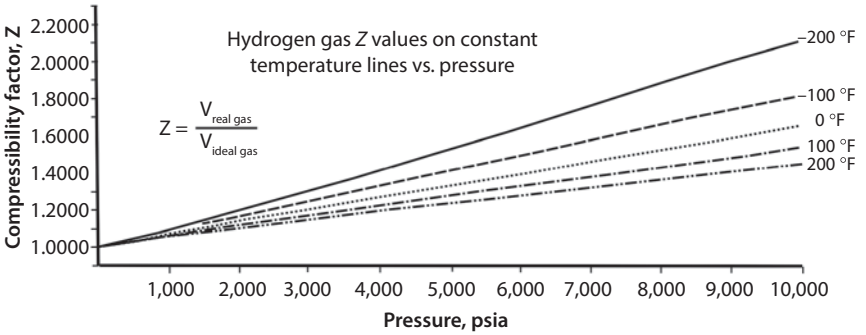

Figure 2.17 Hydrogen gas compressibility factor, *Z;* low to high pressure range. (Modified after Savidge, 2000, figure 2.)

Inasmuch as most stray gas mixtures are primarily methane (>90%), methane is the major component which determines the value of the compressibility factor for a natural gas mixture. Other hydrocarbon components, e.g., ethane, propane, etc., and diluents found in natural gases also contribute to the overall compressibility factor value for real gas mixtures.

Figure 2.17 shows the compressibility factors for hydrogen gas often found in natural gas. The contributions to compressibility by other gases in the stray gas are generally proportional to their mass concentrations. As the components in a mixture change, there is a corresponding change in their contribution to the compressibility factor. For example, for a given mixture consisting of methane and hydrogen at constant temperature and pressure, the compressibility factor value of the mixture will be a mass average weighted value. A compressibility value for methane gas at various low pressures and temperatures can be estimated using Figure 2.14 (NGSMA, 1957).

The compressibility for mixtures of hydrocarbon gases can also be estimated graphically for natural gas knowing only the specific gravity of the gas and using the pseudo-critical temperature and pressure relationships. The NGSMA (1957) presented Figures 2.18 and 2.19 showing specific gravity of the gas vs. critical temperature and pressure of the mixture. Figure 2.14 can then be used to estimate the compressibility

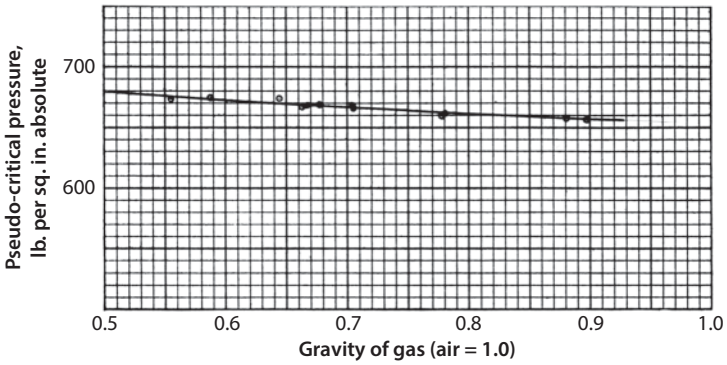

Figure 2.18 Approximate pseudo-critical pressure as a function of natural gas gravity. Specific gravity of air equals 1.0. Pressure is absolute ($p_a = p_g + 14.7$). (After NGSMA, 1957, figure 4, p. 103.)

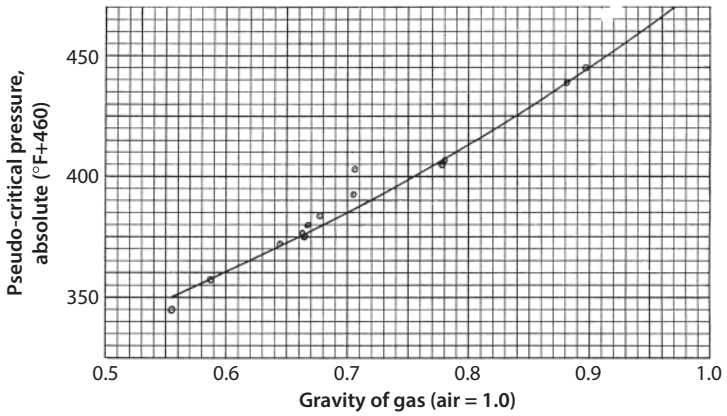

Figure 2.19 Approximate pseudo-critical temperature for natural gases vs. gravity with respect to air. (After NGSMA, 1957, p 103, figure 5.)

factors for a natural hydrocarbon gas knowing the pseudo-critical values of pressure and temperature of the natural gas.

2.5.4 Density of Water

Subsurface water generally is not a fresh water, but has dissolved salts within it. The density difference between the water surrounding the gas and oil globule at any point reflects the buoyancy forces on the globule propelling it toward the surface.

As a liquid, water is almost incompressible and so the density changes little for low changes in pressure. However, changes in salinity and temperature do affect the water density. One can quickly estimate the density of saline water at any depth and temperature by use of density calculators available on the internet. Temperature and salinity are the major factors in determination of the variation of water density as pressure plays a minor role for an almost incompressible fluid. If there is gas within the fluid under pressure, the gas itself is very compressible while the fluid is not. Figure 2.20

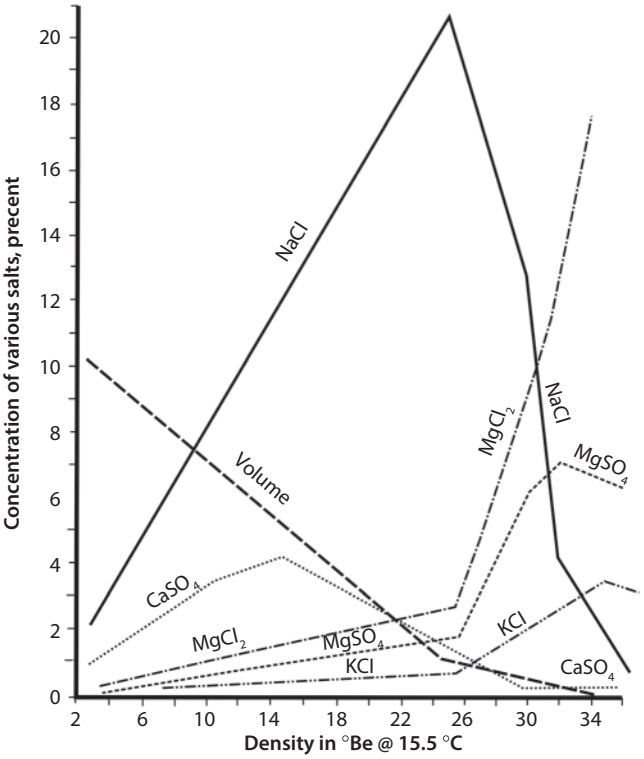

Figure 2.20 Density of water with various concentrations of dissolved salts, °Be = Baume scale. (Modified after Baert *et al.*, 1996.)

illustrates how the density of water varies with the type and concentration of ions in the water. Knowing the concentration of each type of salt, a weighted average density can be approximated for any mixture.

The density of pure water is 1000 kg/m^3, whereas the density of ocean water at the sea surface is about 1027 kg/m^3. A graph (Figure 2.21) to determine the density of water prepared by Class Zone is available on the internet (www.classzone.com/books/earth_science/terc/content/). Figure 2.21 illustrates the interrelationship among temperature, salinity and density. Increasing the salinity of the water (the quantity of dissolved salts) increases the mass of the water per unit volume (density). Temperature also affects the density of seawater by changing the volume of the water. Water expands with higher temperatures and so warmer water has a lower density. Pressure increase has a minor effect on the expansion and contraction of water.

To estimate the density of water (Figure 2.21), find the point where the temperature and salinity values for the water intersect. The line on the graph nearest the point of intersection indicates the density of the water.

2.5.5 Petrophysical Parameters Affecting Gas Migration

There are several factors that determine the magnitude of the force resisting the upward force of buoyancy, e.g. (1) the radius of the pore throats of the rock, (2) the hydrocarbon-water interfacial tension, and (3) wettability.

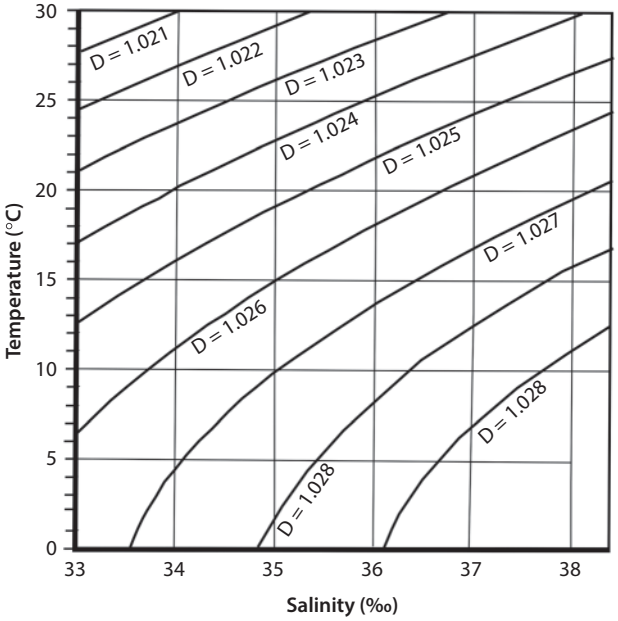

Figure 2.21 Interrelationship among density, temperature (°C) and salinity of water. D = Density of water at a particulatr temperature and salinity, (Modified after Classzone, www.classzone.com/books/earth_science/terc/content/.)

The reliable geological interpretation of the migration of gas through porous media requires knowledge of the petrophysical and reservoir parameters of the formation through which it flows. Petrophysical relationships are based on the laboratory analyses of core samples saturated with formation fluids. Core analyses are conducted under surface (ambient) and subsurface (reservoir) conditions.

2.5.6 Porosity, Void Ratio, and Density

Virtually all detrital rocks are porous (i.e., contain void space) to some extent. The relative volumes of voids and solids can be expressed in terms of (1) porosity and (2) void ratio. With few exceptions, geologists and petroleum engineers prefer the term porosity, whereas soils and civil engineers use the term void ratio. It should be pointed out here that the various disciplines in geology and engineering all have distinct sets of nomenclature and symbols for rock parameters.

Both porosity and void ratio are related to bulk volume of a rock. Bulk volume, V_b, is defined as the sum of the volumes of the voids or pores, V_p, and the solids, V_s:

$$V_b = V_p + V_s \tag{2.11}$$

Porosity, ϕ, is the ratio of the void space to the bulk volume and is usually expressed in percent:

$$\phi = \left(\frac{V_p}{V_b} \right) \times 100 \tag{2.12}$$

When used in an equation, however, the decimal equivalent is usually used, e.g., 0.5 instead of 50%. Comparison charts to aid in visual estimation of porosity are presented in Figure 2.22.

Void ratio, *e*, is defined as the ratio of the voids volume to the solids volume:

$$e = \frac{V_p}{V_s} \tag{2.13}$$

also:

$$e = \frac{\phi}{(1-\phi)} \tag{2.14}$$

or:

$$\phi = \frac{e}{(1+e)}. \tag{2.15}$$

Obviously, porosity can never exceed a value of 100% or 1.0 (fractional porosity), whereas void ratio often exceeds unity in fine-grained sediments and clays. Figure 2.23 shows the relationship between the void ratio and porosity in the commonly occurring range.

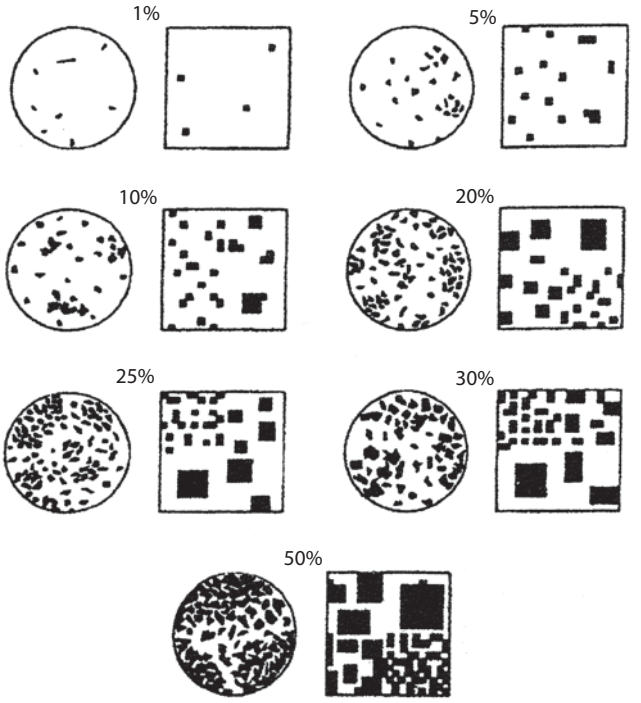

Figure 2.22 Comparison charts to aid visual estimation of porosity. (Circles after Terry and Chilingar, 1955; squares after Folk. 1951.)

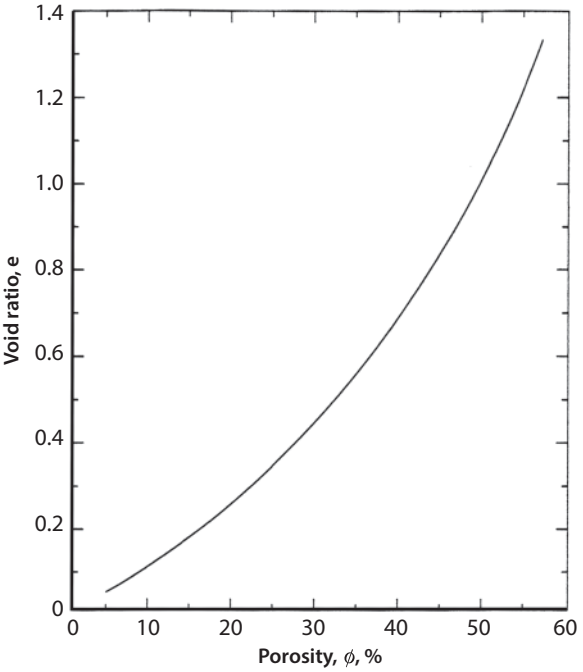

Figure 2.23 Relationship between void ratio and porosity.

Specific weight, γ, is often used in conjunction with porosity and void ratio. It is defined as the weight per unit volume, whereas density, ρ, is the mass per unit volume and is equal to γ/g where g is the gravitational acceleration. The term "density", however, is often used to designate specific weight, which often results in erroneous calculations. Mass, ρ, is attracted by the Earth with a force $\gamma = (\rho \times g)$. For example, if the specific weight of water is equal to 62.4 lb /ft^3, then the density expressed in terms of slugs /ft^3 is equal to 1.94 [= 62.4 (lb/ft^3)/ 32.17(ft/sec/sec)].

Bulk specific weight can be either "dry" or "wet" depending upon the nature of the fluid in the pore spaces. The unit weight of dry sand (only air is present in the pore spaces) is equal to:

$$\gamma_{db} = (1-\phi)\gamma_s \tag{2.16}$$

where γ_{db} = weight per unit of dry bulk volume, and γ_s = specific weight of solids (grains).

The unit weight of wet sand is expressed as:

$$\gamma_{wb} = (1-\phi)\gamma_s + \phi\gamma_f \tag{2.17}$$

or:

$$\gamma_{wb} = \gamma_s - \phi(\gamma_s - \gamma_f) \tag{2.18}$$

where γ_{wb} = weight per unit of wet bulk volume, γ_s = specific weight of solids (grains), and γ_f = specific weight of fluid in the pores.

Quartz sands have an average specific gravity of 2.65 with reference to water [specific gravity = specific weight of a material at 60 °F: (specific weight of water at 60 °F)]. If the weight of one cubic foot of fresh water is assumed to be equal to 62.4 lb, then one cubic foot of solid silica having a specific gravity of 2.65 would weigh 165.4 lb. If one cubic foot of dry sand weighs 137.3 lb, then its dry, bulk specific gravity would be equal to 2.2 (=137.3/62.4). The porosity of this dry sand can be calculated using Eq. 2.16; $\gamma_{db} = (1-\phi)\gamma_s$, or $\phi = \frac{(\gamma_s - \gamma_{db})}{\gamma_s} = \frac{(2.65-2.2)}{2.65} = 0.17$ or 17% If the sand was saturated with water, its bulk specific weight would be equal to the weight of the solids (137.3 lb) plus the weight of the water (0.17×62.4 lb) or 148.06 lb /ft^3.

It can be easily illustrated on using idealized spheres that porosity is dependent upon the method of packing. If packed cubically, then spheres of equal size would have a maximum possible void space of about 47.6% (Slichter, 1897–1898). If packed rhombohedrally, the porosity is reduced to a minimum of about 26% (Figure 2.24). It is obvious that sphere size does not change porosity when unit volumes with sides at least 2 radii in length are examined. In nature, owing to variation in size of grains and their angularity, usually the porosity of a sand or sandstone will be less than the values specified for spherical grains. It has also been demonstrated that in a mixture of spherical particles having different diameters, stacking arrangement does affect porosity. The introduction of a second set of spheres, small enough to fit in the pore space between the larger set, can reduce porosity to about 13%.

Usually, finer-grained sediments exhibit greater porosity when deposited than coarse-grained ones. A well-sorted, well-rounded, loosely compacted medium to

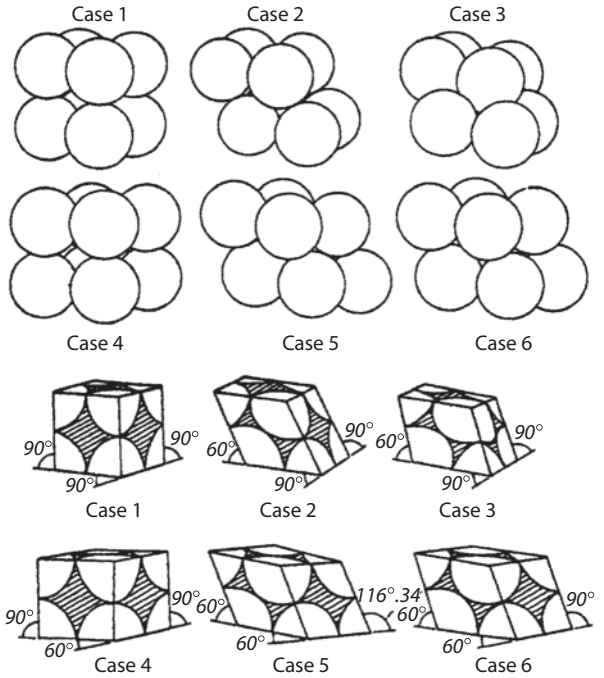

Figure 2.24 Several different ways of packing speres. (After Graton and Frazer, 1933.)

coarse-grained sand may have a porosity of about 37%, whereas poorly sorted fine-grained sand with irregularly shaped grains may have porosity in excess of 50%. An admixture of irregular-shaped, tabular and bladed particles usually gives rise to a higher porosity values because of particle bridging. The wide variability of porosity owing to depositional environment is best illustrated by the greywackes, which may have either a high or a very low porosity value, depending on the amount of fine-grained material filling the pores. Clays and silts may have porosities as high as 50–80% when freshly deposited.

The terms "effective porosity" and "total porosity" are often used in petroleum geology and reservoir engineering studies. These terms differentiate between the interconnected pores through which fluids can move and the total pore space, regardless of its ability to transmit fluid.

The effective porosity as used in the United States is not really effective. It should be called intercommunicating or open. Real effective porosity is the "effective" porosity (as used in the Western world) minus the irreducible fluid saturation depending on wettability (water or oil), which does not participate in the flow of fluids, and is "hiding" in the dead-end pores and fractures. Thus, we recommend using the term "effective" properly.

2.5.7 Permeability

Permeability is the measure of the ability of a porous rock to transmit a fluid under the pressure gradient (differential pressure). The absolute permeability, k, is the ability of a rock to conduct a single fluid (gas, oil, or water) at 100% saturation in the rock pore space with that fluid. Effective/phase permeability is the ability of a rock to conduct one fluid phase (gas, oil, or water) in the presence of other fluid phases. Relative permeability to a fluid is the ratio of effective/phase permeability at a given saturation value to the permeability at 100% saturation (the absolute permeability). The terms $k_{ro}(k_o/k)$, $k_{rg}(k_g/k)$, and $k_{rw}(k_w/k)$ denote the relative permeabilities to oil, gas, and water, respectively. The relative permeability is expressed in percent or as a fraction.

Permeability is measured by an arbitrary unit called the Darcy, D, which is named after Henry d'Arcy, a French engineer, who in 1856 devised a method of measuring the permeability of porous rocks. One Darcy is 1 cm^3 per second of a fluid having viscosity of 1 cP flowing through a 1 cm^2 cross-section of rock under a pressure gradient of 1 atm/cm. Because most reservoir rocks have an average permeability considerably <1 Darcy, the usual measurement units are in millidarcies (mD). Sometimes the term "perm" is used and is equal to 1.127 D.

In the majority of formations there is a simultaneous existence of more than one phase in the pore space (oil and gas; oil and water; gas and water; or oil, gas, and water). The concept of effective permeability implies that all, except for one phase, are immobile. Inasmuch as part of the effective pore space is occupied by another phase, a correction factor must be used. The magnitude of effective permeability depends on wettability, i.e., on whether (1) the mobile phase does not wet the solid mineral surfaces of the rock and, therefore, occupies the central parts of the pores, or (2) the immobile phase wets the solid surfaces and thus tends to concentrate in the smaller pores. The nature, distribution, and amount of immobile phase affect the effective permeability.

The results of effective/phase permeability measurement are shown graphically in the triangular diagram, where the apex represents the 100% saturation point of the respective phase (oil, gas, water). Contour lines of equal permeability to reservoir fluids are drawn in order to evaluate the test results and characteristics of simultaneous multiphase fluid flow (Figure 2.25). Composition of three-phase flow through the porous media (after Leverett, 1941) is illustrated by Figure 2.26. The diagram of relative permeability to oil and to water versus the oil and water saturation is constructed and data

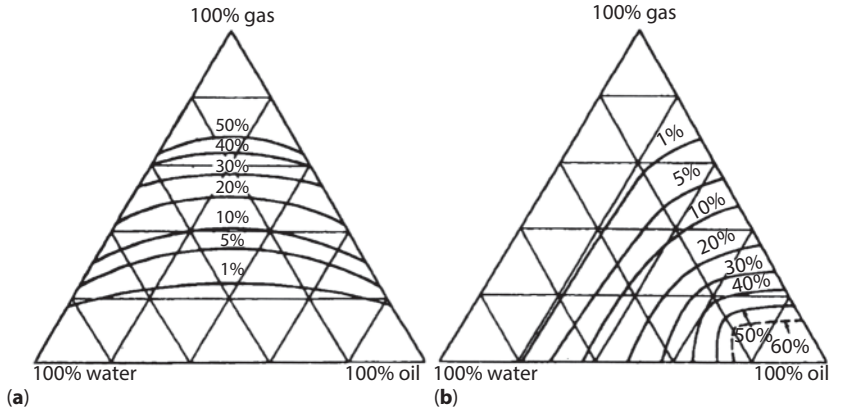

Figure 2.25 Triangle diagram of ternary mixtures (water, oil and gas) with lines of equal relative permeability in %: (a) to gas (as a fnction of water and oil saturation); (b) to oil (as a function of gas and water saturation). (After Leverett, 1940, courtesy of AIME.)

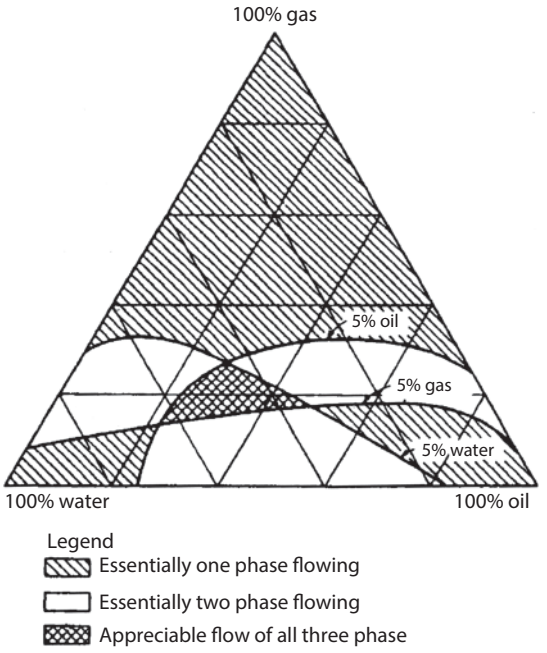

Figure 2.26 Composition of a three-phase flow through the porous media. (After Leverett and Lewis, 1940, courtesy of AIME.)

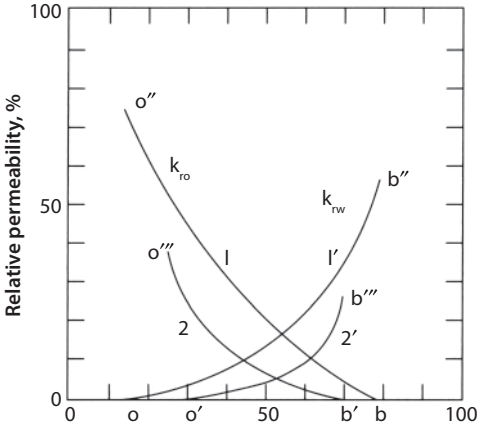

Figure 2.27 Example of relative permeabilities to oil and to water for polar oil + alkaline water (curves 1 and 1′) and for polar oil + hard water (curves 2 and 2′). (Modified after Babalyan, 1956, p. 148.)

points for the relative phase permeability to oil and water in the presence of gas phase are depicted on the diagram. An example of curves of relative permeability to oil and to water vs. water saturation is shown in Figure 2.27.

2.5.8 Free and Dissolved Gas in Fluid

The gas held in solution in a fluid within a hydrocarbon reservoir is not readily free to migrate to areas of lower pressure. During the course of oilfield production operations, as fluids are produced and vacate the reservoir pore structure, the pressure within the reservoir pores decrease, liberating some of the gas previously held in solution by the fluid. This freed gas no longer held in the fluid, can now migrate upward to areas of lower pressure, due to differences in the density between the gas and the surrounding fluids, toward the surface. On its path toward the surface, the freed gas often forms secondary collector zones (pools of gas) under other layers of low-permeability rocks. Due to the natural gas's lower viscosity and higher buoyancy than the liquid holding the dissolved gas, the freed gas attempts to escape along natural and man-made pathways to wellbores that penetrate the caprock and are not properly resealed, to areas of lower pressure. Also man-induced fractures can be generated by: (1) fracturing pressures occurring either during drilling and/or oilfield operations, and (2) subsidence occurring as a result of the production of fluids resulting in the formation of faults and fractures. Once the gas escapes through the caprock, the gas can then continue its migration toward the surface at a faster pace.

2.5.9 Quantity of Dissolved Gas in Water

Significant quantities of methane may be found dissolved in water: between 26 to 32 mg/l. The amount dissolved in water is proportional to the pressure. As shown in Figure 2.28, the higher the pressure, the greater the volume of gas that can be dissolved in water. Baldassare (2012) suggested the following formula to determine the maximum theoretical solubility of methane in water at a particular depth.

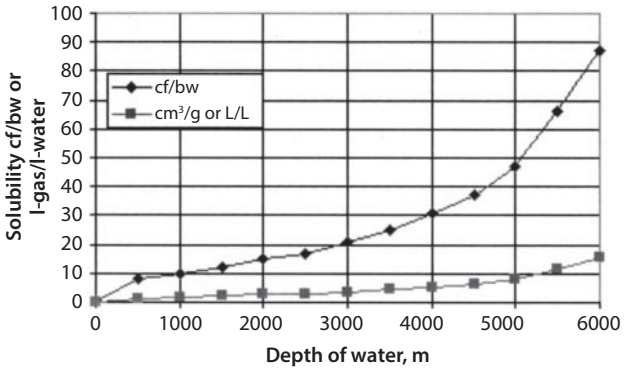

Figure 2.28 Solubility of methane in water at various pressures and temperature. (Modified after www.ipt.ntnu.no/jsg/undervisning/gas/abstracts/vibeke.html; after Bonham, 1978.)

$$C_w = \frac{H_W \times 0.43 \text{ psi/ft} \times 28 \text{ mg/l}}{14.7 \text{ psi}} + 28 \text{ mg/l} \tag{2.19}$$

where:

C_W = maximum theoretical concentration of methane at a particular depth, mg/l.

H_w = depth at which solubility is measured, ft.

As water migrates to the surface of the Earth, the pressure decreases, and the volume of gas held in the water by solubility decreases resulting in an out-gassing or release of flammable methane. This outgassing of the water results in increasing the volume of migrating (*stray*) natural gas.

2.6 Types of Gas Migration

Gas migration from the source to the surface can be either continuous or discontinuous. Continuous gas migration occurs when there is an unbroken saturation of gas from the source to the surface. This type of gas migration is found in the layers of soil from the surface to the top of the water table. Discontinuous gas migration occurs in the form of globules/bubbles (note: a bubble is defined as smaller than a globule) of gas migrating through the water-filled porous rock. This can occur below the water table, where the mechanism of gas migration is diffusion or mechanical, which may work either separately or in combination with each other.

2.6.1 Molecular Diffusion Mechanism

The diffusion of gas is a molecular process. The driving force for this mechanism is the concentration gradient of gas molecules (i.e., there are more molecules of gas in one area than in another). Over time, this system will seek equilibrium through an even distribution of gas molecules in all directions (Figure 2.29). This gas migration-force acts upon the gas at a molecular level.

If one assumes a case where methane gas flow is only by diffusion within a liquid (Figure 2.29), the flow is one-dimensional flowing from areas of higher to lower

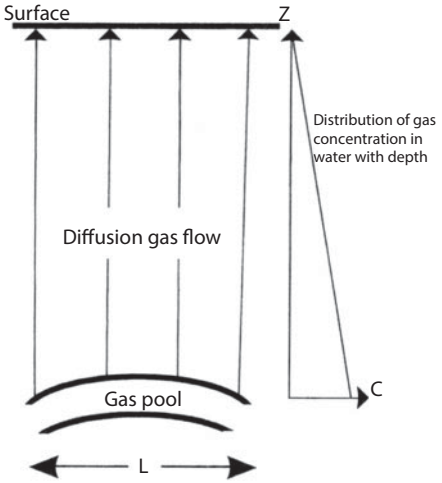

Figure 2.29 Schematic diagram of steady-state diffusion from the gas pool to the surface. C = concentration of gas in water. (Modified after Gurevich *et al*., 1993, p. 224.)

concentrations of methane. The rate of diffusion, *I*, is strongly affected by the porosity and presence of fault and fracture systems. Many other petrophysical properties, (e.g., tortuosity, wettability, widths of pore throats and fractures, etc.) can cause this rate to vary. The exact diffusion flow rate in geologic formations is difficult to establish because of the many variables controlling diffusion rate, which are either unknown or cannot be physically determined. An approximation for the total gas diffusion can be expressed as (Khilyuk *et al*., 2000):

$$I = D\frac{C}{h} \tag{2.20}$$

where: I = the diffusion flow intensity ($cm^3/cm^2/s$); D = the diffusion coefficient for gas moving through water-saturated porous rock (cm^2/s); C = the concentration of gas dissolved in water on the upper boundary of the oil or gas reservoir (m^3/m^3); and h = depth of this boundary (cm). As this equation is only an approximation, the diffusion coefficient, *D,* is the average value for the rock through which the gas diffuses and is assumed to be uniform within the whole path of travel, *h*.

An approximate value of the diffusion flow capacity of geologic formations can be determined as follows. The term *C* represents the solubility of gas in water and the term *C*/*h* is in fact a solubility coefficient: a typical value is 0.3 (m^3/m^3)/MPa, which is equal to 0.003 (m^3/m^3)/m for a column of fresh water. Assuming a diffusion coefficient, *D*, of 10^{-6} cm^2/s, the calculated value for *I* is approximately 3×10^{-11} cm/s for gas diffusion flow through a horizontal cross-sectional area of 1 cm^2. This value is likely larger than the actual values of diffusion flow intensity in the field due to assumption of maximum values that were made to calculate it. Gurevich (1970) measured the gas-saturation values of formation water samples taken during well tests at various depths above the caprock of oil reservoirs. At a distance of several meters above the caprock, the gas content of the water was about one-half or one-third of the maximum gas solubility value in water.

Commonly, the upward diffusion of gas encounters moving water, associated with near-surface fresh-water aquifers. If this water is not totally saturated with gas, the gas moving upwards can be absorbed into the moving water and carried off to other areas. The total quantity of gas that can be absorbed by a unit volume of the water stream is as follows:

$$Q = It = I\frac{L}{v} \tag{2.21}$$

where Q = the quantity of gas absorbed by the water (cm^3); I = the diffusion flow intensity (cm/s); t = time necessary for the water stream to pass above the oil or gas pool(s); L = length of travel path of water through the zone above the oil or gas pool (cm); and v = water velocity (cm/s).

Assigning typical values for a path (L) of 10 km and a flow rate (v) of 1 m/day for the water stream and substituting into Eq. 2.31:

$$Q \approx (3\times10^{-11}\,\mathrm{cm^3/s})\frac{10{,}000\ \mathrm{m}}{1\ \mathrm{m}/86{,}400\ \mathrm{s}}(0.20) \approx 5.2\times10^{-3}\,\mathrm{cm^3} \tag{2.22}$$

Thus, although some writers have given the diffusion process credit for migration of gas to the surface from gas sources, the process of gas diffusion through rocks yields very low values for rate of flow of gas, as demonstrated by the above calculations. This means that there must be other paths, such as faults and fractures, where the gas can migrate faster.

Smith *et al.* (1971) estimated total hydrocarbon losses by diffusion from a gas accumulation at a depth of 1,740 m (5,709 ft), temperature of 70 °C and pressure of 172 atm, at 2.8×10^8 m^3 (99×10^8 ft^3). These values are typical for oil and gas reservoirs in the United States. This data indicates that it would take 140 million years for methane and 170 million years for ethane to migrate to the surface from a depth of 1,740 m by diffusion. This calculation also assumes that the diffusion losses from the reservoir were replaced by source rock gases in order to maintain a gas gradient at a constant concentration and composition. This is an optimistic assumption, i.e., the actual quantities of gases migrating to the surface by diffusion are likely to be even less. Clearly, vertical diffusion from oilfield reservoirs buried at depths around 1,700 m (5,600 ft) cannot be the only mechanism responsible for the volumes of gas being observed in the surface soil over oilfields. Hunt (1979, p. 433) also has pointed out that the vertical diffusion of hydrocarbons from oil and gas reservoirs is too low to account for the quantity of hydrocarbon anomalies found in the surface soil.

In summary, diffusion, as a mechanism working on a molecular level, can move free gas toward the surface. The process, however, is a very slow one, occurring over geologic time. Periods of gas migration for various gases is shown in Table 2.5. Gas held in solution also does not move freely toward the surface. Although the process is slow, all gas eventually migrates to the surface. Given sufficient time, all gases associated with the oil/gas reservoirs will diffuse through the caprocks and overlying formations to the surface. The thickness and integrity of the caprocks (e.g., shales) has a direct effect on the rate of gas diffusion for a particular oil/gas field.

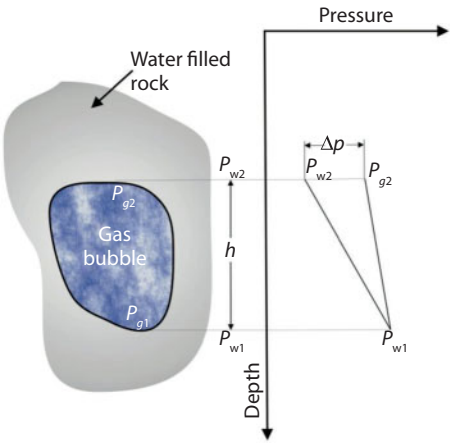

Figure 2.30 Schematic diagram of gas bubble migrating upward. (After guevich *et al.*, 1963, figure 3, p. 226.)

Table 2.5 Time period for gas migration rate and rate of loss to the surface for vertical steady-state diffusion from a depth of 1740 m. (Modified after Smith *et al.*, 1971; in Hunt, 1979, table 9–2. p. 427.)

Type gas	Time to reach surface ($\times 10^6$ years)	Rate of loss to surface (cm^3/m^2/year)
Methane	140	2
Ethane	170	0.16
Propane	230	0.06
Butane	270	0.02

2.6.2 Discontinuous-Phase Migration of Gas

The migration of oil and gas globules through water-filled porous rocks have been investigated by Aschenbrenner and Achauer (1960), Gurevich (1969), and many others. This type of mechanism of flow consists of gas or oil globules migrating through the water-filled rocks having intergranular or micro-fracture porosity. For this type of flow, it is assumed that every migrating globule is larger than the micro-fracture or pore throat.

These globules move slowly through porous rocks with small voids. For small globules, the pressure losses to overcome friction or resistance to flow are often negligible. Except for some very special cases of intensive underground water flows, it is the excess pressure at the top of the gas globule (Figure 2.30) that overcomes the capillary pressure at the upper gas-water interface, where gas displaces water and initiates the upward movement of the gas globule.

Whatever the globule's shape, this excess pressure, Δp is equal to the difference between the specific weights of globule (γ_g) and water (γ_w) times the vertical height of the globule, h:

$$\Delta p = (\gamma_w - \gamma_g)h \tag{2.23}$$

In the case where the specific weight of water (γ_w) is 1.0 g/cm^3, the specific weight of a gas (γ_g) is 0.2 g/cm^3, and depth (h) is 2,000 m, the pressure difference is about 200 kg/cm^2 (Gurevich *et al.*, 1993).

The capillary pressure, P_c, at the upper gas—water interface that resists the upward movement of the globule depends on the values of surface tension, contact angle and pore channel radius. The capillary pressure may be determined using the following equation:

$$P_c = 2\sigma \frac{\cos\theta}{r} \tag{2.24}$$

where σ is the surface tension, θ is the contact angle and r is the radius of the pore channel. To enable the globule to move upwards, the excess pressure should exceed the capillary pressure:

$$\Delta p > p_c \tag{2.25}$$

In order to initiate the upward movement of gas, the minimum vertical height of the bubble must be:

$$h > \frac{2\sigma\cos\theta}{r(\gamma_w - \gamma_g)} \tag{2.26}$$

The value for interfacial tension at the gas—water interface depends on temperature and pressure. It is about 40 dynes/cm at a pressure of 200 kg/cm^2 and a temperature of 60 °C. The angle θ may be assumed to be 60° (if water-wet). The radii of pore throats in coarse, medium and very fine sands are about 0.02, 0.005 and 0.001 cm, respectively. The values of h, necessary for a gas globule to begin moving upwards in these sands will be 2.5, 10.2 and 51.0 cm, respectively. Shales have smaller pore openings and, thus, the gas globule height necessary to overcome capillary forces will be greater. A pore radius of 10 μm and lower is common for shales. Thus, initial heights, h, of at least 5 m are necessary for migration to take place.

In gas pools or gas caps, the height of a continuous gas body almost always exceeds 5 m and often is 20 or 30 m. In most cases, therefore, upward migration of gas through a caprock is possible if the thickness of caprock is greater than the minimum height of gas column necessary to overcome the capillary pressure in water-wet rocks. In recent unconsolidated clays that did not lose their colloidal properties, pore channels are blocked by adsorbed water, partly or completely, at depths at which temperatures are below 50 °C. Thus, gas cannot penetrate such rocks mechanically as a free phase. In this case, the gas must seek fracture systems as pathways for migration.

After gas enters the caprock, its migration rate depends on the rate of water displacement. At low permeabilities of caprocks, migration is very slow and geologic periods of times are required for the gas to reach the surface. (See Gurevich *et al.*, 1993.).

In summary, gas migration occurs when the upward force generated by the height of the gas column is greater than the capillary-force resistance of the rock through which the gas migrates. Some oil/gas reservoirs are composed of thin layers of alternating shale and sandstone. Only in gas-wet rocks, the gas migrates upward from layer to layer until it reaches the top of the water table, and then diffuses to the surface.

2.6.3 Minimum Height of Gas Column Necessary to Initiate Upward Gas Movement

As the gas moves upward through the water in a capillary, several forces act on this column of gas of height, *h*: (1) weight of column of gas (lb) acting downward,

$$W_g = \pi r^2 h \gamma_g \tag{2.27}$$

where *r* is the radius of capillary (ft) and γ_g is the specific weight of gas (lb/ft^3); (2) upward force of water on gas (lb),

$$B = (\pi r^2 h)\gamma_w \tag{2.28}$$

where γ_w is the specific weight of water (lb/ft^3); and (3) capillary force (lb). F_c, pulling the gas downward (in water-wet rocks):

$$F_c = 2\pi r(\sigma_{wg} \cos\theta_{wg}) \tag{2.29}$$

where σ_{wg} is the water-gas interfacial tension and θ_{wg} is the water-gas-rock contact angle. Thus,

$$W_g + F_c = B \tag{2.30}$$

or

$$(\pi r^2 h)\gamma_g + 2\pi r(\sigma_{wg} \cos\theta_{wg}) = \pi r^2 h \gamma_w \tag{2.31}$$

Solving for *h* (ft), one obtains:

$$h = \frac{2\sigma_{wg} \cos\theta_{wg}}{r(\gamma_w - \gamma_g)} = \frac{2\sigma_{wg} \cos\theta_{wg}}{r\Delta\gamma} \tag{2.32}$$

and inasmuch as $\frac{2\sigma_{wg} \cos\theta_{wg}}{\gamma} = p_c^{wg}$, which is the capillary pressure in the water-gas system:

$$h = \frac{p_c^{wg}}{\Delta\gamma} \tag{2.33}$$

In gas-wet systems (possibly some carbonates), the gas starts moving without reaching the minimum height because the capillary pressure aids the upward movement.

2.6.4 Buoyant Flow

In the situation where the gas bubble/globule size is less than that of the flow channel, i.e., a wide fracture, the globule is able to float upwards. As the gas globule moves

upwards due to buoyancy forces, the buoyancy force, B, acts upwards, whereas the drag force, D, and the weight of the gas bubble, W_g are acting down:

$$B = D + W_g \tag{2.34}$$

For a Reynolds Number, N_R, below about 0.4 the drag coefficient, C_d, for a bubble of spherical form is equal to $24/N_R$. Thus for a laminar or viscus flow of the spherical gas bubble having a diameter d in ft, the drag force, D, is equal to:

$$D = C_d \rho \frac{v^2}{2} A = \left[\frac{24}{\left\{ \frac{\rho v d}{\mu} \right\}} \right] \times \rho \times \frac{v^2}{2} \times \left(\frac{\pi d^2}{4} \right) = 3\mu v \pi d \tag{2.35}$$

where ρ is the mass per unit volume in slugs/ft^3, v is the upward velocity of the bubble in ft/sec, A is the largest projected area in ft^2, and μ is the viscosity of the fluid in lb-sec/ft^2 (or slug/ft-sec).

Inasmuch as the buoyant force, B, is acting upward, whereas the drag force, D, and the weight of the gas bubble, W_g, are acting down (see Figure 2.31):

$$D + W_g = B$$

$$3\mu_w v \pi d + \left(\frac{\pi d^3}{6} \right) \gamma_g = \left(\frac{\pi d^3}{6} \right) \gamma_w \tag{2.36}$$

Solving for the upward velocity of bubble, v;

$$v = \frac{d^2 (\gamma_w - \gamma_g)}{18 \mu_w} \tag{2.37}$$

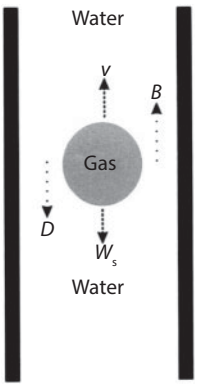

Figure 2.31 Gas bubble (or globule: bubble is smaller than globule) floating up through water in a channel where the diameter of the bubble or globule is smaller than that of the channel. W_s = weight of bubble or globule, B = buoyant force, D = friction drag force and v = upward velocity of the bubble or globule. (After Khilyuk *et al*., 2000, figure 17.5, p. 261.)

where γ_w and γ_g are specific weights of water and gas in lb/cu ft, respectively; d is the diameter of the spherical bubble/globule in ft; μ_w is the viscosity of water in lb-sec/ft^2; and v (upward velocity of the bubble) is in ft/sec.

Assuming: (1) temperature of 25 °C, (2) pressure of 20 kg/cm^2, (3) specific weight of methane gas of about 0.015 g/cm^3, (4) a water viscosity under these conditions of approximately 10^{-2} Poise, and (5) a gas bubble with a radius of 0.1 cm, the critical velocity is equal to 0.22 cm/s. Thus, a bubble of gas can float upwards in a fracture even in a downward moving stream of water that has a velocity < 0.22 cm/s.

2.6.5 Sample Problem (Courtesy of Gulf Publishing Company)

At laminar flow, calculate the rise velocity of a hydrocarbon gas bubble 0.1 mm in diameter through fresh water (Figure 2.31).

Given:

Gas bubble diameter, $d = (0.1 \text{ mm})\left(\dfrac{1\text{ft}}{304.8 \text{ mm}}\right) = 3.28\times10^{-4}$ ft

Specific gravity of water, $SG = 0.998$

Specific weight of water, $\gamma_w = (0.998 \times 62.4 \text{ lb/ft}^3) = 62.27 \text{ lb/ft}^3$

Water viscosity, $\mu_w = 2.089 \times 10^{-5}$ lb-sec/ft^2

(1 Poise = 2.089×10^{-3} lb-sec/ft^2)

Specific weight of gas, $\gamma_g = 0.0422$ lb/ft^3; specific weight of air at 59 °F and 14.7 psia = 0.07651 lb/ft^3; molecular weight of hydrocarbon gas = 16: and molecular weight of air = 29.

The velocity of buoyant rise of the gas bubble is equal to:

$$v = \frac{d^2(\gamma_w - \gamma_g)}{18\mu_w} = \frac{(3.28\times10^{-4})^2(62.27 - 0.0422)}{18(2.089\times10^{-5})}$$

$$= 1.78\times10^{-2} \text{ ft/sec or } 0.54 \text{ cm/sec}$$

2.6.6 Gas Columns

The pressure at any depth (point) in a gas column can be calculated. In a situation, where point 1 is above point 2 in a gas column, Eq. 2.41 can be used to calculate the pressure at point 2:

$$p_2 = p_1 + \frac{\gamma_g \times \Delta L}{144} \tag{2.38}$$

where ΔL, is the distance between points 1 and 2; p_1 is the pressure at point 1 in psi; and γ_g is the specific weight of gas in lb/ft^3.

The equation of state, considering 1 lb of gas, can be expressed as follows:

$$pv_g = z_{ave}NRT_{ave} \tag{2.39}$$

where p = absolute pressure in lb/ft^2, v_g = specific volume in ft^3/lb, z_{ave} = gas compressibility factor, N = number of moles of gas, R = universal gas constant, and T_{ave} = average absolute temperature in °R. Thus:

$$v_g = \frac{z_{ave} N \mathrm{R} T_{ave}}{p} \tag{2.40}$$

Inasmuch as:

$$v_g = \frac{1}{\gamma_g} \tag{2.41}$$

$$\gamma_g = \frac{p}{z_{ave} N \mathrm{R} T_{ave}} \tag{2.42}$$

Substituting Eq. 2.42 into Eq. 2.38:

$$p_2 = p_1 + \left(\frac{p}{144 z_{ave} N \mathrm{R} T_{ave}} \right) \Delta L \,. \tag{2.43}$$

Rearranging:

$$(p_2 - p_1) + \left(\frac{p}{144 z_{ave} N \mathrm{R} T_{ave}} \right) \Delta L \tag{2.44}$$

When $\Delta L \to 0$, Eq. 2.44 can be rewritten in differentials:

$$\frac{\mathrm{d}p}{p} = \frac{\mathrm{d}L}{144 z_{ave} N \mathrm{R} T_{ave}} \tag{2.45}$$

In integral form, Eq. 2.45 becomes:

$$\int_{p_s}^{p_{bc}} \frac{\mathrm{d}p}{p} = \int_0^L \frac{1}{144 z_{ave} N \mathrm{R} T_{ave}} \mathrm{d}X \tag{2.46}$$

where X is a variable of integration.

Thus, after integration,

$$\ln\left(\frac{p_{bc}}{p_s} \right) = \frac{L}{144 z_{ave} N \mathrm{R} T_{ave}} \tag{2.47}$$

and

$$\frac{p_{bc}}{p_c} = e^{\frac{L}{144 z_{ave} N \mathrm{R} T_{ave}}} \tag{2.48}$$

where z_{ave} = average gas compressibility factor computed at the average temperature and pressure, T_{ave} and p_{ave}; N = number of moles of gas; R = universal gas constant (equal to 10.7 for one lb mole of gas); p_s = pressure at the surface, psia; p_{bc} = pressure at the bottom of gas column; L = vertical depth of gas column, ft; and T_{ave} = average temperature in gas column; °R. On simplifying the exponent and considering only one pound of gas:

$$p_{bc} = p_s e^{\frac{LG_g}{53.37 z_{ave} T_{ave}}} \tag{2.49}$$

where G_g = gravity of gas as compared to that of air (SG of air = 1). The average temperature, T_{ave}, in the gas column can be computed from the following equation:

$$T_{ave} = T_s + \left[\left(\frac{L}{2}\right)\left(\frac{dT}{dL}\right)\right] + 460° \tag{2.50}$$

where T_s = surface temperature, °F; L= vertical depth of gas column, ft; and (dT/dL) = geothermal gradient, which is commonly assumed to be about 2 °F/100 ft. It should be noted, however, that the geothermal gradient varies with locality.

2.6.7 Sample Problem 2.2 (Courtesy of Gulf Publishing Company)

A schematic diagram of pressure distribution in a gas-filled wellbore is presented in Figure 2.32.

Above what depth would gas leave the casing through holes formed owing to corrosive formation waters, given the following information:

> Specific gravity of gas, G_g = 0.86 (compared to air); casing depth, D = 4,000 ft; supercompressibility factor, z = 0.95; casing diameter = 7 in; surface casing

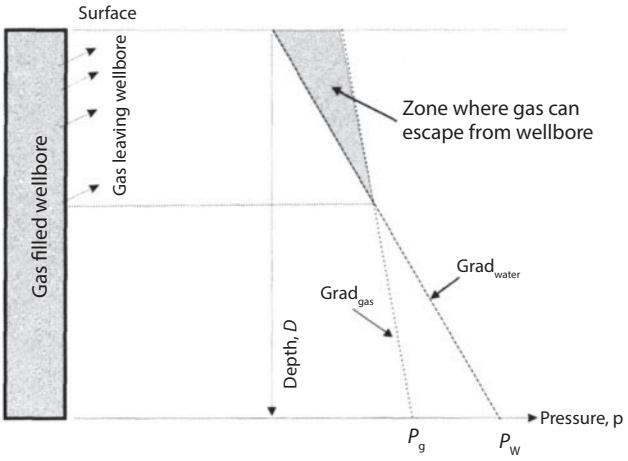

Figure 2.32 Schematic diagram of the pressure distribution in a gas-filled wellbore and in a surrounding water-saturated formation. Arrows indicate potential escape paths of gas through corrosion holes in the casing. P_w = water pressure gradient. (Modified after Gurevich *et al.*, 1993, Figure 6, p. 230.)

pressure, p_{tc} = 180 psig; water table depth = 70 ft below surface; hydrostatic gradient = 0.433 psi/ft; temperature at surface, T_s = 55 °F; geothermal gradient = 2 °F/100 ft.

Solution:

1. $$T_b = 55 + \left[(4000)\left(\frac{2}{100} \right) \right] = 55 + 80 = 135 \text{ °F}$$

$$T_{ave} = \left(\frac{T_s + T_b}{2} \right) = \left(\frac{(55+460)+(135+460)}{2} \right) = 555 \text{ °R}$$

$$p_{bc} = p_{tc} \times e^{\frac{LG_g}{53.3zT_{ave}}} = 194.7\left[e^{\frac{4000\times 0.86}{53.3\times 0.95\times 555}} \right]$$

$$= 220.05 \text{ psia or } 205.35 \text{ Psig}$$

2. $$\text{Gas pressure gradient} = \frac{p_{bc} - p_{tc}}{D} = \frac{(205.35-180)}{4000}$$

$$= 0.00634 \text{ psi/ft}$$

   Hydrostatic gradient = 0.433 psi/ft
   Water table is located at a depth of 70 ft
3. Assume that at depth x, gas would leave casing through corrosion holes.
   Gas pressure at depth x = 180 + 0.00634x, psig.
   Hydrostatic pressure at depth $x = (x - 70) \times 0.433$, psig.
   Gas pressure at depth, x = hydrostatic pressure at depth x.
4. Equating gas pressure and hydrostatic pressure and solving for x,
   x = 492.92 ft.

2.6.8 Continuous-Phase Gas Migration

Continuous gas phase flow from a pool of hydrocarbons to the surface or to another pool, lying at a shallower depth, can occur through vertical and subvertical zones of porous and/or fractured rocks of higher permeability and/or through large open fractures. There must be an unbroken saturation of gas from the source to the final destination.

The continuous phase migration of gas is similar to that of the flow in a pipeline. The cross-sectional area of flow (A) and the velocity of migration (v) control the volumetric rate of flow, Q:

$$Q = Av \tag{2.51}$$

The flow rate of gas is directly related to the pressure drop along the migration path. A naturally occurring pathway of this type could be either a fracture or a fault. An example of a man-made pathway would be where a corehole or wellbore had been drilled, for either oil or water, in a reservoir. The force moving the gas is the pressure drop between the beginning point and the end of the migration path. Gas flows from a higher-pressure area to a lower-pressure area. There are several types of pressure losses that can resist the movement of gas, such as frictional resistance to flow and capillarity.

It is possible to make an order of magnitude estimation of the flow rate in the subvertical column of gas saturating permeable rocks. At any depth, the flow velocity of gas can be estimated (Gurevich, 1993):

$$v = \frac{k}{\mu}(-\text{grad}\, p + \gamma_g) \tag{2.52}$$

where k is the permeability coefficient and γ_g is the specific weight of gas. If bottom and top pressures in the gas column are equal to water pressures, then the value of the pressure gradient (grad p) will correspond to the specific weight of water (1 g/cm^3), i.e., 10^{-3} kg/cm^2/cm. Assuming that density of gas is 0.015 g/cm^3 (at a pressure of 20 kg/cm^2), permeability k is 10^{-2} D and the gas viscosity μ is 1.5×10^2 cP, then the gas velocity will be 7×10^{-4} cm/s or 60 cm per day. Actual rates of the upward gas migration depend on the permeability along the path of migration.

Gas flow through fractures can be thought of as a "pipeline" type flow. In the case of an oilfield, large fractures, faults, or man-made channels (wellbores) can serve as gas-filled paths of migration, or "pipelines." This type of gas flow occurs in the gas-filled zone between the surface and the top of the water table. The force moving the gas is the pressure drop between the point of origin and the end of the path or channel.

The volume of migrating free gas along continuous gas-filled paths is dependent on the width of gas-filled fracture. In general, gas migration through gas-filled paths is capable of producing significant quantities of gas. The volume of gas found at the surface is dependent upon the mechanical aspects of the path traveled by the gas and the pressure gradient. Petrophysical features of the path, such as fracture width, length, saturation with water, tortuosity, absolute and relative roughness of the fracture walls, etc., have a great effect upon the quantities of gas that can move along the path.

Head loss due to friction, h_{lf} (e.g., ft-lb/lb or ft), is equal to:

$$h_{lf} = f\frac{l}{d}\frac{v^2}{2g} \tag{2.53}$$

where f is the friction factor, l is the length of channel (e.g., in ft), d is the equivalent diameter of cross-sectional area (e.g., ft^2), v is the velocity (e.g., in ft/sec), and g is the gravitational acceleration (e.g., in ft/sec/sec).

The fluid flow through open fractures is incomparably easier than through porous media because of lower frictional resistance to flow. It is possible to make an order of magnitude estimation of such gas migration using the Boussinesque's formula (Gurevich *et al.*, 1993):

$$v = \frac{w^2}{12\mu}(-\text{grad}\, p + \gamma_g) \tag{2.54}$$

where w is the fracture width. At the same values of pressure gradient, density and viscosity as in the example above, and assuming w to be 1 cm, v will be equal to 5 m/day.

Thus, the continuous-phase gas migration can produce the greatest volumes of migrating gas, but is less common because it requires a continuous path for the gas to migrate through. Man-made channels (wells) and fault zones are the most likely zones where large volumes of migrating gas flow will occur.

Wellbores penetrating gas/oil reservoirs are filled with gas, oil and water. If the wellbore is filled with gas, the pressure distribution in the gas column can be described by the following formula:

$$p_h = p_b e^{-\frac{0.000341 H \rho}{zT}} \tag{2.55}$$

where p_h is the pressure at any distance H from the wellbore bottom (or top of the fluid level), kg/cm^2; p_b is the pressure at the bottom the wellbore (or top of the fluid level), kg/cm^2; ρ is the gas density relative to that of air (0.7 for methane); z is the average gas super-compressibility (deviation from ideal gas behavior); and T is the average absolute temperature, °K.

In the case of a 3,500-ft (1,068 m) deep wellbore filled with gas in an oil/gas reservoir with a formation pressure (depleted) of 200 psi (14 kg/cm^2), a reservoir temperature of 307 °K, and gas supercompressibility of 0.98, the wellhead pressure, p_h, is 185 psia (13 kg/m^2). If the pressure distribution in the water-saturated formation surrounding the well is hydrostatic, then at a depth of 426 ft (130 m) pressure in the borehole will exceed the pressure outside the wellbore. Above this point, gas can escape into the surrounding formation. In the case where holes are present in the casing (due to corrosion), the gas could leave the wellbore and enter the surrounding formation above a depth of 426 ft ("*escape zone*"). The gas would then migrate toward the surface outside of the casing. (See Sample Problem 2.2.)

2.7 Paths of Gas Migration Associated with Oilwells

Commercial oil production started in Titusville, Pennsylvania, in 1859, when Colonel Drake drilled the famous Drake well. From there, petroleum production expanded globally as more wells were drilled, as the need for more hydrocarbons expanded. Over a 150-year-plus span, hundreds of thousands of core holes, injection wells, and gas-and-oil wells have been drilled around the globe (Ingraffea, 2014).

Allread *et al.* (2015) stated that since 2015, about 50,000 new wells/yr are being drilled in central Canada and the United States (Figure 2.33).

Leaking oil wells have long been recognized as a potential mechanism of subsurface migration of natural thermogenic gases, as well as heavier *n*-alkanes (Ingraffea, 2014). A leaking well in this context is one in which its zonal containment of the formation fluids along the wellbore is compromised due to a structural integrity failure of the cement and/or casing. This loss in integrity can result in direct emissions to the atmosphere and/or subsurface migration of fluids (gas and/or liquids) to ground waters, surface waters and finally the atmosphere. The cement may fail at any time over the life of the well. A number of possibilities for this to occur at the time of drilling and completion of the well are: hydrostatic imbalances caused by inappropriate

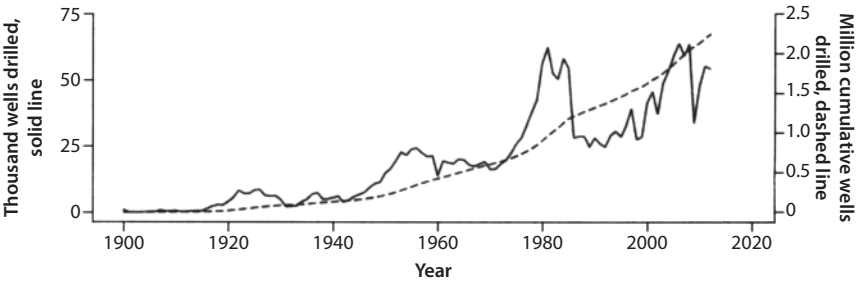

Figure 2.33 The number of oil and gas wells drilled within central provinces of Canada and central U. S. states: Colorado, Kansas, Montana, Nebraska, New Mexico, North Dakota, Oklahoma, South Dakota, Texas, Utah and Wyoming. (Modified after Allread *et al*., 2015, 348:401.)

cement density, inadequately cleaned boreholes, premature gelation of the cement, excessive fluid loss within the cement, high permeability in the cement slurry, cement shrinkage, radial cracking due to pressure fluctuations in the casings, poor interfacial bonding, and normal deterioration due to hydration of the cement with age. Other problems can occur as a result of casing failure, i.e., casing failure due to failed casing joints, casing collapse, and corrosion over a period of time.

Dusseault *et al*. (2000) noted that in North America alone, there are literally tens of thousands of abandoned, inactive, or active oil and gas wells, including gas storage wells that currently leak gas to surface. Much of this migrating stray gas enters the atmosphere directly through and about the wellbores, whereas other portions of this gas may enter the shallow aquifers. Traces of sulfurous compounds in the migrating gas can render fresh water non-potable, or where the methane itself can generate unpleasant effects such as gas locking of household wells, or gas entering household systems to come out when taps are turned on.

The magnitude of gas migrating from wellbores globally has been significant, according to Kotler (2011): "There are at minimum 2.5 million abandoned oil and gas wells (not permanently capped) littering the U.S., and another estimated 20–30 million globally." Many of these oil and gas wells that are leaking contribute to the escape of methane to the surface. Kotler further refers to an Associated Press (AP) investigation in 2010 that was sparked by the BP Deepwater Horizon oil spill, reporting 27,000 abandoned oil wells in the Gulf of Mexico.

Kotler further noted that in Texas, the Railroad Commission of Texas (RRC), which has regulated the oil industry since 1901 (when pipelines were considered another form of interstate transportation, like railroads), reported that as of August 2009, there were 389,000 active and 110,000 abandoned oilwells. The Bureau of Economic Geology at the University of Texas estimated that more than one million wells have been dug in Texas. A 1990 Texas Water Development Board study showed that there were 1.5 million wells in Texas, of which a million had been abandoned. The authors of this book decided to include the results of *all* these different studies to illustrate how many abandoned wells might exist.

Terry Tamminen, former secretary of the California Environmental Protection Agency, stated, as quoted by Kotler: "It's the same in California. We have a century-old oil industry. It is unknown how many wells were abandoned before abandonment

regulations were put in place? Many wells were just wildcatted—who knows where they are or how many there are? Many coreholes were drilled and not properly abandoned. In the Baldwin Field alone, which sits in the center of urban Los Angeles, there are hundreds of abandoned wells."

Many questions lie unanswered pertaining to these unmonitored wells: How securely are these abandoned wells sealed? Many were abandoned prior to the 1940s when cement was seldom used to seal off the petroliferous zone. Many of these wells and coreholes were filled with drilling fluids and then simply shut-in. Not only have these wells not been checked for leakage, but for many of the older wells, not even their location is known. The AP report touched on the oil industry's well-sealing technology, which relies on cement to seal off the oil and gas reservoir from the upper water sands and surface. It was stated that "whether a well is permanently or temporarily abandoned, cement that is improperly applied or aging can crack or shrink after a long period of time," making these abandoned wells "*an environmental minefield*" (emphasis added).

The most important factor is that these wells were shut-in, abandoned, and then forgotten. These wells should be located, checked for leakage, and properly abandoned.

2.7.1 Natural Paths of Gas Migration

The major paths for vertical migration of gas are commonly faults, fractures and wellbores. Vertical paths or channels in the formation can be formed by natural lithification processes, tectonic activities, and/or by man-made activities. These additional paths of migration within the reservoir are often created during drilling operations, which not only create boreholes through the strata, but also induce fracturing of the formation surrounding the wellbore. This problem can be compounded by poor cement bonding between the well casing and formation. Inadequate isolation of the producing formation from the wellbore and/or the well casing can occur with improper cementation of the wellbore. When the man-made pathways are not sealed off, the result is the escape of fluids (gas and liquids). (See Khilyuk *et al*., 2000, p. 264.)

Fractures through which gas can migrate are created in the reservoirs as a direct consequence of many oilfield operations, e.g., drilling, cementing, acidizing, and repressurizing of older and depleted reservoirs.

Faults and fractures are the major natural pathways for the migration of gases. As shown in Figure 2.34, the migrating gases can be trapped in secondary gas traps under layers of shale or other impervious layers during their upward migration, permitting the gas to temporarily gather in collector zones. When the gas migration gets above the water table, continuous gas phase flow can occur. In summary, the production of oil from a reservoir reduces the pressure in the reservoir pores, allowing dissolved gas to move into the pore space vacated by the produced fluids as a free gas, which then can migrate along various paths toward the surface.

In steeply dipping oil-producing formations, as fluids are produced from the reservoir, the free gas separates from the fluids and is able to move up-dip as a consequence of the large difference in density between the free gas and fluids. This phenomenon is often referred to as *gravity drainage* (i.e., oil moving downdip and gas rising updip). Thus production of fluids from the reservoir frees large volumes of gas, which then becomes available for migration toward the surface, e.g., along faults.

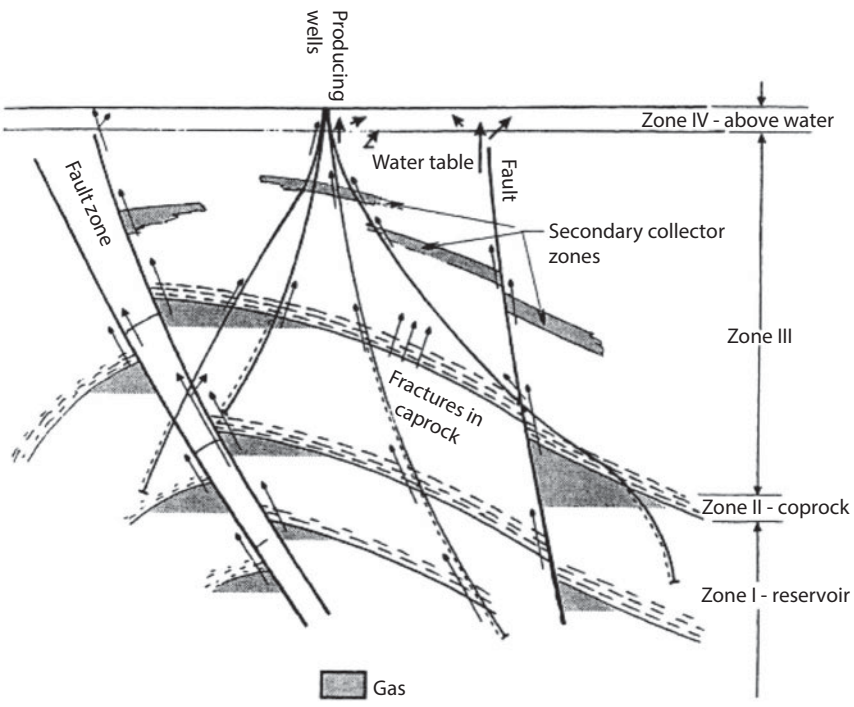

Figure 2.34 Schematic diagram showing potential migration paths for gas from the reservoir to the secondary collection zones and then to the surface. The arrows show several of the various potential paths of gas migration. (After Gurevich *et al.*, 1993, figure 17.)

2.7.2 Man-Made Paths of Gas Migration (boreholes)

It should be noted that not all stray gas originates from hydrocarbon reservoirs, e.g., from leaking transmission/distribution pipelines and wellbores. Other sources of methane gas include microbial processes (decomposition of buried organic matter), landfills, and mining activity.

Revkin (2009) suggested that gas migration cases can be organized into several categories: (a) producing and/or injection wells, (b) abandoned wells and coreholes, (c) repressurized wells (particularly those wells associated with underground storage of natural gas), and (d) pipelines:

a. ***Producing and/or injection wells*** are those wells that involve oil or gas production while the well is being drilled, re-drilled, completed or used for injection, production or sitting idle but not properly abandoned and plugged.
b. ***Abandoned wells and coreholes*** include exploratory coreholes and former producing wells that were previously drilled but have since been shut-in and either not properly plugged or not plugged according to today's standards. Many of these wells lack a history of production and completion and in many cases the exact location of the wellbores is unknown.

c. ***Repressurized wells*** present gas migration problems associated with gas storage, steam injection, and secondary recovery wells. The wells were completed as low-pressure producing wells and are today often being repressured at pressures above their capability to isolate and contain the fluids and gases.
d. ***Pipelines*** are carrying hydrocarbons under pressure, often without corrosion control (cathodic protection, sacrificial anodes, etc.).

2.7.2.1 Producing Wells

Bachu and Watson (2007) noted that all wells are potential candidates for leakage of hydrocarbons. Producing wells are susceptible to developing pathways of gas migration because of the (1) wellbore cement's deterioration with age, (2) improper isolation of the hydrocarbon producing layer from water sands and/or surface, (3) corrosion of the casing, or (4) collapse of the casing itself. The arrows in Figure 2.35 illustrate several possible paths of gas migration along a wellbore due to improper isolation of the producing intervals. Oilwells drilled and completed prior to the 1980s are likely candidates for leakage as they were often completed according to lower standards than those used today and also due to aging of the cement, i.e., the breakdown of cement with time. (The authors of this book estimate the life of a cementing job at about 50 years.)

Bachu and Watson (2007) identified 362,265 producing and nonproducing wells that had been drilled since 1893 in Alberta, Canada, by the end of 2006. Of these wells, 32%

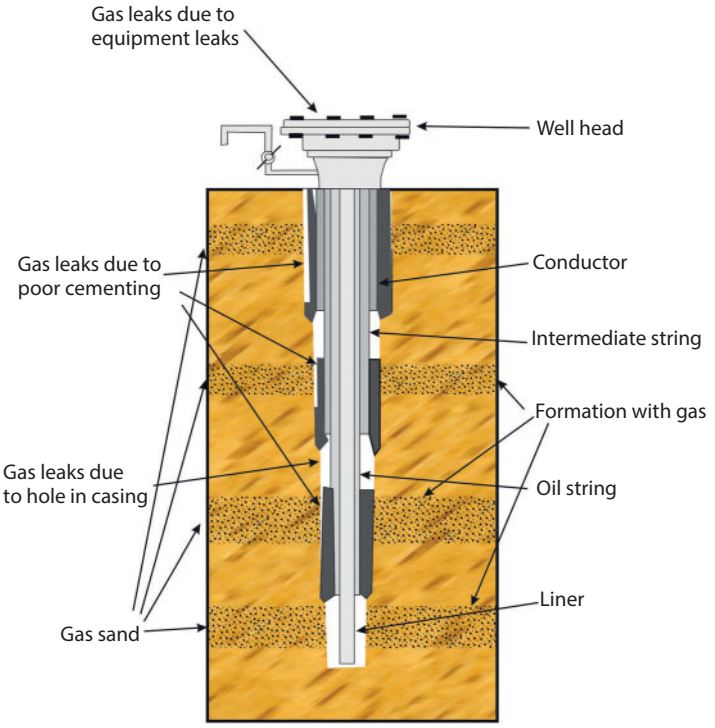

Figure 2.35 Example of several sources for gas leaks for a well. (Modified after Bacu and Watson, 2000.)

(116,550) had been abandoned by 2006. Their study indicated that the migrating gas pathways for these wells were created primarily due to mechanical breakdown of the cement, casing failure (mainly due to corrosion), and abandonment operations.

2.7.2.2 Abandoned Wells

Abandoned wells include exploratory coreholes and former producing wells that were previously drilled but have since have been shut-in and either not properly plugged or plugged according to the standards or practices that were in place at the time. Bacu and Watson (2000) noted that some of these wells were constructed under the Oil and Gas Act (Canada), which was passed in 1984 when new standards for casing, cementing and plugging of wells were established. Prior to that time, many wells were not properly abandoned, and had unknown ownership. Very early drilling practice was to fill the wellbore of a corehole or former producing well with a drilling fluid and no cement.

In their study of leaking wells in Alberta, Canada, Bachu and Watson (2007) found that the potential for leakage inside the casing of abandoned wells utilizing bridge plugs was much higher than that for other types of abandonment procedures. They also found that wells with uncemented casing were the main source of leakage.

In abandoned and idle oilfield wells, migrating gas gradually seeps upwards and accumulates in the upper portion of the wellbore. In time, water is squeezed downward out of the wellbore by gas which has migrated into the upper portions of the wellbore (replacing the water). The upper portion of the gas-filled wellbore has a higher pressure than that of the formations surrounding the well. As a result, the gas seeps out of any openings in the wellbore (such as those where corrosion and tectonic movements have damaged the well casing and cement) into the adjoining rock layers. Often, water in shallow fresh-water sands can be very corrosive, resulting in holes in the casing. Consequently, one can anticipate gas migration into the surface soils from the older wells (Gurevich *et al*., 1993).

2.7.2.3 Repressured Wells

Wells for underground storage of natural gas, secondary recovery, steam injection, etc., are likely candidates for future leakage (gas and/or liquids). Older producing wells used for gas storage reservoirs have a greater potential of leakage because of the aging of cement and expansion of the reservoir due to pressuring the reservoir and breaking down the cement seal. As the original reservoir is produced, pore pressure decreases, effective stress (grain-to-grain stress) increases and the pore structure collapses in order to carry an increasing share of the overburden pressure. This collapse of pore structure permanently alters the abilities of the pores to receive an additional influx of fluids. If at a later time the pore pressure is increased, the collapsed structure may not be capable of confining the gas and/or liquids in the reservoir.

2.7.3 Creation of Induced Fractures during Drilling

Induced fractures may be found in all wells as a result of drilling and are easily visible in image logs and cores. While drilling, the action of the cone drilling bit is a chipping

and crushing action, which breaks off small portions of the rock while creating induced tensile fractures in the formation adjacent to the wellbore. When a drilling bit breaks off a portion of the rock (Figure 2.36a) in the wellbore to deepen the hole, it literally cuts a chip from the rock below the bit because the pressure of the bit against the formation exceeds the tensile strength of the rock. The pressure of the bit on the formation (WOB) at the bottom of the wellbore (Figure 2.36b) also generates induced fractures in the surrounding rock about the wellbore when the concentrated stresses about the borehole exceed that required to cause tensile failure of the rock around the wellbore wall (Aadnoy, 1990). These fractures typically develop as narrow sharply defined features that are sub-parallel or slightly inclined to the borehole axis in vertical wells, extending beyond the wellbore and are potential vertical paths for the future migration of gas.

Lacazette (2001) and Tingay *et al.* (2008) reviewed borehole breakouts and induced fracturing. They prepared a schematic cross-section of the borehole showing that when the stress-induced in the rock exceeds the rocks tensile strength there are: (1) breakouts in the formation wall (chunks of rock breaking off in a wellbore enlarging the wellbore cross-section), and (2) induced fracturing (formation of fractures about the wellbore) of the wall. Figure 2.37 shows (1) the orientation for both the compressive and tensile strengths, (2) the stresses and orientation of breakouts, and (3) the induced fractures relative to the borehole perpendicular to the *in-situ* Earth's stress components. The broken out material is shown in dark grey. These authors noted that hydraulically induced fractures tend to be inclined to the wellbore. The broken-out portion of the wellbore (identified as breakout in Figure 2.37) material is shown in dark gray. In most instances, one of the three principal stresses is oriented vertically, which requires the other two to be oriented horizontally. However, inclined stress-fields do occur, especially in tectonically active areas. Breakouts form in response to the minimum and maximum stress *components* that are oriented perpendicular to the wellbore. These components may or may not be principal stresses depending on the orientation of the wellbore relative to

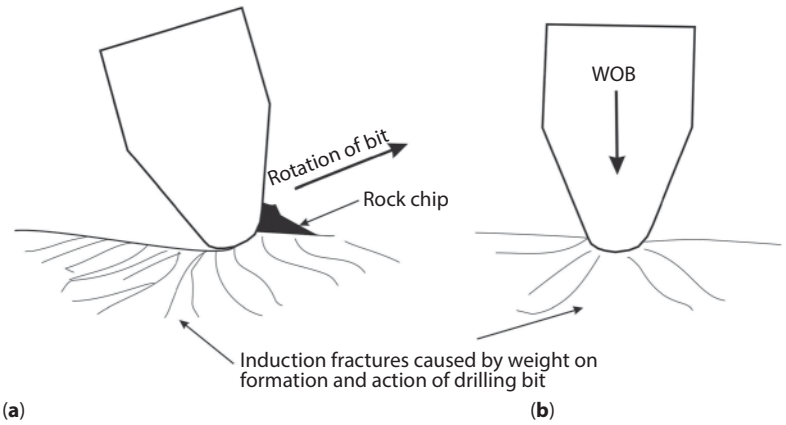

Figure 2.36 Schematic of drill bit-tooth striking bottom of the drill-hole. The tooth of the bit in figure (a) strikes the rock with a force greater than the strength of the rock and chips out a piece of rock and also creates induction fractures. (b) WOB refers to the weight of the rock on the bit which induces fractures in the formation. (Modified after Aadnoy, 1990.)

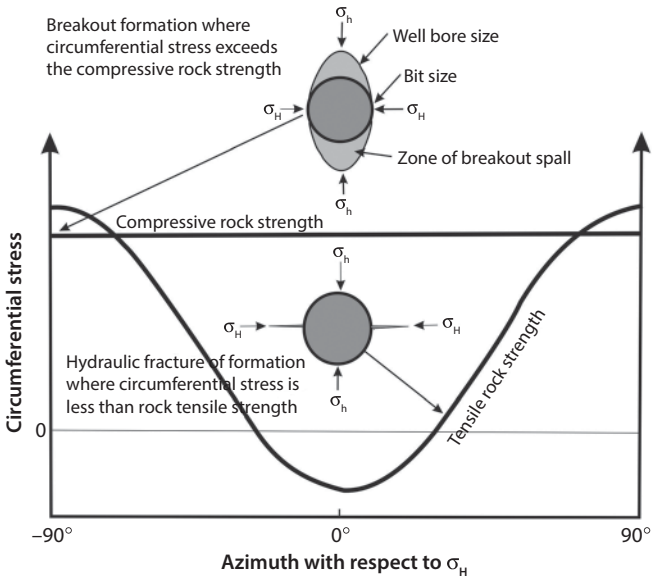

Figure 2.37 Schematic cross-sections of borehole breakout and drilling-induced fracture (DIF; figure adapted from Hillis and Reynolds, 2000). Borehole breakouts form when the circumferential stress around the wellbore exceeds the compressive rock strength and, thus, are orientated parallel to the minimum horizontal stress (σ_H). DIF's form when the circumferential stress exceeds the tensile strength of the well bore wal and are thus oriented parallel to the maximum horizontal stress σ_H. (Modified after Tingay a *et al.*, 2008, figure 1.)

the *in-situ* stress-field. Hydraulic induced fractures tend to be inclined to the wellbore, although they may not form perpendicular to it.

Petal, centerline, and petal-centerline fractures form ahead of the bit during both coring and normal drilling operations. These induced fractures normally extend beyond the diameter of the borehole and are potential pathways for vertical gas migration. Acoustic log can be utilized to identify induced fracturing in a wellbore. Televiewers can sometimes be useful in seeing these fractures in the borehole. Examination of the cores from wellbores can also help to identify various types of induced fracturing.

Lacazette (2001) has noted that increased induced fracturing problems may be encountered in reduced-pressure basins when extended reach wells are drilled through depleted reservoirs. As the wellbore inclination increases, the imbalance between vertical and horizontal stress can result in the formation breakouts leading to widening of the wellbore and, thus, resulting in increased volume of cuttings as well as causing drilling problems, e.g., stuck drillpipe.

Lacazette (2001) proposed the following guidelines to distinguish between the naturally occurring fractures in the formation and induced fractures caused by drilling:

> **Rule 1: The stacking rule**. Induced fractures that do not completely cut the wellbore have a consistent orientation and tend to appear at the same azimuth in the image, whereas natural fractures with a consistent

orientation that does not completely cut the wellbore appear at different azimuths.

Rule 2: The aperture rule. Induced tensile fractures are always open, whereas natural fractures may be open or partially to completely mineralized or gouge-filled.

Rule 3: The continuity rule. The continuity of a fracture trace does not indicate its origin.

Rule 4: The orientation rule. The orientation of a fracture relative to the *in situ* (present day) stress is not indicative of its origin.

Rule 5: The breakout rule. Hydraulically induced fractures form in, and tend to be restricted to, the tensile quadrants of the wellbore wall, which are 90° from the breakouts. Petal fractures, another common type of tensile induced fracture, form ahead of the bit in what will become the compressive quadrants (where breakouts develop). Poorly developed petal fractures tend to be restricted to the compressive quadrants.

Rule 6: The symmetry rule. Individual natural fractures are often symmetrically developed on opposite sides of the borehole. Petal and centerline fractures are nearly always symmetrical, whereas hydraulic fractures are usually asymmetrically developed.

As pointed out by Lacazette (2000), these rules apply to sections of the wellbore where the *in situ* stresses maintain a constant orientation relative to the wellbore. (1) The *in situ* stress can vary in orientation and magnitude along the length of the wellbore due to recent tectonic activity, lithologic changes and other reasons. (2) These rules do not directly address induced shear fractures; however, Rule 1 is applicable.

2.8 Wells Leaking Due to Cementing Failure

2.8.1 Breakdown of Cement

As pointed out by Dusseault *et al.* (2000), there are two principal objectives in primary cementation for oilwells: casing support and zonal isolation. It is zonal isolation that usually raises the most concern, particularly when there is potential for gas migration from the productive zone. The breakdown of cement and resultant leaking of gas from older wellbores is only a question of time as all cements dehydrate as they get older. As a result, cement bonds break down due to volume shrinkage. Cement helps protect the casing from corrosion and collapse.

Either faulty installation of the cement and/or breakdown of the cement over time can result in hydrocarbon leaks through the cement barrier and along the casing and wellbore. Faulty cement application can put the cement isolation of the hydrocarbon productive zone at risk. Cement breakdown can occur either due to improper placement at the time of installation or at a later time as a result of the breakdown as the cement hydrates (ages). Cement problems leading to breakdown of the isolation of the productive zone can be many fold, including: channeling, poor mud cake removal, entrainment of the gas within the cement, and problems with the cement itself, e.g., shrinkage and high cement permeability (Dusseault *et al.*, 2000).

2.8.2 Cement Isolation Breakdown (Shrinkage—Circumferential Fractures)

Particularly in the case of an older well, when production has ceased, the original cement may break down. Bonding breakdown of the cement is often due to cement shrinkage, which also leads to circumferential fractures that are propagated upward by the slow accumulation of gas under pressure behind the casing. Over time, Portland cement continues to dehydrate (loses water) and shrinks creating stresses that lead to circumferential fractures. Various mechanisms, but primarily cement shrinkage can lead to a drop in radial stress. When $\sigma_r < p_o$, a circumferential fracture will open which will lead to a vertical growth of the fracture as shown in Figure 2.38. The gas from the formation develops excessive pressure at the upper leading tip of the fracture extending the vertical height. As shown in Figure 2.39, eventually the fracture will grow toward the surface, and gas will escape the isolated formation to shallower strata or leak at the surface.

To control this shrinkage, Dusseault *et al.* (2000) suggested control of water through the use of superplasticizers and control of macro-shrinkage by using appropriate aggregates in the cement. They also noted that other factors which can lead to cement shrinkage are formation brines high in salt content and salt beds where osmotic dewatering of the cement can occur. Also, dissolved gas, high-curing temperatures and early (flash) set may contribute to cement shrinkage. The ability of the cement to bond to salt, oil sand, high porosity shale, etc., is low. Dusseault *et al.* (2000) noted that the presence of a "*good bond*" on a cement log is in fact not an indicator of bond, but an indicator of intergranular contact maintained by sufficient radial effective stress.

Thus, shrinkage of the cement occurs as the cement ages or if there is too high a water content in the slurry. It is this shrinkage that can give rise to fractures within the cement. While the cement is still in an almost liquid-early-set state, massive shrinkage can occur by water expulsion. Portland Class G cements continue to shrink after setting

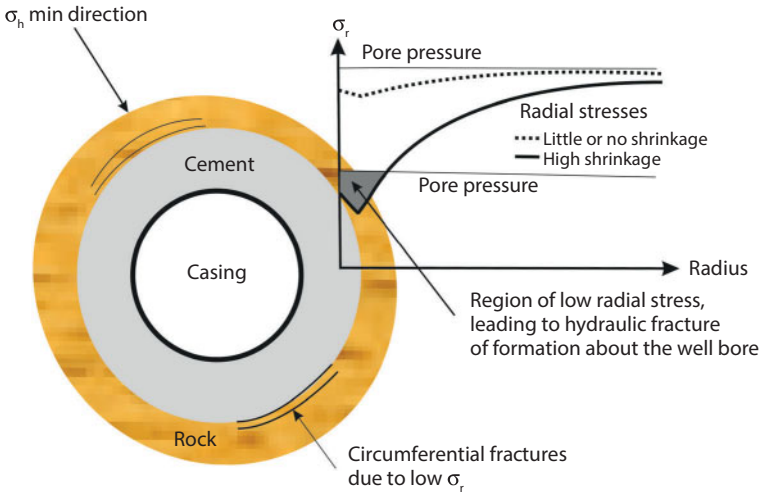

Figure 2.38 Schematic showing radial stresses about a cemented wellbore and casing. Where σ_r = radial stress; P_o = pore pressure. (Modified after Dusseault *et al.*, 2000, figure 2.)

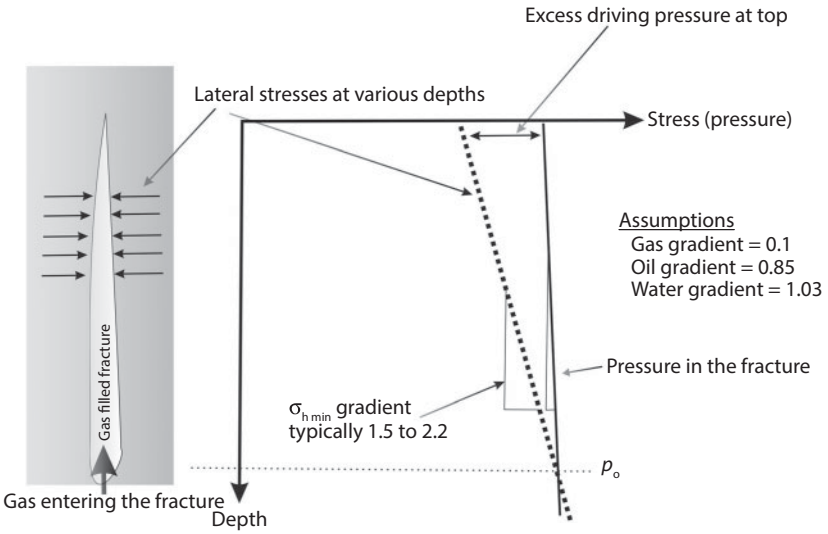

Figure 2.39 A fracture driven by pressure in a cement sheath due to gradient differences. P_o = pore pressure driving the fracture.(Modified after Dusseault *et al.*, 2000, figure 3.)

and during hardening (Dusseault *et al.*, 2000). Additives may be incorporated to alter the cement properties (e.g., wettability), but Portland Class G cement is the base of most oilwell cements. Dusseault *et al.* (2000) noted that slurries are often placed at densities of about 2.0 mg/m^3, but at these low densities cement can shrink and be influenced by elevated pressures (10–70 Mpa) and temperatures (35 to >140 °C) which are encountered in deeper wells. With regard to shrinkage, they stated that the current standards for cement are either not well founded or the criteria are based on a flawed view of the mechanism. There is also a need for better quality oilwell cement formulations for higher pressure and/or temperature applications (Dusseault *et al.*, 2000).

The significance of shrinkage is that older (>50 years) producing wells, along with the many abandoned wells and coreholes worldwide have an increasing potential for gas leakage as their cement gets older and shrinks. Commonly the way the oilwells are handled, is to plug them, cover them up and then forget about them. These plugs, however, do not last forever because of aging of cement along with corrosion of the metal casing. Thus, there is a likelihood that every oil and gas well will eventually leak.

2.8.3 Improper Placement of Cement

It is imperative that the isolation of the oil and gas productive zones by cement (from the upper regions of the wellbore) is properly done. Improper well completion methods can result in a number of pathways for the migration of gas along the wellbore. These include missing cement, channeling of the cement, cracks or fractures in the cement sheath, debonding of the cement to the casing and/or wellbore, and plastic deformation of the cement sheath (Figure 2.41). Some causes for these problems may be the result of poor mud cake removal, shrinkage of the mud cake and/or cement, and cement permeability (Ravi *et al.*, 2002).

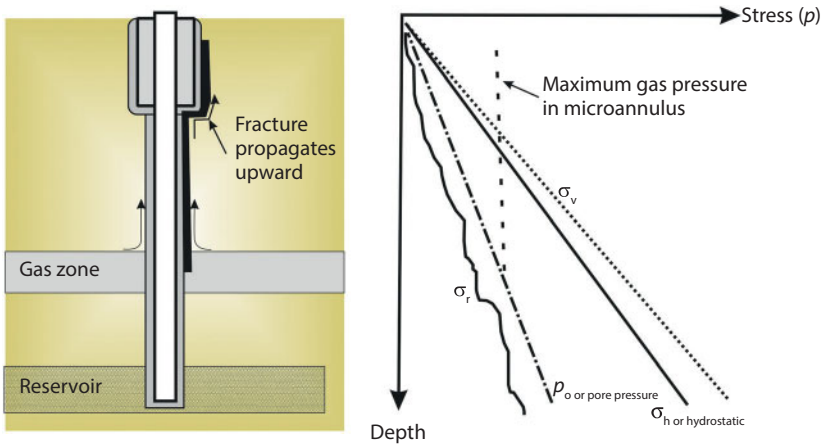

Figure 2.40 A generated fracture in a cased cemented oilwell approaching the surface. Shown in black, beginning in the gas zone where pore pressure exceeds rock strength and then propagates toward the surface. P_o = pore pressure driving the fracture, σ_r, = stress at which rock ruptures, σ_h = stress at hydrostatic pressure, σ_v = maximum stress pressure in microannulus. (Modified after Dusseault *et al.*, 2000, figure 4.)

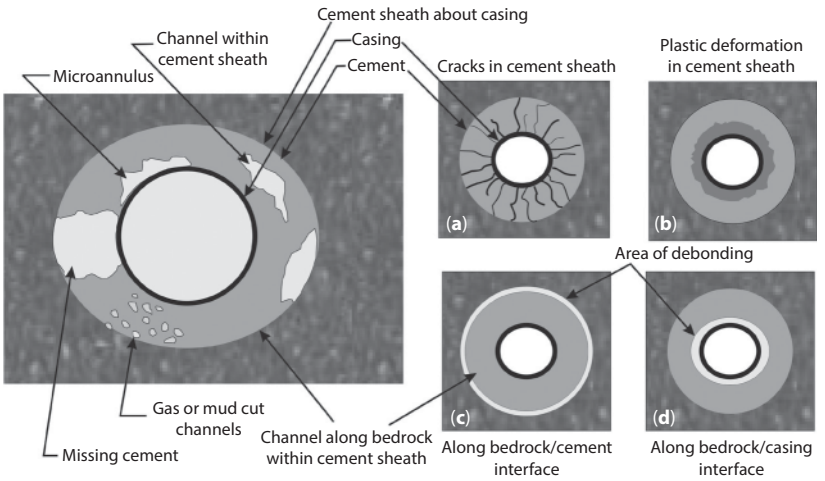

Figure 2.41 Schematics illustrating the effect of various mechanical problems resulting from improper placement of cement in wellbores. (Modified after Ravi *et al.*, 2002 and Newhall, 2006.)

Bonett and Pafitis (1996) have noted that if during the period of placement and setting of the cement paste within the wellbore, the pressure within the annulus drops below that of the formation, gas will migrate from the formation into the cement paste. This invasion of gas into the cement paste may occur in a number of ways other than simple bubbles. As shown in Figure 2.42, gas may flow through the cement as elongated slugs, etc., which can result in channels within the cement as the cement hydrates and hardens. Bonett and Pafitis (1996) describe this gas infiltration as follows:

> ***Stage 1*** – The cement slurry is a dense granular fluid and if the hydrostatic pressure is greater than the formation pressure, gas will not enter the cement paste. However, the hydrostatic pressure begins to drop almost

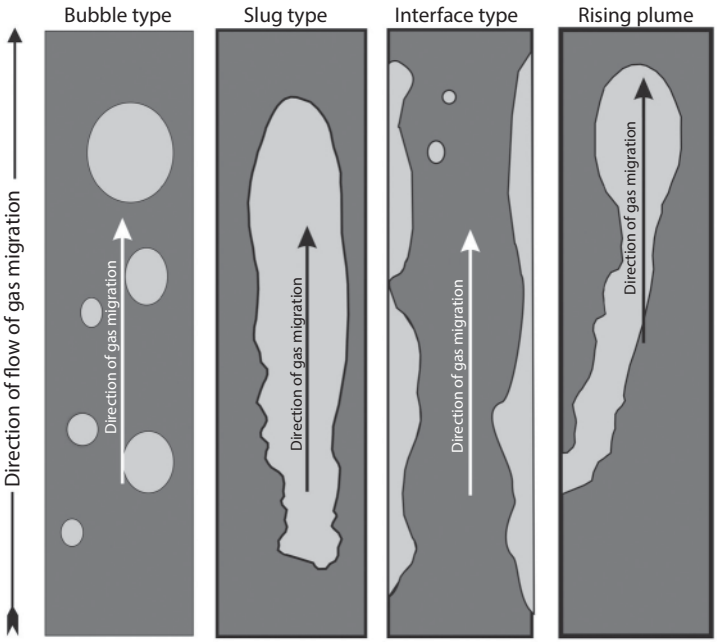

Figure 2.42 Schematic illustrating the different ways gas bubbles (light gray) can migrate through cement prior to its setting (dark gray) that can lead to channeling. (Modified after Bonett and Pafitis, 1996, p. 39.)

immediately because of a combination of gelation, fluid loss and shrinkage of the cement paste. As the cement sets, static gel strength constantly increases, with the rate dependent upon the nature of the slurry. Space for the gas to enter the slurry is provided by the shrinkage of the cement (dehydration). As the cement cures, opportunity for gas to enter the slurry decreases.

Stage 2 – *Cement as a two-phase material*: During Stage 2, a cement column is fully self-supporting and is a matrix of solid particles with interconnected pores containing a fluid phase. The majority of the shrinkage occurs during this phase. This may initiate fractures and disrupt the bonding of the cement to the casing and/or formation. Internal shrinkage creates a secondary porosity in the cement.

Stage 3 – *An elastic solid.* Once dehydration is almost complete, cement becomes an elastic and brittle material, which is isotropic, homogeneous and essentially impermeable to gas infiltration. At this stage, gas can only flow through the fractures and pathways present in the cement matrix.

Major contributing factors resulting from incorrect placement of cement, which create gas migration pathways during the cementing process, were reviewed by Bonett and Pafitis (1996) in Figure 2.43. Incorrect cement densities can result in the flow of natural gas from the formation into the cement. Poor and incomplete removal of mud cake can result in channels along the formation providing future pathways for gas migration up the annulus. Premature gelation leads to loss of hydrostatic pressure control. Excessive fluid loss from the cement gives rise to additional space in the cement paste for natural

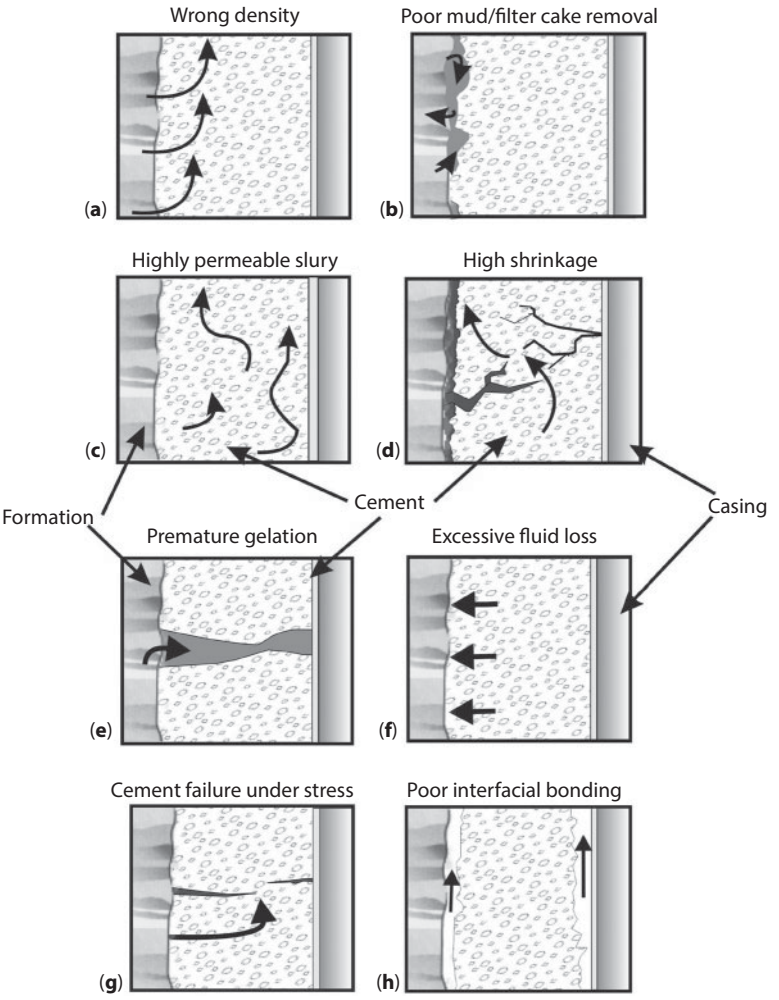

Figure 2.43 Schematics illustrating the effect of various mechanical problems resulting from improper placement of cement in well bores. Arrows indicate direction of fluid flow (gas/liquid). (Modified after Bonett and Pafitis, 1996, figure 1, p. 37.)

gas to enter the cement. Highly permeable slurries result in poor zonal isolation and offer little resistance to gas flow. High cement shrinkage results in increased porosity in the cement sheath that may lead to microannulus. Cement failure under stress results in fracturing of the cement sheath, whereas poor cement bonding to the casing and/or wellbore wall gives rise to channels for gas migration along the wellbore.

2.9 Environmental Hazards of Gas Migration

2.9.1 Explosive Nature of Gas

Many petroliferous basins have experienced fires due to migrating hydrocarbon gases. The lower explosive limit (LEL) of hydrocarbon (oilfield) gases (composed primarily

of methane) occurs when approximately 5% by volume of gas is mixed with 95% by volume of air. This translates into a serious explosion and fire hazard, especially where the gas is capable of migrating into a confined space such as a room or an electrical vault. These hydrocarbon gases are often the result of leakage from gas pipelines and/or seepage of gas from oilfields. If the explosion (LEL) limit is met, a spark can quickly initiate a fire/explosion.

In many areas, homes and commercial structures have been constructed directly over old oilwells that have not been properly sealed, and where mitigation measures have not been taken to seal out the seeping gases.

2.9.2 Toxicity of Hydrocarbon Gas

The U.S. Environmental Protection Agency (EPA) has determined that the primary hazardous air pollutants (HAP) emitted from the oil and natural gas transmission and storage facilities are (*Federal Register*, Volume 63, No. 25 / Feb. 6, 1998): (a) benzene, (b) toluene, (c) ethyl benzene, and (d) xylenes. These compounds are often collectively referred to as the BTEX chemicals. The BTEX chemicals are common aromatic components of crude oil and gas. A detailed discussion of these hazardous components of crude oil can be found in McMillen *et al.* (2001). Although crude oil has variable contents of aromatic hydrocarbons, depending upon its origin, the API rating of the crude oil can be a good predictor of the content of aromatics, especially benzene (see Figure 2.44). A general rule is that, the higher the API gravity of the crude oil, the higher the percentage of aromatics in the crude oil. The formula for calculating API gravity is:

$$\text{API}^\circ \text{ gravity} = \frac{141.5}{SG} - 131.5. \tag{2.56}$$

Generally speaking, 40 to 45 API gravity degree oils have the greatest commercial value because they are rich in gasoline. Condensates are worth slightly less because the natural gasoline has a lower octane value. Heavier crudes are worth less because they require more refinery processing. An overall classification of crudes is presented

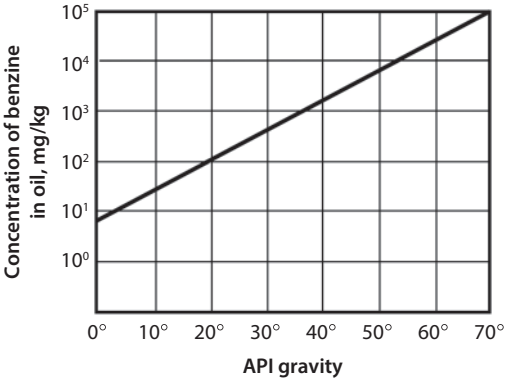

Figure 2.44 Benzene concentrations versus API gravity for 61 crude oils and 14 condensates. (Note: API gravity data were unavailable for eight crude oils). Modified after Rixey, 2001.)

in Figure 2.45. West Texas Intermediate (WTI) is the benchmark crude oil used by the United States to set prices and compare with other oils. Figure 2.46 shows the composition of various API gravity oils. Tissot and Welte (1978) found that 95% of the crude oils produced around the world fall into the hydrocarbon distribution pattern shown in Figure 2.47.

The majority of the world's crude oils have been reported to contain 15% to 40% aromatics. These aromatics are characterized by a double carbon bond, which has been directly linked to the health hazards posed by these chemicals. Benzene and toluene, known human carcinogens, have been linked to leukemia, aplastic anemia, lymphomas and a variety of other cancer-related ailments. Oil and gas production

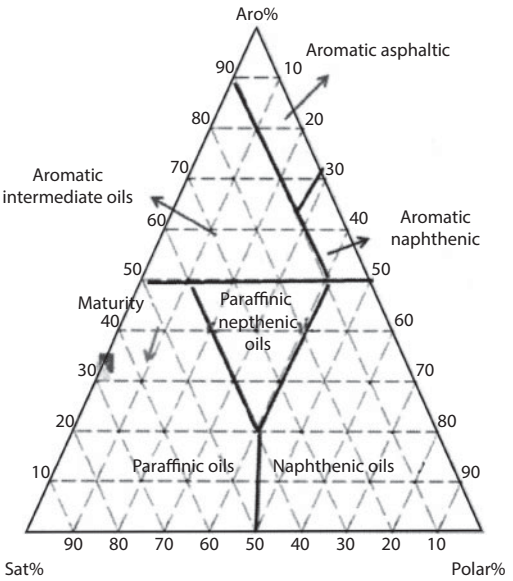

Figure 2.45 Ternary diagram showing the class of composition of the World's crude oils. (Modified after Kamali *et al*., 2012.)

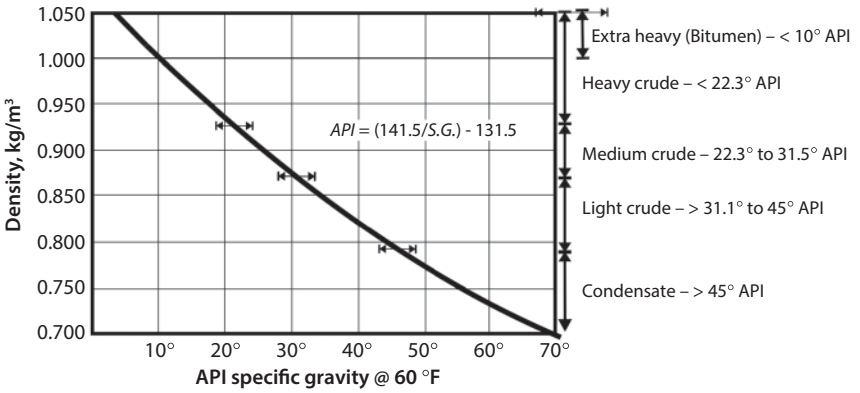

Figure 2.46 API gravity of oil vs density and classification of oil based on API gravity.

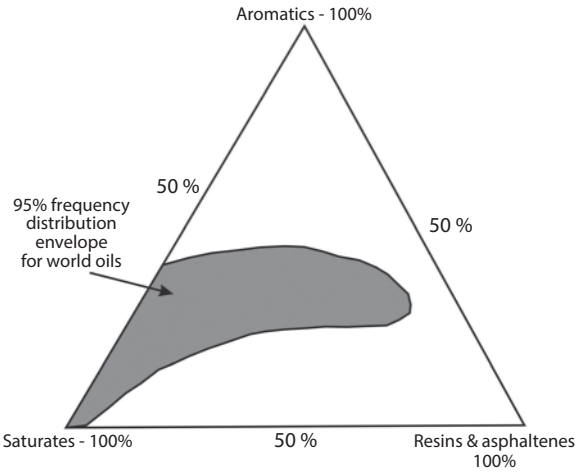

Figure 2.47 Ternary diagram showing the class composition of crude oils. (Modified after Tissot and Welte, 1978.)

facilities handling these potentially dangerous chemicals are required by California law, for example, to provide warnings to the public under the California Health and Safety Code Section 25249.6 (otherwise known as Proposition 65). All facilities must be required to identify the amount or the specific types of chemicals being released to the atmosphere from their operations.

The EPA has identified dehydration equipment as a major source of benzene and toluene air toxics emissions, and has proposed legislation to curtail such emissions, especially in residential areas. Venting of oilfield gases to the atmosphere must be viewed as a hazardous activity, not only due to potential fire and explosion danger, but because oilfield gases may contain appreciable levels of benzene and toluene. Oilfield gases and condensates are known to contain aromatics (benzene, etc.). A typical content of benzene in the oilfield gases can vary between 30 parts per million (ppm) to over 800 ppm. For this reason, the natural gas should always be carefully tested for its benzene content before venting to the atmosphere. Also, vent stack emissions should be carefully monitored.

Additional concerns and precautions must always be taken in and around sour (hydrogen sulfide, H_2S) oilfield operations. Hydrogen sulfide, even in small quantities, can be toxic (hazardous) to human health. Research conducted at the University of Southern California Medical Facility (Kilburn, 1998, 1999) has established central nervous system damage from the neurotoxin effects of hydrogen sulfide even at concentration in air as low as 1 ppm. This is much lower than the workplace standards that have been considered safe in the past. This also highlights the importance of not relying upon workplace standards regarding air toxics emissions in the case of residential areas and school sites. Safety, health, and environmental considerations need to be made a top priority in the land use planning where urban development coexists with the oilfield and gasfield operations.

Many oilfields have a long history of gas migration problems, i.e., explosion, fires, noxious odors, and potential emissions of carcinogenic chemicals such as BTEX. These risks must be seriously examined for all oil and/or gas operations in urban or developed

areas. Although the migration of hydrocarbons has been long recognized, the dangers of fire and explosion were not considered as the primary problem.

2.10 Migration of Gas from Petroleum Wellbores

Many petroliferous basins have been plagued with numerous gas seeps from oilfields (migration of gas from hydrocarbon pools to the surface) that present serious explosion and health risks to the overlying population. Oilfield gases have a propensity to migrate upward to the surface along faults and poorly cemented and/or abandoned wellbores. Furthermore, the upward migrating gases can accumulate in the near-surface collector zones, which are often concealed within the shales in the permeable gravel and sand lenses.

There is a need to carefully evaluate the integrity of casings in many older oilwells because holes in the casing due to corrosion can serve as a primary source for gas migration to the surface. Also, it should be remembered that the bonds between the casing and formation will break down in time. Early oilwells were not always completed with cement. In some cases the wellbore was filled and abandoned with a drilling fluid. Furthermore, the early cement utilized in the oilwells drilled prior to the 1950s was not as competent as that which is available today. Recent studies have shown that even under current standards with today's cements, over 15% of all modern oilwells leak. Many oilwell leaks can be traced to poor well completion and/or abandonment procedures, e.g., poor cementing practices. The writers estimate that the life of cement before deterioration is about 50 years.

Gas migration from the subsurface hydrocarbon pools into inadequately cemented wellbores, with the resultant leakage to the surface, has been a persistent problem in the oil and gas industry for many years. In the case of gas storage reservoirs, pressure and temperature cycling on the cement bonding of wells is an acute problem and can give rise to shoe leaks and loss of bonding between the formation and well casing. To help quantify the annular leakage problem in gas storage wells, a survey was prepared and sent to the American Gas Association's Pipeline Research and Storage Reservoir Supervisory Committee. The survey attempted to determine the magnitude of the annular leakage problem (Marlow, 1989).

Tests showed that even when the most up-to-date cement types and techniques are used, leakage can and will occur in a significant number of cases (Marlow, 1989, pp. 1147, 1148). For example, in a study of 250 well casing jobs over a 15-month period with current cement, 15% of the wells leaked (Waiters and Sabinas, 1980). Many wells are capable of giving rise to very serious environmental problems associated with gas migration to the surface. Even low concentrations of hydrogen sulfide in the gas can further destroy the integrity of both steel and cement. The corrosive action of hydrogen sulfide has defied engineering solutions (Craig, 1993). The topic of corrosion is further discussed in Chapter 6.

2.10.1 Effect of Seismic Activity

Seismic activity is another factor in contributing to the well integrity problem, e.g., in the Los Angeles Basin, CA, the 1971 Sylmar earthquake was responsible for damaging

well casing and cement bonding in several oilfields resulting in well blowouts in the Fairfax area (Salt Lake Oilfield) (Khilyuk *et al*., 2000). It is important to do a systematic examination of the condition of all wells in a field after seismic events to determine the extent of damage to the well casings. If each well leak is only evaluated individually and as an isolated example, without examining the field history and other wells, the true dangers to the public may not be recognized.

2.11 Case Histories of Gas Migration Problems

This section is a review of many case studies illustrating the potential environmental problems inherent with oilfields in developed urban areas. In the case of the Salt Lake Field, for example, gas migrated along the faults and/or wellbores resulting in the Ross Dress for Less department store explosion, Los Angeles, CA. Toth (1996), in his study of the hydrology of this area, noted that the underlying permeable aquifers for this basin can conceal the true magnitude and hazard of lateral gas migration away from the reservoir itself. In the case of Hutchinson, KS, gas migrated horizontally about 7 miles through aquifers from where the explosions and fire occurred within the city. A review of well abandonment records for the Los Angeles Basin for example reveals the potential problem of very serious leakage of gas from wells that were abandoned prior to the use of cement and/or to current standards of completion. Many of the wells within the Los Angeles Basin, CA, were drilled prior to the 1970s, when current cementing standard practices were not used to insure proper placement of the cement and segregation of the productive zone from the wellbore to prevent gas migration. For example, in the Montebello Oilfield (utilized as a repressured gas storage reservoir), several older wells that had been abandoned to make way for a new housing development, were found to be leaking gas to the surface and under the new homes. In order to reabandon the leaking wells under these homes, the homes were torn down, the wells reabandoned and the land where the home had stood was converted to a mini-park. Building a house over an abandoned well is like building a house over a potential "*volcano.*"

Most construction over old wells fail to provide gas detection or other mitigation measures (e.g., as required by the Los Angeles City Methane Ordinance, 1985) in order to deal with potential gas migration hazards. For example, the underground gas storage operations at Playa del Rey involved injection of storage gas under high pressure ($\approx$120 kg/cm^2). Gas inventory studies (Tek, 1987) have shown that leakage is directly proportional to the reservoir pressure maintained for gas storage (Figure 2.48). According to Tek (1987), a gas reservoir after repeated pressure cycling begins to break down and leak gas after 50 years. It is paramount to realize that repressured wells often leak gas.

Proper procedures for continuous monitoring for leaking gas must be developed for gas storage reservoirs in urban areas. The gas storage pressures are typically selected by the operator to maximize the storage volume, and to enhance retrievability of the stored gas when market demands (usually during cold spells when demand for gas increases). According to Khilyuk *et al*. (2000), what often is not considered when repressuring the reservoir is: (1) the potential creation of new fractures within the reservoir if the pressure exceeds the current strength of the reservoir rock, (2) fluid leakage along the faults when they open up as the formation is repressured, (3) the mechanical condition of the aging active wells that may not have been designed to isolate the formation from the

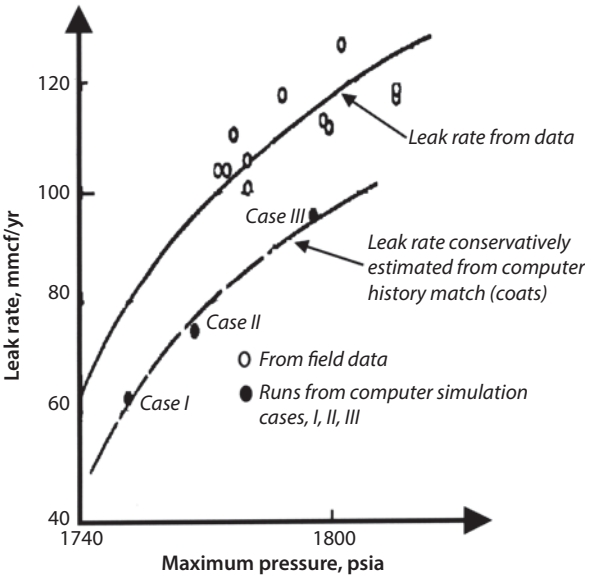

Figure 2.48 Gas leak rate for various maximum reservoir pressures for the Leroy Gas Storage Project. (Modified after Tek, 1987, figure 11.16.)

wellbore under the new pressures, and (4) the existence of a cement barrier isolating the cyclic repressurizing zone for those wells that penetrate or pass through the repressurized interval and all coreholes and abandoned wells that penetrate the repressurized interval. In addition, the operator must continuously monitor the surface soil for leaking gases.

2.11.1 Inglewood Oilfield, CA

The Inglewood Oilfield consists of nine major groupings of layers or pools of intermixed oil and water aquifers located about 9 miles west of the center of Los Angeles, CA. The field, as shown in Figure 2.49, is a faulted anticline. A major fault, the Newport-Inglewood, bisects the field. The reservoir thickness for the total field is over 8,000 ft of alluvial Pliocene and Miocene sediments with the average depth of pools ranging from 950 to 8,400 ft. The discovery well was drilled in 1924. Over 693 wells have been drilled in this field. Many of these well were drilled prior to the 1950s when cementing practices were not recorded or regulated by today's standards.

As the property values were increasing there was interest in developing the property above the Inglewood Oilfield. This field has a history of inadequately abandoned wells leaking fluid (gas and liquids) to the surface during the waterflooding of the Vickers zone. There is also a record of water passing through fault planes within the Vickers waterflood at differential water pressures greater than 150 psi. A large housing development was proposed for the Baldwin Hills area with high retaining walls contemplated to enhance views of the buildings. This project was halted and the property later sold to the State of California for use as a public park (Chilingar and Endres, 2005).

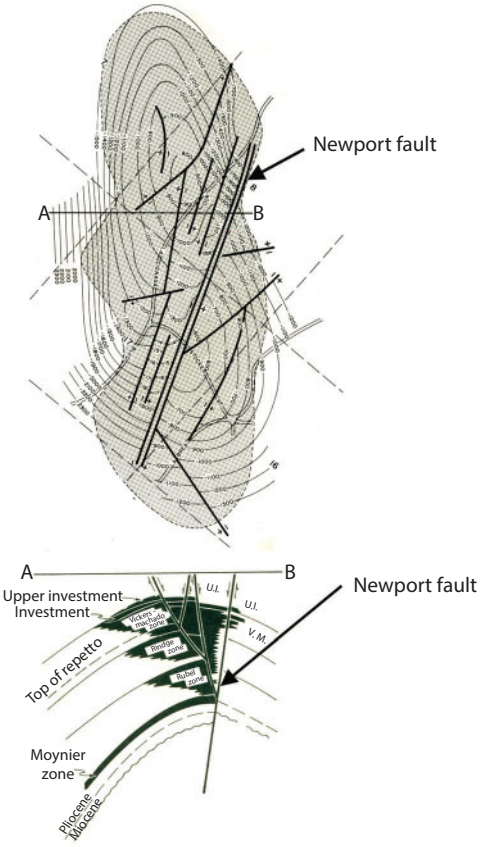

Figure 2.49 Inglewood Oilfield, CA; contours on Vickers-Machado zone. (After California Division of Oil and Gas, 1961, p. 576.)

2.11.2 Los Angeles City Oilfield, CA

The Los Angeles City Oilfield consists of three shallow major groupings of layers of oil and water aquifers located about 1 mile north of the center of Los Angeles, CA. The field, as shown in Figure 2.50, is a shallow faulted homocline. The total thickness of sediments is about 1,500 ft of alluvial Miocene deposits with the average depth of reservoir pools ranging from 375 to 1,700 ft. The discovery well was drilled prior to 1892. About 1,250 wells have been drilled in this field. Almost all the wells were drilled prior to the 1950s and not abandoned by today's standards with many abandoned without the use of cement. Intense residential and commercial development has occurred over this old field and abandoned wells. There is evidence of natural gas leaking to the surface from the reservoir throughout the area.

2.11.2.1 Belmont High School Construction

The Belmont Learning Center, previously proposed to be a high school in downtown Los Angeles, CA, was constructed over the Los Angeles City Oilfield. The site chosen was on a 0.14 km^2 parcel of land. This location is over the shallow oilfield that has a

surface outcrop just north of the building site. The area is also over part of the Elysian Park blind thrust fault system that has a generally east-west trend, which helps explain the uplifting and tilting of petroliferous formation depicted in Figure 2.50.

There are oilwells in the area producing from shallow oil deposits at a depth of no greater than 213 m. Most of the wells producing oil today were drilled in the early 1900s, and lack a proper cement completion to isolate the producing formation from the wellbore. Although the gas production is minimal, all of the produced oilfield production gases are released to the atmosphere in the residential area above the wells. This includes four operational wells at the northwest corner of the school property.

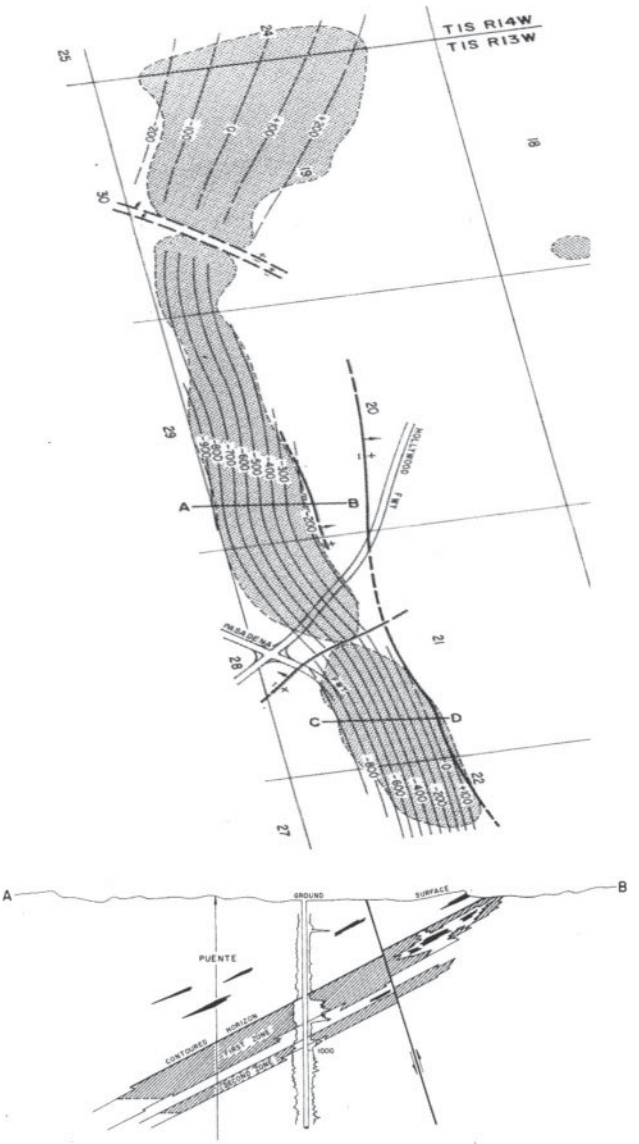

Figure 2.50 Los Angeles Oilfield; contours on top of the 1st Oil Sand. Productive area is shaded. (After California Division of Oil and Gas, 1961, p. 598.)

Environmental studies were undertaken only after construction began. These studies revealed oilfield gas seepage to the surface over most of the 0.14 km^2 parcel and the surrounding area, including the area directly under the proposed school buildings. The project was abruptly halted when gas seepage was detected in the main electrical vault room of the project, just before the power was to be energized.

Soil gas studies revealed that methane (explosive levels) and other gases are migrating to the surface, including toxic gases such as hydrogen sulfide. Measurements at the surface revealed releases to the air of over 300 parts per million (ppm) of hydrogen sulfide (Endres, 1999, 2002). Investigation in the area revealed that the gas migration to the surface is common throughout this area. After a lengthy discussion, the project was completed and used as an administrative center rather than a school site.

This case history clearly identifies the caution required in evaluating the environmental suitability of developed sites located over oilfields where there are migrating hydrocarbon gases, especially in the case of school construction. The State of California has passed recent legislation that requires direct participation by the Department of Toxic Substances Control (DTSC) in the future school site selection process in order to avoid a repeat of the Belmont failure.

2.11.3 Montebello Oilfield, CA

The Montebello Oilfield consists of 13 major groupings of layers or pools of oil and water aquifers located about 5 miles east of the center of Los Angeles, CA. As shown in Figure 2.51, this field consists of a Main and West area anticline and East area faulted

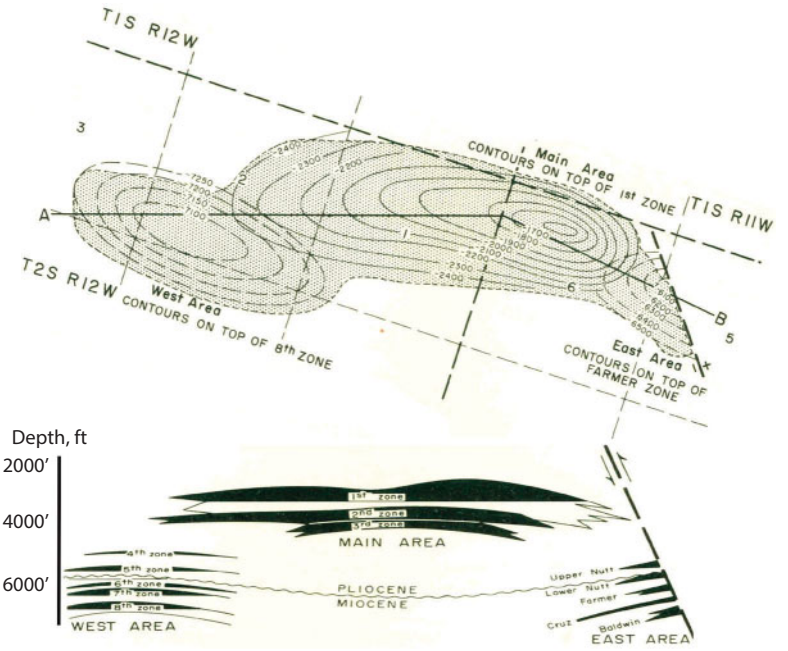

Figure 2.51 Montebello Oilfield; contours on top of the 8th zone. (After California Division of Oil and Gas, 1961, p. 606.)

anticline area. The overall thickness of the deposits is about 6,000 ft of alluvial Pliocene and Miocene sediments with the average depth of pools ranging from 2,200 to 7,000 ft. The discovery well was drilled in 1917. Over 629 wells have been drilled in this field, many prior to the 1950s when cementing practices were neither regulated nor recorded. Overlying this oil field is a dense, highly developed, residential area.

2.11.3.1 Montebello Underground Gas Storage

The partially depleted 8th zone of the Montebello Oilfield (at a depth of 2,236 m) was converted into an underground gas storage operation. Natural gas was transported to the field through interstate pipelines and injected under high pressure (exceeding 105.6 kg/cm^2) into the 8th Zone pool. Methane gas was discovered at the surface coming out around several well wellheads and under existing dwellings. Investigation revealed that this gas had migrated from the gas storage reservoir to the surface though wellbores that had been drilled in the 1930s and, possibly, along faults. In several instances, homes which had been built over abandoned wells had to be torn down in order to provide access for drilling rigs to reabandon wells that were a pathway for gas migration to the surface. Further investigation revealed that the cement used in some of the older abandoned wells was not adequate to seal off the repressured storage gas in the reservoir. After several years of problems with the migration of gas and reabandoning leaking wells, this facility was abandoned.

2.11.4 Playa Del Rey Oilfield, CA

The Playa Del Rey Oilfield, CA, consists of two major groupings of layers or pools of oil and water aquifers located about 13 miles southwest of the center of Los Angeles. This field, as shown in Figure 2.52, consists of an Upper and Lower zone and is an anticline over a basement high. There are about 2,000 ft of alluvial Pliocene and Miocene sediments, with the average depth of pools ranging from 4,000 to 6,400 ft. The discovery well was drilled in 1929. Over 320 wells have been drilled in this field and many when cement was not used or when cementing practices were neither regulated nor recorded. Overlying this oilfield is a dense, highly developed, residential area.

Oil production in the Venice area of the Playa Del Rey Field began in 1929. This area has produced 82% of the oil production of this field. A large reduction in reservoir pressure occurred from 1929 to 1944, when the initial pressures of 1900 psi decreased to about 100 psi.

Nearly all of the oil wells in the Venice area have been abandoned and there is currently little subsidence due to hydrocarbon withdrawal; however, environmental problems exist because of water extraction from the aquifer in the area causing subsidence and potential problems of gas migration through the improperly abandoned wells.

2.11.4.1 Playa del Rey underground Gas Storage

The older wells in this field were drilled, completed, and abandoned prior to the 1950s, which today are vulnerable to the problems of gas migration as a result of: (1) a breakdown of aging of the cement about the wellbore along with additional the chemical breakdown weakening the cement seal between the formation and the wellbore.

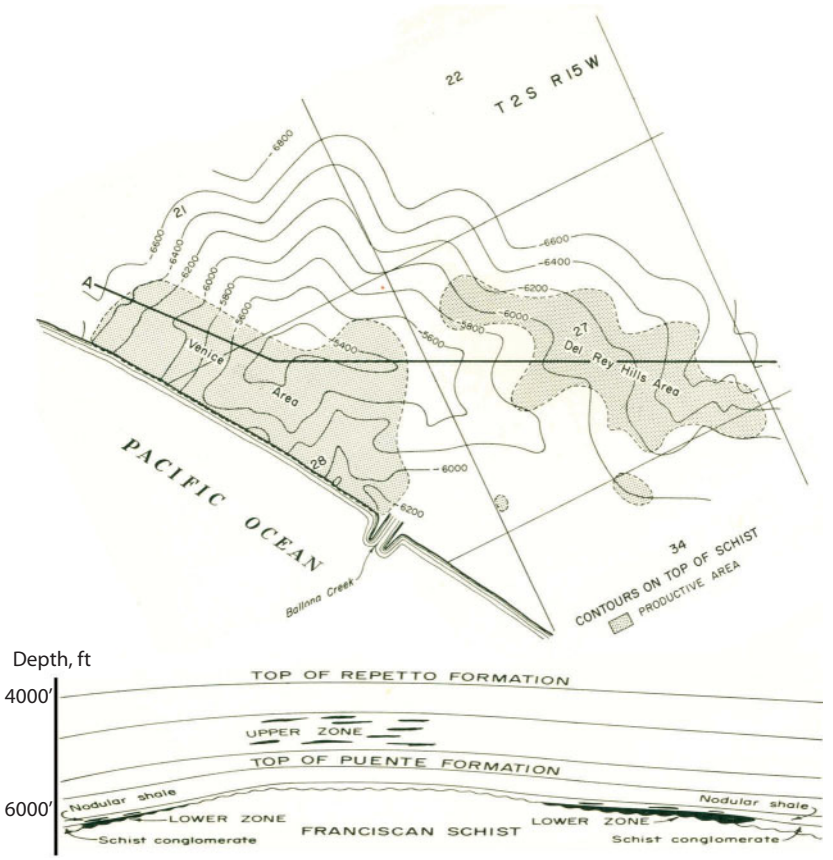

Figure 2.52 Playa Del Rey Oilfield with contours on top of schist conglomerate. (After California Division of Oil and Gas, 1963, p. 634.)

(2) Many of the earlier wells had no cement as a protective barrier. (3) Breakdown of earlier cements as a direct result of seismic activity (earthquakes). (4) Movement along the faults bending or shearing the casing. (5) Holes in the casing due to corrosion. The condition of these older wells in the Del Rey Hills area (see Figure 2.53) is especially critical, because the reservoir underlying this area is now being used to store high-pressure gas (Lower Zone). There is a potential for repressured gas to migrate up from the Lower Zone along many potential vertical pathways and contaminate the upper fresh-water sands in the area as it moves toward the surface.

A portion of the Lower Zone of the Playa Del Rey Oilfield was converted to an underground gas storage operation about 1942. As shown in Figure 2.53, the Venice Oilfield adjoins Playa Del Rey Oilfield to the immediate north. This gas storage reservoir located in the Del Rey Hills area has been laterally leaking (stored gas) into the adjoining Venice Oilfield since the early years of the gas storage operation (Riegle, 1953). There are over 200 abandoned wells throughout this area, including those wells that had to be abandoned in order to accommodate the construction of the Marina Del Rey Boat Harbor.

Many of these wells, which were drilled prior to the 1950s, were not cemented and are located directly below the main surface channel that connects to the Pacific Ocean. Numerous gas seeps at the surface have been observed by the authors of this book

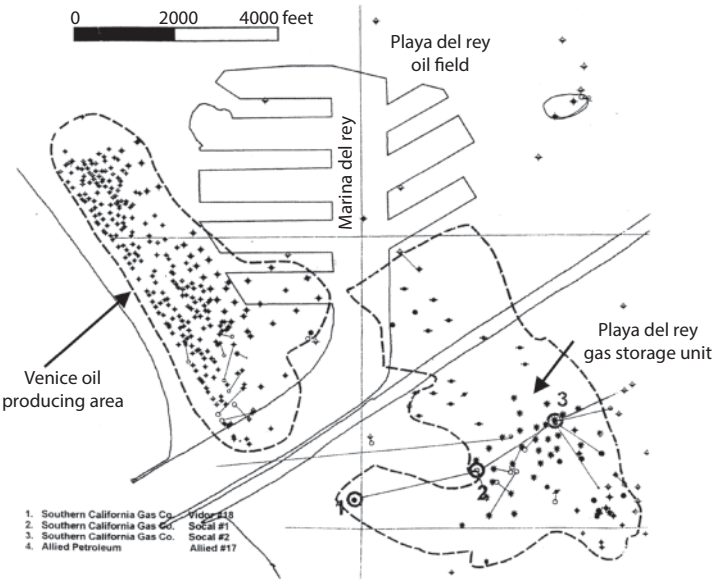

Figure 2.53 Playa del Rey Oilfield showing location of oil-producing areas and gas storage reservoir. (In: Chilingar and Endres, 2006, figure 4.)

within the boat harbor, around the homes in the marina, and in the Ballona Flood Control Channel.

Historically, the Los Angeles River was responsible for depositing a massive gravel layer that extends eastward, providing a highly permeable collector zone. This Gravel Zone begins below the surface sediments at a depth of approximately 15 m (sometimes also referred to as the "15-meter Gravel") and extends to a depth of several hundred feet. The Gravel Zone interconnects many of these wells in the area providing a pathway for gas migration and serves to conceal the identity of those wells that are experiencing the worst leakage.

Gas fingerprinting has established that the leaking well gases match the stored reservoir gases seeping to the surface along the flood control channel and into the surrounding residential areas. This Gravel Zone is saturated with hydrocarbon gases, which are additionally pressurized during the heavy rains. At this time, surface gas seeps can be observed bubbling through the surface brackish water. Probes placed into the 15-meter Gravel Zone have measured gas flow rates as high as 20 to 30 L/min (Chilingar and Endres, 2005). Also, drilling rigs have experienced blowouts as a result of encountering the high-pressure gas zone when drilling to a depth of 15 m.

2.11.5 Salt Lake Oilfield, CA

The Salt Lake Oilfield, CA, is located in Los Angeles, east of the town of Beverly Hills. This field consists of four major groupings of layers or pools of oil and water aquifers and is a stratigraphic trap along two plunging anticlinal noses (Figure 2.54). There are about 1,000 ft of alluvial Pliocene and Miocene sediments with the average depth of pools ranging from 1,000 to 2,850 ft. The discovery well was drilled in 1902. Over 500 wells have been drilled in this field, many when cement was not used or when cementing practices were neither regulated nor recorded.

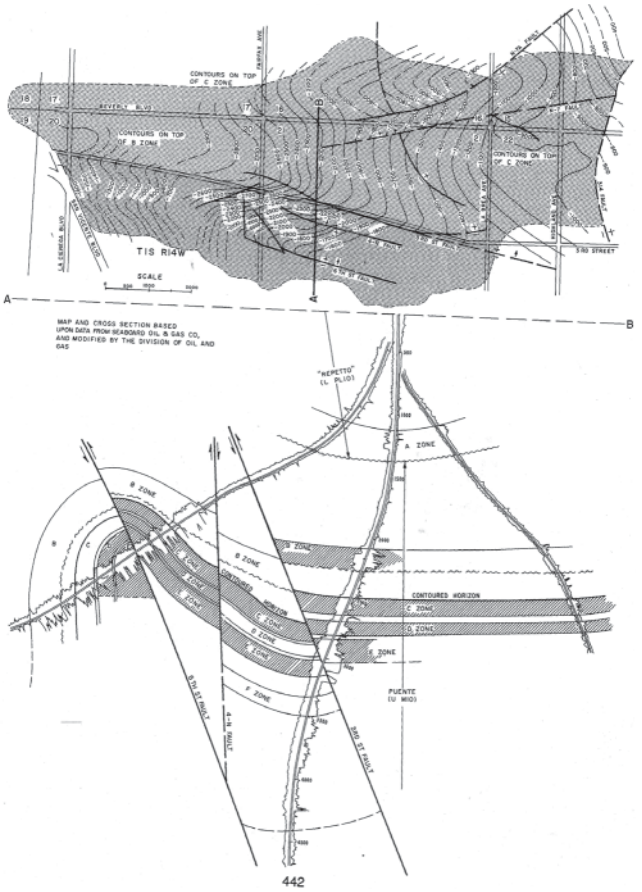

Figure 2.54 The cross-section and structure of the Salt Lake Oilfield. (After California Division of Oil and Gas, 1961, p. 652.)

Overlying this oilfield is a dense, highly developed residential area and the La Brea Tar Pits are a portion of this area. The tar pits are an excellent example of fluids (oil and gas) migrating up along a fault to the surface. After a rainfall in this area, one can observe small bubbles of gas and oil breaking out in surface cracks in the sidewalks and paved areas. The urban area above the Salt Lake Field has had a history of migrating gas, fires and explosions.

2.11.5.1 Ross Dress for Less Department Store Explosion/Fire, Los Angeles, CA

A very serious urban problem due to oilfield gases migrating to the surface, igniting and causing an explosion in the La Brea Tar Pits area occurred on March 24, 1985, at the Ross Dress for Less department store, in the Fairfax area of Los Angeles, CA. This incident resulted in an explosion and fire for several days, that could not be extinguished, injuring over 23 people (Cobarrubias, 1985). The fire was fed by escaping migrating natural gas through cracks in the paved areas. This area was across the street from the La Brea Tar Pits. Investigation revealed that in another nearby area there was a large quantity of subsurface gas migrating to the surface under the Hancock Park Elementary School, located on Fairfax Street near 3rd Street.

The complex pathway for gas migration to the surface included the (1) 3rd Street Fault, (2) an abandoned well and (3) a shallow collector zone (large pocket) of trapped oilfield gas at a depth of approximately 10 m with pressures of approximately 1.8 kg/cm^2. This collector zone had sufficient porosity and permeability to serve as a secondary trap for a large quantity of upward migrating gases. A clay layer over the secondary trap served as a seal until its threshold pressure was exceeded. After the Ross store explosion, permanent soil gas probes were installed to a depth of approximately 4.6 m penetrating this clay layer in order to perform degassing of the collector zone and as an ongoing monitoring of the migrating gases.

Near-surface soil gas studies revealed that the highest concentrations of gases were aligned in an elliptical pattern with the semi-major axis having an exact alignment with a nearby well (the Metropolitan #5 well). Well production records of this well revealed that it was the largest gas producer from the underlying Salt Lake Oilfield. Well records revealed that the well casing had developed leaks as a result of corrosion, located at depths beginning approximately at 1,100 ft (366 m) (Endres *et al.*, 1991; Khilyuk *et al.*, 2000).

The major migration gas pathways were the wellbore of Metropolitan Well #5, and the 3rd Street Fault. Another migration path to the surface for the migrating gas was traced to an abandoned Well #99. To remedy the problem, a vent well was drilled into the collector zone in the parking lot of the Ross store to vent gas to the atmosphere. Detailed gas fingerprinting, primarily utilizing isotopic gas characterization, showed that the Fairfax explosion and fire were caused by migrating gases escaping from the underlying Salt Lake Oilfield (Figure 2.55, Schoell *et al.*, 1993). Identification of migrating gases in the surrounding area revealed that the gas seeps at the adjacent La Brea Tar Pits had resulted from the upward migration of gases from the Salt Lake Field along the 6th Street Fault (Jenden, 1985). The 6th Street Fault slopes downward toward the north and intercepts the oilfield reservoir at the location of the Metropolitan Well #5. Jenden (1985) showed (fingerprinting) that the gas seeps at the La Brea Tar Pits match the leaking gases that caused the Ross department store explosion.

2.11.5.2 Gilmore Bank

On February 7, 1989, a pedestrian walking by the Gilmore Bank building, located across the street from the 1985 explosion site, observed gas bubbling out of the

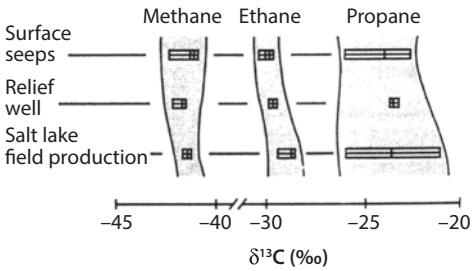

Figure 2.55 Carbon isotope fingerprinting of migrating gas leaking from a shallow Salt Lake Oilfield. (After Schoell *et al.*, 1993, p. 7, figure 8.)

ground in an outside flower planter box. The fire department was immediately called, which led to the discovery of area-wide gas seeps emerging from the cracks in the sidewalks.

Investigation showed that the Anthony ventwell (the well-used to alleviate pressure in the collector zone for the 1985 fire) had become plugged and no longer bled the migrating gas from the collector zone. The area was immediately cordoned off to prevent ignition/explosion of the gas. The ventwell was cleaned out and the migrating gas again vented to the surface.

2.11.5.3 South Salt Lake Oilfield Gas Seeps from Gas Injection Project

In January 2003, serious gas leakage was discovered in the residential area near the Fairfax area (viz., in the vicinity of Allendale St. and Olympic Boulevard, Los Angeles, CA). The oilfield operator had been injecting natural gas into the South Salt Lake Oilfield for approximately 2 years, under elevated pressures to enhance recovery.

Gas began leaking to the surface along abandoned and poorly completed wellbores. In fact, the Division of Oil and Gas records reveal that numerous wells had been drilled and completed in this area before the official well records were maintained. Consequently, the existence and abandonment status of some of these wells is unknown. High-density urban development, largely of apartment buildings, has occurred directly over many of these improperly abandoned older wells.

2.11.5.4 Wilshire and Curson Gas Seep, Los Angeles, CA, 1999

A very serious gas seep at the intersection of Wilshire and Curson streets (south of the La Brea Tar Pits) was discovered in 1999. This required the City of Los Angeles to install a vent pipe on the southwest corner of this intersection in order to direct the oilfield gases into the air above the adjoining three-story commercial building. The odors from the gas emitted from the vent pipe were noticeable throughout the area. The commercial office building to the immediate east of this seep location experienced gas odors. A ventilation system is now operating 24 hr/day within the subterranean parking structure of that building in order to mitigate against the risk of an explosion.

Historical records of the area, reviewed by the writers, revealed that an old abandoned well had been drilled near the location of this seep. However, the high-density commercial development in the area has prevented finding the exact location of the well.

2.11.6 Santa Fe Springs Oilfield, CA

The Santa Fe Springs Oilfield consists of 10 major groupings of layers or pools of oil and water aquifers located about 12 miles southeast of the center of Los Angeles. The structure of this field is a dome (Figure 2.56). The overall thickness of the deposits is about 7,000 ft (alluvial Pliocene and Miocene sediments) with the average depth of pools ranging from 3,580 to 9,100 ft. The discovery well was drilled in 1919. Over 1,283 wells have been drilled in this field and many when cement was not used or when cementing practices were neither regulated nor recorded. Overlying this oilfield is a dense residential area.

Earth Engineering, Inc., Fallbrook, CA, conducted a study for the City of Santa Fe Springs, CA, to determine the migration of gas and integrity of the oilwells in the Santa Fe Springs oilfield in the 1990s. To facilitate this study, a time period was selected after heavy rains in which the well cellars were partially filled with water. This allowed the observation of migrating gas bubbles in the producing well cellars which were seeping to the surface along wellbores and casings. The results were systematically recorded for more than 50 wells in this field, some of which were used for waterflooding operations at pressures approaching 84.4 kg/cm^2. Approximately 75% of the wells surveyed were found to be leaking small amounts of gas.

Waterflooding for enhanced oilfield recovery can be a dangerous practice if one does not monitor the maximum injection pressures at which the hydraulic fracturing of the formation and sheaths of cement in the wellbore can occur. These fractures could create new pathways for the migration of gas toward the surface. Repressurization of an oilfield by way of water or gas injection requires careful examination of the age and integrity of the cement for the producing, injecting and abandoned wells throughout the oilfield. A soil gas monitoring program must be implemented in the vicinity of each well and surface fault to define the overall leakage of gas to the surface.

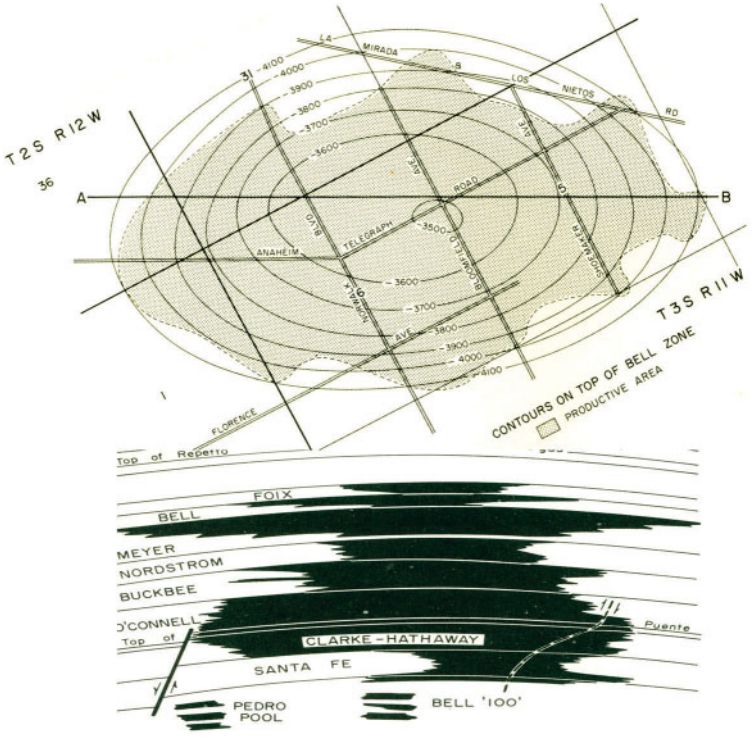

Figure 2.56 Structure and cross-section of the Santa Fe Springs Oilfield. Contours on the top of the Bell Zone. After California Dvision of Oil and Gas. 1961, p. 662.)

2.11.7 El Segundo Oilfield, CA

The El Segundo Oilfield has a depth of about 3,000 ft. Gas that was stored in the early 1970s, migrated into the adjoining geologic formations. Gases were detected in a nearby Manhattan Village, CA, housing development that was under construction. As a result, the construction was stopped. To protect the housing development, a $750,000 passive venting system was installed to prevent the buildup of gases, which may cause an explosion, and the injection project was shut down.

2.11.8 Honor Rancho and Tapia Oilfields, CA

Castaic gas storage is located in the depleted Castaic Hills Oilfield (Figure 2.57) near the producing Honor Rancho (Figure 2.58) and Tapia (Figure 2.59) oilfields. Figure 2.60 shows the relationship of the three oilfields. The arrows show the direction of gas migration. The Tapia oilfield producing zone has an average depth of 1,050 feet. The Honor Rancho has several producing levels ranging from an average depth of 3,800 to 6,400 feet. Gas from the gas storage project broke into producing wells of the Honor Rancho and Tapia oilfields. Indications of gas migration along faults at the surface included killing of oak trees along the surface trace of faults in the area. Gas bubbles were also noted in a nearby water reservoir. The helium content identified the migrating gas as originating from the gas storage project at the Castaic Field because the native natural gas has very low helium content, whereas the imported gas from Texas does contain helium.

2.11.9 Sylmar, CA — Tunnel Explosion

In 1971, a tunnel (approximately 5 miles long) in the Sylmar area of Southern California was being excavated for a future water project. The excavation had proceeded uneventfully until the tunneling machine encountered a fault plane. The fault was filled with natural gas that had migrated from a nearby oilfield. Natural gas from that oilfield had migrated along the fault plane and had filled the fault zone. The tunneling machine, upon contacting the gas-saturated fault zone, set off an explosion. Consideration of gas-saturated fault zones had not been a part of the design of this project. Seventeen workers were killed in the explosion.

2.11.10 Hutchinson, KS — Explosion and Fires

A natural gas explosion destroyed part of the downtown area of Hutchinson, KS, on January 17, 2001. The next day, a second natural gas explosion under a mobile home park, outside of the city, occurred killing two people. The migrating gas and the associated gas created additional gas-water geysers reaching heights of 30 feet. The source of the gas leaks was traced to an underground repressurized natural gas storage reservoir located in a prior oilfield. This prior oilfield was located nearly 7 miles from the site of the explosions. The gas had migrated from the reservoir, through faults into

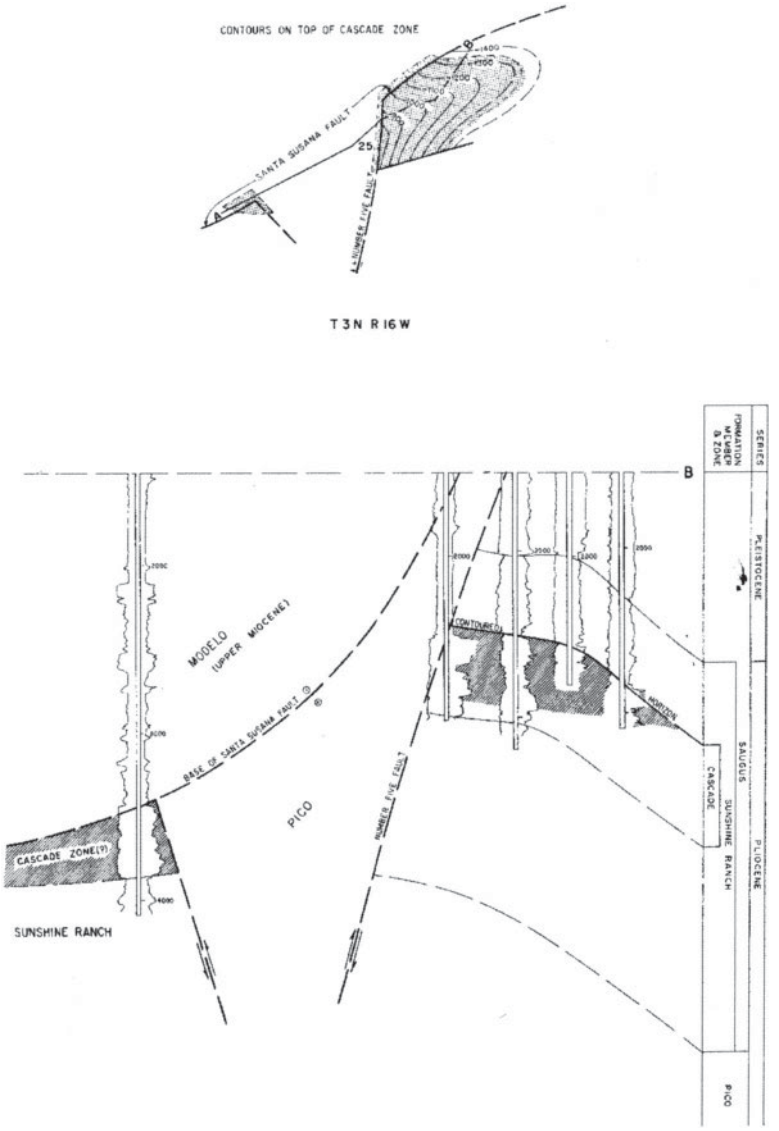

Figure 2.57 Contours on top of Cascade zone and structure for the Castaic Hills Oilfield, CA. (After California Division of Oil and Gas, 1974.)

a permeable water aquifer. The water, in turn, carried this gas to the explosion site. Investigation has revealed that virtually no monitoring was in place in order to prevent this disaster.

The emergency response teams initially had no clue as to the cause of disaster. For example, the fire department was unable to extinguish the flames, illustrating the lack of preparedness for such an event. In the case of the 1985 Fairfax explosion, the fire department had been called and had responded to gas odors in the area 30 minutes before the explosion.

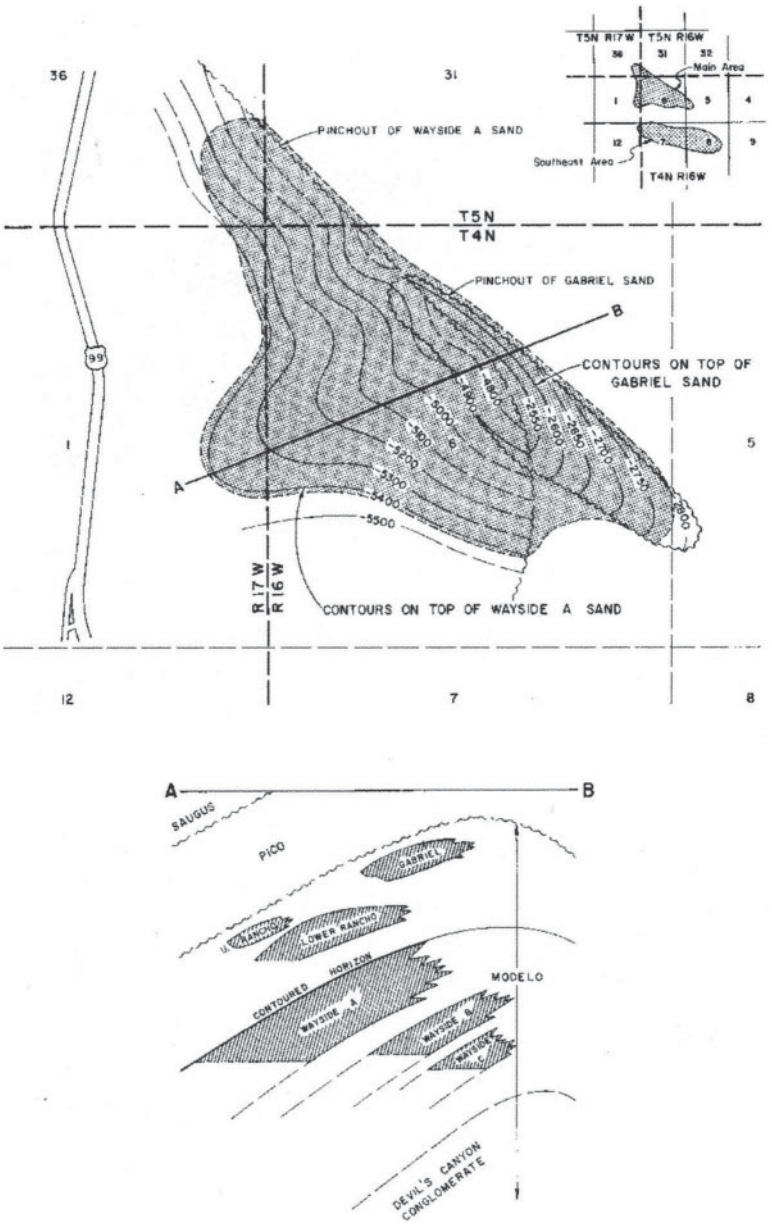

Figure 2.58 Contours on top of Wayside A Sand and Gabriel Sand along with structure for the Honor Rancho Oilfield. (After California Division of Oil and Gas, 1974.)

2.11.11 Huntsman Gas Storage, NE

Located in southwestern Nebraska, the Huntsman Gas Storage Field was a depleted 4,800-ft deep gas field prior to its conversion to gas storage. Gas leakage occurred from this field into the adjoining oil- and gas-producing field several miles away.

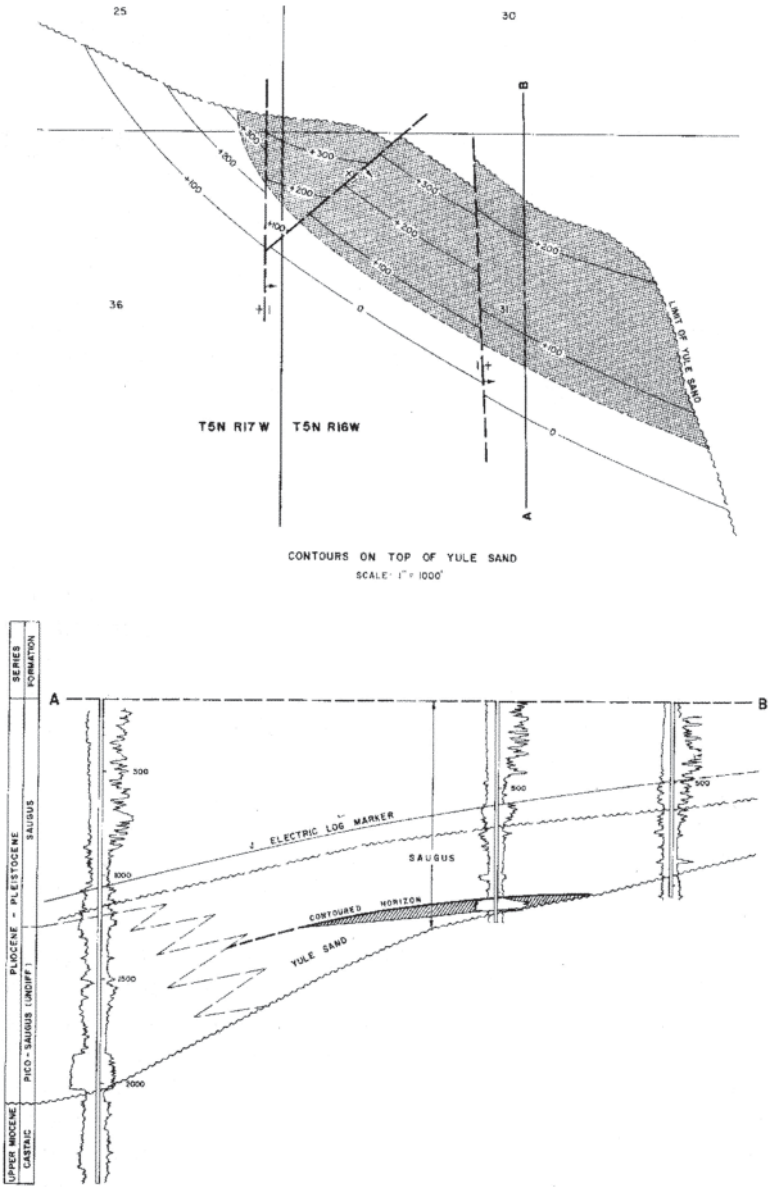

Figure 2.59 Contours on top of the Yule Sand and structure of the Tapia Oilfield, CA. (After California Division of Oil and Gas, 1974.)

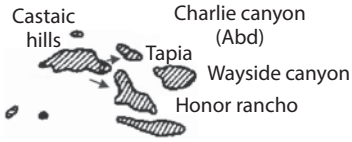

Figure 2.60 Physical relationship of the Castaic Hills, Honor Rancho and Tapia Oilfields, CA. Arrows show the prevailing direction of gas migration. (After California Division of Oil and Gas, 1974.)

A different company handled production. In this case, a large lateral gas migration occurred through the barrier (fault), which several experts had thought to be impermeable. The gas company purchased gas from the oil company. In fact, they purchased the migrating gas several times over, as the gas was recycled between the two fields. Isotopic analysis proved that the gas company was purchasing its own gas.

2.11.12 Mont Belvieu Gas Storage Field, TX

In October 1980, a serious gas leak developed in a salt dome gas storage field beneath Mont Belvieu, TX, located 33 miles east of Houston. The gas seepage was detected when an explosion ripped through the kitchen in a house. This explosion occurred when the homeowner turned on the dishwasher and the spark of electricity ignited the gas mixture. More than 50 families were evacuated from their homes as a result of the explosion caused by the gas leak. A flash fire caused by the gas that had seeped into the home burned the housewife. The gas consisted of a mixture of ethane and propane with traces of butane. The concentration of these gases ranged from 2% to 14% by volume. The gas storage company had noted an "unexplained" drop in the reservoir pressures in September 1980. The event caused severe financial difficulties for the city, which paid for housing and lodging of the displaced families.

Isotopic gas identification results showed that the source of gas was the gas storage facility.

2.11.13 Leroy Gas Storage Facility, WY

The Leroy Gas Storage project lies about 100 miles northeast of Salt Lake City. Shell Oil Co. drilled the first well in the summer of 1951. After testing, it was decided that the Thaynes would be a good storage formation (Figures 2.61 and 2.62). Additional wells were drilled and completed in 1970 through 1972. The Federal Power Commission approved this storage project on November 17, 1972.

Gas migration to the surface was first confirmed during the latter part of November 1978 through bubbling of gas in a nearby creek and pond. The gas migrated from the reservoir and was trapped in a secondary collector formation (Figure 2.63). The gas leaked from this storage to the surface and was, overall, a result of corrosion problems in wellbores and migration of gas along the fault plane. The gas leakage was confirmed by identification of the formation of bubbles in the adjacent creek and pond. The rate of gas loss to the project was estimated to be (Tek, 1987, p. 323):

$$q_1 = 3.74 \times 10^{-7} (p_g^2 - 1.600^2)^n \tag{2.57}$$

where q_1 is the daily leak rate in MMCF/D and p_g is the maximum gas bubble pressure in psia. The exponent n was assumed to be equal to 1.0. The variation of leak-rate versus formation pressure is shown in Figure 2.48.

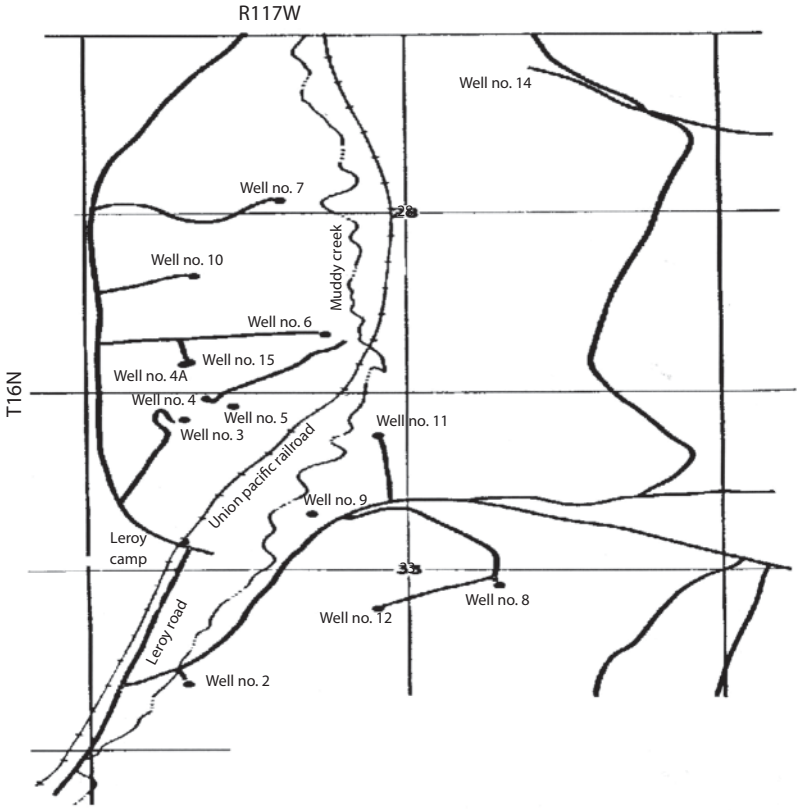

Figure 2.61 Surface map illustrating road (solid lines) and well locations for the Leroy Gas Storage Project, WY. (After Tek, 1987, figure 11.7, p. 316.)

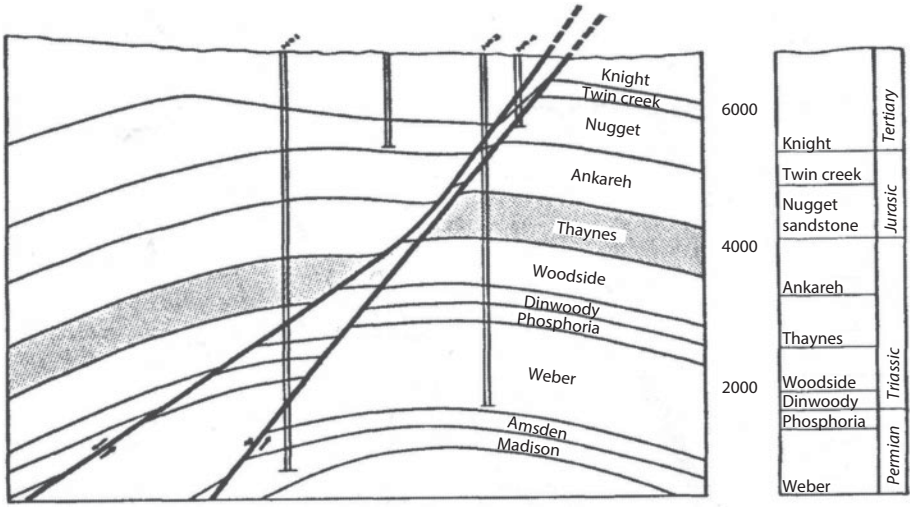

Figure 2.62 Lithologic cross-section and stratigraphic sequence of the Leroy Gas Storage Project, WY. (After Tek, 1987, figure 11.8, p. 317.)

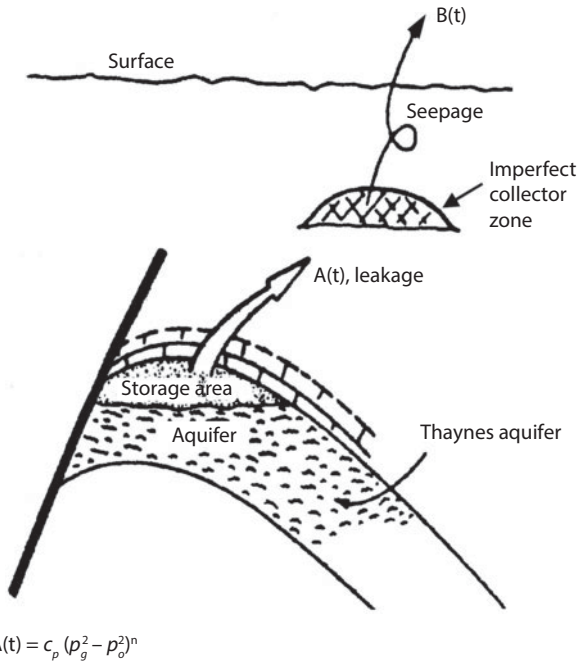

Figure 2.63 Schematic representation of gas leakage from the Leroy Gas Storage Project. c_p = performance coefficient for leak, MMCF/D/psi^2, P_o = maximum storage pressure, psia. After Tek, 1987, figure 11.12, p. 323.

2.12 Conclusions

The history of environmental problems throughout the world has demonstrated the need to exercise a high degree of vigilance. Subsidence and gas migration are common to all oilfields, Land use planning and governmental decisions regarding allowing massive real estate development over and adjacent to the oilfields has often ignored the health and safety risks to the public posed by these operations. The most important lesson to be learned from these problems is the need to carefully evaluate and continue to monitor all wells which can serve as the primary pathways for the migration of oilfield gases to the surface; and be aware that the faults can provide pathways for the migrating gases. In order to exercise a high degree of vigilance regarding the environmental hazards posed by oilfield operations, it is necessary to take the following steps:

1. ***Gas migration monitoring***: Close attention must be given to the need of ongoing monitoring for gas migration into the near-surface soils and under developed areas that are impacted by historical oil production. This is particularly true where there are many old and abandoned wells drilled prior to the 1950s. Cement was often not used in many of these older wells and even when used in wells drilled prior to the 1950's, was of a poorer quality and breaks down with time. It is also very important to monitor gas migration near the fault zones.

2. ***Soil and groundwater monitoring***: Soil and groundwater should be carefully evaluated at construction sites for toxic contamination before development is allowed to proceed. This requires an evaluation of the underlying aquifers, which become a ready target for the oil and gas contamination. It is also necessary to determine what mitigation measures may be necessary to protect against migration of explosive and sometimes toxic oilfield gases into residential and commercial structures. This will be an ongoing problem in many areas that must employ gas detectors, vent pipes, membrane barriers and ventilation systems in order to protect against the gas migration hazards.
3. ***Air toxics monitoring***: The release of toxic material from hydrocarbons from all surface operations, wellheads and pipelines must be carefully monitored and recorded in order to protect the public health, especially from the release of such chemicals as benzene, toluene, ethyl benzene, xylene (viz., the BTEX aromatic hydrocarbons) and hydrogen sulfide. Monitoring of toxic emissions is also required in the operation of vapor recovery equipment (release of gases to the atmosphere). Analysis of all produced gases should be made and recorded in order to be aware of any toxic hazards and to take corrective action.
4. ***Prohibition of building over and near abandoned wells***: No construction should be allowed over any abandoned wellbore or corehole. Prior to permitting any construction, all oil and gas wells near a proposed construction site must be carefully evaluated.
5. ***Land planning:*** Issuance of new building permits should require adequate room to provide access for a drilling rig to reenter old wells, if and when they begin leaking gas.

References and Bibliography

Aadnoy, B. S., 1990. Inversion technique to determine the in-situ stress field from fracturing data. *J. Petrol. Sci. Engin.*, 4:127–141.

Aalmanac, L. A., 2010. Internet: "The Los Angeles Basin - A Huge Bowl of Sand".

Allison M. L. (2001) *The Hutchinson Gas Explosions: Unraveling a Geologic Mystery*. Kansas Bar Association, 26th Annual KBA/ KIOGA Oil and Gas Law Conference vi:1–29.

Allread, B. M., Smith, W. K., Twidwell, D., Haggerty, J. H., Running, S. W., Naugle, D. E. and Fuhlendorf, S. D., 2015. Ecosystem services lost to oil and gas in North America. *Science*, 348: 401–402, April 24.

Ambah, S. A., Chilingar, G. V. and Beeson, C. M., 1965. Application of electrokinetic phenomena in civil and petroleum engineering. *N. Y. Acad. Sci.,* 118:585–602.

Aoyagi, K. and Asakawa, T., 1980. Primary migration theory of petroleum and its application to petroleum exploration. *Org. Geochem.,* 2:33–43.

Aoyagi, K., Kazama, T. Sekiguchi, K. and Chilingarian, G. V., 1985. Experimental compaction of Na-montmorillonite clay mixed with crude oil and seawater. *Chem. Geol.,* 49:385–392.

Aoyagi, K., Aoyagi, L., Kobayashi, N., Kazama, T., Sawa, T. and Sasaki, S., 1975. Compaction of clays under high pressure and programming temperature. *I. Jpn. Assoc. Pet. Technol.*, 40:111–116 (in Japanese).

Aschenbrenner, B. C. and Achauer, C. W., 1960. Minimum conditions for migration of oil in water-wet carbonate rocks. *AAPG Bull.*, 44(2):235–243.

Asquith, G. and Krygowski, D., 2004. Basic well log analysis. *AAPG Methods in Exploration #16*, AAPG, Tulsa, OK, 244 pp.

Bachu, S. and Watson, T., 2007. Factors affecting or indicating potential wellbore leakage, *SPE Paper* #106817**,** Alberta Energy and Utilities Board, Alberta Geological Survey, http://www.albertasurfacerights.com/upload/files/SBachuTWatson%20%20Potential%20Wellbore%20Leakage.pdf

Baert, P., Bosteels, T. and Sorgeloos, P., 1996. *Manual on the Production and Use of Live Food for Agriculture*, Fisheries and Agriculture Department. http://www.fao.org/docrep/004/w3732e/w3732e0q.htm

Baldassare, P.G., 1998. Stray gas migration and applications in the use of isotope geochemistry, Pennsylvania Department of environmental protection. www.bfenvironmental.com/pdfs/Baldassare_final.pdf

Betler, S., 1963. Los Angeles, CA, Dam Collapse, Dec., //www/3gendisasters.com/California/12352/los-angeles-ca-dam-cllapse-dec-1963.

Beresnev, I. and Johnson, P., 1994. Elastic-wave stimulation of oil production: A review of methods and results. *Geophysics*, 59:1000.

Beresnev, I., 2006. Theory of vibratory mobilization of nonwetting fluids entrapped in pore constrictions. *Geophysics*, 71(6).

Berner, U., 1989. *Entwicklung und Anwendung empirischer Modelle fur die Kohlenstoffisotopenvariationen in Mischungen thermogener Erdgase*, Ph.D. thesis, Technische Universitat Clausthal, Germany.

Berner, U., and E. Faber, 1988. Maturity related mixing model for methane, ethane and propane, based on carbon isotopes. *Org. Geochem*., 13:67–72.

Bonett, A. and Pafitis, D., 1996. Getting to the root of gas migration. *Oil Review*, Spring, p. 36–49.

Burst J. F., 1969. Diagenesis of Gulf Coast clayey sediments and its possible relation to petroleum migration. *Am. Assoc. Pet. Geol. Bull*., 53:73–93.

Buryakovsky, K., Chilingar, G. V., Rieke, H. H. and Shin, S., 2012. *Fundamentals of the Petrophysics of Oil and Gas Reservoirs*, Wiley-Scrivener, Salem, MA, 374 pp.

California Department of Water Resources, *Baldwin Hill Reservoir*, Chapter 2, Lessons from Notable events, Internet, http://www.saveballona.org/gasoilfields/Lesson-BHDamGC.pdf.

California Division of Oil and Gas, 1961. *California Oil and Gas Fields -- Maps and Data Sheets*, Vo1.2, California Div. Oil and Gas Publ., San Francisco, CA.

California Division of Oil and Gas, 1991. *California Oil and Gas Fields,* Vo1.2, California Div. Oil and Gas Publ. No. TR 12, Sacramento, CA.

Castle, R. O. and Yerkes, R. F., 1976. Recent surface movements in the Baldwin Hills, Los Angeles County, California — a study of surface deformation associated with oil field operations. *U.S. Geol. Surv. Prof. Pap. 882*, 125 pp.

Chapman, R. E., 1983. *Petroleum Geology*. Elsevier, Amsterdam, pp. 245–251.

Chilingar G. V. and Knight, L., 1960. Relationship between pressure and moisture content of kaolinite, illite and montmorillonite clays. *Am. Assoc. Petrol. Geol. Bull*., 56:796–802.

Chilingar, G. V. and Adamson, L. G., 1964. Does some migration of oil occur in a gaseous form? *Internat. Geol. Congr*. Sec. 1, Part 1:64–70.

Chilingar, G. V., El-Nassir, A. and Stevens, R. G., 1970. Effect of direct electrical current on permeability of sandstone cores. *J. Petrol. Tech.*, 22:830–836.

Chilingar, G. V., and Endres, B., 2005. Environmental hazards posed by the Los Angeles Basin urban oilfields: an historical perspective of lessons learned. *Envir. Geol*., 47:302–317.

Chilingar, G. V., Katz, S., Fedin, L., Fedin, A., Khilyuk, L. and Liu, M., 2015. Primary versus secondary migration of oil. *J. Sustainable Energy Engr.*: 1–8.

Chilingar, G.V., Khilyuk, L.F., and Katz, S.A., 1996. Pronounced changes in upward natural gas migration as precursors of major seismic events. *J. Petrol. Sci. Eng.,* 14:133–136.

Chilingarian, G. V. and Wolf, K. H., 1975. *Compaction of Coarse- Grained Sediments*, 1. Developments in Sedimentology, 18A. Elsevier, Amsterdam, 552 pp.

Chilingarian, G.V., Donaldson, E.C., and Yen, T. F., 1995. *Subsidence Due to Fluid Withdrawal*. Dev. Petrol. Sci. 41, Elsevier, Amsterdam, 498 pp.

Claypool, G. E. and Kaplan, I. R., 1974. The origin and distribution of methane in marine sediments. In: I. R. Kaplan (ed.) *Natural Gases in Marine Sediments*, Plenum Press, New York, NY, pp. 99–140.

Cobarrubias, J. W., 1985. *Task force report on the March 24, 1985 methane gas explosion and fire in the Fairfax area, City of Los Angeles*. Department of Building and Safety, 58 pp.

Coleman, D. D., Liu, C. L., Hackley, K. C. and Pelphrey, S. R., 1995. Isotopic identification of landfill methane. *Environ. Geosciences*, 2:95–103.

Copley, T., 2012. The simple facts on stray gas migration, http://energyindepth.org/marcellus/the-simple-facts-on-stray-gas-migration/

Cordell, R. J., 1972. Depths of oil origin and primary migration: a review and critique. *AAPG Bull.*, 56:2029–2067.

Craig, B. D., 1993. *Sour-Gas Design Considerations*. Soc. Petrol. Eng., Inc., Monogr. vol. 15.

Denton, J. E. et al., 2001. *Prioritization of toxic air contaminants under the Children's Environmental Health Protection Act*, California Environmental Protection Agency Final Report.

Dickey, P. A., 1975. Possible primary migration of oil from source rock in oil phase. *AAPG Bull.*, 59:337–345.

Dodson, C. R. and Standing, M. B., 1944. Pressure-volume-temperature and solubility relations for natural gas-water mixtures. *Drilling and Production Practices, API*: 173–179.

Donaldson, E. C. and Alam, W., 2013. *Wettability,* Gulf Publishing Company, Houston, TX, 336 pp.

Dusseault, M. B., 2000. Why oilwells leak: cement behavior and long-term consequences, *SPE Paper 64733*.

Endres, B. L., 1999. An evaluation of the oil and gas migration hazards existing at the Belmont Learning Center Complex, *Belmont Blue Ribbon Commission Hearings*, Oct.

Endres, B. L., 2002. *Why the Belmont Learning Center Requires the Preparation of a Subsequent Environmental Impact Report* (EIR), Los Angeles Unified School District School Board Hearing, Aug. 15.

Endres, B. L., Chilingarian, G. V. and Yen, T.F., 1991. Environmental hazards of urban oilfield operations. *J. Petrol. Sci. Eng.*, 6:95–106.

Endres, B. L., Chilingarian, G. V. and Pokinwong, P., 2002. Environmental hazards and mitigation measures for oil and gas field operations located in urban settings. *Can. Int. Petrol. Conf.*, Calgary, Alberta, Canada, June 13.

Environmental Consultants, B. F., 2015. Methane and Other Gases in Drinking Water and Groundwater. http://www.Water-research.net/index.php/methane

Faber, E., 1987. Zur isotopengeochemie gasformiger Kohlen wasserstoffe. *Erdol Erdgas Kohle*, 103:210–218.

Faber, E., Stahl, W. J. and Whiticar, M. J., 1992. Distinction of bacterial and thermogenic hydrocarbon gases. In: R. Vially (ed.), *Bacterial Gas*, Paris, Editions Technip, pp. 63–74.

Fedin, L. M., Fedin, K.L. and Fedin, A. K., 2013. *Basics of Increasing Heavy Oil Recovery*, Dolyam, Simpheropol, 112 pp. (in Russian).

Geertsma, J., 1973. Land subsidence above compacting oil and gas reservoir. *J. Petrol. Tech.*, 25(6):734–744.

Geber, M. I. and Dvali, M. F., 1961. *Natural Compressed Gases as a Probable Factor in Migration of Oil from Source Rocks*, GosTopTechlzdat, Leningrad, 83pp.

God, T. and Soter, S., 1980. The deep-earth gas hypothesis. *Sci. Am.*, 242:154–161.

Gulf Coast Midwest Energy Partners, 2015. Facts about crude Oil, http://benergypartners.com/Facts_About_Crude_Oils.html

Guevich, A. E. and Chilingarian, G. V., 1993. Subsidence over producing oil and gas fields, and gas leakage to the surface. *J. Pet. Sci. Eng.*, 9: 239–250.

Guevich, A. E., Endres, B. L., Robertson, Jr., J. O. and Chilingarian, G. V., 1993. Gas migration from oil and gas fields and associated hazards. *J. Pet. Sci. Eng.*, 9: 223–238.

Gurevich, A. E., 1969. *Processes of Ground-Water, Oil, and Gas Migration*. Nedra Publishers, Leningrad, 112 pp. (in Russian).

Hamilton, D.H. and Meehan, R.L., 1971. Ground rupture in the Baldwin Hills. *Science*, 172:333–344.

Hedberg, H. D., 1964. Geological aspects of origin of petroleum. *Am. Assoc. Pet. Geol. Bull.*, 48:1755–1803.

Hillis, R. R. and Reynolds, S. D., 2000. The Australian Stress Map. *J. Geol. Soc.*, London. 157:915–921.

Hunt, M., 1979. *Petroleum Geochemistry and Geology*. Freeman and Co., San Francisco, CA, 617 pp.

IMC, 2016. Classifications of Crude Oil - International Marine Consultancy. www.imcbrokers.com/blog/overview/detail/classifications-of-crude-oil

Ingraffea, A. R., 2012. Fluid migration mechanisms due to faulty well design or construction: an overview and recent experiences in the Pennsylvania Marcellus Play. *PSE - Physicians Scientists & Engineers for Healthy Energy*, Oct.

Ingraffea, A. R., Wells, M. T., Santoro, R. I., and Shonkoff, S. B. C., 2014. *Assessment and Risk Analysis of Casing and Cement Impairment in Oil and Gas Wells in Pennsylvania, 2000–2012*, Cary Institute of Ecosystem Studies, Millbrook, N.Y., May 30th.

Jenden, P. D., Kaplan, I. R., Poreda, R. J. and Craig, H., 1988. Origin of nitrogen-rich gases in the California Great Valley: Evidence from helium, carbon and nitrogen isotope ratios. *Geochimica et Cosmochimica Acta*, 52(4):851–861.

Jenden, P. D., 1985. *Analysis of Gases in the Earth's Crust*, Final Report to the Gas Research Institute for the period 1 January 1982-28 February 1985, Contract No. 5081-360-0533:110 pp.

Kamali, M. R., Abolghasemi, A., Bagheri, R. and Kadkhoday, A., 2013. Petroleum geochemistry and oil-oil correlation of the Fahliyan and Surmech reservoirs in the Garangan and Chilingar oilfields, the Dezful embayment (SW Iran). *J. Petrol. Explor. Prod. Tech.*, 3:85–92.

Kaplan, I. R., 1994. Identification of formation processes and source of biogenic gas seeps. Isr. *J. Earth Sci.*, 43:297–308.

Kapyelyshnikov, M. A., 1954. Migration and accumulation of dispersed petroleum in sedimentary rocks. *Dokl. Akad. Nauk USSR*, 99(6):1077–1078.

Katz, S. A., Khilyuk, L. F. and Chilingarian, G. V., 1994. Interrelationships among subsidence owing to fluid withdrawal, gas migration to the surface and seismic activity. Environmental aspects of oil production in seismically active areas. *J. Petrol. Sci. Eng.,* 11:103–112.

Khilyuk, L. F., Chilingar, G. V., Robertson, J.O. and Endres, B. L., 2000. *Gas Migration — Events Preceding Earthquakes.* Butterworth-Heinemann, Woburn, Massachusetts, 389 pp.

Kilburn, K.H., 1998. *Chemical Brain Injury.* Van Nostrand Reinhold, New York, 416 pp.

Kilburn, K.H., 1999. Evaluating health effects from exposure to hydrogen sulfide: central nervous system dysfunction. *Environ. Epidemiol. Toxicol.,* 1:207–216.

Kotler, P., 2011. *Abandoned Oil and Gas Wells are Leaking*, https://zcomm.org/zmagazine/abandoned-oil-and-gas-wells-are-leaking-by-steven-kotler/

Kouznetsov, O. L., Simkin, E. M. and Chilingar, G. V., 2001. *Physical Bases of Acoustic and Vibrational Effects on Oil and Gas Deposits*, Izd. Mir, Moskow, 260 pp.

Kouznetsov, O. L., Simkin, E. M., Chilingar, G. V. and Katz, S., 1998. Improved oil recovery by application of vibro-energy to waterflooded sandstones. *J. Petrol. Sci. and Engr*., 19:191–200.

Kouznetsov, O. L., Simkin, E. M., Chilingar, G.V., Gorfunkel, M. and Robertson, J., 2002. Seismic techniques of enhanced oil recovery: Experimental and field results. *Energy Sources,* 22:877–890.

Kouznetsov, O. L., Sidorov, V. I., Katz, S., and Chilingar G. V., 1994. Interrelationship among seismic and short-term tectonic activity, oil and gas production, and gas migration to the surface. *J. Petrol. Sci. Eng.,* 13:57–63.

Lacazette, A., 2000. Distinguishing natural from induced fractures in image logs, http://www.naturalfractures.com/5.3.btm

Lacazette, A. 2001. Internet: Al Lacazette's Natural Fractures.com

Lee, J. J., 2012. *Regulatory Reponses to Stray Gas Incidents* -- The Pennsylvania Experience (PDF), Ground Water Protection Council Stray Gas Conference, Cleveland, OH, 24 July.

Lee, K., 1976. Calculated Horizontal Movements at Baldwin Hills, CA., Inter. Assoc. of Hydro. Sci., Anaheim Symposium, Dec.

Leverett, M. C., 1941. Capillary behavior in porous solids. Trans. AIME TP 696, 142:152–169.

Mah, R. A., Ward, D. M., Baresti, L. and Glass, T., 1977. Biogenesis of methane. Annu. Rev. Microbiol., 31:109–131.

Mah, R. A. and Sussman, C., 1967. Microbiology of anaerobic sludge fermentation, I Enumeration of the nonmethanogenic anaerobic bacteria. *Appl. Microbiol*., 16:358–361.

Marcellus Shale Coalition, 2012. *Responding to Stray Gas Incidents (PDF)*. Ground Water Protection Council Stray Gas Conference, Pittsburgh, PA, 16 Oct.

Marlow, R. S., 1989. Cement bonding characteristics in gas wells. *J. Petrol. Technol.*, Nov:1146–1153.

McAuliffe, C., 1966. Solubility in water of paraffin, cycloparaffin, olefin, acetylene, cycloolefin, and aromatic hydrocarbons. *J. Phys. Chem*., 70:1267–1275.

McMillen, S. J., Magaw, R. I. and Carovillano, R. I., 2001. *Risk-based decision-making for assessing petroleum impacts at exploration and production sites*. Petroleum Environmental Research Forum and the United States Department of Energy.

NGSMA, 1957. *Engineering Data Book*, Natural Gasoline Supply Men's Association Seventh Edition. Natural Gasoline Association of America, Tulsa, OK.

Penn State Extension, 2012. *Water Facts #24: Methane Gas and Its Removal from Water Wells in Pennsylvania* (PDF), University Park, PA, 8 Oct.

Perry Jr., E. A. and Hower, J., 1972. Late stage dehydration in deeply-buried pelitic sediments. *Am. Assoc. Pet. Geol. Bull.,* 56:2013–2021.

Poreda, R. J., Jeffery, A. W, A., Kaplan, I. R., and Craig, H., 1988. Magmatic helium in subduction-zone natural gases. *Chemical Geology*, 71:199–210.

Powers, M. C., 1967. Fluid-release mechanisms in compacting marine mudrocks and their importance in oil exploration. *Am. Assoc. Pet. Geol. Bull*., 51:1240–1254.

Price, L. C. and Schoell, M., 1995. Constraints on origins of hydrocarbon gas from composition of gases at their site of origin. *Nature*, 378:368–371.

Price, L. C., 1976. Aqueous solubility of petroleum as applied to its origin and primary migration. *AAPG Bull*., 60:213–244.

Pride, S., Flekkfay, E. and Aursio, O., 2008. Seismic stimulation for enhanced oil recovery. *Geophysics*, 73:23–35.

Ramos, G. and Thackrey, T., 1985. *Los Angeles Times* article.

Ravi, K. and Bosma, M., 2002. *Improve the Economics of Oil and Gas Wells by Reducing the Risk of Cement Failure*. IADC/SPE Drilling Conference, Dallas, February 26–28, IADC/SPE 74497.

Revkin, A, 2009. *Stray gas migration associated with oil and gas wells*. Pennsylvania Department of Environmental Protection, Bureau of Oil and Gas Management, 15 pp.

Rice, D. D., 1993. Biogenic gas: controls, habitats, and resource potential. In: D. G. Howell (ed.), *The Future of Energy Gases* - U.S. Geological Survey Professional Paper 1570, United States Government Printing Office, Washington, pp. 583–606.

Rice, D. D and Claypool, G. E., 1981. Generation, accumulation and resource potential of biogenic gas. *AAPG Bull*., 65:5–25.

Riegle, J.R., 1953. Gas storage in the Playa del Rey oil field. In: *Summary of Operations, California Oil Fields*. State of California Division of Oil and Gas, San Francisco, CA., 39(2):17–33.

Rieke III, H. H. and Chilingarian, G. V., 1974. *Compaction of Argillaceous Sediments*. Developments in Sedimentology, 16. Elsevier, Amsterdam, 424 pp.

Rixey, W. G., 2001. An evaluation of benzene risk. In: McMillen, S.J., Magaw, R.J., and Carovillano, R.L. (eds.), *Risk-based decision-making for assessing petroleum impacts at exploration and production sites*. Petroleum Environmental Research Forum and the United States Department of Energy, pp. 156–173.

Roof, J. G. and Rutherford, W. M., 1958. Rate of migration of petroleum by proposed mechanisms. *AAPG Bull*., 42:963–980.

Santos, R. G., Loh, W., Bannwart, A. C., and Trevisan, O. V., 2014. An overview of heavy oil properties and its recovery and transportation methods. *Braz. J. Chem. Eng*. vol. 31 no. 3, São Paulo July/Sept.

Savidge, J. L., 2000. *Compressibility of Natural Gas*, internet: help.intellisitesuite.com/Hydrocarbon/papers/1040.pdf, 26 pp.

Schoell, M., 1983. Genetic characterization of natural gases. *AAPG Bull.,* 67:2225–2238.

Schoell, M., 1988. Multiple origins of methane in the earth. *Chemical Geology*, 71:1–10.

Schoell, M., Jenden, P. D., Beeunas, M. A. and Coleman, D. D., 1993. Isotope analysis of gases in gas field and gas storage operations. *SPE No. 26171, SPE Gas Technol. Symp*., Calgary, Alberta, Canada, June 28–30, pp. 337–344.

Schowalter, T. T., 1999. *Mechanics of Secondary Hydrocarbon Migration and Entrapment*, AAPG data pages, http://www.searchanddiscovery.com/documents/97018/mechan.htm

Schumacher, D. and Abrams, M. A. (eds), 1994. *Hydrocarbon Migration and Its Near-Surface Expression*. AAPG Mem. 66:360 pp.

Serruya, C., Picard, L. and Chilingarian, G. V., 1967. Possible role of electric currents and potentials during diagenesis (Electrodiagenesis). *Sediment. Petrol*., 37:695–698.

Smith, J. E., Erdmn, J. G. and Marris, D. A., 1971. Migration, accumulation and retention of petroleum in the earth. In: *Proc. 8th World Petroleum Congress*, Moscow. Applied Science Publishers, London, pp. 13–26.

Sundberg, K. R., 1994. Surface geochemistry applications in oil and gas exploration. *Oil and Gas J.*, 6:47–58.

Tek, M. R., 1987. *Underground Storage of Natural Gas*. Contributions in petroleum geology and engineering, No. 3, G. V. Chilingar (ed.), Gulf Publishing Co., Houston, TX, 389 pp.

Terry, D. and Chilingar, G. V., 1955. Summary of concerning some additional aids in studying sedimentary formation by M.S. Shvetsov. *J. Sediment. Petrology*, 25(3):229–234.

Tingay, M., Reinecker, J. and Muller, B., 2008. Borehole breakout and drilling-induced fracture analysis from image logs. *World Stress Map Project*, 8 pp.

Tissot, B. P. and Welte, D. H., 1978. *Petroleum Formation and Occurrence*. Springer, Berlin, Heidelberg, New York.

Titus, C. H. Wittle, J. K. and Bell, C. W., 1985. Apparatus for passing electric currents through an underground formation. *U.S. Patent 4495990*, 29 Jan.

Toth, J., 1996. Thoughts of a hydrogeologist on vertical migration and near-surface geochemical exploration for petroleum. *AAPG Mem*., 66:279–283.

Waiters, L. T. and Sabinas, F. L., 1980. *Field evaluation of method to control gas flow following cementing. SPE Paper* 9287 presented at the 1980 SPE Annual Technical Conference, Dallas, TX, Sept. 21–24.

Ward, D. M., Mah, R. A. and Kaplan, I. R., 1978. Methanogenesis from acetate. *App. Env. Microbiol.*, 35:1185–1192.

Weatherford laboratories, 2011. *Determining the Origin of Hydrocarbon Gas Shows and Gas Seeps (Bacterial Gas vs. Thermogenic Gas) Using Gas Geochemistry.* http://www.gaschem.com/determ.html

Welte, D. H., 1972. Petroleum exploration and organic geochemistry. *J. Geochem. Explor*., 1:117–136.

Wentworth. C. M., Ziony, J. I., and Buchanan, J. M., 1969. *Preliminary Geologic Environmental Map of the Greater Los Angeles Area, California*.

Whittaker, M. J., 1994. Correlation of natural gases with their sources. In: L. B. Magoon and W. G. Dow (eds.), *The Petroleum System, From Source to Trap*, AAPG:261–283.

Wittle, J. K., Hill, D. G. and Chilingar, G. V., 2008. *Direct Current Stimulation for Heavy Oil Production*. Paper 2008-374. Second World Heavy Oil Congress. Edmonton, March 10–12.

Wittle, J. K., Hill, D. G. and Chilingarian, G. V., 2011. *Direct Electric Current Oil Recovery (EEOR)*. A new approach to enhancing oil production. *Energy Source* Part A, 33:805–822.

Woese, C. R. and Wolfe, R.S. (eds.), 1985. *Archaeobacteria*, Vol III. In: *A Treatise on Structure and Function*. Academic Press, New York, NY.

Zaks, S. L., 1952. Effect of rock and bound water on value of pressures at which oil/gas system is transformed into one-phase gas condition. *Dokl. Akad. Nauk USSR*, 86:1017–1020.

Zaks, S. L., 1955. Toward question of migration and accumulation of petroleum. *Dokl. Akad. Nauk USSR*, 105:332–334.

Zhuze, T. P. and Yushkevich, G. N., 1959. Solubility of oil and its heavy fractions in compressed gases. *Trudy Inst. Nefti Akad. Nauk*, 13:626–274.

Environmental Aspects of Oil and Gas Production.
John O. Robertson and George V. Chilingar.
© 2017 Scrivener Publishing LLC. Published 2017 by John Wiley & Sons, Inc.

3

Subsidence as a Result of Gas/Oil/Water Production

3.1 Introduction

Much of the Earth's surface consists of layers of alluvial material. Some of these porous layers contain fluids and are identified as aquifers. There are two types of aquifers, confined and unconfined. An unconfined aquifer has no caprock (similar to an unsealed tank without a top) and fluids can easily migrate either in or out of this type of aquifer without affecting the support of the overburden as the fluid does not help support the weight of the formation above it. When surface pressure is applied to the unconfined aquifer, the pressure of the overburden is carried totally by the rock-matrix skeletal structure of the rock.

Confined aquifers have a caprock or impervious interval that prevents fluids from either percolating into the aquifer from above or migrating out of the aquifer (similar to a sealed tank). The difference between a layer of confined and unconfined aquifer is that in a confined aquifer, fluids within the aquifer help support the overlying weight. Withdrawal of fluid from a confined aquifer results in reduction of the pressure of the pore fluid as the fluid (produced) is withdrawn from the aquifer, resulting in the rock-matrix skeletal structure of the rock then carrying a greater share of the overburden pressure. Hydrocarbon reservoirs are confined aquifers. (See Poland and Davis, 1960.)

The withdrawal of fluids (oil, water, and/or gas) from subsurface confined aquifers/reservoirs can result in the subsidence of the Earth's surface. Fluids that exist in the pore space or fractures of confined aquifers are under pressure. The pressure of the fluid within that pore space along with the strength of the rock-matrix skeletal structure of

the rock help support the overlying formation (load). If fluids (oil, water, and/or gas) are withdrawn from the pores of a subsurface aquifer, a decrease in fluid pressure may occur giving less support of the overlying formation. This reduction of pore pressure can result in the partial compaction of the subsurface aquifer, to the level where the pore structure and remaining fluid pore pressure can now support the overlying load.

The two fluids that occur in subsurface aquifers beneath the surface of the Earth are water (groundwater) and hydrocarbons (crude oil and/or natural gas). Upon reduction of pore pressure as a result of the production of fluid, there is often a collapse of the rock-matrix skeletal structure of the rock to compensate for the reduction of pore pressure supporting the overburden. This collapse in a subsurface aquifer is not elastic and the deformation of the pore structure is permanent. Table 3.1 lists a few cities throughout the world that have experienced these subsidence problems due to removal of water and/or hydrocarbons from underlying aquifers.

Chilingarian and Donaldson (1995) have pointed out that subsidence events are rarely considered as immediate major disasters, certainly nowhere near the scale of an earthquake, tsunami, volcanic eruption or landslide. However, the slow subsidence of an urban area over a long period of time can cause as much economic damage as earthquakes in which damage occurs over a short period of time. Subsidence problems manifest themselves in various ways. The following selected global examples portray problems associated with subsidence: (1) The extraction of natural gas caused land subsidence in the Po Delta of Italy and also in the large Groningen Gasfield of the Netherlands. (2) Widespread harbor subsidence resulted from oil production in the

Table 3.1 Subsidence found in various cities as a result of fluid withdrawal. (Modified after Nelson, 2015.)

City, Country	Maximum recorded subsidence	Approximate area of subsidence (km^3)	Cause of subsidence
Long Beach/Los Angeles, CA, U.S.A.	9.00 m (≈29.25 ft)	50 km^3	Hydrocarbon production
San Joaquin Valley, CA, U.S.A.	8.80 m (≈28.6 ft)	13,500 km^3	Groundwater production
Mexico City, Mexico	8.50 m (≈27.6 ft)	225 km^3	Filled in lake with sediments
Tokyo, Japan	4.50 m (≈14.5 ft)	3,000 km^3	Coastal sediments
San Jose, CA, U.S.A.	3.90 m (≈12.7 ft)	800 km^3	Coastal sediments
Osaka, Japan	3.00 m (≈10 ft)	500 km^3	Coastal sediments
Houston, TX, U.S.A.	2.70 m (≈8.8 ft)	12,100 km^3	Coastal sediments
Shanghai, China	2.63 m (≈8.5 ft)	121 km^3	Coastal sediments
Niigata, Japan	2.50 m (≈8.1 ft)	8,300 km^3	Coastal sediments
Nagoya, Japan	2.37 m (≈7.7 ft)	1,300 km^3	Coastal sediments
New Orleans, LA, U.S.A.	2.00 m (≈6.5 ft)	175 km^3	Deltaic sediments
Taipei, China	1.90 m (≈6.1 ft)	130 km^3	Costal sediments
Bangkok, Thailand	1.00 m (≈3.2 ft)	800 km^3	River sediments
Venice, Italy	0.22 m (≈0.7 ft)	150 km^3	Costal sediments
London, England	0.30 m (»1.0 ft)	295 km^3	River sediments

Wilmington Oilfield, Los Angeles/Long Beach, CA. (3) Seabed subsidence occurring around the North Sea Ekofisk production platforms resulting in a threat to the safety of personnel and equipment. (4) The rapid draw-down of the groundwater table by over-pumping in arid and semi-arid agricultural regions can result in abrupt ground failure. (5) Excessive withdrawal of groundwater creating large earth fissures in the farming area of Wadi al Yatimah and destruction of new tourist facilities at Al Afiaj lakes of western and central Saudi Arabia. 6) Widespread ground subsidence in the large metropolitan areas, e.g., Osaka, Japan, and London, England, resulted from excessive pumping of water from aquifers.

If all subsidence of the Earth's surface was uniform due to fluid production, the elevation of all supported structures, within the area of subsidence would uniformly decrease in elevation and there would be few environmental problems; however, the layers of Earth's sediments are not homogeneous, they are heterogeneous and so the amount of collapse of the rock structure can vary from one area to another within the area of subsidence. This variation in subsidence is often referred to as differential subsidence. Differential subsidence may result in: (1) cracking of concrete highways, curbs and sidewalks, (2) weakening foundations and structures of buildings, (3) breaking of pipelines and leaking sewers, (4) breaking in earthen dams, and (5) generation of fractures in the Earth's surface through which gas and/or fluids can then migrate to the surface.

Some of the earliest recorded examples of subsidence due to ground water withdrawal are Osaka, Japan (noted in 1885); London, England (noted in 1865), and Mexico City, Mexico (noted in 1929). One of the earliest recognized examples of subsidence caused by withdrawal of hydrocarbons is Goose Creek Oil Field, Texas (noted in 1918), described by Pratt and Johnson (1926). The phenomenon of subsidence has been investigated by many and today it is recognized that withdrawal of fluids from a confined reservoir likely will result in the compaction of the reservoir rocks, reflected as subsidence at the surface.

A detailed analysis of subsidence has been presented by Chilingarian et al. (1995) and Donaldson and Chilingarian (1997). In summary, subsidence as a result of fluid withdrawal occurs when the reservoir fluid pore pressures are reduced and the grain-to-grain pore structure along with the existing pore pressure of the fluid in the reservoir rocks lack the strength to resist deformation upon the transfer of load from the fluid phase to the grain-to-grain contacts needed to support the overburden pressure.

The principal lithological and structural characteristics of the subsiding areas in oilfields commonly include the following characteristics:

1. Sediments are unconsolidated and lack appreciable cementation.
2. Porosity of the sands is high (>30%).
3. The sediments are of Miocene age or younger.
4. Producing formations are located at depths <2000 m.
5. Aquifer thickness is >30 m.
6. Overburden is composed of structurally weak rocks.
7. Tension-type faulting, often with a graben, is present.
8. Sands are interbedded with clays, silts and/or siltstones, and shales.
9. Pore pressure is greatly reduced by production

3.2 Theoretical Compaction Models

Subsidence over fluid producing (oil, water, and gas) formations is caused by the reduction of pore (fluid) pressure within the producing formation through the removal of fluids within the pores and increasing effective stress. Thus, (effective, grain-to-grain, stress, p_e) = (total overburden stress, p_t) – n (pore or fluid pressure, p_p):

$$p_e = p_t - np_p \tag{3.1}$$

Rieke and Chilingarian (1974, p, 6), however, proved experimentally that exponent n is about one. Thus,

(effective stress {grain-to-grain} stress, p_e)
= (total overburden pressure, p_t) – (pore or fluid pressure, p_p) (3.2)

The overburden pressure, p_t is equal to the specific weight of the overlying water-saturated rock (γ_b) multiplied by the depth (D):

$$p_t = \gamma_b \times D \tag{3.3}$$

During sedimentation, the stresses (p_e, p_t, p_p) can attain temporary equilibrium with different degrees of support assumed by the rock-matrix skeletal structure and the fluids occupying the pores ($p_t = p_p + p_e$). Gravitational stress (mass of the overburden) is transmitted vertically through the grain-to-grain contacts. Hydrostatic stress from the mass of the interstitial water above the compacting rocks is transmitted through the water column. Another stress that aids grain redistribution is the viscous drag caused by movement of water downward and toward producing wells.

Chilingarian *et al.* (1995) found that clay and sand layers compact to almost the same extent. The principal difference is the plastic behavior of the clay bodies, because of the extremely low effective permeability to water, which must be expelled in order for compaction to take place. Over a period of years, however, the slow contribution of shales and clays to compaction (and subsequent subsidence) can be of major importance (Van der Knap and Van der Vis, 1967).

The concept of the compaction process can be explained by use of a mechanical model that is composed of a perforated round metal plate and enclosing cylinder which contains a metal spring and water (Figure 3.1). In this analogy, the spring represents the compactable sediment grains, water represents the fluid in the pore space, and the size of perforations in the metal plate is a measure of permeability.

A useful expression in studying compaction is the ratio of the fluid stress, σ_w, to the total stress, σ (see Hoffman and Johnson, 1965):

$$\lambda = \frac{\sigma_w}{\sigma} = \frac{p_p}{p_1} \tag{3.3}$$

When stress is initially applied to the closed system, λ has a value of 1 and the system is overpressured. At the final compaction stage, when the load is carried entirely

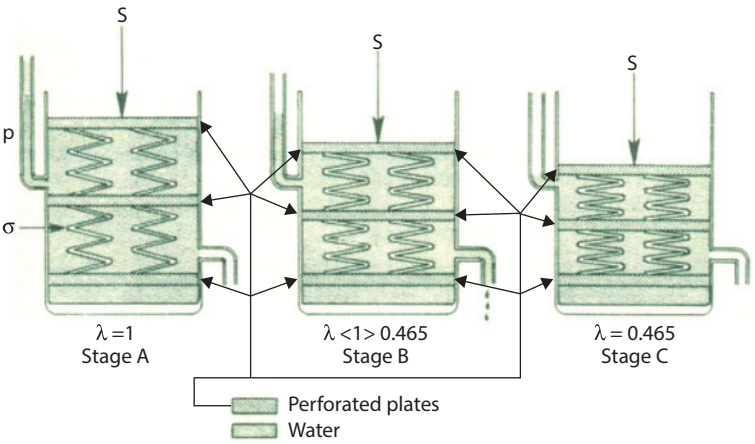

Figure 3.1 Simplified schematic representation of clay compaction (concept after Terzaghi and Peck, 1948, p. 84; In: Holtman and Johnson, 1965, p. 718.). σ = grain-to-grain bearing strength; *S* = axial component of total stress (overburden pressure); *p* = fluid pressure; and λ = ratio of the pore stress to total stress: σ = S – p. Stage A: overpressured system; water is not allowed to escape. Stage B: water is allowed to escape: springs carry part of the applied load. Stage C: compaction equilibrium; load is supported by the springs and the water (water pressure is simply hydrostatic). (Modified after Rieke and Chilingarian, p. 93, 1974.)

by the skeletal structure (spring), λ is equal to 0. At the final stages of compaction, the applied load is supported jointly by the skeletal structure and intergranular water (hydrostatic) and the value of λ is approximately equal to the normal pressure gradient, i.e., 0.465psi/ft. This value is typical of the normal pressure gradient in the U.S. Gulf Coast. The lithostatic (geostatic or overburden) pressure gradient is considered to be about 1.0 psi/ft (0.3231 kg $cm^{-2}m^{-1}$) of depth. The hydrostatic pressure can vary from locality to locality dependent upon the specific weight of the water (due to the varying degree of salinity).

The spring analogy often fails to agree with the actual compaction values of clay in the field as the pressure conditions in the field are often not uniform throughout the thickness of the clay mass as they are in the test cylinder.

According to Allen *et al.* (1971), subsidence due to withdrawal of fluids occurs when (a) reservoir fluid pressures are lowered, (b) reservoir rocks are compactable (usually uncemented) and/or are unable to effectively resist deformation upon the transfer of load from the fluid phase to the grain-to-grain contacts, and (c) overburden lacks internal self-support and can easily deform downward.

When the hydrostatic head is lowered, the overburden support is decreased and grain-to-grain load increases. As a result, sands and silts compact by grain rearrangement and crushing, whereas plastic flow occurs in argillaceous sediments. Water from clays and shales moves into associated sands and, consequently, there is a decrease in volume of fine-grained sediments. The relative contribution of sands and of clays to compaction varies with depth and with the geologic history. According to Allen *et al.* (1971), at very shallow depths clays and silts are usually the major compacting materials, whereas at greater depths (300–1,000 m) sands constitute the major compacting material.

Susceptibility of the formation to subsidence is dependent upon many factors, such as the degree of compaction due to (1) previous depth of burial during geologic time, (2) types of clays, (3) shape and size of sand grains, and (4) relative proportions of interbedded clays and sands.

As pointed out by Allen *et al.* (1971), the concept of overburden load and load transfer is extremely important, because upon fluid removal subsidence would not occur unless there is a load transfer. The maximum amount of load transfer possible at a particular depth is equal to the fluid pressure (hydrostatic pressure) at that point.

The manner in which the load change could occur upon production of fluids is illustrated in Figure 3.2. Initially, the geostatic pressure gradient (0.91 psi/ft.) is equal to the sum of the intergranular pressure gradient (0.48 psi/ft.) and hydrostatic pressure gradient (0.43 psi/ft.). Assuming no residual fluid in the pores, the buoyant effect of the water is lost and the intergranular load is increased as the fluid level is lowered from A to B, for example. Geostatic load decreases (curve 3 shifts to curve 3b, Figure 3.2) as

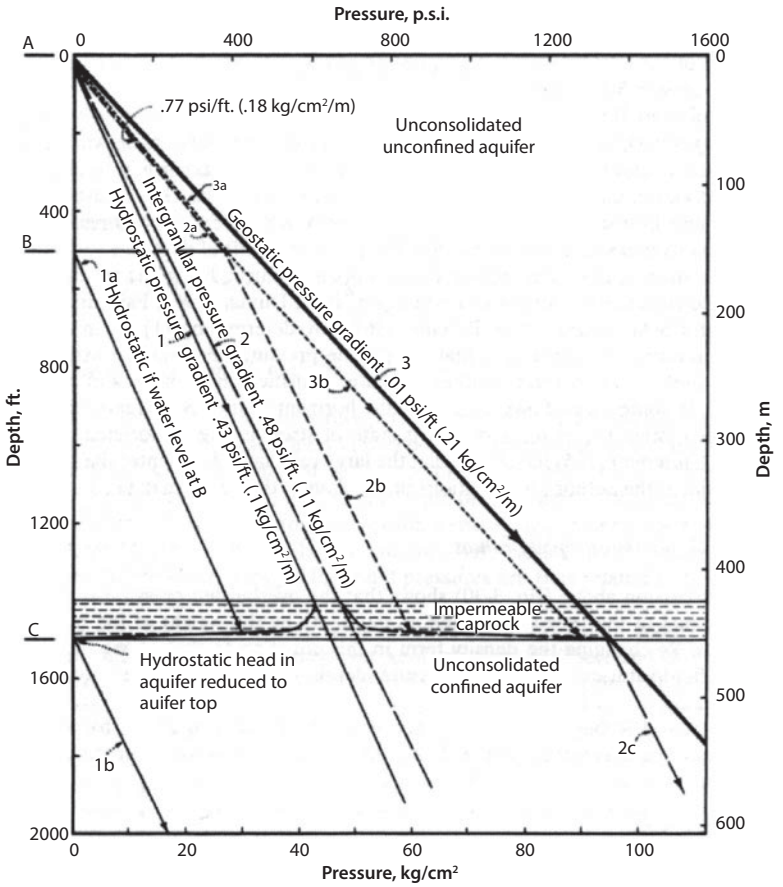

Figure 3.2 Illustration of load transfer owing to water-level drop or reduction in pore-water pressure in unconfined and confined aquifers. Geostatic, hydrostatic and intergranular pressure gradients are plotted assuming that solids and water have specific gravities of 2.7 and 1.0, respectively, and that porosity is equal to 35%. (Modified after Allen *et al.*, 1971, figure 4, p. 285. Courtesy of Enciclopedia della Scienza e dell Tecnica, Mondadori.).

water is removed. The intergranular and geostatic loads are equal if the pores are dry (curve 2b, Figure 3.2). Compaction can occur if the intergranular load is increased. In the case of a confined aquifer, which has a relatively impermeable cover (caprock), as the fluid level is lowered from A to C, the intergranular load gradually increases until it becomes equal to the geostatic load (curve 2 shifts to curve 2c, Figure 3.2). If pore spaces still contain some residual water, the intergranular load and geostatic load are not equal below the level C.

Upon the reduction in pore-water pressure and consequent load transfer in the aquifers, pressure gradients are set up across the interfaces of interbedded siltstones, shales, and clays. As a result, water movement occurs from these fine-grained beds into coarse-grained aquifers. The volumetric rate of flow depends on the permeability of clays and silts, pore-water pressure drop, length of the drainage paths, viscosity of water, and cross-sectional area of flow. According to Allen *et al.* (1971), in shallow, unconsolidated sediments consisting of interbedded clays, silts, and sands, which have void ratios of about 0.6 or greater, clays and silts are the major compactible materials upon dewatering. On the other hand, at depths of 300 m or greater and/or where the void ratios are below 0.6, the sands constitute the major compacting material.

In Figure 3.3, void ratio is plotted versus applied pressure for sand, silt, and clay cores. At void ratios of 0.6 or greater and pressures of about 30 kg/cm^2, sands are as compactible as clays, or even more compactible. Clays having high void ratios are very compactible at high pressures. Void ratio-versus-pressure data obtained by Roberts (1969) shows that in the 1,000–20,000 psi pressure range, certain sands may be at least as compressible as the typical clays, if not more compressible.

At a depth of 3,000 ft, Boston Blue Clay could undergo about 6% compression (Figure 3.4), i.e., for an initial stratum thickness of 100 ft, a total settlement of approximately 6 ft may occur. Compression of the oil sand, which was disturbed and repacked into an initially loose condition, could result in a settlement only 15% lower than that of the Blue Clay (Roberts, 1969, p. 375).

At a depth of 5,000 ft, the Blue Clay could undergo 5.5–6% compression. At this depth various sands could undergo 1–7.5% compression (Roberts, 1969, p. 375).

At a depth of 8,000 ft, the Blue Clay could undergo about 5% compression, whereas various sands could undergo compressions varying from about 2 to 10%. At this depth a 20–40 mesh Ottawa Sand is about twice as compressible as the Blue Clay (Roberts, 1969, p. 375). Figure 3.5 illustrates the relationship between void ratio and applied pressure for oil sands. Figure 3.6 shows the relationship between porosity and depth of burial for shales and argillaceous sediments.

3.3 Theoretical Modeling of Compaction

The porosity or pore volume of elastic sediments and rocks decreases with increasing depth. This decrease in porosity is a measure of the amount of compaction undergone in the argillaceous sediment since deposition. There is a problem in evaluating the effects of depositional rates and geologic age in developing a simple sediment compaction model. Nevertheless, empirical data suggest that the effect of age and depositional rates are predictable.

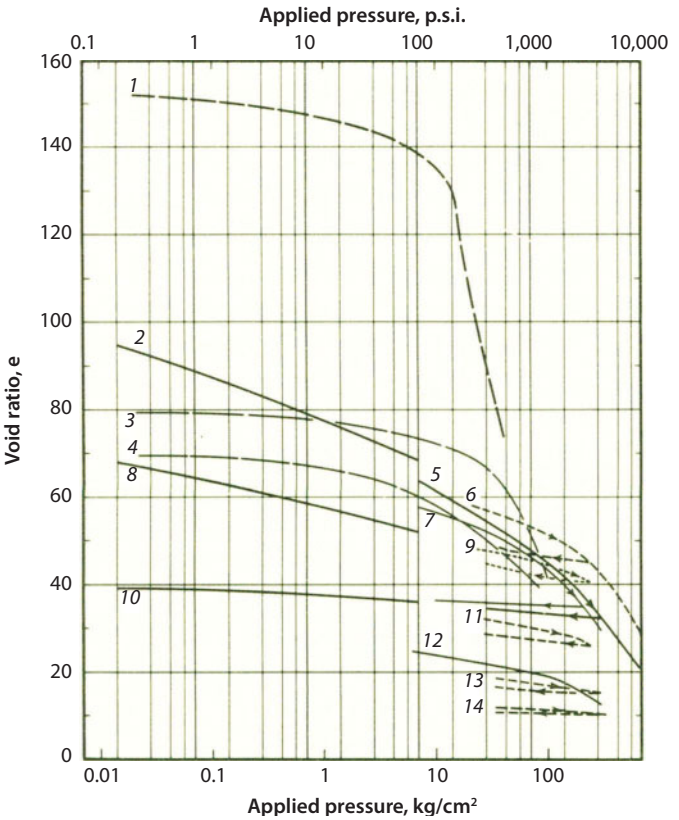

Figure 3.3 Relationship between void ratio and applied pressure for sand, silt and clay cores obtained at different depths from various areas. 1 = Corcoran Clay (depth of 425 ft); 2 = very loose sand; 3 = Corcoran Clay (depth of 735 ft); 4 = silt (depth of 1,345 ft); 5 = average Wilmington, California sands (depth of 2,000–4,000 ft); 6 = average Wilmington, California siltstones (depth of 2000–2,900 ft); 7 = sand from Maracaibo, Venezuela (depth of 3,000 ft); 8 = intermediate compacted sand; 9 = average Wilmington, California siltstone (depth of 3,000 ft); 10 = very compacted sand; 11 = average Wilmington, California siltstone (depth of 3,100–3,500 ft); 12 = clay from Maracaibo, Venezuela (depth of 3,104 ft); 13 & 14 = average Wilmington, California, siltstones (depth of 3,600–6,000 ft). (After Allen and Mayuga. 1969. In: Chilingarian *et al.*, 1995, p. 187, figure 3.11.)

Although the effect of temperature on formations is difficult to evaluate, experiments by Warner (1964, pp. 50–79) suggested that at temperatures less than 200 °F, temperature may not have a significant effect (other than in accelerating compaction-rates). Most compaction models utilize clay minerals of an idealized size and shape, which are influenced by mechanical rearrangement during burial. The following theories, presented below, are intended to enable the reader to better visualize the interrelationship among pressure, porosity reduction, and interstitial fluid release in argillaceous sediments.

3.3.1 Terzaghi's Compaction Model

Terzaghi (1943) introduced the effective stress concept. The effective stress concept was first empirically formulated on the basis of laboratory experiments. This approach assumes that the load, L (overburden pressure), applied to a unit of fluid-filled soil or

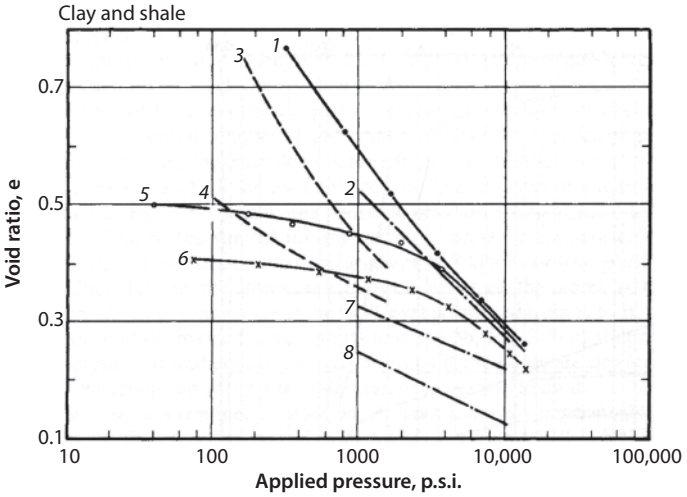

Figure 3.4 Relationship between void ratio and applied pressure for clay and shale. Curve 1 = undisturbed Boston Blue Clay; Curves 2,7 & 8 = clay cores from Venezuela (depths of 2,486 to 4769 ft); Curves 3 & 4 = compressed curves for plastic clays with liquid limits of 80 and 30% with a P. I. of 50 & 12, respectively (Skempton, 1953); Curve 5 = undisturbed shale (C11); and Curve 6 = undisturbed shale (C5). (After Roberts, 1969, figure 1, p. 369. In: Chilingarian *et al.*, 1995, p. 188, figure 3.12.)

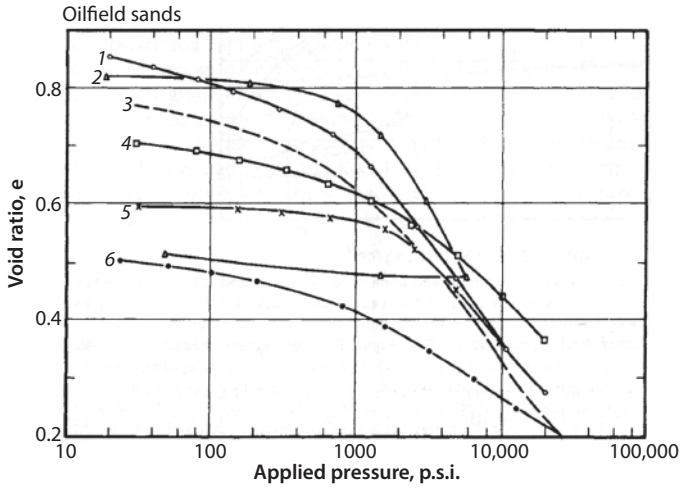

Figure 3.5 Relationship between void ratio and applied pressure for oilfield sands. Curve 1 = remolded(25.10); Curves 2 & 6 = remolded (M.I.T. Geol. Dept.); Curve 3 = undisturbed (1.1); Curve 4 = undisturbed (25.1); Curve 5 = remolded (25.13). (After Roberts, 1969, figure 4, p. 372. In: Chilingarian *et al.*, 1995, figure 3.12, p. 183.)

rock, is supported by the solid frame (grain-to-grain stress, σ_e, or p_e) and the pore pressure increase, Δp. The support provided by the solid frame, within this scheme, was also called effective stress (σ_e or p_e). Effective stress does not correspond to any actual stress in a rock, but is the stress in the model medium and is an average stress (computed value) on a horizontal plane (see Gurevich and Chilingarian, 1993):

$$\sigma_e = L - \Delta p \tag{3.5}$$

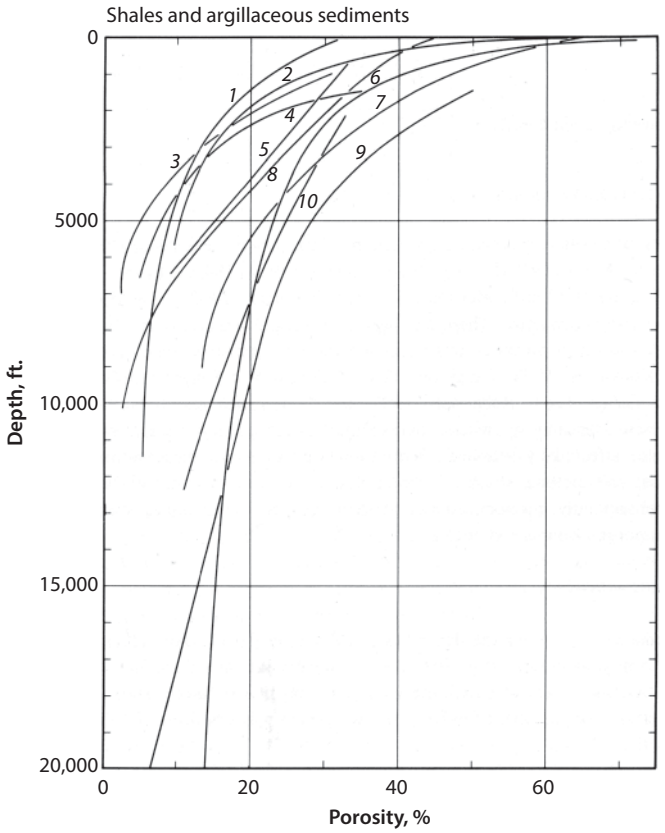

Figure 3.6 Relationship between the porosity and depth of burial for shales and argillaceous sediments. Source: Curve I = Proshlyakov (1960); Curve 2 = Meade (1966); Curve 3 = Athy (1930); Curve 4 = Hosoi (1963); Curve 5 = Hedberg (1936) Curve 6 = Dickinson (1953); Curve 7 = Magara (1968); Curve 8 = Weller (1959); Curve 9 = Ham (1966); and Curve 10 = Foster and Whalen (1966). (After Rieke and Chilingarian, 1974, p. 42, figure 17.)

In the Terzaghi model, physical meanings of measured values are quite definite: L represents a new, additional load applied to a physical body in mechanical equilibrium and Δp is the elastic response of the pore fluid to the total (elastic, reversible, and plastic, irreversible) deformation of the specimen. Terzaghi assumed that effective stress, σ_e, is the stress in the solid frame under these conditions (Gurevich, 1980).

In a dynamic situation, hydrostatic uplift and elastic response act together. Thus, the physical meaning of the effective stress concept being applied to deformations of rocks *in situ* is rather obscure physically and often leads to confusion. This is especially true because the effective-stress concept completely ignores both the nature of deformations and mechanical properties of rocks that are deformed. This concept does not take into account the fact that not just a small piece, but rather a large mass of rocks is being deformed as a single unit. Thus, when deformation cannot be reduced to a one-dimensional model, some additional problems arise. For example, the generation of a vertical tension and strain of rocks in the course of subsidence of formations above a compacting reservoir is not compatible with the effective-stress concept: the overburden

weight is not fully transmitted to the reservoir but, nevertheless, compaction continues (Gurevich and Chilingarian, 1993).

Additional problems with the effective-stress concept arise because of heterogeneity of the rock and its mechanical properties, and the presence of fractures. Owing to heterogeneity, some scale effects arise and should be taken into account (Bell and Dusseault, 1991; Enever *et al.*, 1990; Ito *et al.*, 1990; Ratigan, 1990).

Another source of confusion is the disagreement on whether or not compressibility of sediments and rocks obtained from compaction tests in the laboratory and those *in situ* differ. There is a dependence of compressibility on loading history and according to some investigators, the measured degree of compaction *in situ* is lower than those predicted from laboratory tests.

Radioactive bullet surveys in the Groningen gas field showed that the actual compaction values were three times lower than the amount predicted (Mess, 1979). It is important to know, however, whether uniaxial or hydrostatic compaction equipment was used in the laboratory. For example, when using hydrostatic compaction apparatus, the compressibility of unconsolidated sands are often about twice as high as those obtained when using uniaxial compaction apparatus.

3.3.2 Athy's Compaction Model

According to Athy (1930) compaction represents a simple process of squeezing out the interstitial fluids and thereby reducing the porosity. In relatively pure shales a definite relationship exists between porosity and depth of burial as shown in Figures 3.6 and 3.7. After sediment has been deposited and buried, the pore volume may be further modified by: (1) deformation and granulation of the mineral grains; (2) cementation; (3) solution; (4) recrystallization; and (5) squeezing together of the grains. Upon continued application of overburden stress, the porosity is reduced and bulk density is increased. Athy (1930) pointed out that the amount of compaction is not directly proportional either to reduction in pore volume or increase in bulk density because of the above-mentioned processes.

3.3.3 Hedberg's Compaction Model

Hedberg (1936) stated that because of the numerous processes involved in compaction, it is not possible to express satisfactorily pressure-porosity relationships for clays and shales throughout the entire depth range by any one simple equation. Hedberg (1936) determined the porosities of shale core samples taken from Venezuelan wells from depths of 291 ft to 6,175 ft. An analysis of this data, led Hedberg (1936) to propose a compaction process consisting of three distinct stages:

> The ***first stage*** consists mainly of the mechanical rearrangement and dewatering of the clayey mass in the pressure interval from zero to 800 psi. During this period of dewatering, there is a rapid decrease in porosity for small increments of additional overburden pressure. Expulsion of free water and mechanical particle rearrangement are dominant in the porosity range from 90% to 75%. Some adsorbed water is also lost during this stage. Between a porosity of 75% and 35%, adsorbed water is expelled from the sediment.

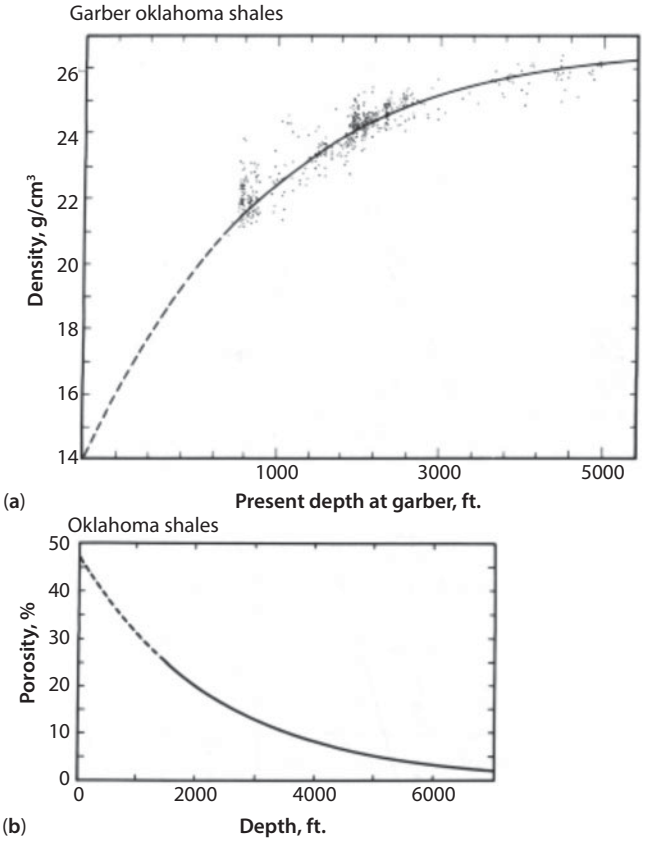

Figure 3.7 (a) Relationship between bulk density and depth for Oklahoma shales. (b) Relationship between porosity and depth for Oklahoma shales. (After Athy, 1930, Figures 2 and 3, pp 12 & 13. In: Rieke and Chilingarian, 1974, p. 37, figure 14. Courtesy of the American Association of Petroleum Geologists.)

In the ***second stage*** mechanical deformation of the clay structure occurs below a porosity of 35% where the clay particles come in closer contact with each other. As a result, there is a greater resistance to further reduction in porosity.

The ***third and final stage*** is recrystallization with porosities less than 10%. The main compaction mechanism during this stage is recrystallization under high pressures. Reduction of the pore volume occurs slowly and only with large pressure increments. The larger crystals may grow at the expense of the smaller ones, and a gradual transition may occur from a shale to a slate and then to phyllite.

3.3.4 Weller's Compaction Model

Weller (1959) described a compaction process very similar to the one proposed by Hedlberg (1936). Weller's composite porosity depth curve shown in Figure 3.8 represents an equilibrium condition in a continuous column of ordinary mud and shale. This

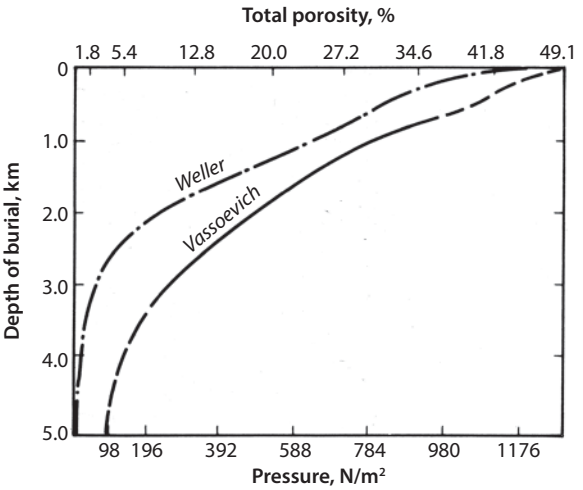

Figure 3.8 Relationship between porosity, depth of burial and overburden pressure. N = unit of force (Newton) = 102 g-force = 10^5 dynes. (After Weller and Vassoevich, in: Kartsev *et al.*, 1969, in: Rieke and Chilingarian, 1974, p. 43, figure 18.)

curve is based on Terzaghi's, Athy's, and Hedberg's data. The porosity-depth relationships can be distorted by the occurrence of carbonates and sands in shales and by abnormally overpressured zones. In addition, application of laboratory soil-compression tests to buried sediments presents some problems.

Weller (1959) proposed a compaction process starting with a mud at the surface having a porosity between 85% and 45%. As the overburden pressure increases owing to sedimentation, the interstitial fluids are expelled from the pore space (porosity ranges from 45% to 10%). As a result, there is rearrangement of the mineral grains and development of closer packing. Compaction at this stage is related to the yielding of clay minerals between the more resistant grains. Weller theorized that at about 10% porosity, the non-clay mineral grains are in contact with each other, and the clays are being squeezed into the void space. Further compaction (porosity < 10%) requires deformation and crushing of the grains.

3.3.5 Teodorovich and Chernov's Compaction Model

Teodorovich and Chernov (1968) suggested the following stages in the compaction of productive Apsheron horizons in Azerbaijan:

> The ***first stage*** occurs at burial depths of 0 to 8–10 m where there is a rapid compaction. Porosity in clays decreases from 66% to 40%, whereas that of sandstones-siltstones decreases from 56% to 40%. Large amounts of water are squeezed out during this stage.
>
> During the ***second stage*** there was a rapid decrease in the compaction rate in the intervals from 8–10 m to 1,200–1,400 m. During this stage, porosities of the shales and sandstones-siltstones decrease to about 20%.

The ***third stage*** (burial to a depth of 1,400 to 6,000 m) is characterized by slow compaction. The absolute porosity of sandstones-siltstones at a depth of 6,000 m decreases to approximately 15% to 16%, whereas that of shales to 7% to 8%.

3.3.6 Beall's Compaction Model

Beall (personal communication, 1970), proposed a simple model for consolidation of elastic muds, based on the data from offshore well core samples, Louisiana, the JOIDES Deep Sea Drilling Project, and from high-pressure experiments on marine muds. The initial stage of compaction (down to a depth of approximately 3,300 ft) primarily involves expulsion of fluids by mechanical processes as in the other proposed theories. Approximately 50% of the total consolidation is reached at a very shallow depth. The average calculated pore throat diameters during the first stage are around 6Å. During the second stage (approximately at depths of 3,300 to 8,000 ft) about 75% of total compaction is complete, and pore throat widths in the clays approach 1Å. The fluid pressures remain hydrostatic. During the third-stage of compaction there is an extremely slow decrease of porosity with depth, and pore throat diameters are generally less than 1Å. According to Beall, NaCl filtration could probably take place during the third stage resulting in the expulsion of progressively less saline fluids to associated permeable sands, if the latter are present. In Beall's model, overburden pressure between 8,000 to 12,500 psi would be required to initiate NaCl filtration in marine muds. In the absence of permeable sands, the excess fluid pressure may be generated during the third stage.

3.3.7 Katz and Ibrahim Compaction Model

Katz and Ibrahim (1971) presented a mechanical model for explaining compaction and fluid expulsion from shales. Their model is based on Terzaghi and Peck's simple piston and spring analogy (see Figure 3.9). The Katz and Ibrahim model is based on the compaction of an argillaceous layer between two permeable sand layers. As proposed by Terzaghi and Peck, the argillaceous sediment is represented by a series of springs and perforated disks. The perforated disks represent low-permeability clays, which restrict the escape of fluids, whereas the springs represent the deformable clay matrix. Sudden loading on the model corresponds to a rapid sedimentation rate. Water contained in the spaces between the perforated disks represents the interstitial fluid. If a stress is applied suddenly to the system, the water between the disks initially will support the entire load.

After a brief period of time, the water will be forced through the perforations in the disks either in an upward or a downward direction, depending on the relative magnitudes of pressure in the compacting systems, without lateral flow.

As the top and bottom disks move closer to the internal disks, the springs will begin to carry part of the applied load (Figure 3.9). Consequently, the fluid pressure between the external disks will decrease. When the disks approach each other, it will become difficult for the pore fluid to escape from inside the system. Katz and Ibrahim (1971) mentioned that the gradual decrease of permeability from the center toward the top and bottom of the model could be represented either by a decrease in the number of

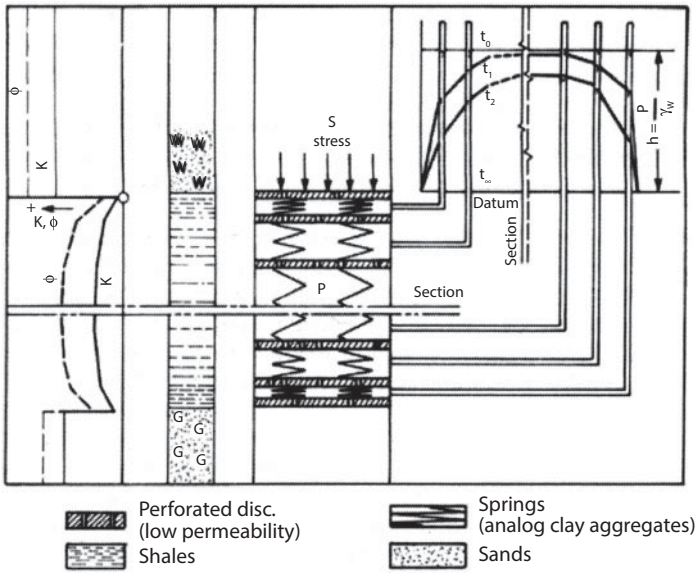

Figure 3.9 Schematic representation of clay compaction, porosity and permeability relationships and creation of abnormally high formation fluid pressures. Where k = permeability; ϕ = porosity; t = time; p = pore pressure; γ_W = specific weight of water; h = height to which fluid will rise in the tubes; this represents the pressure head (P/γ_w); W = water and G = gas. (Modified after Katz and Ibrahim, 1971, figure 12, courtesy of Soc. Pet. Eng., in: Rieke and Chilingarian, 1974, p. 319, figure 170.)

openings in the disks per unit length in the model or by an increase of the number of disks per unit length in the model. Higher fluid potential is shown to exist in the central portion rather than in the upper or lower portions of the model. This means it takes more time for the fluid in the center of the model to escape than at the outer boundaries.

The behavior of the Katz and Ibrahim mechanical model is in general agreement with the observed performance of overpressured formations in the U.S. Gulf Coast area. The model illustrates the reasons for the higher porosity for undercompacted shales, the extreme drop in permeability with increasing lithostatic pressure, and entrapment of high interstitial fluid pressure in the shales.

3.4 Subsidence Over Oilfields

Formation pressure drops in petroleum reservoirs during fluid production (water/oil/gas) often result in subsidence if there is no influx of water. If there is an influx of water, the quantity of subsidence could be less than anticipated. This reduction in pore pressure within reservoir rocks may result in the influx of water from the adjoining formation in waterdrive reservoirs. If the influx of water is not sufficient to totally replace the produced fluids, a greater percentage of the overburden load will be then carried by the skeletal structure of the rock (the grain-to-grain stress is increased). This eventually will be reflected at the Earth's surface as land subsidence. Compaction occurs in both the reservoir rocks and the overlying layers of rock as the pore skeletal structure

adjusts itself to carry the additional stress. The area of subsidence as a result of subsurface fluid production is about twice as large as the area of the reservoir. Subsidence (differential) at the surface can cause engineering and ecological problems. These include structural damage, rupture of casings, and disruption of pipelines (Barends *et al.*, 1995; In Chilingarian *et al.*, 1995; Dobrynin and Serebryakov, 1989).

Tapping the earth for ground water and/or hydrocarbons has resulted in many areas in sinking of the land surface due to loss of pore pressure. An excellent example is the subsidence in East Mesa geothermal field, CA, where there was withdrawal of large quantities of hot brine for geothermal power. Fluid pressures in petroleum and geothermal reservoirs are often reduced by as much as 2,000 to 4,000 psi from the initial pressure, whereas those in ground-water reservoirs are reduced by 200 to 600 psi (460 to 600 ft head of water).

Dramatic and damaging effects of subsidence occurred above the Wilmington Oilfield in Long Beach, CA, in the 1940s and 1950s. This sinking (see Figure 3.10) occurred over an area of 22 sq mi and gave rise to a subsidence bowl up to 27 ft deep, causing damages in excess of $150 million to the above structures. The vertical subsidence was accompanied by a horizontal movement of as much as 9 ft, directed inward toward the center of the bowl of subsidence. The bowl is underlain by 6,000 ft of sediments of Recent to Miocene ages that uncomfortably overlie a basement schist of Pre-Tertiary age. Seven oil-producing zones extend from a depth of about 2,500 ft to 6,000 ft. The average porosity of productive zones, containing 23% to 70% sand, ranges from 24% to 34%.

Similar areas of land subsidence related to exploitation of oil and gas fields include: (1) Goose Creek, Texas; (2) Lake Maracaibo, Venezuela; (3) Niigata, Japan; and (4) Po Delta, Italy.

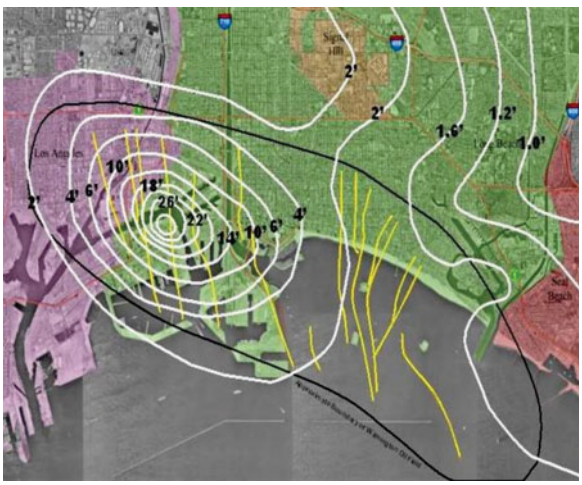

Figure 3.10 Subsidence of Long Beach, CA, area between 1928 and 1962 of the Wilmington Oilfield, CA. The subsidence shown in the upper right is due to fluid withdrawal from the Long Beach (Signal Hill) oilfield, whereas that in the foreground is due to fluid withdrawal from the Wilmington oilfield. Lines of equal subsidence are in feet (–2', –4', –6', –10', –14', –22', –27' and –29'). (Courtesy of City of Long Beach Department of Oil Properties, CA.; http://www.lon beach. ov/lb a/about-us/oil/subsidence/)

Marsden and Davis (1967, p. 95) and Poland and Davis (1969) described several techniques of measuring the compaction of underground strata:

1. Bullets of radioactive material are shot into the rock at measured intervals in the wellbore from a firing mechanism (gun) lowered down the hole. A gamma ray detector is then periodically lowered into the well on a cable to determine the changes (lessening) in distances between the radioactive markers.
2. The vertical compression of casing (steel pipe) that lines the well is measured. Inasmuch as casing is usually cemented to the rock surrounding it, the vertical compression of the rock will shorten the pipe length. Casing comprises 30- or 40-ft pipe joints. Magnetic flux at the collar joining two pipe lengths is different from the flux along the length of the pipe. Thus, a magnetometer can be used to locate the successive collars and measure the shortening of individual pipe lengths. Shortening as low as 1/2 inch in a 40-ft joint can be detected. The shortening also can be measured by marking the pipe with radioactive pellets at definite intervals.
3. Compaction recorders are used, which consist of a heavy weight emplaced in the formation below the bottom of a well casing. Cable, which is attached to the anchor weight (200–300 1b), extends to the land surface and is counter-weighted (in 50-lb increments) to maintain constant tension. The cable is free to move at its upper end. The amount of cable rise above the land surface is continuously measured by a recorder, as subsidence occurs. When amplified, the record can reveal subsidence as small as 1/10 mm.
4. Floats, quartz rods and transducers are employed, which enable measurement of vertical and horizontal strains and tilts of the land (Marsden and Davis, 1967, p. 99).

Additional information may be found in Colazas and Strehle (1995, pp. 324–327).

3.4.1 Rate of Subsidence

In addition to the grain response to increased stress in the rock-matrix skeletal structure, the subsurface reservoir as a whole undergoes several types of changes adjusting to the imbalance of forces caused by fluid withdrawal. Loosely cemented rocks undergo permanent rearrangement of grains and pore spaces resulting in the loss of porosity and permeability. This type of compaction induced by the mobility of grains is only partially reversible if the fluid pressure is later increased by water injection or natural recharge. Thus, indiscriminate fluid production can lead to a permanent loss of the capacity of an aquifer or a reservoir to contain (and to conduct) fluids.

Information published on total and annual rates of subsidence may be relatively abundant but it tends to be incomplete. This information often gives the impression that there is an approximate maximum amount of subsidence; however, to get at definite values of the subsidence rates one must know the pressure decline rates, reservoir thickness, depth, and lithology of reservoir and overlying rocks. In a few cases, subsidence

reached ≈10 m. In the San Joaquin Valley, CA, by 1970, the largest subsidence due to groundwater withdrawal was 8.5 m (28 ft). In the Wilmington Oilfield, CA, total subsidence due to hydrocarbon and water withdrawal was ≈9 m. Lesser values of subsidence for other oilfields are in the order of 0.9–1.5 m (3.5 ft) in the Los Angeles Basin, CA. The annual rate of subsidence is dependent on the rate of pore pressure decline, and may be as high as 0.6 m (2 ft) per year. In San Joaquin Valley, average annual rate of subsidence due to water withdrawal, was up to 2.4 m (8 ft) for 10 years (1959–1969), i.e., 24 cm (0.8 ft) per year. In the Wilmington Oilfield, annual subsidence rate in some areas was as high as 70 cm (2.3 ft), with the total subsidence for a three-year period (from 1951 to 1954) being 2.1 m (7 ft). Globally, high rates of about 0.3 m (1 ft) per year are often encountered [25 cm (0.84 ft) per year in Taipei Basin, Taiwan; and 32 cm (1.07 ft) per year (in 1960) in Tokyo, Japan] while lower rates in the order of several cm per year are also common.

3.4.2 Effect of Earthquakes on Subsidence

Green (1972) investigated the movement of benchmark elevations in California affected by earthquakes. The two principal types of earthquakes studied were those causing (1) surface faulting and (2) shaking, with the former being uncommon at the present time as the majority of earthquakes in California are relatively deep-seated. Earthquakes are normally reported in terms of magnitude (M), which is a measure of the energy released at the source (1 to 10 on the Richter scale) and epicenter, i.e., location on the surface directly above the quake. Intensity, which is a measure of the severity of ground motion at a particular point on the earth's crust (I to XII on the modified Mercelli scale), is of prime importance in studying the effect of the magnitude of earthquakes on subsidence. According to Green (1972), the largest earthquake during the past 20 years in California (Kern County, 1952, $M = 7.7$) resulted in a maximum vertical displacement of 4 ft and a maximum horizontal displacement of 2–3 ft. The 1971 earthquake in San Fernando Valley in California ($M = 6.6$) resulted in maximum vertical and horizontal movements of 3 and 5 ft, respectively. Green (1972) showed a direct relationship between the anomalous settling of benchmarks and increased shaking. The amount of energy released at a particular source does not appear to be as important as the secondary effect of ground shaking.

3.4.3 Stress and Strain Distribution in Subsiding Areas

Distribution of stress and strain within the rock mass above the compacting hydrocarbon reservoir is the most important feature of subsidence from a viewpoint of fracturing of rocks and increase in vertical permeability. Several points should be emphasized.

Horizontal tension is the highest in the zone around the central core of the subsidence bowl where horizontal compression predominates (Figure 3.11). Horizontal displacement in the Wilmington Oilfield reached a maximum of about 3.66 m (Allen, 1973; Kosloff *et al.*, 1980). This extension can be presented, for example, as four new 0.5 mm-wide fractures per each meter in the zone of tension. These deformations, which released tensile strain and caused earthquakes, gave rise to open fractures, both lateral and vertical. The latter can become avenues for gas migration from the oilfields.

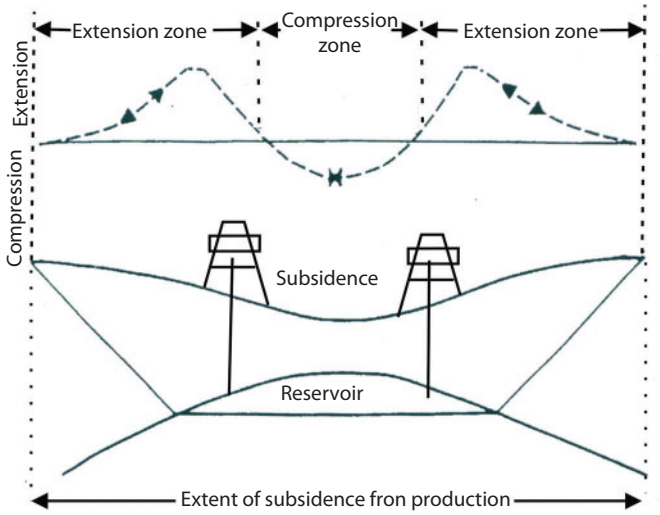

Figure 3.11 Schematic diagram of compressive and tensile stress distribution in subsiding formation due to fluid withdrawal. (Modified after Gurevich and Chilingarian. 1993, figure 1, p. 224.)

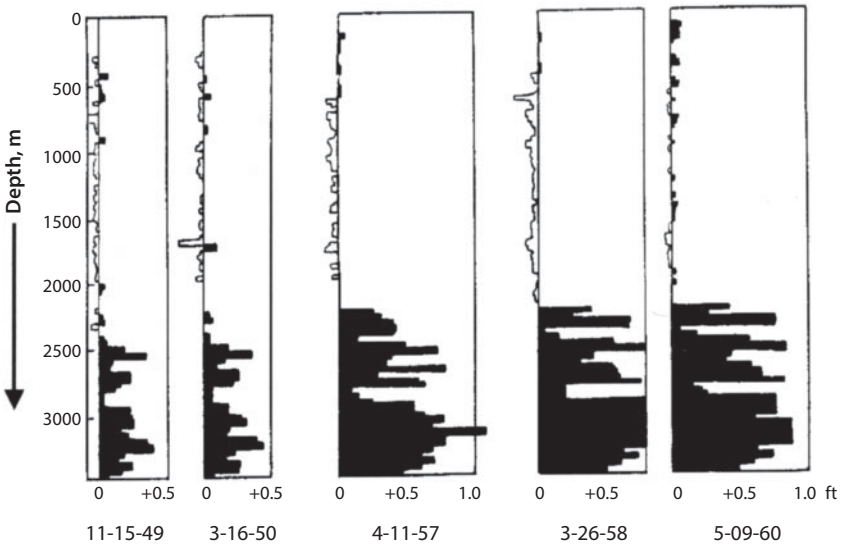

Figure 3.12 Schematic of casing count surveys of a typical well in the Wilmington Oilfield. (Modified after Poland ad Davis, 1969; in: Gurevich and Chilingarian, 1993, figure 2, p. 244.)

Vertical tension is the highest in approximately the same zone. Figure 3.12, modified after Poland and Davis (1969), shows measured elongations in five successive moments. This combination of horizontal shear stress with vertical tension caused several small earthquakes (Lee, 1979; Kosloff *et al.*, 1980). As Kosloff *et al.* emphasized; "The hypocenters were at shallow depths between 450 and 550 m in bedded shale formation. The fault planes were always close to horizontal (Richter, 1958; Mayuga, 1965; Kovach, 1974). Locations of epicenters for the Wilmington Oilfield are shown in

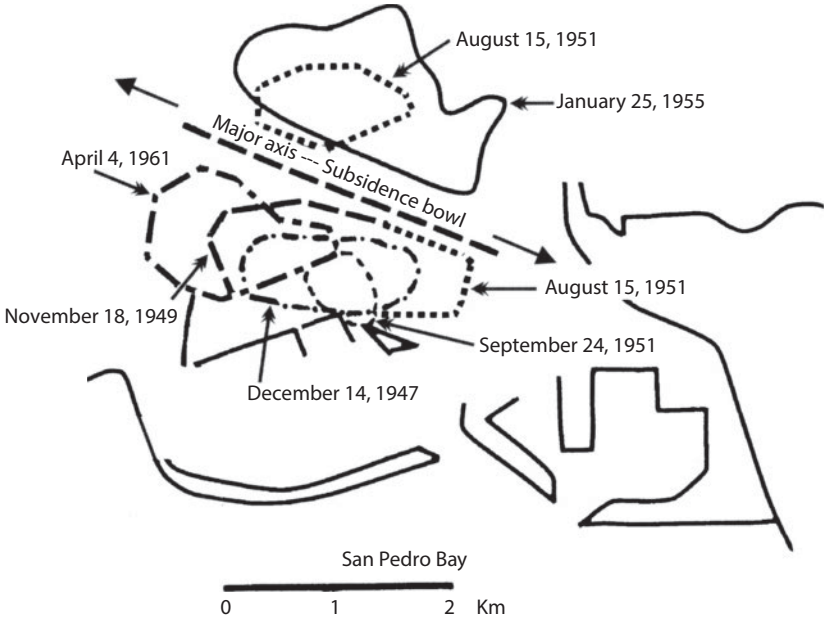

Figure 3.13 Locations of epicenters and slip planes of subsidence earthquakes, Wilmington Oilfield, Long Beach, CA. (After Kosloff *et al.*, 1980 figure 3, p. 245. In: Gurevich and Chilingarian, 1993.)

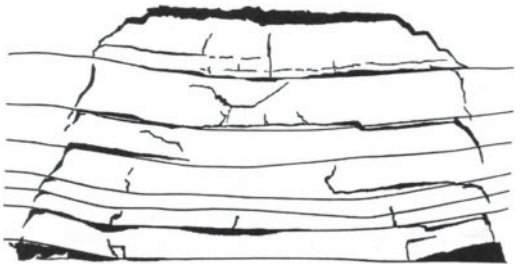

Figure 3.14 Deformation pattern of strata above longwall extraction with strong overburden (physical model). (After Whittaker and Reddish, 1989; in: Gurevich and Chilingarian, 1993, figure 4, p. 254.)

Figure 3.13 modified after Kosloff *et al.* (1980). It is these deformations, that released tensile strain and caused earthquakes, also formed open fractures, both lateral and vertical.

It is necessary to emphasize that the very fact of the existence of vertical tensile strains and elongations above the compacting reservoir is direct evidence that the weight of the overburden is not transmitted fully to the compacting rocks due to the bridge-effect of overlying formations. That means that the effective-stress concept and models based on it do not exactly fit this deformation. In a sense, the existence of vertical tensile strain means that a reservoir compacts faster than the overlying beds bend down. Thus, beds break apart vertically. It is worth noting that in the case of sand production, when extraction of sand forms a cavity around the borehole, this effect will be enhanced and deformation similar to those shown in Figure 3.14 (Whittaker and Reddish, 1989), may be possible.

The role of the strength of formations above a compacting reservoir is also indicated by a time lag in subsidence. Meyer and Fowley (1988) noted that "surface subsidence commonly lags behind cumulative production."

This means that for some time compaction of the reservoir is compensated not by equal subsidence but by vertical extension of the formation above the reservoir, while the deformation zone slowly expands upwards. Thus, first fractures should form in the caprock of a depleting reservoir. This may impair the reliability of the caprock and provide some paths for the leakage of gas from the pool.

Generally, gas/oil/water production lowers the formation pressure and results in surface subsidence. However, in the case of some hydrocarbon reservoirs which are water driven, the influx of water from the surrounding aquifer will reduce the pressure drop due to the production of fluids. Only if the influx of water is not sufficient to replace the produced fluids there will be subsidence as in other types of hydrocarbon reservoirs.

3.4.4 Calculation of Subsidence in Oilfields

The area of subsidence, as shown in Figure 3.11, due to fluid withdrawal is about twice as large as the reservoir from which the fluids are withdrawn. The type of subsidence for hydrocarbon reservoirs is generally differential, resulting in structural damage, rupture of well casings, disruption of pipelines, etc. (Barends *et al.*, 1995; Chilingarian *et al.*, 1995a&b, Dolbrynin and Serebryakov, 1989).

Geertsma (1973), along with a study by Yerkes and Castle (1976) identified oilfields with "*extreme*" subsidence. These fields primarily consisted of gas-depletion reservoirs with large vertical production zones in poorly consolidated alluvial sediments similar to those found in the L.A. Basin. Generally, the large vertical production interval consists of independent pools of oil and/or water aquifers. Their studies, suggested the following contributions to "*extreme*" subsidence: (1) There is a significant reduction in reservoir pressure as a result of high volumes of produced fluid (oil, gas and water) over the production life of the hydrocarbon field. (2) The major mechanism for production is dissolved gas drive (gas-depletion). (3) Production is obtained from a large vertical interval. (4) Fluids (oil and gas) are contained in loose or weakly cemented (poorly consolidated) sediments. (5) The producing reservoirs have a rather small depth of burial compared to their lateral dimensions.

Extreme Subsidence has been an environmental problem in several instances caused by oilfield fluid production within the L.A. Basin (Wentworth *et al.*, 1969). Subsidence is the result of the reduction of pore pressure within the reservoir resulting from fluid production where the pore pressure helps support the geologic overburden. The resulting increase in the effective stress on the pore structure partially collapses the structure, resulting in the compaction of sediments which is propagated to the surface, typically causing a bowl-shaped subsidence as shown in Figure 3.15 at the surface, centered over an oilfield. G. V. Chilingar has suggested that the area of actual surface subsidence can encompass and affect about four times the surface area of the reservoir itself or twice its lateral dimensions. The maximum vertical subsidence occurs at the center of the reservoir.

Wilmington Oilfield subsidence reached approximately 8.5 m before corrective action was taken by implementing a massive water injection program (see Figure 3.15).

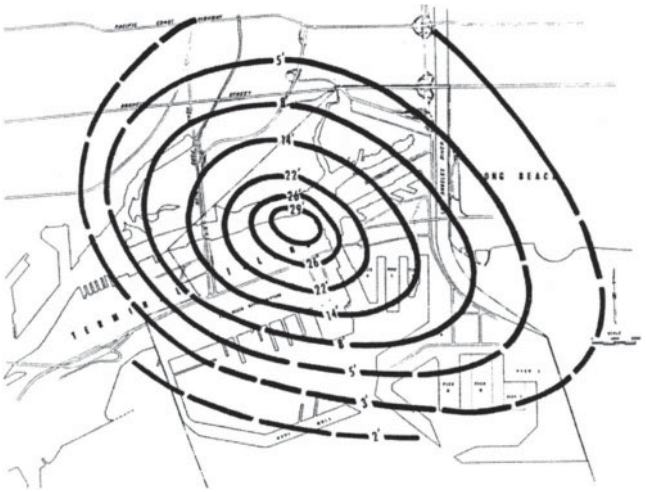

Figure 3.15 Total subsidence in Wilmington Oilfield area in 1954. (In: Chilingarian *et al.*, 1995, p. 296, figure 6.8.)

Experience has shown that subsidence can be minimized by a subsidence-monitoring program and repressurizing the formation by reinjecting produced water. Standard subsidence-monitoring that can be used throughout the world (Endres *et al.*, 1991) is the Global Positioning Satellite System (GPS). Many subsidence problems of the past can be directly traced to the failure to perform adequate monitoring and reinjecting fluids to prevent subsidence. Conventional surveying and now satellite geodesy permit determination of both vertical and horizontal movements of the land surface above oilfields with great accuracy and at relatively minimal cost.

Vertical reservoir subsidence due to compaction (a reduction in reservoir thickness) is the result of the partial collapse of sediments (pore space) in those reservoirs where the pore pressure partially supports the overburden pressure. The total overburden pressure (p_t) is supported by the pore pressure (p_p) and the grain-to-grain or effective pressure (p_e), i.e., $p_t = p_p + p_e$. As the pore pressure decreases due to fluid production, the effective stress in the rock matrix structure increases causing a compaction of the formation. When the reservoir lateral dimensions are large compared to the vertical height, Geertsma (1973) suggested that reservoirs deform predominately in the vertical plane. Vertical compaction can be characterized for a reservoir by the vertical strain in the reservoir: $E_z = \frac{dz}{z}$, or $E_z = c_m dp$. The vertical reservoir coefficient of compressibility may be defined as $c_m = \frac{1}{z}\frac{dz}{dp}$. Due to the nature of the structure of reservoirs, c_m is usually not a constant, but rather a function of $\Delta p = (p_i - p_c)$, the difference between current reservoir pressure, p_c, and initial pressure, p_i. The coefficient of vertical compressibility, c_m is dependent upon a number of factors, such as rock type, degree of cementation, porosity, depth of burial, etc. Figure 3.16 presents a general relationship between porosity and the coefficient of vertical compressibility for unconsolidated sediments at depths of 1,000 m and

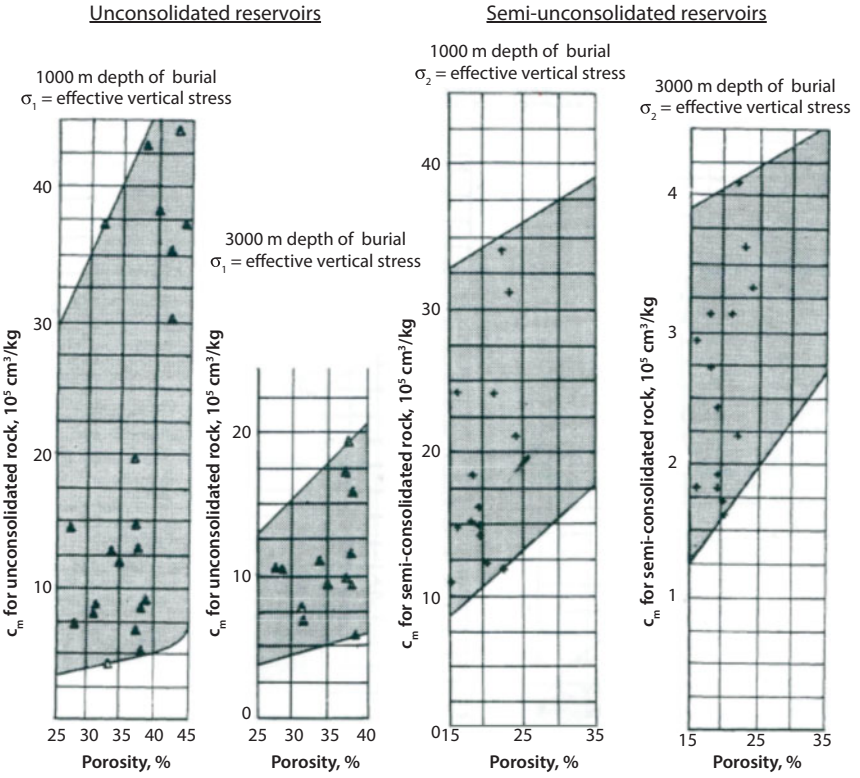

Figure 3.16 Uniaxial compaction coefficient c_m (vertical axes) for unconsolidated and semi-consolidated sandstone reservoirs. The effective vertical stresses σ_1. range from 100 to 200 kg/cm^2, correspondin to a depth of burial of 1000 m and σ_2 = 300 to 600 kg/cm^2 for a depth of burial of 3000 m for normal pressure reservoirs. (Modified after Geertsma, 1973, figures 1 & 2. 736 & 738.)

3,000 m. Geertsma (1973) suggested that the vertical compaction coefficient, c_m, could range between 20 to 40 $\times$ 10^{-5} cm^2/kg for sediments similar to those found within the L.A. basin. For detailed analysis, see Geertsma (1973) and Chiligarian *et al.* (1995).

In regard to subsidence, the main factors that dominate reservoir compaction behavior are: (1) the reduction in reservoir pressure as a result of the production of fluids, (2) the vertical extent over which this pressure reduction takes place, and (3) the order of magnitude of the relevant physical deformation properties of the reservoir itself. The combination of large vertical production intervals and/or thick stacking of producing pools (layered reservoirs) of unconsolidated sediments can result in significant or *extreme* vertical surface subsidence. It should also be noted that a sizable degree of compaction can be expected even in a well-consolidated rock for the particular conditions of large pore-pressure reductions and a sufficiently large vertical producing interval.

Figure 3.17 illustrates the interrelationship among earthquakes, gas migration, and subsidence resulting from oilfield production (Chilingarian *et al.*, 1995).

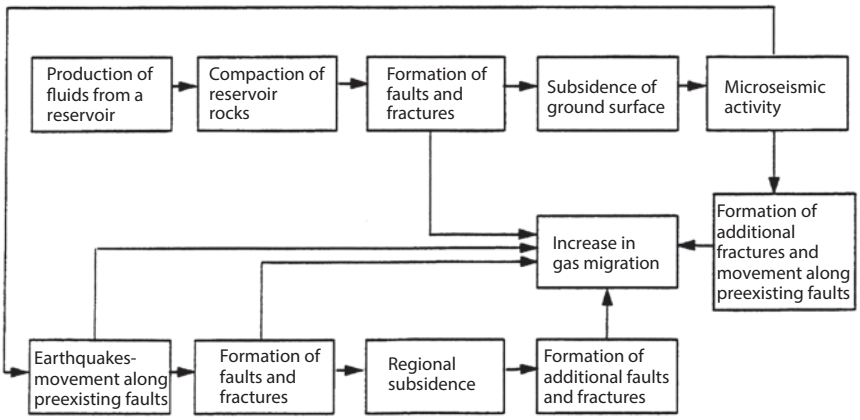

Figure 3.17 Schematic diagram of system relationships among production of fluids, compaction, subsidence, and seismic activity. (After Chilingarian *et al.*, 1995, figure D-1, p. 461.)

3.4.5 Permeability Seals for Confined Aquifers

A permeability seal (caprock) is required in order to have a closed or leaky-proof compaction system in a confined aquifer for hydrocarbon systems. Bradley (1975) described seals in three dimensions, that is, top, bottom and lateral containment of the fluids within the sediment body. The bottom seal for hydrocarbon reservoirs can be simply the density difference between water and hydrocarbons (Bradley, 1975, p. 971).

Lateral or horizontal permeability seals can be faults, lateral diagenetic and lithologic changes in facies, or existence of evaporite bodies. Vertical seals arise from lithologic changes, fault displacement or diagenetic changes. Myer (1968) stated that the thickness of a seal may be variable, but it is assumed to be thin with respect to both thickness and lateral extent of an abnormal pressure zone. Pressure changes can be abrupt laterally across faults or vertically across bedding.

Bradley (1975) stated that the manner in which a seal is maintained is an enigma. High pore pressures generated by compaction and aqua-thermal pressuring at great depth could fracture the argillaceous sediments. If the sediments are relatively unconsolidated, such vertically directed fracturing would be self-sealing owing to the plastic nature of the argillaceous sediments. Another healing mechanism could be the precipitation of minerals resulting from the release of pressure (Bradley, 1975) and/or a decrease in temperature across this boundary, as described by Lewis and Rose (1970).

Seals in the geologic column have existed over a long period of geologic time and many have survived destruction during tectonic activity. The fact that permeability seals remain intact suggests that the above-mentioned mechanisms may heal any damage to these barriers. (For further discussion, see Powley, 1990.)

3.4.6 Fissures Caused by Subsidence

Tensile horizontal strain can cause fissures on the Earth's surface (Guacci, 1979; Beckwith *et al.*, 1991; Holzer, 1984; Lister and Secrest, 1985; Love et al., 1987; Pewe *et al.*, 1987; Pampeyan *et al.*, 1988; Contaldo and Mueller, 1991; Haneberg *et al.*, 1991; Keaton and Shlemon, 1991). Mostly, large surface fissures are caused by withdrawal of water from

shallow aquifers, as a rule, alluvial. Withdrawal of oil or water with dissolved gas, with substantial formation pressure decline, also causes surface deformation, which mostly consists of horizontal displacements and fractures (Pratt and Johnson, 1926; Strehle, 1989). Full depth of cracks and fissures should be investigated.

Origin and occurrence of earth fissures with dewatering of phreatic aquifers in Arizona, California, and Nevada have been studied by Holzer (1984). A common mechanism of fissure generation is localized differential compaction of unconsolidated aquifer material over bedrock irregularities. Association of earth fissures with zones of variable aquifer thickness suggests the occurrence of differential compaction (Jachens and Holzer, 1979). Differential compaction is the dominant source of horizontal tension causing earth fissures in the Picacho Basin, Arizona. An analysis of tensile strains at fissures at the times of their formation ranged from 0.1% to 0.4% (see Figure 3.18).

The deepest reported fissure [more than 16.8 m (55.1 ft)] was located near Pixley in the San Joaquin Valley, California (Guacci, 1979). It was 0.8 km (0.5 mile) long and 2.4 m (8 ft) wide. The fissure was open to a depth of 1.8 m (6 ft) (Figure 3.19). Reported

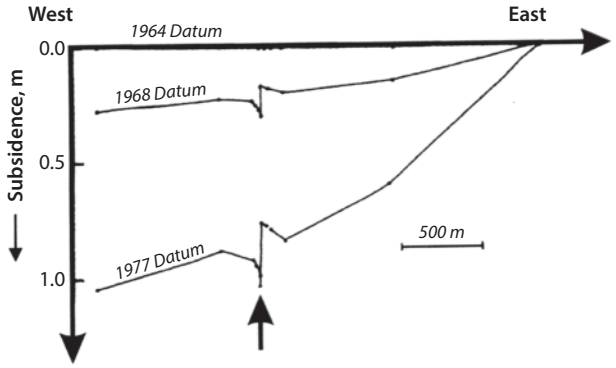

Figure 3.18 Subsidence profiles across the Picacho Fault, AZ. (Modified after Holzer and Thatcher, 1979; in: Gurevich and Chilingarian, 1993, figure 6, p. 247.)

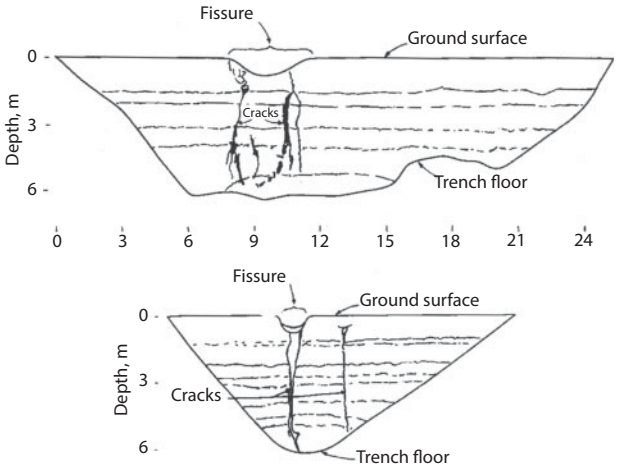

Figure 3.19 Trench logs of the Pixly fissure, San Joaquin Valley, CA. I I 21 24 (Modified after Guacci, 1979; in: Gurevich and Chilingarian, 1993, figure 5, p. 246.)

cracks attributed to hydro-compaction extended up to 4.4 m (14.5 ft) deep and were no more than 1 cm (0.4 in) wide (Beckwith *et al.*, 1991). Contaldo and Mueller (1991) studied 13 discrete locations in the Mimbres Basin in southwestern New Mexico. They found that measurable fissure depths range from less than 0.3 to 12.8 m, whereas the width of fissures ranged from an incipient hairline to 9.7 m (see Figure 3.19). Little is known about the full depth of these cracks and fissures, which is important from the potential gas migration viewpoint.

Kreitler (1977), Gabrish and Holzer (1978), Holzer and Thatcher (1979), and Van Sickle and Groat (1981) have studied the effect of subsidence on faulting. Holzer and Thatcher (1979) investigated changes of surface altitudes on both sides of the Picacho fault (Figure 3.18). They simulated the process of differential movements of fault sides and showed that the difference in altitude changes of sides depends on the angle of a fault. Physically, it is quite clear that existing faults will provide differential movements of their sides if a shear stress exists, relative to the fault plane. The widths of old and new fractures should be studied from the upward gas migration viewpoint.

The issue of the full depth range of fissures to the producing formation, which is very important from the gas migration/leakage viewpoint, remains unexplored. It is suggested by the authors that surface cracks likely extend much deeper than measured. This problem needs extensive examination.

3.5 Case Studies of Subsidence over Hydrocarbon Reservoirs

3.5.1 Los Angeles Basin, CA, Oilfields, Inglewood Oilfield, CA

An instructive review of subsidence rates in the Los Angeles Basin, CA, can reveal serious environmental urban problems, as a result of subsidence, that have been caused by oilfield production. Chilingarian *et al.* (1995) found that subsidence exists over virtually every oilfield and producing horizon in the Los Angeles Basin. Figure 3.20 shows the location of oilfields located in the Los Angeles Basin.

The Inglewood Oilfield, discovered on September 1924, lies under the western half of the Baldwin Hills area. It covers an area of about 4.9 km^2. In 1963, there were more than 600 producing wells. The Inglewood Oilfield consists of nine major groupings of layers or pools of intermixed oil and water aquifers located about 9 miles west of the center of Los Angeles. The field, as shown in Figure 3.21, is a faulted anticline. The thickness of the deposits in the field is over 8,000 ft (alluvial Pliocene and Miocene sediments) with the average depth of pools ranging from 950 to 8,400 ft. The discovery well was drilled in 1924. Over 693 wells have been drilled in this field; many prior to the 1950s when cementing practices were not recorded or regulated by today's standards (see California Division of Oil and Gas, 1961).

Historically, there has been little urban development above the reservoir and so environmentally the development of the field has presented few problems; however, there is a record of abandoned and production wells leaking fluid to the surface during the development of the waterfloods in the Vickers zone. There is also a record of water passing through fault planes within the Vickers waterflood at differential water

Figure 3.20 Distribution of oilfields in the Los Angeles Basin, CA. (After California Division of Oil and Gas, 1961.)

pressures greater than 150 psi. Due to the lack of urban development and monitoring for this field, subsidence is likely present but basically unrecorded with the exception of the area of the Baldwin Hills Dam failure.

3.5.1.1 Baldwin Hills Dam Failure

On December 14, 1963, at about 11:15 a.m., an unprecedented flow of water was heard in the spillway pipe at Baldwin Hills Dam in the Inglewood Oilfield area of Los Angeles County. A short time later the earthen dam failed and water broke violently through the downstream-face of the dam (causing property damage to 60 homes located below the dam and six deaths) flooding a 4-square-mile area.

The Inglewood Oilfield lies under the area of the site of the water reservoir on the south and west. The nearest reported production from the Inglewood Oilfield, at the time of the reservoir failure, was from three wells within 213 m of the south rim of the dam.

The Baldwin Hills earthen dam formed a large water reservoir that held water in a highly developed residential portion of Los Angeles and was located over a large oilfield with two large-active faults. Although an ongoing surveillance for leaks within spillways had been carried out, no monitoring for oilfield subsidence had been undertaken.

The owner of the dam, the Los Angeles Department of Water and Power, had operated the dam continuously from July 1951 until its failure on December 14, 1963.

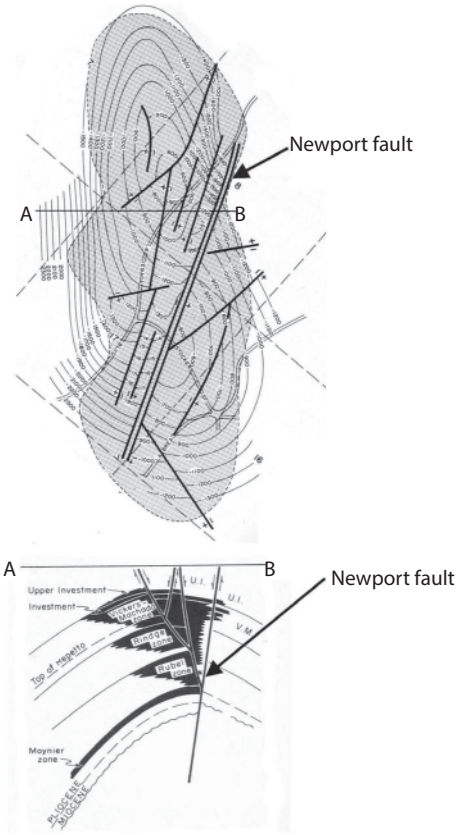

Figure 3.21 Structure and contour map of the Inglewood Oilfield showing location of the Newport Fault. Contours on the Vickers-Machado zone. (After California Division of Oil and Gas, 1961, p. 561.)

Analysis of this catastrophe revealed that the earthen dam failure was due to differential subsidence of the earth which correlated directly with the Inglewood Oilfield fluids production. The total area of subsidence resembled an elliptical bowl with its center about 805 m west of the reservoir and centered over the oilfield. Subsidence at the reservoir site was about 0.9 m, compared to nearly 3.4 m at the subsidence bowl (Figure 3.22). Noteworthy was the fact that the southwest corner (viz., direction of maximum subsidence) had dropped more than the northeast corner, resulting in differential settlement across the dam of approximately 0.15 m. Figure 3.23 shows the subsidence of several local benchmarks between 1918 and 1974. Furthermore, a review of survey data from 1934 to 1961 and 1963 showed lateral movement in the direction of subsidence depression.

The Inglewood-Newport Beach Fault (an active major strike-slip fault) bisects this area with numerous tension relief faults branching off the main fault (see Figure 3.21). There was potential for differential movement along individual fault blocks. Indeed, a post-accident investigation revealed that differential fault block movement had caused rupturing of the asphaltic membrane used as a water seal over the floor of the dam.

Although fluid extraction and resultant subsidence were the prime contributors to the rupture of the reservoir, there is substantial evidence to indicate that water injection

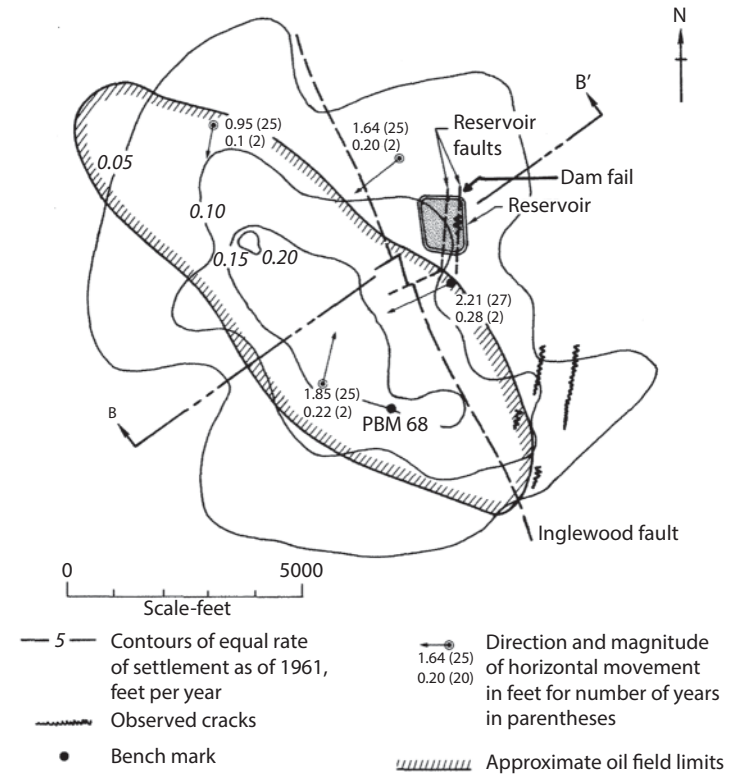

Figure 3.22 Horizontal movements and subsidence rates in the area of the Baldwin Hills Dam. (Modified after Lee, 1976, p. 301, figure 1.)

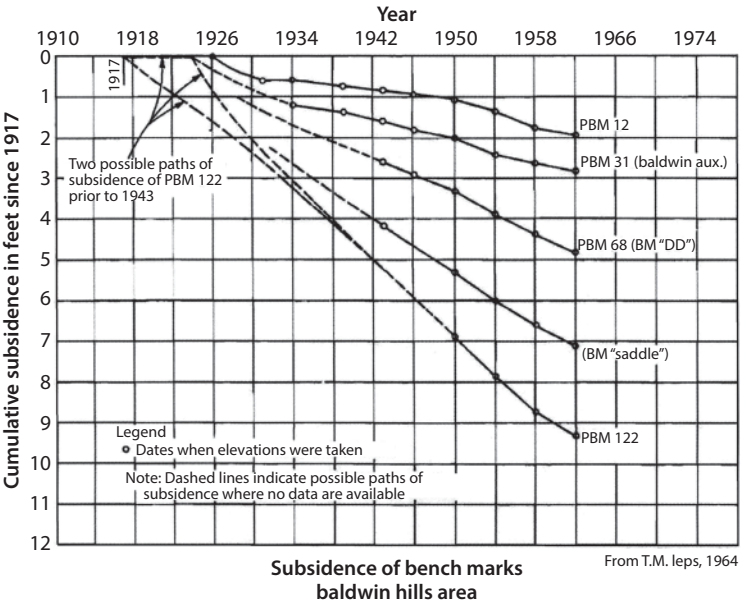

Figure 3.23 Subsidence of benchmarks, Baldwin Hills Dam area, Los Angeles, CA. (After California Department of Water Resources, Baldwin Hills Reservoir, Apr. 1964, figure 2.5, p. 8.)

to stimulate oil production was also a contributing factor as it caused differential uplift in portions of the reservoir and possibly led to fault movement (Hamilton and Meehan, 1971).

The main lesson to be learned is that differential subsidence was responsible for this disaster and property loss, which could have been avoided if proper monitoring for subsidence had been undertaken. Virtually every oilfield in the Los Angeles Basin has experienced similar subsidence as a result of fluid production (Chilingar and Endres, 2004).

3.5.1.2 Proposed Housing Development

Recently, a large housing development was proposed for the Baldwin Hills area, virtually over the mentioned subsidence area. Large retaining walls (exceptionally high) were contemplated to enhance views. If the project had been completed, these retaining walls would have been extremely vulnerable to a known geologically active and subsidence-prone area. The project was halted and the property later sold to the State for use as a public park (Chilingar and Endres, 2005).

This case history of the dam failure highlights the importance of proper planning and monitoring of the land movement in an area that has been heavily impacted by major faulting, oilfield subsidence, and secondary recovery. The problem was not uniform subsidence, but rather differential subsidence resulting in vertical stress on the dam. Although not discussed, there is also a likely problem of migration of gas from this oilfield, which currently does not pose a hazard as there is a lack of urban development over the Inglewood Oilfield.

3.5.2 Los Angeles City Oilfield, CA

The Los Angeles City Oilfield, CA, consists of three shallow major groups or layers of oil and water aquifers located about 1 mile north of the center of Los Angeles. The field, as shown in Figure 3.24, is a faulted homocline. The total thickness is about 1,500 ft of alluvial Miocene sediments with the average depth of pools ranging from 375 to 1,700 ft. The discovery well was drilled prior to 1892. About 1,250 wells have been drilled in this field. Many of these wells were drilled prior to record keeping. The wells drilled prior to the 1950s were not abandoned by today's standards. Intense residential and commercial development has occurred over this old field (see California Division of Oil and Gas, 1961).

3.5.2.1 Belmont High School Construction

The Belmont Learning Center, a proposed high school in downtown Los Angeles, was constructed over the Los Angeles City Oilfield. The site chosen was on a 0.14 km^2 parcel of land. This location is over the shallow oilfield that has a surface outcrop just north of the building site. The area is also part of the Elysian Park blind thrust fault system that has a generally east-west trend, which helps explain the uplifting and tilting of the petroliferous formation.

Oil wells in the area continue to produce from shallow oil deposits at a depth no greater than 213 m. Most of the wells producing oil today were drilled in the early 1900s,

Figure 3.24 Los Angeles Oilfield, contours on top of 1st Oil Sand. Productive area is shaded. (After California Division of Oil and Gas, 1961, p. 598.)

and lacked a proper cement completion. Although the gas production is minimal, all of the produced oilfield production gases are released to the atmosphere in the residential area above the wells. This includes four operational wells at the northwest corner of the school property.

Environmental studies, undertaken only after construction began, revealed oilfield gas seepage to the surface over most of the 0.14 km^2 parcel and the surrounding area, including the area directly under the school buildings. The project was abruptly halted when gas seepage was detected in the main electrical vault room of the project, just before the power was to be energized.

Soil gas studies revealed that methane (explosive levels) and other gases are migrating to the surface, including toxic gases such as hydrogen sulfide. Measurements at the surface revealed releases to the air of over 300 parts per million (ppm) of hydrogen sulfide (Endres, 1999, 2002). Investigation in the area revealed that the migration to the surface was common in this area. After a lengthy discussion, the project was completed and used as an administrative center rather than a school site.

This case history clearly identifies the caution required in evaluating the environmental suitability of developed sites located over oilfields, where there are migrating hydrocarbon gases, especially in the case of school construction. The State of California has passed recent legislation that requires direct participation by the Department of Toxic Substances Control (DTSC) in the future school site selection process in order to avoid a repeat of the Belmont failure.

3.5.3 Playa Del Rey Oilfield, CA

The Playa Del Rey Oilfield consists of two major groups or layers/pools of oil and water aquifers located about 13 miles southwest of the center of Los Angeles. This field, as shown in Figure 3.25, consists of Upper and Lower zones and is an anticline over a basement high. The overall thickness of the sediments is about 2,000 ft (alluvial Pliocene and Miocene) with the average depth of pools ranging from 4,000 to 6,400 ft. The discovery well was drilled in 1929. Over 320 wells have been drilled in this field and many when cement was not used or when cementing practices were neither regulated nor recorded. Overlying this oilfield is a dense, highly developed, residential area (see California Division of Oil and Gas, 1961).

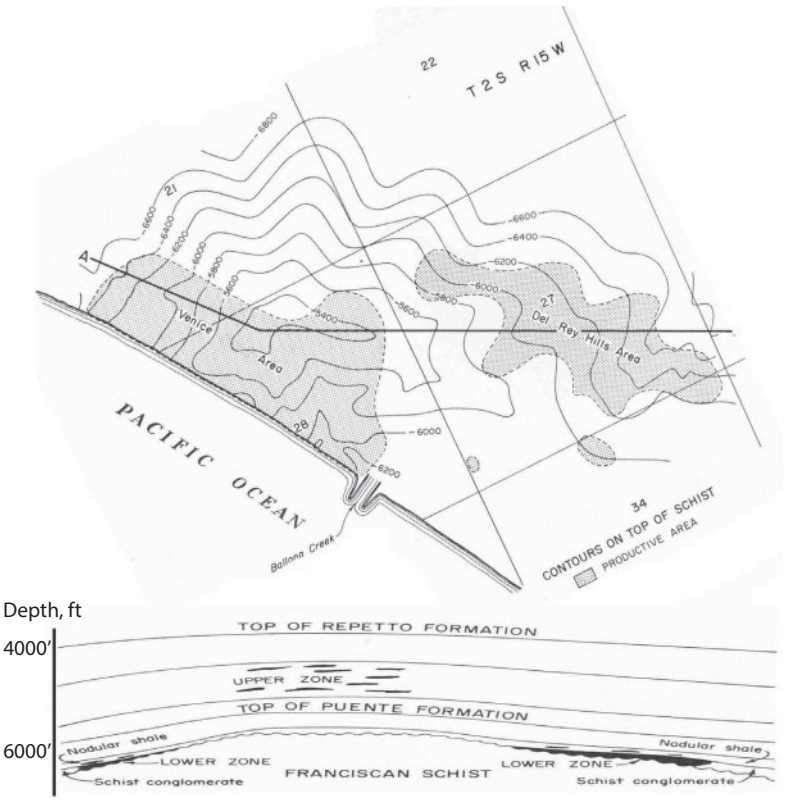

Figure 3.25 Playa Del Rey Oilfield with contours on top of the Franciscan Schist. (After California Division of Oil and Gas, 1963, p. 634.)

3.5.3.1 Playa Del Rey Marina Subsidence

The oldest periodic leveling surveys of the land over the Playa Del Rey Oil Field were made by the U.S. Coast and Geodetic Survey in 1925 to 1927 and 1931 to 1932. During this period of 6 years as much as 5 in. of subsidence was observed. Studies of old topographic surveys indicate that the Venice area has had little subsidence prior to the 1920s. A later survey in 1936 indicated that rate of subsidence had increased to 1 in. per year. Based upon later surveys, the subsidence rate appeared to decrease over the years from 1936 to 1970 (see Figure 3.26). Since 1964, the average rate of subsidence along Balboa Creek appears to be related to the depletion of ground water in underlying aquifers. Subsidence in the area of the Venice Oilfield is likely caused by a combination of oilfield production and regional ground water extraction (DOGGER). Today, the subsidence in this area appears to be primarily due to water withdrawals from the groundwater aquifer and possibly the compaction of sands, silts and muds near the surface. Little subsidence monitoring has occurred since 1970 despite the fact that fluids continued to be produced. The Marina Del Rey breakwater overlying this portion of the oilfield is likely subsiding as is the coastal area.

Oil production in the Venice area of the Playa Del Rey Field began in 1929. This area has produced 82% of the oil production of this field. A large reduction in reservoir pressure occurred from 1929 to 1944, when the initial pressures of 1,900 psi decreased to about 100 psi. Nearly all of the oil wells in the Venice area have been abandoned and there is currently little subsidence from hydrocarbon withdrawal; however, environmental problems exist as there is water extraction from the aquifer in the area and potential problems of gas migration through improperly abandoned wells (see Chilingar and Endres, 2004).

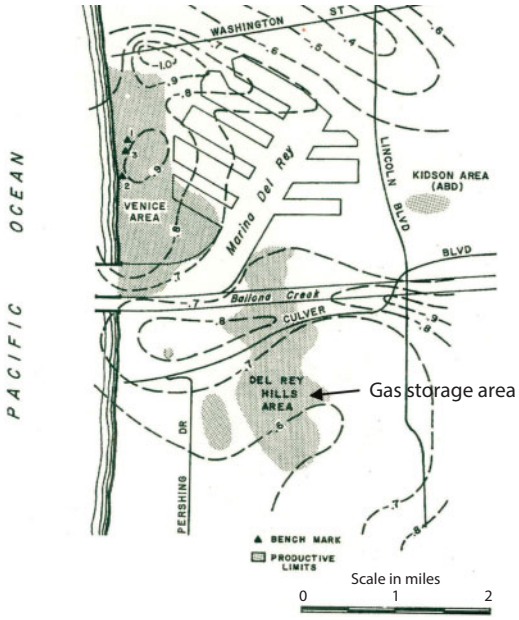

Figure 3.26 Subsidence in the Playa Del Rey Oilfield. Vertical movement in feet occuring between 1937 to 1970. (After California Division of Oil and Gas, 1961.)

3.5.4 Torrance Oilfield, CA

The Torrance Oilfield consists of three major groups of layers/pools of oil and water aquifers located about 8 miles southwest of the Long Beach, CA. This field as shown in Figure 3.27 consists of a faulted anticline and is considered by many as an extension of the Wilmington Oilfield. The overall thickness of the sediments is about 1,500 ft (alluvial Miocene) with the average depth of pools ranging from 3,100 to 4,400 ft. The discovery well was drilled in 1922. Over 1,541 wells have been drilled in this field, many of which were not cemented. Overlying this oilfield is a dense, highly developed, residential area. (See California Division of Oil and Gas, 1961.)

According to the California Division of Oil and Gas (1961), the greatest amount of subsidence in the Torrance Oilfield amounted to 0.8 ft from 1953 to 1970 and occurred where the Torrance Oilfield abuts the Wilmington Oilfield. In a 12-year period prior to 1953, subsidence reached 0.2 ft. Although subsidence is not a great problem for the Torrance Field, it presented a serious problem for the Redondo Beach marina area which overlies a portion of the Torrance Oilfield.

3.5.5 Redondo Beach Marina Area, CA

The Redondo Beach Oilfield is the western extension of the Torrance Oilfield located under the harbor area of the City of Redondo Beach (Figure 3.27). This area is about

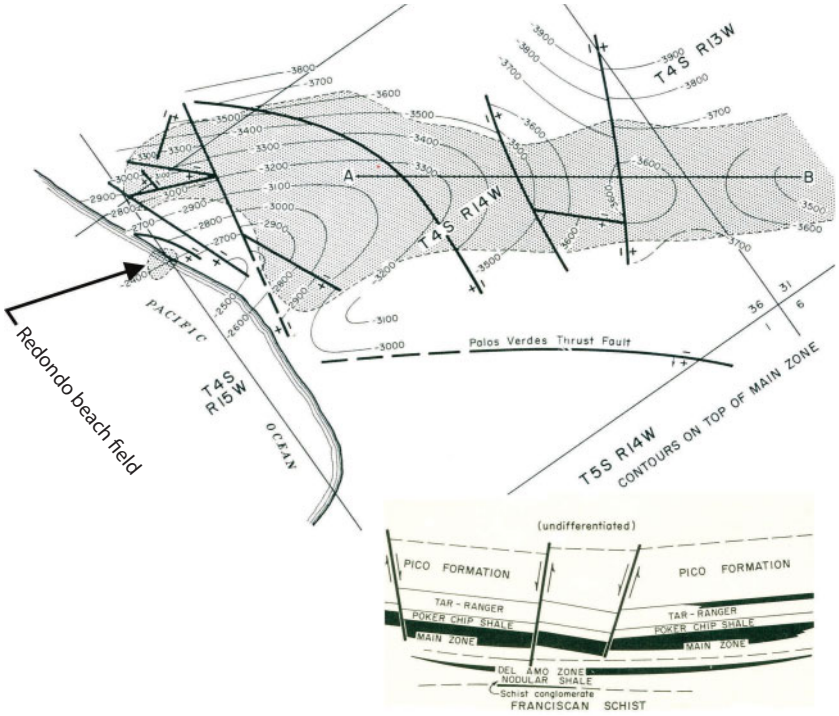

Figure 3.27 Torrance Oilfield showing the geologic structure on the top of Main Zone. The Redondo Beach Oilfield is an extened portion of the Torrance Oilfield as shown above. (After the California Division of Oil and Gas, 1961, p.674.)

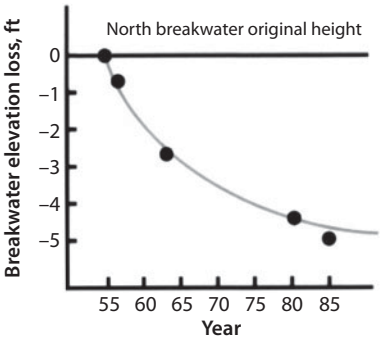

Figure 3.28 Changes in the North Redondo Beach breakwater elevation during the period of 1955 to 1980. (Data obtained from U.S. Army Corps of Engineers; in: Robertson *et al.*, 2012.)

12 miles northwest of the city of Long Beach, CA. This edge area of the Torrance Oilfield consists of layers of hydrocarbon-bearing sands intermixed with layers of water-bearing sands. Initial production in this area was initiated in 1943, but the area remained relatively undeveloped until the City of Redondo Beach authorized drilling of directional wells under the marina and breakwater area. Thus, the fluid production (oil and water) from this area increased significantly.

During a winter storm in January 1988, waves overtopped a breakwater constructed by the U.S. Army Corps of Engineers built to protect the Redondo Beach King Harbor Boat Marina and surrounding commercial structures. Subsidence had lowered the height of the breakwater (Figure 3.28), which resulted in the destruction of the Portofino Inn and many facilities in the area.

The heights of benchmarks used by the U.S. Army Corps of Engineers to construct the breakwater were based on a U.S. Coast and Geodetic Survey of 1945. These benchmarks were assumed to be fixed, but were actually lower due to the subsidence as a result of the high fluid production from the Redondo Oilfield. The Corps of Engineers were not aware of subsidence in this area until 1985. The surveys in 1985 showed the breakwater crests to be as much as 1.5 m below the original design elevations. The breakwater no longer had the necessary height to protect the city. Nothing was done to protect the harbor or to warn the commercial establishments prior to the storm of January 1988. This disaster could have been averted if the subsidence had been recognized and the breakwater elevation increased to the proper levels (see Chilingar and Endres, 2004).

3.5.6 Salt Lake Oilfield, CA

The Salt Lake Oilfield is located in Los Angeles, CA, east of the town of Beverly Hills. This field consists of four major groups of layers/pools of oil and water aquifers and is a stratigraphic trap along two plunging anticlinal noses (Figure 3.29). The overall thickness of sediments is about 1,000 ft (alluvial Pliocene and Miocene) with the average depth of pools ranging from 1,000 to 2,850 ft. The discovery well was drilled in 1902. Over 500 wells have been drilled in this field, many when cement was not used or when cementing practices were neither regulated nor recorded (see California Division of Oil and Gas, 1961).

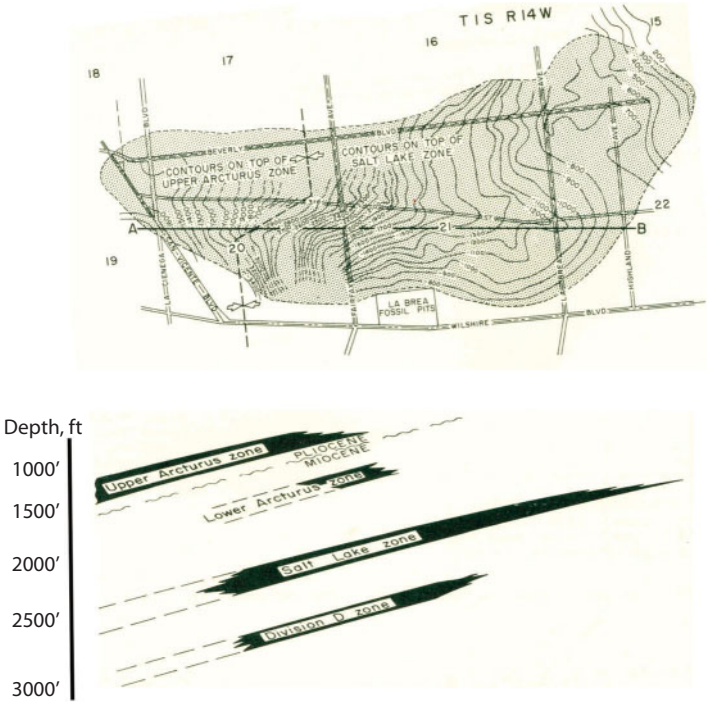

Figure 3.29 The cross-section and geologic structure of the Salt Lake Oilfield. (After California Division of Oil and Gas, 1961, p. 652.)

Overlying this oilfield is a dense, highly developed, residential area and the La Brea Tar pits. The tar pits are an excellent example of fluids (oil and gas) migrating up along a fault to the surface. After a rainfall in this area, at cracks in the sidewalks, paved areas, and roads, one can observe small bubbles of gas. When captured, this gas burns when ignited. Further examination of the paved areas after the rainfall shows small quantities of oil that has been carried by the gas and water to the surface. The area over the Salt Lake Oilfield has had a history of fires and explosions. It is also subjected to surface subsidence, which is reflected in broken sidewalks, paved areas, etc.

3.5.7 Santa Fe Springs Oilfield, CA

The Santa Fe Springs Oilfield consists of 10 major groups of layers/pools of oil and water aquifers located about 12 miles southeast of the center of Los Angeles. The structure of this field is a dome (Figure 3.30). The overall thickness of the sediments is about 7,000 ft (alluvial Pliocene and Miocene) with the average depth of pools ranging from 3,580 to 9,100 ft. The discovery well was drilled in 1919. Over 1,283 wells have been drilled in this field and many when cement was not used or when cementing practices were neither regulated nor recorded. Overlying this oilfield is a residential area. (See California Division of Oil and Gas, 1961.) Many of the concrete buildings, sidewalks, paved streets show evidence of cracking, which is probably due to differential subsidence.

The authors determined the integrity of operational oilwells in the Santa Fe Springs Oilfield in the 1990s. To facilitate this review, a time period was selected after heavy

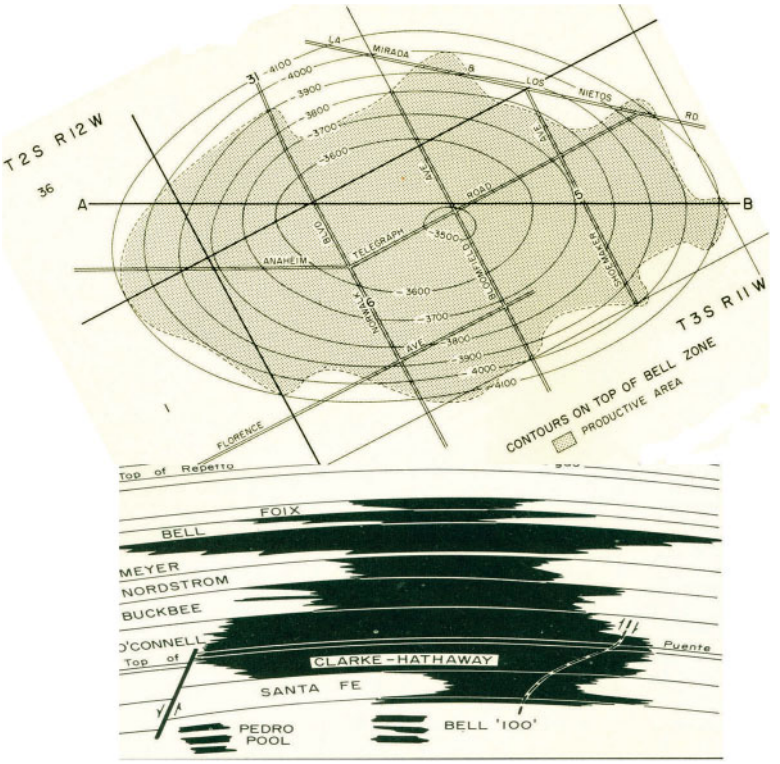

Figure 3.30 Structure and cross-section of the Santa Fe Springs Oilfield. Conturs on to of the Bell Zone. (After California Division of Oil and Gas, 1961, p. 662.)

rains in which the well cellars were partially filled with water. This allowed observation of gas bubbles seeping to the surface along the side of the well casings. Results were systematically recorded for more than 50 wells, some of which were used for waterflooding operations at pressures approaching 84.4 kg/cm^2. Approximately 75% of the wells were found to be leaking small amounts of gas.

Waterflooding for enhanced oilfield recovery can be a dangerous practice if one does not monitor the maximum injection pressures that could result in hydraulic fracturing of the formation, as these fractures could form pathways for the migration of gas toward the surface. Repressurization of an oilfield by way of water injection or gas injection also requires careful examination of the integrity of both the producing and the abandoned wells throughout the oilfield. A soil gas monitoring program must be implemented in the vicinity of each well and surface fault, to detect the leakage of gas to the surface.

3.5.8 Wilmington Oilfield, Long Beach, CA

The Wilmington Oilfield is located approximately 20 miles south of downtown Los Angeles, California in the Wilmington-Long Beach Harbor area (see Figure 3.31). The field is one of a chain of oil accumulations that overlie a basement high extending for approximately 21 miles in a southeasterly direction from the Torrance Oilfield to

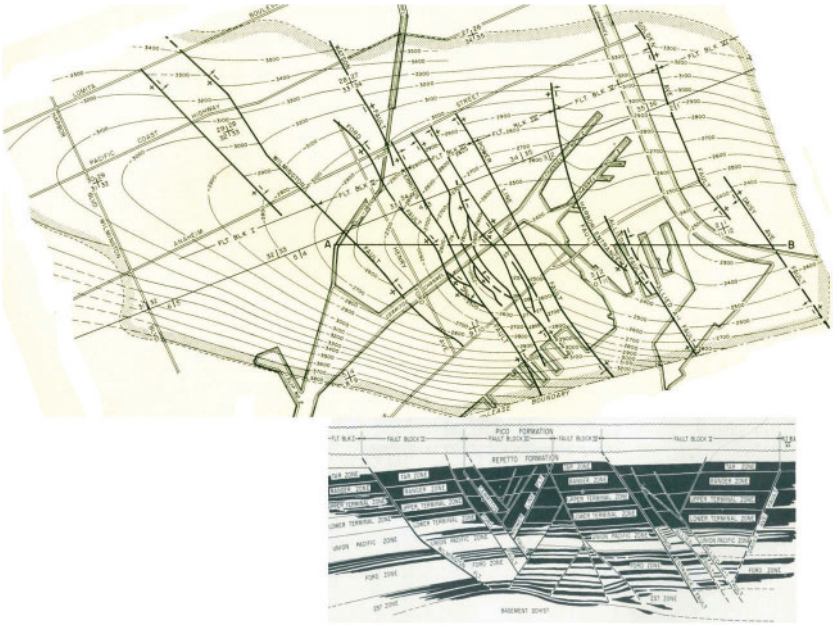

Figure 3.31 Structure and cross-section of the Wilmington Oilfield. Contours on top of the Ranger Zone. (After California Division of Oil and Gas, 1961, pp. 684 & 685.)

the Huntington Beach offshore pool. The Wilmington oilfield consists of five major groups of layers/pools of oil and water aquifers and is a gentle faulted anticline overlying the Franciscan Schist. The overall thickness of sediments is about 4,500 ft (alluvial Pliocene and Miocene) with the average depth of pools ranging from 2,200 to 11,000 ft. The discovery well was drilled in 1932 (Colazas and Strehle, 1995; in: Chilingarian *et al.*, 1995). Over 6,150 wells have been drilled in this field, many when cement was not used or when cementing practices were neither regulated nor recorded. Overlying this oilfield is a dense, highly developed, industrial, residential, and major seaport area.

The Wilmington Oilfield was officially discovered in 1931, but intensive development did not begin until 1936. By 1951, yearly production was more than 50 million barrels of oil, along with about 53,000 MMcf of gas. By 1965, approximately 3,500 wells had produced about one billion barrels of oil from 7,825 acres. Until 1965, production was confined to the western portion of the Wilmington Oilfield. With the successful solution to the subsidence problem in this portion, development was started in the eastern portion (Long Beach Unit) which extends east of the harbor area in the City of Long Beach. From the Wilmington Oilfield's discovery in 1931 to the end of 1990, more than 2.34 billion barrels of oil and 1.1 billion Mcf of gas have been produced from the Wilmington Oilfield. Current daily production is about 71,000 barrels of oil and 1,081,000 barrels of water. Remaining reserves for the field are approximately 600 million barrels (Colazas and Strehle, 1995; in: Chilingarian *et al.*, 1995).

According to Colazas and Strehle (in: Chilingarian *et al.*, 1995), more than 1,000 wells were drilled during the initial development of the field from 1932 to 1942. The rapid

rate of fluid production led to a subsidence problem. First noticed in 1941, with a drop of more than a foot, it wasn't initially clear what was causing the subsidence. In 1953, a $30-million program of waterflooding was initiated to slow down the rate of subsidence. Figures 3.32 and 3.33 demonstrate a 9-meter subsidence at the center of the depression in 1954. Reinjected water has helped slow down the rate of subsidence and in some areas the surface has rebounded due to water injection. The area affected by subsidence was about 50 km^2.

Since the early 1940s, the Wilmington Oilfield has been plagued by an unusually large amount of land subsidence. This was an especially critical problem because the

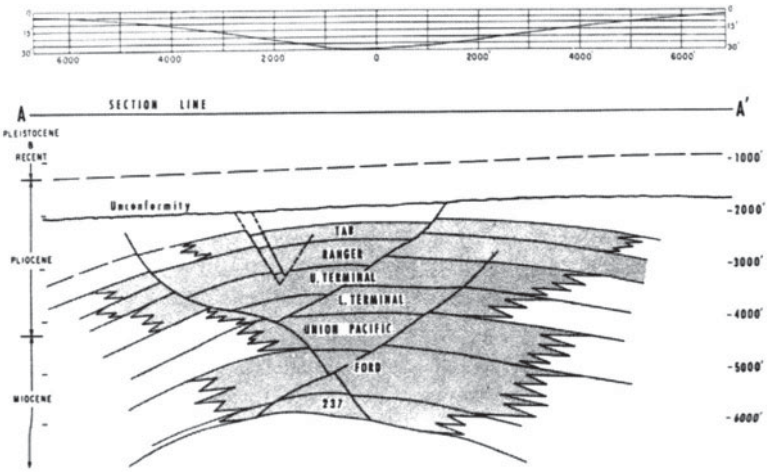

Figure 3.32 Northwest-southwest cross-section of the Wilmington Oilfield showing profile of subsidence bowl on top of the Wilmington anticline. (After Colazas, 1971; in: Chilingarian *et al.*, 1995, p. 297, figure 6.10.)

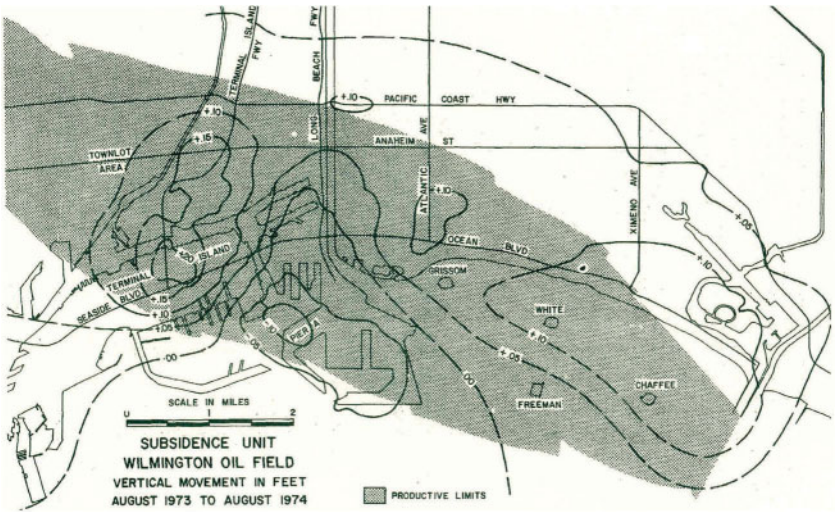

Figure 3.33 Wilmingtion Oilfield subsidence unit: 1973 to 1974 subsidence in feet. (After California Division of Oil and Gas, Sixth Annual Report.)

field is located under the Long Beach and Los Angeles Harbor areas. The City of Long Beach, U.S. Navy, and Southern California Edison Company engaged qualified engineers, geologists and soil experts to investigate the causes and assist in finding a solution to the potential destruction of the industrial, port and naval facilities within this area of subsidence. They concluded that restoration and maintenance of subsurface pressures by injection of water would reduce further subsidence. The result of this decision was one of the largest waterflooding programs in the world. (See Colazas and Strehle, 1995; in: Chilingarian *et al.*, 1995, p. 286.)

Currently, field injection of water is in excess of 1.2 million barrels per day into 700 injection wells. With this program in effect, subsidence was stopped. In the areas of maximum repressuring the surface has rebounded over 1 foot.

The sequence of rocks encountered in the Wilmington Oilfield, including the depth, net and gross thickness of the sediments, are presented in Tables 3.2 and 3.3 and in Figures 3.32, 3.34 and 3.35. Zone names, boundaries and markers within the zones are those designated by the City of Long Beach, its contractors and other operators in the Wilmington Oilfield. (See Colazas and Strehle, 1995; in: Chilingarian *et al.*, 1995, p. 287.)

The oil-bearing formations in the Wilmington Oilfield range in thickness from 6,400 to 7,500 ft. The age of these formations ranges from Jurassic (?) for the Catalina Schist-Basement complex to the early Pliocene (Repetto) for the Tar Zone.

There are seven recognized productive zones in the field. In increasing depth sequence these are the Tar, Ranger, Upper Terminal, Lower Terminal, Union Pacific, Ford and 237-Basement. Table 3.2 lists these zones, their approximate depths at the crest of the anticline, gross thickness and net oil sand thickness. (See Colazas and Strehle, 1995; in: Chilingarian *et al.*, 1995, p. 290.) The upper four zones are of great economic importance, not only because they have produced the greatest amount of oil, but also because they have made the greatest contribution to subsidence. In addition, they have been the subject of numerous compression tests conducted by investigators. Colazas and Strehle (1995; in: Chilingarian *et al.*, 1995) have described the most productive zones in the Wilmington Oilfield as follows (See Figure 3.35):

1. The **Tar Zone** consists primarily of unconsolidated fine- to coarse-grained, fairly well sorted lenticular sands, with soft, light brown to olive green interbedded siltstones. The sands average approximately 40% of the bulk of the zone.
2. In the **Ranger Zone**, the top of the Miocene is found near the "G" electric log marker (see Figure 3.34). The Ranger Zone consists of alternating layers of fine- to coarse-grained, fairly well to poorly sorted unconsolidated sands. The Pliocene siltstones are firm, sandy and have a distinctive brown to olive green color, whereas the Miocene siltstones and shales are dark brown to grey, becoming progressively darker with depth. The Miocene shales are well laminated, diatomaceous and are locally referred to as "poker chip" shales. They average approximately 40% of the bulk of the zone. (See Colazas and Strehle, 1995; in: Chilingarian *et al.*, 1995, p. 290.)
3. The **Upper Terminal Zone** consists primarily of soft to easily friable very fine-to medium-grained, fairly well sorted arkosic sands, interbedded

Table 3.2 Geologic formation data, oil producing zones and summary of reservoir data for the various zones of the Wilmington Oilfield, CA. (After Colazas, 1971; in: Chilingarian *et al.*, 1995, table 6.1, p. 288.)

Age	Formation	Form. Thick., ft	Prod. zone	Elect. log mark.	Zone thick., ft	Sand interval in zone	Oil gravity, °API	Average porosity, %	Aver. perm., mD	Lithology and remarks
Recent	Unnamed	± 1000	Gaspur		± 189					Fresh water sands, gravels and clays
Pleistocene	San Pedro		200/400 Silverado		± 220 ± 600					
Pliocene	Upper Pico	± 800	Upper Pico		± 800					Alternating sands and siltstones
	Middle Pico	0 to 200	Upper Pico		0 to 200					Sands and siltstones
Unconformity										
Pliocene	Repetto	700 to 1400	Tar	Old area, *S* to *F* New area, *T* to F_o	300 to 400 200 to 400	± 40	12 to 15	35	± 1000	Grey and green shales, siltstones & sands at top grading too brown and fine grained at bottom
			Upper Ranger	Old area *F* to *G* New area F_o to *G*	400 to 500 600 to 700	± 40	12 to 25	35	700 to 1500	
Miocene	Puente	± 5,300	Lower Ranger	Old area *G* to *HX* New area *G* to HX_1	150 to 250	± 30	12 to 25	35	700 to 1500	Hard brown shales and sands; sands are fine and unconsolidated at top, becoming firmer coarser grained at bottom
Unconformity										
	Upper Mohnian		Upper Terminal	Old area *HX* to *AA* New area *HX* to *AA*	400 to 850 400 to 900	50 to 70 60 to 80	14 to 25 14 to 25	35 35	450 450	
			Lower Terminal	*AA* to *AE*	500 to 800	60 to 80	20 to 31	30	450	
			Union Pacific	*AE* to *AM*	400 to 900	25 to 30	27 to 32	20 to 25	150	
			Ford	*AM* to *BA*	750 to 1200	25 to 35	28 to 32	25	100	
			"237"	*BA* to basement	200 to 2650	20 to 40	28 to 32	25	275	
Unconformity										
Jurassic	Basement				± 100					Schist, fractured

with layers of claystone, siltstone and occasional hard sandstone calcareous members locally referred to as "shells". The lower sand members are generally coarser than the upper members. The sands average approximately 70% of the bulk of the zone.

4. The **Lower Terminal Zone** consists primarily of sands that are similar to the Upper Terminal Zone, but somewhat coarser and more massive,

Table 3.3 Depth and thickness of Wilmington Oilfield oil zones. (After Colazas, 1971; in: Chilingarian *et al.*, 1995, table 6–11, p. 291.)

Productive Zone	Depth, ft	Zone gross thickness, ft	Net oil zone thickness, ft
Tar	2,050 to 2,350	200 to 400	50 to 95
Ranger	2,350 to 2,850	400 to 750	220 to 420
Upper Terminal	2,850 to 3,350	600 to 750	400 to 500
Lower Terminal	3,350 to 3,850	700 to 800	450
Union Pacific	3,850 to 4,500	900 to 950	230 to 285
Ford	4,500 to 5,400	950 to 1,200	500 to 600
"237"	5,400 to 5,600	2,650	75
Basement (Schist)	±5,600		

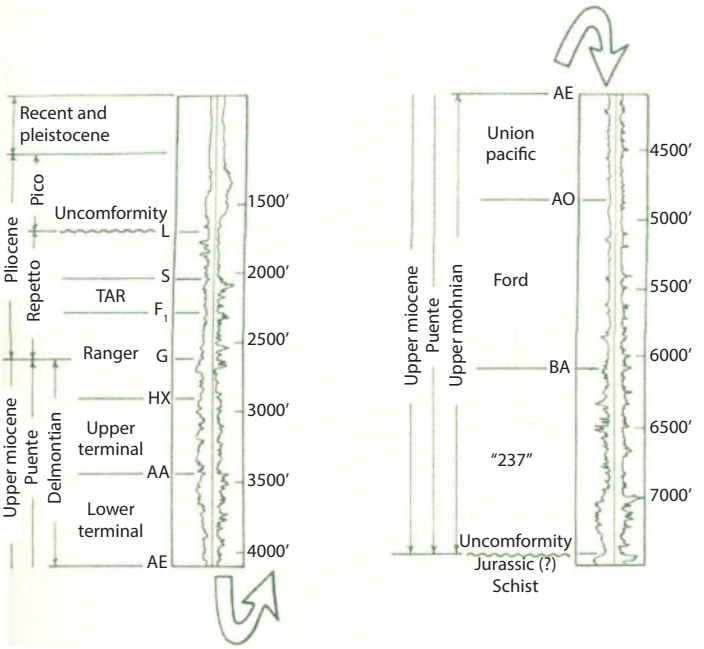

Figure 3.34 Composite electric log showing stratigraphic sections and markers of the Wilmington Oilfield. (After Colazas, 1971; in: Chilingarian *et al.*, 1995, p. 287, figure 6.2.)

becoming firmer with depth. The siltstones and shales are well indurated and have a dark grey color. The sand content is estimated at 60% to 80% of the bulk of the zone.

The lower three zones are comprised of the Union Pacific, Ford and 237 zones and consist primarily of thin to massive sands ranging in grain size from fine to coarse and pebbly. The shales vary from soft claystones and mudstones to true, hard, dense shales. Generally, the amount of subsidence in these zones is considered to be small. (See Colazas and Strehle, 1995; in: Chilingarian *et al.*, 1995, p. 291.)

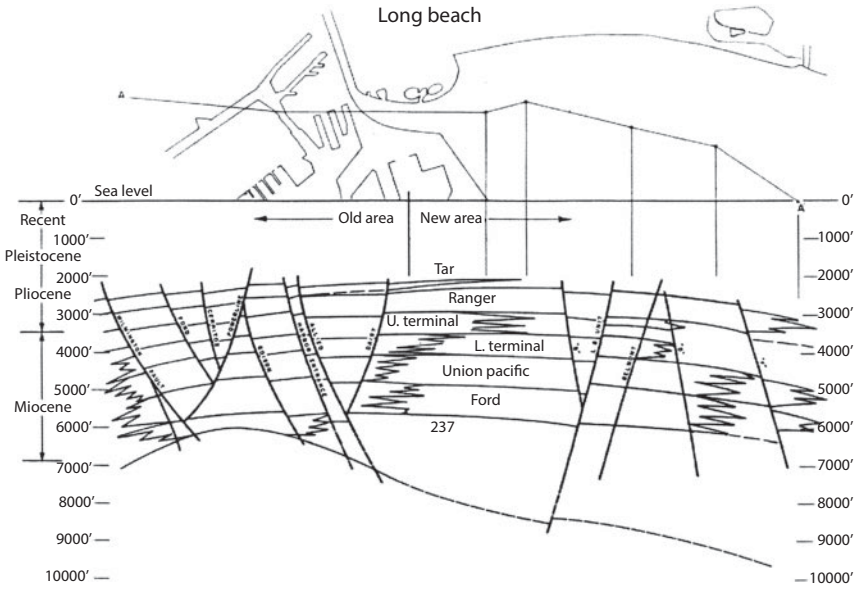

Figure 3.35 Geologic section along axis of Wilmington Anticline showing approximate water/oil limits. (After Mayuga, 1970; in: Chilingarian *et al.*, 1995, p. 289, figure 6.3.)

The sands of the Union Pacific and Ford zones are thin-bedded to massive, fine-to coarse-grained, fairly well to poorly sorted and are interbedded with hard, dense, dark grey to black siltstones and shales. Hard sandstone members, previously called "shells," are more prevalent in these formations. Usually, during coring operations the core barrel has to be pulled out of the hole in order for the "shells" to be drilled with a rock bit and, thus, resume coring operations. The Union Pacific Zone is thinly bedded, with the sands becoming massive, coarse and pebbly in the lower part of the Ford Zone. The degree of induration of sediments is, in general, directly related to the depth of burial. The hard dense shales in the deeper horizons grade to siltstones, soft claystones and mudstones. (See Colazas and Strehle, 1995; in: Chilingarian *et al.*, 1995, p. 291.)

The 237 Zone consists of 2,000 ft of massive, poorly sorted, locally friable to well cemented arkosic sandstones interbedded with dense black shales. The lower 650 ft consist of black, dense, locally fractured, well-bedded shale, with brown phosphate nodules and occasional thin interbeds of hard, medium- to coarse-grained sandstone. The fractured nodular shale and the upper 100 ft of fractured basement is oil productive in the East Wilmington portion and is known as the "D-118" sub-zone.

The Wilmington Oilfield structure is a large, broad, asymmetrical anticline having a northwest-southeast axial trend. The low angles of dip of the unconsolidated beds near the crest, the presence of tension faulting and the heavy overburden result in an unstable structure susceptible to compaction. The structure is cut by numerous major and minor faults thus dividing it into hundreds of fault blocks, down-dropped wedges and individual reservoirs.

The Wilmington Oilfield geologic structure and the geologic structures surrounding it are extremely complex. Flow paths and pressure conduits exist peripheral to the field and there is no guarantee that all fluids injected into the reservoirs for subsidence

control will remain within the Wilmington Oilfield structure. As a matter of fact, chances are they will not. Constant surveillance and monitoring of pressures are and will be of extreme importance for a considerable time into the future in order to prevent a renewal of Long Beach's past disastrous subsidence.

According to Colazas and Strehle (1995; in: Chilingarian *et al.*, 1995, p.291), geodetic leveling surveys established that the San Pedro-to-Seal Beach coastal areas have been naturally subsiding since the early 1900s. Since the 1930s, survey crews from the cities of Los Angeles and Long Beach, the United States Coast and Geodetic Survey, and other agencies have regularly conducted leveling surveys across the Wilmington area. Generally, during this time, the surveys indicated an average subsidence rate of between 0.02 and 0.04 ft per year.

During the summer of 1941, the U.S. Coast and Geodetic Survey conducted a first order leveling survey from the cities of Redondo Beach and San Pedro to a point east of Long Beach over the same level network they had established in 1931. This latest survey showed a subsidence of 0.2 ft at the west city boundary of Long Beach with a gradual increase to 1.3 ft at the easterly end of Terminal Island and then gradually decreasing to practically zero under the City of Long Beach. Inasmuch as the area of maximum subsidence coincided with a Navy dewatering project for the construction of a dock, it was thought that subsidence would stop and perhaps part of the lost elevation would be recovered when the dry dock construction was completed. In July 1945, the U.S. Coast and Geodetic Survey confirmed leveling surveys of the Long Beach Harbor Department which indicated that the easterly end of Terminal Island had subsided 4.2 ft from 1931 to 1945. The results of these surveys and other data indicated that progressive ground movement, oilfield development and fluid production were perhaps dependent events.

Subsidence has caused a great deal of damage because the surface land was the center of a busy port and industrial area. By 1962, the rate of subsidence had been greatly reduced as a result of reinjection of water and subsidence was limited to an area of 8 km^2 as a result of waterflooding. Up to this date, little uplift from waterflooding had occurred. The cumulative subsidence costs to 1962 were estimated at $100 million (http://www.longbeach.gov/lbgo/about-us/oil/subsidence/). Figure 3.36 shows the relationship between the cumulative production (oil and water production less water injection) and cumulative total subsidence for the Wilmington Oilfield from 1937 to 1967 (Mayuga and Allen, 1998). A historic presentation of net oil production, water injection and subsidence is presented in Figure 3.37.

Along with the problems of subsidence, there also have been several minor earth movements between 1947 and 1952. These earthquakes were caused by slippage along several nearly horizontal planes of shale located at depths between 1,500 ft and 2,000 ft. Well damage in the Wilmington area alone was in the millions of dollars. A large amount of horizontal movement was also occurring on the surface. Most surface and near structures such as railroads, pipelines, and transit sheds were cracked, buckled, and bowed due to subsidence (Colazas and Strehle, 1995; in: Chilingarian *et al.*, 1995, p. 294).

While various studies were being made by experts to determine what was causing subsidence, the subsiding area continued to grow, gradually assuming shape of a 20-square-mile area of Long Beach, CA, shown in Figure 3.10. The subsidence rate increased to a maximum in 1951 when the center of the bowl was sinking at a rate

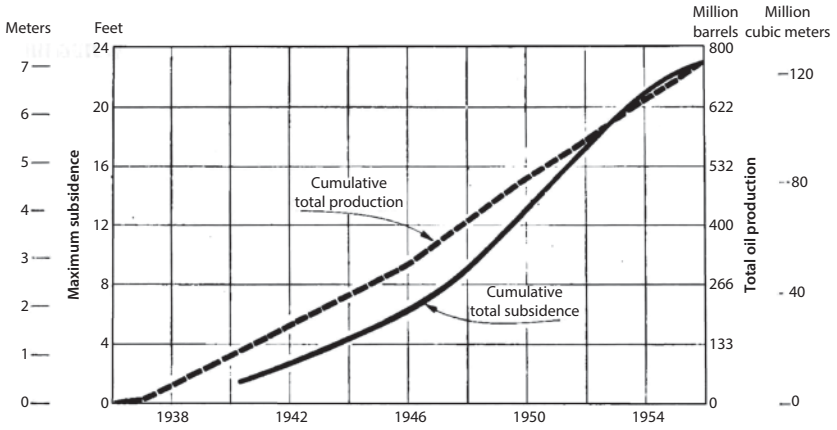

Figure 3.36 Curve showing cumulative total production versus cumulative total subsidence of the Wilmington Oilfield, CA (After Mayuga and Allen, 1998.)

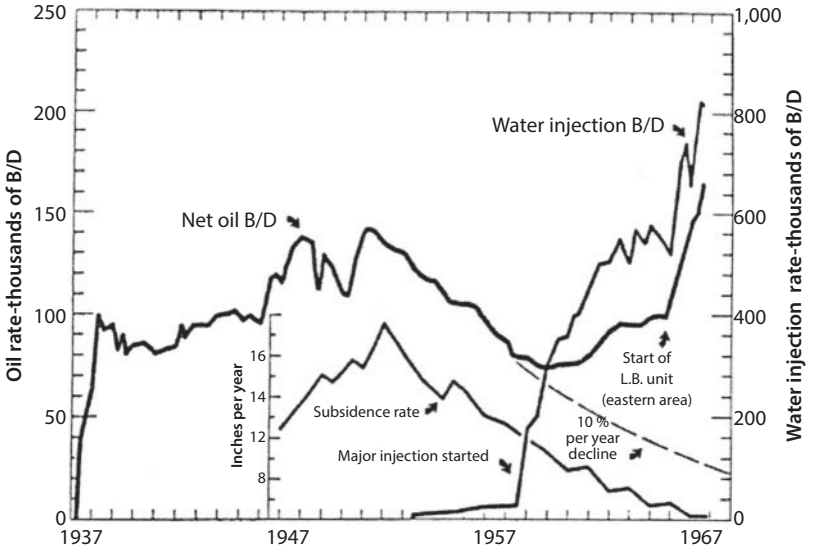

Figure 3.37 Historical oil production, water injection and subsidence in the Wilmington Oilfield, CA. (After Mayuga and Allen, 1998.)

of more than 2 ft per year and the field had attained its maximum production of oil and gas (see Figure 3.37). Cumulative subsidence reached 15 ft. By 1952, the ground elevation of the Navy Shipyard had sunk below high tide water. By 1958, the total area affected covered over 20 square miles. Horizontal surface movements of more than 10 ft accompanying vertical subsidence caused extensive damage to the existing structures, oil wells, and the U.S. Navy installations. Early 1940s groundwater pumping contributed to subsidence, but the majority of the subsidence resulted from the oil and gas extraction. An average of 42 gallons of water per gallon of oil have been produced by this oilfield (http://www.longbeach.gov/lbgo/about-us/oil/subsidence/).

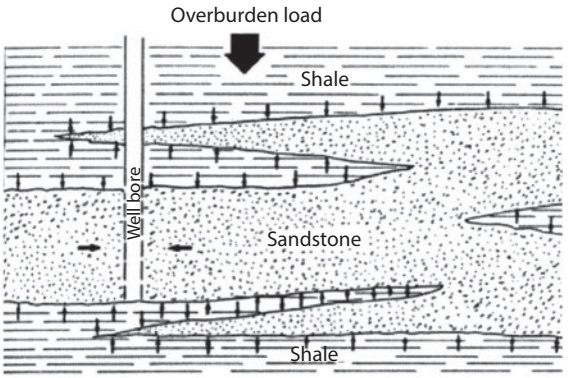

Figure 3.38 Diagrammatic shale-water flow to low-pressure permeable sands. (After Colazas and Strehle, 1995; in: Chilingarian *et al.*, 1995.)

Gilluly *et al.* (1948) prepared a report on subsidence for the Wilmington Oilfield. A modification of this report was later published in the Bulletin of the Geological Society of America (1949). After considering a number of possible causes for subsidence, they demonstrated that the progressive surface depression was likely due to compaction of sediments in the oil zones. They examined the evidence and found that the history of the surface movement since 1937 could be explained by compaction of reservoir sands.

At about the same time, Harris (1945) made an extensive study for the U.S. Navy, reaching the same conclusion except that he attributed the subsurface compaction to the reservoir shales.

Hudson (1957) and other investigators considered all the following factors in their examination of compaction and surface subsidence in the Wilmington Oilfield:

1. Lowering of hydraulic head due to groundwater withdrawals.
2. Oil reservoir sand compaction owing to fluid withdrawals.
3. Compaction of shales and siltstones interbedded with the oil sands.
4. Surface loading by structures.
5. Vibrations due to land usage.
6. Regional tectonic movements.
7. Lack of rigidity of the Wilmington structure.
8. Movements along known faults in the field.
9. A lack of preconsolidation in the sediments.

Most investigators who have studied the problem concluded that withdrawals of fluids from the oil zones and the consequent lowering of pressure within these zones resulted in compaction of the oil sands and the interbedded siltstones and shales. The relative amounts of compaction between the sands and shales can be inferred from both laboratory compaction and porosity tests and from oilfield operational practices and measurements.

Subsequent to the early studies, some of which concluded that shales were the compacting material and some that sands were, more data has been accumulated and new

interpretations prepared. For example, based upon extensive laboratory compaction studies, Chilingarian *et al.* (1995), concluded that sands are just as compactible as clays.

Allen and Mayuga (1969) attributed Wilmington Oilfield subsidence to the following causes: (1) reservoir pressure decline due to rapid development and production of fluids; (2) the unconsolidated reservoir sands having little or no cementation; (3) the thin, interbedded shales being susceptible to drainage; (4) the relatively flat overburden supplying a constant load; (5) the lack of severity of folding causing a weak structure that is incapable of supporting the overburden; and (6) normal tension faulting, which weakens the Wilmington structure, whereas compressional faulting would have strengthened it.

The actual mechanics of compaction are believed to include rearrangement of sand grains, plastic flow of soft minerals, some plastic deformation of sand grains, and perhaps some crushing of grains or breakage of sharp corners in exceptionally low-pressure reservoirs or pools. Limited crushing of sand grains was observed in the laboratory but the samples were dry and the pressure ranged to 2,500 psi.

Due to the high permeability of the sands, a fairly rapid shift in grain-to-grain loading results when fluid pressures are lowered, creating a rapid loss of pore volume. In the case of the shales, however, their extremely low permeability results in a slow transfer of load from the pore fluids to the skeletal structure as the fluids are slowly forced from the shales into the relatively lower pressured and more permeable sand members (Figure 3.38).

The length of time required for the Wilmington sands and shales to approach equilibrium has been investigated by Allen and Mayuga (1969), Colazas (1971), Converse Engineering Company (1957) and numerous other investigators. The general conclusion of all investigators was that the degree of compaction is a function of unit thickness, depth of burial, cementation, and permeability. Generally, the deeper the burial, the less the compaction due to the existing natural consolidation state of the sediments.

According to van der Knaap and van der Vlis (1966), the time for a Venezuelan shale or clay layer to reach equilibrium increases as the square of the thickness. They found that thin shales or clay layers reached equilibrium within a few days to a few weeks, whereas an 8-ft shale might require 16 years and a 20-ft shale might require upwards of 50 years (Figure 3.39).

Sawabini *et al.* (1974) determined the effective bulk compressibility $\left[\frac{1}{V_{bi}}\left(\frac{\partial V_b}{\partial p_e}\right)_{p_t T}\right]$ and pore compressibility $\left[\frac{1}{V_{pi}}\left(\frac{\partial V_p}{\partial p_e}\right)_{p_t T}\right]$ of unconsolidated sands from the Wilmington Oilfield, where V_{bi} = initial bulk volume of sample, cm^3; V_{pi} = initial pore volume of sample, cm^3; p_e = effective pressure ($p_t - p_p$), psi; p_t = total overburden pressure, psi; and p_p = pore pressure, psi. There is an inverse relationship between the effective (grain-to-grain) pressure and the compressibility. The effective bulk compressibility ranged from 7.4×10^{-4} to 3×10^{-5} psi^{-1} in the 0 to 3,000 psi effective pressure range; whereas the effective pore volume compressibility ranged from 1×10^{-3} to 1×10^{-4} psi^{-1}. The void ratios in the same pressure range varied from 0.85 to 0.18.

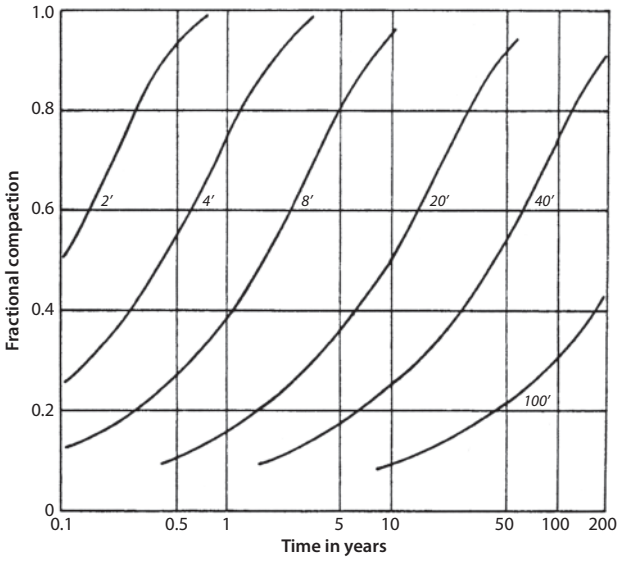

Figure 3.39 Fractional compaction of clay layers of various thickness following instantaneous drop in reservoir pressure. (After van der Knaap and van der VIis, 1966; in: Colazas and Sterhle, 1995, figure 6.12, p. 300.)

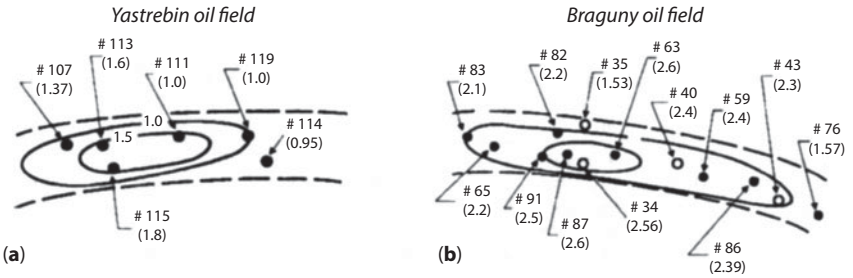

Figure 3.40 Subsidence of the Earth's surface at the Yastrebin Oilfield (A) and Braguny Oilfield (B). Solid circles indicate borehole locations; numbers between parentheses are Δh_{calc}, values in m. In the case of open circles, Δh_{mean} values are measured. (After Dobrynin and Serebryakov, 1989, figure 124, p. 282; also in: Serebrybryakov and Chilingar, 2000, figure 2, p. 425.)

3.5.9 North Stavropol Oilfield, Russia

Ternova and Belov (1965, in: Dobrynin and Serebryakov, 1989) described subsidence at the North Stavropol Oilfield in Russia. Maximum subsidence of 14.1 cm was observed during 1961–1962 after 5–6 years of production (Figure 3.40). They proposed the following formula for the determination of subsidence (Δh) of the productive horizon:

$$\Delta h = h \Delta p \beta^* \tag{3.4}$$

where h is the thickness of compacting formation, Δp is compacting pressure (MPa), and β^* is the coefficient of formation compressibility (MPa^{-1}). Eq. 3.4 takes into consideration only the productive horizon. Because the only subsidence considered in Eq. 3.4 is that of

the productive horizon, the actual surface subsidence was five times higher than that calculated by this equation.

$$\beta^* = \phi_f \beta_b + \beta_m \tag{3.5}$$

where ϕ_f is the producing formation porosity (fraction), β_b is bulk compressibility of liquids (cm^2/kg), and β_m is matrix compressibility (cm^2/kg). Pore compressibility, β_p, is equal to

$$\beta_P = \frac{1}{V_p}\left(\frac{dV_p}{dp_p}\right) \tag{3.6}$$

where V_p is volume of the pores (cm^3), and p_p is pore (fluid) pressure (kg/cm^2). The formula for the coefficient of irreversible compaction (β_i, MPa^{-1}) (Dobrynin, 1970) is:

$$\phi = \phi_o e^{-0.014\beta_i D} \tag{3.7}$$

where ϕ_0 is the initial porosity of clays after deposition, and ϕ is porosity of clays at a burial depth D (m).

The compaction of associated shales must also be considered when studying subsidence. The Braguny and Yastrebinoye oilfields in the Tersko-Sunzhenskaya region of Russia were examined using geophysical data for the boreholes. The initial average (weighted) porosity of the producing zone, ϕ_{a1}, was

$$\phi_{a1} = \frac{\sum_{i=1}^{h} \phi_i h_i}{\sum_{i=1}^{h} h_i} = \frac{V_p}{V_b} \tag{3.8}$$

where ϕ_i and h_i are the porosity (%) and thickness of the ith layer (in m), and V_p (m^3) and V_b (m^3) are the pore volume and bulk volume, respectively.

Upon decrease in the pore pressure by production of fluids, the porosity decreases to ϕ_{a2}:

$$\frac{\phi_{a1}}{\phi_{a2}} = \frac{\frac{V_p}{V_b}}{\frac{(V_p - V\Delta V_p)}{(V_b - V\Delta V_b)}} = \frac{1-\left(\frac{\Delta V_b}{V_b}\right)}{1-\left(\frac{\Delta V_p}{V_p}\right)} \tag{3.9}$$

where ΔV_b, and ΔV_p are changes in the bulk volume (m^3) and pore volume (m^3), respectively.

Inasmuch as $\Delta V_p \approx \Delta V_b$, Eq. 3.9 can be also written as $\Delta V_b = S\Delta h$ and $V_b = Sh$: ΔV…=Sh

$$\frac{\phi_{a1}}{\phi_{a2}} = \frac{1-\left(\frac{\Delta V_b}{V_b}\right)}{1-\left(\frac{\Delta V_p}{V_p}\right)} = \frac{1-\frac{\Delta h}{h}}{1-\frac{\Delta h}{\phi_{a1} h}} \tag{3.10}$$

where S is the area of deposits (m^2), and h is the thickness of formation (m). Also,

$$\frac{\phi_{a_1}}{\phi_{a_2}} = \exp[\overline{\beta}_p (p_1 - p_2)] \tag{3.11}$$

where $\overline{\beta}_p$ is the weighted average coefficient of pore compressibility (MPa^{-1}), and p_1 and p_2 are, respectively, initial and final low reservoir pressure due to production (MPa^{-1}).

Thus, from Eq. 3.10:

$$\frac{\Delta h}{h} = \frac{\exp[\overline{\beta}_p (p_1 - p_2)] - 1}{\frac{1}{\phi_{a1}} \exp[\overline{\beta}_p (p_1 - p_2)] - 1} \tag{3.12}$$

Eq. 3.12, therefore, can be used to estimate the amount of subsidence, depending on the drop in the formation pressure due to production ($p_1 - p_2$). Obviously, it is necessary to determine h, ϕ_{a1}, and $\overline{\beta}_p$.

The thickness of the formation can be determined using geophysical logging methods (electrical, radioactive, and sonic). Curves for the normally compacted clays are prepared on a semi-logarithmic scale (Dobrynin and Serebryakov, 1978). Figure 3.41 illustrates the zones of abnormally low pore pressure as indicated by an increase in the specific resistivity (ohm-m). The thickness of the formation, h, is 394 m.

In a new region, which was not studied, the value of h necessary for estimating Dh is established using an analogy with other regions taking into account the lithological and hydrodynamic characteristics of the area. The ϕ_{a1} is determined using geophysical data:

$$\phi_{a1} = \frac{\sum h_{ss}}{h} \phi_{ss} + \frac{\sum h_{sh}}{h} \phi_{sh} \tag{3.13}$$

where $\sum h_{ss}$ and $\sum h_{sh}$ are the sums of thicknesses for sandstones and shales in the low-pressured zone, respectively (m), and ϕ_{ss}, and ϕ_{sh} are the initial porosities (%) of sandstones and shales, respectively.

In order to determine $\overline{\beta}_p$ in the area of pressure reduction, one can use the following methods: (1) repeated leveling measurements of the Earth's surface (repeated measurements of borehole altitudes after pore pressure reduction), using Eq. 3.12; and (2) repeated measurements in boreholes using radioactive logging before and after production.

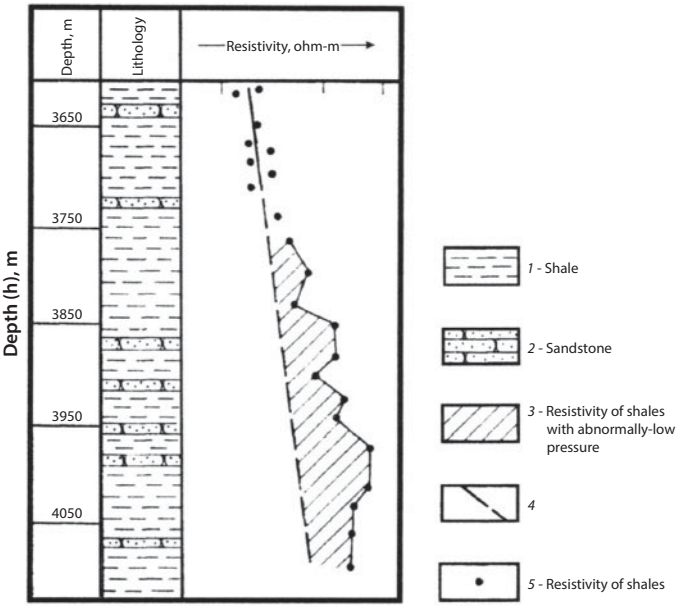

Figure 3.41 Abnormally low formation pressure in the borehole Number 83, Braguny Oilfield, Russia. Lithology: 1 = shale; 2 = sandstone; 3 = abnormally low pressure zones; 4 = curve for normaly compacted clays; 5 = resistivity of shales (ohm-m). (After Dobrynin and Serebraykov, 1989, Figure 122, p. 272; also in: Serebraykov and Chilingarian, 2000, figure 1, p. 413.)

Table 3.4 Values of $\overline{\beta}_p$ determined on the basis of repeated leveling for the Braguny Oilfield, Russia. (After Dobrynin and Serebryakov, 1989; in: Chilingar *et al.*, 2002, table 13.1, p. 356.)

Borehole number	Depth of interval, m	Interval thickness, m	Porosity, ϕ, %	$\sum h_{sh}$, m	$\sum h_{ss}$, m	Δh_{meas}, m	Δh_{calc}, m	$\overline{\beta}_p \times 10^4$, MPa^{-1}
34	3,533–3,953	420	15.9	317	103	2.56	2.39	8.6
35	4,073–4,420	347	16.1	278	69	1.53	2.00	6.1
40	3,638–4,045	407	15.8	295	112	2.4	2.30	8.3
43	3,840–4,220	380	15.9	283	97	2.39	2.16	8.9

Changes in density divided by the average density of the formation $\left(\frac{\Delta\rho_f}{\rho_f}\right)$ is about equal to $\left(\frac{\Delta h}{h}\right)$. Thus, one can determine $\overline{\beta}_p$ from Eq. 3.12 without repeated leveling. In new regions, $\overline{\beta}_p$ is estimated using analogy with other regions having similar lithology and hydrodynamic conditions.

The weighted average porosity was determined from Eq. 3.13. The f_{ss} and f_{sh} were determined from graphs and analytical functions of porosity versus depth for the Tersk-Sunzhen petroliferous area of Russia, based on data obtained from repeated leveling surveys after 15 years of production (Table 3.3). Using the average value of 8×10^{-4} MPa^{-1} for $\overline{\beta}_p$, Δh_{calc} was calculated in boreholes in which repeated leveling was performed. The values obtained (Δh_{calc}) were compared with those determined by leveling (Δh_{meas}). Average absolute error in four boreholes was 0.24 m. Thus (Δh_{calc}) can be obtained using the average $\overline{\beta}_p$ value (Table 3.4).

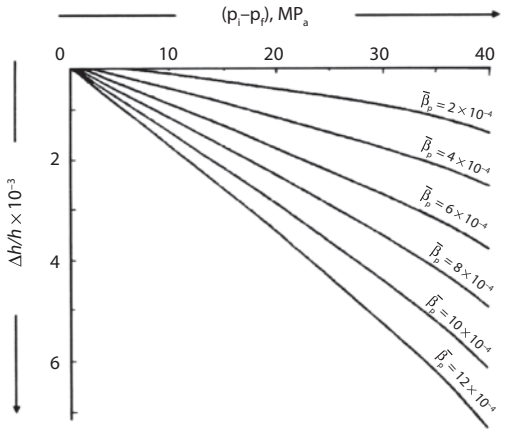

Figure 3.42 Relationship between $\Delta h/h$ and formation pressure drop due to production $(\Delta p = p_i - p_f)$ in MPA^{-1}; Δh = subsidence, m; h = formation thickness, m; p_i; = initial formation pressure, MPa^{-1}; p_f = final formation pressure after a certain amount of production, MPa^{-1}; ϕ = initial porosity = 15.9%; and numbers on curve are β_p = weighted Pore compressibility. (After Dobryin and Serebryakov, 1989; in: Serebryakov and Chilingarian. 2000. figure 3, p. 415.)

Table 3.5 Subsidence of the Earth's surface (Δh) at the Tersk-Sunzhen petroliferous area using $\overline{\beta}_p = 8 \times 10^{-4}$ MPa^{-1}. (After Dobrynin and Serebryakov, 1989; in: Chilingar *et al.*, 2002, table 13.2, p. 357.)

Borehole no.	Interval depth, m	Interval thickness, m	Porosity, Φ, %	$\sum h_{sh}$, m	$\sum h_{ss}$, m	Pressure drop, MPa	Δh, m
Braguny oilfield							
59	3,635 to 4,057	422	15.9	319	103	38.4	2.4
63	3,507 to 3,963	456	15.9	345	111	36.4	2.6
65	3,667 to 4,062	395	15.8	287	108	37.9	2.2
76	4,222 to 4,506	284	15.7	198	86	37.9	1.57
82	3,635 to 4,047	412	15.8	299	113	36.3	2.2
83	3,706 to 4,100	394	15.7	275	119	36.4	2.1
86	3,696 to 4,161	465	15.9	351	114	34.6	2.39
87	3,459 to 3,944	485	16.0	381	104	35.6	2.58
91	3,491 to 3,978	487	15.7	340	147	35.1	2.5
Yastrebinoe oilfield							
107	3,587 to 3,977	390	16.1	317	73	23.2	1.37
111	3,502 to 3,900	398	16.0	312	86	25.4	1.52
113	3,578 to 3,923	345	16.0	271	74	29.0	1.5
114	3,773 to 4,002	229	16.1	186	43	27.4	0.95
116	3,443 to 3,881	441	15.9	333	108	27.4	1.8
119	3,654 to 3,890	236	16.0	185	51	28.4	1.0

Based on data calculated using Eq. 3.12, a relationship between $\frac{\Delta h}{h}$ and pressure drop after production $(p_1 - p_{a1})$ (where p_1 is the initial pressure and p_{al} is the lower pressure after production) was established (Figure 3.42). Using this figure, Dobrynin and Serebryakov (1989, pp. 280–281) estimated the subsidence (Δh) of the Earth's

surface during production from the Cretaceous deposits of the Tersk-Sunzhen petroliferous area of Russia. Figure 3.40 shows the subsidence of the Earth's surface during the 1969–1984 period above the Braguny and Yastrebin oilfields, with the maximum subsidence corresponding to the crestal areas of anticlines (maximum production).

The amount of compaction of the producing formation (and resulting subsidence of the Earth's surface) can be predicted from the decrease in pore pressure due to production or *vice versa*. The method presented here is simple and accurate, provided compressibilities are properly determined or estimated (see Rieke and Chilingarian, 1974), which is commonly not the case.

3.5.10 Subsidence over Venezuelan Oilfields

Venezuela's total remaining reserves of heavy, extra heavy crudes and bitumen which are producible by primary and cyclic steam technology are 156.1×10^9 bbl. This can be increased by an additional 136.1×10^9 bbl by use of steam drive, thus resulting in a total of 292.2 billion barrels (292.2×10^9 bbl). An important portion of these reserves, mainly of heavy and extra heavy crude oils, has been exploited for many years in the Bolivar Coastal and Boscan oilfields using well established technologies and at competitive costs. Of these two areas, the Bolivar Coastal Fields, is the most affected by reservoir compaction and subsidence. In these two areas, original reserves of heavy and extra heavy oil, amounted to 33.8×10^9 bbl, of which 19.0×10^9 bbl remain. These reserves include only those producible by primary means (mainly compaction). These reserves can be increased by further application of steam drive, which has proven to be very successful in the C-3/C-4 and M-6 projects in the Bolivar Coastal Fields at Tia Juana and the Jobo project in eastern Venezuela, where recoveries in some cases were as high as 40% of STOIP are expected. Inasmuch as most of the heavy and extra heavy Bolivar Coastal Field crudes are suitable for this process, the future additional recoveries by steam drive are estimated to be 11.0×10^9 bbl (Borregales and Salazar, 1987).

The huge heavy, extra heavy and bitumen accumulations in the Orinoco Belt contain some 1.18×10^{12} bbl of oil. Approximately 10.1% of the Orinoco Belt's STOIP is producible by already demonstrated primary and cyclic steam technology, yielding recoverable reserves of 135.4×10^9 bbl. Application of already existing steam drive technology to the heavy, extra heavy and bitumen accumulations in place in the Orinoco Belt will yield an additional future recovery of 136.1×10^9 bbl (Finol and Farouq Ali, 1974). All of the Orinoco Belt reserves are found in unconsolidated sands and are consequently predisposed for future reservoir compaction and subsidence (Finol and Sancevic, 1995, p. 339).

With respect to production, Venezuela has always been an important producer of heavy oil, owing to the Bolivar Coastal Fields, which have also been affected by reservoir compaction and subsidence. The first commercial development took place in 1917 in the heavy oil Mene Grande field in the Lake Maracaibo Basin, 14 km to the southeast of the Bachaquero Field, the southernmost of the BCF. At present, the total productive capacity of the country is 2.6×10^6 BOPD of which 40% (or 1.0×10^6 BOPD) is heavy and extra heavy oil. Throughout its history, the Venezuelan oil industry has produced some 14.8×10^9 bbl of heavy and extra heavy oil, mostly by compaction/subsidence, which has affected the Bolivar Coastal Fields.

Cyclic steam injection at depths of up to about 4,000 ft (1,220 m) has been practiced in Venezuela for over 22 years and has resulted in an accumulated production of over 1.0×10^6 bbl. Two large-scale steamflood projects, the M-6 project in Tia Juana, Bolivar Coastal Field, which has been in operation since 1977, and the Jobo Project in eastern Venezuela, which has been in operation since 1981, jointly contribute 25,000 BOPD to the production of heavy and extra heavy crudes. The cyclic steam injections as well as steamflood projects cause further compaction and subsidence (Finol and Sancevic, 1995, p. 339).

3.5.10.1 Subsidence in the Bolivar Coastal Oilfields of Venezuela

The first oilfield in the area of the Mene Grande Field was discovered in 1914. The first prolific well in what was to become the Bolivar Coastal Fields was drilled near a surface oil seep and completed in 1917, but it was not until 5 years later when the Shell R-4 well blew out (at an estimated 100,000 BOPD) that sufficient stimulus was provided for development.

The Bolivar Coastal Fields are located on the eastern margin of Lake Maracaibo and comprise the Tia Juana, Lagunillas and Bachaquero fields (Figure 3.43). When the Bolivar Coastal Fields are considered jointly, they constitute one of the largest oilfields outside of the Middle East and contain heavy and extra heavy crudes having gravities lower than 20° API.

There are several types of traps in the Bolivar Coastal Fields: (1) asphalt seals in the oil seepage areas; (2) fault and fold traps; (3) lithological variations that form permeability barriers in the producing members; and (4) stratigraphical

Figure 3.43 Bolivar Coastal Fields (BCF). (After Finol and Sancevic, 1995; in: Chilingarian *et al.*, 1955, p. 341.)

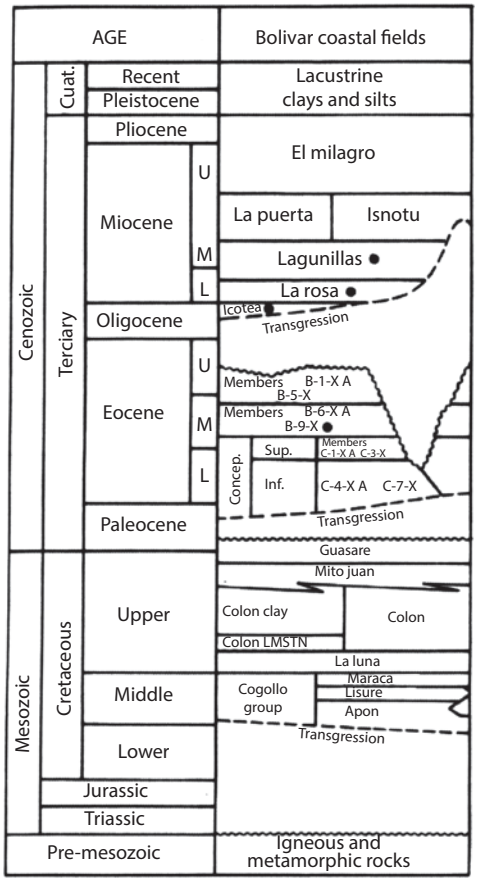

Figure 3.44 Stratigraphic section of Bolivar Coastal Fields. (After Finol and Sancevic, 1995; in: Chilingarian *et al.*, 1995, p. 343, figure 7.30.)

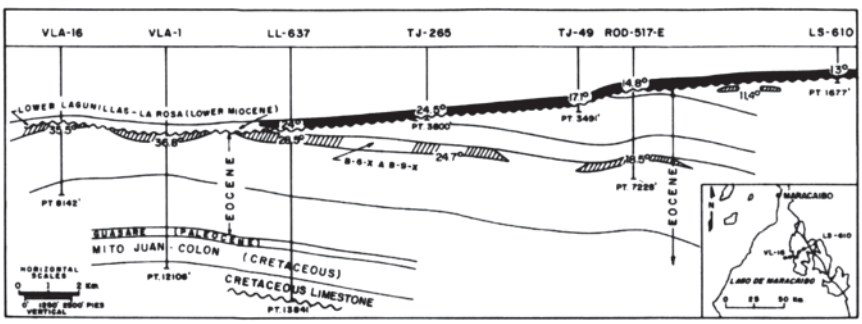

Figure 3.45 A northeast-southwest crosssection through the Bolivar Coastal Fields (BCF). After Finol and Sancevic, 1995; in: Chilingarian *et al.*, 1995, p. 344, figure 7.4.)

unconformity traps, caused by erosion of Eocene sandstones and sealing by overlying Oligocene—Miocene shales. Although many trap units have been recognized in the BCF, a southwest—northeast cross-section of the Bolivar Coastal Fields (Figure 3.44 and Figure 3.45) show the Oligocene—Miocene monocline

seal, close to the surface or on the surface, is the most important trap of heavy and extra heavy crudes.

Energy-wise, the main primary driving mechanisms in the Bolivar Coastal Fields are solution gas drive, reservoir compaction and water-drive. The gravity of the oil varies between 8° and 22° API for heavy and extra heavy oil production, and is in the 22–43° API range for minor quantities of medium and light oil (Bockmeulen *et al.*, 1983).

On land, portions of the Bolivar Coastal Fields reservoirs have crude gravities in the range of 8–18° API, at moderate depths of 100–4,000 ft, net oil sand thicknesses of 50–600 ft, a high porosity of 30–40%, permeability of 1–8 D, initial oil saturation of 80%, and high *in situ* oil viscosity of 100–10,000 cP. Development of the land portions of the Lagunillas field started in 1926, and the first signs of subsidence were observed in this field's land operations in 1929. Development of the onshore Tia Juana and Bachaquero fields, and the Mene Grande Oil Co. and Creole concessions on the lake started in the mid-1930s and even later, and where subsidence was also observed. However, it was only before and after World War II that considerable surface subsidence above the three Bolivar Coastal Fields reservoirs occurred, which was due to sharp increases in production. It was at that time that it became evident that the three producers: Shell (onshore), Mene Grande (narrow strip along the shore in shallow water), and Creole (on the lake, in deeper water) were developing different production policies as dictated by the different surface conditions. The areas most affected by subsidence were on land (Shell) and on the lake, close to the shoreline (Mene Grande) operations. Creole's operations were in deeper water, less affected by subsidence where the policy was to maintain the installations (platforms, etc.) above the water level in case more serious subsidence developed in future. The properties of oil vary, from the northeast to the southwest, with the more viscous lower-API gravity oils in the onshore portion of the reservoir and the less viscous, somewhat lighter, higher API gravity oils in the deeper lake portions of the reservoirs (Finol and Sancevic; in: Chilingarian *et al.*, 1995, p. 345).

Owing to the fact that the Bolivar Coastal Fields reservoirs are at relatively moderate depths (1,000–4,000 ft), contain heavy and extra heavy crudes, and are at low pressures, the wells producing from these reservoirs require artificial lift (sucker-rod pumping equipment). At first the wells in unconsolidated sands utilized installation of slotted or wire-wrapped liners to help prevent sand entry into the wellbores; however, this technique was replaced by gravel packing with a slotted liner. This was more effective in controlling sand entry into the wellbore and decreased the number of liner failures, e.g., wells sanding up, and, consequently, reducing the number of workovers and well-repair jobs (Finol and Sancevic; in: Chilingarian *et al.*, 1995, p. 345).

3.5.10.2 Subsidence of Facilities

Prior to the start of oil operations in the Bolivar Coastal Fields in 1926, the eastern coasts of Lake Maracaibo were typical of lacustrine environments: flat and swampy (Lagunillas in Spanish means small lagoons or marshes) barely above lake level and composed mostly of sandy-silty soils. These swamps were separated from the lake by a comparatively narrow strip of land slightly higher than the lake water level, so that these strips were flooded during high tides, storms and strong onshore winds. The

coastal plains are characterized by savannas with gentle slopes (0–8 in/km), extending from the western foothills of the Ziruma Mountain Range to the coast. The area includes the deltas of the Tamare, Pueble Viejo, Machango and Misoa rivers. Shallow gutters connecting the swamps and the lake afforded drainage of flood waters during the rainy season from the shore to the lake and, during the dry season, from the lake into the swamps (Finol and Sancevic; in: Chilingarian *et al.*, 1995, p. 346).

For a number of years oilfield operations were concentrated on the onshore coastal strip of land of the Tia Juana, Lagunillas and Bachaquero fields, so that additional small earthen dikes were built by hand labor along the shore, often using foreshore vegetation as breakwaters. During this early period, subsidence was not yet apparent, but in 1929 the Lagunillas dike was breached and the resulting flooding of the camp area drew attention to this phenomenon. For the first time, this led to the suspicion of the occurrence of ground subsidence because the foreshore became permanently submerged and the vegetation started to disappear, leaving the earthen dike exposed to wave action. Once observed, it was hoped that the subsidence phenomenon would not persist and an attempt was made to protect the earthen dike against wave erosion by use of various improvised materials to resist water-breaks, such as junk (old tank plates, corrugated iron sheets, etc.), building palisades, clay facing, grooved wooden sheet piling with pine boards, facing with gravel and bitumen, etc. All of these types of protection, obviously, failed and it was soon realized that the improvised structures had to be replaced by a more permanent structure, particularly over those parts of the shore where most of the subsidence occurred. Consequently, a concrete protection of the dike and a drainage system was built to protect the area from flooding (Finol and Sancevic, 1995, p. 346).

Almost from the start of the subsidence, it also became necessary to construct inner dikes and a drainage system to dispose of the run-off by pumping it into the lake. A system of bench marks was installed in 1939 and precise levels were taken at periodic intervals to check further ground subsidence. The overall subsidence pattern for this area is shown in Figure 3.46. Figure 3.47 reflects the subsidence measured at the bench mark (BM) AB in this area.

As new oil was discovered, both north and south of Lagunillas, the oil companies extended their operations and established new oilfields. Tia Juana to the north and Bachaquero to the south also had to be protected by means of the construction of polders similar to the one in Lagunillas. The Mene Grande Oil Company, exploiting their concessions in the lake on a narrow strip along the coast and the Standard Oil (Creole), with their activities in deeper lake waters, had their bases of operation on the Bolivar Coast, either in Lagunillas or in Tia Juana. Both companies also began to protect their installations from the lake waters by means of small hand-built earth dams (Finol and Sancevic, 1995, p. 347).

Given the experience of the Dutch in coastal engineering and land reclamation, the VOC was asked in 1937 by Mene Grande and Standard to undertake the design and carry out the construction of properly engineered Earth dikes. Initially, these dikes were built along the coast as "simple" elevated roads behind a sheet-piled construction. The continued subsidence made it necessary to uplift and widen the dikes continually. With time, the initial simple elevated roads became fully developed earth dams. Figure 3.48 shows the cross-section of succession of raising the dike at this location as subsidence progressed.

According to Finol and Sancevic (1995), on the basis of historic subsidence predictions (Figures 3.48 and 3.49), it's expected that the Tia Juana and Bachaquero dikes

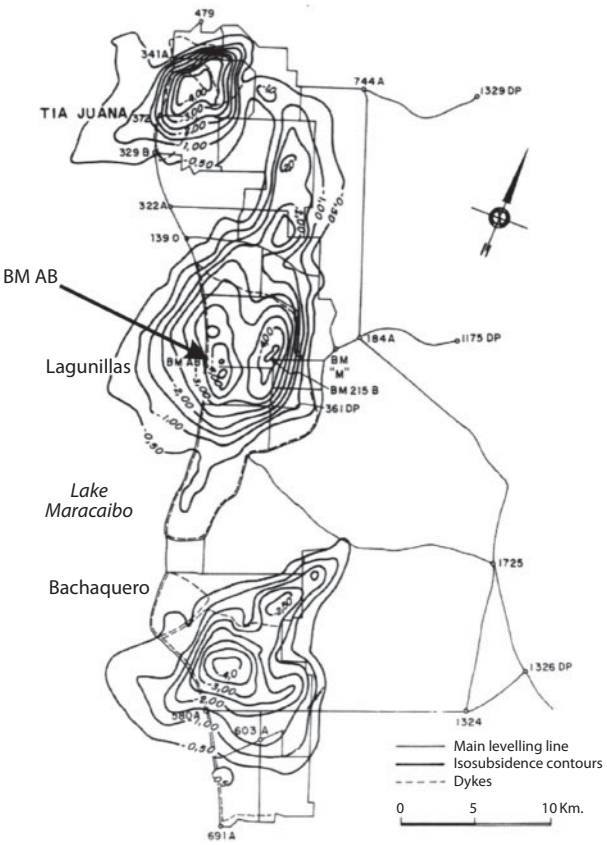

Figure 3.46 Main leveling network and subsidence contours. (After Finol and Sancevic, 1995; in: Chilingarian *et al.*, 1995, p. 350, figure 7.8.)

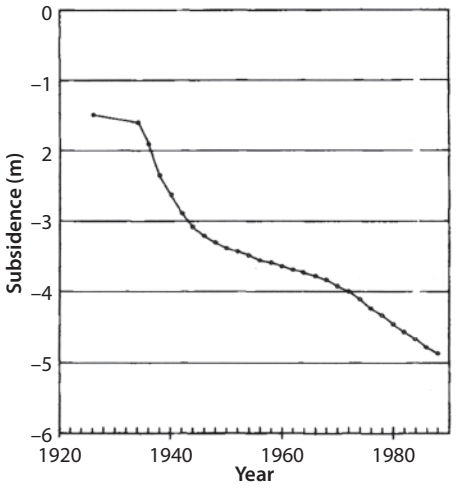

Figure 3.47 Cumulative subsidence of bench mark (BM) AB (see Figure 3.47 for location). (After Finol and Sancevic, 1995; in: Chilingarian *et al.*, 1995, p. 350, figure 7.9.)

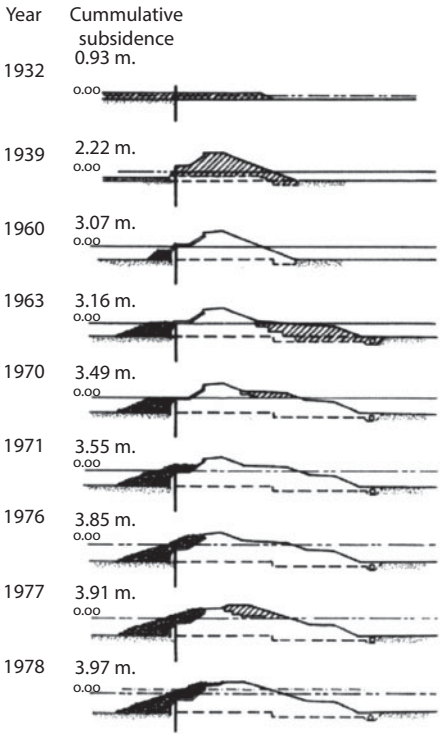

Figure 3.48 Progressive raising of the dike with respect to time. (After Finol and Sancevic, 1995; in: Chilingarian *et al.*, 1995, p. 348, figure 7.5.)

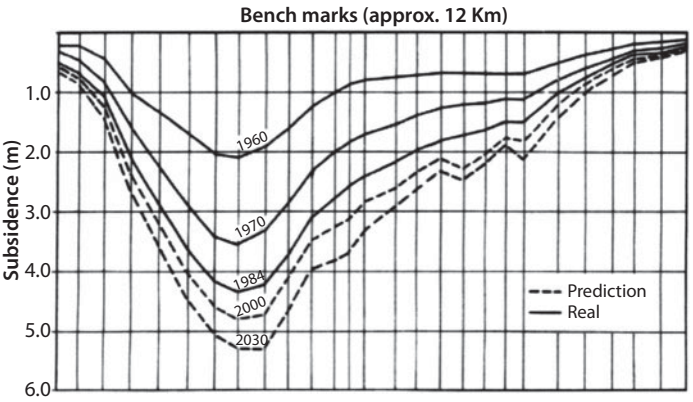

Figure 3.49 Subsidence history and prediction along the Bachaquero dike. (After Finol and Sancevic, 1995; in: Chilingarian *et al.*, 1995, p. 349, figure. 7.6.)

will have to be raised an additional 1.0–1.5 m, whereas the Lagunillas dike may have to be raised 4.0 m, because additional subsidence is expected, due to the exploitation of superposed reservoirs, Laguna and Lower Lagunillas (Figures 3.50 and 3.51).

As construction proceeded, the coastal protection system gradually took shape and proper "*polders*" were produced in the Tia Juana, Lagunillas and Bachaquero/ Pueblo

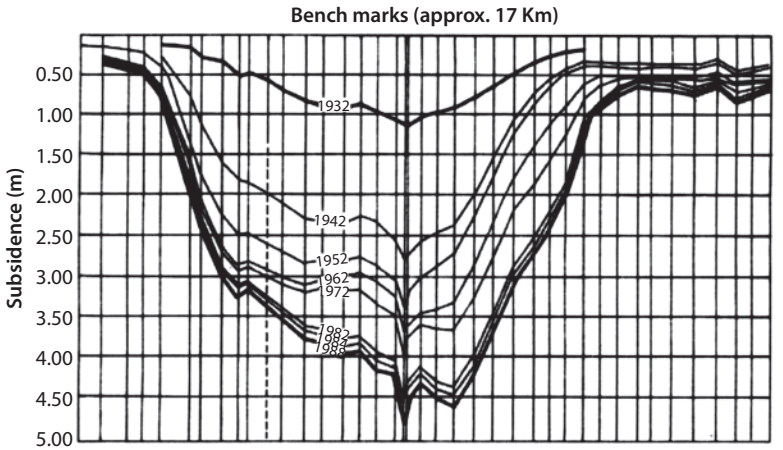

Figure 3.50 Subsidence history and prediction along the Lagunillas dike. (Modified after Finol and Sancevic, 1995; in: Chilingarian *et al.*, 1995, p.349, figure 7.7.)

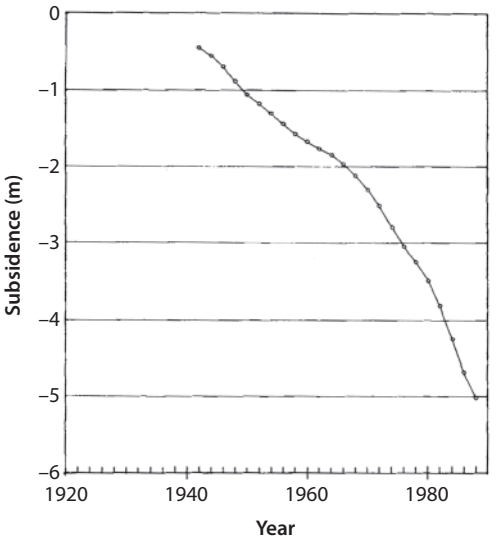

Figure 3.51 Cummulative subsidence of bench mark (BM) 215 B (see Figure 3.46 for location). (After Finol and Sancevic, 1995; in: Chilingarian *et al.*,1995, p. 351, figure 7.9.)

Viejo consisting of: (1) a coastal dike to protect the subsided area from lake water flooding; (2) inner diversion dikes to prevent run-off from the area outside moving into the subsided polder area; (3) drainage channels to convey the water to the pumping stations constructed along the coast; and (4) pumping stations to dispose of the water over the dike and into the lake (Finol and Sancevic; in: Chilingarian *et al.*, 1995, p. 347).

As shown by Finol and Sancevic (1995, p. 355), the main driving mechanism for the reservoirs is compaction. Thus, repressurizing of Venezuelan reservoirs is problematic; stopping subsidence by water injection, for example, results in lower production and

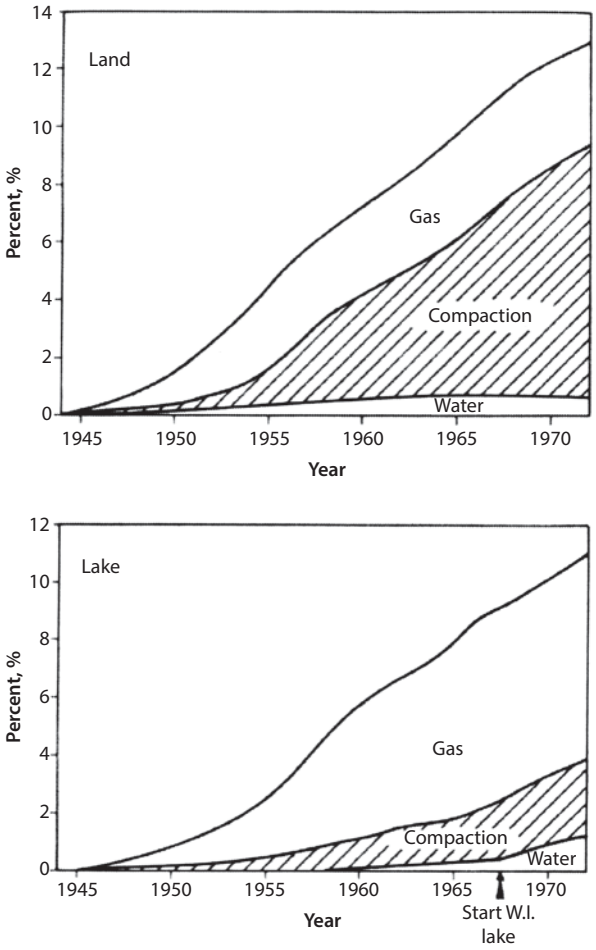

Figure 3.52 The relative contributions of various drive mechanisms, Bachaquero Reseervoir, Venezuela. Reservoir volumes of free gas, compaction, and invaded water (percent of initial pore volume). (After Merle *et al.*, 1975; in: Finol and Sancevic, 1995; in: Chilingarian *et al.*, 1995, p. 355, figure 7.13.)

recovery. This problem was faced by a small group of experts on compaction/subsidence sent to Venezuela by the DOE in 1983[1]. Figure 3.52, presents the relative contributions of various drive mechanisms in the Bachaquero Reservoir, Venezuela, with respect to time.

According to Finol and Sancevic (1995), water injection must be limited to portions of reservoirs where the mobility ratios (M) of displacing and displaced fluid are not extremely adverse. On land, portions of Bolivar Coastal Fields, the high-viscosity, low-gravity crude oil recoveries are negatively affected by water injection. Even more so, injection of high-mobility gas contributes to the losses of reserves.

Nunez and Esojido (1976) found that a straight-line relationship exists between the subsidence and reservoir withdrawal in strongly subsiding oilfields after an initial period of low subsidence when solution gas-drive predominates as the reservoir energy mechanism. One should keep in mind that the incremental subsurface volumes

[1]Professor G. V. Chilingar was a member of the delegation headed by Prof. E. Donaldson.

of produced gas, oil and water is approximately equal to the incremental surface subsidence volumes (Finol and Sancevic, 1995; in: Chilingarian *et al.*, 1995, p. 356).

The cyclic steam injection process (steam soaking and huff-and-puff) contributes to additional compaction/subsidence. Steam injection, however, was responsible for the rejuvenation of the onshore Bolivar Coastal oilfields (see Finol and Sancevic, 1995, for details).

3.5.11 Po-Veneto Plain, Italy

There are several subsiding basins overlying hydrocarbon-bearing reservoirs in the Po-Veneto Plain of Italy shown in Figure 3.53. Over the last 30 years, land subsidence has occurred due to production of fluids. The fluids consist of predominantly dissolved methane-bearing brine water. Several confined aquifers have been produced in this plain.

Brighenti *et al.* (1995) have presented in detail the geologic history of this plain with its aquifers. They noted that the Po-Veneto Plain is a wide sedimentary basin, which has experienced intense and differential subsidence due to fluid withdrawal. In certain areas of this plain, the depth to the base of the Pliocene sediments exceeds 8,000 m and that the Pleistocene sediments at times measure 3,000 m in thickness. This Pliocene sedimentary subsiding basin extends beyond the confines of the current Plain and is included as a part of the Apennine area and the northern and eastern Pre-Alps. Considerable volumes of terrigenous sediments have been deposited in subsidence basins. There is a prevalence of sedimentation over the subsidence during most of the recent Quaternary, as a result of which the sea withdrew and continental alluvium covered the marine sediments. In some subsidence areas the thickness of the alluvium layer reaches 400–500 m.

The entire Plain has a vast and complex regional hydraulic system, nourished from its sides (Alps and Apennines) by surface waters with the formation of fluvial fans. There is a deep and complex aquifer system, characterized by a hydrodynamism towards the east (Brighenti *et al.*, 1995; in: Chilingarian *et al.*, 1995, p. 217).

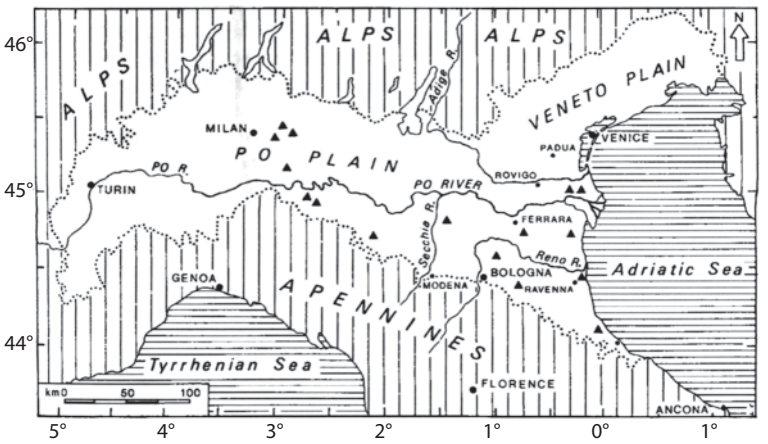

Figure 3.53 Simplified view of the Po-Veneto Plain. The triangles indicate main hydrocarbon reservoirs. After Btrighenti *et al.*, 1995; in: Chilingarian *et al.*, 1995.)

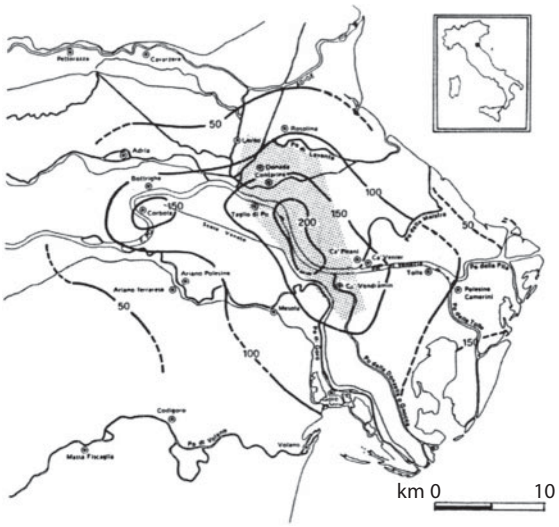

Figure 3.54 Land subsidence in the Po Delta in the period of 1951 to 1962 expressed in cm. The grey area indicates the area in which in 1960 the withdrawal of gas-bearihg water was discontinued. (After Borgia *et al.*, 1985a; in Chilingarian *et al.*, 1995, p. 239, figure 5.18.)

The search for oil and gas has helped in defining the geology of this petroleum basin (Brighenti *et al.*, 1995). The petroleum basin is characterized by a wide and diversified spectrum of hydrocarbon generation and migration (Mattavelli *et al.*, 1983; Borgia and Ricchiuto, 1985; Borgia *et al.*, 1987). The central-eastern part of the Plain is characterized by the presence of numerous biogenic gas reservoirs (which are almost always autochthonous), located particularly in the vicinity of the plicated systems (submerged Apennine area). During the Pliocene-Pleistocene there was a widespread formation of structural stratigraphic traps which allowed for gas retention in this area. The development of biogenic gas was favored by the abundant and long-lasting sedimentation. This gas, which is very light isotopically, was formed by immature sediments at a low temperature. In certain areas, e.g., Ravenna, the gas formed and accumulated in large quantities after synsedimentary tectonic activity in the presence of thick sand and clay banks. This resulted in the formation of abnormally deep biogenic gas (Brighenti *et al.*, 1995, in: Chilingarian *et al.*, 1995, p. 217).

3.5.11.1 Po Delta

The Po Delta (Figure 3.54) was the first major subsidence area studied closely in Italy. Subsidence, which reached its peak in the early 1950s, was caused by the withdrawal of gas-bearing waters (Borgia *et al.*, 1982). A schematic cross-section of the Po Plain sediments is shown in Figure 3.55. This subsidence was aggravated by the overlapping effects of: (1) recent land reclamation, (2) the natural settlement of young soils, (3) the rise in the average sea level (about 1 mm/year over the past century with a sharp increase in the past 20 years), and (4) an added effect of the embankment of the drainage system, which prevented river sediments from spreading onto the surrounding area (Bondesan and Simeoni, 1983). As a result, today the middle section of the delta as

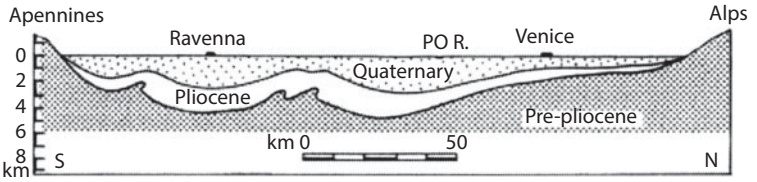

Figure 3.55 Schematic cross-section of the Po Basin. (After Brighenti *et al.*, 1995; in Chilingarian *et al.*, 1995, p. 239, figure 5.19.)

shown in Figure 3.55, appears "*spoon-shaped*", with a depression of over 3 m deep in the middle. The survival of the whole basin is dependent on the effectiveness of the man-made water control works (Brighenti *et al.*, 1995). This is especially critical at its eastern edge bordering on the sea where there has been subsidence of the order of 2 m in the last 40 years (Brighenti *et al.*, 1995; in: Chilingarian *et al.*, 1995, p. 238).

A detailed description of the geology can be found in Brighenti *et a1*. (1995). Looking at the subsidence area, it is bounded to the north by the lower course of the Adige River and to the south by the northern section of the Ferrara Province. Thus, it is located in the eastern part of the Po Plain covered by fairly thick Quaternary sediments of marine and continental origin.

In the past, there was a brisk extraction of gas-bearing waters from Quaternary reservoirs over a surface area of about 1,000 km^2. Large quantities of gas dissolved in the brine were stored in these reservoirs. There is a considerable accumulation of gas-bearing waters; with an estimated several dozens of billions of cubic meters of solution gas dissolved in water. The gas-bearing interstitial brines are quite similar to sea water in their composition. They are, however, characterized by a lower salinity (5–27 g/1) and can be interpreted as residual, brackish water, sea water, or a mixture of freshwater and fossil waters (Brighenti *et al.*, 1995; in: Chilingarian *et al.*, 1995, p. 240).

Although the existence of gas reservoirs has been known for a long time, their systematic exploitation began only in the late 1930s, at a time of great shortage of oil in Italy. In the post-war period, production gradually increased and in the late 1950s reached 300 million scum per year. Based on drilling, the gas-bearing Quaternary layers reach down to a depth of about 800 m. Five horizontal, often not well-defined layers can be distinguished between 100 and 600 m (Brighenti *et al.*, 1995; in: Chilingarian *et al.*, 1995, p. 240).

At the height of development, about 1,700 wells were in production, drawing water primarily from strata down to a depth of 600 m. It is estimated that a total of over 3,700 wells were drilled, especially in the Rovigo Province. The average well depth, estimated at about 200 m in the first decade of exploitation activity, increased steadily as deeper aquifers were developed. Initially, water flowed spontaneously from the wells. As fluid production lowered the reservoir pressure, there was a decrease in the hydraulic head and submersible pumps and/or gas lift became necessary to produce the wells.

The gas was separated from the brackish water and the water was discharged into a surface drainage system. The gas was sent to compression plants. A gas pipeline network, extending approximately over a length of 650 km and connected to the national gas pipelines, was established in this area to convey gas to gasworks in several nearby towns, including Padua and Venice.

Due to its low GWR ratio (1–1.4 scum/m^3), extraction of gas in the delta area involved massive brine water withdrawals, estimated at 3 billion scum. This, in turn, caused substantial subsidence of the hydraulic head, which originally almost reached the land surface. At this time, the relationship between pore-pressure change and sediment compaction was not undisputed, as large-scale subsidence was also known to occur in the Po Delta due to the production of fluids long before gas extraction was started.

According to Brighenti *et al.* (1995), during 1845–1875, considerable natural subsidence was recorded, with peaks of 70–80 cm. Elevation measurements conducted between 1884–1887 and 1950 revealed average sinking rate in the middle of the delta area of about 0.5 cm/year.

In the 1950s, when the land-subsidence became greater, subsidence was regarded by many as a temporary accentuation of known phenomena. However, the progressive impairment of the area (decreased embankment clearance, reverse gradients of canals, and lowering of drainage plants) turned out to be an impending threat to the local population who were hit by frequent floods. It was then decided that a number of field measurements (mainly topographic and piezometric surveys) should be made by private and public institutions (Brighenti *et al.*, 1995).

Just a few examples are sufficient to reveal the severity and the impact of subsidence. In the withdrawal areas, subsidence of the water-table surfaces down to a depth of 50 m was recorded. At this time, subsidence proceeded at a rate of up to 25–30 cm/year in the middle area of the delta (Figure 3.54) and reached a total of 2.5 m over the 1951–1962 period. The average land subsidence of the whole delta in the same period was estimated at 115 cm. Inasmuch as a considerable amount of the data suggested that gas-bearing water extraction was the main cause of the phenomenon, a committee appointed by the Italian government stopped gas production over the 25,000-acre area where subsidence was greatest (Figure 3.54, shaded area). This step, implemented in 1960, proved highly successful in showing a close relationship between subsidence and gas production. As a result, this committee decided to extend this policy over all the delta (1961) and, later, in the remaining areas, i.e., in the entire Rovigo Province in 1963 and Ferrara Province in 1965.

The average subsidence rate in the delta area and the natural gas production per year are presented as a function of time in Figure 3.56. As shown, the sinking decreased rapidly once production of the gas-bearing water was discontinued. The discontinuance of the water extraction activities caused the surface of the water-table to rise rapidly. The subsidence rate decreased exponentially with time. Based on recordings at a number of bench marks (Zambon, 1967), the relationship between sinking (h, m) and time (t, yr) can be expressed by the following equation:

$$h = h_o e^{-kt} \tag{3.14}$$

where h_o = maximum sinking, and k is a dumping constant varying from 0.24 to 0.70.

A change in elevation with respect to a surface bench mark does not allow the thickness of layers to be established, unlike well measurements using extensometers. Figure 3.57 demonstrates the length variations of a nearly 700 m deep well located close to Ca' Vendramin (within the grey area of Figure 3.54) obtained through measurements carried out during a period of about 3.5 years, starting from May 1960, using a specially

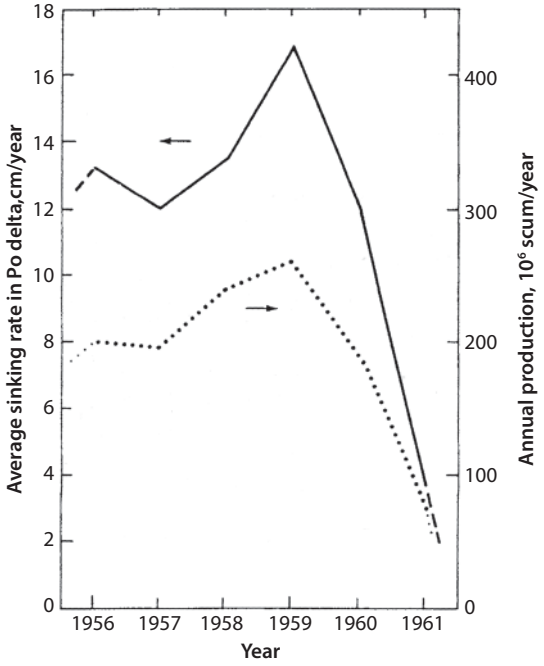

Figure 3.56 Average sinking rate (solid line) and annual gas production (dashed line) in the period of 1956–1961 in the Po Delta. (After Borgia *et al.*, 1985a; in: Chilingarian *et al.*, 1995, p. 243, figure 5.22.)

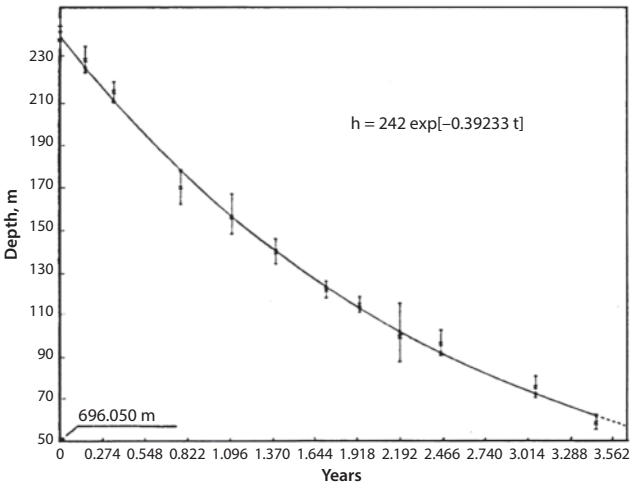

Figure 3.57 Depth variation of a nearly 700-m deep well located in the Po Delta, measured by means of a moveable extensometer. h = depth (m), t = time (years). (After Borgia *et al.*, 1982; in: Chilingarian *et al.*, 1995, p. 244, figure 5.23.)

designed movable extensometer (Borgia *et al.*, 1982). These measurements showed that ground-sinking was related to the compaction of layers up to a depth of 700 m. This was further proved by the fact that total well shortening, over the period under consideration, turned out to be very close to the subsidence values as measured through specially performed geometric leveling, deviation being less than 8%. Moreover, even the

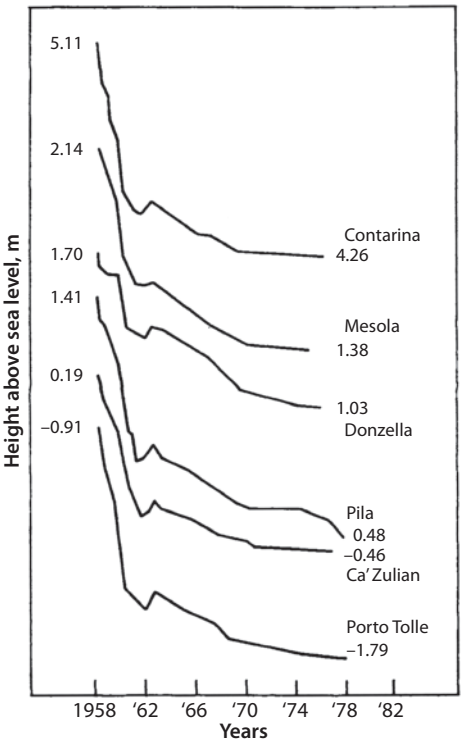

Figure 3.58 Soil-sinking charts of some significant bench marks updated in 1978; heights are expressed in meters and refer to sea level. (Brighenti *et al.*, 1995; in: Chilingarian *et al.*, 1995, figure 5.25, p. 246.)

dumping constant ($k = 0.39$) was in agreement with the values obtained using surface measurements (see Brighenti *et al.*, 1995, in: Chilingarian *et al.*, 1995, p. 295).

Other series of tests were carried out in three abandoned wells close to the previous one, ranging from 180 to 415 m in depth. The data obtained were in agreement with that shown by specially designed leveling. This confirmed the reliability of extensometer measurements.

As pointed out by Brighenti *et al.* (1995; in: Chilingarian *et al.*, 1995, p. 295) the delta area displays unique hydraulic and environmental conditions, where sea, river and continental environments coexist in a delicate equilibrium. The understanding of the system was enhanced from the recordings at times of greatest stress and in the following stages during attainment of equilibrium.

The ground-sinking charts of some significant benchmarks based on the most recent measurements are presented in Figure 3.58. This data confirms the gradual rebound of land, starting in the early 1960s. Figure 3.58 suggests that subsidence has not stopped, because human activities certainly did not stop when the gas extraction was discontinued.

In its terminal course the river tends to become deeper, thus impairing the stability of embankments (Figure 3.59). Thus in time, may turn out to be a somewhat critical factor, as here the level of the river is greater than the surface of the land (Brighenti *et al.*, 1995).

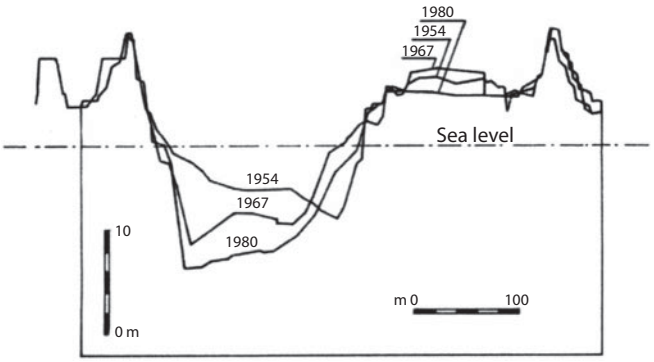

Figure 3.59 Examples of variation in the cross-section of the Po River which occurred near Polesella, Rovigo Province, Italy, with time. (After Bondesan and Bizzari, in: Brighenti *et al.*, 1995; in: Chilingarian *et al.*, 1995, figure 5.26, p. 247.)

According to Brighenti *et al.*, (In: Chilingarian *et al.*, 1995, p. 245) efforts have been made to find a remedy, whenever possible, for the disruptive effects in areas where ground-sinking was highest. Measures taken or about to be taken pursue a dual goal: (1) to control floods and restore the water balance, and (2) to prevent the sea from eroding away the land (Montori, 1983; Carbognin *et al.*, 1984; Gambardella and Mercusa, 1984). In spite of this action, some areas nevertheless had to be abandoned. The "spoon" shape of the delta and the depressions resulting from land reclamation in the northern area of the Ferrara Province (southern part of Po Delta) require that water be drained mechanically, as extensive areas are below sea level by a few meters. Ground-sinking, therefore, impaired the performance of the drainage equipment.

Damage to irrigation works and the canal system was also caused by a reduced gradient (or even reverse gradient) of canals. Hence a major part of the water supply system had to be rebuilt (Brighenti *et al.*, 1995; in: Chilingarian *et al.*, 1995, p. 246).

River and sea embankments suffered functional damage as a result of a change in pattern and increase in stresses. They had to be repeatedly raised and strengthened in order to prevent blowouts and offset the weakening of embankment structures resulting from increased loading. Further increase in loading on sea embankments was brought about by the lowering of the sea bed, which, in turn, was due to a decrease in the transport of solids by rivers. This resulted in flooding of some beaches and made it necessary to build dams designed to recover at least part of the damaged land, but frequently with disfiguring effects on the landscape.

Based on the experience with Japanese reservoirs having similar features (Marsden, 1980), a feasibility study was conducted on the possibility of maintaining pressure by the injection of de-gassed water back into the formation. One of the issues dealt with was the simulation of a pilot field using a numerical model (Borgia *et al.*, 1985). Among other things, it appeared that the effects of exploitation could be kept within reasonable limits even in the presence of extreme and exceptionally unfavorable anisotropies. Moreover, the simulation proved to be an advantageous tool in selecting

the distribution of wells and their rates (Brighenti *et al.*, 1995; in: Chilingarian *et al.*, 1995, p. 247).

In their excellent contribution, Brighenti *et al.* (1995, in: Chilingarian *et al.*, 1995, p. 246) also discussed subsidence mainly due to water withdrawal in Ravenna, Bologna, Modena, and Venice areas of Italy.

3.5.12 Subsidence Over the North Sea Ekofisk Oilfield

The North Sea is located in the western portion of the Northwest European Basin. The Mid North Sea-Ringkobing-Fyb strikes east-west across the North Sea from Denmark to the United Kingdom at 55° to 56°N (Figure 3.60). It divides the North Sea area of

Figure 3.60 Location map of the North Sea oilfields. (After the Petroleum Resources of the North Sea Energy Administration; in: Chilingarian *et al.*, 1995, p. 324, figure 8.1.)

the Northwest European Basin into two smaller subbasins: the southern North Sea and the northern North Sea basins. A detailed discussion of the geology, production and problems of this field are presented by Zaman *et al.* (1995; in: Chilingarian *et al.*, 1995, p. 373.)

The northern North Sea Basin consists of several subbasins, platforms, plateaus, grabens, and embayments. Most of the major hydrocarbon accumulations are associated with the Central and Viking grabens. These grabens form part of the same Mesozoic rift system but they are different especially in the age of the producing reservoirs and type of structural traps containing hydrocarbons. Almost all of the fields currently producing oil are located in two grabens and one subbasin: (1) the Viking or East Shetland Basin, (2) Central grabens and (3) the Moray Firth (Zaman *et al.*, 1995, in: Chilingarian *et al.*, 1995, p. 373).

The southern North Sea Basin includes a belt of natural gas fields that extend from southern England through the North Sea, the Netherlands, and northern Germany to Poland. Permian Rotliegendes Sandstone is the main reservoir in this area. It also contains natural gas accumulations in tilted fault blocks, horsts, faulted domes and anticlines (Dietzman *et al.*, 1983). The North Sea covers several smaller sedimentary and structural basins of different geologic ages. The rocks range in age from Paleozoic to Tertiary and consist of sandstones, shales, carbonates and evaporites. The most productive of the salt-induced domes are located in the Norwegian sector of the Central Graben where the Ekofisk and other nearby fields, commonly referred to as the Ekofisk complex, produce hydrocarbons from Upper Cretaceous and Lower Paleocene chalk (Dietzman *et al.*, 1982; also in: Chilingarian *et al.*, 1995, p. 373).

The Ekofisk field is located in the Central Graben in the southern part of the Norwegian sector of the North Sea (Sulak and Danielson, 1989). It is the largest of six fractured chalk fields operated by Phillips Petroleum Co. Norway on behalf of the Phillips Norway Group. Water depth in the area is about 235 ft (72 m).

The presence of massive Danian limestone is the key to Ekofisk success. The porosity of the limestone is 30% in a relatively homogeneous and clean section. Primary matrix permeability can be lower than 1 mD in some sections. However, extensive natural fracturing is found in all Ekofisk wells which results in an average 12 mD permeability to oil, calculated from well test pressure analysis. Additional Ekofisk reservoir data is shown in Table 3.5 (Snyder, 1971).

A cross-section of the sedimentary basin running north to south through the area is shown in Figure 3.61. Salt domes and ridges pushing up from the basin floor create anticlinal structures in the sedimentary layers. Seismic maps of the area reveal many such structures with different sizes and shapes, which have probably increased the reservoir permeability by contributing to fracturing in the massive, brittle Danian carbonates (Snyder, 1971).

3.5.12.1 Production

Norway's first significant oil production from the North Sea was obtained in 1971, whereas in the case of the U.K., it was 1975. Most of the oil accumulations found to date are located in the Moray Firth, the Viking Graben, or the Central Graben. As of

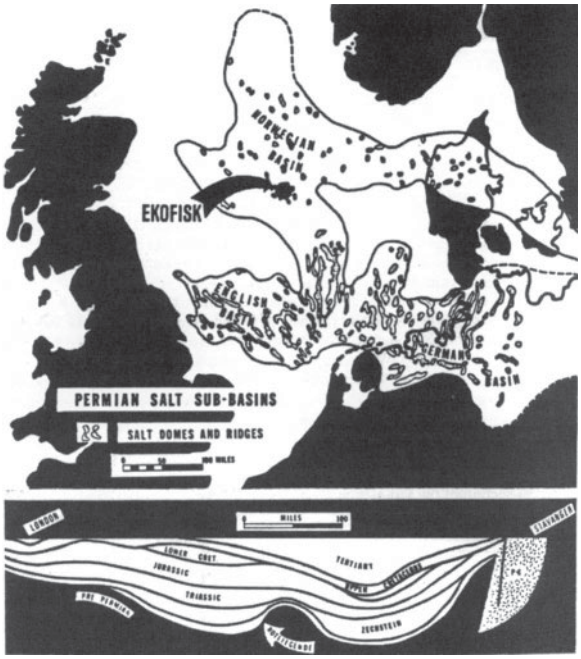

Figure 3.61 Promising structures within the major sedimentary basin that runs north to south through the North Sea, based upon seismic data. Ekofisk production is from 700 ft of lower Tertiary limestone as illustrated in the basin cross-section on a line from Norway to England. (After Snyder, 1971; in: Chilingarian *et al.*, 1995, p. 376, figure 8.2.)

January 1, 1982, there were at least 242 developed and undeveloped oilfields in the North Sea that originally contained about 96 billion barrels of oil in place and had an estimated proved reserves of 19.8 billion barrels and undeveloped reserves of 5.7 billion barrels of oil remaining to be recovered. Cumulative production until then was 3.6 billion barrels, giving a total estimated ultimate oil recovery of 29.1 billion barrels and a recovery efficiency of 30.5% of the original oil-in-place (Zaman *et al.*, 1995; in: Chilingarian *et al.*, 1995, p. 373).

Oil production from the North Sea has increased steadily since its inception in 1971 with the exception of a very minor reversal in 1973. Since then output reached a rate of 216 thousand barrels of oil per day in 1975, doubled in 1976, doubled again by 1980, and in 1981 oil production was estimated to be about 2.3 MM bopd (Dietzman *et al.*, 1983).

Production at the Ekofisk started in July 1971 and reached a peak rate of 349,000 B/D (55,500 m^3/d) in 1976.

3.5.12.2 Ekofisk Field Description

The Ekofisk reservoir is large and shaped like a shallow, elliptical dome about 22,000 ft (67 m) wide and 30,800 ft (9,390 m) long. The crest of the reservoir is approximately 9,500 ft (2,900 m) below sea level, and the pay zone is nearly 1,000 ft (300 m) thick. The reservoir initially contained undersaturated volatile oil with the properties listed in Table 3.6.

Table 3.6 Ekofisk reservoir data. (After Snyder, 1971; in Chilingarian *et al.*, 1995, table 8.1, p. 375.)

Total porosity, %	30
Permeability to oil, mD	12
Temperature, °F	268
Solution GOR, ft^3/bbl	1707
API gravity, °	35.6
Initial BHP, psia	4135
Bubble point pressure, psia	5560

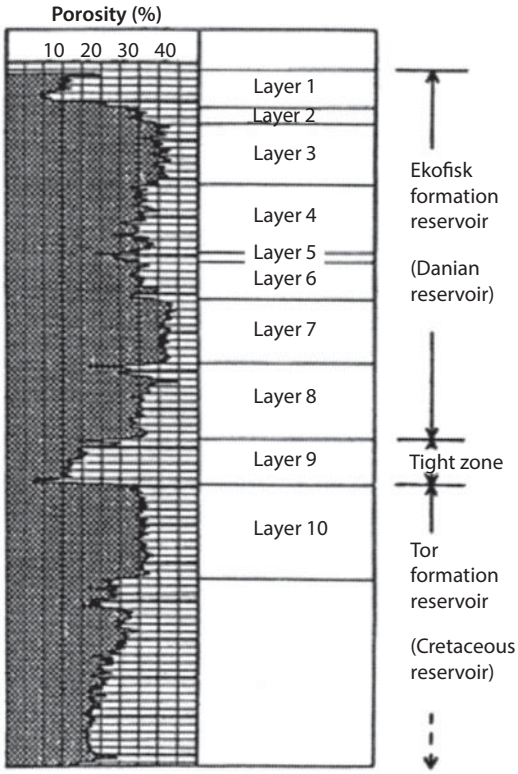

Figure 3.62 Representative porosity log from an Ekofisk well. (After Boade *et al.*, 1989; in: Chilingarian *et al.*, 1995, p. 378, figure 8.3.)

The Ekofisk Formation, which is located at a depth of 9,500 ft is of Danian of the Paleocene Period, whereas the Tor Formation, which underlies Ekofisk Formation, is of the Cretaceous Period. The Tight zone, which exists between the Ekofisk and the Tor formations, forms an impermeable barrier between the two producing formations (Figure 3.62). The porosity of chalks ranges from 25% to 48% with permeabilities up to 100 mD. The overall pay thickness reaches 1000 ft and more (Boade *et al.*, 1989).

The reservoir is covered with a 9,300-ft thick overburden, mostly composed of clays and shales interbedded with silty streaks. The overburden is overpressured below about 4,500 ft. Permeability is extremely low (10^{-6} to 10^{-9} D), and there is no indication of pressure communication between the reservoir layers and overlying sediments (Sulak and Danielson, 1989.

3.5.12.3 Enhanced Oil Recovery Projects

Enhanced oil recovery methods have significantly increased the oil and gas production from the seven fields. The excess gas which could not be sold was injected back resulting in high gas injection rates. Waterflooding was initiated in 1987 to cover the Tor Formation in the northern two-thirds of the field (Sylte *et al.*, 1988; Hallenbeck *et al.*, 1989). It was expanded in 1988 to include the southern portion of the Tor field as well as to the Lower Ekofisk. Nitrogen injection into the crest of the Upper Ekofisk was also planned to start in late 1993 (Thomas *et al.*, 1989). Production from the Ekofisk field has increased steadily. Two-thirds of that increase is due to waterflood response. The other third is due to an effective remedial work program implemented over the past few years as well as improved communications across disciplines which has reduced the well failures (Sulak, 1991).

3.5.13 Platform Sinking

In the early 1980s, after more than a decade of production, it was noticed that the Ekofisk platforms were sinking. A boat-landing on the east side of the Ekofisk complex was more or less under water, whereas it had previously been visible in the 1970s. The same was true for a landing on the horizontal bracing on the jacket below the 2/4-C platform. Initially no one gave any attention to check if the platforms really were sinking. In fact, many natural conditions can contribute to the variation of sea level. Late in the fall of 1984, however, the matter was given serious attention. It started with sounding measurements on the bridges to check clearance margins for anchor-handling boats. The results were compared with the relevant data from 1974. Photographs taken in the early and mid-1970s were also compared with recent ones (Wiborg and Jewhurst, 1986; Kvendseth, 1988). In November 1984, through measurements from fixed platform references to Kogan sea level, it was finally concluded that the platforms indeed were sinking. This was predicted much earlier by Professor George V. Chilingar given the very high compressibility of chalk. By 1984, the seafloor in the Norwegian Sea was discovered to have subsided by more than 10 ft as a result of production-induced reservoir compaction (Sulak, 1991).

The effective stress on the rock (the difference between the overburden load on the rock and the pore pressure within the rock) increases as additional hydrocarbons and water are withdrawn and reservoir pressure declines. Certain rocks, under such conditions, exhibit a sudden increase in compressibility. This sudden increase in compressibility, coupled with a large irreversible deformation, is called *pore collapse* (Smits *et al.*, 1988). Several investigators have observed this phenomenon in the laboratory also (e.g., Blanton, 1981; Newman, 1983). The compaction resulting from the pore collapse in the reservoir rocks is transmitted through the overburden causing the seafloor to subside

according to Zaman *et al.* (1995, in: Chilingarian *et al.*, 1995, p. 380). Pore collapse is believed to be the main cause of reservoir compaction and the seafloor subsidence in the Ekofisk Field.

The Phillips Group had discussed the subsidence of the seafloor as a possibility in their application for test production in 1970. But it could not be noticed easily *in situ* because the subsidence occurred millimeter by millimeter over the years and the people accustomed to sights on an everyday basis could not notice it. Another point is that the measurements taken between the structures in the Ekofisk complex showed no change in elevation from one structure to another, because all structures in the area were moving down as a unit, at approximately the same rate. Also, the Phillips engineers noted that the Ekofisk reservoir is more than 10,000 ft deep, and subsidence was never reported over a 10,000 ft deep reservoir (Kvendseth, 1988). They described methods of measurement of the reservoir compaction and the resulting surface subsidence. Both temporary and permanent solutions to overcome the problem were discussed. A brief description of the factors that affect the subsidence of the ground was provided. This was followed by a discussion of various approaches adopted by research workers to investigate the characteristics and mechanics of reservoir rocks, and to model the observed behavior. Two-dimensional and three-dimensional numerical simulations of the compacting field were undertaken by different investigators.

According to Zaman *et al.* (1995), as a result of compaction and consequent subsidence, it was necessary to raise the Ekofisk complex, at a cost of about $1 billion. It should be kept in mind that compaction drive made a significant contribution to the recovery of hydrocarbons. Sulak *et al.* (1989) used a three-dimensional reservoir simulator and a three-dimensional (3D) finite element (FE) model to relate rock compressibility to porosity, rock type, reservoir pressure, and areal and vertical location. Boade *et al.* (1988) simulated compaction/subsidence using FE geomechanics model DYNFLOW.

3.6 Concluding Remarks

Bending of rock formations, due to subsidence, results in compression, extension, and shear, which lead to fracturing of rocks. Fractures tend to occur at the periphery of a subsiding basin. Fracturing of rocks damages wellbores and sometimes induces technological earthquakes. These fractures may form avenues for the migration of natural gas from the oilfields to the surface.

The fact that fluid withdrawal for hydrocarbons is generally from point sources (not evenly distributed over the areal extent of the produced formation) and that the formations above the hydrocarbon reservoir are not composed of homogenous sediments (or in even layers) subsidence tends to be differential. Damage to subsurface pipelines, foundations of buildings, structures, sidewalks, streets and paved areas can often be minimized by recognition of the problem and use of repressuring the reservoir by waterflooding. This type of corrective measure, utilizing water to replace the produced fluids can have beneficial results. This measure helps to maintain the structural integrity of the surface facilities, prevent aquifer invasion by surrounding fluid of greater pressure, e.g., sea water, and help support the pore structure of the formation itself. All

economic future development should consider all aspects of production and consequent subsidence because *subsidence occurs in most oilfields*.

References and Bibliography

Allen, D. R. and Chilingarian, G. V., 1995. Mechanics of sand compaction. In: G. V. Chilingarian and K. H. Wolf (Eds.), *Compaction of Coarse-Grained Sediments*, 1, Elsevier, Amsterdam, pp. 423–477.

Allen, D. R. and Mayuga, M. N., 1969. The mechanics of compaction and rebound, Wilmington Oil Field, Long Beach, California, U.S.A. In: *Land Subsidence.* I.A.S.H.—Unesco, Publ. no.89 AIHS, 2:410–423.

Allen, D. R., 1968. Physical changes in reservoir properties caused by subsidence and repressuring operations. *J. Pet. Technol*., 2:23–29.

Allen, D. R., Chilingar, G. V., Mayuga, M. N. and Sawabini, C. T., 1971. Studio e previsione della subsidenza. *Enciclopedia della Scienza e della Tecnica*. Arnoldo Mondadori Editore, pp.281–292.

Applin, P. and Applin, E. R., 1965. Comanche Series and associated rocks in subsurface in central and south Florida, *U.S. Geol. Sur., Prof. Pap*. 447:84 pp.

Armstrong, F. C. and Oriel, S. S., 1965. Tectonic development of Idaho-Wyoming thrust belt. *Bull. Am. Assoc. Pet. Geol*., 49:1847–1866.

Baars, D. L., 1966. Pre-Pennsylvanian paleotectonics - key to basin evolution and petroleum occurrences in Paradox Basin, Utah and Colorado. *Bull. Am. Assoc. Pet. Geol*., 50:2082–2111.

Bara, J. P., 1960. Laboratory studies in loessial foundations and embankment samples - Sherman Dam- Farewell Unit, Nebraska. *U.S. Bur. Reclam., Earth Lab*., Denver, Colo., Rep., EM-572, 17 pp.

Barbat, W. F., 1958. The Los Angeles Basin area, California; in: L. G. Weeks (Editor), Habitat of oil. *Bull. Am. Assoc. Pet. Geol*., Tulsa, OK, pp 62–77.

Barrends, F. B. J., Carbognin, L., Gambolati, G., and Steedman, R. S., 2005. *Land Subsidence*, Proc. 7th Int'l. Symp. Land Subsidence, Shanghai, P. R. China, 171 pp.

Beal, L H., 1965. Geology and mineral deposits of the Bunkerville mining district, Clark County, Nevada. *Nev. Bur. Mines Bull*., 63:96 pp.

Beckwith, G. H., Slemmons, D. B. and Weeks, R. E., 1991. Use of low-sun angle photography for identification of subsidence-induced fissures. In: A. I. Johnson (Ed.), *Land Subsidence*, IAHS Publ., 200:261–269.

Bell, J. S. and Dusseault, M. B., 1991. Scale effects and the use of borehole breakouts as stress indicators. In: A. Pinta da Cunha (Ed.), *Scale Effects in Rock Masses*, Balkema, Rotterdam, pp. 327–337.

Biot, M.A., 1941. General theory of three-dimensional consolidation. *J. Appl. Phys*., 12(5):155–164.

Bissell, H. J., 1962a. Pennsylvanian and Permian rocks of Cordilleran area. In: *Pennsylvanian System in the United States - a Symposium*. *Am. Assoc. Pet. Geol.*, Tulsa, OK, pp.188–262.

Bissell, H. J., 1962b. Permian rocks of parts of Nevada, Utah, and Idaho. *Bull. Geol. Soc. Am.*, 73:1083–1100.

Bissell, H. J., 1962c. Pennsylvanian-Permian Oquirrh Basin of Utah. In: *Geology of the Southern Wasatch Mountains and Vicinity, Utah*. Brigham Young Univ. Geol. Stud., 9(1):26–49.

Bissell, H. J., 1970. Realms of Permian tectonism and sedimentation in western Utah and eastern Nevada. *Bull. Am. Assoc. Pet. Geol*., 54:285–312.

Blanton, T. L. III, 1981. Deformation of chalk under confining pressure and pore pressure. *J. Soc. Pet. Engr*., 21(1):43–50.

Bloom, A. L., 1967. Pleistocene shorelines: a new test of isostasy. *Bull. Geol. Soc. Am*., 78:1477–1494.

Boade, R. R., Chin, L. Y. and Siemers, W. T., 1989. Forcasting of Ekofisk reservoir compaction and subsidence by numerical simulation. *J. Pet. Technol*., 41(7):723–728.

Bockmeulen, H., Barker, C. and Dickey, P. A. 1983. Geology and geochemistry of crude oils, Bolivar Coastal Fields, Venezuela. *Bull. Am. Assoc. Pet. Geol*., 67(2):242–270.

Bondesan, M. and Simeoni, U., 1983. Dinamica e analisi morfologica statistica dei litorali del delta del Po e alle foci dell'Adige e del Brenta. *Mem. Sci. Geol*., 36:1–48.

Borgia, G. C. and Ricchiuto, T., 1985. Genesi e correlazione degli accumuli gassiferi superficiali, dell' Appenino Emiliano. *Acque Sotterranee*, 2(3):15–27.

Borgia, G. C., Brighenti, G. and Vitali, D., 1982. Misure estensimetriche del compattamento del sottosuolo per produzine di acqua o idrocarbutri in aree soggette a subsidenza. *Quademo AMGA*, 4:1–24.

Borgia, G. C., Brighenti, G., Mesini, E., and Vitali, D., 1987. In-situ measurements of compaction due to water or hydrocarbon production. *Proc. XXI-th Congr. IAH*, Rome Italy, 13 pp.

Borgia, G. C., Elmi, C., and Ricchiotu, T., 1987. Correlation by genetic properties of the shallow gas seepage. *Proc. XIII-th Int. Meeting Organic Chemistry*, Venice, Italy.

Borregales, C. and Salazar, A.,1987. *The Future for In-Situ Recovery;, Treatment, Trqnsportation of Heavy Oil in Venezuela*. Topic 17 on Recovery of Extra Heavy Oils, Natural Bitumens and Shale Oils, 12th World Petroleum Congress, Houston, TX.

Bradley, J., 1975. Abnormal formation pressure. *Bull. Am. Asoc. Pet. Geol*., 59:957–973.

Brighenti, G, Borgia, G. C. and Mesini, E., 1995. Subsidence studies in Italy, pp. 215–276. In: G. V. Chilingarian, E. C. Donaldson and T. F. Yen, 1995, *Subsidence Due to Fluid Withdrawal*, Elsevier Science, 498 pp.

Brill Jr., K. G., 1952. Stratigraphy of the Permo-Pennsylvanian zeugogeosyncline of Colorado and northern New Mexico. *Bull. Geol. Soc. Am*., 63:809–880.

Brown Jr., R. D. and Hanna, W. F., 1971. Aeromagnetic evidence and geologic structure, Northern Olympic Peninsula and Strait of Juan de Fuca, Washington. *Bull. Am. Assoc. Pet. Geol*., 55:1939–1953.

Bucher, W. H., 1933. *The Deformation of the Earth's Crust*. Princeton University Press, Princeton, N.J., 518 pp.

Bullard, E., Everett, J. E. and Smith, A. G., 1965. The fit of the continents around the Atlantic. *R. Soc. Lond. Philos. Trans*., Ser. A, 258:41–51.

Carbognin, L., Gatto, P. and Marabini, M., 1984. Correlation between shoreline variations and subsidence in the Po River Delta, Italy. *Proc. 3rd Int. Symp. Land Subsidence*, Venice, IAHS Publ., 151:309–320.

Chamberlain, C. K, 1971. Bathymetry and paleoecology of Ouachita geosyncline of southeastern Oklahoma as determined from trace fossils. *Bull. Am. Assoc. Pet. Geol*., 55:34–50.

Chase, C. G. and others, 1970. History of sea-floor spreading west of Baja California. *Bull. Geol. Soc. Am*., 81:491–498.

Chilingar, G. V. and Endres, B., 2004. Environmental hazards posed by the Los Angeles Basin urban oilfields: an historical perspective of lessons learned. *Environmental Geology*, 47:302–317.

Chilingar, G. V., Khilyuk, L. F., and Katz, S. A., 1996. Pronounced changes of upward natural gas migration as precursors of major seismic events. *J. Petrol. Sci. and Engr*., 14:133–136.

Chilingar, G. V., Mannon, R. W. and Rieke III, H. H., 1972. *Oil and Gas Production From Carbonate Rocks*, Am. Elsevier, New York, NY, 408 pp.

Chilingarian, G. V. and Wolf, K. H., 1975. *Compaction of Coarse--Grained Sediments*, 1. Developments in Sedimentology, 18A. Elsevier, Amsterdam, 552 pp.

Chilingarian, G. V., Donaldson, E. C., and Yen, T. F., 1995. *Subsidence Due to Fluid Withdrawal*. Dev. Petrol. Sci. 41, Elsevier, Amsterdam, 498 pp.

Chipping, D. H., 1972. Early Tertiary paleogeography of central California. *Bull. Am. Assoc. Pet. Geol*., 56:480–493.

Christiansen, F. W., 1952. Structure and stratigraphy of the Canyon Range, central Utah. *Bull. Geol. Soc. Am*., 63:717–740.

Clark, L. M. (Editor), 1954. *Western Canada Sedimentary Basin*. Am. Assoc. Pet. Geol., Tulsa, Okla., 521 pp.

Cline, L. M., 1970. Sedimentary features of Late Paleozoic flysch, Ouachita Mountains, Oklahoma. *Geol. Assoc. Can., Spec. Pap*., 7:85–101.

Colazas, X. C. and Strehle, R. W., 1995. Subsidence in the Wilmington Oilfield, Long Beach, CA, U.S.A.; in: G.V. Chilingarian, E. C. Donaldson and T. F. Yen, *Subsidence Due to Fluid Withdrawal*, Elsevier Science, Amsterdam, 498pp.

Colle, J., Cooke Jr., W. F., Denham, R. L., Ferguson, H. C., McGuirt, J. H., Reedy Jr., F. and Weaver, P., 1952. Volume of Mesozoic and Cenozoic sediments in Western Gulf Coastal Plain of United States. *Bull. Geol. Soc. Am*., 63:1193–1200.

Coney, P. J., 1970. The geotectonic cycle and the new global tectonics. *Bull. Geol. Soc. Am*., 81:739–748.

Contaldo, G. J. and Mueller, J. E., 1991. Earth fissures and land subsidence of the Mimbres Basin, Southwestern New Mexico, U.S.A. In: A. I. Johnson (Ed.), *Land Subsidence*. IAHS Publ., 200: 301–310.

Cramer, H. R., 1971. Permian rocks from Sublett Range, southern Idaho. *Bull. Am. Assoc. Pet. Geol*., 55:1787–1801.

Crittenden Jr., M. D., 1963a. New data on the isostatic deformation of Lake Bonneville. *U.S. Geol. Surv., Prof. Pap., 454-E*, 31 pp.

Crittenden Jr., M. D., 1963b. Effective viscosity of the Earth derived from isostatic loading of Pleistocene Lake Bonneville. *J. Geophys. Res.,* 68:5517–5530.

Crittenden Jr., M. D., Schaeffer, F. E., Trimble, D. E. and Woodward, L. A., 1971. Nomenclature and correlation of some Upper Precambrian and Basal Cambrian sequences in western Utah and southeastern Idaho. *Bull. Geol. Soc. Am*., 82:581–602.

Crosby, G. W., 1968. Vertical movements and isostasy in western Wyoming overthrust belt. *Bull. Am. Assoc. Pet. Geol*., 52:2000–2015.

Currie, J.B., 1967. Evolution of stress in rocks of a sedimentary basin. Rock Mechanics in Oilfield Geology. *Drilling and Production. Proc. World Petrol. Congr*., Mexico City, Mexico. Elsevier, Amsterdam, pp. 1–51.

Dallmus, K. F., 1958. Mechanics of basin evolution and its relation to the habitat of oil in the basin. In: L G. Weeks (Editor), *Habitat of Oil*, Am. Assoc. Pet. Geol., Tulsa, OK, pp. 883–931.

Dana, J. D., 1873. On some results of the Earth's contraction from cooling. *Am. J. Sci*., 3rd Ser., 5:430; 6:717.

Dewey, J. F., 1969. Evolution of the Appalachian-Caledonian orogen. *Nature*, 22:124–129.

Dietz, R. S. and Holden, J. C., 1966. Miogeosynclines in space and time. *J. Geol*., 74:566–583.

Dietz, R. S., 1972. Geosynclines, mountains, and continent-building. In: J. T. Wilson (Ed.), *Continents Adrift*, Sci. Am., pp. 124–132.

Dietz, R. S., Holden, J. C. and Sproll, W. P., 1970. Geotectonic evolution and subsidence of Bahama Platform. *Bull. Geol. Soc. Am*., 81:1915–1928.

Dietzman, W. D., Rafidi, N. R., and Ross, T. A., 1983. *The Petroleum Resources of the North Sea,* DOE/EIA-0381, Energy Information Administration, U.S. Department of Energy, 103 pp.

Dobrynin, V. M. and Serebryakov, V. A., 1989. *Geologic-Geophysical Methods of Predicting Abnormal Formation Pressures*. Nedra, Moscow, 285 pp.

Donaldson, E. C. and Chilingarian, G. V., 1997. Review of subsidence due to groundwater withdrawal. *Second Ann. Symp. Groundwater Resources and Groundwater Quality Protection*, Jan. 9–10, National Cheng Kung Univ., Tainan, Taiwan, pp. 247–264.

Drake, C. L., Ewing, M. and Sutton, J., 1959. Continental margins and geosynclines: The east coast of North America north of Cape Hatteras. In: *Physics and Chemistry of the Earth*, 5. Pergamon, New York, NY, pp. 110–198.

Endres, B. L., Chilingar, G. V., and Yen, T.F., 1991. Environmental hazards of urban oilfield operations. *J. Petrol. Sci. Eng*., 6:95–106.

Enever. J. R., Walton, R. J., and Wold, M. B., 1990. Scale effects influencing hydraulic fracture and overcoming stress measurements. In: A. Pinta da Cunha (Ed.), *Scale Effects in Rock Masses*, Balkema, Rotterdam, pp. 317–326.

Finol, A. and Farouq Ali, S. M., 1974. Numerical simulation of oil production with simultaneous ground subsidence. SPE European Spring Meeting, Amsterdam, May 29–30; *Soc. Petro. Engr. J*., October: 411 enrule 424: *Trans. AIME*, 259 (1975):411–424.

Finol, A. and Sancevic, Z. A., 1995. Subsidence in Venezuela, pp. 337–370, in: G. V. Chilingarian, E. C. Donaldson and T. F. Yen, *Subsidence due to Fluid Withdrawal*, 1995, 500 pp.

Fukuo, Y., 1969. Visco-elastic theory of the deformation of confined aquifer. In: Land *Subsidence. I.A.S.H.--Unesco, Publ*. No.89 AIHS, 2:547–562.

Gabrish, R. K. and Holzer, T. L., 1978. Fault control of subsidence, Houston, TX. Discussion. *Ground Water*, 16(1):51–55.

Galloway, D., Jones, D., and Ingebritsen, S.E., 1999. *Land Subsidence in the United States*, U.S.G.S. Circular 1182, Geol., 21st Sess., pp.5–16.

Gambardella, F. and Mercusa, G. 1984. Land subsidence in the delta area of River Po: damages and repairing works. *Proc. 3rd Int. Symp*., Venice. IAHS Pub., 151:309–320.

Gilluly, J., Johnson, H. R. and Grant, U. S., 1945. *Subsidence of the Long Beach Harbor Area, California*, Report to the Board of Harbor Commissioners, City of Long Beach, 152 pp.

Guacci, G., 1979. The Pixley fissure, San Joaquin Valley, California; in: S. K. Saxena (Ed.), *Evaluation and Prediction of Subsidence*, ASCE Publ., New York, NY, pp. 303–319.

Gurevich, A. E., Endres, B. L., Robertson, Jr., J. O. and Chilingarian, G. V., 1993. Gas migration from oil and gas fields and associated hazards. *J. Pet. Sci. Eng*., 9:223–238.

Gurevich, A. E. and Chilingarian, G. V., 1993. Subsidence over producing oil and gas fields, and gas leakage to the surface. *J. Pet. Sci. Eng*., 9, 239–250.

Gurevich, A. E., 1980. *Handbook of Groundwater Motion Exploration*, Nedra Publishers, Leningrad, 216 pp. (In Russian.)

Hallenbeck, L. D., Sylte, J. E., Ebbs, D. J., and Thomas, L. K., 1989. Implementation of the Ekofisk field waterflood. *SPE Paper 19838*, *SPE Ann. Technol. Conf*., San Antonio, TX, 12 pp.

Hamilton, D. H. and Meehan, R. l., 1971. Ground rupture in the Baldwin Hills. *Science*, 172:333–344.

Haneberg, W. C., Reynolds, C. B. and Reynolds, I. E., 1991. Geophysical characterization of soil deformation associated with earth fissures near San Marcial and Deming, New Mexico. In: A. I. Johnson (Ed.), *Land Subsidence*, IAHS Publ., 200: 271–280.

Harris, F. R., 1945. *Report of Subsidence of the Terminal Island-Long Beach Area, California*. Report to the Commander of the Long Beach Naval Shipyard, 137 pp.

Holmes, A., 1944. *Principles of Physical Geology*, 1st ed. Nelson, London. (2nd ed. 1965, 1288 pp.)

Holzer, T. L. and Thatcher, W., 1979. Modeling deformation due to subsidence faulting. In: S. K. Saxena (Ed.), *Evaluation and Prediction of Subsidence*. ASCE Publ., New York, NY, pp. 349–357.

Holzer, T. L., 1984. Ground failure induced by groundwater withdrawal from unconsolidated sediments. In: T. L. Holzer (Editor), Man-induced Land Subsidence. *Geol. Soc., Am. Rev. Eng. Geol*., VII:67–105.

Hottman, C. E. and Johnson, R. K., 1965. Estimation of formation pressures from log-derived shale properties. *J. Pet. Technol*., 6(6):717–722.

Hsu, K. J., 1958. Isostasy and a theory of geosynclines. *Am. J. Sci*., 256:305.

Hudson, F. S., 1957. *Subsidence of Long Beach Harbor Area*. Report to the City of Long Beach, 66 pp.

Ito, T., Hayashi, K., and Abe, H., 1990. Scale effect in breakdown pressure of hydraulic fracturing stress measurements. In: A. Pinta da Cunha (Ed.), *Scale Effects in Rock Masse*s. Balkema, Rotterdam, pp. 289–295.

Jacquin, C. and Poulet, M. J., 1970. Study of the hydrodynamic pattern in a sedimentary basin subject to subsidence, *45th Ann. Fall Meet. Soc. Pet. Engrs., Am. Inst. Min. Metall. Engrs.*, Houston, Texas, Presented *Paper No. SPE 2988*, 6 pp.

Jachens, R. C. and Holzer, T. L., 1979. Geophysical investigation of ground failure related to groundwater withdrawal—Picacho Basin, *Groundwater*, 17(6):574–585.

Kartsev, A. A., Vagin, S. B. and Baskov, E. A., 1969. *Paleohydrogeology*. Nedra, Moscow, 150 pp.

Keaton, J. R. and Shlemon, R. J., 1991. The Fort Hancock earth fissure system, Hudspeth County, Texas: Uncertainties and implications. In: A. I. Johnson (Ed.), *Land Subsidence*. IAHS Publ., 200:281–290.

Kreitler, C. W., 1977. Faulting and land subsidence from groundwater and hydrocarbon production, *Land Subsidence Symposium, Paris. Int. Assoc. Hydrol. Sci*., pp. 435–446.

Khilyuk, L. F., Chilingar, G. V., Robertson Jr., J. O. and Endres, B. L., 2000. *Gas Migration--Events Preceding Earthquakes*, Butterworth-Heinemann, Woburn, Massachusetts, 389 pp.

Kosloff, D., Scott, R. F. and Scranton, J., 1980. Finite element simulation of Wilmington oil field subsidence: 1. Linear modeling. *Tectonophysics*, 65:339–368.

Kovach, R. L., 1974. Source mechanism for Wilmington Oilfield, California, subsidence earthquakes. *Bull. Seismol. Soc. Am*., 64:699–711.

Kvendseth, S. S., 1988. *Giant Discovery: A History of Ekofisk Through the First 20 Years*, Phillips Petroleum Co., Norway, 224 pp.

Lee, K. L., 1979. Subsidence earthquakes at a California oil field. In: S. K. Saxena (Editor), Evaluation and Prediction of Subsidence, *Eng. Found. Conf. ASCE*, pp. 549–564.

Lister, L. A. and Secrest, C. D., 1985. Giant desiccation cracks and differential surface subsidence, Red Lake Playa, Mojave County, Arizona. *Am. Assoc. Eng. Geol. Bull*., 22:299–314.

Lofgren, B.E. and Klausing, R.L., 1969. Land subsidence due to ground-water withdrawal, Tulare Wasco area, California. *U.S. Geol. Surv., Prof. Pap*., 437B, 103 pp.

Lofgren, B. E., 1969. Field measurements of aquifer-system compaction, San Joaquin Valley, California, U.S.A.; in: *Land Subsidence*. I.A.S.H.,Unesco, Publ. no. 88 AIHS, 1:272–284.

Love, D. W., Remers, R. F., Hawley, J. W., Johnpeer, G. D., and Bobrow, D. J., 1987. Summary of geotechnical investigations near Espanola, New Mexico. In: C. Menges (ed.) *Quaternary Tectonics Landform Evolution, Soil Chronologies and Glacial Deposits*. N. M. Dept. of Geol., Albuquerque, NM, pp. 133–157.

Louis, C. R. and Rose, C. S., 1970. A theory relating high temperatures and overpressures. *J. Pet. Technol*., 22:11–16.

Marsden, S. S., 1980. The status of dissolved gas in Japan. *Pet. Eng. Int*., 52(6):23–24.

Marsden, S. S. and Davis, S. N., 1967. Geological subsidence. *Sci. Am*., 216(6): 93–100.

Mattavelli, L., Ricchitto, T., Grignani, D., and Schoell, M., 1983. Geochemistry and habitat of natural gases in Po Basin, northern Italy. *Bull. Am. Assoc. Pet. Geol*., 67(12):2239–2254.

Merle, H. A., Kentie, C. J. O., van Opstal, G. and Schneider, G. M. C., 1975. The Bacaquero study – a composite of the behavior of a compaction drive/solution gas drive reservoir. 5th Annual Fall Conference, Dallas, TX. SPE pap. 5529, *J. Pet. Technol.*, 1976, I:1107–1115.

Mess, K. W., 1979. On the interpretation of core compaction behavior. In: S. K. Saxena (Ed.), *Evaluation and Prediction of Subsidence*. ASCE Publ., New York, NY, pp. 76–91.

Meyer, R. F. and Powly, D. E., 1988. Subsidence and the petroleum industry: an overview. *AAPG Bull*., 72(2):223.

Mikasa, M., 1963. *Consolidation of Soft Clays, A New Consolidation Theory and Its Application*. Res. Inst. Kajima Construction Co. Ltd., Publ. Office, Japan.

Montori, S., 1983. Effetti della subsidenza sui teritorio di bonifica. *Proc. Workshop "Subsidenza del Territorio e Problemi Emergenti,* Bologna, 11 pp.

Newman, G. H., 1983. The effect of water chemistry on laboratory compression and permeability characteristics of some North Sea chalks. *J. Pet. Technol*., 35(5):976–980.

Okumura, T., 1969. Analysis of land subsidence in Niigata; in: *Land Subsidence*. I.A.S.H.-Unesco, Publ. no.88 AIHS, 1:130–143.

Pampeyan, E. H., Holzer, T. L., and Clarke, M. M., 1988. Modern ground failure in the Garlock Fault zone, Fremont Valley, California. *Geol. Soc. Am. Bull*., 100:677–691.

Pewe, T. L., Raymond, R. H., and Schumann, H. H., 1987. Land subsidence and earth-fissure formation in eastern Phoenix metropolitan area, Arizona. In: G. H. Davis and E. M. van den Dolder (Editors), *Geologic Diversity of Arizona and Its Margins -Excursions to Choice Areas*. Ariz. Bur. Geol. Min. Tech., Geol. Surv. Branch, Spec. Pap., 5:199–211.

Poland, J. F. and Davis, G. H., 1969, Land subsidence due to withdrawal of fluids. In: *Reviews in Engineering Geology*, II. Geol. Soc. Am., New York, NY, pp. 187–269.

Powley, D. E., 1990. Pressures and hydrogeology in petroleum basins. *Earth-Sci. Rev.,* 29:215–226.

Pratt, W. E. and Johnson, D. W., 1926. Local subsidence of the Goose Creek Oil Field. *Geology*, XXXIV (7, Part I):577–590.

Ratigan, J. L., 1990. Scale effects in the hydraulic fracture test associated with the estimation of tensile strength. In: A. Pinta da Cunha (Ed.), *Scale Effects in Rock Masses*. Balkema. Rotterdam, pp. 297–306.

Richter, C. F., 1958. *Elementary Seismology*. Freeman, San Francisco, CA, 768 pp.

Rieke, H.H., III and Chilingarian, G.V., 1974. *Compaction of Argillaceous Sediments*. Developments in Sedimentology, 16. Elsevier, Amsterdam, 424 pp.

Roberts, J. E., 1969. Sand compression as a factor in oil-field subsidence. In: *Land Subsidence*, I.A.S.H.-Unesco, Publ. no. 89 AIHS, 2:368–376.

Robertson, J. O., Chilingar, G. V., Khilyuk, L. R., and Endres, B**.,** 2012. *Environmental Hazards from the Los Angeles Basin oilfields*, CA. *E6-193-22 UNESCO-EOLSS*, 45 pp.

Sandhu, R. S. and Wilson, E. L., 1969. Finite element analysis of land subsidence. In: *Land Subsidence*. I.A.S.H.-Unesco, Publ. no. 89 AIHS, 2: 393–400.

Sawabini, C. T., Chilingar, G. V. and Allen, D. R., 1974. Compressibility of unconsolidated arkosic oil sands. *Soc. Petrol. Engr. J*., 14:132–138.

Scheidegger, A. E. and O'Keefe, J. A., 1967. On the possibility of the origination of geosyncline by deposition. *J. Geophys. Res*., 72(24):6275–6278.

Serebrykov, V.A. and Chilingarian, G.V., 2000. Prediction of subsidence: relationship between lowering of formation pressure and subsidence due to fluid withdrawal. *Energy Sources*, 22(5):409–416.

Smits, R. M. M., de Waal, J. A., and van Kooten, J. F. C., 1988. Prediction of abrupt reservoir compaction and surface subsidence caused by pore collapse in carbonates. *Soc. Pet. Engr. Form. Eval*., 3(2):340–346.

Snyder, R. E., 1971. Phillips in the North Sea: massive Danian limestone key to Ekofisk success. *World Oil*, 172(6):51–52.

Strehle, R. W., 1989. Subsidence hazards — a history. In: S. M. Testa (Ed.), *Environmental Concerns in the Petroleum Industry*. AAPG Publ., pp. 107–116.

Sulak, R. M. and Danielsen, J., 1989. Reservoir aspects of Ekofisk subsidence. *J. Pet. Technol.*, 41(7):723–728.

Sulak, R. M., 1991. Ekofisk field: The first 20 years. *J. Pet. Technol.*, 43(10):1265–1271.

Sylte, J. E., Hallenbeck, L. D., and Thomas, L. K., 1988. Ekofisk formation pilot waterflood. *Proc. Soc. Petrol. Engrs. Ann. Technol. Conf.*, Houston TX, Oct., pp. 153–167.

Taylor, D. W., 1948. *Fundamentals of Soil Mechanics*. Wiley, New York, NY, 700 pp.

Ter-Martirosyan, Z.G. and Ferronsky, V.I., 1969. Some problems of time-soil compaction in pumping liquid from a bed. In: *Land Subsidence*. I.A.S.H.-Unesco, Publ. no.88 AIHS, 1:303–314.

Terzaghi, K. and Peck, R. B., 1948. *Soil Mechanics in Engineering Practice*. Wiley, New York, NY, 566 pp.

Terzaghi, K., 1926. Simplified soil tests for subgrades and their physical significance. *Public Roads*, 7:153–162.

Terzaghi, K., 1936. Simple tests determine hydrostatic uplift. *Eng. News Rec.*, 116 (June 18):872–875.

Terzaghi, K., 1943. *Theoretical Soil Mechanics*, Wiley, New York, N.Y., 510 pp.

Thomas, L. K., Dixon, T. N., Pierson, A. G., and Hermansen, H. 1989. Ekofisk nitrogen injection, *SPE Paper 19839. SPE Ann. Techol. Conf.*, San Antonio, TX, Oct 8–11, 16 pp.

Van der Knaap, W. and Van der Vlis, 1967. On the cause of subsidence in oil producing areas. *Proc. 7th World Pet. Congr.*, Mexico City, pp. 85–95.

Van Sickle, V. R. and Groat, C. G., 1981. Subsidence and induced faulting: key environmental issues in geopressured geothermal resource development. *5th Louisiana Geol. Surv., Louisiana State Univ. and U. S. Gulf Coast Geopressured Energy Conf. Proc.*, Paris, pp. 325–330.

Weeks, L. G., 1952. Factors of sedimentary basin development that control oil occurrence. *Bull. Am. Assoc. Pet. Geologists*, 36:2071–2124.

Wentworth, C. M., Ziony, J. I., and Buchanan, J. M., 1969. *Preliminary Geologic Environmental Map of the Greater Los Angeles Area, California.*

Wiborg, R. and Jewhurst, J., 1986. Ekofisk subsidence detailed and solutions assessed. *Oil Gas J.*, 84(7):47–51.

Zaman, M. M., Abdulraheem, A., and Roegiers, J. C., 1995. Reservoir compaction and surface subsidence in the North Sea Ekofisk Field, pp. 373–423; in: G. V. Chilingarian, E. C. Donaldson, and T. F. Yen, 1995. *Subsidence Due to Fluid Withdrawal*, Elsevier Science, 498 pp.

Zambon, M., 1983. Subsidenza del territorio e problemi emergenti. Proc. Workshop, "*Subsidenza del Territorio Problemi Emergenti*." Bologna, 22 pp.

Zambon, M., 1967. Abbassamenti del suolo per estazioni di acqua e di gas. Deduzioni ed indirizzi logicamente conseguenti per la sistemazione del delta del fiume Po. *Proc. XXIII-th Congr. Nazionale delle Bonifiche,* Roma, 34 pp.

Environmental Aspects of Oil and Gas Production.
John O. Robertson and George V. Chilingar.
© 2017 Scrivener Publishing LLC. Published 2017 by John Wiley & Sons, Inc.

4

Effect of Emission of CO_2 and CH_4 into the Atmosphere

4.1 Introduction

A major environmental concern is the production and burning of hydrocarbons and the releasing of carbon to the atmosphere. It is thought by some, without scientific evidence, that humans are putting carbon (in the form of carbon dioxide, CO_2, or methane, CH_4) into the atmosphere and that this anthropogenic carbon is responsible for *global warming*.

Syante Arrhenius, a Swedish scientist, was the first to claim that fossil fuel combustion may eventually result in enhanced global warming (Maslin, 2004; in: Enzler, 2015). He proposed that there was a relationship between atmospheric carbon dioxide concentrations in the atmosphere and global temperature. Since then, the concept has been taken as obvious by many without "*verification*" (Budyko, 1997; Global warming, 1993; Greenhouse effect, 1989). The arguments for, against, and why global warming occurs have grown within the scientific community since his proposal. In examining the relationship between temperature and carbon content in the atmosphere it is critical that we examine not just the recent history, but also the Earth's historical geologic data. The Earth's climatic changes, as demonstrated in the Antarctic ice, for the last 800,000 years, have been cyclic periods of cooling and warming.

A theory of global warming states that heating of the atmosphere occurs as a direct result of additional carbon dioxide (CO_2) and methane (CH_4) that is added to the Earth's atmosphere produced by man's activities (anthropogenic). As a result, the

petroleum industry has often been "*singled out for blame*" for the release of carbon (methane and carbon dioxide) into the atmosphere as it produces and handles hydrocarbons. There are some who believe that today's increase in atmospheric carbon dioxide, can be entirely attributed to human activities related to release of CO_2 or CH_4 to the atmosphere.

A survey of several thousand scientists conducted by the University of Illinois found that 82% believe that human activity in generating CO_2 has been a significant factor in changing mean global temperatures. Climatologists who are active in research showed the strongest consensus on this cause of global warming, with 97% agreeing human activity plays a primary role. Those familiar with hydrocarbons and climate, e.g., petroleum geologists and engineers along with meteorologists were among the biggest doubters, with only 47% to 64%, respectively, accepting the concept of human involvement as a primary cause of global warming. Delingpole (2015) reported that Steven Goddard, 2015, has shown evidence that NASA and NOAA have adjusted the raw temperature values to indicate global warming. He also pointed out that Hansen in a 1989 report observed that over the previous 50 years (which was also a period of significant increase in the production of greenhouse gases) there had been little temperature change. In fact, this period appears to be one of global cooling throughout much of the United States.

However, Greenberg (2015) reported that the members of the U.S. Senate voted 98-1 that climate change is real and not a hoax.

Today, with more information available, more scientists are beginning to openly disagree with prior concepts that the CO_2 released by humans is the cause for increased global temperature (Chilingar *et al*., 2009 and Chilingar *et al*., 2014). In fact, as demonstrated in this chapter, CO_2 cannot be the driving force to higher global temperatures as shown by both the historic geologic and adiabatic data. These authors note that the scientific community, throughout the world, is today currently divided on the issue of whether man's activities are truly responsible for global warming or if global warming is a natural process, e.g., the positional interrelationship between the sun and Earth, volcanic activity and other factors related to natural causes. The authors present arguments brought forward by scientists such as Sorokhtin *et al*. (2003, 2004 and 2006), Chilingar and Khilyuk (2007), Chilingar *et al*. (2009), Chilingar *et al*. (2014) and many others examining the various "*carbon cycles*" of Earth and their relationship to global temperature.

This chapter is divided into three sections: (1) historic geological evidence showing a historic cycling of temperature long before human existence, (2) adiabatic theory and (3) effect of methane gas in the atmosphere. The historic portion has several subsections: (a) geologic evidence that the Earth's global temperature has historically been cyclic for the past 800,000 years, and (b) that the geologic temperature vs. CO_2 data, indicate that the increase in CO_2 did not raise global temperature as the increase in CO_2 concentration in the atmosphere occurred after an increase in global temperature (by about 800 to 1,000 years). The adiabatic analysis shown at the end of this chapter is consistent with the presented historic data, demonstrating that temperature fluctuation affects the percentage of carbon content in the atmosphere and not the other way around.

4.2 Historic Geologic Evidence

4.2.1 Historic Record of Earth's Global Temperature

The historic geologic record of temperature (and carbon dioxide) is presented in Figure 4.1. This figure shows that Earth's global temperature and % carbon in the atmosphere have varied greatly over geologic time without a distinctive relationship. This geologic record also shows that the Earth has often been much hotter and more humid than it is today. Heib (2009) has noted that the only period of the Earth's history that appears to have similar values of global temperature and atmospheric carbon content is 300 million years ago during the late Carboniferous Period.

Temperature and % carbon in atmosphere data for the Earth's lower atmosphere has been obtained from several studies of gas bubbles that were trapped in the ice overlying Antarctica. The data from studies of Antarctic ice cores yield a 400,000-year to 800,000-year record of global temperature with a deviation of about 10 °C. Dillon plotted the deviation of temperature relative to the 2000 A.D. temperature for the past 400,000 years (Figure 4.2). This figure indicates a historic temperature cycle (≈100,000 years) of cooling and warming of the Earth's lower atmospheric global temperature. The Earth's global temperature cycle of warming and cooling occurred long before human activities.

Today, some investigators suggest that Earth's global temperature is currently warming; however, Monctkon (2015) in a review of Earth's lower atmosphere, obtained by satellite, has noted little evidence of either warming or cooling for the past 17 years.

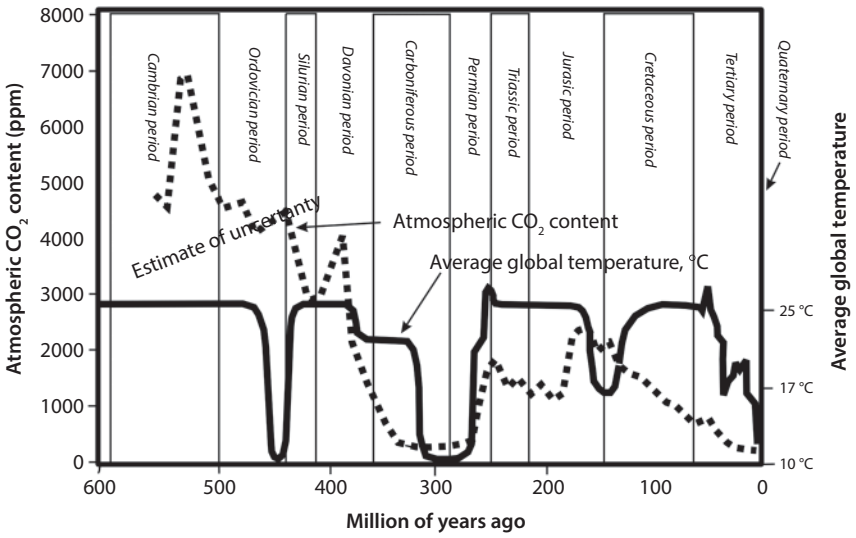

Figure 4.1 Schematic showing the relationship between average global temperature (solid line) and atmospheric carbon dioxide (dashed line) over geologic time. The late Carboniferous to Early Permian Period (315 mya to 270 mya) is the only time in the last 600-million years when both the atmospheric carbon dioxide content and temperatures were as low as they are today. (Modified after Hieb, M, 2009, in: Climate and the Carboniferous Period, http//www.geocraft.com/MVFossils/Carboniferous_climate.html., data for temperature obtained from Scotes and CO_2 after Berner, 2001.)

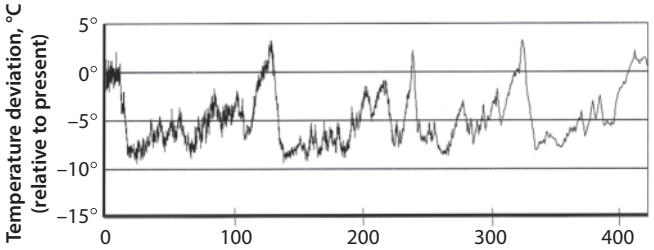

Figure 4.2 Deviation of Earth's lower atmospheric temperature from 2000 A.D. for the last 400,000 years. (Modified after Dillon, 2015. Data for temperature sources: Satellite stratosphere data (2000–1979); Southern hemisphere ground temp. data (1979–1871); Vostok ice core data (1871–422 k B.P.).)

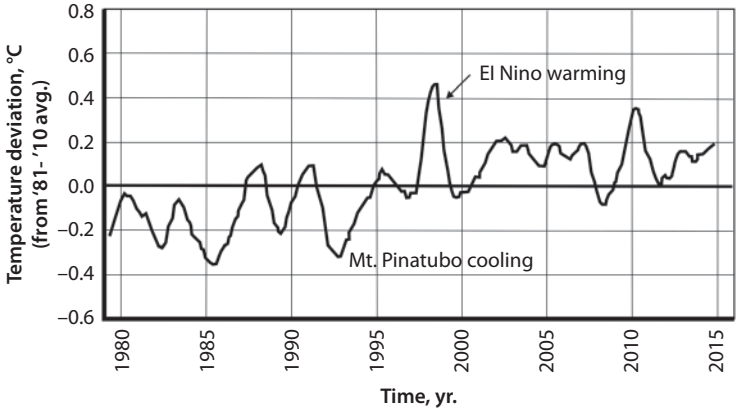

Figure 4.3 Running centered 13-month average of UAH satellite-based temperature of the global lower atmosphere (version 6.0) from 1979 to June 2015. (Modified after Bastasch, 2015.)

Bastasch (2015) in a similar study using data taken by satellite found no evidence of global warming over the past 22 years (Figure 4.3). A review of temperature deviation data over the past 2,000 years reveals that temperature has been mildly cyclic over this period and that we are currently in a "*modern warmer period*" cycle that may not have reached its peak global temperature (Figure 4.4). An examination of Figure 4.4 indicates an overall gentle cooling period from 1000 to 1700 AD and that the current warming period is not exceptional.

Hiebe (2009) has suggested that we are currently in an ice age climate period. However, "for the last 10,000 years we have enjoyed a warm but temporary interglacial vacation." This is reflected in geological records, e.g., (1) ocean sediments and ice cores from permanent glaciers that have formed in the last 750,000 years and (2) interglacial periods that occur at 100,000-year intervals (see Figure 4.2). Hiebe (2009) also suggested that these cycles have been occurring for the past 2–4 million years although the Earth's temperature appears to have been cooling for the past 30 million years.

In conclusion, the Earth's global temperature has been cycling about every 100,000 years about 10 °C due to natural causes and not as a result of human

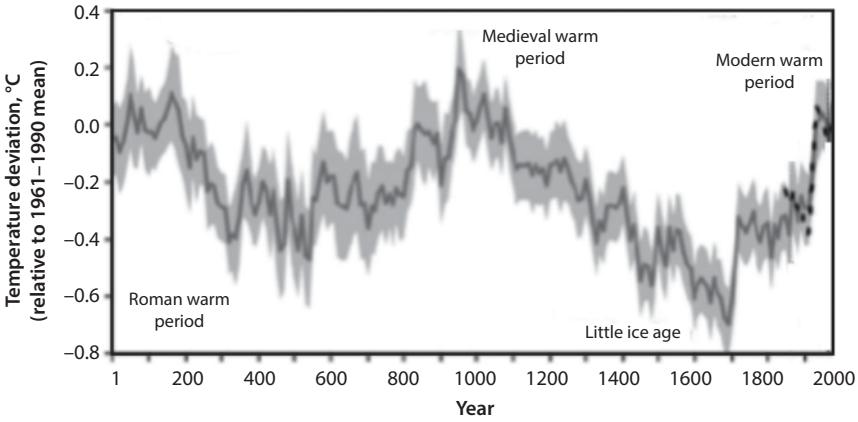

Figure 4.4 A reconstruction of temperature deviation, to the 1961–1900 mean for the Earth's northern hemisphere during the last two millennia. This shows that the current warm period is not exceptional. (Modified after Geografiska Annaler, 2010.)

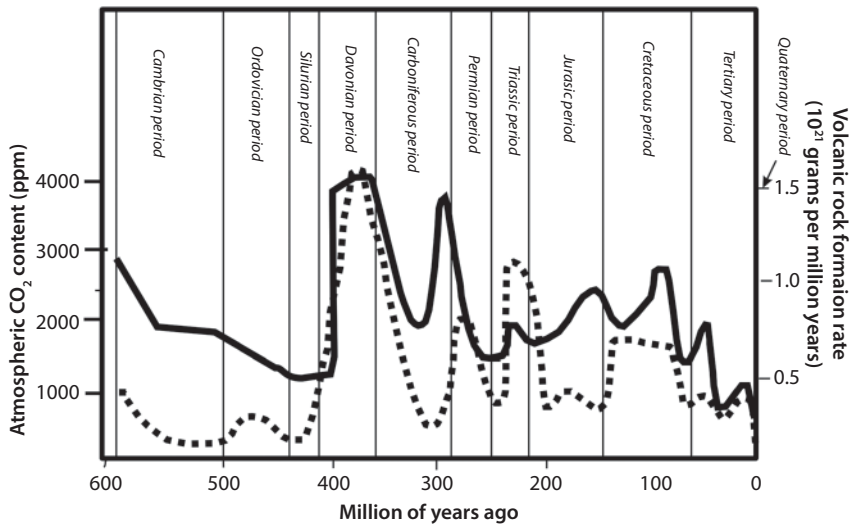

Figure 4.5 Schematic showing relationship between the CO_2 content in the atmosphere (dashed line) and the volcanic activity on Earth (solid line). (Modified after Archer, 2010.)

influence, e.g., sun-Earth relationship and volcanic activity, for a minimum of the last 800,000 years.

4.2.2 Effect of Atmospheric Carbon Content on Global Temperature

Figure 4.1 illustrates that there appears to be little relationship between global temperature and the percentage carbon content in the atmosphere during much of the Earth's geologic history. Global temperature appears to be independent from % carbon in the atmosphere. Archer (2010) found a relationship between % CO_2 content in the atmosphere and volcanic activity throughout geologic history (see Figure 4.5).

A record of the past 800,000 years is preserved, in gas bubbles, in the ice cover of the Antarctic, which is a source of historic data of global temperature and % carbon in the atmosphere. Several important studies have been made:

1. Fischer *et al.* (1999) studied air trapped in bubbles in Antarctic ice cores, around the last three glacial periods. This study of air trapped in the bubbles within the ice revealed a record of temperature and the carbon content in the atmosphere for the past 400,000 years. These high-resolution records from the Antarctic ice cores show that carbon dioxide concentrations increased by 80 to 100 parts per million by volume 400 to 600 years after the warming of the last three deglaciations. The carbon content of the atmosphere increased after the temperature had increased (Figure 4.6). Despite strongly decreasing temperatures, the high carbon dioxide concentrations in the atmosphere can be sustained for many years during glaciations before it is absorbed back into the carbon cycle.
2. Monnin *et al.* (2001), who studied ice cores from the Dome Concordia, Antarctica, found that CO_2 concentrations in the atmosphere increased after the global temperature increased after a period of ≈1000 years. His findings are consistent with the earlier work of Fisher *et al.* (1999).
3. Caillon *et al.* (2003) investigated the Vostok ice cores, and also found that the atmospheric CO_2 content increased after (800 ± 200-years) after the temperature had increased.

All these investigators independently had a similar conclusion that temperature increases preceded an increase in the CO_2 content of the atmosphere. Therefore, the evidence is that increases in global temperature results in increasing the carbon content

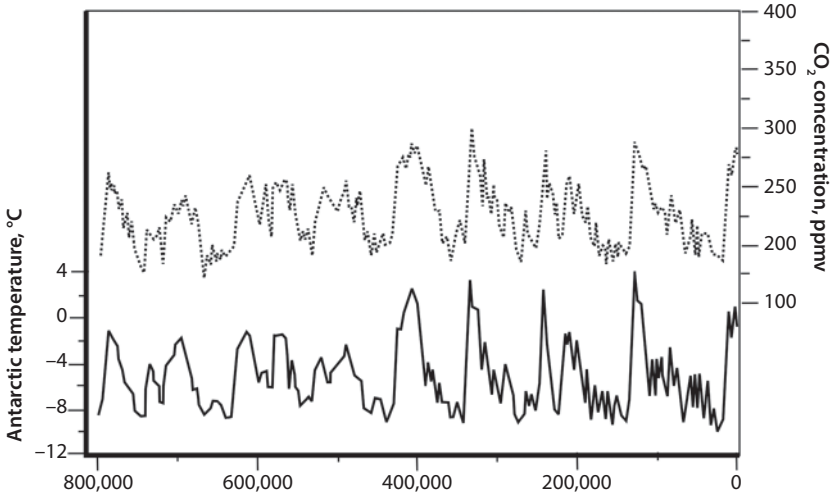

Figure 4.6 800,000-year record of atmospheric CO_2 content and a reconstruction of temperature from Antarctic ice cores. Temperature values in solid line and percent CO_2 in atmosphere in dashed line. (Modified after Shakun, 2012.)

in the atmosphere and that there is no evidence that the change of carbon content in the atmosphere changes global temperature.

Evans (2010) summarized his findings on the relationship between atmospheric carbon dioxide content and global temperature. He noted that if the atmospheric carbon dioxide content increased after global temperature increases, then there is no justification for claiming that increased carbon dioxide content in the atmosphere can increase the global temperature. Examining only the supposed human-generated carbon emissions and global temperature one can note that there is a significant lag between the human emissions of carbon content to the atmosphere and the temperature increase (Figure 4.7). This also assumes that the increase in temperature is due to the increased CO_2 emissions and no other factors, e.g., sun/Earth relationship and volcanism. Giving further support to the position that CO_2 emissions are not a factor, Evans (2010) noted that the global warming trend was initiated prior to 1700; however, the additional emissions by humans were negligible from 1850 to 1940, showing that there is no possibility that humans initiated global warming. Evans (2010), looking at this data, questioned that there has been any significant global warming since 1998. Inasmuch as a quarter of all human emissions have occurred in the past 12 years, why have we not seen more global warming?

Jones (2009) stated that perhaps human emissions of CO_2 have merely aggravated the current global warming trend. He also pointed out that 85% of all human emissions have occurred after 1945. The post-World War II industrialization greatly accelerated human emissions (see Figure 4.7).

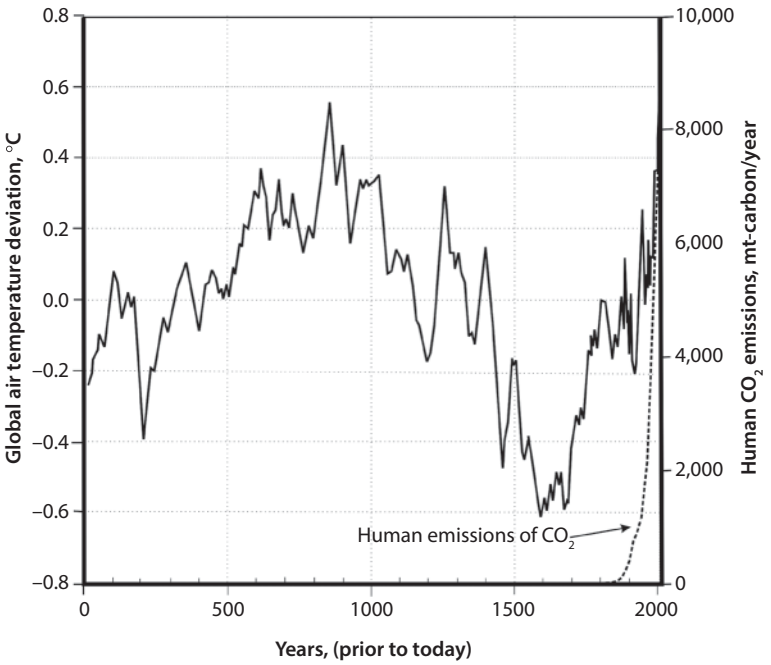

Figure 4.7 Schematic showing relationship between global air temperature vs. human CO_2 emissions from 16 AD to 2010. (Evans, 2010, states that these emission figures are not perfect because they omit some minor causes, e.g., deforestation; however, these are relatively minor). Evans also noted that the temperatures from 1850 to 1980 are suspect because they come from land-thermometers. (Modified after Evans. 2010.)

Bastasch (2015) has reviewed satellite temperature data during a 22-year period (1979–2015) of increased human emissions (see Figure 4.7) and found little or no global warming even though the CO_2 emissions significantly increased during this period (Figure 4.3).

Hieb (2009) noted that the global temperature and atmospheric concentrations of carbon dioxide (CO_2) in the Early Carboniferous Period, were approximately 1500 ppm (parts per million), but by the Middle Carboniferous they had declined to about 350 ppm -- comparable to the average CO_2 concentrations today. Figure 4.7 does not support a direct relationship between human-generated carbon in the atmosphere and global temperature. Figure 4.7 does show, however, that an increase in global temperature could have affected the carbon content in the atmosphere.

Earth's atmosphere today contains about 380 ppm CO_2 (0.038%) as compared to a higher concentration in former geologic times. The CO_2 content of our present atmosphere (like the Late Carboniferous atmosphere) is low. Hieb (2009) noted that in the last 600 million years of Earth's history only the Carboniferous Period and our present age (Quaternary Period) have witnessed CO_2 levels lower than 400 ppm. He also noted that historically the concentration of CO_2 in the atmosphere has been much higher, e.g., during the Jurassic Period (200 mya), average CO_2 concentrations were about 1800 ppm or about 4.7 times higher than today. The highest concentrations of CO_2 during all of the Paleozoic Era occurred during the early history of Earth (Cambrian Period) when it was, nearly 7000 ppm -- about 18 times higher than today. Possibly, the CO_2 content of the atmosphere of Pre-Cambrian time explains extensive formation of dolomites (Chilingar, 1956) and scarcity of fossils due to high Mg/Ca ratio of sea water.

The Carboniferous Period and the Ordovician Period were the only geologic periods during the Paleozoic Era when global temperatures were as low as they are today (Hieb, 2009). The Late Ordovician Period was also an Ice Age, whereas, at the same time, CO_2 concentrations then were nearly 12 times higher than today, 4400 ppm. According to the greenhouse theory, Earth should have been exceedingly hot. Instead, global temperatures appear to be no warmer than they are today. Again, the carbon dioxide content in the atmosphere appears to have had little effect on global temperature. Clearly, other factors besides atmospheric carbon dioxide content (e.g., temperature of the oceans and volcanism) influence Earth temperatures and global warming/cooling.

4.2.3 Sources of CO_2

To answer the question of where the source of CO_2 is coming from, one must look at the Earth's carbon cycle and in particular where carbon is stored on the Earth (Figure 4.8). There are several different forms of carbon that one needs to track in the Global Carbon Cycle (Archer, 2010):

1. Inorganic-C in rocks, e.g., bicarbonate and carbonate.
2. Organic-C, e.g., organic plant material.
3. Carbon gases such as CO_2, volcanism and solution gas in the oceans.
4. Methane gas, CH_4.
5. Carbon monoxide, CO.

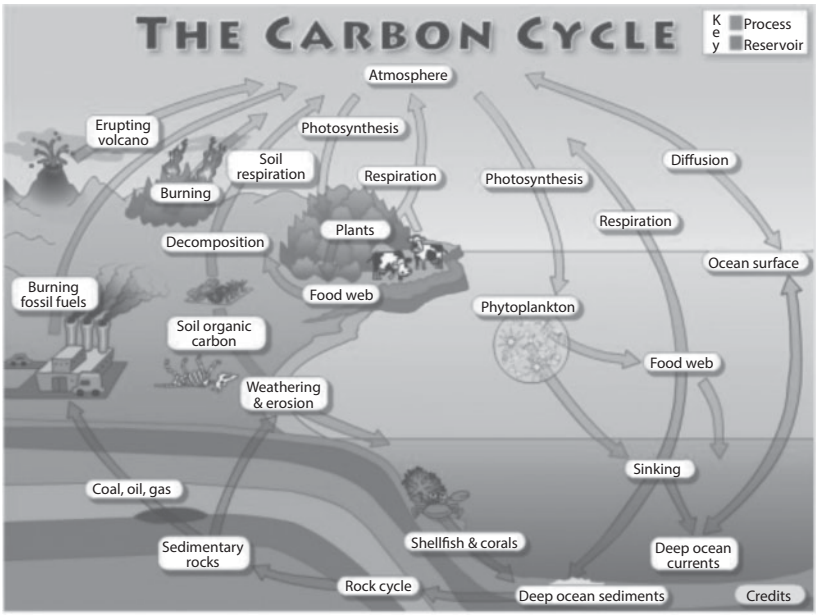

Figure 4.8 Pathways of carbon in the carbon cycle showing storage areas of carbon, e.g., ocean, atmosphere, vegetation, and rock. The ocean is one of the largest storage areas of carbon (After Earth Labs, http://serc.carleton.edu/eslabs/carbon/index.html).

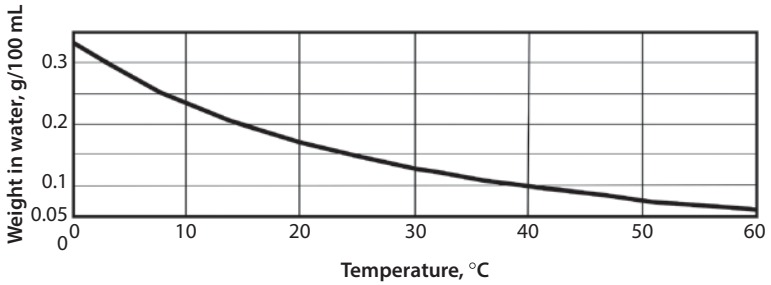

Figure 4.9 Relationship between the temperature and the solubility of CO_2 in water. (Data obtained from Wallace, 2009.)

Although there are several pathways of carbon cycling, the ocean/atmospheric cycle is one of the largest. As the global temperature and ocean temperature increase (see Figure 4.9), a large volume of CO_2 previously dissolved in the ocean water is released to the atmosphere due to the loss of solubility in warmer water. The oceans are a great storehouse of CO_2, covering about 72% of the Earth's surface. Therefore, an increase in global temperature will directly give rise to an increase in the quantity of CO_2 in the atmosphere.

Another source of carbon to enter the atmosphere is volcanism. The carbon cycle for outgassing from the Earth's interior is shown in Figure 4.10. Archer (2010) has shown that over geologic history, there is a close relationship between the atmospheric CO_2 content and volcanic activity (Figure 4.5) exists. During higher periods of volcanic activity, CO_2 concentration in the atmosphere is higher; therefore, increased CO_2 concentration in the atmosphere can also be related to volcanic activity. Figure 4.11 shows the volcanic activity from 1850 to 2010.

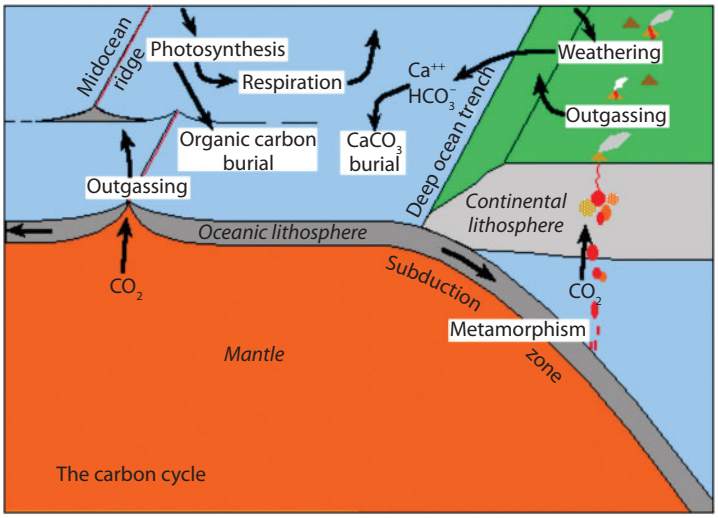

Figure 4.10 Sources of Carbon looking at the rock cycle showing outgassing from the Earth's interior at Midocean ridges, hotspot volcanoes and subductiuon-related volcanic (breakdown of carbonates, etc. volcanism. (After http//www.columbia.edu/-v"d1/carbon.htm).

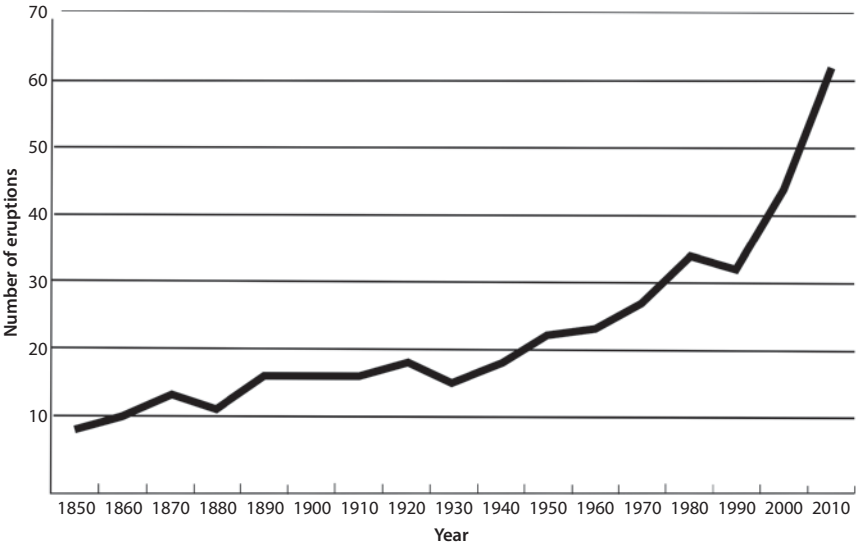

Figure 4.11 Global volcanism over time by decade from 1850 to 2010. There has been a general increase in volcanism over the past 100 years. (Modified after http://informacaoincorrecta.blogspot.com/2011/08/porque-nibiru-nao-existe.html)

In summary, the increase of CO_2 in today's atmosphere is likely due to: (1) The release of dissolved CO_2 from the ocean water occurring as a result of the increase in ocean temperature due to the sun's irradiation. (2) The exponential increase in volcanic activity from 1950 through 2010. (3) Human activities. Currently, the increase in the CO_2 content in the atmosphere has often been attributed to only human activity.

4.3 Adiabatic Theory

4.3.1 Modeling the Planet Earth

The adiabatic theory of the greenhouse effect shows that the temperature distribution in a planet's troposphere (including the Earth's troposphere) at pressures >0.2 atm (2.0265×10^1 kPa) under the greenhouse effect theory can be determined using the following equation:

$$T = b^{\alpha}\left[\frac{S(1-A)}{\sigma\left(\frac{\frac{\pi}{2}-\psi}{\frac{\pi}{2}}\times 4+\frac{\psi}{\frac{\pi}{2}}\times 2\times\frac{2}{1+\cos\psi}\right)}\right]^{\frac{1}{4}}\left(\frac{p}{p_o}\right)^{\alpha} \tag{4.1}$$

where: S (=1.367×10^6 erg/cm^2 s) is the solar constant (flow of the solar energy reaching the Earth); σ (=5.67×10^{-5} erg/cm^2 s °C^4) is the Stefan-Boltzmann constant; A is the planet's reflectivity (albedo) (for the Earth, A ≈ 0.3); b is a scaling factor; α is the adiabatic exponent; $\alpha = \frac{(\gamma-1)}{\gamma}$ and $\gamma = \frac{c_p}{c_v}$, where c_p and c_v, are the specific heats of gas at constant pressure and constant volume, respectively; ψ is the precession angle of the revolving planet (for the present-day Earth, $\psi = 23.44°$). At $\psi = 23.44°$. the denominator in Eq. 4.1 is equal to 3.502 rather that 4.0 in the classic format at $\psi = 0$.

According to current measurements, average near-surface Earth temperature at $p = p_o = 1$ atm (1.01324×10^2 kPa) is approximately equal to 288 K or +15 °C (Bachinsky *et al.*, 1951). Factor b can be determined under the condition that the present-day average Earth's surface temperature is equal to 288 K at $\alpha = 0.1905$. In such a case, $b = 1.597$, and for the nitrogen-oxygen atmosphere composition, $b^{\alpha} = 1.093$. For a different composition of troposphere, the factor b remains the same, but the b^a value changes depending on the adiabatic exponent α (Sorokhtin 2006).

If the specific heat at a constant pressure (c_p) is expressed in cal/g °C, and the universal gas constant R = 1.987 cal/mol °C, the relationship between the adiabatic exponent α and the composition and humidity of troposphere can be presented by the following equation:

$$\alpha = \frac{\mathrm{R}}{\mu(c_p + C_w + C_r)} \tag{4.2}$$

$$c_p = \frac{[p_{N_2}c_p(\mathrm{N_2}) + p_{o_2}c_p(\mathrm{O_2}) + p_{co_2}c_p(\mathrm{CO_2}) + p_{\mathrm{Ar}}c_p(\mathrm{Ar})]}{p} \tag{4.3}$$

where R = 1.987 cal/mol °C is the gas constant; μ is the molar weight of atmospheric mixture (for the Earth, $\mu \approx 28.9$E); $p_{N_2} = 0.7551$; $p_{CO_2} = 0.00046$ and $p_{Ar} = 0.0128$ atm are the partial pressures of the corresponding gases (Voitkevich *et al.*, 1990); $p \approx 1$ atm is the total atmospheric pressure at sea level; $c_p(N_2) = 0.248$, $c_p(O_2) = 0.218$ cal/g °C;

$c_p(CO_2)$ = 0.197 cal/g °C; c_p(Ar) = 0.124 cal/g °C are specific heats of nitrogen, oxygen, carbon dioxide and argon at constant pressure (Naumov *et al*., 1971); C_p and C_r are the correction factors with the dimension of specific heat (taking into account the total heating effect of the water vapor condensation process C_w in a humid atmosphere and the absorption of heat from the Earth and sun C_r by *greenhouse gases*).

From Eq. 4.2;

$$(C_w + C_r) = \frac{\mathrm{R}}{\mu \cdot \alpha} - c_p \tag{4.4}$$

At $\psi = 23.44^{\circ}$ and $A \approx 0.3$, the best fit of the theoretical temperature distribution (Eq. 4.1) within the Earth's troposphere to the averaged empiric data occurs at $\alpha = 0.1905$ and $b^{\alpha} = 1.093$. For a dry air mixture of the Earth's atmosphere, c_p = 0.2394 cal/g °C. Thus, using Eq. 4.4 for the absorbing-infrared-radiation humid air of the troposphere with the temperature gradient of 6.5 °/km, the $C_r + C_w$ = 0.1203 cal/g °C. For planets with atmospheres of a different composition these parameters should be understood as the description of any thermophysical or chemical processes resulting in the heat release (at $C_r + C_w > 0$) or absorption (at $C_r + C_w < 0$) within the troposphere.

To determine the C_r and C_w, factors, it is necessary to involve the characteristic temperatures T_s and T_e of a planet (Sorokhtin 2001):

$$C_r = \frac{\mathrm{R}}{\mu\alpha}\left(\frac{(T_s - T_e)}{T_s}\right) \tag{4.5}$$

$$C_w = \frac{\mathrm{R}}{\mu\alpha}\frac{T_e}{T_s} - c_p \tag{4.6}$$

On substituting the values of Earth's parameters into Eqs. 4.5 and 4.6 ($\alpha = 0.1905$, μ = 28.9, c_p = 0.2394 cal/g °C, T_s = 288 K, T_e = 263.5 K and R = 1.987 cal/mol °C), one obtains C_r = 0.0306 cal/g °C; C_w = 0.0897 cal/g °C; and $C_r + C_w$ = 0.1203 cal/g °C. Eq. 4.4 gives the same results.

The adiabatic model (Eq. 4.1) was verified with the standard temperature distribution in the troposphere (Bachinsky *et al*., 1951). The results of the comparison [at y = 23.44° and p_o = 1 atm (1.01324×10^2 kPa)] are presented in Figure 4.12.

4.3.2 Modeling the Planet Venus

A much more stringent check of the universality of the derived patterns is a computation of temperature distribution in the troposphere of Venus. It is performed based on the given pressure of 90.9 atm (92.1035×10^2 kPa), solar constant, $S = 2.62 \times 10^6$ erg/cm^2, precession angle $\psi \approx 3.18°$, and the molecular weight μ = 43.5 (Marov 1986; Venus 1989). The results are also presented in Figure 4.13. The best fit of the theoretical temperature distribution with its empirical values occurs at the adiabatic exponent α = 0.1786 and b^{α} factor of 1.429 (b = 7.37). For Venus, c_p = 0.2015 cal/g °C, T_s = 735.3 K and T_e = 230.5 K. Then, C_r = 0.1756 cal/gm °C, C_w = 0.1213 cal/g °C and $C_q = (C_r + C_w)$ = 0.0543 cal/g °C. The C_r parameter determines the absorption of the planet's heat

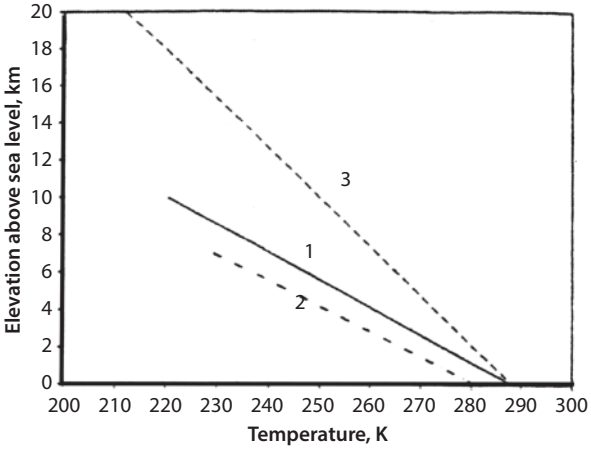

Figure 4.12 Averaged temperature distributions in the Earth's troposphere using Eq. 4.1: Model 1 - Earth's troposphere with a nitrogen-oxygen atmosphere; Model 2 - Earth's atmosphere composed totally of carbon dioxide; and Model 3 - Earth's atmosphere composed totally of methane. All other parameters of models 2 and 3 are the same as in model 1. (After Chilingar *et al.*, 2009, p. 1210, figure 2.)

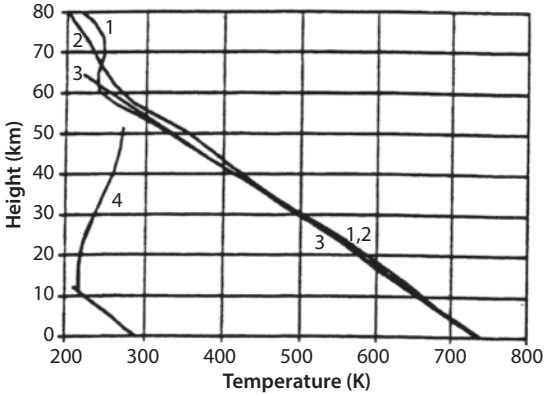

Figure 4.13 Distribution of experimentally determined temperature within the Earth's troposphere and stratosphere (curve 4: Bachinsky *et al.*, 1951) and within the Venetian troposphere (curves 1 and 2: Venus, 1989) as compared to the theoretical distributions (curves 4 and 3). Constructed in accordance with the adiabatic theory of the greenhouse effect. Temperatures are in Kelvin. (After Chilingar *et al.*, 2009.)

radiation by atmosphere. Its relatively elevated value is apparently due to a high atmospheric pressure and very hot troposphere. Inasmuch as $C_w < 0$ for Venus troposphere (especially in its lower and middle layers), endothermic reactions predominate (dissociation of some chemical compounds, for instance, dissociation of the sulfuric acid into SO_3 and water). For the upper layer of the Venetian troposphere (at the elevations between 40 and 60 km) $C_w > 0$. Therefore, the exothermic chemical reactions (e.g., the reduction of sulfuric acid) and condensation of water vapor in the clouds prevail.

As Figure 4.13 shows, theoretical temperature distribution in the Venetian troposphere, which is completely different from the one on Earth, fits quite well to the

empirical data quoted in Venus (1989). The range of relative error through the elevations up to 40 km is 0.5–1.0%. Theoretical temperatures at the elevations ranging from 40 to 60 km are positioned between two series of empirical data corresponding to the measurement at the Venetian high and low latitudes. At the higher altitudes where $p < 0.2$ atm (Venetian tropopause), the presented theory is not valid. This cannot be accidental and most likely is an indication of the validity of the presented theory for the troposphere layer.

The temperature distributions presented in Figure 4.13 were constructed based on the adiabatic theory of temperature distribution and are in effect the first theoretical models of the Earth's and Venus's tropospheric heat regime, i.e., the models for the planets with totally different atmospheric parameters. The obtained close fit of the theoretical model to experimental data is a strong testimony to the validity of the adiabatic theory of greenhouse effect. The results of comparison indicate that the average temperature distribution in a planetary troposphere is determined by the solar constant, the planet's albedo (a measure of the reflectivity of the earth's surface. Ice, especially with snow on top of it, has a high albedo), the mass (pressure) of atmosphere, heat-absorbing capacity of its gaseous mixture, and the planet's precession angle.

By definition, the greenhouse effect ΔT is the difference between the planet's surface average temperature T_s. and its effective temperature T_e:

$$\Delta T = T_s - T_e \tag{4.5}$$

Average temperature for the entire Earth's surface is approximately 288 K or +15 °C. Its effective temperature ($\psi = 0$) is $T_e = 255$ K or −18 °C. Thus, the present-day value of the greenhouse effect for the Earth is +33 °C. If we take into account that the present-day Earth's precession angle is $\psi = 23.44°$, then the effective temperature of Earth turns out to be $T_e = 263.49$ K (Sorokhtin 2006).

This adiabatic model allows one to estimate the effect of so-called "greenhouse gases" on the temperature regimes of the Earth's troposphere and its greenhouse effect. For asymptotic estimates, the writers assumed that the nitrogen-oxygen Earth's atmosphere is completely replaced by a carbon dioxide one and, then, by a methane one, with the same atmospheric pressure, $p_s = 1$ atm (1.01324×10^2 KPa). The adiabatic exponents are determined from Eq. 4.2 and 4.3 at $\mu_{CO_2} = 44$, and $c_p = 0.197$ cal/gm °C, $\mu_{CH_4} = 16$, and $c_p = 0.528$ cal/gm °C. Thus, $\alpha_{CO_2} = 0.1423$ and $\alpha_{CH_4} = 0.1915$. Substituting these a values into Eq. 4.1 with the same b factor value of 1.597, one can construct the temperature distribution in the hypothetical carbon dioxide and methane atmospheres. The corresponding near-surface temperature of the hypothetical carbon dioxide atmosphere will be 281.5 K (6.4 °C) lower than that at the nitrogen-oxygen composition of the atmosphere, and for the methane atmosphere it will be 288.1 K, which is just 0.1 °C, above the usual average Earth's temperature of 288 K. One needs to remember, however, that the carbon dioxide atmosphere is denser, whereas the methane atmosphere is lighter so that the same pressures in these atmospheres will be reached at different elevations than those in the nitrogen-oxygen atmosphere,

$$h_{CO_2} = h_{N_2+O_2} \frac{\mu_{N_2+O_2}}{\mu_{CO_2}} \tag{4.7}$$

and

$$h_{CH_4} = h_{N_2+O_2} \frac{\mu_{N_2+O_2}}{\mu_{CH_4}} \tag{4.8}$$

where $\mu_{N_2+O_2} (= 28.9)$ is the molar weight of the nitrogen-oxygen atmosphere, and $\mu_{CO_2} (= 44)$ and $\mu_{CH_4} (= 16)$ are the molecular weights of carbon dioxide and methane, respectively. The constructed temperature distributions within the hypothetical totally carbon dioxide and totally methane atmospheres are shown in Figure 4.14 together with the already presented (Figure 4.13) temperature distribution in the existing nitrogen-oxygen atmosphere.

Thus, for the hypothetical carbon-dioxide atmosphere with the same near-surface pressure of 1 atm, the average Earth's surface temperature declines by approximately 6.5 °C (and not increases significantly as commonly believed). Besides, due to a higher molecular weight of carbon dioxide, temperature within the entire thickness of such a troposphere is always lower than in the nitrogen-oxygen troposphere.

For a hypothetical methane atmosphere, the near-surface temperature at sea level remains almost unchanged, because $\alpha_{N_2+O_2} = 0.1905 \approx \alpha_{CH_4} = 0.195$. At the same time, in the troposphere it is higher than that for the nitrogen-oxygen atmosphere, inasmuch as $\mu_{CH_4} (= 16) < \mu_{N_2-O_2} (= 28.9)$, because the methane atmosphere is much thicker than the nitrogen-oxygen one. That is why in the mountainous areas surface temperature may significantly increase under such atmosphere.

Similarly, for a hypothetical nitrogen-oxygen Venetian atmosphere at the same pressure of 90.9 atm, its surface temperature will rise from 735 to 795 K (462–522 °C; see Figure 4.14.

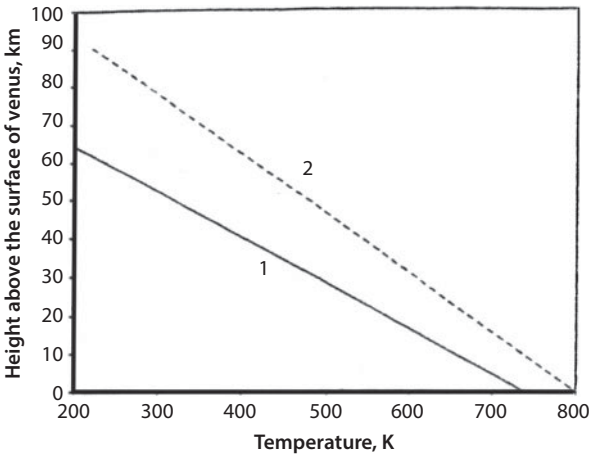

Figure 4.14 Averaged temperature distributions in the Venetian troposphere based on Eq. 4.1: (curve 1) Venus's carbon dioxide troposphere and (curve 2) the temperature distribution for a hypothetical model of the nitrogen-oxygen troposphere for Venus with all other conditions being equal. (After Chilingar *et al*., 2009, p. 1210, figure 3.)

These estimates show that saturation of the atmosphere with carbon dioxide, with all other conditions being equal, results not in an increase but in a decrease of the greenhouse effect and average temperature within the entire layer of the planet's troposphere. This happens despite intense absorption of the heat of radiation by CO_2. The physical explanation of this phenomenon is clear: molecular weight of carbon dioxide is 1.5 times higher and its heat-absorbing capacity is 1.2 times lower than those of the Earth's air. As a result, see Eqs. 4.2 and 4.3, the adiabatic exponent for a carbon dioxide atmosphere, at the same conditions, is about 1.34 times lower than that for a nitrogen-oxygen humid air: $a_{N_2+O_2} = 0.1905$. On Venus, the correction factors C_w and C_r are different from those on Earth, and a parameter is different from the carbon dioxide adiabatic exponent. Thus, a carbon dioxide atmosphere may be compared with a thin, dense blanket with a lower heat-absorbing capacity, whereas a nitrogen-oxygen atmosphere is like a downy (fluffy) blanket, characterized by a higher heat-absorbing capacity.

From the thermodynamic viewpoint, the explanation of this phenomenon consists in the fact that the heat release from the troposphere occurs mostly due to air mass convection, which is a much more efficient mechanism than heat transfer by radiation. After the greenhouse gases absorb the heat of radiation, the energy of this radiation is converted into energy of thermal oscillations of gas molecules. This, in turn, leads to the expansion of the gas mixture and its rapid rise to the stratosphere, where due to the rarified nature of the stratosphere, the excess heat is radiated into space.

Therefore, in a troposphere with elevated carbon dioxide content the convection of the atmospheric gases will accelerate substantially.

There is direct experimental data indicating that the fluctuations of the carbon dioxide partial pressure are the effect, and not a cause, of temperature changes (Khilyuk and Chilingar, 2003; Chilingar and Khilyuk 2007). Based on the data obtained from the Antarctic ice cores there is a correlation between temperature fluctuations and changes in the partial pressure of carbon dioxide obtained from the air bubbles in the Antarctic ice sheets of Vostok Station. However, a detailed study of the Vostok Station ice cores showed that the temperature fluctuations preceded the corresponding changes in CO_2 concentration in the cores (Monin and Sonechkin 2005). Fischer *et al.* (1999) and Mokhov *et al.* (2003) also showed that the changes in CO_2 concentration in the atmosphere occur after the global temperature changes, on an average by about 500–1,000 years. This is the time needed for a complete stirring of the upper (active) oceanic layer, which is the main "controller" of carbon dioxide partial pressure in the atmosphere.

Thus, the data derived from the Antarctic core studies indicate that the temperature changes over the past 800,000 years had always preceded the corresponding changes in the CO_2 concentrations of ice cover. This is indisputable evidence to the fact that the changes in CO_2 concentrations of the atmosphere are the effect of the global temperature changes, and not their cause.

Figure 4.13 shows the temperature distributions for Earth's atmosphere in: (1) totally carbon dioxide, (2) totally methane, and (3) Earth's troposphere. The temperature effects of the greenhouse gas emissions are in the same direction (but much lower in value) in proportion to the concentrations of these gases in the nitrogen-oxygen atmosphere($CO_2 \approx 4.6\times10^{-4}$ and $CH_4 \approx 1.2\times10^{-6}$).

For instance, the cooling effect for carbon dioxide will be about 2,200 times, and the heating effect for methane, 800,000 times smaller. Therefore, saturation of the

atmosphere with carbon dioxide can result only in the accelerated convective mass exchange in the troposphere, and lead to climate cooling (not heating), whereas an increase in methane concentration in the atmosphere practically has no effect on the Earth's climate.

4.3.3 Anthropogenic Carbon Effect on the Earth's Global Temperature

The human generated carbon effect on the Earth's climate is often evaluated on the emotional perception of the fact that greenhouse gases absorb heat of radiation. One can estimate the quantitative effect of anthropogenic carbon dioxide releases into the Earth's atmosphere on the climate applying the adiabatic theory of greenhouse effect.

Various estimates of the volume of current carbon dioxide released by burning of natural fuels are on the order of 7–10 billion tons or 1.9–2.7 billion tons of carbon per year. This large amount of CO_2 not only changes the composition of the atmospheric gas mixture and decreases its heat-absorbing capacity, but also slightly increases the atmospheric pressure. These two factors operate in opposite directions. As a result, the average atmospheric temperature of the Earth is not significantly changed. Using Eq. 4.1, after differentiation and transition to finite differences (see also Khilyuk and Chilingar 2003), and assuming that $p_s \approx 1$ atm, one can obtain the following equation:

$$\Delta T_s \approx T\alpha\Delta p_s \tag{4.9}$$

where ΔT_s, is the change in temperature at sea level attributed to the corresponding change in atmospheric pressure Δp_s (average Earth's temperature T = 288 K) and the adiabatic exponent $\alpha = 0.1905$. For instance, under the doubled carbon dioxide concentration in the Earth's atmosphere from 0.046 to 0.092 mass % (as anticipated by the year 2100), the pressure increase Δp_s would reach 0.46 mbar. Using Eq. 4.9, $\Delta T_s \approx +0.025$ °C. This temperature rise is not associated with the change in the atmosphere's composition, but only with some increase in the atmospheric pressure. Thus, the anthropogenic carbon dioxide releases into the atmosphere have no practical influence on the greenhouse effect in the atmosphere.

According to Henry's law, most of the carbon dioxide released into the atmosphere is dissolved in the oceanic water, and upon hydration of the oceanic crust it is bound in carbonates (some CO_2 is taken up by plants). Part of the atmospheric oxygen, together with carbon, is also fixed in carbonates.

Therefore, instead of some increase in the atmospheric pressure one might expect its slight decrease, which results in a slight climate cooling (rather than its significant warming as suggested by some ecologists). In addition, upon hydration of oceanic crust rocks, part of carbon dioxide is reduced to methane. Currently, due to formation of carbonates and methane generation, 2.3×10^8 tons/year of carbon dioxide are removed from the ocean, and, therefore, from the atmosphere. The potential of this CO_2 removal mechanism, however, is much higher. Although the period of this geochemical cycle is over 100 years, the effect is cumulative over the time.

Together with the man-made carbon dioxide, some oxygen is removed from the atmosphere. Based on the CO_2 molecular stoichiometry, almost 2.3 g of oxygen is removed from the atmosphere with each gram of carbon. Provided the ocean and

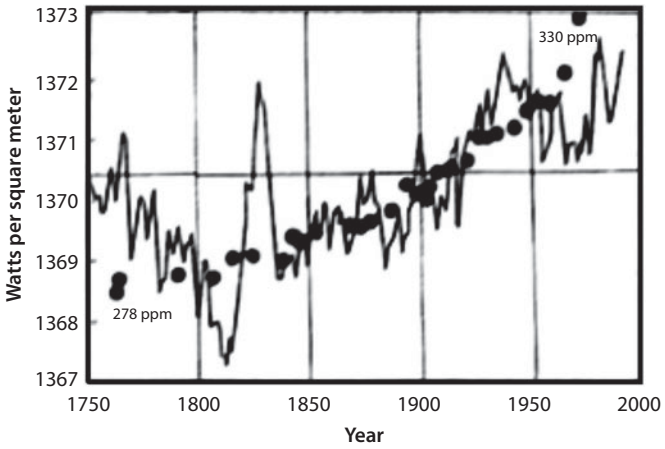

Figure 4.15 Solar irradiance (W/m^2) and CO_2 concentrations in atmosphere (p-pmv) in Northern Hemisphere (solid dots). (Modified after Hoyt and Schatten, 1997.)

vegetation absorb all excessive CO_2 after the year 2100, this should result in a decline of atmospheric pressure approximately by 0.34 mbar and, therefore, in the additional climate cooling by -8.2×10^{-3} K ≈ -0.008 °C. In reality, however, life activity of the plants should almost completely restore the equilibrium distorted by humans (accelerated biomass growth). This would restore the climatic balance.

One can summarize our findings as follows:

1. The anthropogenic impact on the global atmospheric temperature is negligible, i.e., 5% (Matthews, 1998).
2. Changes in the solar irradiation (global temperature) precede the corresponding changes in the carbon dioxide concentration in the atmosphere (e.g., see Figure 4.15).
3. The saturation of an atmosphere with carbon dioxide could lead to its cooling (and not vice versa).
4. The global natural processes drive the Earth's climate: "climate will change, either warmer or colder, over many scales of time, with or without human interference" (Gerhard, 2014).
5. Any attempt to mitigate undesirable climatic changes using restrictive regulations are condemned to failure, because global forces of nature are at least 4 orders of magnitude greater than the available human controls.

From the above estimates, one can conclude that even significant releases of anthropogenic carbon dioxide into the Earth's atmosphere practically do not change average parameters of the Earth's heat regime.

4.3.4 Methane Gas Emissions

Methane molecules have a high capacity of absorption of the infrared photons. According to estimates of the U.S. Environmental Protection Agency (EPA), the GWP

(Global Warming Potential) of methane is 21 times higher than the GWP of carbon dioxide over the 100-year time span. Light methane released in the atmosphere ascends into its upper layers where it initially reacts with ozone, ultimately producing (through the chain of reactions) water and carbon dioxide.

This process of chemical reactions can be summarized in the following equation:

$$CH_4 + O_3 + \text{solar radiation} \rightarrow CO_2 + H_2O + H_2 \tag{4.10}$$

Hydrogen rises into the stratosphere, whereas water vapor and methane gas form light clouds in the vapor layers of the troposphere (at the border of troposphere and stratosphere).

The "greenhouse gases" involved in the reaction absorb infrared radiation at different parts of the infrared spectrum. The rate of oxidation primarily depends on availability of the free OH radicals. The estimated life-time of methane in the atmosphere (estimated by IPCC and adapted by the EPA) is in the range of 8–12 years.

Based on these considerations one can consider the global warming (cooling) effect of the methane released as the effect of supplying additional amounts of CO_2 corresponding to the amount (and corresponding absorption capacity) of CO_2. (For every molecule of CH_4 one can substitute 21 molecules of CO_2). Thus, one can analyze the radiation warming (cooling) effect of methane as the effect of additional concentration 21 times 1.8 ppm of CO_2. This additional concentration of CO_2 (37.8 ppm) leads to cooling of the atmosphere as a result of increased convection in the lower layers of the troposphere. Oxidation of methane is a main source of water vapor in the upper troposphere. The methane gas together with the water vapor shields the Earth's surface from the solar irradiation thus lowering the average Earth surface temperature.

The U.S. government is preparing regulations to reduce methane emissions by more than 40% over the next 10 years. Does this mean that we have to stop developing huge deposits of hydrates all over the world? The EPA reported that ≈29% of all methane emissions in 2012 came from the petroleum industry.

The major sources of methane on the Earth are: (1) volcanic activity, (2) marshes and tundra, (3) rice paddies, (4) cattle, (5) oil and gas production, and (6) natural gas migration (see Chapter 2) to the Earth's surface. A great volume of methane is emanated as a result of volcanic eruptions. Yasamanov (2003) estimated about 5×10^{15} g of CH_4 are released yearly to oceanic water at the spreading zones of mid-ocean ridges. The amount of methane released to the atmosphere from marshes and tundra is estimated between 5×10^{13} and 7×10^{14} g annually. From tundra, the amount of CH_4 released is about 4×10^{13} g/year. Enteric fermentation contributes 2×10^{13} to 2×10^{14} g/year. The total amount of methane released annually into the atmosphere from natural sources is estimated at the level of 2.3×10^{15} g. Methane is also generated as a result of human activities. Rice paddies produce about 5×10^{14} g of methane annually. Oil and gas production and related operations add up to 9×10^{14} g of methane annually, which is one order of magnitude lower than the amount of methane released from the natural sources. A great amount of methane is released to the atmosphere as a result of gas migration to the Earth's surface from coal, oil,

and gas deposits and the Earth's mantle (Khilyuk *et al*., 2000). The total amount from the latter source has not been estimated at the present time. Probably, it is around 5×10^{15} g/year, whereas the fossil fuels burning contribute only 1×10^{13} g/year of methane to the atmosphere.

The content of methane in the atmosphere has been gradually increasing over the last century. In spite of the fact that the methane content constitutes only about 1.8 ppm in the Earth's atmosphere, the national and international policy makers declared the methane gas extremely dangerous to the Earth's climate because of a high potency (about 100 times more potent than CO_2 over the time span of 20 years) of its molecules to absorb the infrared radiation. Together with the growing contents of CO_2 and other greenhouse gases it is supposedly capable of causing drastic changes in the Earth's climate. According to the conventional anthropogenic theory of global warming, as a result of absorption of the infrared radiation by the molecules of the greenhouse gases, these molecules intercept infrared photons in the lower layer of troposphere warming the Earth's climate. This anthropogenic theory is the "scientific" basis for strong political and economic actions against further expansion of fracking, for example, in the shale-gas production.

The conventional anthropogenic theory (backed and promoted by IPCC and other national and international organizations over the last 25 years) completely ignores the main physical phenomena of the heat transfer in the atmosphere. In particular, it assumes that the heat transfer in the atmosphere occurs exclusively by radiation. Meantime in the lower dense layer of troposphere it occurs mostly by convection (67% by convection, 8% by radiation, and 25% by water vapor condensation (Sorokhtin *et al*., 2007)), which is intensified considerably with an additional release of the so-called greenhouse gases. Moreover, analyzing the postulates in the conventional theory one can find out that this theory completely ignores the fact that molecules of methane and other greenhouse gases (H_2O, for example) intercept the infrared solar irradiation in the upper layers of stratosphere and, thus, prevent overheating of Earth.

4.3.5 Monitoring of Methane Gas Emissions

In an excellent article, Rossenfoss (2015) discussed the need for better monitoring of methane gas emissions. According to the EPA, the natural gas emissions would rise by 25% by 2025 without further action.

According to the EPA, since 1990, the industries natural gas emissions are down by 16%. Rossenfoss (2015) stated that this was mainly due to (1) reduced emissions from controlled devices, (2) installation of plunger lift systems, and (3) green well-completion methods, which capture gas that once escaped from fluids flowing back after fracturing.

Based on the study done by the consulting firm ICF (commissioned by EDF), the added cost of a 40% reduction in emissions from natural gas production processing and delivery system would cost about 1 cent per MCF produced using available technology.

Rossenfoss (2015) showed that great strides have been made by oil/gas companies in the field of emission control. Operators should regularly monitor and maintain their gas-producing wells and equipment.

In conclusion, the authors believe that a voluntary effort on the part of the oil/gas industry to reduce emissions is better than EPA's planned regulations.

References

Allen, D. *et al*., 2015. Methane emissions from process equipment of natural gas production sites in the United States. *Env. Sci. & Technol*., 49:641–648.

Archer, D., 2010. *The Global Carbon Cycle*. http://globalchange.umich.edu/blobalchange1/current/lectures/kling/carbon_cycle/html

Bachinsky, A. U., Putilov, V. V. and Suvorov, N. P., 1951. *Handbook of Physics*. Uchpedgiz, Moscow, 380 pp.

Bastasch, M., 2015. Satellites: Earth is nearly in its 22nd year without global warming. http://dailycaller.com/authoir/michaelb/.

Brandt *et al*., 2014. Methane leaks from North America natural gas system. *Science*, 14 Feb.

Chilingar, G. V. and Khilyuk, L. F., 2007. Humans are not responsible for global warming. *SPE 109202*, Paper presented at SPE Technical Conference and Exhibition, Anaheim, California, 11–14 November, pp. 1–12.

Chilingar, G. V., Sorokhtin, O. G. and Khilyuk, L. F., 2014. Do increasing contents of methane and carbon dioxide in the atmosphere cause global warming? *Atmospheric and Climatic Sciences (ACS)*, 4:819–827.

Chilingar, G. V., Sorokhtin, O. G. and Khilyuk, L., 2009. Greenhouse gases and greenhouse effect. *Environ. Geology*, 58:1207–1213.

Chilingar, G.V., 1956. Relationship between Ca/Mg ratio and geologic age. *Bull. Am. Assoc. Petrol. Geol*., 40(a):2256–2266.

Delingpole, J., 2015. *Global Warming* '*Fabrication*' by NASA and NOAA. http://www.breitbart.com/london/2014/06/23/global-warming-fabricated-by-NASAand-NOAA/

Dillon, R. S., 2015. *Scientific Facts and Climate Change: CO_2 and Global Cooling*. 62 pp.

Enzler, S. M., 2015. *History of the greenhouse effect and global warming*. http:www.lenntech.com/greenhouse-effect/global-warming-history.htm#ixzz3fLgle620.

EPA, 2010. Methane and nitrous oxide emissions from natural sources. *U. S. Environmental Protection Agency*, Washington, DC, USA.

Evans, D., 2010. *Is the Western Climate Establishment Corrupt, part 5: CO_2 Emissions versus Temperature?* http://joannenova.com.au/2010/10/is-the-western-climate-establishment-corrupt-part-5.

Fischer, H., Wahlen, M., Smith, I., Mastronianni. D. and Deck, B., 1999. Ice core records of atmospheric CO_2 around the last three glacial terminations. *Science,* 283:1712–1714.

Geografiska Annaler, 2010. *Physical Geography*, 92 A(3):339–351, September.

Gerhard, L. C., 2004. Climate change: conflict of observational science, theory and politics. *Bull. Am. Assoc. Petrol. Geol*., 88(9): 1211.

Gore, A., 2006. *Inconvenient Truth*. Rodale Books, 328 pp.

Greenberg, J., 2015, Climate scientists "fabricated" temperature data. *Fox News*, February 13th at 10:11 a.m.

Hieb, M., 2009. *Climate and the Carboniferous Period*. http://www.geocraft.com/WVFossils/Carboniferous_climate.html.

Howarth, R., W., Santoro, R. L., and Ingraffes, A., 2011. Methane and the greenhouse gases footprint of natural gas from shale formations. *Climatic Change Letters*, DOI:10.1007s 10584-011-0061-5.

Keigwin, I. D., 1996. The little ice age and medieval warm period in the Sargasso Sea. *Science*, 274:1504–1508.

Khilyuk, L. F. and Chilingar, G. V., 2004. Global warming and long-term climatic changes: a progress report. *Environ. Geol.*, 46:6–7.

Khilyuk, L. F. and Chilingar, G. V., 2006. On global forces of nature driving the Earth's climate. Are humans involved? *Environ. Geol.*, 50:899–910.

Khilyuk, L. F. and Chilingar, G.V., 2003. Global warming: are we confusing cause and effect? *Energy Sources*, 25:357–370.

Kotlyakov, V. M., 2000. *Glaciology of the Antarctic*. Moscow, Nauka, 432 pp.

Landau, L. D. and Lifshits, E. M., 1979. *Statistical Physics*, Part 1. Moscow: Nauka, 59 pp.

Landscheidt, T., 2003. New little ice age instead of global warming? *Energy and Environment*, 14:327–350.

Legates, D. R., 2012. Carbon dioxide and air temperature: who leads and who follows. *Cornwall Alliance*.

Marov, M. Y., 1986. *Planets of the Solar System*. Moscow, Nauka, 320 pp.

Matthews, M. Jr., 1998. Who's afraid of CO_2? *Nast. Center for Policy Analysis*. http://www.ncpa.org/pub/ba256.

Mokhov, I. I., Bezverkhniy, V. A. and Karpenko, A. A., 2003. Milankovitch cycles and evolution of the climatic regime and atmospheric composition evolution based on the ice core data from the Antarctic "Vostok" Station. *Mater. Glaciol. Stud.*, 95:3–8.

Monckton, C. 2014. *Updated Global Temperature: No global warming for 17years*. http://www.climatedepot.com/2014/03/04/

Monin, A. S., Sonechkin, D. M., 2005. *Climate fluctuations based on observation data: the Triple Sun Cycle and Other Cycles.* Moscow, Nauka, 191 pp.

Monnin, E. A., Indermuhle, A., Dallenbach, J., Fluckiger, B., Stauffer, T. F., Stocker, D., Raynaud, D. and Barnoa, J. M., 2001. Atmospheric CO_2 concentrations over the last glacial termination. *Science*, 291;112–114.

Naumov, G. V., Ryzhenko, B. N. and Khodakovsky, I. L., 1971. *Handbook of Thermodynamic Values (for Geologists)*, Atomizdat, Moscow, 240 pp.

NOAA, 2015. *8 reasons why climate change critics are wrong*. http://energysocialnetwork.com/blog/8-reasons-why-climate-change-critics-are-wrong.

Robinson, A. B., Baliunas, S. L., Soon. W. and Robinson Z. W., 1998. Environmental effects of increased atmospheric carbon dioxide. *J. Am. Physicians and Surgeons*, 3:171178.

Robinson, A. B., Robinson, N. E. and Soon, W., 2007. Environmental effects of increased atmospheric carbon dioxide. *J. Am. Physicians and Surgeons*, 12:79–90.

Rossenfoss, S., 2015. Pressure to reduce methane emissions highlights the need for better monitoring. *J. Petrol. Eng.*, 67(3):46–57.

Shakun, J., 2012. *Global warming controversial*: "Temperature vs CO_2: which is the cause and which is the effect?" http://www.abovetopsecret.com/form/thread826768/pg1

Sorokhtin, O. G., 1990. Greenhouse effect of atmosphere in the geological history of Earth. *Doklady AN SSSR*, 315, 3:587–592.

Sorokhtin, O. G., 2001. Greenhouse effect: myth and realty. *Bull. RAEN*, 1(1):8–21.

Sorokhtin, O. G., 2006. *Evolution and Forecast of Changes in Earth's Global Climate*. Institute of Computer Studies; NITs Regular and Chaotic Dynamics, Moscow-lzhevsk, 88 pp.

Sorokhtin, O. G., Chilingar, G. V. and Khilyuk, L. F., 2007. *Global Warming and Global Cooling. Evolution of Climate on Earth*. Elsevier Amsterdam, 330 pp.

Sorokhtin, O. G., Chilingar, G. V., Khilyuk, L. F., and Gorfunkel, M., 2006. Evolution of the Earth's Global Climate. *Energy Sources*, 28:1–19.

Sorokhtin, O. G., Chilingarian, G. V. and Sorokhtin, N. O., 2011. *Evolution of Earth and Its Climate (Birth, Life and Death of Earth)*. Developments in Earth and Environmental Sciences 10, Elsevier, 576 pp.

Venus, 1989. (*Atmosphere, Surface, Internal Structure*), I Nauka, Moscow, 482 pp.

Voitkevich, G. V., Kokin, A. V., Miroshnikov, A. E. and Prokhorov, V. G., 1990. *Handbook of Geochemistry*. Nedra, Moscow, 480 pp.

Wallace, E., 2009. *Forced Carbonation*: *Stupid Easy*. http://chanticleersociety.org/forums/p/843/5678.aspx

Yasamanov, N. A., 2003. Modern global warming: causes and ecological consequences, *Bull. Dubna Int. University for Nature, Society, and Man*, 1(8):12–21.

Environmental Aspects of Oil and Gas Production.
John O. Robertson and George V. Chilingar.
© 2017 Scrivener Publishing LLC. Published 2017 by John Wiley & Sons, Inc.

5

Fracking

by Michael D. Holloway

5.1 Introduction

Trapped natural gas can be released from rocks[1] and that is what is being accomplished now throughout North America and other parts of the world. One hundred years ago, no one thought it possible, and very few contemplated the idea. Natural gas, which is primarily methane, has been proven to be an excellent fuel source. It can be safely burned to create heat to power engines, boilers in factories and homes, as well as powering turbines for generating electricity. Projections on natural gas volumes trapped underground suggest a near inexhaustible supply of this product; yet, such abundance spawns controversy. A popular and economical technique that relies on the gas from subterranean sources requires fracturing the rock. This practice can be carried out artificially (induced) using high-powered pumps and various liquid compounds. This technique, combined with new horizontal directional drilling techniques, has enabled the harvest and distribution of natural gas.

The following literature list contains information used either to support fracking or as a tool to oppose it.

5.2 Studies Supporting Hydraulic Fracturing

Interstate Oil and Gas Commission, "States' Experience with Hydraulic Fracturing" 2003.

[1]Yen, T. F. and Chilingarian, G. V. 1976. *Oil Shale, Developments in Petroleum Science*, 5. Elsevier, Amsterdam, 292 pp.

U.S. EPA, "Evaluation of Impacts to Underground Sources of Drinking Water by Hydraulic Fracturing of Coalbed Methane Reservoirs", 6/2004.

U.S. Department of Energy and Ground Water Protection Council, "Modern Shale Gas Development in the United States: A Primer", 4/2009.

U.S. Department of Energy and Ground Water Protection Council, "State Oil and Gas Regulations Designed to Protect Water Resources", 5/2009.

IF International, "Analysis of Subsurface Mobility of Fracturing Fluids", 2009.

NY State Department of Environmental Conservation, "DRAFT Supplemental Generic Environmental Impact Statement", 9/2009.

MIT Energy Initiative, "The Future of Natural Gas: An Interdisciplinary MIT Study, Interim Report", 9/2010.

5.3 Studies Opposing Hydraulic Fracturing

Oil & Gas Accountability Project of EARTHWORKS, "Our Drinking Water at Risk: What EPA and the Oil and Gas Industry Don't Want Us to Know about Hydraulic Fracturing", 4/2005.

Natural Resources Defense Council "Drilling Down: Protecting Western Communities from the Health and Environmental Effects of Oil and Gas Production", 10/2007.

Southern Methodist University for Environmental Defense Fund, "Emissions from Natural Gas Production in the Barnett Shale Area and Opportunities for Cost-Effective Improvements", 1/2009.

NYC Department of Environmental Protection and Hazen and Sawyer, "Impact Assessment of Natural Gas Production in the New York City Water Supply Watershed", 12/2009.

Harvey Consulting LLC, Review of NY State's Draft Supplemental Generic Impact Statement, 12/2009.

Texas Commission on Environmental Quality, "Health Effects Review of Barnett Shale Formation Area Monitoring Projects", 1/2010.

Valid points are made on both fronts. The major concern of those against fracking is the overall health and well-being of people close to a well site, as well as the land, water, and air that could potentially be adversely affected. It is highly advisable that the reader obtain his own copies of these reports if he wishes to delve deep into this topic.

Hydraulic fracturing is one of the most contentious and misunderstood issues, even down to its name (is it frac or frack?). The aim of this chapter is not to deliver a highly technical explanation of the process or to lay out results of study after study that have been conducted on both sides of the subject.

No sides are taken in the following pages. This work is not intended to be pro-industry or anti-fracturing. Namely, it aims to educate the general public on what hydraulic fracturing really is, how it is conducted, and what possible harms may or may not come as a result.

In today's society, it is easy for organizations (be it the general media, political groups, local organizations, unions, or religious associations) to spread their beliefs to the public and push whatever agenda or ideals they may have. These beliefs could be successfully

put forward with good intentions, successfully put forth with bad intentions, or, in many cases, put forward with good intentions but having a negative result. Sadly, it seems human nature dictates that the first opinion heard or the opinion heard the loudest and expressed with the most hyperbole will be what the public comes to believe. In time, once something is believed by enough people and stated as "fact" long enough, the general public will no longer even bother looking into facts, and it will become part of the fabric of beliefs in our society.

As previously stated, the intention in this chapter is not to give opinions or try to sway beliefs, but to give facts in the most straightforward and clear way possible and hopefully give enough background knowledge to initiate further study.

As far as hydraulic fracturing is concerned, the aspect given the most attention by press and most concerned organizations is the impact it may have on the environment. The question of environmental impact through fracking is, to say the least, a very emotional topic and by far the most polarizing issue; however, a great deal of analysis indicates that the most significant environmental risks attributed to fracking are similar to risks long associated with all drilling operations, including groundwater contamination due to inadequate cementing and/or well construction, risks associated with trucking, leaks from tanks and piping, and spills from waste handling. This all-encompassing list has given industry all of the ammunition needed to claim that effects attributed to hydraulic fracturing are overstated, not based on good science, or related to processes other than hydraulic fracturing.

Due to the great ongoing controversy over alleged impacts from fracking, many public groups have become deeply suspicious of the trustworthiness and overall motives of the oil and gas industry. These suspicions are continuously intensified by:

1. ongoing mistrust of data and findings due, in great part, to semantics, and
2. the reluctance of industry to disclose the chemical makeup of fracking fluids and the additives used to enhance hydraulic fracturing.

5.4 The Fracking Debate

A very large portion of negativity toward hydraulic fracturing is actually attributable to processes other than hydraulic fracturing. In the discussions between industry and the public, a great deal of this problem can boil down to an issue of semantics: the oil and gas industry has a narrow view of what fracking entails (including just those processes related to the actual process of fracking while on location conducting the fracking operation), whereas the general public is more inclined to include many more activities commonly related to fracking (water and sand trucking, product and equipment transport and storage, water disposal) under the heading of "fracking." This can cause misunderstandings and skewed data, in that many of the processes included by the general public are utilized in many, if not all, drilling practices, and are hard to put solely under the heading of "fracking," when in actuality they could just as easily be under the heading "completions" or "production."

One important message that can be taken away from this chapter is how to drive this technology *safely*.

5.5 Production

Gas reservoirs are classified as conventional or unconventional:

5.5.1 Conventional Reservoirs

Wells in conventional gas reservoirs produce from sandstones and carbonates (limestones and dolomites) that contain gas in interconnected pore spaces that allow flow to the wellbore. Gas moves from one pore to another through smaller pore-throats that create permeable flow through the reservoir. In conventional natural gas reservoirs, the gas is often sourced from organic-rich shale (source rock) proximal to the more porous and permeable sandstone or carbonate.

5.5.2 Unconventional Reservoirs

Wells in unconventional reservoirs produce from low permeability (tight) formations such as tight sands and carbonates, coal, and shale. In unconventional gas reservoirs, the gas is often sourced from the reservoir rock itself (tight gas sandstone and carbonates are an exception). Because of the low permeability of these formations, it is typically necessary to stimulate the reservoir to create additional permeability. Hydraulic fracturing of a reservoir is the preferred stimulation method for gas shale. Differences between the three basic types of unconventional reservoirs include:

- **Tight Gas:** Wells produce from regional low-porosity sandstone and carbonate reservoirs. The natural gas forms outside the reservoir, and migrates into the reservoir over time (millions of years). Many of these wells are drilled horizontally, and most are hydraulically fractured to enhance production.
- **Coal Bed Natural Gas (CBNG):** Wells produce from the coal seams, which act as source and reservoir of the natural gas. Wells frequently produce water as well as natural gas. Natural gas can be formed by thermogenic alterations of coal or by biogenic action of indigenous microbes on the coal. There are some horizontally drilled CBNG wells, and some that receive hydraulic fracturing treatments. However, some CBNG reservoirs are also underground sources of drinking water, and as such, there are restrictions on hydraulic fracturing. CBNG wells are mostly shallow, as the coal matrix does not have the strength to maintain porosity under the pressure of significant overburden load.
- **Shale Gas:** Wells produce from low permeability shale formations that are also the source for the natural gas. The natural gas volumes can be stored in a local macro-porosity system (fracture porosity) within the shale, or within the micro-pores of the shale, or it can be adsorbed onto minerals or organic matter within the shale. Wells may be drilled either vertically or horizontally, and most are hydraulically fractured to stimulate

production. Shale gas wells can be similar to other conventional and unconventional wells in terms of depth, production rate, and drilling.

Figure 5.1 presents a comparison between conventional well structure and wells using hydraulic fracturing.

Drilling conventional wells and those to be used in hydraulic fracturing begin in much the same ways. The basic well construction steps are:

- An initial length of steel pipe, called conductor casing, is inserted into a vertical wellbore soon after drilling begins. This is done to stabilize the well as it passes through the shallow sediments and soils near the surface.
- Once conductor casing is set, operators continue drilling and insert a second casing, called surface casing, from the ground surface and extending past the depth of all drinking water aquifers.
- After allowing the cement behind the casings to set (cementing is described in detail in the following section), operators continue drilling for approximately 10 to 50 feet before stopping to test the integrity of the cement process by pressurizing the well.
- In horizontal wells, after drilling the horizontal section of the well, operators run a string of production casing into the well and cement it in place.
- Operators then perforate the production casing using small explosive charges at intervals along the horizontal wellbore where they intend to hydraulically fracture the shale.
- Acid stage: consists of pumping several thousand gallons of water mixed with a dilute acid such as hydrochloric or muriatic acid. This serves to clear cement debris in the wellbore and provide an open conduit for other frack fluids by dissolving carbonate minerals and opening fractures near the wellbore.

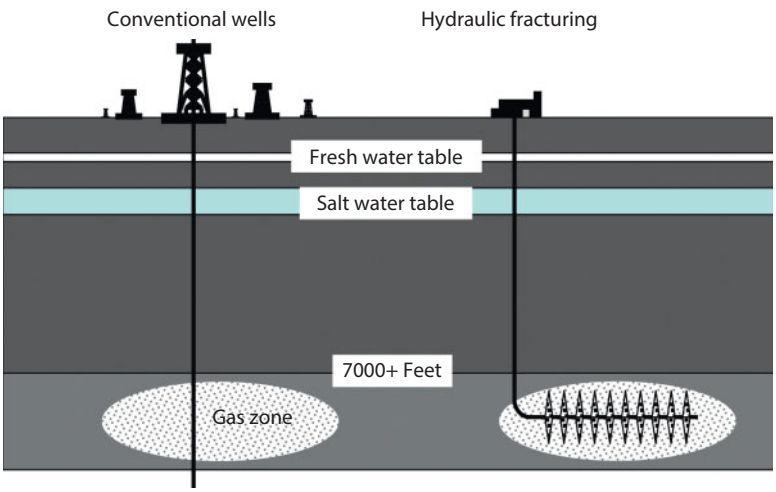

Figure 5.1 Comparison of well sites.

- Pad stage: consists of pumping approximately 100,000 gallons of slickwater without proppant material. The slickwater pad stage fills the wellbore with the slickwater solution (described below), opens the fractures, and helps to facilitate the flow and placement of proppant material.
- Prop sequence stage: consists of several sub-stages of pumping water with proppant material (fine mesh sand or ceramic material, intended to keep open, or "prop," the fractures created and/or enhanced during the fracturing operation after the pressure is reduced). This stage may collectively use several hundred thousand gallons of water. Proppant material may vary from a finer particle size to a coarser particle size throughout this sequence.
- Flushing stage: consists of pumping fresh water sufficient to flush the excess proppant from the wellbore.

Other additives commonly used in the fracturing solution include:

- A dilute acid solution, as described in the first stage, used during the initial fracturing sequence. This cleans out cement and debris around the perforations to facilitate the subsequent slickwater solutions employed in fracturing the formation.
- A biocide or disinfectant, used to prevent the growth of bacteria in the well that may interfere with the fracturing operation. Biocides typically consist of bromine-based solutions or glutaraldehyde.
- A scale inhibitor, such as ethylene glycol, is used to control the precipitation of certain carbonate and sulfate minerals.
- Iron control/stabilizing agents such as citric acid or hydrochloric acid, are used to inhibit precipitation of iron compounds by keeping them in a soluble form.
- Friction reducing agents, also described above, such as potassium chloride or polyacrylamide-based compounds, used to reduce tubular friction and subsequently reduce the pressure needed to pump fluid into the wellbore. The additives may reduce tubular friction by 50% to 60%. The friction-reducing compounds represent the "slickwater" component of the fracking solution.
- Corrosion inhibitors, such as n-dimethyl formamide, and oxygen scavengers, such as ammonium bisulfite, are used to prevent degradation of the steel well casing.
- Gelling agents, such as guar gum, may be used in small amounts to thicken the water-based solution to help transport the proppant material.

Occasionally, a cross-linking agent is used to enhance the characteristics and ability of the gelling agent to transport the proppant. These compounds may contain boric acid or ethylene glycol. When cross-linking additives are added, a breaker solution is commonly added later in the frack stage to break down the gelled solution into a less viscous fluid so that it can be readily removed from the wellbore without carrying back the sand/proppant.

Table 5.1 Well comparisons, lists various sites also known as plays throughout North America.

Name of the gas shale basin	Barnett	Fayetteville	Haynesville	Marcellus	Woodford	Antrim	New Albany
Estimated Basin Area, square miles	5,000	9,000	9,000	95,000	11,000	12,000	43,500
Depth, ft.	8,500	7,000	13,500	8,500	11,000	2,200	2,000
Thickness, ft.	To 600	To 200	To 300	To 200	To 220	To 120	To 100
Depth to Base of Treatable Water, ft.	1,200	500	400	850	400	300	400
Rock ColumnThickness between Top of Play and Bottom of Treatable Water, ft.	7,300	6,500	13,100	7,650	10,600	1,900	1,600
Total Organic Carbon, %	4.5	9.8	4.0	12	14	20	25
Total Porosity, %	4 -	8	9	10	9	9	14
Gas Content,SCF/Ton	up to 350	up to 220	up to 330	up to 100	up to 300	up to 100	up to 80
Water Production,Barrels water/day	N/A	N/A	N/A	N/A	N/A	5–500	5–500
Well spacing,acres	60 to 160	80 to 160	40 to 560	40 to 160	640	40 to 160	80
Original Gas-In- Place, TCF	327	52	717	1,500	23	76	160
Technically Recoverable Resources	44	41.6	251	262	11.4	20	19.2

5.6 Fractures: Their Orientation and Length

5.6.1 Fracture Orientation

Hydraulic fractures are formed in the direction perpendicular to the least stress. Based on experience, horizontal fractures will occur at depths less than approximately 2,000 ft because the Earth's overburden at these depths provides the least principal stress. If pressure is applied to the center of a formation under these relatively shallow conditions, the fracture is most likely to occur in the horizontal plane, because it will be easier to part the rock in this direction than in any other. In general, therefore, these fractures are parallel to the bedding plane of the formation.

As depth increases beyond approximately 2,000 ft, overburden stress increases by approximately 1 psi/ft, making the overburden stress the dominant stress. This means the horizontal confining stress is now the least principal stress. Since hydraulically induced fractures are formed in the direction perpendicular to the least stress, the resulting fracture at depths greater than approximately 2,000 ft will be oriented in the vertical direction. In the case where a fracture might cross over a boundary where the principal stress direction changes, the fracture would attempt to reorient itself perpendicular to the direction of least stress. Therefore, if a fracture propagated from deeper to shallower formations, it would reorient itself from a vertical to a horizontal pathway and spread sideways along the bedding planes of the rock strata.

5.6.2 Fracture Length/Height

The extent that a created fracture will propagate is controlled by the upper confining zone or formation, and the volume, rate, and pressure of the fluid that is pumped. The confining zone will limit the vertical growth of a fracture because it either possesses sufficient strength or elasticity to contain the pressure of the injected fluids, or an insufficient volume of fluid has been pumped. This is important because the greater the distance between the fractured formation and the USDW, the more likely it will be that multiple formations possessing the qualities necessary to impede the fracture to occur. However, while it should be noted that the length of a fracture can also be influenced by natural fractures or faults, as shown in a study that included micro-seismic analysis of fracture jobs, natural attenuation of the fracture will occur over relatively short distances due to the limited volume of fluid being pumped and dispersion of the pumping pressure, regardless of intersecting migratory pathways.

5.7 Casing and Cementing

Typically, the casing and cementing of wells is accomplished in multiple phases, working inward from the largest diameter casing to the smallest.

- First, the surface casing is inserted.
- Cement is then pumped down the inside of the casing, forcing it up from the bottom of the surface casing into the annular space between the outside of the surface casing and the drilled wellbore.
- Once a sufficient volume of cement to fill the annulus is pumped into the casing, it is usually followed by pumping water into the casing until the cement begins to return to the surface in the annular space. This process of cementing is called "circulation" and ensures that the entire annular space fills with cement from below the deepest groundwater zone to the surface, which, when done properly, protects the aquifer.
- After the surface casing is completed and set, the well is drilled to the pay zone. Upon reaching the pay zone, production casing is set at either the top extent of, or into, the producing formation. This zone is then cemented by the same process as before.

As can be expected when working in underground formations, sometimes a well will be extended into a formation that is difficult to cement because of high formation porosity or high water flow. This condition can be detected by personnel during drilling operations or by observing that more cement is being pumped downhole than the calculated area of the annulus. When this happens, additives (such as cellophane flake and calcium chloride) can sometimes be added to the cement to seal off such zones, quicken the cement hardening process, and prevent downhole loss of the cement into formation.

When completed properly, sealing of annular spaces with cement creates a hydraulic barrier to both vertical and horizontal fluid migration, essentially eliminating subsurface releases and blowouts. Consequently, the quality of the initial cement job is

one of the most critical factors in the prevention of fluid movement into groundwater resources. If well cementing and casing is improperly or poorly done, leakage into an aquifer of fluids that flow upward in the annulus between the casing and the borehole can occur; this is the greatest potential pollution risk.

Well integrity issues resulting in leakage can be divided into two categories:

- Annular flow: fluids move up the wellbore by traveling up the space between the borehole formation and cement or between the cement and the casing
- Leak flow: fluids move in a radial direction out of the well and into the adjacent formation.

5.8 Blowouts

The simple definition of a blowout is an uncontrolled fluid release occurring during the drilling, completion, or production of oil and gas wells. Blowouts occur rarely when high pressures are encountered in the subsurface or due to valve or some other type of mechanical failure. What is normally brought to mind when one hears the term "blowout" is an explosion that goes with a catastrophic well blowout. As used here however, this term also includes the smaller above and below ground blowouts.

Blowouts may take place at the surface (wellhead or elsewhere) or subsurface (naturally high pressure, or may be artificially induced in the wellbore during hydraulic fracturing during completion operations, but not during pumping). A high percentage of blowouts occur due to casing or cement failure, allowing high-pressure fluids to escape up the wellbore and flow into subsurface formations. The potential environmental consequences of a blowout depend mostly on:

- The timing of the blowout relative to well activities, which determines the nature of the released fluid such as natural gas or pressurized fracturing fluid.
- Occurrence of the escape of containments through the surface casing or deep in a well.
- The risk receptors, such as freshwater aquifers or water wells that are impacted.

5.8.1 Surface Blowouts

Surface blowouts at the wellhead can result in a major safety hazard to workers and may also result in surface spills. Surface blowouts are primarily prevented through proper well construction, maintenance, and ensuring well integrity.

5.8.2 Subsurface Blowouts

Subsurface blowouts, due to high gas pressure or mechanical failures, happen in both regular and hydraulically fractured wellbores. However, fractured wells have the

incremental risk of potential failures caused by the high pressures of fracturing fluid during the process.

In the event of a blowout in the subsurface, a major problem due to the limited ability to discern what is happening in the subsurface, blowout preventers are used to automatically shut down fluid flow in the wellbores. Subsurface blowouts may pose both safety hazards and environmental risks. For example, when a blowout preventer engages to prevent flow from reaching the surface, the fluid may be forced through weaknesses in the casing and cement below the blowout preventer into the surrounding formations and aquifers. Blowout preventers are important safety devices; however, like all mechanical devices, they have been known to fail.

5.9 Horizontal Drilling

When drilling a horizontal well, operators begin turning the drill bit when they near the production zone so the wellbore runs through the formation horizontally. It can extend out to 10,000 feet, which vastly increases contact with the production zone compared to vertical drilling.

5.10 Fracturing and the Groundwater Contamination

Studies indicate that environmental risks associated with hydraulically fractured wells are similar to those associated with all production wells, including surface and subsurface spills and releases, gas migration and groundwater contamination due to faulty well construction, blowouts, leaks and spills of waste water, and chemicals stored on pad sites.

5.11 Pre-Drill Assessment

If fresh-water aquifer contamination is a concern, many concerned parties (both in industry and in the environmental sector) believe shallow-water monitoring wells should be drilled at the perimeters of the pads, with samples taken as needed. Collecting samples from these water wells before drilling would then be done to establish a base line set of analytical data to show water conditions prior to drilling operations. In fact, some states have enacted regulations to establish pre-drilling groundwater quality through a baseline monitoring program. The baseline sampling would then be followed by regular monitoring during all phases of operations, including hydraulic fracturing. This process could serve two purposes:

- Provide very early warning in case of a well construction leak.
- Eliminate the operation as a potential source of pollution in some areas of concern because it will show that constituents were present in water wells before shale gas development began.

High-quality analytical data before, during, and after production processes have been increasingly collected to document baseline and post-drilling groundwater

quality through wells installed at the well pad. However, one obvious shortcoming of this protocol is that typical horizontal lengths may range from 2,000 ft to 6,000 ft, with extremes of 12,000 ft or more. Therefore, if water monitoring wells are not located at the well pad, they could be located anywhere from 2,000 to 12,000 ft from the location of the actual fracturing process.

The following discussion is based on an excellent workshop by Lloyd Hetrick of the U.S. Environmental Protection Agency (EPA). The seminar was titled Hydraulic Fracturing Study Technical Workshop #2 March 10–11, 2011, a *Well Integrity Case Study* by Lloyd H. Hetrick. The presentation defined well integrity by one simple outcome: the prevention of vertical migration of gas and fluids in order to protect drinking water resources. A generic shale development well was presented, beginning with its basis of design, then construction, an operational phase, and ultimately its plugging and abandonment.

Regulations, industry standards, and best practices will be addressed, as will failure categories and relative failure rates at each phase of the well's life cycle. This case study will also raise relevant issues that have not been fully discussed here, such as the difference between exploration and development phases, development well economics, the potential for well integrity impacts from adjacent well activities, and a time line perspective.

A brief process description for oil and gas projects might be helpful. Years before a well is drilled, significant geological and geophysical "G&G" work is performed to identify prospective areas. During this time, offset wells are studied to identify subsurface hazards that may be present in order to avoid or mitigate them. Once a prospect is defined, mineral leases are acquired, additional G&G and reservoir analysis performed, and well design determined for specific drilling locations. The first group of wells drilled are called "exploratory" and intended to define the commercial value of the prospect. Exploratory wells require extra time to gather data on the quality of the reservoir and are also used to identify well construction efficiencies for the development phase. Once the project transitions from exploration to development, each well has to pass an economic hurdle to be drilled.

Regardless of being exploratory or development, responsible oil and gas companies have a strong business incentive to protect the environment, mineral reserves, and the well itself [1]. It is almost always more difficult and costly to reenter and repair a well than addressing design deficiencies during construction.

The case study by Hetrick mentioned earlier, although generic, is not unlike the Marcellus, Eagle Ford, and other unconventional plays with multiple hydrocarbon zones. Even though only one reservoir is the current development objective, additional reservoirs are candidates for future development. Accordingly, only the most relevant technical items such as failure modes will be included and even then, will be greatly abbreviated. For example, if corrosion is considered to be the primary failure category, the technical discussion will end there with no deeper look into the true root cause failure mode such as galvanic corrosion, sulfide stress cracking, etc. Federal and state environmental laws protect underground sources of drinking water (USDWs). The term USDW is used synonymously with the term "protected water" and refers to an aquifer with less than 10,000 mg/l total dissolved solids (TDS) [2]. State mineral law regulates the extraction and conservation of minerals unless on federal BLM or BIA land, where federal mineral laws apply. In either case, the regulatory agency that oversees mineral

extraction is also the primary regulator for protecting USDWs during oil and gas exploration and production activities [3, 4]. Protected water and hydrocarbons have natural separation [5] in most situations. There are however, areas of the country where methane is routinely found to exist naturally in USDWs [6, 7] and has been associated with bubbles in rivers as early as the mid-1800s [8]. There are also locations where methane vents to the surface via natural pathways having nothing to do with oil and gas extraction activities [9, 10]. It has been estimated from a review of Pennsylvania regulatory records that over 95% of the complaints that oil and gas activities had contaminated private water wells were actually due to preexisting or other land use activities [11]. These naturally occurring migrations are not limited to methane, as towns named Oil Springs, KY [12], Oil Springs, Ontario [13], and historical sites such as Seneca Oil Spring, NY [14] and Brine Springs, TX [15] all attest that oil and brine have been observed migrating to the surface dating back to the 1600s.

5.12 Basis of Design

A development well is drilled only if there is confidence that the estimated recoverable hydrocarbon reserves will provide an acceptable economic rate of return, given the cost to construct and operate the well. For an unconventional gas play, development wells tend to have generational designs where a group of wells will have a similar drilling, casing, cementing, perforating, and hydraulic fracturing design. Over time as more wells are drilled, experience provides opportunities to correct any design deficiencies and improve drilling efficiencies, and well performance. Subsequent generations of wells, therefore, are seldom designed exactly the same.

Individual wells, regardless of their generational status, receive detailed engineering analysis and planning that is communicated to the site well supervisor in the form of a written drilling and completion procedure. These planned sequence of activities also incorporate regulatory compliance and industry best practices.

5.13 Well Construction

5.13.1 Drilling

A typical onshore well is a conductor pipe that is driven, drilled, or augered into the ground by a construction crew or "spud rig" prior to the drilling rig's arrival. This conductor pipe is a structural component that sometimes is not needed at all. Conductor pipe most often does not reach the top and does not penetrate the base of protected water; therefore, it is not involved in protecting USDWs from vertical migration of fluids. Accordingly, failure categories for the conductor pipe will not be discussed.

The surface hole is drilled to a prescribed depth below the base of protected water. This depth is most often provided by the State Oil and Gas Regulator, as in Oklahoma [16], or the State Environmental Protection Regulator, as in Texas [17], or not specifically provided other than to protect all USDWs encountered, as in Pennsylvania [18]. In this latter situation, oil and gas operators typically research a Pennsylvania

Groundwater Information System (PaGWIS) database and local water well driller's records to generate a hydro-geological map in order to determine depths of water that need to be protected.

The surface hole is not left open for more than a few hours while being drilled, cased, and then cemented back to surface. Those zones left open during this brief period are all USDWs, so vertical migration of fluids does not present a significant threat during surface hole drilling. The surface hole on our case study well is drilled in a few hours on day #1 of the drilling operation.

The surface casing string is the primary barrier to prevent fluids from the wellbore from entering protected water as the well is being drilled to the next casing setting depth. Unlike the conductor pipe, surface casing is always required, and is typically specified by regulation to be of "suitable and sufficient" quality [19] or "suitable for all drilling and operating conditions such as tension, burst, collapse" [20]. For all casing strings, industry best practices provide extensive guidance on the selection of proper casing size, grade, weight, and connections, plus procedures for field handling, inspection, and testing [21–27].

Failure categories for the surface casing and all other casing strings can be divided into the following five categories [28]. It should be noted that two of these categories, mechanical and corrosion, may be secondary to cement failures where a failed cement sheath can lead to buckling or external corrosion that would not have otherwise occurred. Failure categories, their respective failure modes, relative failure rates, and remedial options are discussed below:

- Materials: defects, tolerance busts, not getting the quality of pipe specified.
- Connections: wrong connection selected for the service, improper makeup.
- Wear and handling: internal wear from drilling, external damage from handling.
- Mechanical: tensile, burst, collapse, buckling, cyclic loading.
- Corrosion: internal vs external; galvanic, CO_2, sulfide stress, hydrogen induced cracking.

Materials defects are supplier dependent, and can be managed by inspections and other supply chain quality control efforts. Connection problems are most often related to improper makeup and can be minimized by on-site supervision. Wear for the surface casing string is seldom a concern and occurs as a result of other problems encountered while drilling the well. Mechanical problems with the surface casing are very few when compared to deeper casing strings that are exposed to higher pressures and temperatures. External corrosion presents the highest failure category for surface casing. Remedies may include external coatings, cement squeezes, and cathodic protection systems.

The surface casing string's cement job provides the primary barrier against vertical migration of fluids into protected water for the entire life of the well. In the context of USDW protection, the importance of getting a good primary cement job on the surface casing string cannot be overstated. Remedial cementing options do not provide high success rates for zonal isolation and should be considered only for contingency

purposes. Of all regulations for onshore wells, the rules for surface casing cementing contain the most stringent requirements for hole size versus casing size, centralization, cement quality, cement quantity, cement placement techniques, and quality assurance than for any other casing string [29]. Failure to properly cement the surface casing string triggers both agency notification and corrective actions [30]. The surface casing on our case study well is cemented on day #2 of the drilling operation.

There is a significant body of information published on cement selection and cementing best practices [31–34]. There is also a significant body of information available on cementing failure rates [35–36]. This Well Integrity Case Study will focus on those conditions that directly relate to zonal isolation for the protection of USDWs, briefly discussing three failure categories, with their respective modes and relative failure rates, and remedial options:

- Insufficient cement volume: underestimated annular volume, lost circulation.
- Low bond strength: poor slurry design, poor management of hydrostatic head pressure.
- Micro-annulus, cracking, plastic deformation: thermal and pressure effects, cyclic loads.

Cement failure rates are directly proportional to the ability to evaluate the top of and quality of the cement sheath. Cement tops can be identified by a temperature log, relative cement bond quality can be identified by a Cement Bond Log or CBL, while absolute cement bond quality requires a combination of logging, testing, and engineering analysis [37].

For all three cement failure categories, remedial options are not optimum; including pumping in from the top, spotting from the top via a small work string, or by perforating and squeezing. It should be noted that two of these three remedies; 1) pumping in from the top and 2) perforating and squeezing, might add new problems for zonal isolation if not properly executed.

There is a strong correlation between the gas migration and uncemented or poorly cemented casing strings. There is also a strong correlation between external casing corrosion and the absence of a good cement sheath [35–36]. After the surface casing has been successfully tested, the float collar, float shoe, and approximately 10 feet of new formation are drilled. Another integrity test is then performed, a Formation Integrity Test (FIT), which tests both the casing shoe and new formation together. This is not a leak-off test and does not test the limits of the shoe and formation. Rather, the FIT provides an assessment of the wellbore's ability to withstand additional pressure in case of an influx of fluids and allows for safer drilling to the next casing point [38].

The next sections of well, which for this case study includes an intermediate and production casing section, are essentially a repeat of the surface casing section described above, except that:

- The design depth for intermediate and production casing strings are not as comprehensively regulated (as for the surface casing depth) other than to provide safe drilling operations.

- The regulations concerning hole size versus casing size, centralization, cement quality, cement quantity, cement placement techniques, and quality assurance for intermediate and production casing strings are not as specific (as for the surface casing) other than to provide safe drilling operations.

Although this case study well has been drilled, cased, and cemented over a 30-day period, the first two days are the most critical for zonal isolation of USDWs where the foundation for well integrity is determined.

5.13.2 Completion

After the production casing is perforated, the formation is hydraulically fractured, frack fluids are unloaded from the formation, and production operations commence. This is basically the well's configuration for the rest of its life as it relates to protecting USDWs.

Prior to performing the hydraulic frack, the production casing is tested to anticipated frack pressure plus a safety factor, as is the frack tree and all of the surface pumping equipment and lines. During the frack, all casing annuli are monitored, as are the injection rate, injection pressure, and slurry properties. If during the frack job, significant pressure is found on the intermediate casing annulus, or there is any indication of communication with the surface casing annulus, the frack job is shut down and not resumed until corrective actions are made so that only the intended zone is subject to frack pressures.

Refracks are similar to original fracks as discussed above, with the exception that a frack string or wellhead saver might be used to protect older production casing strings and wellheads from frack pressures. This is a case-by-case situation that requires additional testing and engineering analysis in order to protect both the well and USDWs during refrack operations.

As the well is produced, reservoir pressures tend to drop and liquid rates tend to rise; therefore, devices for lifting liquids, such as a tubing string with pumping or gas lift equipment, become necessary. This internal configuration can have an impact on USDW protection and is addressed during the operations phase.

Figure 5.2 is a schematic of the various layers in a typical site casing design.

5.13.3 Well Operations

Prudent operators monitor all casing annuli on a regular basis to be able to detect sustained casing pressure or SCP. This condition could be caused by thermal expansion of annular fluids, packer or liner leaks, leaks into the annulus from inner tubing or casing strings, or from annular migration due to poor zonal isolation.

All states have rules for reporting and responding to the loss of well integrity, which includes gas and fluid releases, non-thermal SCP, and other abnormal situations [39], as does the BLM [40], as do best industry practices [41]. The Commonwealth of Pennsylvania has new rules that require quarterly mechanical integrity testing and annual reporting for all operating wells [42].

Adjacent well operations may have an impact on mechanical integrity of a well. Hydraulic fracturing of another well near a zone that is not protected, or not adequately

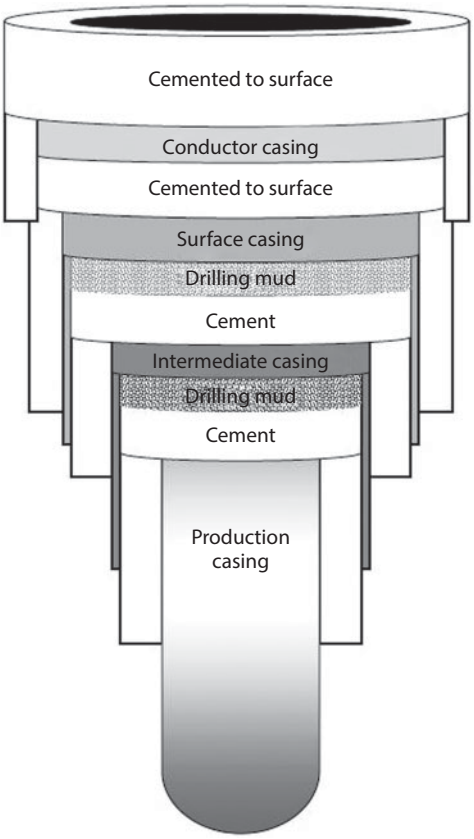

Figure 5.2 Well casings.

protected for the conditions imposed, can lead to unwanted well-to-well communication. This is currently a void where regulations and industry practices have not fully recognized that well integrity can become a neighborhood issue.

5.13.4 Well Plug and Abandonment P&A

Similar to well construction regulations and industry practices, well P&A also has comprehensive guidance to prevent vertical migration of fluids into USDWs. There is a clear guidance for plug location, cement (quantity, quality, placement techniques), testing, and reporting [43–45]. Regulations may also specify that only approved cementing contractors perform plugging, require independent on-site supervision, and require post-cement job certifications by operator and the cementing company. There are also significant industry studies and best practices for well P&A [46, 47].

The vertical migration issues in P&A wells are directly related to the quality of the original primary cement job during well construction. Those wells with gas migration to the surface prior to well P&A were likely to continue to have gas migration to the surface after P&A. Additionally, those wells which were plugged with bridge plugs and dump bailed cement on top were found to be more prone to leakage than wells plugged with cement that was circulated or squeezed in place [35, 36].

5.14 Summary

Well integrity and well construction are inextricably linked, regardless of the completion technique selected. Primary cementing is the critical step for preventing vertical migration of fluids during the well's productive life, and afterwards. State and federal regulations address casing and cementing with prescriptive rules and reporting requirements, while industry employs a large body of technical studies and best practices. There are five identified casing failure categories: materials, connections, wear/handling, mechanical, and corrosion. These are not as problematic for zonal isolation as three identified cementing failure categories: insufficient cement volume, low bond strength, and cement sheath damage.

For hydraulically fractured completions, significant bodies of industry technical information and best practices have been published. State and federal regulations address hydraulic fracturing with rules and reporting requirements that are continuously adapting to keep pace with technology advancements [48]. The potential for unwanted communication between adjacent wells during hydraulic fracturing is a concern. State and federal regulations are largely silent on this issue; however, there are extensive industry studies on this practice.

5.15 Failure and Contamination Reduction

The following are several key areas to be addressed in order to develop a pad site that is both safe for the environment as well as being productive.

5.15.1 Conduct Environmental Sampling Before and During Operations

Many of the contaminants that have been attributed to fracking, such as methane gas, occur naturally in groundwater and soil. If post-fracking contamination of soil or water is found, and there is no pre-fracking baseline against which the contamination can be compared, it could be difficult for the well operator to demonstrate that such contamination was pre-existing. This type of uncertainty increases the risk of regulatory scrutiny and litigation. Some states, like Wyoming, already require pre-drilling disclosures. Consider engaging a qualified environmental consultant to test water and soil before fracking begins. Air modeling or monitoring should also be performed during operations to help demonstrate that emissions are under control.

5.15.2 Disclose the Chemicals Used in Fracking Operations

This may be the issue that generates the most attention from state legislators and environmentalists. All of the states that recently have enacted fracking-related statutes (e.g., Texas, Colorado, Ohio, and Pennsylvania) have included sections that not only address the disclosure of chemicals used, but also provide some level of protection for trade secrets. The energy industry as a whole has supported this approach and generally agrees that while the disclosure of the chemicals used is appropriate, companies should not be forced to publish their exact fracking fluid "recipes." Companies have

also come to recognize that there are benefits to using environmentally friendly chemicals as much as possible. For example, when the public is advised that the guar gum used to gel frack water is the same ingredient commonly found in ice cream and bakery products, this type of disclosure tends to negate the fear associated with the use of "unknown" chemicals.

5.15.3 Ensure that Wellbore Casings are Properly Designed and Constructed

The U.S. Department of Energy demonstrated that the risks of a properly constructed well contaminating an aquifer as a result of fracking are remote. The most significant risks come instead from poorly constructed casings that might leak into groundwater. Thus, many state legislatures have enacted strict regulations that govern the manner in which casings are to be constructed, tested and monitored. Once again, the industry as a whole has already embraced these efforts to ensure that wells are properly built and should continue to implement improved technologies as they become available.

5.15.4 Eliminate Venting and Work toward Green Completions

On April 17, 2012, the EPA issued the first federal air standards for natural gas wells that are hydraulically fractured. A key component of the final rules is the implementation of a process known as "green completion." The process separates gas and liquid hydrocarbons from the flowback and is expected to yield a nearly 95% reduction in greenhouse gases. Although green completions were not mandatory until January 2015, companies used this time to acquire the necessary equipment. Until then, flaring was used to minimize the impact of these gases upon the environment.

5.15.5 Prevent Flowback Spillage/Leaks

Millions of gallons of flowback can be generated by fracking just one well. The flowback will include sand, chemicals (i.e., biocides, surfactants, gelling agents), brine, and dissolved solids. If the flowback is not contained properly, it can leak into nearby surface water and soil, thereby harming the environment and increasing the risk for various types of litigation and regulatory action. One way to minimize such risks is to ensure that all flowback pits are properly lined. A preferred method would be a "closed system" that eliminates the pit altogether and routes the flowback directly to the storage tanks prior to offsite treatment and disposal.

5.15.6 Dispose/Recycle Flowback Properly

The EPA and the states share responsibility for implementing the Clean Water Act (CWA) programs. The effluent guidelines program prohibits the on-site direct discharge of flowback from fracking wells into the water. While some flowback is transported to publicly owned treatment works (POTWs), and significant amounts are still injected into underground wells for disposal, there is an increasing trend to recycle the

flowback. Recycling can significantly reduce the amount of water needed for fracking activities. This is an extremely important consideration in those areas experiencing drought conditions. In addition, if the recycling is done near the drilling pad, it can also curtail the truck traffic needed to deliver the water and remove the flowback, thereby lowering transportation and off-site disposal costs.

5.15.7 Minimize Noise and Dust

Fracking activities at the drill pad can be loud. When they occur in urban areas or near residential communities, efforts are frequently undertaken to abate the noise by surrounding the drill pad with noise blankets, sound curtains, or wall barrier systems. Truck traffic also has the potential to generate significant levels of noise and dust. As indicated above, reducing the amount of traffic at the drill pad by recycling is one way to combat these potential problems. Other ways include the use of centralized pump stations and multi-well drilling techniques that reduce the number and size of pads needed for fracking. Spraying service roads with treated production water and brine is also permitted in some states to reduce dust, but care must be taken not to apply such liquids near vegetation, residences, or drainage ditches.

5.15.8 Protect Workers and Drivers

The *New York Times* has reported that the most dangerous jobs associated with fracking are not at the drilling rig but on the road. Drivers working at oil and natural gas wells reportedly work longer hours than drivers in other industries, and are thereby subjected to fatigue and a greater risk of having an accident. That is not meant to minimize the risks faced by drilling crews who obviously could be exposed to many potential jobsite hazards if proper safety precautions are not followed. While certain exemptions for oil and gas truckers were upheld by the Federal Motor Carrier Safety Administration, the exemptions have come under closer scrutiny in the last 2 years. The need for companies to enforce OSHA regulations and other safety rules implemented by the industry to protect its workers is of critical importance.

5.15.9 Communicate and Engage

Nearly every group that has generated a set of Best Management Practices has emphasized the importance of communicating with nearby residents, local governments, and other stakeholders. Misinformation can be quickly spread through the Internet. First impressions, although mistaken, can be difficult to reverse. The Investor Environmental Health Network (IEHN) recommends that the fracking industry identify communities potentially impacted, address their major concerns, and establish a mechanism for resolving conflicts. Companies should be prepared to direct persons with legitimate questions to websites that provide answers that are scientifically and factually accurate. Several such websites exist, such as http://www.energyindepth.org/. The need for patience must also be stressed, since many of the discussions that involve fracking are emotionally charged.

5.15.10 Record and Document

Sloppy record keeping gives plaintiffs, regulators, and juries too much leeway to draw erroneous conclusions. If documentation should have been kept, but was not, there will almost always be an inference that the "lost" documents were adverse to the interests of the company. Sloppy record keeping reflects poorly on a company's overall reputation even though the company may have an excellent history of actual environmental compliance and worker safety. It is also important to recognize that in this fast-paced age of instant communications with emails and text messages, virtually all of those communications can be converted to documents that must be produced if litigation occurs.

5.16 Frack Fluids

The use of hydraulic fracturing for oil and gas exploration in the United States has become highly controversial. One of the greatest points of contention between the public and industry is the makeup of frack fluids and their possible impacts on public health and the environment. This has become such a hot topic with many segments of the public for two reasons:

1. if a concern exists about the pumping of fluids into any structure, then the most concern will naturally be centered on what is being pumped, and
2. a great deal of suspicion arose and was intensified when the oil and gas industry initially balked at disclosing the chemical makeup of fluids used to enhance hydraulic fracturing.

This has become a major argument point for the concerned public because, basically, "if there is nothing to hide, why not disclose it?"

To make this contentious subject a little clearer, this section will provide descriptions of why frack fluids are needed, what general chemicals are needed and used, relative amounts of chemicals in frack fluid composition, the different types and uses of proppants, a discussion on slickwater, and a discussion on present regulations and standards for industry disclosure of frack fluid compositions.

There are a great deal of varied chemicals used every day in oil production wells during all phases of drilling, completions, and production. These chemicals can include cement used to seal the annulus to protect the pipe and surrounding formation from damage through wells exceeding the producing and stimulation requirements placed on the pipe, temperature, and even natural ground stresses. An example is corrosion inhibitors. These chemicals help pipe and connection seals remain within the design specifications to prevent failures. Corrosion prevention and treating chemicals may also be necessary due to operational and field changes, even after well completion and during production.

These chemicals can be used in much the same fashion in fracturing; however, chemicals in well operation are applied in smaller quantities, at lower pressure, and in a regular maintenance-driven schedule during a well's life. Just like the maintenance-driven chemicals utilized during operations, chemicals serve numerous necessary functions

to ensure successful, safe, and efficient hydraulic fracturing operations. The following provides a comprehensive look at common chemical additives utilized in the current fracturing industry.

5.17 Common Fracturing Additives

There is no one formula for how much each of the following additives are used in a given fracturing fluid; however, the following section is intended to present a brief description of some of the most commonly used additives and a general percentage breakdown of each that has been widely reported. Each well differs in the number, type, and amount of additives used (the term "additives" is used to include water, sand, and chemicals to allow for a discussion of each under one heading) in a successful fracture treatment. Typically, between 3 and 12 additives are used, depending on the conditions of the specific well to be fractured and characteristics of the surrounding formations. Additives utilized in hydraulic fracturing operations are intended to serve specifically engineered uses, such as biocides to control microorganism/bacterial growth, corrosion inhibitor to prevent corrosion, viscosity agents to carry the proppant, gelling agents to improve proppant placement, friction reduction to decrease pump friction and reduce treating pressure, and acids to help remove drilling mud up build damage.

Fluids (*typically water*)*:* usually approximately 98–99% of the total volume; used to create the fractures in the formation and to carry a propping agent (typically silica sand) that is deposited in the induced hydraulic fractures to keep them from closing up.

Hydrochloric acid (HCl): from 5% to 25% in solution used to help dissolve minerals and help remove damage near the well bore by cleaning out cement around the perforations; also helps to initiate fissures in the rock matrix.

Corrosion inhibitor (*typically ammonium bisulfate*)*:* usually approximately 0.2%–0.5% of total acid volume, resulting in approximately 5–10 gallons; used only in instances when acid is used to prevent corrosion.

Biocides (typically sodium hypochlorite or chlorine dioxide): usually approximately 0.005%–0.05% of the total volume; used to control bacterial growth in the water injected into the well and prevent corrosion.

Friction reducers (*typically polyacrylamide based compounds*)*:* usually approximately 0.025% of total volume; used to reduce pipe friction and pressure in the piping required to pump fluids.

Gelling agents (*guar gum and cellulose*)*:* not often used; used to thicken water-based solutions and help in suspension and transport of proppants into formation.

Crosslinking agent (*boric acid, titanate and zirconium*)*:* used to enhance abilities of the gelling agent to aid in the transport of proppant material.

Breaker solution: when cross-linking additives are added, a breaker solution is commonly added in the frack stage to cause the enhanced gelling agent to break down into a simpler fluid so that it can be readily removed from the wellbore without carrying back the sand/ proppant material.

Iron control and stabilizing agents (*citric acid and acetic acid*)*:* used to keep iron compounds in soluble form to prevent precipitation.

Surfactant: usually approximately 0.5 to 2 gallons per 1,000 gallons of frack fluid; used to promote flow of the fluids used in the fracturing process.

Scale Inhibitor (*ethylene glycol*)*:* seldom used; used to control the precipitation of specific carbonate and/or sulfate minerals.

Proppants (*sand, resin coated sand, or man-made ceramic particles*)*:* usually approximately 1–1.9% of total volume; used to hold fissures open so that gas and oil can be extracted.

"Ingredients" of fracking fluids have everyday uses; scale inhibitors have the same chemicals as windshield washer fluid; friction reducers have the same chemicals as many makeup products; surfactants are basically the same as shampoo products; proppants are play sand; and hydrochloric acid is a swimming pool cleaner.

5.18 Typical Percentages of Commonly Used Additives

Fracturing fluids are varied to meet the specific needs of each location; however, evaluating the widely reported percentage volumes of the fracturing fluid components reveals the relatively small volume of different chemicals that are present. Overall, the concentration of various chemicals in most fracturing fluids is a relatively consistent 0.5% to 2%, with water and proppants making up the remaining 98% to 99.5%. It should be kept in mind, however, that a typical fracturing job uses upwards of 5 million gallons of fracturing fluid.

As one can imagine, the overall composition of fracturing fluids varies among companies and the drilling location. Fracturing fluids typically contain:

Approximately 90% water.
Approximately 9.5% proppant materials.
Approximately 0.5% chemicals: this percentage varies, but is typically between 0.5–1.0% by weight of total fluid.

As described in previous sections, the chemical additives are included in fracking fluids to tailor the fluids to the requirements of the specific geological situation. The chart below (Figure 5.3) demonstrates typical volumetric percentages of additives that were used for a typical hydraulic fracturing treatment of a shale horizontal well.

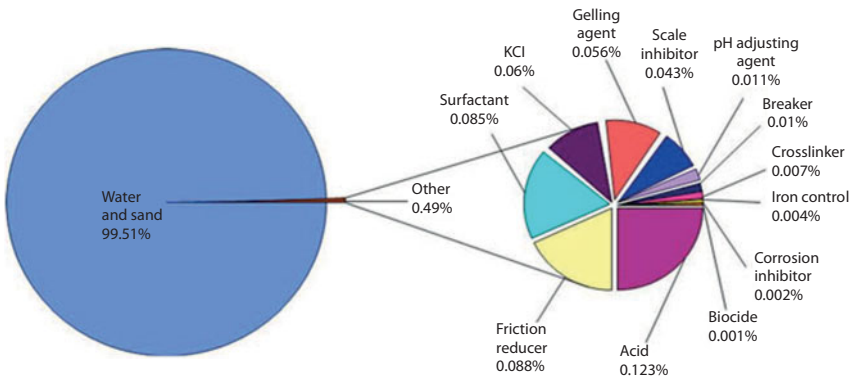

Figure 5.3. Volumetric percentages of additives in fracturing fluids.

5.19 Chemicals Used in Fracking

The common chemicals used at a fracking site are presented in Table 5.2. One of the problems associated with identifying chemicals is that some chemicals have multiple names. For example, Ethylene Glycol (Antifreeze) is also known by the names Ethylene alcohol; Glycol; Glycol alcohol; Lutrol 9; Macrogol 400 BPC; Monoethylene

Table 5.2 Chemicals used in fracking.

Chemical name	CAS	Chemical purpose	Product function
Hydrochloric Acid	007647-01-0	Helps dissolve minerals and initiate cracks in the rock	Acid
Glutaraldehyde	000111-30-8	Eliminates bacteria in the water that produces corrosive byproducts	Biocide
Quaternary ammonium chloride	012125-02-9	Eliminates bacteria in the water that produces corrosive byproducts	Biocide
Quaternary ammonium chloride	061789-71-1	Eliminates bacteria in the water that produces corrosive byproducts	Biocide
Tetrakis hydroxymethyl-phosphonium sulfate	055566-30-8	Eliminates bacteria in the water that produces corrosive byproducts	Biocide
Ammonium persulfate	007727-54-0	Allows a delayed breakdown of the gel	Breaker
Sodium chloride	007647-14-5	Product stabilizer	Breaker
Magnesium peroxide	014452-57-4	Allows a delayed breakdown of the gel	Breaker
Magnesium oxide	001309-48-4	Allows a delayed breakdown of the gel	Breaker
Calcium chloride	010043-52-4	Product Stabilizer	Breaker
Choline chloride	000067-48-1	Prevents clays from swelling or shifting	Clay stabilizer
Tetramethyl ammonium chloride	000075-57-0	Prevents clays from swelling or shifting	Clay stabilizer
Sodium chloride	007647-14-5	Prevents clays from swelling or shifting	Clay stabilizer
Isopropanol	000067-63-0	Product stabilizer and / or winterizing agent	Corrosion inhibitor
Methanol	000067-56-1	Product stabilizer and / or winterizing agent	Corrosion inhibitor
Formic acid	000064-18-6	Prevents the corrosion	Corrosion inhibitor
Acetaldehyde	000075-07-0	Prevents the corrosion	Corrosion inhibitor
Petroleum distillate	064741-85-1	Carrier fluid for borate or zirconate crosslinker	Crosslinker
Hydrotreated light petroleum distillate	064742-47-8	Carrier fluid for borate or zirconate crosslinker	Crosslinker
Potassium metaborate	013709-94-9	Maintains fluid viscosity as temperature increases	Crosslinker
Triethanolamine zirconate	101033-44-7	Maintains fluid viscosity as temperature increases	Crosslinker
Sodium tetraborate	001303-96-4	Maintains fluid viscosity as temperature increases	Crosslinker
Boric acid	001333-73-9	Maintains fluid viscosity as temperature increases	Crosslinker
Zirconium complex	113184-20-6	Maintains fluid viscosity as temperature increases	Crosslinker
Borate salts	N/A	Maintains fluid viscosity as temperature increases	Crosslinker
Ethylene glycol	000107-21-1	Product stabilizer and / or winterizing agent.	Crosslinker
Methanol	000067-56-1	Product stabilizer and / or winterizing agent.	Crosslinker

(*Continued*)

Table 5.2 Cont.

Chemical name	CAS	Chemical purpose	Product function
Polyacrylamide	009003-05-8	"Slicks" the water to minimize friction	Friction reducer
Petroleum Distillate	064741-85-1	Carrier fluid for polyacrylamide friction reducer	Friction reducer
Hydrotreated light petroleum distillate	064742-47-8	Carrier fluid for polyacrylamide friction reducer	Friction reducer
Methanol	000067-56-1	Product stabilizer and / or winterizing agent.	Friction reducer
Ethylene glycol	000107-21-1	Product stabilizer and / or winterizing agent.	Friction reducer
Guar gum	009000-30-0	Thickens the water in order to suspend the sand	Gelling agent
Petroleum distillate	064741-85-1	Carrier fluid for guar gum in liquid gels	Gelling agent
Hydrotreated light petroleum distillate	064742-47-8	Carrier fluid for guar gum in liquid gels	Gelling agent
Methanol	000067-56-1	Product stabilizer and / or winterizing agent.	Gelling agent
Polysaccharide blend	068130-15-4	Thickens the water in order to suspend the sand	Gelling agent
Ethylene glycol	000107-21-1	Product stabilizer and / or winterizing agent.	Gelling agent
Citric acid	000077-92-9	Prevents precipitation of metal oxides	Iron control
Acetic acid	000064-19-7	Prevents precipitation of metal oxides	Iron control
Thioglycolic acid	000068-11-1	Prevents precipitation of metal oxides	Iron control
Sodium erythorbate	006381-77-7	Prevents precipitation of metal oxides	Iron control
Lauryl sulfate	000151-21-3	Used to prevent the formation of emulsions in the fracture fluid	Non-Emulsifier
Isopropanol	000067-63-0	Product stabilizer and / or winterizing agent.	Non-Emulsifier
Ethylene glycol	000107-21-1	Product stabilizer and / or winterizing agent.	Non-Emulsifier
Sodium hydroxide	001310-73-2	Adjusts the pH of fluid to maintain the effectiveness of other components, such as crosslinkers	pH adjusting agent
Potassium hydroxide	001310-58-3	Adjusts the pH of fluid to maintain the effectiveness of other components, such as crosslinkers	pH adjusting agent
Acetic acid	000064-19-7	Adjusts the pH of fluid to maintain the effectiveness of other components, such as crosslinkers	pH adjusting agent
Sodium carbonate	000497-19-8	Adjusts the pH of fluid to maintain the effectiveness of other components, such as crosslinkers	pH adjusting agent
Potassium carbonate	000584-08-7	Adjusts the pH of fluid to maintain the effectiveness of other components, such as crosslinkers	pH adjusting agent
Copolymer of acrylamide and sodium acrylate	025987-30-8	Prevents scale deposits in the pipe	Scale inhibitor
Sodium polycarboxylate	N/A	Prevents scale deposits in the pipe	Scale inhibitor
Phosphonic acid salt	N/A	Prevents scale deposits in the pipe	Scale inhibitor
Lauryl sulfate	000151-21-3	Used to increase the viscosity of the fracture fluid	Surfactant
Ethanol	000064-17-5	Product stabilizer and / or winterizing agent.	Surfactant
Naphthalene	000091-20-3	Carrier fluid for the active surfactant ingredients	Surfactant
Methanol	000067-56-1	Product stabilizer and / or winterizing agent.	Surfactant
Isopropyl alcohol	000067-63-0	Product stabilizer and / or winterizing agent.	Surfactant
2-Butoxyethanol	000111-76-2	Product stabilizer	Surfactant

glycol; Ramp; Tescol; 1,2-Dihydroxyethane; 2-Hydroxyethanol; HOCH2CH2OH; Dihydroxyethane; Ethandiol; Ethylene glycol; Glygen; Athylenglykol; Ethane-1,2-diol; Fridex; M.e.g.; 1,2-Ethandiol; Ucar 17; Dowtherm SR 1; Norkool; Zerex; Aliphatic diol; Ilexan E; Ethane-1,2-diol; 1,2-Ethanedio.

This multiplicity of names can make a search for chemicals somewhat difficult and frustrating. However, a search for a chemical by the CAS number (see Table 5.2) will return the correct chemical even if the name on the fracturing record does not match. For example, if the fracturing record listed the chemical hydrogen chloride, a search for it by name using a chemical search site may not get a result. But if a search is made for CAS # 007647-01-0, it might return hydrochloric acid, which is another name of hydrogen chloride. Therefore, by using the CAS number, the issue of multiple names for the same chemical can be avoided.

5.20 Proppants

As discussed earlier, proppants are simply materials (typically silica sand, resin coated silica sand, or manufactured ceramics) used to prop open the open fractures to promote flow and eventual extraction of hydrocarbons. As simple as proppants may seem, the estimated amount of proppant used in industry has grown tenfold since 2000. In some regions, it is not uncommon to see upwards of 4 million pounds of proppant used per well, and for proppant to represent up to 5% of well costs. The growth in proppant usage is generally attributed to operators realizing better well completion techniques with more proppant per stage and better well pad techniques with more laterals and fracturing stages per pad.

The first frack job was conducted in 1947, utilizing approximately 20,000 pounds of uncoated frack sand, whereas manufactured ceramic proppant was not first used until 1983, or 36 years later. Then, approximately 1 year later, resin-coated proppant was first introduced. As with most all technologies, as new techniques continue to develop, proppants will surely evolve further to increase effectiveness and efficiency in hydraulic fracturing.

The most important characteristics for a proppant are particle size distribution, crush resistance, shape, and sphericity (or roundness). Proppant materials are carefully sorted for size and sphericity to provide an efficient conduit for production of fluid from the reservoir to the wellbore. Grain size is critical because a proppant must reliably fall within certain size ranges to coordinate with downhole conditions and completion design. (See Figure 5.4. Proppant size and placement.)

Proppant shape and hardness qualities are very important to the efficiency and effectiveness of a fracturing operation. A coarser proppant allows for higher flow capacity due to the larger pore spaces between grains, but it may break down or crush more readily under high closure stress. Rounder and smoother proppant shapes give rise to better permeability. (See Figure 5.5. Proppant's shape)

Another important quality that must be taken into consideration is the proppant's hardness with respect to the formation. If the proppant is unable to embed in the formation, something referred to as point load occurs, which leads to higher flow capacity,

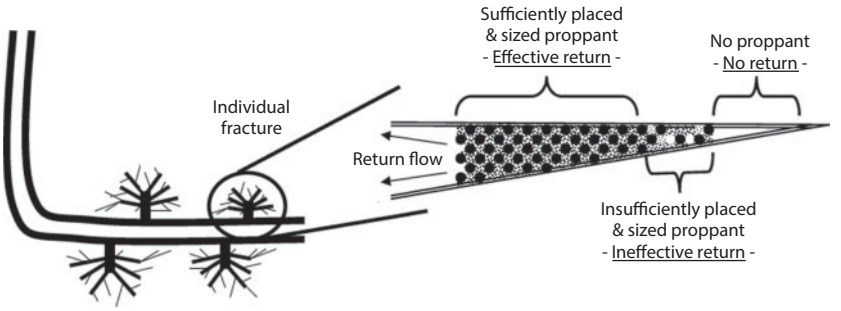

Figure 5.4 Proppant size and placement.

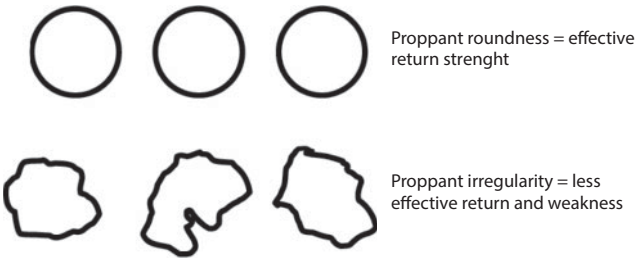

Figure 5.5 Proppant's shape.

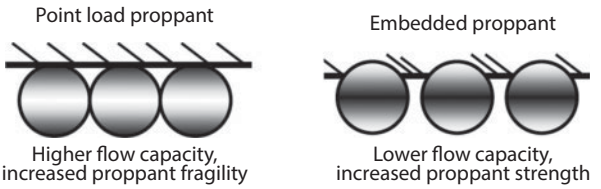

Figure 5.6 Proppant hardness.

but the proppant will break more easily. However, if the proppant is able to embed in the formation, it is referred to as embedment, which results in the load pressure spreading out over the proppant area, increasing the breaking point, but also lowering the flow capacity. Embedment is also a function of particle size. (See Figure 5.6. Proppant hardness)

The logistics in procuring and transporting proppants can be daunting. Logistical considerations include coordination of manufacturing material resources, transportation costs and possibly a substantial monetary investment in equipment necessary for processing and material handling facilities.

5.20.1 Silica Sand

The type of sand utilized for proppants is silica sand, which is, by far, also the most commonly used type of proppant. Silica sand, unlike many other "ingredients" of frack

fluid, is more of a natural resource than an engineered product. Silica sand proppant is made up of the most common mineral in the Earth's continental crust i.e., quartz. Even though silica sand is a relatively common material, silica sand used for proppant is a specifically selected product. The quality of silica sand used as a proppant depends on the original depositional environment and some slight mechanical processing, if necessary. Silica sand used for proppant is chosen for its round spherical shape and commonly graded particle distribution.

In addition to the oil and gas industry, there is some competition with other industries for silica sand. Industrial-grade silica sand has a wide range of uses. This resource is also commonly used in the manufacture and preparations of various types of glass, in water filtration, sand blasting, as a fill, ingredients in industrial concrete, in the metal casting industry to make cores and molds, and in the creation of highly flame-resistant industrial molds and construction materials for the kilns used in the manufacture of the sintered ceramic and bauxite proppants.

There are some possible hazards related to the use of certain proppants. Because of the fine grains of silica sand, it can present a health risk if not properly handled. Care must be taken to keep the silica sand out of the lungs during use; all materials containing more than 0.1% of silica sand must be clearly labeled. Workplace health applications also need to be in place and enforced: failure to wear a proper respirator or mask can result in lung irritation, and prolonged exposure can cause a chronic condition known as silicosis. Silicosis is a form of lung disease resulting from occupational exposure to silica dust over a period of years, causing a slowly progressive fibrosis of the lungs, impairment of lung function, and even a heightened susceptibility to tuberculosis. Silicosis can also progress and worsen even after someone is no longer exposed to the silica dust, causing long-term effects and shortness of breath years later. In 2000, the World Health Organization determined that crystalline silica is "associated with silicosis, lung cancer, and pulmonary tuberculosis" in classifying it as a Group I carcinogen "based on sufficient evidence of carcinogenicity in humans and experimental animals."

5.20.2 Resin-Coated Proppant

As the name suggests, and to describe in the most simplistic of terms, resin-coated proppant is exactly that: silica sand coated with resin. Resin coating silica sand proppant is utilized for two main functions:

1. to spread the pressure load more uniformly in order to improve the crush resistance of the silica sand particles, and
2. to keep grains together after being broken by a high closure stress from downhole pressure and temperature. This not only prevents broken pieces from flowing into the borehole, but also prevents these broken pieces from returning to the surface during flowback production operation.

Currently, there are two types of resin-coated proppants, *Pre-cured* and *Curable*. Pre-cured is the "original" technology, in which the resin coating on the silica sand grains is fully cured prior to injection into the fractures. The newer, curable technology has

often been described as having a coating that is not completely "baked" or hardened. Curable resin-coated proppants which is used at a little more than half cure, so that when the proppant is pumped downhole it can finish curing in the fractures under downhole pressure and temperature. The advantage of curable proppant technology is that it allows the individual proppant grains to bond together in the fracture, resulting in the grains bonding together uniformly in strength when temperature and pressure reach high levels.

5.20.3 Manufactured Ceramics Proppants

A third commonly used type of proppant is the manufactured ceramic proppant. This is a proppant generally manufactured from a type of ceramic material, typically non-metallurgic bauxite or kaolin clay. Bauxite is an aluminum ore from which most aluminum is extracted, whereas kaolin is one of the most common clay minerals, occurring in abundance as a result of chemical weathering of rocks in hot, moist climates like tropical rainforest areas.

Both bauxite and kaolin are utilized as proppants because of their superior strength characteristics, which are further enhanced through a process known as sintering. The sintering process is conducted in high-temperature kilns that are used to bake the bauxite or kaolin powder after it has been properly sized. This process decreases the water content in the bauxite and kaolin to make them more uniformly shaped for roundness and spherical shape. The desired results of this process are that the manufactured ceramic proppants can be engineered to withstand high levels of downhole pressure (closure stress).

5.20.4 Other Types of Proppants

As more is learned through the ongoing processes and further advances are made in technology, additional types of proppants will be developed. One current trend is toward the usage of "waste" material, including glass, metallurgical slags, and even rock cuttings produced to the surface during oil and gas drilling. The reuse of rock cuttings from drilling operations is especially attractive, since not only does it reuse a common waste product in industry, but it also utilizes sources indigenous to the locality. This will cut down not only the wastes but also overhead costs. Such operations will require work with landfills, metallurgical operations, and glass companies to recycle and reuse their wastes in lieu of land filling.

5.21 Slickwater

Slickwater is a more dilute, predominately water-based fracturing fluid that utilizes a limited amount of sand, friction reducers, and other chemicals. Slickwater is prepared in order to create a lower viscosity fracturing fluid to allow for an easier escape out of the created hydraulic fracture. Due to its low viscosity, slickwater can also be pumped down the wellbore at a higher rate.

5.22 Direction of Flow of Frack Fluids

As discussed previously, hydraulic fracturing involves the use of pressure applied by a fluid to create a new fracture or enlarge natural fractures present in the rock. These fractures extend in a planar style in general directions perpendicular to the plane of the least principal stress in the rock, following what is called "fracture direction." These hydraulic fractures are most commonly vertical (until contact is made with a rock of different structure, texture, or strength to stop the fracture growth), and may extend laterally several hundred feet away from the wellbore. These fracture barrier rocks, which stop the upward or downward growth of fractures are very common. Fracture height growth may extend up to a few hundred feet or more, but will likely be quickly limited by one of the dozens of rock barriers above the pay zone. Driving a fracture upwards through several thousand feet of rock is simply not possible, given the limits imposed by natural barriers and stresses of the rocks above the pay zone.

Pumping of a single frack stage may be limited to anywhere from 20 minutes to 4 hours, depending on the design and intent of the frack. This period of high-pressure operation is normally the only time most wells will experience pressure high enough to reverse fluid flow into the formation. However, the required travel time for fluid to flow from the shale to aquifer under those pressures would be years. Any flow of frack fluid toward an aquifer through open fractures would be reversed during flowback.

Chemicals returning from a well after fracture are a fraction (usually between 20% or less for chemicals and about 40% for polymers) of what was pumped down the well. Most corrosion inhibitors, scale inhibitors, and surfactants adsorb onto minerals such as clays in the formation. Those that do not adsorb may bleed back very slowly, usually in a concentration of approximately 5–10 parts per million of water. The hydrochloric acid is typically used up within inches of the frack entry point and yields calcium chloride, water, and a small amount of CO_2. Thus no live acid is returned to the surface.

5.23 Subsurface Contamination of Groundwater

An increasingly common concern expressed about hydraulic fracturing is that operations create fractures extending past the target formation to aquifers, allowing fracturing fluids to migrate into the drinking water supplies. There are several factors that would prevent this from occurring:

- This would require hydro-fractures to extend several thousand feet beyond the upward boundary of the target formation through many layers of rock.
- Geologists estimate that usually there is at least a half mile of rock between the natural gas deposits and the groundwater.
- Impermeable shale acts as a barrier to vertical propagation of both natural and artificial fractures.
- After hydraulic fracturing is completed, the fluid flow is toward – not away from – the well as gas enters the wellbore during production.

Studies have shown that failure of the cement or casing surrounding the wellbore poses a far greater risk to water supplies than hydraulic fracturing.

5.23.1 Water Analysis

Groundwater contamination can adversely affect property values, the image of a community, economic development, and the overall quality of life shared by all. Clean water at a reasonable cost is essential, and in many parts of the country, groundwater is the only economical water source available. Once groundwater has been contaminated, it is usually very difficult and costly to clean. Even small contamination sites often cost many thousands of dollars to clean up. The quality of water from private water supplies, such as those from wells at individual homes, is not regulated. It is the responsibility of the well owner to ensure a safe drinking water supply. Although there are a few requirements for water quality testing and monitoring of private wells (i.e., in some areas, testing is required at the time of property transfer), it is recommended that all well owners have their water tested periodically. While "complete" drinking water analyses can be expensive and are generally unnecessary for the private well owner, it is recommended that private water supplies be tested routinely for common contaminants including total coliform bacteria, nitrates, and lead. These contaminants can occur in well water due to agricultural activity, septic system use, household chemical use/ disposal, age of the plumbing, or industrial activity. The frequency of water testing and the contaminants to test for depend on factors such as the potential sources of pollution and the type of well. Another consideration is ensuring that the private well complies with proper well construction standards.

A water's taste, smell, or color is not necessarily an indicator of water quality. Many of the most hazardous contaminants are undetectable to the senses. The only way to detect most pollutants is by testing.

Before hydraulic fracturing operations begin in a new area, American Petroleum Institute guidance (API - HF1) recommends a baseline assessment program that includes the sampling of nearby water wells be conducted prior to hydraulic fracturing operations. Fresh water wells should also be sampled following hydraulic fracturing operations. At least one U.S. state (Colorado) requires the sampling of certain water wells in various areas of the state as part of its regulatory program. Another state (Pennsylvania) has regulations that presumptively place the burden of proof on any oil and gas company to demonstrate that it has not caused deterioration of the quality of groundwater used for drinking water purposes in the vicinity of oil and gas wells in the event of a contamination complaint.

In order to obtain valid results from sampling, it is important to follow proper sampling and analysis protocols. One should contact a state or EPA-certified laboratory for sampling containers and instructions. Proper protocols may include:

1. using appropriate containers and seals;
2. purging of the well prior to sample capture;
3. collection at points before water treatment equipment;
4. following sample container filling procedures;
5. following storage and holding time requirements;
6. utilizing appropriate analysis methods; and
7. following appropriate quality control/ quality assurance protocols.

Sampling should be conducted by someone familiar with sampling procedures. Analyses should be conducted by an accredited laboratory using appropriate analysis methods. One may be able to obtain a list of qualified laboratories by contacting a local health department, state water quality agency shown on the regulations by state page, or county extension agent.

It is important for landowners to have an oil and gas operational sampling and analysis of their groundwater conducted by a professional for constituents that may provide a reasonable baseline for post-fracturing analysis. The National Ground Water Association maintains a list of groundwater professionals that the reader can review to help find someone in the local area for assistance. The following is a good basic list of constituents that should be considered for analysis prior to oil and gas operations.

- Major cations and anions
- pH
- Specific Conductance
- Total Dissolved Solids
- Benzene, Toluene, Ethyl benzene, Xylene (BTEX)/Diesel range organics (DRO)/Gasoline
- Range organics (GRO)
- Total petroleum hydrocarbons or oil & grease (HEM)
- Arsenic
- Barium
- Calcium
- Chromium
- Iron
- Magnesium
- Selenium
- Boron
- Sodium
- Chloride
- Potassium
- Bicarbonate
- Dissolved Methane

Once hydraulic fracturing has taken place and a record of the actual chemicals used is available, it would be advisable to consider having a sampling and analysis conducted on the groundwater for the chemicals shown on the record that match those listed above or those that are byproducts, reaction products, or daughter products of those listed above. This is important because many of the chemicals used in hydraulic fracturing will be degraded, oxidized, or otherwise modified during the fracturing process. Thus, simply looking for the chemicals on the list shown above may not yield enough information for a comparative analysis. However, to minimize costs for the landowner, an alternative analysis should be conducted for at least (1) Total Dissolved Solids (TDS), which is a measure of the combined content of all inorganic and organic substances contained in liquid and (2) dissolved methane. An increase in the concentration of either of these constituents could indicate that further, more complete sampling and analysis should be conducted.

The reader can learn more about the toxicity characteristics of chemicals by searching for the chemical using the name or CAS number on the USEPA National Center for Computational Toxicology website. USEPA also maintains a Drinking Water Hotline that is available Monday-Friday from 8:30 AM-4:30 PM Eastern Time at 1-800-426-4791.

Only a trained professional such as a toxicologist or a physician can state if the water is safe to consume. The reader should not use the information obtained from the USEPA Toxicology website, or any other website to make decisions regarding the safety or drinkability of water.

One of the most graphic and widely publicized issues related to hydraulic fracturing is the notion that it causes methane gas to emit from water wells, in some instances in ignitable concentrations. However, methane has always been a relatively common contaminant in water wells and can be the result of natural or man-made causes.

There are several possible causes for methane gas to be found in water wells unrelated to hydraulic fracturing operations. These include naturally forming biogenic methane caused by the decay of organic materials or natural seeps of thermogenic methane that have been coming to the surface for millions of years.

5.23.2 Possible Sources of Methane in Water Wells

As discussed in Chapter 2, many water wells are liable to produce some level of odorless methane through sources such as agriculture, livestock, wetlands, landfills, and other sources allowing biogenic gas to form through decaying vegetation. In addition to these natural causes, it is also quite possible to have detectable methane content in a water well caused by a nearby improperly constructed gas or oil well. A third possible cause of methane in water wells is from the penetration of coal formations that are saturated with fresh water. Coals can have as much as 90% or higher organic content with adsorbed gas which can desorb as water is pumped from the area, e.g., a water well.

There are literally thousands of natural oil, gas, and salt water seeps that come to the surface. The earliest historical written record of natural oil and gas seeps in the Western Hemisphere was Sir Walter Raleigh's account of Pitch Lake in Trinidad in 1595. Well-known current oil and gas seeps in the United States include the La Brea Tar Pits and McKittrick Tar Pits in California and the "Eternal Flame Falls" of the Shale Creek Preserve, a section of the Chestnut Ridge Park in New York.

5.24 Spills

Another major concern for hydraulic fracturing well production is the potential for spills or releases at the well pad site or during transportation. Oils from well releases, in their concentrated form with chemical additives pose a higher risk while being transported or stored on-site than when injected into the subsurface during hydraulic fracturing.

Common sources of spills at the pad site include the mechanical failure at the drill rig and other operating equipment, storage tanks, pits, and even leaks or blowouts at

the wellhead. Leaks or spills may also occur during transportation (by truck or pipeline) of materials and wastes to and from the well pad. As in most all of these cases, surface water and groundwater are the primary risk receptors. Root causes of on-site and off-site releases can be accidents, inadequate facilities management or staff training, or even illicit/illegal dumping.

In the event of spills, effective containment is a major factor in minimizing the impacts on human health and the environment when a spill occurs. Containments, including berms around tank batteries, double walls in tanks and vessels, and catch pans and basins for smaller storage containers, are the first line of defense against spills.

5.24.1 Documentation

The Clean Water Act addresses spills and other accidental releases. A main component of spill prevention is the Spill Prevention Control and Countermeasures (SPCC) plan prepared to assure that adequate responses, materials, and personnel are available to respond to releases. Most states require an SPCC plan or equivalent for oil and gas operations as well as a statewide plan for response to spills and other releases. SPCC plans include prevention and control measures along with contact information, site-specific maps and details, reporting and cleanup requirements, and specifications for proper materials handling.

5.25 Other Surface Impacts

Drilling operations require significant above-ground development. In addition to possible spill scenarios related to the well pad itself, other possible surface impact scenarios are also quite common. Lease roads may need to be built and gathering infrastructure installed to bring the product from the wellhead to a delivery point or a pipeline. The pipeline itself, including installation and the remaining easement, may require the development of several acres of land.

Total land use and resulting impacts to the environment can be reduced by drilling multiple wells from a single well pad, which is a very common practice on horizontal hydraulic fracturing well pads. Nonetheless, with so many wells being drilled and the related infrastructure development, it is imperative that industry and regulatory bodies do as much as possible to minimize the overall impact on local communities, habitats, and road systems.

5.26 Land Use Permits

Land use decisions affect a wide range of stakeholders, including landowners, adjacent neighbors, surrounding communities, and community leaders. Permitting procedures will need to consider the needs of each of these stakeholders and include concise and enforceable preventative and remediation strategies to help provide minimal impact and maximum restoration of the land associated with well pads and production. Proper oversight also needs to be provided to help manage soil erosion and transport of

sediment into streams and other water bodies, prevent damage to ecological habitats, and avoid destroying habitats.

During the construction phase for a well pad or infrastructures, the quality of surface water resources may be impacted by runoff, particularly during storms. Shale gas development will also affect forests and ecological habitat on a large scale. Development studies indicate that many well pads are constructed in forest clearings, resulting in the clearing of thousands of acres of habitat for well pads and associated road infrastructure.

5.27 Water Usage and Management

Flowback water is the portion of injected fluid that returns to the wellbore after the downhole hydraulic fracturing process is completed and the fluid pressure is relieved. Flowback water is then brought back to the surface for treatment, recycling, and/or disposal. The initial fluid withdrawn from the wellbore actually consists of a mixture of the flowback water and saline water from the formation, referred to as "produced" water.

There is much concern over the use of water for fracking. Consider the following table (Table 5.3).

The source for Table 5.3 is the Chesapeake Energy 2009 presentation to the Ground Water Protection Council, citing Chesapeake well estimates for shale gas and a U.S. Department of Energy water use report. Coal plant water consumption: "Energy Demands on Water Resources," U.S. Department of Energy, December 2006, http://www.sandia.gov/energy-water/docs/121- RptToCongress-EWwEIAcomments-FINAL.pdf. NYC water consumption: New York City Department of Environmental Protection,

Table 5.3 Volume of water required for development of various resources.

Energy resource	Volume of water used per MMBTU of energy produced
Shale Natural Gas	0.60–1.80
Natural Gas	1 to 3
Coal (no slurry transport)	2 to 8
Coal (with slurry transport)	13 to 32
Nuclear (processed uranium ready to use in plant)	8 to 14
Conventional Oil	8 to 20
Synfuel-Coal Gasification	11 to 26
Oil Shale Petroleum	22 to 56
Tar Sands Petroleum	27 to 68
Synfuel-Fischer Tropsch (Coal)	41 to 60
Enhanced Oil Recovery (EOR)	21 to 2,500
Fuel Ethanol (from irrigated corn)	2,510 to 29,100
Biodiesel (from irrigated soy)	14,000 to 75,000

(Courtesy of Chesapeake Energy)

Golf course consumption: Colorado State University Agricultural and Resource Policy Report, April 2004.

According to Chesapeake (2009), the amount of water it uses to frack an average shale well is the same as that consumed by a coal-fired power plant in 12 hours. This amount is consumed by New York City in 7 minutes. A golf course consumes the same amount in 25 days with the same amount every month.

5.27.1 Flowback Water

Flowback water contains some or all of the following: sand and silt particles (from the shale or returned proppants), clay particles that remain in suspension, oil and grease from drilling operations, organic compounds from the hydraulic fracturing fluids and the producing shale, and total dissolved solids from the shale. The amount of injected fluid returned as flowback ranges widely from 20% to 80%. The flowback period can range anywhere from hours to weeks. As continued withdrawal proceeds, the flowback water becomes more saline as the relative amount of produced water increases.

Proper management of the flowback and produced water streams has been a major issue of the hydraulic fracturing controversy. Issues arise from the spills, both on location and during transport of these water sources to the proper disposal. Disposal of flowback water has historically been permitted using injection wells in some areas and by discharge to publicly owned treatment works in others. However, discharge to publicly owned treatment works, which is necessitated by less desirable subsurface conditions for underground injection wells in the eastern United States, has become controversial and has been prohibited by some states, while other states require pretreatment before discharge to a publicly owned treatment works.

5.27.2 Produced Water

Produced water is the formation water that is produced along with the oil and gas. Produced water originates as a natural water layer that lies under the hydrocarbons in oil and gas reservoirs.

5.27.3 Flowback and Produced Water Management

Flowback water and produced water is commonly stored on a temporary basis in on-site pits or tanks before removal by truck or pipeline for reuse, treatment, or disposal. These pits or tanks are another possible source of leaks or spills. Lining of pits, or lack thereof, for flowback water and produced water depends on company policies and regulatory requirements, which vary from state to state.

Even in cases where liners are used, they may leak either with time and wear or because of improper installation and upkeep. These leaks result in releases to the subsurface, and have led many to question the use of pits in favor of closed-loop steel tanks and piping systems. Storing flowback water and produced water in enclosed steel tanks, a process many companies have already adopted, has led to a reduction in the risk of releases while improving water retention for subsequent reuse. The following Chart 5.1 presents a list of the various substances found in the produced water.

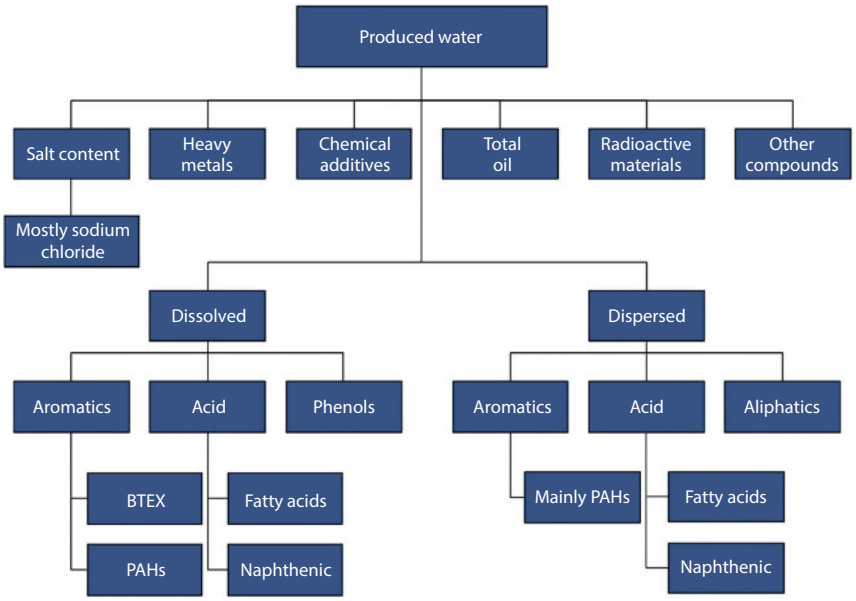

Chart 5.1 Contaminants in produced water.

5.28 Earthquakes

With improving technology and detection methods, the United States Geological Survey has compiled data showing that the number of damaging earthquakes has remained constant. Also, their data indicate that there appears to be no direct connection between the hydraulic fracturing and damaging earthquakes. However, fracturing into a moderate size fault may produce seismic energy sufficient to create measurable signals at instruments very close to the fracturing site.

Data has shown that the hydraulic fracturing process, while not necessarily creating damaging earthquakes, does create a large number of micro-seismic events, or micro-earthquakes. The magnitudes of these micro-seismic events are generally too small to be detected at the surface. The biggest micro-earthquakes have a magnitude of about 1.6, which is insignificant.

5.29 Induced Seismic Event

Pumping fluids in or out of the Earth's subsurface has the potential to cause seismic events. These seismic events, when attributable to human activities, are called "induced seismic events." Seismic events are dependent upon the sub-surface geology of the site. Every site is unique. Much work is underway to model the likelihood of seismic events due to pumping flow-back into the wellbore for safe disposal. The factors that induce seismicity include:

- The presence, orientation, and physical properties of nearby faults.
- The volumes, rates, pressures, and temperatures of fluids being injected or withdrawn.

5.30 Wastewater Disposal Wells

Tens of thousands of injection wells have been drilled and operate in production areas to dispose of the flowback water and produced water generated by oil and gas production operations. This flowback and produced water injection for disposal has also been suspected and, in some cases, determined a likely cause for induced seismicity in the past several decades. Unlike production wells, those used only for flowback and produced water disposal normally do not undergo detailed geologic review prior to construction.

5.31 Site Remediation

The requirements for the plugging and abandoning of production wells at the end of their life cycle is determined by state agencies. States also have oversight for specifying site restoration requirements.

The common objective in the site restoration for drillpads and other infrastructure requirements is to restore the site to its former condition and use. Prior to release of the location for other uses, operators are required to (1) test for contamination, (2) clean up, (3) restore the location to prior drainage patterns, and (4) reinvigorate the site within a reasonable time.

5.31.1 Regulatory Oversight

The different processes of shale gas development are regulated at almost all levels of government. However, the principal regulatory authority generally lies within each state. Not only is the primary regulatory authority at the state level, but many federal requirements have also been delegated to the state level. State agencies typically administer the federal environmental regulations and also are tasked with writing and enforcing their own regulations, governing nearly all phases of oil and gas operations.

In addition to problems encountered through differing states managing production facilities by differing regulations, most oil and gas regulations were written before the hydraulic fracturing became the industry that it is today and do not adequately address fracturing processes. In general, few regulations are currently directed specifically to hydraulic fracturing. Many regulations are directed to broader environmental laws for air, water, waste, and land development. However, state and federal regulations are currently being developed and and/or revised to focus on:

- Proper cementing and casing of wells.
- Disclosure of hydraulic fracturing chemicals.
- Proper management and disposal of flowback and produced water.

In addition to having concise and relevant regulations, it is also very important to have adequate enforcement of regulations both by the office and field staff conducting inspections.

Regulations should focus on the most urgent issues, such as spill prevention, which may pose a greater risk of interacting with receptors than hydraulic fracturing itself. Most recorded violations are associated with overall gas drilling operations rather than being specific to hydraulic fracturing processes: surface spills, improper disposal of oil and gas wastes, problems with leaking pits or tanks, and administrative issues are typically the most common violations.

5.31.2 Federal Level Oversight

Hydraulic fracturing is subject to many federal regulations (as is the case for other oil and gas operations), but also receives a great number of exemptions to regulations that normally would have been applicable. This is partly to do with what is known as "process knowledge." Process knowledge is related work which is carried out by a different company or subsidiary within the same organization to save costs or resources with the industry. As processes are continuously conducted under the same protocols, the same results occur with wastes and regulations; therefore, it can self-regulate. This is meant as a time- and resource-saving area for regulatory agencies. This has also led to cooperative efforts between regulatory agencies and the industry to optimize the effectiveness of regulations. However, in some states, similar requirements that are exempted from federal regulation are imposed at the state level.

5.31.3 State Level Oversight

States have been delegated a great deal of oversight and management for hydraulic fracturing regulations and enforcement. However, with a great deal of regulations having been enacted prior to hydraulic fracturing becoming the topic, it is today (particularly in states not having previous extensive oil and gas development), new or additional industry-specific regulations, such as chemical management requirements, may be needed to minimize surface and subsurface disturbances and impacts on environmentally sensitive areas.

To help alleviate this, a number of organizations and activities are underway, including the Groundwater Protection Council (GWPC) and State Review of Oil and Natural Gas Environmental Regulations (STRONGER), to research and develop state regulation of oil and gas operations.

5.31.4 Municipal Level Oversight

Municipal oversight is provided for mostly secondary processes related to oil and gas developments that are not regulated by the state and/or federal entities. These include traffic management, road maintenance and repair, land usage, and bridge zoning.

5.32 Examples of Legislation and Regulations

The following laws and regulations are associated with varying phases and protocols of shale gas development:

- Clean Water Act (CWA): Oil and gas operators must obtain a storm water permit under the Clean Water Act for the construction and operation of a well pad and access road that is one acre or greater. Also, the CWA prohibits the dumping of any pollutant into U.S. waters without a permit. Typically, facilities that may generate storm water runoff must obtain a storm water permit for this runoff. However, the CWA does not require oil and gas operators to obtain a permit for uncontaminated "discharges of storm water runoff from . . . oil and gas exploration, production, processing, or treatment operations."
- Clean Air Act (CAA): Recently proposed Clean Air Act regulations are intended for operators to control volatile organic compound emissions from flowback during the fracturing process by using volatile organic compound capture techniques called "green completion."
- Endangered Species Act (ESA): Operators must consult with the Fish and Wildlife Service and potentially obtain an incidental "take" permit if their operations may affect endangered or threatened species by well development.
- Migratory Bird Treaty Act (MBTA): Operators are held strictly liable for any harm to migratory birds, and must ensure that maintenance of surface pits or use of rigs does not attract and harm these birds.
- Emergency Planning and Community Right-to-Know Act (EPCRA) and Occupational Safety and Health Act (OSHA): Operators must meet safety requirements in a myriad of work processes such as working at heights, tank entry, excavation, medical surveillance, first aid, and chemical storage. Operators must also maintain material safety data sheets for certain hazardous chemicals that are stored on site in threshold quantities.
- Comprehensive Environmental Responsibility, Compensation, and Liability Act (CERCLA): Operators must report releases of hazardous chemicals of threshold quantities and may potentially be liable for cleaning up spills.
- Resource Conservation and Recovery Act (RCRA): Most wastes from hydraulic fracturing and drilling are exempt from the hazardous waste disposal restrictions, meaning that states – not the federal government – have responsibility for disposal procedures for the waste.
- Safe Drinking Water Act (SDWA): Hydraulic fracturing operators also are exempt from the Safe Drinking Water Act, which requires that entities injecting substances underground prevent underground water pollution. The SDWA applies only to waste from fracturing and drilling that is disposed of in underground injection control wells. If operators use diesel fuel in fracturing, however, they are not exempt from SDWA.

5.33 Frack Fluid Makeup Reporting

Of all the issues related to hydraulic fracturing, the issue of frack fluid makeup reporting may be the one that generates the most attention from state legislators and the

concerned public. An overriding reason for this level of concern is greatly related to semantics and the refusal of many companies to openly disclose frack fluid makeup sooner.

The detailed composition of the additives has been controversial because, until recently, companies that manufacture fracturing fluid components have insisted the exact composition was proprietary, and some components should, therefore, not be reported. Over the last few years, however, a greater number of voluntary disclosures and state-based disclosure laws have resulted in increased disclosure in the details of frack fluid composition. In spite of a great deal of positive ground made in the pursuit of full disclosure of frack fluid ingredients, there is not yet a clear understanding of what the full list of chemicals or their impact on the environment might be.

In a helpful compromise between industry and the concerned public, recently enacted frack fluid makeup reporting regulations have stipulations that not only address the disclosure of chemicals used but also provide some level of protection for proprietary trade secrets. The energy industry as a whole has supported this approach (see e.g., www.Fracfocus.org) and generally agrees the disclosure of the chemicals used in frack fluid makeup is appropriate and necessary. However, industry maintains that proprietary information should not be forced into publication.

Continued movement toward detailed disclosure of chemicals present in hydraulic fracturing fluid will enable a continued analysis of the chemicals potential impact and will help address and alleviate public concern over their risk to water resources.

5.33.1 FracFocus

As stated on the website, FracFocus is a national hydraulic fracturing chemical registry managed by the Ground Water Protection Council and Interstate Oil and Gas Compact Commission, two organizations whose missions both revolve around conservation and environmental protection. The site was created to provide the public access to reported chemicals used for hydraulic fracturing within their area. To help users put this information into perspective, the site also provides objective information on hydraulic fracturing, the chemicals used, the purposes they serve, and the means by which groundwater is protected.

The stated primary purpose of FracFocus is to provide factual information concerning hydraulic fracturing and groundwater protection. It is not intended to argue either for or against the use of hydraulic fracturing as a technology. It is also not intended to provide a scientific analysis of risk associated with hydraulic fracturing. While FracFocus is not intended to replace or supplant any state governmental information systems, it is being used by a number of states as a means of official state chemical disclosure. Currently, eight states, Colorado, Oklahoma, Louisiana, Texas, North Dakota, Montana, Mississippi, and Pennsylvania use FracFocus in this manner.

5.34 Atmospheric Emissions

Air emissions from shale gas operations occur at the drillsite during drilling and fracturing and at ancillary off-site facilities such as pipelines and natural gas compressors.

The on-site emissions include dust, diesel fumes, fine particulate matter (PM 2.5), and methane. Air emissions have become a major component of the shale gas controversies.

A principal concern for shale gas emissions is related to the volatile organic carbon (VOC) compounds. Depending on the composition of the gas produced from the shale, VOCs are typically rich in the BTEX (benzene, toluene, ethylene, xylene) compounds. However, the role of VOCs as smog precursors (they combine with NOx in the presence of sunlight to form smog) is the main source of concern with these compounds. Ozone, a primary constituent of smog, and NOx are two of the five "criteria pollutants" of the Clean Air Act (CAA). The Fort Worth area in the Barnett shale play has been designated "non-attainment" for ozone under the CAA, which means that the established standard is not met for ozone concentration in the atmosphere. The role of VOCs in forming smog and their contribution to the elevated levels of ozone is the reason for the focus on VOC emissions from shale gas activities.

However, the contribution of shale gas activities to ozone levels is highly controversial. For example, investigations in the Fort Worth, Texas, area have found that most VOCs are not associated with natural gas production or transport. Allegations that VOC and NOx emissions from natural gas production from Barnett Shale activities play a significant role in ozone formation have been strongly contested. Records of the Texas Commission on Environmental Quality (TCEQ) monitoring program since 2000 actually show overall decreases in the annual average concentration of benzene, one of the VOCs, during the period of early shale gas development in the Fort Worth area. It should be noted that ozone formation occurs as a consequence of the absorption of the solar UVR by the atmosphere. (See Chilingar *et al*., 2013, *J. Sustainable Energy*, Vol. 1, No. 2, pp. 161–168.)

Public concern over air quality and the need for more precise information led to more focused emissions studies sponsored by local governments or private foundations. The first – and most controversial – of these studies was at DISH, Texas, where elevated levels of benzene, xylene, and naphthalene were found from a set of 24 samples and four residences. DISH was originally named Clark. In November 2005, the community accepted an offer to rename itself "DISH" (all capital letters) as part of a commercial agreement with a satellite television company. Another study in a very active area of shale gas production located about 7 or 8 miles from DISH found that shale gas was responsible for less than half of the VOCs (43%) in the atmosphere, with motor vehicle emissions contributing most of the rest (45%).

Modeling studies indicate that 70% to 80% of benzene is from fugitive emissions of natural gas, but that other VOC constituents are from motor vehicle emissions. In portions of Western states such as Wyoming, air emissions from oil and gas activities are the largest source of VOCs and related high ozone levels. In Sublette County, Wyoming, for example, ozone levels in the winter routinely exceed the EPA 8-hour standard, resulting in air quality that is sometimes worse than in Los Angeles, CA.

Allegations that the emission of VOC constituents such as benzene is "widespread" or is present in "prevalent" amounts in shale gas operations appear not to be supported when comparisons are made with air quality standards or when the relative amounts are compared to other sources such as vehicle exhausts. The relative contribution of shale gas activities in relation to conventional oil and gas development and other sources

such as vehicle exhaust emissions must be taken into account in reports such as those from Wyoming and Fort Worth.

Venting or flaring of natural gas may take place during the fracturing and flowback phase of shale gas well development. However, many operators use "green completions" to capture and sell rather than vent or flare methane produced with flowback water. On-site fugitive emissions of methane may take place from other sources as well, such as pressure relief valves of separators, condensate tanks, and produced water tanks. Although natural gas is confined in pipelines from production wells to the point of sale, methane emissions may also occur from off-site gas processing equipment and compressors, notwithstanding the economic motive to minimize loss of natural gas. The extent to which Best Management Practices (an industry term for the low-emissions completions, low-bleed valves, etc.) result in reduced methane and fugitive losses of methane. (See Chapter 2.)

5.35 Air Emissions Controls

Shale gas development is subject to both federal and state air emissions regulations established by the Clean Air Act (CAA) and state-level legislation. Many of the CAA provisions are delegated from the U.S. EPA to the various states' environmental agencies. The major air pollutant sources of shale gas drilling and fracturing are the drilling and associated equipment, tanks and pits for flowback water, flared gas, and methane sources at the wellhead and from pipelines and compressors.

Oil, gas, and shale gas operations in particular are subject to regulations for "criteria pollutants" (sulfur dioxide, nitrogen oxides, ozone, particulate matter, carbon monoxide, and lead) and "hazardous air pollutants" (HAPs, including 187 compounds). However, these regulations focus on "major" sources, which generally do not include oil and gas operations for the sources listed above specifically. If regulated at all, oil and gas sources of criteria pollutants and HAPs fall under state minor source programs. The strictest criteria air pollutants regulations apply to areas not meeting established maximum ambient air standards, which are referred to as "nonattainment" areas. Air quality regulations are, far and away, the most cumbersome regulations related to the oil and gas industry. Unfortunately, air regulation discussions will invariably result in the use of the phrase "it depends" more than in pretty much any other discussion one could possibly have. Most confusion related to air regulations stems from the way they are written: they can and often are based on any combination of equipment type, locations, date of manufacture, date of equipment order, date of reconstruction, whether the equipment is considered mobile or not, etc. These regulations are written such that one piece of equipment may be covered by several different regulations, to the point that even the regulatory employees are often as confused as industry personnel.

In an attempt to clear up some of the confusing points of air regulations, the following section is broken into discussions on some common sources and types of air emissions and an overview of a few of the common air regulations and permits related to the oil and gas industry.

5.35.1 Common Sources of Air Emissions

Air emissions can come from any number of sources, both related to and not related to the oil and gas industry. Non-industry examples are large sources such as refineries, factories, and power plants, and smaller sources such as dry cleaners and gas stations, mobile sources such as cars, buses, planes, trucks, and trains, and naturally occurring sources such as natural windblown silt/sand/dust, and even volcanic eruptions. All of these sources contribute to the overall breakdown of air quality. However, keeping in line with the overall context of this book, the discussion in this section will be concentrated on air emissions and regulations related to the oil and gas industry.

Air emissions from shale gas operations can occur at the drillsite during drilling and fracturing operations. Air emissions, including diesel fumes, fine particulate matter, and methane, also occur at off-site facilities such as pipelines, natural gas compressors, evaporation pits, and pig launch receiver/launchers. In addition to those emissions linked directly to oil and gas facilities, air emissions are also attributed to trucks used to transport equipment, fracturing fluid ingredients, and water to the wellpad, drilling rigs, compressors, tanks, and pumps.

A principal concern for shale gas emissions is volatile organic compounds (VOC) such as propane, BTEX (benzene, toluene, ethylene, and xylene) constituents, and the six principal criteria pollutants named by the EPA, nitrogen dioxide (NO_2), ozone (O_3), sulfur dioxide (SO_2), particulate matter (PM), carbon monoxide (CO), and lead (Pb).

5.35.2 Fugitive Air Emissions

Fugitive air emissions are air emissions that escape from equipment through normal use, routine maintenance, or small leaks. This can be through equipment such as pumps, valves, flanges, compressors, and process drains. There are generally four categories of emissions:

- Normal operations: emissions during expected operating scenarios.
- Planned maintenance, start-up and shut-down: emissions during normal operations that are expected and predictable.
- Scheduled maintenance start-up and shut-down: unexpected emissions that are expected but not necessarily predictable.
- Emission events: emission events that are not authorized, scheduled, or planned.

Three sources of emissions commonly related to fracking operations are flare emissions, liquid storage tank emissions, and loading/unloading emissions:

- Flare emissions: flare emissions result from the pilot light, combusted waste, and uncombusted waste (depending on flare efficiency). These can result in the release of NO_x, CO, VOCs, SO_2, H_2S (in some areas), HAPs, CO_2, and methane.

- Liquid storage tank emissions: liquid storage tank emissions are categorized as working, breathing, and flash emissions. These can result in the release of VOCs, HAPs, H_2S (in some areas), CO_2, and methane. Liquid storage tank emissions are most commonly controlled utilizing vapor-recovery units and condensers.
  - Working emissions occur during tank filling and draining.
  - Breathing emissions result from normal daily fluctuations in temperature and pressure.
  - Flash emissions result from a high pressure stream being directed into an atmospheric tank.
- Loading/Unloading emissions: loading/unloading emissions result from hose disconnects when petroleum liquids are loaded into trucks, rail cars, tankers, or even ships, and can also occur when the vapor space in a tanker truck is displaced by fluids. These can also result in the release of VOCs, HAPs, H_2S (in some areas), CO_2, and methane, and are normally controlled utilizing vapor recovery units, incineration through flaring or thermal oxidizers, and carbon systems.

In addition to emissions related directly to fracking operations, emissions related to the oil and gas industry also include fugitive emissions of methane from other sources as well, such as pressure relief valves of separators, condensate tanks, and produced water tanks. Controls to prevent and mitigate fugitive emissions are generally comprised of a leak detection and repair program (commonly referred to as LDAR) and maintenance. Emissions from gas production come from:

- Direct emissions (methane venting during frack cleanup, lost gas or fugitive emissions, and $CO_2$from fuel combustion).
- Indirect emissions from trucks (pumpers and processing equipment used in drilling, fracturing and production).
- Off-site gas processing equipment such as natural gas in pipelines and compressors from production wells to the point of sale.

5.36 Silica Dust

Silica dust is an emission source that is becoming more of a fracking industry concern. As discussed throughout this chapter, fracking commonly requires large volumes of sand and water to be pumped into wells at high pressures to break up tight formations, like shale, which have trapped oil and gas. Therefore, many truckloads of sand must be offloaded and transferred before being mixed with water and other chemicals and pumped downhole. The dust produced, which may contain up to 99% crystalline silica, is a health concern due to the risk of silicosis, a progressive and disabling lung disease.

5.36.1 Stationary Sources

A "stationary source" is, as the name suggests, a non-mobile piece of equipment that emits an air pollutant. Some states have specified time periods, such as 6 months, that are also used to define a stationary source.

While not specific to fracking operations, common stationary sources in the natural gas industry as a whole include compressor engines, turbines, generators, tanks, reboilers or associated equipment, boilers, vaporizers, flares, etc. Stationary sources may be subject to different requirements depending on the amount and type of air pollutant emitted and the quality of the air in the vicinity of the source.

5.37 The Clean Air Act

The federal Clean Air Act provides the principal framework for national, state, and local efforts to protect air quality. Under the CAA, the Office of Air Quality Planning and Standards Organization (OAQPS) is responsible for setting standards known as national ambient air quality standards (NAAQS), for pollutants that are considered harmful to people and the environment.

As with other types of regulations, state and local agencies take the lead in carrying out the requirements of the CAA. Each state has to develop and implement plans that outline how to control air pollution as required by the CAA. In doing this, state and local governments will need to conduct air monitoring, facility inspections, and conduct permit management and enforcement. Also, as with other types of regulations, individual states may have stronger air quality laws than the federal regulation, but they may not have weaker pollution limits than those set by the EPA.

The Clean Air Act regulates many aspects of the construction and operation of oil and gas facilities, including compressor engines, flares, and other emission sources. Under the CAA, many stationary sources of air pollution cannot legally operate until an air permit is obtained and compliance requirements are in place and met.

The CAA has several programs to protect public health and welfare and enhance the quality of the nation's air resources, including New Source Performance Standards (NSPS – found in 40CFR Part 60), National Emission Standards for Hazardous Air Pollutants (NESHAP – found in 40CFR Part 63), NSR, and Prevention of Significant Deterioration (PSD). Depending on the level and source of emissions, various types of air permits may be required.

5.38 Regulated Pollutants

Regulated pollutants that result from emissions at oil and gas locations are generally separated into two main categories:

1. National Ambient Air Quality Standard (NAAQS) Criteria Pollutants: there are six NAAQS criteria pollutants that are generally regulated by county.
2. National Emission Standards for Hazardous Air Pollutants (NESHAP): there are 187 HAPS that are regulated on a "source by source" basis, and are considered more difficult to monitor than criteria pollutants.

5.38.1 NAAQS Criteria Pollutants

There are six principal criteria pollutants classified by the EPA as criteria pollutants: nitrogen dioxide (NO_2), ozone (O_3), sulfur dioxide (SO_2), particulate matter (PM), carbon monoxide (CO), and lead (Pb). Criteria pollutants are more of an "industry based regulation," or in other words, government regulation of an industry as a whole (Table 5.4). The Clean Air Act, which was last amended in 1990, requires the EPA to

Table 5.4 NAAQS criteria pollutants.

Pollutant		Primary/ Secondary	Averaging time	Level	Form
Carbon Monoxide (CO)		primary	8 hours	9 ppm	Not to be exceeded more than once per year
			1 hour	35 ppm	
Lead (Pb)		primary and secondary	Rolling 3 month average	0.15 μg/m^3 [(1)]	Not to be exceeded
Nitrogen Dioxide (NO_2)		primary	1 hour	100 ppb	98th percentile of 1-hour daily maximum concentrations, averaged over 3 years
		primary and secondary	1 year	53 ppb [(2)]	Annual Mean
Ozone (O_3)		primary and secondary	8 hours	0.070 ppm [(3)]	Annual fourth-highest daily maximum 8-hour concentration, averaged over 3 years
Particle Pollution (PM)	$PM_{2.5}$	primary	1 year	12.0 μg/m^3	annual mean, averaged over 3 years
		secondary	1 year	15.0 μg/m^3	annual mean, averaged over 3 years
		primary and secondary	24 hours	35 μg/m^3	98th percentile, averaged over 3 years
	PM_{10}	primary and secondary	24 hours	150 μg/m^3	Not to be exceeded more than once per year on average over 3 years
Sulfur Dioxide (SO_2)		primary	1 hour	75 ppb [(4)]	99th percentile of 1-hour daily maximum concentrations, averaged over 3 years
		secondary	3 hours	0.5 ppm	Not to be exceeded more than once per year

[(1)] In areas designated nonattainment for the Pb standards prior to the promulgation of the current (2008) standards, and for which implementation plans to attain or maintain the current (2008) standards have not been submitted and approved, the previous standards (1.5 μg/m^3 as a calendar quarter average) also remain in effect.

[(2)] The level of the annual NO_2 standard is 0.053 ppm. It is shown here in terms of ppb for the purposes of clearer comparison to the 1-hour standard level.

[(3)] Final rule signed October 1, 2015, and effective December 28, 2015. The previous (2008) O_3 standards additionally remain in effect in some areas. Revocation of the previous (2008) O3 standards and transitioning to the current (2015) standards will be addressed in the implementation rule for the current standards.

[(4)] The previous SO_2 standards (0.14 ppm 24-hour and 0.03 ppm annual) will additionally remain in effect in certain areas: (1) any area for which it is not yet 1 year since the effective date of designation under the current (2010) standards, and (2) any area for which implementation plans providing for attainment of the current (2010) standard have not been submitted and approved and which is designated nonattainment under the previous SO_2 standards or is not meeting the requirements of a SIP call under the previous SO_2 standards (40 CFR 50.4(3)), A SIP call is an EPA action requiring a state to resubmit all or part of its State Implementation Plan to demonstrate attainment of the require NAAQS.

set National Ambient Air Quality Standards (40 CFR part 50) for pollutants considered harmful to public health and the environment. The CAA identifies two types of national ambient air quality standards. Primary standards provide public health protection, including protecting the health of "sensitive" populations such as asthmatics, children, and the elderly. Secondary standards provide public welfare protection, including protection against decreased visibility and damage to animals, crops, vegetation, and buildings.

5.39 Attainment versus Non-attainment

"Attainment" and "non-attainment" describe the air quality in a given area (usually broken down by county) for any of the six established criteria pollutants. An area with levels below the established standards for all six criteria pollutants is referred to as an attainment area. A county that does not meet the standards, or is considered to contribute to elevated levels in nearby areas that do not meet the standards, is called a non-attainment area. Industry located in non-attainment areas are held to much more stringent air emission standards than those located in attainment areas. Since an area is compared to established levels for all six criteria pollutants, an area may be designated attainment for some pollutants and non-attainment for others. Once an area is determined to be non-attainment, it is then further broken into tiered levels of non-attainment: marginal, moderate, serious, severe, and extreme. This classification is determined based on the number of pollutants and the levels that exceed the limits.

In addition to "attainment" and "non-attainment," two more possible classifications for NAAQS criteria pollutants are "unclassified" and "maintenance." Areas that move from non-attainment to attainment retain many of the more stringent rules of attainment areas and are referred to as maintenance areas and areas with insufficient air quality data for classification are referred to as unclassified areas and are treated the same as attainment areas.

5.40 Types of Federal Regulations

There are various types of Clean Air Act regulations and permits. Oil and gas operations, and shale gas in particular, are subject to numerous regulations such as those related to the six criteria pollutants and 187 hazardous air pollutants mentioned earlier. The following is a brief discussion of some of the most common types related to the oil and gas industry.

5.41 MACT/NESHAP

Unlike the relatively small number of criteria pollutants, there are 187 separate designated hazardous air pollutants (listed pollutants that increase mortality of serious, irreversible, or incapacitating illness). The MACT/NESHAP hazardous air pollutant regulations are "risk-based regulation" and are established on the "source by source"

criteria for each separate piece of equipment; for example, boiler MACT and reciprocating internal combustion engine MACT (NESHAP Quad ZZZZ). Also, since these are risk-based regulations of separate pieces of equipment, there are no established attainment designations of across the board acceptable levels.

5.42 NSPS Regulations: 40 CFR Part 60

In accordance with the Clean Air Act, reconstructed or modified sources are potentially subject to a New Source Performance Standard (NSPS), which is exactly what the name describes, standards set up to manage and determine possible new sources for emissions. If a facility is a new, reconstructed, or modified source, it could be considered a potentially affected source under the NSPS. NSPS standards are in place to create higher standards of performance and maintenance as new equipment is brought into service. New equipment is automatically covered by NSPS and additional sources are added as reconstructed or modified.

A source is "reconstructed" if the components of an existing stationary source are replaced and/or repaired and the fixed capital costs exceed a specified percentage of the cost of constructing a comparable new source. The specified percentage is determined by the applicable air regulation. New-source performance standards may be applied to sources reconstructed after the proposal of the standard if it is technologically and economically feasible to meet the standards.

A source is "modified" if any physical or operational change to an existing facility is made that results in an emission increase of any pollutant to which the standard applies, such as horsepower increase or engine conversion.

Consequently, an existing facility containing an existing (*older*) emission unit, which might not be subject to the NSPS due to the age of the unit, could still become subject to regulation under NSPS if reconstructed or potentially modified.

5.42.1 NSPS Subpart OOOO

NSPS Subpart OOOO (Quad OOOO) regulations, finalized by the EPA on August 16, 2012, centered on gas production, transmission and distribution, are generally considered the most concentrated on fracking operations. Therefore, this regulation will be discussed in greater detail than those regulations centered on oil and gas as a whole.

5.42.2 Facilities/Activities Affected by NSPS OOOO

The following is a brief overview of activities/equipment requirements regulated under NSPS OOOO to reduce VOC emissions from sources constructed, reconstructed or modified after August 23, 2011:

- **Natural gas well completions**
  For natural gas wells that use hydraulic fracturing, new regulations require companies to control and reduce emissions during flowback.

The goal of the new standard is to reduce VOC emissions generated during flowback activity. In the past, the general industry practice was to vent the gas generated during flowback. Starting October 15, 2012, these new standards require flowback emissions to be routed to a completion combustion device, usually a flare. After January 1, 2015, flowback will be required to implement "green completions" where flowback vapors will be routed to the gas gathering line. If this is infeasible due to lack of infrastructure, vapors will be routed to a completion combustion device (i.e., flare). The only exceptions to implementing this regulation are if the completion could potentially result in a fire hazard or explosion or if local ordinances restrict the use of flares, such as during a burn ban.

- **Storage vessels**
  EPA regulates storage vessels that handle crude oil, condensate, and produced water at production and gathering/booster stations to reduce emissions by 95%. Storage vessels with VOC emissions of greater than 6 tons per year (tpy) must install emission controls to reduce emissions to less than 6 tpy. Operators must demonstrate compliance by developing emission calculations and include them in annual reports submitted to EPA or the delegated state agency. A storage vessel is exempt, however, if skid mounted (i.e., mobile) and is at the site less than 180 consecutive days.
- **Pneumatic controllers**
  Pneumatic controllers at processing plants and production facilities also have requirements under this new EPA regulation. At gas processing plants, each continuous bleed natural gas driven pneumatic controller must operate at a zero bleed rate (i.e., instrument air) by October 15, 2012. At production facilities, each continuous bleed natural gas driven pneumatic controller must operate at a bleed rate of 6 standard cubic feet per hour (SCFH) or less. Intermittent bleed and no-bleed controllers are exempt from this regulation.

  The goal of this part of the regulation is to encourage controllers to use low-bleed, intermittent-bleed or non-gas-driven devices in the future. Operators can claim exceptions if a high continuous bleed rate controller is required for functional needs, including but not limited to response time, safety, and positive actuation.
- **Compressors**
  The compliance date for both centrifugal and reciprocating compressors was October 15, 2012. For wet seal centrifugal compressors, the regulation stipulates that operators reduce emissions from each centrifugal compressor wet seal fluid degassing system by 95% through routing gas to controls.

  For reciprocating compressors, the new rule requires operators to replace rod packings before the compressor has operated 26,000 hours or prior to 36 months from last replacement or date of startup for the unit, whichever is later.

5.43 Construction and Operating New Source Review Permits

In addition to federal air regulations, there are also several differing types of permits governing new source construction compliance which vary by state. These include construction permits, used to regulate construction and modification of sources and prevent significant deterioration affects to non-attainment areas, and operating permits, authorizing the operation of larger emission sources and to keep these sources more accountable to federal standards.

Prevention of significant deterioration (PSD) is a construction of the air pollution permitting program designed to ensure that air quality does not degrade beyond the NAAQS levels. The PSD permit includes a requirement to comply with ambient air quality levels and to install "best available control technology" (BACT) for criteria pollutants emitted in significant levels.

5.44 Title V Permits

Title V permits are operating permits that grant larger air emission sources the permission to operate. Title V permits include all air standards and requirements that apply to that source, including emissions limits, monitoring protocol, and record-keeping requirements. This permit is used to identify all of the applicable air quality requirements for a site. It also requires that the site demonstrate compliance with the requirements on an ongoing basis, often semi-annually. The main purpose of a Title V permit is intended to be a single point of reference for all regulations at the permitted location. However, along with the intended gathering of all the regulations in one document, Title V permits also include a great deal of additional unnecessary administrative protocols.

5.45 Chemicals and Products on Locations

A common point of contention for residents in oil producing areas is on-site storage of chemicals and products. For decades, one of the biggest drivers for public concern has been the identity and amounts of chemicals stored on pad locations during all phases of the well completion and production process. This can include fuels used on location, the makeup of drilling fluids (water-based, oil-based or synthetic), fracking chemicals and additives stored on locations, chemicals kept on-site during ongoing production, and even the products (produced water and/or oil) stored on-site as recovered from the well during operations.

People safely use chemicals every day: dish soap, gasoline, motor oil, bleach, hydrogen peroxide, and vinegar are some examples. The same chemicals are frequently used in workplaces, but are often in a higher concentration and volume, which could pose a higher risk for individuals. As an example, 3% hydrogen peroxide is used to clean skin abrasions or as a mouthwash at home, and some folks use concentrations as high as 35% for treating swimming pool water.

Companies produce and distribute products with concentrations of hydrogen peroxide at levels between 3% and 35%, so one must be able to recognize which products are

generally safe and which products require precautions to be handled and used safely. The important information to take away from this section includes:

- How to recognize that a chemical product may present a hazard.
- Know where to get information that explains the hazards.
- Know who to ask for help and assistance at any time.
- Understand what GHS means and the reason for its implementation.
- Understand the difference between GHS and HCS 2012.

It is also important that one is able to recognize the changes to hazard communication. The most important among these are:

- Label information and changes.
- Safety data sheet information and format.
- The difference between the numerical rating systems.
- Chemical hazards and classification.
- Chemical Labels.
- Safety Data Sheets (Formerly known as Material Safety Data Sheets).
- Detection of and protection from hazardous chemical exposure.

Many people in the chemical industry, as well as those directly or even indirectly related to the industry, should understand what Hazard Communication is. OSHA's Hazard Communication standard is published in the Code of Federal Regulations at 29 CFR 1910.1200. The standard was first published in 1983. The standard has been revised since then, with the most recent and sweeping changes made in March 2012 to conform to the United Nations Globally Harmonized System of Classification and Labeling of Chemicals (or GHS). Hazard Communication is designed to ensure that employers and employees are equipped with proper information to facilitate safe storage and handling of chemicals.

The general public would be surprised at how little chemical and products are stored on-site during construction, drilling, and frack operations. For the most part, oilfield operations have become such a streamlined and efficient operation that operators will know how much of a given chemical product will be necessary and, for the most part, make all attempts to have the chemicals arrive on location as close to when needed as possible to avoid storage. This process is beneficial to the operator in that it cuts down on the time taken up by storing chemicals only to return for them when needed, cuts down on waste from unused or outdated chemicals, cuts down on equipment needed to maneuver chemicals if they are delivered directly to the point of need, allows for more working space on the pad, and helps avoid a great deal of logistical problems related to maneuvering equipment around storage areas.

Once production operations are in place and wells begin producing the fluids (produced water and oil) are often stored on-site in large tanks while awaiting transport offsite. Safeguards put in place to protect the environment and public from tank releases include consistent measurements by pumpers, high level shut down sensors, continued equipment observations and maintenance, and secondary containments in place around the tanks to contain any fluids that may be released from tanks. Secondary

containments may be constructed of properly packed and integrity-tested earthen materials or up to specifically designed and manufactured metal containments with plastic liners. Secondary containments must be sufficiently large to contain all the fluids that could possibly escape the tanks plus sufficient extra space for "waste case scenario" rainfall. Rainfall amount is calculated for each region of the country based on historic amounts.

Even with attempts to minimize the amount of on-site storage, some chemical and product storage is unavoidable, and there are very valid concerns, including potential spills, leaks, tank or container overfill, and even the chance of traffic accidents on location or roadways leading to releases of chemicals and/or products. Release events could range from relatively small amounts from equipment leaks to possibly hundreds of barrels from tank release. Two regulatory measures in place to manage and oversee on-site chemical storage conditions are requiring Spill Prevention Countermeasure and Control (SPCC) plans and SARA reporting.

SPCC plans are documents required by all facilities having the potential to discharge oil to navigable waters of the United States and meeting one or both of the following: greater than 1,320 gallons (31.4 bls) aggregate above ground storage in equipment, drums, tanks, storage tanks greater than 55 gallons in size, or greater than 42,000 gallons total underground storage capacity. Aggregate refers to adding up separate amounts of all storage vessels. There can be one 1,320-gallon tank or ten 132-gallon tanks, which are equal under the SPCC requirements. Also, determining the "potential to discharge oil to navigable waters of the U.S." is left up to regulatory discretion. Simply, SPCC plans are engineer-stamped documents that must be created for all facilities meeting the above conditions that include a list of spill response procedures, an emergency notification phone list, inspection procedures and schedule, training requirements, site figures, site chemical and product storage vessel types and sizes, and containment calculations to prove sufficient containment is given to contain the largest possible spill amount.

SARA reporting, or possibly better known as the federal "right to know," requires quarterly and annual reporting of chemical storage details (types of chemicals, amounts, and dates of storage) for all facilities that used more than 10,000 pounds per year of the chemical exceeding the threshold quantity. This requirement means a facility storing more than 10,000 pounds of a given chemical in a year must report that chemical and its amount. This program is intended as the "right to know" for emergency responders and emergency services that may respond to an emergency situation on the location so that they will be able to adequately prepare for what may be stored on-site. The drawback of this program as related to the oil and gas industry is that, with quarterly reporting, by the time a chemical has been reported, the oilfield function requiring the chemical has normally been long completed and the chemicals are no longer on-site. This basically means that once the chemical is reported as being on a location, it is no longer there. As previously stated, oilfield operations have become such a streamlined process that if one knows what has been reported for a previous location by a specified operator, one can, for the most part, expect much the same chemicals and products stored at the following locations. If one wants to know what chemicals are used at a site, a copy of the Material Safety Data Sheet of the chemicals used must be requested.

5.46 Material Safety Data Sheets (MSDS)

Any time a company produces for sale, or uses, a chemical, a Material Safety Data Sheet (MSDS) has to be written on the product and on file when used. Occupational Safety and Health Administration (OSHA) estimates that there are over 650,000 hazardous chemicals used daily in the United States, and that hundreds more will be added this year alone. To address the physical and health hazards of these chemicals, OSHA finalized the Hazard Communication Standard (HCS) on November 25, 1983. The purpose of the HCS is to "ensure that the hazards of all chemicals produced or imported are evaluated, and that information concerning their hazards is transmitted to employers and employees" (29 CFR 1910.1200(a)[1]).

Employers are under obligation to use labels, MSDS, and other information to evaluate both the physical and health hazards created by the use of chemicals at their workplace, establish a program that addresses these hazards, and train workers to minimize exposure to them. According to an OSHA Executive Summary: "Chemical information is the foundation of workplace chemical safety programs. Without it, sound management of chemicals cannot occur. The HCS has made provision of hazard information about chemical products an accepted business practice in the United States. There is now a whole generation of employers and employees who have never worked in a situation where information about the chemicals in their workplace is not available."

Manufacturers or importers of chemicals must create or obtain a MSDS for every hazardous chemical that they produce or import (29 CFR 1910.1200(g)), and supply the appropriate one with a customer's first purchase, and any time the MSDS changes (29 CFR 1910.1200(g)(6)(i)). Employers are not required to evaluate information on a MSDS (29 CFR 1910.1200(d)(1)). They do, however, have a duty to study and to use it to "develop, implement and maintain... a written hazard communication program" to ensure the safety of their workers (29 CFR 1910.1200(e) (1)). To help address worker safety "at all times," OSHA requires employers to make MSDS "readily accessible during each work shift to employees when they are in their work area(s)" (29 CFR 1910.1200(g) [8]). OSHA permits electronic and other forms of access to MSDS, as long as there are "no barriers to immediate employee access in each workplace" (29 CFR 1910.1200(g) [8]).

5.47 Contents of an MSDS

Frack site workers, as well as anyone working in an industry or market that uses chemicals, will have access to an MSDS for any chemical with which they may have contact. Consumer products also have MSDSs. In fact, the local hardware store has a complete file of MSDSs for all the consumer chemicals they sell, and many department stores do as well. If the reader ever wants to know the dangerous effects of a particular insecticide or cleaner, he can refer to the MSDS for detailed information. The information contained within an MSDS can be a bit foreboding. Like pharmaceuticals and over-the-counter medications, the warnings typically are meant to take into consideration any and all dangers that may happen upon exposure. Without a working knowledge of the terms and criteria put forth in the MSDS, the layperson could quickly become horrified

with the prospect of using a product only to experience dizziness, dry mouth, or shortness of breath (which seems to be the universal response to everything from aspirin to Zoloft®).

5.48 Conclusion

In conclusion, the author believes that hydraulic fracturing can be done safely if done properly.

State Agency Web Addresses

Alabama, Geological Survey of Alabama, State Oil and Gas Board http://www.ogb.state.al.us/ogb/ogb.html

Arkansas, Arkansas Oil and Gas Commission http://www.aogc.state.ar.us/

Colorado, Colorado Department of Natural Resources, Oil and Gas Conservation Commission http://cogcc.state.co.us/

Illinois, Illinois Department of Natural Resources, Division of Oil and Gas http://dnr.state.il.us/mines/dog/index.htm

Indiana, Indiana Department of Natural Resources, Division of Oil and Gas http://www.in.gov/dnr/dnroil/

Kentucky, Kentucky Department for Energy Development and Independence, Division of Oil and Gas Conservation http://www.dogc.ky.gov/

Louisiana, Louisiana Department of Natural Resources, Office of Conservation http://dnr.louisiana.gov/cons/conserv.ssi

Michigan, Michigan Department of Environmental Quality, Office of Geological Survey http://www.michigan.gov/deq/0,1607,7-135- 3306_28607---,00.html

Mississippi, Mississippi State Oil and Gas Board http://www.ogb.state.ms.us/

Montana, Montana Department of Natural Resources and Conservation, Board of Oil and Gas http://bogc.dnrc.mt.gov/default.asp

New Mexico, New Mexico Energy, Minerals and Natural Resources Department, Oil Conservation Division http://www.emnrd.state.nm.us/OCD/

New York, New York Department of Environmental Conservation, Division of Mineral Resources http://www.dec.ny.gov/energy/205.html

North Dakota, North Dakota Industrial Commission, Department of Mineral Resources Oil and Gas Division https://www.dmr.nd.gov/oilgas/

Ohio, Ohio Department of Natural Resources, Division of Mineral Resources Management http://www.ohiodnr.com/mineral/default/tabid /10352/Default.aspx

Oklahoma, Oklahoma Corporation Commission, Oil and Gas Conservation Division http://www.occ.state.ok.us/Divisions/OG/newweb/og.htm

Pennsylvania, Pennsylvania Department of Environmental Protection, Bureau of Oil and Gas Management http://www.dep.state.pa.us/dep/DEPUTATE/MI NRES/OILGAS/oilgas.htm

Tennessee, Tennessee Department of Environment and Conservation, State Oil and Gas Board http://www.tennessee.gov/environment/boards /oilandgas.shtml

Texas, The Railroad Commission of Texas http://www.rrc.state.tx.us/index.html

West Virginia, West Virginia Department of Environmental Protection, Office of Oil and Gas http://www.wvdep.org/item.cfm?ssid=23

References

1. Interstate Oil and Gas Compact Commission, "Hydraulic Fracturing, Texas Regulations Protect Surface and Ground Water".
2. Case Study for Well Integrity over a Full Life Cycle, Lloyd H. Hetrick, PE, CSP, EPA Technical Workshop #2 on Well Construction and Integrity, Theme #3 Mechanical Integrity, March 11, 2011.
3. 40 CFR 144.3 Safe Drinking Water Act, definition for USDW.
4. Texas Administrative Code Title 16, Part 1, Rule 3.7 and Title 16, Part 1, Rule 3.8 (b).
5. 43 CFR 3162.1 (a) Onshore Oil and Gas Order #2, Drilling Operations.
6. U.S. Energy Information Administration, "The Geology of Natural Resources", February 14, 2011.
7. Pennsylvania Department of Environmental Protection, "Methane Gas and Your Water Well", November 2009.
8. The National Academies, "Management and Effects of Coalbed Methane Produced Water in the United States", 2010.
9. *New York Times*, "Nature's Cheapest Fuel, The Natural Gas of the Delaware Valley Likely to Be Utilized", March 15, 1886.
10. Western New York Trails.com "Eternal Flame Falls – Chestnut Ridge Park, Orchard Park, New York", December 2010.
11. American Geophysical Union Blogosphere, "Natural Gas Seeps in Western NY", November 2010.
12. Penn State University College of Agricultural Sciences, "Gas Well Drilling and Your Private Water Supply", March, 2010.
13. Wikipedia, Oil Springs, Kentucky.
14. Wikipedia, Oil Springs, Ontario, Canada.
15. Wikipedia, Seneca Oil Spring, NY.
16. Texas Landmarks and Vanished Communities, Salt Creek and Brine Springs, TX.
17. Oklahoma Administrative Code 165:10-3-1.
18. Texas Administrative Code Title 16, Part 1, Rule 3.13 (a)(2)(C).
19. Pennsylvania Code Title 25 Chapter 78.83.
20. Oklahoma Administrative Code 165:10-3-4 (c)(1).
21. Pennsylvania Code Title 25 Chapter 78.84 (a).
22. API Spec 5CT "Specification for Casing and Tubing" Eighth Edition, 2006.
23. NACE MR0175 / ISO 15156 "Materials for use in H2S Containing Environments in Oil and Gas Production", Second Edition, 2009.
24. API RP 5C1 "Recommended Practice for Care and Use of Casing and Tubing", Eighteenth Edition, 2010.
25. API RP 5C5 "Recommended Practice on Procedures for Testing Casing and Tubing Connections", Third Edition, 2003.
26. API RP 5A5 "Field Inspection of New Casing, Tubing, and Plain-end Drill Pipe", Seventh Edition, December, 2009.
27. API RP 5B1 "Gaging and Inspection of Casing, Tubing, and Line Pipe Threads", Fifth Edition, 2010.
28. API RP 5A3 "Recommended Practice on Thread Compounds for Casing, Tubing and Line Pipe", Third Edition, 2009.
29. Department of Energy, Sandia National Labs "Euler Buckling of Geothermal Well Casing" Rechard and Schuler, April, 1983.
30. Texas Administrative Code Title 16, Part 1, Rule 3.13 (b)(2) (A) thru (G).

31. Texas Administrative Code Title 16, Part 1, Rule 3.13 (a)(1).
32. API RP 65 "Isolating Potential Flow Zones During Well Construction" Part 2, First Edition May, 2010.
33. API Spec 10A "Specification for Cements and Materials for Well Cementing" December, 2010.
34. API RP 10B (1 thru 6) "Recommended Practice for Testing Well Cements".
35. API Spec 10D "Specification for Bow-Spring Centralizers", Sixth Edition, 2002.
36. SPE 106817 "Evaluation of the Potential for Gas and CO_2 Leakage Along Wellbores", Watson and Bachu, March, 2007.
37. Alberta Energy and Utilities Workshop "Factors Affecting or Indicating Potential Wellbore Leakage", Watson and Bachu, March, 2007.
38. API Technical Report 10TR1 "Cement Sheath Evaluation" Second Edition 2008
39. SPE 105193 "Improving Formation Strength Tests and Their Interpretation" van Oort and Vargo, February, 2007.
40. Texas Administrative Code Title 16, Part 1, Rule 3.17 (a) & (b).
41. 43 CFR 3162.5-2 Onshore Oil and Gas Order #2, Drilling Operations.
42. API RP 90 "Annular Pressure Management for Offshore Wells", First Edition, August, 2006.
43. Pennsylvania Code Title 25 Chapter 78.88(e).
44. Texas Administrative Code Title 16, Part 1, Rule 3.14.
45. Oklahoma Administrative Code 165:10-11.
46. Pennsylvania Code Title 25 Chapter 78.91 thru 78.98.
47. API Bulletin E3 "Environmental Guidance Document: Well Abandonment and Inactive Well Practices for U.S. Exploration and Production Operations", First Edition, June, 2000.
48. SPE 28349 "Issues and Techniques of Plugging and Abandonment of Oil and Gas Wells", Calvert and Smith, September, 1994.
49. SPE 140482 "State and Federal Regulation of Hydraulic Fracturing: A Comparative Analysis", Arthur, Hochheiser and Coughlin; January, 2011.

Bibliography

Andrews, Anthony *et al*., October 2009, (PDF). Unconventional Gas Shales: Development, Technology, and Policy Issues. Congressional Research Service. http://www.fas.org/sgp/crs/misc/R40894.pdf

Biello, David, March 2010. "What the Frack? Natural Gas from Subterranean Shale Promises U.S. Energy Independence--With Environmental Costs". *Scientific American*. http://www.scientificamerican.com/article.cfm?id=shale-gas-and-hydraulic-fracturing

Committee on Energy and Commerce, U.S. House of Representatives, April 18, 2011. Chemicals Used in Hydraulic Fracturing (Report). http://democrats.energycommerce.house.gov/sites/default/files/documents/Hydraulic%20Fracturing%20Report%204.18.11.pdf

Fjaer, E., 2008. "Mechanics of hydraulic fracturing." *Petroleum related rock mechanics*. Developments in petroleum science (2 ed.). Elsevier. p. 369. ISBN 978-0-444-50260-5. http://books.google.co.uk/books?id=l6CfasFxhzYC&pg=PA369&lpg=PA369

"Frac job". *Oilfield Glossary*. Schlumberger. http://www.glossary.oilfield.slb.com/Display.cfm?Term=frac%20job

Laubach, S.E.; Reed, R.M., Olson, J.E., Lander, R.H. & Bonnell, L.M., "Coevolution of crack-seal texture and fracture porosity in sedimentary rocks: cathodoluminescence observations of regional fractures." *Journal of Structural Geology* (Elsevier) 26(5), 967–982, 2004. doi:10.1016/j.jsg.2003.08.019. http://www.sciencedirect.com/science/article/pii/S0191814103001858

McKibben, Bill, 8 March. "Why Not Frack?". *New York Review of Books* 59(4), 2012. http://www.nybooks.com/articles/archives/2012/mar/08/why-not-frack/

Office of Air and Radiation, U.S. Environmental Protection Agency, November 2010. "General Technical Support Document for Injection and Geologic Sequestration of Carbon Dioxide: Subparts RR and UU Greenhouse Gas Reporting Program." Office of Air and Radiation U.S. Environmental Protection Agency. http://www.epa.gov/climatechange/emissions/downloads10/Subpart-RR-UU_TSD.pdf

Whitten, Jack E, Courtemanche, Steven, R., Jones, Andrea, R., Penrod, Richard, E., and. Fogl, David B., (Division of Industrial and Medical Nuclear Safety, Office of Nuclear Material Safety and Safeguards), June 2000. "Consolidated Guidance About Materials Licenses: Program-Specific Guidance About Well Logging, Tracer, and Field Flood Study Licenses (NUREG-1556, Volume 14)." US Nuclear Regulatory Commission. http://www.nrc.gov/reading-rm/doc-collections/nuregs/staff/sr1556/v14/#_1_26

Environmental Aspects of Oil and Gas Production.
John O. Robertson and George V. Chilingar.
© 2017 Scrivener Publishing LLC. Published 2017 by John Wiley & Sons, Inc.

6

Corrosion

6.1 Introduction

Corrosion is responsible for numerous environmental problems, e.g., structural damage to the hydrocarbon-producing facilities. Fresh-water systems can become contaminated and unsuitable for drinking water due to contamination by hydrocarbons as a result of leakage resulting from corrosion of pipelines carrying hydrocarbons or natural gas from reservoirs or a nearby leaking well. Structures such as hydrocarbon storage tanks, pipelines, oilwells, ships, railcars, tanker trucks, offshore well platforms, etc., are subject to the harmful effects of corrosion. When the structural integrity of these facilities is weakened by corrosion, they no longer can contain their fluids, threatening the environment and public safety. Chapter 2 includes the discussion of the migration of gas escaping from these facilities when corrosion destroys the containment capability. The total cost of the corrosion should include damage to the facility and the environment due to pollution. The total cost of environmental damage, however, is often difficult to assess and expensive to correct (Bennett, 1978).

Evaluating the environmental damage within which a corroded structure is located should also be considered when evaluating corrosion control. Reduction of corrosion by modifying the environment immediately surrounding a facility, such as improving drainage, can be a simple and effective way to reduce the rate of corrosion.

Oilfield production environments can range from practically a zero rate of corrosion to severely high rates of corrosion. Crude oil at normal production temperatures (less than 120 °C) without dissolved gases is not, by itself, corrosive (www.corrosioncost.com). It is the water and ions within the oil that create the problem, e.g., metals oxidize in the presence of oxygen.

In 1975, Cron and Marsh (1983) identified the cost of corrosion in the United States as $70 billion, of which $10 billion was considered avoidable. Estimates gathered by the authors of this book estimate the total cost of all corrosion in the United States to have increased in 2014 to about $350 billion. The authors estimate that in 2014 the petroleum industry alone suffered a loss of about $90 billion in corrosion costs: (a) gas/oil transmission, about $40 billion; (b) petroleum refineries, about $20 billion; and (c) oil and gas exploration and production about $40 billion. To save money by reducing this cost, the principles of corrosion must be understood in order to effectively select materials and to design, fabricate, and utilize metal structures for the optimum economic life of facilities and safety in operation.

Corrosion in various forms causes many drillpipe failures while drilling wells, adding significantly to drilling costs of wells. Corrosion can occur: (1) during drilling of deep wells, (2) using higher-strength steels to drill these wells, (3) in the presence of higher stresses, (4) using lower-pH drilling fluids, etc. In all these cases, there is an increased susceptibility of metals to failure due to corrosion.

Corrosion is often not only a major cause of damage to metals in wells but also in production facilities and pipelines. Corrosion damage results in costly maintenance of these facilities (repairs and replacements) in addition to the loss of production. It should also always be remembered that there are additional environmental costs due to hydrocarbon contamination.

To better understand corrosion and its costs, one must first understand what corrosion is and what causes it.

6.2 Definitions

6.2.1 Corrosion

In 1946, the American Electrochemical Society defined corrosion as the "destruction of a metal by chemical or electrochemical reaction with its environment." The destruction of metals by corrosion can occur by: (a) direct chemical attack at elevated temperatures in a dry environment, and (b) by electrochemical processes at lower temperatures in a water-wet or moist environment. Corrosion occurs because metals tend to revert (oxidize) to more stable forms in which they were initially found in nature, i.e., oxides, sulfates, sulfides, or carbonates.

Inasmuch as the corrosion mechanism (oxidation) is the same for all metals and alloys, differing only in degree, it is useful to examine the mechanism of corrosion for iron.

In the case of electrochemical reaction, the magnitude of electrochemical potential for a particular metal determines the tendency of the reaction to proceed, whereas the resistance offered by the corrosion products, to the continued progress of the reaction, determines the rate of corrosion.

6.2.2 Electrochemistry

Chemical reaction is caused by an external voltage (voltage caused by a chemical reaction) as in an electrochemical cell. In general, electrochemistry deals with oxidation

and reduction reactions. The following electrical terms are widely used in electrochemistry and corrosion science:

6.2.3 Electric Potential

Electric potential (E) is defined as the capacity of an electric field to do work; it is measured in volts (1 volt = 1 joule/coulomb; joule = 10^7 ergs [energy or work]; coulomb = quantity of electricity; ampere = 1 coulomb/sec). Electric potential can be described as follows:

$$E = \frac{I}{R}. \tag{6.1}$$

6.2.4 Electric Current

Electric current (I) is a movement of electrically charged particles, and is measured in amperes as follows:

$$I = \frac{E}{R} \quad \text{(Ohm's Law)} \tag{6.2}$$

6.2.5 Resistance

Resistance determines the amount of current that flows through an object for a given voltage. The resistance (R) is measured in ohms (volt/ampere).

6.2.6 Electric Charge

Electric charge (C) is the quantity of electric charge in coulombs (1 coulomb is the amount of electric charge transported by a current of 1 ampere in 1 second):

$$C = I \times t \tag{6.3}$$

where I is the electrical current in amperes and t is the time in seconds. Faraday is the larger unit for the electric charge (one Faraday is approximately equal to 96,500 coulombs).

6.2.7 Electrical Energy

Electrical energy is the energy made available by the flow of electric charge through an electrical conductor. The SI unit of electrical energy is the joule:

$$1\,J = 10^7 \text{ ergs} \tag{6.4}$$

6.2.8 Electric Power

Electric power: the unit of electric power is the watt (W) (one watt is one joule per second):

$$1W = 1\left(\frac{J}{s}\right) = 1V \times 1A \tag{6.5}$$

$$1 \text{ HP} = 746 \text{ watts} \tag{6.6}$$

The interrelationship among electrical potential (E), electrical current (I), and resistance (R) in a metallic circuit is presented in Figure 6.1.

In an electrical circuit, there are four main resistances to the current flow between the anode and cathode: R_m = resistance between anode and cathode along the metallic path; R_a = resistance at the anode due to surface films and retardation of anodic reactions (retardation of current flow; polarization); R_e = resistance of electrolyte path; and R_c = resistance at the cathode due to surface films and retardation of cathodic reactions (retardation of current flow; polarization). Thus, the total cell resistance R_t is equal to:

$$R_t = R_m + R_a + R_e + R_c \tag{6.7}$$

6.2.9 Corrosion Agents

Common components in fluids that promote the corrosion of steel in drilling and producing operations are oxygen, carbon dioxide, hydrogen sulfide, salts, and organic acids. The destruction of metals is influenced by various physical and chemical factors that localize and increase corrosion damage.

Conditions that promote corrosion include:

1. Energy differences in the form of stress gradients or chemical reactivities across the metal surface in contact with corrosive solution.

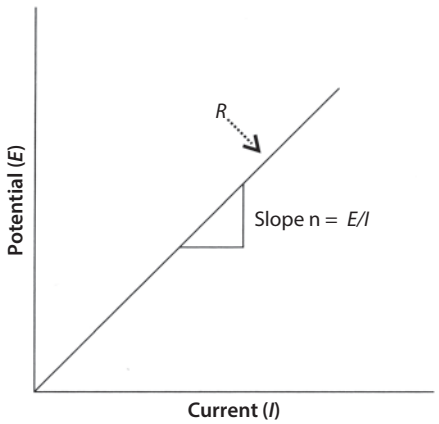

Figure 6.1 Interrelationship among electrical potential (E), current (I) and resistance (R). (After Chilingar *et al.*, 2008, Figure 1.1, p. 4.)

2. Differences in concentration of salts or other corrodents in electrolytic solution.
3. Differences in the amount of deposits, either solid or liquid, on the metal surfaces, which are insoluble in the electrolyte solutions.
4. Temperature gradients over the surface of the metal in contact with corrosive solution.
5. Compositional differences in the metal surface.

6.3 Electrochemical Corrosion

Four conditions must be present to complete the electrochemical reactions and corrosion circuit:

1. **Presence of a driving force or electrical potential**. Difference in reaction potential at two sites on the metal surface must be sufficient to drive electrons through metal, surface film, and liquid components of the corrosion circuit.
2. **Presence of an electrolyte**. Corrosion occurs only when the circuit between anodic and cathodic sites is completed by an electrolyte present in water.
3. **Presence of both anodic and cathodic sites**. An anodic and cathodic area must be present to support the simultaneous oxidation and reduction reactions at the metal-liquid interface. Metal at the anode area is oxidized.
4. **Presence of an external conductor**. A complete electron-electrolytic circuit between anodes and cathodes of the metal, through (a) the metal surface films, (b) surrounding environment, and (c) fluid-solid interfaces, is necessary for the continuance of corrosion.

Corrosion will continue as long as the four above conditions are present. When any one of the above conditions is not present, corrosion will stop.

The presence of water in the environment surrounding the metal, provide the conducting paths for both corrodents and corrosion products. The corrodents may be a dissolved gas, liquid, or solid. The corrosion products may be: (1) ions in solution, which are removed from the metal surface; (2) ions precipitated as various salts on metal surfaces, and/or (3) hydrogen gas.

The conditions needed to promote various types of corrosion can be found in most industrial facilities. The basic electrochemical reactions, which occur simultaneously at the cathodic and anodic areas of metal causing many forms of corrosion damage, are:

1. At the cathode, the hydrogen (or acid) ion (H^+) removes electrons from the cathodic surface to form hydrogen gas (H_2) (Figure 6.2):

$$2e^- + 2H^+ \rightarrow 2H^o \rightarrow H_2 \text{ (in acidic solution)} \tag{6.8}$$

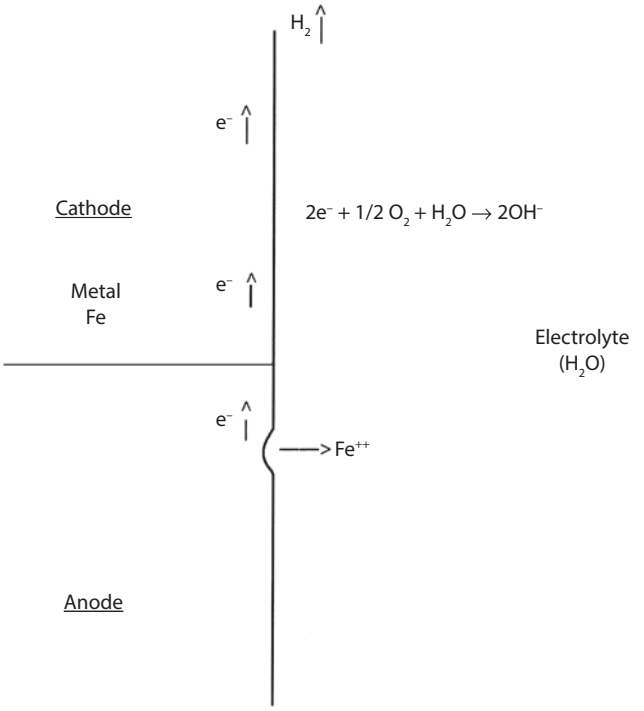

Figure 6.2 Schematic diagram of electrochemical reactions. (After Chilingar *et al.*, 2008, figure 1.2, p. 60.)

If oxygen is present, electrons are removed from the metal by reduction of oxygen (see Figure 6.3):

$$4e^- + O_2 + 4H^+ \rightarrow 2H_2O \text{ (in acidic solution)} \tag{6.9}$$

$$4e^- + 2H_2O + O_2 \rightarrow 4OH^- \text{ (in neutral or in alkaline solution)} \tag{6.10}$$

2. At the anode, a metal ion (e.g., Fe^{2+}) is released from its structural position in the metal through the loss of the bonding electrons and passes into solution in the water as soluble ion or reacts with another component of the environment to form scale. The principal reaction is:

$$Fe - 2e^- \rightarrow Fe^{2+} \tag{6.11}$$

An illustration of galvanic corrosion is presented in Figure 6.4.

Thermodynamic data indicate that the corrosion process in many environments of interest should proceed at very high rates of reaction. Fortunately, experience shows that the corrosion process behaves differently. Studies have shown that as the process proceeds, an increase in concentration of the corrosion products develops rapidly at the cathodic and anodic areas. These products at metal surfaces serve as barriers that tend

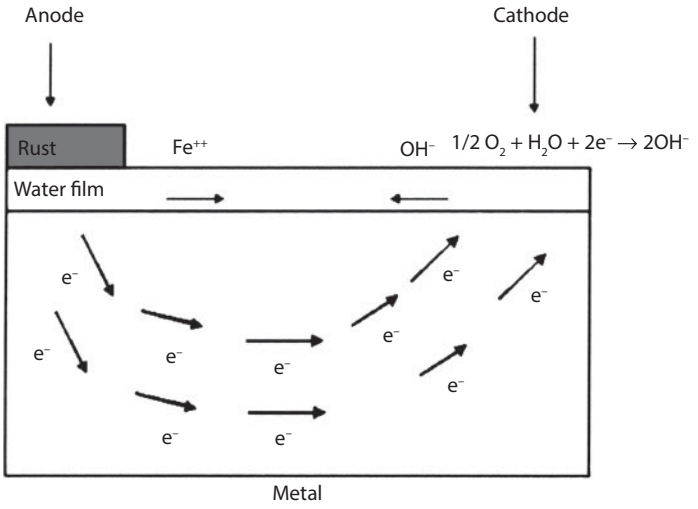

Figure 6.3 Schematic diagram of electrochemical process. (After Chilingar *et al.*, 2008, figure 1.3, p. 7.)

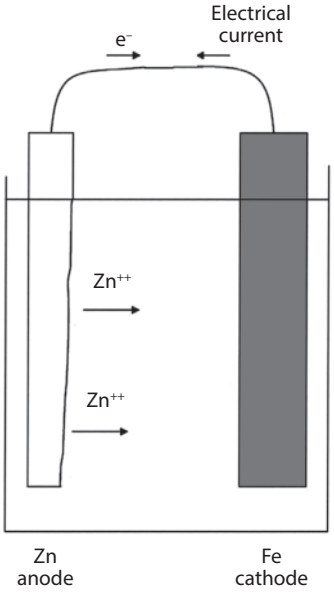

Figure 6.4 Corrosion cell showing flow of electrons and electrical current. Corrosion occurs at the anode. (After Chilingar *et al.*, 2008, figure 1.4, p. 8.)

to retard the corrosion rate. The reacting components of environment may be depleted locally, which further tends to reduce the total corrosion rate.

The potential differences between cathodic and anodic areas decrease as corrosion proceeds. This reduction in potential difference between electrodes upon current flow is termed polarization. The potential of anodic reaction approaches that of the cathode

and potential of the cathodic reaction approaches that of the anode. Electrode polarization by corrosion is caused by:

1. changing the surface concentration of metal ions,
2. adsorption of hydrogen gas at cathodic areas,
3. discharge of hydroxyl ions at cathodes, and
4. increasing resistance of electrolyte and film of metal-reaction products on the metal surface.

Changes (increase or decrease) in the amount of these resistances by the introduction of materials or electrical energy into the system will change both the corrosion currents and rate.

One practical method to control corrosion is through cathodic protection, whereby polarization of the structure to be protected is accomplished by supplying an external current to the corroding metal. Polarization of the cathode is forced beyond the corrosion potential. The effect of the external current is to eliminate the potential differences between the anodic and cathodic areas on the corroding metal. Removal of the potential differences stops local corrosion action. Cathodic protection operates most efficiently in the systems under cathodic control, i.e., where cathodic reactions control the corrosion rate.

Some materials may cause an increase in polarization and retard corrosion by adsorbing on the surface of the metals and thereby changing the nature of the surface. Such materials act as inhibitors to the corrosion process. On the other hand, some materials may reduce the polarization and assist corrosion. These materials, called depolarizers, either assist or replace the original reaction and prevent the buildup of original reaction products.

Oxygen is the principal depolarizer that aids corrosion in the destruction of metal. Oxygen tends to reduce the polarization or resistance, which normally develops at the cathodic areas, with the accumulation of hydrogen at these electrodes. The cathodic reaction with a hydrogen ion is replaced by a reaction in which electrons at the cathodic areas are removed by oxygen and water to form hydroxyl ions (OH^-) or water:

$$4e^- + O_2 + 4H^+ \rightarrow 2H_2O \text{ (in acid solution)} \tag{6.12}$$

$$4e^- + 2H_2O + O_2 \rightarrow 4OH^- \quad \text{(in neutral and alkaline solution)} \tag{6.13}$$

Polarization of an electrode surface reduces the total current and corrosion rate. Though the rate of metal loss is reduced by polarization, failures may increase if incomplete polarization occurs at the anodes. For example, inadequate anodic corrosion inhibitors will reduce the effective areas of the anodic surfaces and thus localize the loss of metal at remaining anodes. This will result in severe pitting and destruction of metal.

Resistance to the corrosion process generally does not develop to the same degree at the anodic and cathodic areas. These resistances reduce the corrosion rate, which is controlled by the slowest step in the corrosion process. Electrochemical corrosion

comprises a series of reactions and material transport to and from the metal surfaces. Complete understanding of corrosion and corrosion control in a particular environment requires knowledge of each reaction that occurs at the anodic and cathodic areas.

6.3.1 Components of Electrochemical Corrosion

The various components that are involved in the process of corrosion of metal are: (1) the metal, (2) the films of hydrogen gas and metal corrosion products, (3) liquid and gaseous environment, and (4) the several interfaces between these components. Metal is a composite of atoms that are arranged in a symmetrical lattice structure. These atoms may be considered particles that are held in an ordered arrangement in a lattice structure by bonding electrons. These electrons, which are in constant movement about the charged particles move readily throughout the lattice structure of metal when an electric potential is applied to the system. If bonding electrons are removed from their orbit about the particle center, the resulting cation will no longer be held in the metal's crystalline structure and can enter electrolyte solution (see Chilingar *et al.*, 2008).

Electrochemical corrosion is simply the process of freeing these cations from their organized lattice structure by removal of the bonding electrons. Inasmuch as certain of the lattice electrons move readily within the metal under the influence of electrical potentials, the locations on the surface of the metal from which the cations escape and the locations from which the electrons are removed from the metal need not be and generally are not the same. Corrosion will not occur unless electrons are removed from some portion of the metal structure.

All metals are polycrystalline with each crystal having a random orientation with respect to the next crystal. The metal atoms in each crystal are oriented in a crystal lattice in a consistent pattern. The pattern gives rise to differences in spacing and, therefore, differences in cohesive energy between the particles, which may cause preferred corrosion attack. At the crystal boundaries the lattices are distorted, giving rise to preferred corrosion attack. In the manufacture and processing of metals, in order to gain desirable physical properties, both the composition and shape of crystal may be made nonuniform, distorted, or preferably oriented. This may increase the susceptibility of the metal to corrosion attack (see Chilingar *et al.*, 2008).

Undistorted single crystals of metals experience comparatively little or no corrosion under the same conditions, which may destroy commercial pieces of the same metal. Compositional changes in metal alloy crystals and crystal boundaries, which are present in steels and alloys, can promote highly localized corrosion.

6.3.1.1 Electromotive Force Series

Oxidation takes place when a given substance loses electrons or a share of its electrons. On the other hand, reduction occurs when there is a gain in electrons by a substance. A substance that yields electrons to something else is called a reducing agent, whereas the substance that gains electrons is termed an oxidizing agent. Thus electrons are always transferred from the reducing agent to the oxidizing agent. In the example below, two electrons are transferred from metallic iron to cupric ion:

$$Fe^0 + Cu^{2+} \rightarrow Fe^{2+} + Cu^0 \tag{6.14}$$

Examples of oxidation and reduction processes are presented below:

$$Zn^0 \rightarrow Zn^{2+} + 2e^- \text{ (Oxidation)} \tag{6.15}$$

$$Cu^{2+} + 2e^- \rightarrow Cu^0 \text{ (Reduction)} \tag{6.16}$$

The emf series is presented in Table 6.1. Potentials given are those between the elements in their standard state at 25 °C and their ions at unit activity in a solution at

Table 6.1 The electromotive force series or the electrode potential of an element according to decreasing tendency to release electrons.

Element	Electrode reaction	Standard electrode potential in volts, *E* @ 25 °C
Lithium	$Li = Li^+ + e^-$	+3.05
Potassium	$K = K^+ + e^-$	+2.922
Calcium	$Ca = Ca^{++} + 2e^-$	+2.87
Sodium	$Na = Na^+ + e^-$	+2.712
Magnesium	$Mg = Mg^{++} + 2e^-$	+2.375
Beryllium	$Be = Be^{++} + 2e^-$	+1.85
Aluminum	$Al = Al^{+++} + 3e^-$	+1.67
Manganese	$Mn = Mn^{++} + 2e^-$	+1.029
Zinc	$Zn = Zn^{++} + 2e^-$	+0.762
Chromium	$Cr = Cr^{+++} + 3\ e^-$	+0.74
Gallium	Ga = Ga+++ + 3e$^-$	+0.53
Iron	$Fe = Fe^{++} + 2e^-$	+0.44
Cadmium	$Cd = Cd^{++} + 2e^-$	+0.402
Indium	$In = In^{+++} + 3e^-$	+0.34
Thallium	$Tl = Tl^+ + e^-$	+0.336
Cobalt	$Co = Co^{++} + 2e^-$	+0.277
Nickel	$Ni = Ni^{++} + 2e^-$	+0.25
Tin	$Sn = Sn^{++} + 2e^-$	+0.136
Lead	$Pb = Pb^{++} + 2e^-$	+0.126
Hydrogen	$H_2 = 2H^+ + 2e^-$	+0.00
Copper (cupric)	$Cu = Cu^{++} + 2e^-$	–0.345
Copper (cuprous)	$Cu = Cu^+ + e^-$	–0.522
Mercury	$2Hg = Hg^{++} + 2e^-$	–0.789
Silver	$Ag = Ag^+ + e^-$	–0.80
Palladium	$Pd = Pd^{++} + 2e^-$	–0.987
Mercury	$Hg = Hg^{++} + 2e^-$	–0.854
Platinum	$Pt = Pt^{++} + 2e^-$	–1.20
Gold	$Au = Au^{+++} + 3e^-$	–1.50
Gold	$Au = Au^+ + e^-$	–1.68

25 °C. A plus (+) sign for E^0 shows that, for the above conditions, the reduced form of the reactant is a better reducing agent than H_2. On the other hand, a negative (–) sign indicates that the oxidized form of the reactant is the better oxidizing agent than H^+. Thus, in general, any ion is a better oxidizing agent than those ions above it.

Any metal can displace any other metal (in ionic form), that occupies a lower position in the activity series, from a solution of any salts of the latter metal, if the metal to be displaced is not very far above hydrogen. In the latter case, there will be a preponderance of hydrogen gas evolution. Examples below demonstrate this:

$$Ca^0 + Sn^{2+} \rightarrow Ca^{2+} + Sn^0 \tag{6.17}$$

$$Ca^0 + 2H^+ \rightarrow Ca^{2+} + H_2 \uparrow$$

$$Ca^0 + Zn^{2+} \rightarrow Ca^{2+} + Zn^0 \tag{6.18}$$

6.3.1.2 Actual Electrode Potentials

In the emf series, each metal can reduce (or displace from solution) the ion of any metal below it in the series, providing all of materials have unit activities. The activity of a pure metal in contact with a solution does not change with the environment. The activity of an ion, however, changes with concentration, and activity of a gas changes with its partial pressure.

An electrode reaction, in which a metal M is oxidized to its ion M^+, liberating n electrons, may be represented by the relation: $M = M^{n+} + ne^-$. The actual electrode potential of this reaction may be calculated from the standard electrode potential by use of the following expression:

$$E = E^0 - \frac{RT}{nF} \ln(M^{n+}) \tag{6.19}$$

where E = actual electrode potential at the given concentration (volts): E^0 = standard electrode potential (volts); R = universal gas constant, 8.315 volt coulombs/K; T = absolute temperature (K); n = number of electrons transferred; F = Faraday, 96,500 coulombs; M^{n+} = concentration of metal ions.

At 25 °C, 3.303 RT/F = 0.05915 and the formula (Eq. 6.19) becomes

$$E = E^0 - \frac{0.05915}{n} \log_{10}(M^{n+}) \tag{6.20}$$

The actual electrode potential for a given environment may be computed from the above relation. Table 6.2 shows how the actual electrode potentials of iron and cadmium vary with change in concentration of the ions. It is apparent from Table 6.2 that iron will reduce cadmium when their ion concentrations are equal, but the reverse holds true when the concentration of cadmium ion becomes sufficiently lower than that of the ferrous ion.

The standard electrode potentials are a part of the more general standard oxidation-reduction potentials. Many books on physical chemistry contain a general expression for calculating the actual oxidation-reduction potential from the standard oxidation-reduction potential.

Table 6.2 Variation in actual electrode potential of iron and cadmium with a change in concentration of ions.

	Activity, moles/kg water			
	1	**0.1**	**0.01**	**0.001**
Reaction	**Actual electrode potential, volts**			
$Fe = Fe^{++} + 2e^{-}$	+0.440	+0.470	+0.499	+0.529
$Cd = Cd^{++} + 2e^{-}$	+0.402	+0.431	+0.461	+0.490

6.4 Galvanic Series

Dissimilar metals exposed to electrolytes exhibit different potentials or tendencies to go into solution or react with the environment. This behavior is recorded in tabulations in which metals and alloys are listed in order of increasing resistance to corrosion in a particular environment. Coupling of dissimilar metals in an electrolyte will cause destruction of the more reactive metal, which acts as an anode, and provides protection for the less reactive metal, which acts as a cathode.

6.4.1 Cathode/anode Area Ratio

When the ratio of area of cathodes to that of anodes (C/A ratio) is high, the corrosion rate at anodes will be high. On the other hand, when the C/A ratio is low, the corrosion rate at anodes will be low. Thus, in the case of Figure 6.5a, the steel rivets will be heavily corroded and the two plates will soon fall apart when immersed in seawater.

In the case of Figure 6.5b, on the other hand, there will be only slight corrosion of both copper rivets and steel plates upon immersion in seawater.

6.4.2 Polarization

Electrochemical cells in which a chemical reaction produces a current can be called primary cells.

In many primary cells, hydrogen liberated at the cathode soon coats the cathode with bubbles. This diminishes the surface at which electrons can be accepted and, thus, results in an increased resistance to the current flow, i.e., polarization (see Figure 6.6).

If some good oxidizing agent is placed in contact with the cathode to accept electrons more readily than does the oxonium ion (H_30^+), hydrogen gas liberation will occur. This is called depolarization.

Excellent treatment of the subject can be found in Jones (1988, p. 162), who presented the polarization diagram of zinc corroding in acid (Figure 6.7).

6.4.3 Corrosion of Iron

In many corrosion problems, the important differences in reaction potential are not those between dissimilar metals, but are those that exist between separate areas interspersed over all the surface of a single metal. These potential differences result from

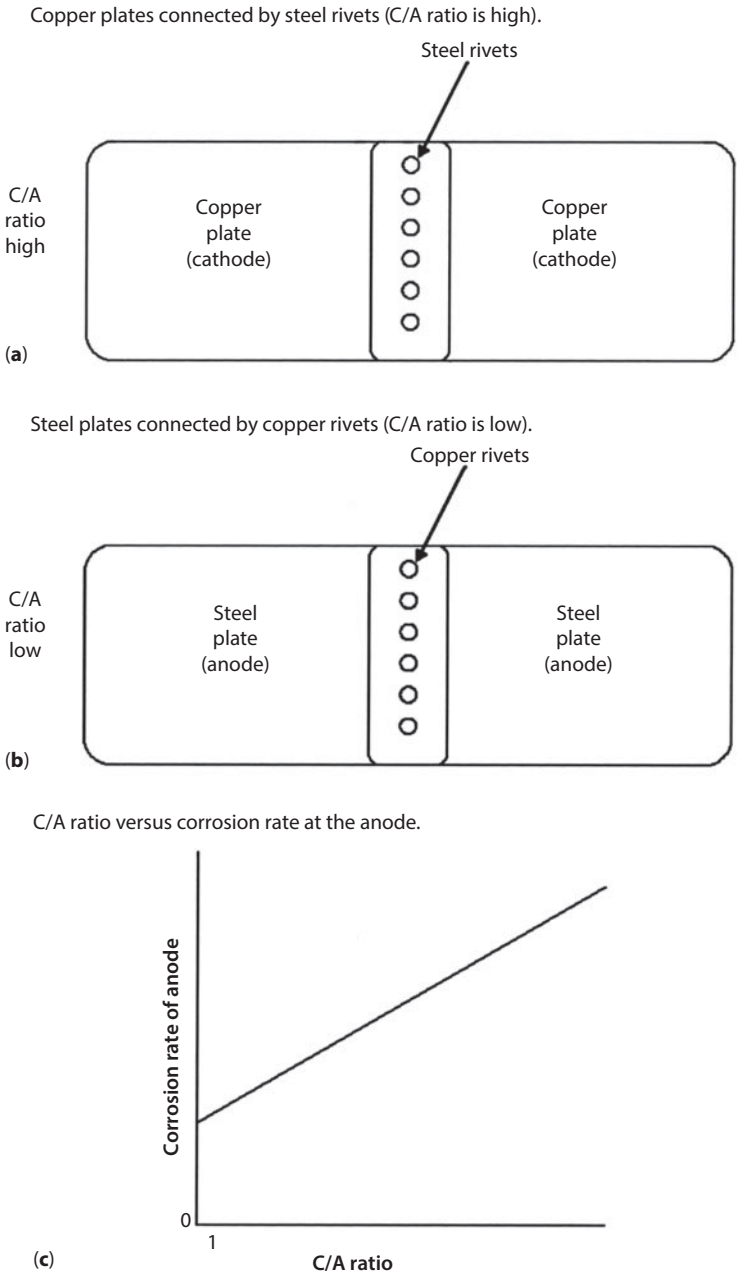

Figure 6.5 Effect of the ration of the area of cathode to the area of anode on corrosion rate. (After Chilingar *et al*., 2008, figure, 1.5, p. 15.)

local chemical or physical differences within or on the metal and can be caused by variations in:

1. grain structure
2. stresses
3. scale

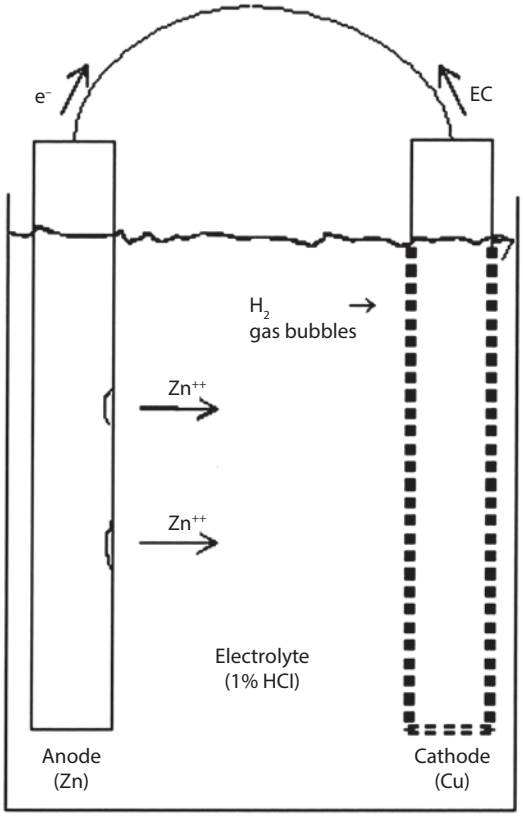

Figure 6.6 Zn-Cu cell and polarization. (After Chilingar *et al.*, 2008, Figure 1.6, p. 16.)

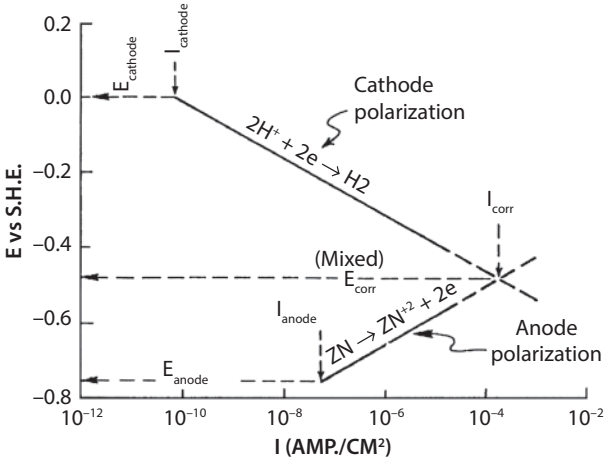

Figure 6.7 Polarization diagram of zinc corroding in acid. E_{corr} = mixed (corrosion) potential where oxidation and reduction are occurring equally, i.e., zinc dissolution is equal to hydrogen as evolution. (Modified after Jones, 1988, p. 163, figure 1A 3.)

4. inclusions in the metal
5. grain boundaries
6. scratches or other surface condition.

Steel is an alloy of iron with only small amounts of carbon (normally containing 0.2 to 1.5% carbon) with Fe_3C and trace amounts of other elements. Iron carbide (Fe_3C) is cathodic with respect to iron.

Inasmuch as in typical corrosion of steel the anodic and cathodic areas lie side by side on the metal surface, in effect it is covered with both positive and negative sites. During corrosion, the anodes and cathodes of metals may interchange frequently.

6.4.4 Gaseous Corrodents

Gaseous corrodents include oxygen, hydrogen sulfide, and carbon dioxide.

6.4.4.1 Oxygen

Oxygen dissolved in drilling fluids is a major cause of drillpipe corrosion. As a depolarizer and electron acceptor in cathodic reactions, oxygen accelerates the anodic destruction of metal. The high-velocity flow of drilling fluids over the surfaces of drillpipes continues to supply oxygen to the metal and is destructive at concentrations as low as 5 ppb. The presence of oxygen magnifies the corrosive effects of the acid gases (H_2S and CO_2). The inhibition of corrosion promoted by oxygen is difficult to achieve and is not practical in the drilling fluid system. Removal of oxygen from the drilling fluid by physical deaeration, followed by chemical removal of residual oxygen, is recommended. (See Chilingar *et al.*, 2008.)

Oxygen corrosion of drillpipe can also occur while the pipe is out of the hole. Pitting can develop rapidly under particles of mud solids that are left on the pipe. Pits provide the sites for further local attack of the drillpipe while it is in service. Proper cleaning of the drillpipe with fresh water to remove the salts and mud solids is recommended. Cleaned drillpipe should be sprayed with a protective coating prior to storage.

The control of corrosion in water-handling facilities requires the complete exclusion and removal of oxygen from the water throughout the facilities. Oilfield brines, which usually exhibit an oxygen demand, should react with dissolved oxygen in the water. Unfortunately, the brines usually contain soluble organics which interfere with this reaction. An oxygen scavenger with the appropriate catalysts is usually required for the complete removal of oxygen from the waters.

Oxygen can enter produced brines by exposure to air through open tank hatches, pump seals, flotation and filtration systems, and other points throughout water-handling facilities. Oxygen can also enter produced fluids in low-pressure pumping wells and in gas- and oil-gathering systems.

The strong depolarization properties of oxygen create localized attack of metal in areas of lower oxygen concentration, such as in crevices, pits, and in areas under deposits on the metal. Even in trace quantities, oxygen in brines can create severe pitting of metal.

Inhibition of oxygen-induced corrosion in production facilities has been difficult to attain. Corrosion control effort should be directed to both the exclusion of oxygen from

production and water-handling facilities and the complete removal of oxygen from oilfield waters.

The method used to remove dissolved oxygen from water can be either mechanical or chemical. Mechanical methods are useful in reducing dissolved oxygen to values less than 1 ppm. The water is then treated chemically for complete removal of oxygen. A common mechanical method used in the oilfield to strip dissolved oxygen from water is by a countercurrent flow of water with oxygen-free gas through a flash and stripper operation. This process was described by Weeter (1965). Oxygen content can be reduced economically by vacuum deaerators to about 0.3 ppm. According to Cron and Marsh (1983, p. 1037), vacuum is best obtained by the use of steam injectors in series. Chemical scavengers for the removal of oxygen are sodium sulfite, bisulfites, and hydrazine:

$$Na_2SO_3 + \frac{1}{2}O_2 \rightarrow Na_2SO_4 \tag{6.21}$$

$$N_2H_4 + O_2 \rightarrow N_2 + 2H_2O \tag{6.22}$$

The reaction rates are complex in many water systems and are affected by temperature, pH, hydrogen sulfide content, and the presence of catalysts. Snavely and Blount (1969) and Snavely (1971) have shown that:

1. SO_2 or Na_2SO_3 is not effective for scavenging oxygen from sour waters, and H_2S must be removed prior to treatment.
2. Hydrozine is not sufficiently reactive for scavenging O_2 at ambient temperatures, except in the presence of Cu^{2+}.

Although stoichiometrically 8 ppm of Na_2SO_3 is required to react with 1 ppm of dissolved oxygen, in actual practice 10 ppm is used. In the case of hydrazine, 1 ppm is required to scavenge 1 ppm of oxygen. Tests of oxygen scavenger reaction rates and chemical scavenger and catalyst requirements should be made in each case.

6.4.4.2 Hydrogen Sulfide

Hydrogen sulfide is most damaging to drillpipe by promoting sulfide cracking or embrittlement. General corrosion attack by hydrogen sulfide is also significant and is influenced by the presence of carbon dioxide, oxygen, and salts. The nature of the attack on metal is related to the alloy composition and strength of steel. The corrosion of mild steel in distilled water containing hydrogen sulfide was studied by Watkins and Wright (1953). Their data indicated that a high concentration of hydrogen sulfide may inhibit corrosion of mild steel.

High concentrations of hydrogen sulfide are catastrophic; however, in the case of high-strength steels, producing rapid embrittlement. The influence of hydrogen sulfide, brine, and carbon dioxide mixtures upon corrosion rates of mild steels was studied by Meyer *et al.* (1958).

The removal of dissolved gases (oxygen, hydrogen sulfide, and carbon dioxide) from drilling fluids is an important step in minimizing corrosion damage to drillpipe. The primary object of removing hydrogen sulfide from drilling fluids is the safety of personnel, because H_2S is extremely toxic. The limit for repeated exposure is 10 ppm.

Exposure to concentration of 800+ ppm may result in death. Drilling fluids must, therefore, be treated to neutralize hydrogen sulfide gas as it enters the drilling fluid by flow from the formation or from the cuttings. If the presence of hydrogen sulfide is expected, the pH of drilling fluids should be held above 10. The reactions with caustic soda are as follows:

$$\text{pH} = 7.0 : \text{H}_2\text{S} + \text{NaOH} \rightarrow \text{NaHS} + \text{H}_2\text{O} \tag{6.23}$$

$$\text{pH} = 9.5 : \text{Na HS} + \text{NaOH} \rightarrow \text{Na}_2\text{S} + \text{H}_2\text{O} \tag{6.24}$$

Hydrogen sulfide scavengers are also added to drilling fluids for the purpose of pretreatment or removal of this gas. These materials include (1) carbonate, chromate, and oxides of zinc; (2) iron oxide; and (3) copper carbonate. Copper carbonate should not be used for the purpose of pretreatment or in excess of the sulfide requirement due to the possible corrosive effects.

Ironite® Sponge®, which is the product of a reaction (controlled oxidation) using highly reactive, specially formulated chemical-grade iron powder as the raw material, can be used as an H_2S scavenger. It consists mainly of Fe_3O_4 and is characterized by high surface area (10 m^2/kg or approximately 50,000 sq ft/lb). The specific gravity of the dry material is around 4.5–4.6 g/cm^3, and particle size ranges from 1.5 to 50.0 mm, with 90% being between 2 and 20 mm. Inasmuch as the material retains very little magnetism, it is not attracted to drillpipe or casing. Ironite® Sponge® reacts with H_2S according to the following equations:

$$\text{Fe}_3\text{O}_4 + 4\ \text{H}_2\text{S} \rightarrow 3\ \text{FeS} + 4\ \text{H}_2\text{O} + \text{S} \tag{6.25}$$

$$\text{FeS} + \text{S} \rightarrow \text{FeS}_2 \tag{6.26}$$

$$\text{Fe}_3\text{O}_4 + 6\ \text{H}_2\text{S} \rightarrow 3\text{FeS}_2 + 4\ \text{H}_2\text{O} + 2\ \text{H}_2 \tag{6.27}$$

The first two reactions predominate in basic environment, whereas the third reaction occurs in acidic environment. One pound of material (0.453 kg) reacts with 0.7 lb (0.318 kg) of H_2S. The speed of reaction can be expressed by the following equation:

$$\frac{\mathrm{d}S}{\mathrm{d}t} = -3000 \times S_t^2 \times (H^+)^{1.06} \times I \tag{6.28}$$

where S_t = total dissolved sulfides in filtrate, ppm; t = time, min; H^+ = hydrogen ion concentration, moles/L; I = Ironite® Sponge® concentration, lb/bbl (0.351 kg/m^3).

Replacement of water-base drilling fluids with oil-base systems provides protection to drillpipe by eliminating the electrolyte that is essential to corrosion. The oil-base systems contain some emulsified water, alkalinity of which must be maintained. The H_2S gas, which is carried by oil-base drilling fluid, must be removed by the gas separators and vacuum degassers. The removed gases must then be neutralized for the protection of personnel.

Hydrogen sulfide causes failure of production equipment by acid attack and hydrogen penetration of steel which results in blistering and cracking. Hydrogen sulfide forms iron sulfide scale, which is cathodic to the metal and promotes localized attack under the scale and the penetration of hydrogen into the metal.

The control of corrosion in H_2S environments requires:

1. The proper selection of materials including the use of low-hardness steels with a maximum hardness of Rockwell C-22.
2. The application of inhibitors.
3. The complete exclusion and removal of oxygen from waters in petroleum production.

The transmission of sour or acid gases should be preceded by drying to a dew point, which is below the minimum temperature of exposure within the facilities.

6.4.4.3 Carbon Dioxide

Carbon dioxide is present in most formation fluids as a component of formation gases and in solution in water and oil. Carbon dioxide dissolves in water and oil. Upon dissolution in water, carbon dioxide forms carbonic acid:

$$CO_2 + H_2O \rightarrow H_2CO_3 \tag{6.29}$$

$$H_2CO_3 \leftrightarrow H^+ + HCO_3^- \tag{6.30}$$

$$HCO_3^- \leftrightarrow H^+ + CO_3^{2-} \tag{6.31}$$

As the partial pressure of carbon dioxide increases, more acid ions are formed and the water becomes more corrosive.

According to Cron and Marsh (1983, p. 1034), the characteristic appearance of CO_2 corrosion is the deep, rounded pits with sharp edges. CO_2 corrosion is especially prevalent in areas of turbulence. The partial pressure of CO_2 can be used as a yardstick to predict corrosion. The following relationships have been found:

1. A partial pressure of CO_2 above 30 psi usually indicates that corrosion will occur.
2. A partial pressure of 3 to 30 psi indicates that corrosion may occur.
3. A partial pressure below 3 psi indicates that corrosion generally is not serious.

Carbon dioxide is usually removed from drilling fluids by degassers and adjusting the pH. Alkalinity is preferably adjusted with caustic soda, to avoid scaling or precipitation of carbonates.

6.4.5 Alkalinity of Environment

The pH (hydrogen ion activity) of water influences the corrosion rate of steel. The effect of pH on the corrosion of steel is dependent upon metal composition, stresses, oxygen concentration, and the type of acid that controls the pH.

In a high alkaline range, the corrosion reaction is under anodic control and proceeds at high rates:

$$O_2 + Fe - 2e^- \rightarrow FeO_2^{2-} \tag{6.32}$$

In the neutral range and in mild alkaline solutions, the corrosion rate is under cathodic control, which provides some corrosion protection. Ferrous hydroxide, which provides a protective layer on the metal surface, forms in this environment. The actual corrosion rate is dependent upon the diffusion of oxygen to metal surface. Corrosion increases with increasing oxygen concentration and abrasion and in the presence of turbulent, high-velocity flow, which is often imposed on drillpipe.

In the acid pH range, corrosion is under anodic control and the metal composition influences the corrosion rates extensively. Trace elements in steel and stresses affect the corrosion damage. The type of acid in solution determines the pH at which corrosion increases rapidly with evolution of hydrogen gas. The hydrogen evolution starts at pH near 4, with corrosion accelerating as pH is reduced. Hydrogen evolution at pH of about 4 occurs in the presence of strongly disassociated acids.

Carbonic acid from the solution of carbon dioxide reacts with iron at a pH of 6 with the evolution of hydrogen gas causing severe corrosion. This illustrates the importance of pH control throughout the system where carbon dioxide is present. Relationship of failure by embrittlement (sulfide cracking) to pH is also likely.

6.4.6 The influence of pH on the Rate of Corrosion

The most important corrosion control measure is to remove oxygen, carbon dioxide, and hydrogen sulfide (soluble gases) from the system. The effectiveness of both corrosion inhibitors and pH is enhanced by the removal of soluble gases.

6.4.7 Sulfate-Reducing Bacteria

The influence of sulfate-reducing bacteria in the corrosion process has been the subject of extensive investigations. The subject is complex and the reader is referred to the comprehensive treatment of the subject by Davis (1967) (also see Chilingar and Beeson, 1969). Microbial corrosion has not been significant in the corrosion of drillpipe.

Sulfate-reducing bacteria have produced serious corrosion to well casing as reported by Doig and Wachter (1951). Pitting occurred on the external surface of casing where drilling fluid was present between the casing and the wall of the hole. The low pH of the mud and presence of organic nutrients were favorable for growth of sulfate-reducing bacteria. The pH favorable for bacterial growth ranges from 5 to 9. Bacteria will thrive in areas of stagnant flow even in high-pH systems, however, provided other requirements, i.e., temperature and contents of organic nutrients, salts, and oxygen are satisfied. Sulfate-reducing bacteria are anaerobic and thrive only in the absence of oxygen. In an aerated mud system, oxygen is depleted in stagnant areas, e.g., along the walls of mud pits and behind the casing. This allows sulfate-reducing bacteria to grow with the evolution of H_2S:

$$H_2SO_4 + 8\ H^+ + \text{bacteria} \rightarrow H_2S + 4\ H_2O \tag{6.33}$$

Thus, hydrogen atoms formed at cathodic areas of metal are removed and utilized to reduce sulfates to sulfides. The end products are live bacteria and corroded iron. The bacterial attack of organic additives of drilling fluids may result in excessive use of mud chemicals and a rapid reduction of pH. The mud will become more corrosive under these conditions. Thus, bacteria must be controlled by the use of high pH (e.g., 10.5) or bactericides.

6.4.8 Corrosion in Gas-Condensate Wells

Corrosion in gas-condensate wells presents serious problems which cannot be predicted accurately. A rigorous corrosion control program, with conscientious monitoring of equipment condition, properties of produced fluids, and corrosion rates, is required to maintain corrosion control.

Analysis of the problem by NGAA (1953) and the NACE Committee on Condensate Well Corrosion (1979) provided several guidelines for control of corrosion. The NGAA (1953) statistical studies showed that corrosion was likely in condensate wells with:

1. Depths greater than 5,000 ft.
2. Bottom-hole temperatures above 160 °F.
3. Bottom-hole pressures above 1,500 psi.
4. CO_2 partial pressures above 30 psi.

As the gas wells were drilled deeper than ≈10,000 ft, the corrosion problem became more complex. Hilliard (1980) in laboratory and field studies has noted that the effects of gas composition, pressure, temperature, velocity, and composition of produced water modify the simple relationships between these factors and the corrosion of steel. For example, corrosion due to CO_2 decreases at high temperatures due to a passivation effect. Temperature has not been related clearly to the CO_2 partial pressure, composition of water, or other properties. Hydrogen sulfide at low concentrations reactivates the corrosion.

Presence of water or electrolytes in contact with metal is essential for corrosion to proceed. Water may contact tubing in a gas well from the bottom to the wellhead or be present in a limited area within the well as a result of condensation of vapor. Corrosion in deep gas wells is difficult to monitor except by iron count, caliper logs, and inspection. Corrosion monitoring at the surface does not reveal behavior that is representative of conditions within the well.

Gatzke and Hausler (1983) described an empirical relationship between corrosion rate vs. production rates of water and gas. The corrosion rates are derived from iron counts in the interior areas of tubing. Figures 6.8 and 6.9 illustrate the relationship between corrosion rate and brine and gas productions.

Adequate placement of corrosion inhibitors in deep hot gas wells is complicated by problems of evaporation of carrier fluid and removal of inhibitor by the flow of produced condensate and gas. Methods of inhibitor application are:

1. Squeezing of inhibitor into the formation, which may impair well productivity.
2. Batch treatment down the tubing, which may not reach the corrosive areas in deep wells.
3. Continuous injection of inhibitor through a separate line to the bottom.

The continuous injection method with appropriate inhibitor and carrier fluid is the most effective procedure. An excellent discussion of corrosion characteristics and control practices in deep hot gas wells was presented by Annand (1981).

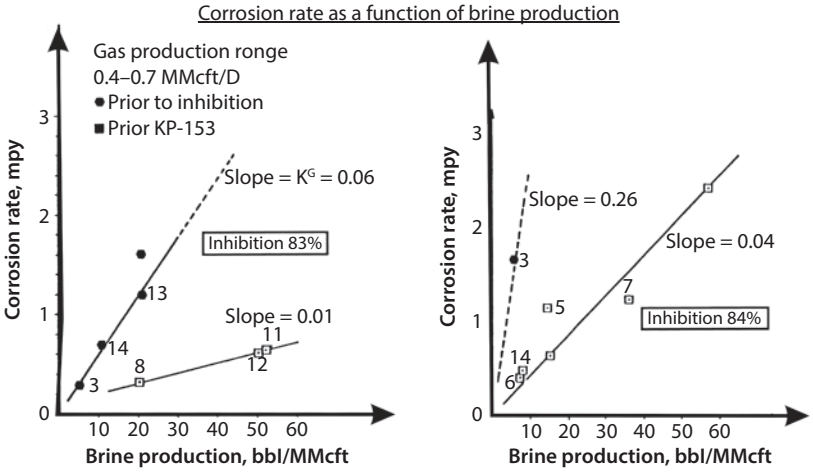

Figure 6.8 Empirical relationship between corrosion rate and brine production for the interior areas of tubing. (Modified after Gatzke and Hausler, 1983; in: Chilingar *et al*, 2008, p. 29, figure 1.13.)

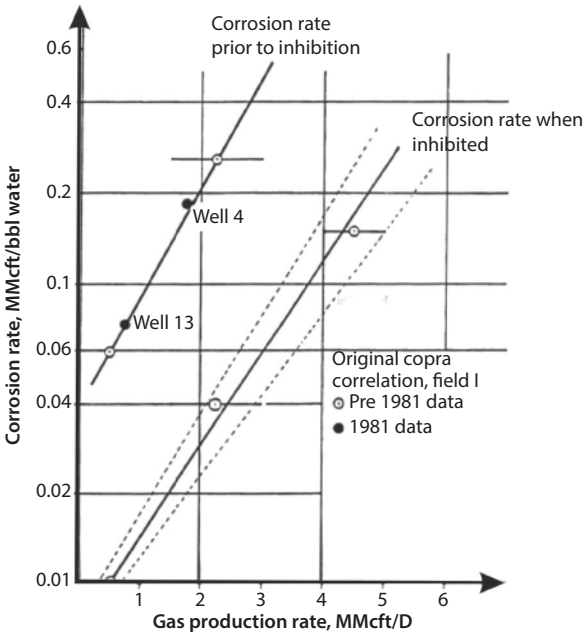

Figure 6.9 Relationship between corrosion rate and gas production inside tubing for gas production. (Modified after Gatzke and Hausler, 1983; in: Chilingar *et al*., 2008, p. 30, figure 1.14.)

6.5 Types of Corrosion

One can divide the types of corrosion on the basis of appearance of corrosion damage, mechanism of attack, industry section, and preventive methods. There are many types and causes of corrosion. In the oil and gas production industries, corrosion is usually

classified into four different types. This classification is mostly based on the types of corrosion in the oilfield (see Oxford and Foss, 1958):

1. Sweet corrosion
2. Sour corrosion
3. Oxygen corrosion
4. Electrochemical corrosion

One can also classify corrosion types as follows (see http://www.corrosiondoctors.org/Forms/fretting.htm):

1. Uniform attack
2. Pitting corrosion
3. Crevice corrosion
4. Galvanic corrosion
5. Erosional corrosion
6. Fretting corrosion
7. Cavitation
8. Intergranular corrosion
9. Stress corrosion
10. Dealloying (selective leaching)
11. Environmental cracking
12. Fatigue
13. Exfoliation

According to Bertness *et al.* (1989, p. 559), destruction of metal is influenced by various physical and chemical factors which localize and increase corrosion damage.

The conditions which promote corrosion include:

1. Energy differences in the form of stress gradients or chemical reactivities across the metal surface in contact with corrosive solution.
2. Differences in concentration of salts or other corrodants in electrolytic solution.
3. Differences in the amount of deposits, either solid or liquid, on the metal surfaces, which are insoluble in the electrolytic solutions.
4. Temperature gradients over the surface of the metal in contact with corrosive solution.
5. Compositional differences in the metal surface.

Although one can differentiate between different types of corrosion, one should realize, that in practice usually more than one type of corrosion can take place.

6.5.1 Sweet Corrosion

Sweet corrosion is generally characterized first by simple metal dissolution followed by pitting. The corrodant is H^+, derived from carbonic acid (H_2CO_3) and the dissolution

of CO_2 in the produced brine. The pitting leaves distinctive patterns (e.g., "mesa" corrosion), attributable to the metallurgical processing used in manufacturing the tubing. "Ringworm" corrosion is caused when welding is not followed by full-length normalizing of the tubular pipe after processing.

Naphthenic acids and simple organic acids indigenous to crude oil also contribute to corrosion (PetroWiki, 2015). Corrosion inhibitors and CRAs are effective in mitigating sweet corrosion.

Sweet corrosion is a common type of corrosion in the oilfield and can be defined as the deterioration of metal due to contact with carbon dioxide, fatty acids, or other similar corrosive agents, but excluding hydrogen sulfide (H_2S). One can recognize sweet corrosion by pitting on the surface of the steel. Carbon dioxide systems are one of the more common environments in the oilfield industry where corrosion occurs. Carbon dioxide reacts with the moisture in the environment and forms a weak carbonic acid (H_2CO_3) in water, which then reacts with metal (however, this reaction occurs very slowly):

$$CO_2 + H_2O \leftrightarrow H_2CO_3 \tag{6.34}$$

$$H_2CO_3 + H_2O \leftrightarrow H_3O^+ + HCO_3^- \tag{6.35}$$

$$Fe + H_2CO_3 \rightarrow FeCO_3 + H_2\uparrow \tag{6.36}$$

Corrosion induced by CO_2 is a function not only of CO_2 partial pressure and temperature but also the composition of crude oil. Crude oils contain surface-active chemicals (some oils contain more than others). These chemicals (e.g., resins and asphaltenes) can impact the corrosion process, at least for low-alloy steels. For a fixed brine composition, WOR, temperature, and pressure, corrosion in the presence of some crudes can be negligible, whereas in the presence of others, it can be extreme under identical environmental conditions (Jasinski, 1986). Sweet corrosion generally results in the deposition of insoluble $FeCO_3$ (siderite) on the steel surface. It has been suggested that this selectivity to oil composition relates to the physical morphology of the $FeCO_3$ corrosion product: a compact tight film can protect the steel, whereas a loose, poorly adherent film does not (Jasinski, 1986).

Corrosion rates in a CO_2 system can reach very high levels (thousands of mils per year), but corrosion can be effectively inhibited. The reaction of CO_2 with water will decrease pH [$pH = -\log H_3O^+$] which will cause corrosion. With increasing solubility of carbon dioxide in water, corrosion will increase. The solubility is determined by the temperature, pressure, and composition. Pressure increases the solubility, whereas temperature decreases the solubility.

Sweet corrosion always occurs in gas-condensate wells. Condensate wells produce water with pH below 7 at the wellhead and commonly as low as 4 at the bottom of some wells (Oxford and Foss, 1958). This is due to:

1. High CO_2 contents of gas; usually up to 3%.
2. High total pressure, ranging from 1,000 to 8,000 psi at the wellhead.
3. Presence of organic acids, such as acetic acid (CH_3COOH).

Erosion by high-velocity gas stream aggravates the corrosion.

6.5.2 Sour Corrosion

The deterioration of metal due to contact with hydrogen sulfide and moisture is called "*sour corrosion*." Although hydrogen sulfide is not corrosive by itself, it becomes a severely corrosive agent in the presence of water. The general equation of sour corrosion can be expressed as follows:

$$H_2S + Fe + H_2O \rightarrow FeS_X + 2\,H + H_2O \tag{6.37}$$

Blistering, embrittlement and sulfide stress cracking (Stress Corrosion Cracking (SCC) and subclasses of SCC) all stem from the same cause: the presence of H_2S in the system and at the metal surface. The roots of the problem are in the mechanism for the cathodic discharge of hydrogen. The mechanism discussed involves two steps:

$$2H^+ + 2e^- = 2H^o \tag{6.38}$$

and

$$2H^o \rightarrow H_2 \tag{6.39}$$

(i.e., the proton is first reduced to a hydrogen atom on the metal surface (H), followed by the combination of two hydrogen atoms to yield hydrogen gas. Hydrogen sulfide inhibits the combination of hydrogen atoms (as does arsenic and some other corrosion inhibitors) (PetroWiki, 2015). Accordingly, hydrogen atoms penetrate into the metal where they can cause the blistering problems (Brondel, 1994).

This hydrogen entry into low-strength steels can result in hydrogen blisters, if there is a macroscopic defect in the steel such as an inclusion. Such a void can provide a space for the hydrogen atoms to form the hydrogen gas. Pressure builds and blisters form resulting in rupture and leakage (PetroWiki, 2015).

Embrittlement (hydrogen-induced cracking and hydrogen embrittlement cracking) causes failure at stresses well below the yield strength of the steel. This phenomenon usually occurs only with high-strength, hard steels, generally those having yield strengths of 90,000 psi or higher. Tubing and line pipe (electric welded and seamless) are susceptible to this effect. The dominating factor is the metallurgical structure of the steel relating to its method of manufacture (PetroWiki, 2015).

SSC cracking failure requires only low concentrations of H_2S. The time to failure decreases as stress increases. Cracking tendency increases as pH decreases. SSC can be thought of in the same language as that used in describing hydraulic fracturing. There is a critical "stress intensity factor" below that at which a fracture (crack) will not propagate. This factor is related linearly to tensile strength. Some of this problem has been attributed to the effects of cold working on the alloys. Alloys that were stress relieved were found to be more resistant to SSC (Treseder and Badrack, 1997).

Wells producing hydrocarbon liquids, with the hydrogen sulfide, are less susceptible to SSC, pitting, and weight loss. For example, certain Canadian condensate wells have produced fluids with 40 mol% H_2S and 10% CO_2 for 30 years without serious corrosion problems. Stability is associated with a protective iron sulfide film, wetted by the oil/liquid hydrocarbon. These wells also had a BHT of 90 °C. Iron sulfide films are less effective in preventing corrosion above 110 °C (Treseder and Badrack, 1997).

One can recognize the sour corrosion by the black deposit, i.e., iron sulfide deposit on the surface of steel. The scale tends to cause faster corrosion because the iron sulfide plays the role of cathode, whereas the steel acts as the anode where corrosion occurs. Sour corrosion results in deep pitting on the equipment. Also, the hydrogen released in the above reaction can embrittle the steel causing sulfide stress cracking (SSC). The presence of CO_2 and/or O_2 aggravates sour corrosion. The incidents of sour corrosion in refineries vary according to the sulfur content of oil blends used. Amine units are the hot spots for sour corrosion. The following refinery units are the places where sour corrosion is considerable (http://www.ionscience.com/Pages/HydroApp.htm#B ac):

1. Amine columns
2. CDU lower reflux circuits
3. Catalytic crackers
4. Coker gas recovery systems
5. Diesel drier overhead accumulators
6. Fuel gas mixing drums and knockout drums
7. Flame knockout drums
8. Compressor suction drums
9. Gas compressors
10. Hot wells
11. Gas/oil pre-saturators, strippers, and absorbers
12. Hydrocracker reactor effluent air coolers
13. High-pressure sour gas separators
14. Low-pressure sour gas separators
15. Off-gas knockout pots
16. On-site flare knockout drums
17. Recycle gas knockout drums
18. VBU flare knockout drums
19. Sour fuel gas knockout drums
20. Sour gas gathering lines, absorber towers, knockout drums, flash drums
21. Sour water strippers
22. Sour flare lines
23. Vacuum off-gas knockout drums

6.6 Classes of Corrosion

Numerous types of steel destruction can result from the corrosion process, which are listed under the following classes of corrosion:

6.6.1 Uniform Attack

The entire area of the metal corrodes uniformly resulting in thinning of the metal. This often occurs to drillpipe, but usually is the least damaging of different types of corrosive attacks. Uniform rusting of iron and tarnishing of silver are examples of this form of corrosion attack.

6.6.2 Crevice Corrosion

Crevice corrosion is an example of localized attack in the shielded areas of metal assemblies such as pipes and collars, rod pins and boxes, tubing, and drillpipe joints. Crevice corrosion is caused by concentration differences of corrodants over a metal surface. Electrochemical potential differences result in selective crevice or pitting corrosion attack. Oxygen dissolved in drilling fluid promotes crevice and pitting attack of metal in the shielded areas of drillstring and is the common cause of washouts and destruction under rubber pipe protectors.

6.6.3 Pitting Corrosion

Pitting is often localized in a crevice but can also occur on clean metal surfaces in a corrosive environment. An example of this type of corrosion attack is the corrosion of steel in high-velocity seawater, low-pH aerated brines, or drilling fluids. Upon formation of a pit, corrosion continues as in a crevice but, usually, at an accelerated rate.

6.6.4 Intergranular Corrosion

Metal is preferentially attacked along the grain boundaries. Improper heat treatment of alloys or high-temperature exposure may cause precipitation of materials or nonhomogeneity of the metal structure at the grain boundaries, which results in preferential attack. Weld decay is a form of intergranular attack. The attack occurs in a narrow band on each side of the weld owing to sensitizing or changes in the grain structure due to welding. Appropriate heat-treating or metal selection can prevent the weld decay. Ringworm corrosion is a selective attack which forms grooves around the pipe near the box or external upset end. This type of selective attack is avoided by annealing the entire pipe after the upset is formed.

6.6.5 Galvanic or Two-metal Corrosion

Galvanic corrosion may occur when two different metals are in contact in a corrosive environment. The attack is usually localized near the point of contact.

6.6.6 Selective Leaching

Selective leaching occurs when one component of an alloy is removed by the corrosion process. An example of this type of corrosion is the selective corrosion of zinc in brass.

6.6.7 Cavitation Corrosion

Cavitation damage results in a sponge-like appearance with deep pits in the metal surface. The destruction may be caused by purely mechanical effects in which pulsating pressures cause vaporization with formation and collapse of bubbles at the metal surface. The mechanical working of the metal surface causes destruction, which is amplified in a corrosive environment. This type of corrosion attack, e.g., is found in pumps

and may be prevented by increasing the suction head on the pumping equipment. A net positive suction head should always be maintained not only to prevent cavitation damage, but also to prevent possible suction of air into the flow stream. The latter can aggravate corrosion in many environments.

6.6.8 Erosion-corrosion

The combination of erosion and corrosion results in severe localized attack of metal. Damage appears as a smooth groove or hole in the metal, such as in a washout of the drill-pipe, casing, or tubing. The washout is initiated by pitting in a crevice which penetrates the steel. The erosion-corrosion process completes the metal destruction. The erosion process removes the protective film from the metal and exposes clean metal surface to the corrosive environment. This accelerates the corrosion process. Impingement attack is a form of erosion-corrosion process, which occurs after the breakdown of protective films. High velocities and presence of abrasive suspended material and the corrodants in drilling and produced fluids contribute to this destructive process. The combination of wear and corrosion may also remove protective surface films and accelerate localized attack by corrosion. This form of corrosion is often overlooked or recognized as being due to wear. The use of inhibitors can often control this form of metal destruction. For example, inhibitors are used extensively for protection of downhole pumping equipment in oilwells.

6.6.9 Corrosion Due to Variation in Fluid Flow

Velocity differences and turbulence of fluid flow over the metal surface cause localized corrosion. In addition to the combined effects of erosion and corrosion, variation in fluid flow can cause differences in concentrations of corrodants and depolarizers, which may result in a selective attack of metals. For example, selective attack of metal occurs under the areas which are shielded by deposits from corrosion, i.e., scale, wax, bacteria, and sediments, in pipelines and vessels.

6.6.10 Stress Corrosion

The stress corrosion is produced by the combined effects of stress and corrosion on the behavior of metals. An example of stress corrosion is that local action cells are developed due to the residual stresses induced in the metal and adjacent unstressed metal in the pipe. Stressed metal is anodic, whereas the unstressed metal is cathodic. The degree to which these stresses are induced in pipes varies with (1) the metallurgical properties, (2) cold work, (3) weight of the pipe, (4) effects of slips, notch effects at tool joints, and (5) presence of H_2S gas. In the oil fields, H_2S-induced stress corrosion has been instrumental in bringing about sudden failure of drillpipes (Chilingar *et al.*, 2008).

6.7 Stress-Induced Corrosion

Because of extra energy supplied by the stress, the portion of the same metal exposed to a higher stress acts as an anode. This can be demonstrated by placing a bent nail into seawater (Figure 6.10). The initial points of corrosion attack (formation of rust) will

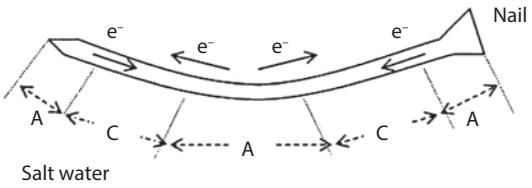

Figure 6.10 Bent nail in seawater showing the flow of electrons (and electrical current)--stress cell. (After Chilingar *et al.*, 2008, p. 41, figure 2.1.)

be the more stressed areas, i.e., the head, the point, and middle portion of the nail as shown in Figure 6.10, with discoloration of water with rust in the vicinity.

In general, the more stressed part of a metal structure acts as an anode where corrosion occurs. Thus, "stress begets rust!"

Hydrogen collects on the pipe as a film of atomic hydrogen which quickly combines with itself to form molecular hydrogen gas (H_2). The hydrogen gas molecules are too large to enter the steel and, therefore, usually bubble off harmlessly.

In the presence of sulfide, however, hydrogen gradient into the steel is greatly increased. The sulfide and higher concentration of hydrogen atoms work together to maximize the number of hydrogen atoms that enter the steel. Once in the steel, atomic hydrogen is converted to molecular hydrogen, which gives rise to a high stress in the metal (hydrogen-induced stress). Presence of atomic hydrogen in steel reduces the ductility of the steel and causes it to break in a brittle manner.

The amount of atomic hydrogen required to initiate sulfide stress cracking appears to be small, possibility as low as 1 ppm. Sufficient hydrogen must be available, however, to establish a differential gradient required to initiate and propagate a crack. The H_2S concentration as low as 1–3 ppm can produce cracking of highly stressed and high-strength steels (Wilhelm and Kane, 1987).

According to Cron and Marsh (1983, p. 1035), very low concentrations of H_2S (0.1 ppm) and low partial pressures (0.001 atm) can cause SSC. The time to failure is decreased with increasing concentration of H_2S and increasing stress. Maintaining a high temperature prevents cracking, because SSC does not occur at temperatures above ≈180 °F.

Stress-corrosion cracking can occur in most alloys, and the corrodants which promote stress cracking may differ (few in number for each alloy). Cracking can occur in both acidic and alkaline environments, usually in the presence of a chloride ion and/or oxygen.

Engineers should monitor the condition of tubular goods (casing, pipelines, etc.) in areas that are subsidence-prone due to fluid (oil, water) withdrawal (see Chilingar *et al.*, 2013). Faults and fractures form as a result of subsidence, which can cause appreciable stress in the casing. In turn, stressed metals are corrosion-prone.

6.7.1 Cracking in Drilling and Producing Environments

Hydrogen embrittlement (sulfide cracking) and corrosion fatigue are two forms of cracking that are associated with drilling and producing environments.

6.7.1.1 *Hydrogen Embrittlement (Sulfide Cracking)*

Hydrogen embrittlement occurs as a sudden cracking of metal, caused by the entrapment of hydrogen within the lattice structure. The cracking of the metal may proceed in a stepwise rupturing manner. The corrosion process in an acid environment produces atomic hydrogen:

$$Fe + 2H^{+} \rightarrow Fe^{2+} + 2H^{0} \quad \text{(atoms)} \tag{6.40}$$

$$Fe - 2e^{-} \rightarrow Fe^{2+} \quad \text{(anode)} \tag{6.41}$$

$$2H^{+} + 2e^{-} \rightarrow 2H^{0} \quad \text{(cathode)} \tag{6.42}$$

Some of the hydrogen atoms that are formed in the cathodic reaction penetrate the metal with subsequent formation of molecular hydrogen. The remaining hydrogen atoms combine to form molecules of hydrogen gas at the metal surface. The adsorption of hydrogen atoms by the metal causes a loss in ductility and cracking of high-strength steels.

Materials which interfere with the pairing of atoms of hydrogen to form hydrogen gas at the cathodic areas of metal enhance the penetration of atomic hydrogen into the steel. Hydrogen sulfide in drilling fluids supplies sulfide ions, which prevent the pairing of hydrogen atoms to form hydrogen gas. Thus, the penetration of atomic hydrogen into steels is promoted by the presence of hydrogen sulfide. The time to failure by hydrogen embrittlement is shortened by increasing:

1. Concentration of hydrogen sulfide
2. Stress
3. Strength and hardness of steel

This behavior was studied by Hudgins *et al.* (1966). The embrittlement (sulfide stress cracking [SSC]) occurs generally in steels with yield strengths above 90,000 psi or above Rockwell C-20-22 hardness. Lower-strength steels are not subject to SSC; however, they are subject to hydrogen blistering.

6.7.1.1.1 Hydrogen Blistering

Hydrogen penetration into low-strength steel may cause blistering, which appears as bumps on the metal surface. The hydrogen atoms form hydrogen molecules at points of defect in the metal. The hydrogen gas cannot penetrate into nor escape from the crystalline structure. The pressure of hydrogen gas increases sufficiently to part the metal, create a void, and raise a blister on the steel surface.

6.7.1.2 *Corrosion Fatigue*

Cyclic stresses at high levels cause fatigue failure of metal. In a corrosive environment, the progress of fatigue is accelerated by the electrochemical corrosion. Corrosion fatigue is the combined action of corrosion and fatigue (cyclic stressing), which results in early fracture of metal. Corrosion fatigue is a principal cause of drillpipe failures. By establishing limits to the stresses repeatedly applied to metal, fracture by metal fatigue in a noncorrosive environment can be avoided. The *endurance limit* is the maximum

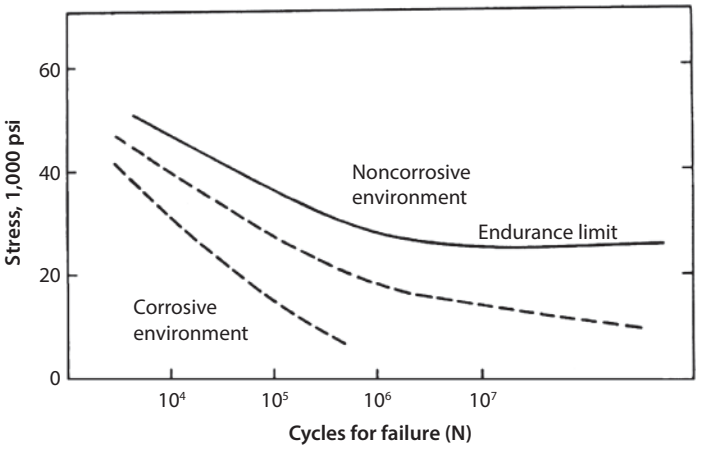

Figure 6.11 Relationship between endurance strength of steel (stress) and number of cycles needed for the occurrence of failure in corrosive and noncorrosive environments. (Modified after Bertness, 1957, p. 131, figure1. In: Chilingar *et al.*, p. 45, figure 2.4.)

cyclic stress level which can be applied to a metal without a fatigue failure. In an environment with continued corrosion, instead of exhibiting an endurance limit, metal will fail due to the growth of corrosion fatigue cracks. The time to failure or number of stress cycles necessary to cause failure is decreased with increasing severity of corrosive environment and level of stress as illustrated in Figure 6.11.

Corrosion fatigue is enhanced by corrodents in a corrosive environment which cause pitting of steel, such as oxygen and acid gases (H_2S and CO_2), which are often present in drilling and produced fluids. Increasing the strength of steels will not improve the resistance to corrosion fatigue. Instead, it may shorten the number of cycles to failure.

High-strength steels are more susceptible to pitting than the low-strength steels.

Notches or scratches, such as the ones caused by tongs or slips, and corrosion under protectors will accelerate corrosion fatigue failure.

Inhibitors, which reduce the corrosion and the entry of corrosion-generated hydrogen into the rods, can reduce the frequency of corrosion fatigue failures provided that stress is within a reasonable range. Examples of field test of inhibitors for control of corrosion fatigue are discussed by Martin (1980, 1983).

6.8 Microbial Corrosion

The term microorganism encompasses five major groups of organisms (Bryant *et al.*, 1989, p. 423):

1. Viruses
2. Fungi
3. Algae
4. Protozoa
5. Bacteria

These are organisms that exist as an individual cell or undifferentiated aggregates of cells (cells that are not differentiated into tissues that have distinct functions). The size of these microbial cells is so small that a microscope is required for observation. The viruses are the smallest form of recognized microbial life. They are not cells because they differ in many respects from the multifunctional cells: the viruses are much simpler in structure containing only protein and nucleic acid surrounded by a lipid or protein membrane and they do not reproduce by growth followed by division as cells do. Viruses must use other living cells in order to reproduce (Bryant *et al*., 1989).

A second division of microorganisms is the eukaryotic microbes which include:

1. Fungi
2. Algae
3. Protozoa

Eukaryotic microbes are distinguished from viruses and bacteria by virtue of possession of true nucleus, which is enclosed by a membrane that contains the genetic material of the cell (the deoxyribonucleic acid [DNA]), organized into structures known as chromosomes. Eukaryotic microorganisms also have specialized organelles in their cells, such as Golgi bodies that conduct specialized functions of transport of materials within the cell and secretion of materials to the exterior (Gaudy and Gaudy, 1980). Although eukaryotic microbes are probably responsible for some microbial plugging problems of injection wells, they are not important to enhanced oil recovery processes at this time; therefore, the reader is referred to the literature for additional information on them (Bryant *et al*., 1989).

The third division of microorganisms that can be distinguished by its physical characteristics is the prokaryotes (bacteria). The prokaryotes are in general about 10 times smaller than eukaryotes and the structural features within the cells are not distinguishable with an optical microscope. The intracellular features of some prokaryotes can be observed by staining, but an electron microscope is required for detailed structural observation. The only food utilized by prokaryotes (bacteria) comprises soluble molecules that can be assimilated through the cell wall. On the other hand, the eukaryotic protozoa contain a flexible membrane that can surround particles of food to form a vacuole where digestion of the food takes place (Bryant *et al*., 1989).

Bacteria have two distinctive structural features: (1) a rigid cell wall that determines the shape of the organisms, which may be either cylindrical or spherical; and (2) flagella which are responsible for the movement of mobile organisms. Differences in the cell walls of bacteria furnish the basis for classification into two broad groups: gram-positive and gram-negative bacteria. The cell wall of gram-positive bacteria consists of multiple layers of peptidoglycan, cross-linked through amino acid bridges, and teichoic acids bonded to the peptidoglycans. The three-dimensional network of molecules provides a strong (rigid) structure. The wall of the gram-negative bacteria also contains peptide glycan; however, the wall is very thin and surrounded by a lipid layer of lipoprotein and lipopolysaccharide, sometimes referred to as the outer membrane. Different bacterial morphologies are shown in Figure 6.12.

There are many species of bacteria having a variety of sizes and shapes. Some have flagella that are used for movement within an aquatic environment. Bacteria that are

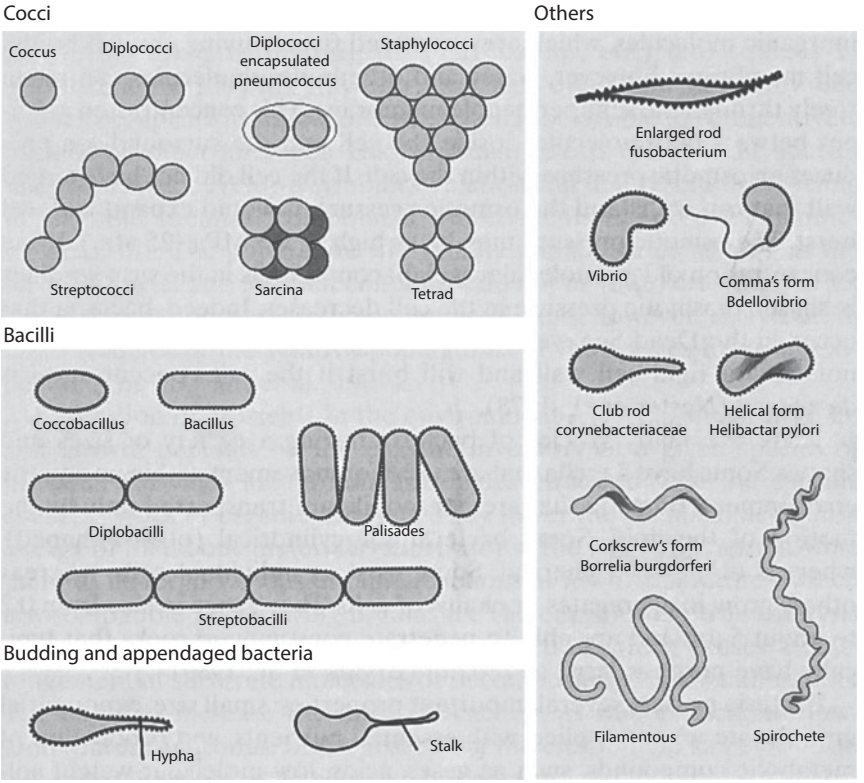

Figure 6.12 Schematic diagrams of bacterial morphology. (http://en wiki edia.org.)

not mobile are transported only by motion of the fluid. Some bacteria are cylindrical (or rod-shaped), whereas others are spherical. Some exist as individual cells, whereas others grow in aggregates or chains of cells. They range in size from 0.2 to about 5 μm and are able to penetrate consolidated rocks that typically have pores as large as 100 μm (Bryant *et al.*, 1989).

Bacteria possess several important properties: small size, exponential growth rate when supplied with essential nutrients, and production of metabolic compounds, such as gases, acids, low-molecular-weight solvents, surfactants, and polymers. Various types of bacteria also tolerate harsh environments similar to those encountered in subsurface geological formations, such as high salinity, high pressure, and high temperature. Also, many bacteria are anaerobic (grow in the absence of oxygen).

Populations of microbes are found everywhere in nature; in fact, they are even found in areas that will not support life. The actual species growing in a particular environment comprise those that have been able to successfully adapt to the prevailing environmental and nutritional conditions and the extremes of variations of those conditions. They also have been the most successful in competition with other microbes that may have entered the particular ecosystem. There may be several species living in an area, apparently as a homogenous population.

In assessing microbial nutrient requirement and their metabolic products, it is more appropriate to classify the microbes according to their ability to utilize oxygen, as

discussed previously. Numerous cultures (pure and mixed) are capable of synthesizing a variety of biochemical products using petroleum fraction and substrates. The range of metabolic products from microbial consumption of petroleum is very broad, depending on (Bryant *et al.*, 1989):

1. Pressure
2. Temperature
3. Salinity
4. pH
5. Presence or absence of oxygen
6. Supporting nutrients available for cell metabolism (nitrogen, phosphorus, minerals, etc.).
7. The specific bacterial cell interaction with petroleum (Donaldson and Clark, 1982).

Obligate aerobes are organisms that must have oxygen for their metabolism and growth, but they can exist dormant in the absence of oxygen. The bacteria decompose sugars to energy, carbon dioxide and water, and often acids: $C_6H_{12}O_2 + 8O_2 = 6CO_2 + 6H_2O$ + energy. When the microbes are furnished with hydrocarbons and an ample supply of oxygen, a wide variety of products will result which depend on:

1. The type of microbe
2. Environmental conditions
3. The specific type of hydrocarbon substrates

The products may be carbon dioxide, low-molecular-weight acids, phenols, or biopolymers (proteins, polyanionic, lipids, glycolipids, or polysaccharides). The compounds are waste product from the microorganisms and some may even be toxic if accumulated in the surrounding fluid.

Obligate anaerobes cannot utilize free oxygen; in fact, small quantities of oxygen (10 ppm) are even toxic to some anaerobes. Spores produced by some anaerobes, however, can remain dormant for long periods in aerobic environment, germinating when they enter anaerobic environments. The anaerobes use low-molecular-weight organic compounds, such as sugars, as a source of carbon and energy. In the process of metabolism, the microbes release various products. Sugars undergo anaerobic fermentation yielding acids, alcohols, ketones, aldehydes, carbon dioxide, and hydrogen. Some species of anaerobic genus *Clostridium* have been found to produce all these compounds (Grula *et al.*, 1983). These anaerobes also may reduce sulfur occurring as inorganic sulfates, or as part of the molecular structure of organic compounds, to hydrogen sulfide. Petroleum reservoirs have been known to become sour (produce large quantities of H_2S with the hydrocarbons) when infected by *Desulfovibrio* bacteria from injected water in secondary recovery (Crawford, 1983). Anaerobes also can produce chemicals, some of which are surface-active agents that lower the oil-water interfacial tension and promote emulsification of oil. The anaerobic bacteria also may produce biopolymers (primarily polysaccharides).

Facultative bacteria can change their metabolism for growth either in an oxidizing or reducing environment. Their products of metabolism are quite similar to those

described above. They may produce hydrogen sulfide from organic sulfides and inorganic sulfates, and reduce the low-molecular-weight compounds (sugar, aldehydes, etc.) to methane, hydrogen, and carbon dioxide. In some environments, they produce biosurfactants and biopolymers.

The three classes of bacteria mentioned above are generally mesophilic (existing within a temperature range of 20–50 °C). There are also thermophilic and caldoactive bacteria that can live at temperatures ranging from 40 to 100 °C. They reduce sugars and other carbohydrate compounds to methane and carbon dioxide, while reduction of sulfur compounds yields hydrogen sulfide. They are used in the secondary (anaerobic) treatment of sewage (Bryant *et al*., 1989).

6.8.1 Microbes Associated with Oilfield Corrosion

A great deal of the early work by microbiologists working with petroleum was oriented toward the control of the deleterious effects of microorganisms in oilfields. Numerous reports of the presence of microbes in reservoirs have been published (Crawford, 1983; Lazar and Constantinescu, 1985; Singer, 1985). These reports discuss the microbial population increases that occur with application of secondary oil recovery methods where the injected water is exposed to the atmosphere in open ponds. Lazar and Constantinescu (1985) found abundant microbial flora indigenous in oilfield formation waters, which included species of *Bacillus, Pseudomonas, Micrococcus, Mycobacterium, Clostridium, and Escherichia*. Spore-forming bacilli and some cocci were usual bacteria found in deep reservoirs, whereas aerobic pseudomonas and facultative anaerobes were the dominant species in shallow reservoirs. Pseudomonas are one of the most difficult microbes to control in industrial water systems; they exhibit a high rate of growth and can produce a slime that apparently protects them from biocides to some extent and also results in plugging of the reservoir rock pores (Chakrabarty, 1982). *Escherichia* is reported to contain hydrogenase, an enzyme that utilizes molecular hydrogen and may be associated with cathodic hydrogen depolarization, causing corrosion of steel casings and pipes in the oilfield. Natural mixed population of microorganisms growing in oil wells and in petroleum reservoirs produce chemicals that corrode production equipment and plug reservoirs. Sulfate-reducing bacteria cause a sweet crude to turn sour (produce hydrogen sulfide), which has happened in the Wilmington Oilfield, CA (Gates and Parent, 1976).

Several patents deal with biocides that are recommended for injection into reservoirs to control indigenous microbial flora. Some examples of these biocides include formaldehyde, benzene, toluene, and several quaternary ammonium compounds (Jack and Thompson, 1983). Other processes involve the use of physicochemical methods for bacterial control, including treatment of refinery waste waters and filtering of injection water to remove microorganisms.

Many corrosion problems in the oilfield are caused by hydrogen sulfide produced *in situ* by *Desulfovibrio*. The hydrogen sulfide also reacts with iron in the reservoir, producing ferrous sulfide which oxidizes to ferric sulfide in the produced water.

Bacteria that form slime (some form of polysaccharides), such as *Achromobacter* sp. and *Flavobacterium* sp., will adhere to each other forming a large mass. They also adhere to the walls of the pores, causing severe plugging problems at injection wells (McCoy and Costerton, 1982).

Ivanov and Belyaev (1983) showed that a population of aerobic bacteria around the injection well, which is receiving oxygen and nutrients dissolved in the injected water, produce low-molecular-weight oxygen compounds. The latter are utilized as essential food for growth by *Desulfovibrio* and other anaerobic bacteria in the oxygen-depleted region beyond the vicinity of wellbore.

6.8.2 Microbial Interaction with Produced Oil

Microorganisms have been shown to be normal inhabitants of interstitial waters (Singer, 1985). Microbial metabolism on petroleum in the subsurface, particularly where surface waters carry oxygen and nutrients to the oil deposit, can reduce the value of the crude oil because the aerobic bacteria use the paraffin as carbon source (Crawford, 1983). A staff report in World Oil (Anonymous, 1972) claimed that 10% of the world's crude oil has been destroyed, and another 10% considerably reduced in value by microorganisms.

Singer *et al*. (1983) reported that microbial oxidation of specific sulfur- or nitrogen-containing components of crude oil is feasible. Microorganisms that oxidize specific sulfur- and nitrogen-containing aromatic compounds in crude oils have been isolated. These isolates exhibit specificity for sulfur- and nitrogen-containing aromatic compounds. They are unable, however, to oxidize or grow on a variety of other hydrocarbons, including aliphatic alkanes, cycloalkanes, and mono-polynuclear hydrocarbons. Isolates identified to date can metabolize only under strictly aerobic conditions. In a related study, Fedorak *et al*. (1983) found that several isolates of pure and mixed bacterial cultures could degrade the aromatic compounds in Prudhoe Bay oil.

Inasmuch as microbial enhanced oil recovery (MEOR) is gaining in popularity, corrosion engineers should become more familiar with microbial corrosion (see Donaldson *et al*., 1989).

6.8.3 Microorganisms in Corrosion

Involvement of microorganisms is the main distinction between abiotic corrosion and microbial corrosion which forms a biofilm layer at the metal-solution interface. Microorganisms change the surrounding environment of the metal surface and consequently enhance and facilitate the corrosion process.

The most common microorganisms found in the oilfield waters are presented in Table 6.3.

6.8.3.1 Prokaryotes

Bacteria are prokaryotic microorganisms. The bacteria involved in the corrosion process are a part of the sulfur cycle in nature. Aerobic *Thiobacillus* is a well-known bacteria causing corrosion. Due to their metabolic activity, they oxidize sulfur and produce sulfuric acid. They proliferate in the soils near sulfur plants and in conduits with sour produced water. According to Videla (1996, p. 34), there are two types of processes involved in the sulfur cycle:

1. Assimilatory sulfate reduction
2. Dissimilatory sulfate reduction

Table 6.3 Microorganisms found in oilfield waters. (Modified after Jones, 1988, p. 130.)

Microorganism	Definition, activity, and control
Sulfide-producing bacteria	Most important is *Desulfovibrio dsesulfuricans*, the sulfate reducer that metabolizes sulfate ions ($SO_4^{=}$) in water to form H_2S. Controlled by limiting aerobic bacteria growth and biocides treatment. Thermophilic *Clostridium nigrificans* sulfide producer: also *Clostridium tetani*.
Iron bacteria	Composed of bacteria cells, surrounded by gelatinous iron oxide excretion. Controlled via chemical treatment of producing sand; detergent-acid treatment. *Gallionella*, *Crenothrix* and *Sphaerotilus* are common genera.
Slime formers	Aerobic and facultative bacteria and fungi. Controlled by elimination of dissolved oxygen and treatment with biocides. *Pseudomonas*, *Flavobacterium*, *Nocordia*, *Aspergillus*, *Aerobacter*, and *Micrococcus* are common genera.
Sulfur oxidizers	Oxidize sulfur and produce sulfuric acid. Aerobic bacteria. Examples of genera are *Beggiatoa* and *Thiobacillus*. Controlled best by removing the sulfur nutrient.
Algae and diatoms (plants)	Grow in open and sunlit waters; green-color slimes. Controlled by copper compounds.
Protozoa	Live on smaller organisms in contaminated, open aqueous environments. Controlled with biocides

In the assimilatory sulfate reduction, sulfate is used by microorganisms as the sulfur source in metabolic process involving reduction of sulfates to organic sulfides. On the other hand, in the dissimilatory sulfate reduction, sulfate is used as the terminal electron acceptor to produce hydrogen sulfide in the anaerobic respiration. *Desulfovibrio desulfuricans* is one of the most famous corrodents of the former category.

Iron-oxidizing bacteria are microorganisms that are involved in the corrosion process. These bacteria generally oxidize Fe^{2+} to Fe^{3+}, which usually precipitates as ferric hydroxide. The families of microorganisms include:

1. *Caulobacteraceae*
   a. *Gallionella*
   b. *Siderophacus*
   c. *G. ferruginea*
2. *Clamidobacteriaceae*
   a. *Sphaerotilus*
   b. *Leptothrix*
3. *Crenothiaceae*
   a. *Crenothrix*
   b. *Clonothrix*

6.8.3.2 Eukaryotes

As mentioned earlier, the main eukaryotic microorganisms are fungi, algae, and protozoans. The most well-known fungus associated with microbial corrosion is *Hormoconis resinae*, which can grow on a wide range of organic compounds including hydrocarbons. According to Videla (1996, p. 41), the *Hormoconis resinae* (1) facilitate the formation of pits at the fixation points of tank walls, (2) produce organic acids (which are corrosive to aluminum), (3) consume nitrates, and (4) create redox conditions for passivity breakdown.

In the case of algae, corrosion occurs as a result of metabolic production of oxygen (algae produce oxygen when exposed to light photosynthesis). Some species produce organic acids. Corrosion generally occurs as blockage of pipes in cooling water towers, creating pH changes which affect water treatment efficiency (Videla, 1996). Among the algae associated with microbial corrosion, the most relevant are *Navicula, Oscillatoria*, and *Ulothrix*.

6.8.4 Different Mechanisms of Microbial Corrosion

According to Videla (1996), microbial corrosion involves different kinds of mechanisms:

1. Production of compounds, due to metabolic bacterial activities, which change the medium to a corrosive one.
2. Respiration characteristics.
3. Consumption of corrosion inhibitor.
4. Acceleration of corrosion reaction rate at the anode and cathode.
5. Removal of the protective film on metal surfaces.

Microorganisms can produce surfactants, inorganic acids, carboxylic acids, or sulfide ions (in the case of sulfate-reducing bacteria (SRB), which will convert the environment to highly corrosive.

Microorganisms can also increase the corrosion rate at the anode and cathode. At the anode, organic acid production by different types of fungi causes corrosion, whereas sulfide anions are produced as a consequence of dissimilatory reduction of sulfates by SRB in anaerobic conditions. In the case of sulfate-reducing bacteria, the production of H_2S at the cathode facilitates corrosion.

As shown in Figure 6.13, sulfate reducers can also proliferate under a layer of aerobic organism slime deposit in aerated water.

6.8.5 Corrosion Inhibition by Bacteria

Some bacteria can also inhibit corrosion. The inhibition generally occurs as a result of biofilm formation on the surfaces of metals or alloys, which slows down anodic and/or cathodic reactions. The biofilm increases the electrolyte resistance of the circuit.

Microorganisms' respiratory metabolic processes can also modify the oxygen concentration at the metal--solution interface (see Videla, 1996, p. 122).

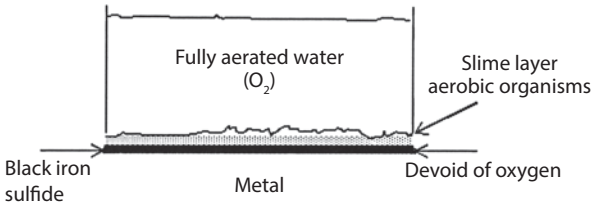

Figure 6.13 Schematic diagram of sulfide corrosion under aerobic slime deposit. Corrosion of iron by H_2S, generated by sulfate reducers. (After Chilingar *et al.*, 2008, p. 64, figure 3.4.)

Table 6.4 Bacterial control agents. (After Jones, 1988, p.134; in: Chilingar *et al.*, 2008. table 3.2, p. 65.)

Bacterial control Agents:
Alkyl-aryl quaternary ammonium chlorides
Chlorine-hypochlorites[1]
Aldehydes
Chlorinated phenols
Fatty amines and salts
Alkyl thiocarbamates
Acrolein

[1]See Henry and Heinke (1996) for details

There are three types of bioinhibitors:

1. Bioinhibitors with oxidizing properties
2. Bioinhibitors dissolving oxygen to form a biofilm
3. Adsorption-type bioinhibitors

Guiamet *et al.* (1987) and Videla *et al.* (1988) have reported that *Serratia marcescens* decreases the medium corrosiveness.

6.8.6 Microbial Corrosion Control

Methods for controlling the microbial corrosion include:

1. Use of biocides
2. Use of corrosion inhibitors
3. Cathodic protection
4. Material selection

Inasmuch as most of the corrosion inhibitors are either expensive or harmful to humans and the ecosystem, only few chemicals are being used in oilfield and water transport systems. Some of these chemicals are presented in Table 6.4.

A biocide is a chemical substance capable of killing different forms of living organisms. Biocides are used in the fields of agriculture, forestry, and mosquito control. There are two main categories of biocides:

1. Antimicrobials: include germicides, antibiotics, antibacterials, antivirals, antifungals, antiprotozoans, and antiparasites (also spermicides).
2. Pesticides: include fungicides, herbicides, insecticides, algicides, molluscicides, miticides, and rodenticides.

Biocides can also be added to other materials (typically liquids) to protect the material from biological infestation and growth. For example, certain types of quaternary ammonium compounds (quats) can be added to pool water or industrial water systems to act as an algicide, protecting the water from infestation and growth of algae. Chlorine can be added in low concentrations to water as one of the final steps in wastewater treatment as a general biocide to kill microorganisms, algae, etc. It is often impractical to store and use poisonous chlorine gas for water treatment, so alternative methods of effectively adding chlorine are used. Adding hypochlorite solutions to pools, etc., is one possible solution. Hypochlorite can gradually release chlorine into the water (see Henry and Heinke, 1996, for details). Even more convenient are compounds such as sodium dichloro-s-triazinetrione (dihydrate or anhydrous), sometimes referred to as dichlor, and trichloro-s-triazinetrione, sometimes referred to as trichlor. These compounds are stable while solid and may be used in powdered, granular, or tablet form. When added in small amounts to pool water or industrial water systems, the chlorine atoms hydrolyze from the rest of the molecule forming hypochlorous acid (HOC1), which acts as a general biocide killing germs, microorganisms, algae, etc. Halogenated hydantoin compounds are also used as biocides (http://en.wikipedia.org/).

Chlorine gas hydrolyzes in water to form hypochlorous acid (prime disinfecting agent):

$$Cl_2 + H_2O \leftrightarrow HOC1 + H^+ + Cl^- \tag{6.43}$$

Hypochlorous acid, in turn, dissociates into H^+ and hypochloritc (OCl^-).

$$HOC1 \leftrightarrow H^+ + OC1^- \tag{6.44}$$

HOC1 plus OCl^- are called free available chlorine, available for disinfection.

Disinfection of water by ozone (O_2) is called ozonation. Ozone is a powerful oxidizer of inorganic and organic impurities and is effective against *Cryptosporidium*.

Ultraviolet (UV) radiation is not very effective for turbid effluent and is relatively expensive compared to chlorination. Its advantage is the fact that no chemical residues are left after treatment.

6.9 Corrosion Related to Oilfield Production

There are many sources of corrosion in the oilfield industry. There are also many ways that the rate of corrosion can be reduced or slowed down. This section examines several methods of slowing the process down for various types of oilfield operations.

6.9.1 Corrosion of Pipelines and Casing

Pipelines and well casing are similar in the fact that they both consist of iron pipe which is susceptible to internal and external corrosion. As noted by the Corrosion Doctors

(Corrosion Doctors, 2015), in some instances, pipe can deteriorate slowly, e.g., in certain cases some pipeline life has been reliably targeted at 70 years or more, while other pipelines have been built which have exhausted their useful life after 1 year of operation. Apart from the quality of the construction, coatings, inhibitors, cathodic protection systems, etc., the factors which affect pipeline life include nature of the product, nature of the external environment, operating conditions and quality of maintenance.

In the early 1990s there was recognition of the increasing threat of corrosion to pipeline integrity as the pipelines aged (Corrosion Doctors, 2015):

1. Corrosion was the major cause of reportable incidents in North America.
2. Corrosion was the major cause of pipeline failures in the Gulf of Mexico.
3. Corrosion in one pipeline in North America required over $1 billion in repairs.

The corrosion-related cost to the transmission pipeline industry is approximately $5.4 to $8.6 billion annually. This can be divided into the cost of failures, capital, and operations and maintenance (O&M) at 10%, 38%, and 52%, respectively. The environmental cost was not included in these figures.

Internal corrosion of metal (pipe) in the presence of water is a typical problem. In fact, most oil and gas production includes co-produced water which makes corrosion a pervasive issue throughout the industry. Age of pipe and presence of corrosive materials such as carbon dioxide (CO_2) and hydrogen sulfide (H_2S) can exacerbate this problem. The external and internal pipe corrosion may be caused by the presence of one or combination of the following (Rahman and Chilingarian, 1995):

1. Presence of corrosive formation water (having high salinity).
2. Presence of bacterially generated H_2S
3. Presence of electrical currents
4. Presence of corrosive completion fluids
5. Presence of faults which cross the borehole (this gives rise to weak, damaged steel zones susceptible to corrosion).

In oilfields, electrolytic corrosion is the primary source of casing corrosion. The current flow may originate from (1) potential gradients between the formations traversed by the casing, (2) potential difference between the well casing and long flowline, or (3) electrical grounding systems and connecting flowlines.

The origin of stray currents is not always easy to determine. The use of a voltmeter across an open flowline-to-wellhead flange, however, will show whether or not the electrical current is entering the well, i.e., whether or not electrons are leaving the casing.

6.9.2 Casing Corrosion Inspection Tools

A variety of tools and interpretation techniques are employed to monitor corrosion because a large amount of information is required for interpretation from both single and multiple casings. Four types of tools are considered here (Cryer *et al.*, 1987):

1. Electromagnetic casing corrosion detection
2. Multi-finger caliper tool (mechanical)
3. Acoustic tool
4. Casing potential profile tool

6.9.3 Electromagnetic Corrosion Detection

In essence, electromagnetic corrosion detection tools consist of a number of electromagnetic flux transmitters and receivers that are linked by the casing string(s) in much the same way as the core in a transformer links the primary and secondary coils (see Rahman and Chilingarian, 1995).

For a qualitative measure of the average circumferential thickness of multiple casings (Cryer *et al.*, 1987), the phase shift between the transmitted and received signals is measured. The phase shift related to the thickness of the casing is as follows:

$$\phi = 2\pi t\sqrt{\mu\sigma f} \tag{6.45}$$

where t = combined thickness of all casings, σ = combined conductivity of all casings, μ = combined magnetic permeability of all casings, and f = tool frequency.

By increasing f, the depth of investigation can be reduced to include only the inner casing and values of σ and μ can be determined. Increasing f still further provides an accurate measure of the ID of the inner casing string. All three measurements can be made simultaneously to provide an estimate of overall view of material losses.

For a more detailed analysis of the inner casing string, a multi-armed pad-tool can be used which generates a localized flux in the inner wall of the casing by means of a central, high-frequency, pad-mounted signal coil. Flux distortions, measured at the two adjacent receivers or "*measure*" coils, are indicative of inner pipe corrosion.

In a second measurement, electromagnets located on the main tool body generate a flux in the inner casing. Again, the presence of corrosion will induce a flux leakage, which is measured by the two measure coils. This measure is a qualitative evaluation of total inner casing corrosion.

6.9.4 Methods of Corrosion Measurement

The multi-finger caliper tool consists of a cluster of mechanical feelers that are distributed evenly around the tool. Each of these feelers gives an independent measurement of the radius. The small size of feelers allows small anomalies in the inner casing wall to be detected and measured. The multi-finger caliper gives an accurate representation of the changes in the internal diameter of the casings (Watfa, 1989; in: Rahman and Chilingarian, 1995).

6.9.5 Acoustic Tool

The acoustic tool consists of eight high-frequency ultrasonic transducers. The transducers act as receiver and transmitter, as two measurements are obtained from each

transducer: (1) internal diameter, which is measured from the time interval of signal emission to the echo return; and (2) the internal casing thickness.

6.9.6 Potential Profile Curves

Corrosion damage to the casing can be detected easily using the casing potential profile tool. This tool measures the voltage drop (IR drop) across a length of casing (e.g., 25 ft) between two contact knives (see Figure 6.14).

Logging (from bottom to the top) is done at intervals equal to the spacing of the knife contactors. Voltage (IR) drops are then plotted versus depth (casing potential profile). As shown in Figure 6.14, readings on the left (–) side of zero indicate that current flows down the pipe, whereas positive values (+) show that flow is upward. Consequently, the curve sloping to the left from the bottom indicates a corroding zone (anode), where electrons are leaving the casing (see Jones, 1988).

6.9.7 Protection of Casing and Pipelines

As pointed out by Jones (1988), the primary causes of external casing corrosion are: (1) corrosion by completion fluids, (2) aggressive formation water, (3) bacterially generated H_2S, and (4) electrical currents. Casing can be protected by one or combination of the following:

1. Using wellhead insulator (electrical insulation of well casing from the flowline).
2. Cementation (placement of a uniform cement sheath around casing).

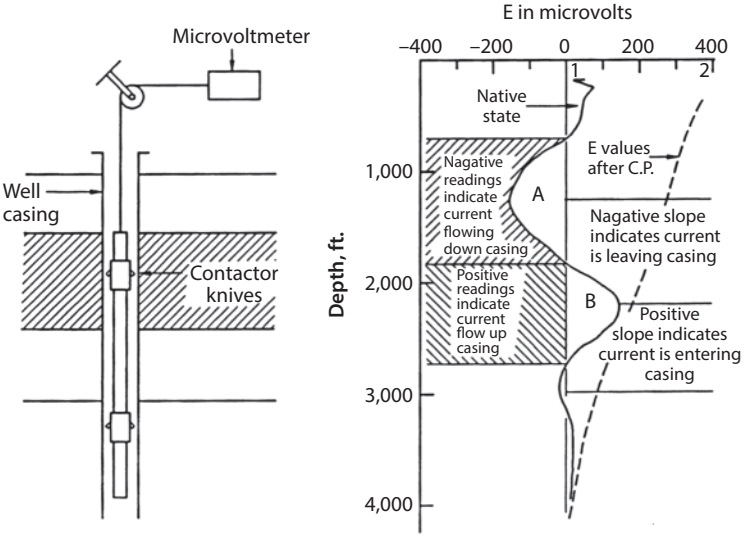

Figure 6.14 Casing potential profile test equipment and example of plotting data. Modified after Jones, 1988, p. 66, figures 1 & 2; in: Chilingar *et al.*, 2008, p. 102, figure 5.3.)

3. Placing completion fluids around casing which has not been cemented (these fluids should be oxygen-free, high-pH, and thixotropic).
4. Cathodic protection
5. Proper choice of steel grades

Wellhead insulation – Use of electrical insulation stops current flow down the casing from the surface and reduces both internal and external casing corrosion. Dielectric insulation materials for both screw and flange joints are commonly used to insulate casing from flowlines. Insulation of wells by connecting them to a single battery is often recommended. It should be noted that when the flowline is at high potential due to cathodic protection, it may induce interference corrosion. In this case, the insulating joints may be partially shunted or wellhead potential elevated by attaching a sacrificial anode (Figure 6.15). Heat-resistant material should be selected for hot, high-pressure wells to prevent failure of insulation materials (also see Jones, 1988, p. 64).

Cementation – In addition to wellhead insulation, the best available procedure of reducing casing failure due to external corrosion is placement of a uniform cement sheath opposite all formations, containing aggressive waters, e.g., formation waters rich in chlorine and sulfate. Diffusional supply of chlorine and sulfate ions to the surface of the casing can be inhibited by reducing porosity and permeability of the cement sheath. Most API oil well cements contain tricalcium alumina, which forms complex salts of calcium chloroaluminate upon contact with chlorine ions, and calcium sulfoalumina hydrates upon contact with sulfate ions. Both of these reaction products lead to the formation of porous and permeable set cement. Upon long exposure to these environments, the cement matrix begins to deteriorate and ultimately collapses, leaving the casing without any protection (Rahman and Chilingarian, 1995).

Full-length cementing of surface casing and production casing is advisable, especially for deep wells. Pozzolan blended ASTM type I cement (API Class B or C), which is resistant to chlorine and sulfate attack and at the same time develops strong cement matrix, can be used, for example. Additives such as fuel ash, blast furnace slag, or silica

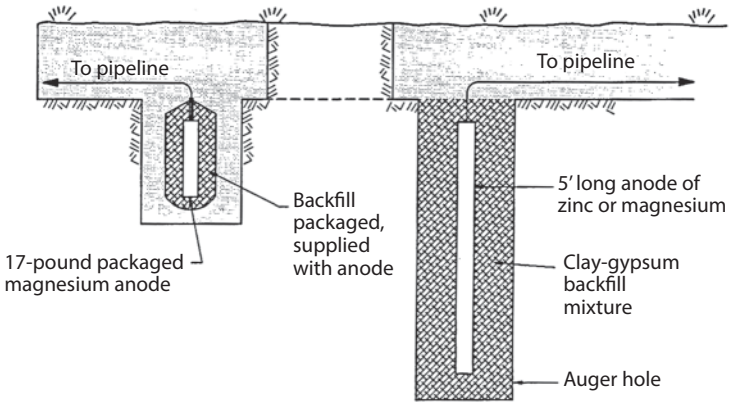

Figure 6.15 Installation of galvanic anodes. (Modified after NACE, Houston, TX, Control of Pipeline Corrosion, 1979, figure 8.6; in: Chilingar *et al.*, 2008, p. 103, figure 5.4.)

flour are added to the cement to improve its properties (porosity, permeability, and strength) (Chilingar *et al*., 2008).

6.9.8 Casing Leaks

In repairing the casing leaks in casing or pipelines, one can either:

1. isolate the leak with a packer (inexpensive), or
2. replace the pipe, e.g., casing (much more expensive).

Casing leaks can cause loss of production and, possibly, eventual loss of a well. The log of cumulative leaks is often a linear function of time (Figure 6.16). The curve is often an approximate one, because in many situations casing leaks can go undetected for a long time. In many cases, however, the extrapolation of the leak frequency versus time curve is surprisingly accurate and can aid in economic analysis (feasibility of cathodic protection).

As pointed out by Cron and Marsh (1983), it is important to determine whether the leaks are due to external or internal corrosion, because cathodic protection can prevent only the external corrosion. In their classical paper, Cron and Marsh (1983, p. 1036) also stated that electrical insulation at wellhead may interrupt a current as high as several amperes. It is important to insulate the casing completely from the large surface structures or apply cathodic protection to these structures as well.

6.9.9 Cathodic Protection

Cathodic protection is used in many oilfields to protect the pipe against internal and external corrosion (see Figure 6.17). Corrosion occurs at the anode, as electrons leave the anodic area and move toward the cathodic areas. If electrons are forced into the anodic areas, corrosion will not occur.

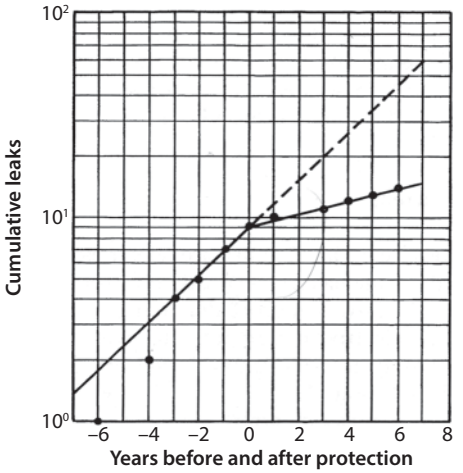

Figure 6.16 Leak frequency, Clairmont Field, Kent County, TX. (After Kirklen, 1973, figure 4; in: Chilingar *et al*., 2008, figure 5.5, p. 107.)

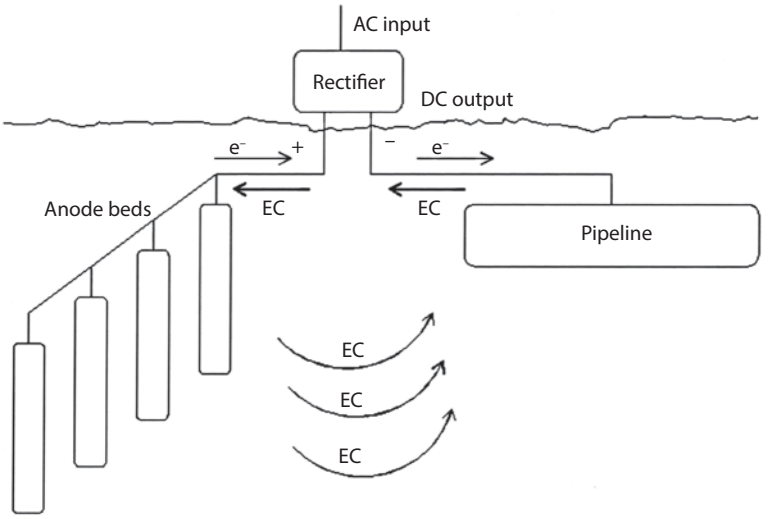

Figure 6.17 Schematic diagram of cathodic protection for a pipeline. (In: Chilingar *et al.*, 2008, p. 73, figure 4.2.)

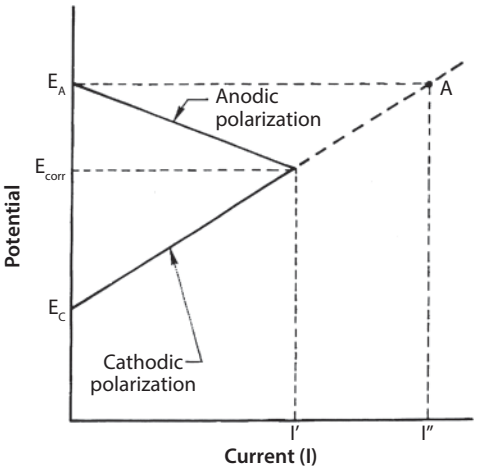

Figure 6.18 Diagram illustrating the theory of cathodic protection. *I*" = current required to produce complete cathodic protection. Current must exceed equilibrium corrosion current *I'* to provide any protection. Corrosion will cease when the flow of cathodic current (*I*") increases cathodic polarization to the open circuit potential (E_A) of the anode as shown at point A. (After Chilingar *et al.*, 2008, p. 72, figure 4.1.)

The first step in the control of external casing corrosion is to provide a complete cement sheath and bond between the pipe and formation over all external areas of the casing strings.

Cathodic protection involves supplying electrons to the metal to make the potential more negative. Complete protection is achieved when all the surface area of the metal acts as a cathode in the particular environment (see Figure 6.18).

The increase in electronegative potential can be achieved by use of sacrificial anodes (magnesium, aluminum, and zinc) or by an impressed direct current. The potentials required for protection differ with the environment and the electrochemical reactions which are involved. For example, Blount (1970) noted that iron corroding in neutral aerated soil has a reduction potential of 0.579 V. The potential is limited by the activity and solubility of ferrous hydroxide. If iron is exposed to H_2S in an oxygen-free environment, the potential is increased to 0.712 V and is controlled by the solubility of ferrous sulfide.

Measurements of potential are made by use of reference half-cells. The copper-copper sulfate half-cell is widely used for potential measurements of pipe in soils. The criteria for protection of iron with this half-cell are- 0.85 V in aerated soil and –0.98 V in an H_2S system.

The two types of cathodic protection most commonly used in the oilfield are:

1. Galvanic
2. Impressed current

When anodes (e.g., aluminum) are electrically coupled to steel (immersed in the same electrolyte), cathodic protection current is generated. As a result of oxidization of aluminum, electrons are forced into the steel, because electrochemical potential of aluminum is higher than that of steel. Inasmuch as aluminum is consumed in the process, it is called a "*sacrificial anode*."

In the case of impressed-current cathodic protection, rectifiers are used-to convert alternating current to direct current. The negative side of the direct current is connected to the casing, whereas the positive side is connected to the buried anodes. The anode material in this case is essentially inert.

Interference bond on an insulating flange at a catholically protected casing is shown in Figure 6.19. In the absence of bond, the interference current on the electrically

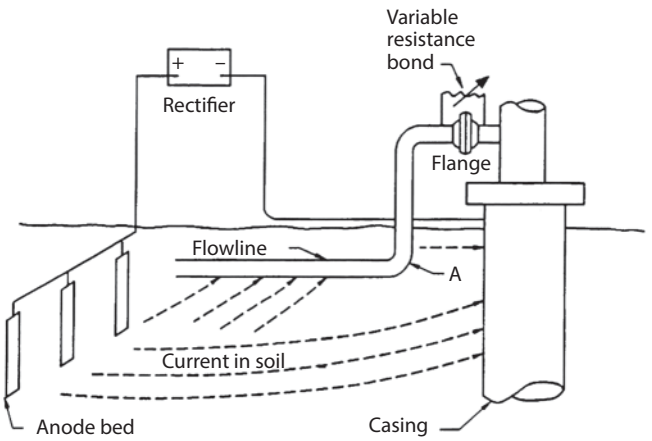

Figure 6.19 Adjustable interference bond across an insulating (isolating) flange connecting a buried flowline to cathodically protected casing. (After Jones, 1988, p. 34, figure 14.6; in: Chilingar *et al*., 2008, p. 110, figure 5.7.)

isolated flowline would leave through the soil at point A, causing corrosion of the flowline (Jones, 1988).

As shown in Figure 6.19, the insulating flange electrically isolates the casing from the surface equipment. This confines the cathodic protection current to the casing.

6.9.10 Structure Potential Measurement

The relative potential values of buried pipes in the soil must be measured to (Jones, 1988):

1. determine if protection is needed,
2. determine the location of anodes,
3. determine how much current must be supplied, and
4. check if the protection has been achieved or not.

Relative potential is usually measured in comparison to a reference electrode, which is usually ($Cu/CuSO_4$) electrode in soils, whereas Ag/AgC1 half-cell is used in the seawater. The reference electrode is connected to positive (+) terminal of a potentiometer and the pipeline is connected to the negative (–) terminal (see Figure 6.20).

Several pipe-to-soil potentials over the distance along the pipeline are measured, and consequently plotted to determine the hot spots, where the pipe is more subject to corrosion. Usually, these occur in zones of lowest soil resistivity (Jones, 1988).

6.9.11 Soil Resistivity Measurements

To determine if the cathodic protection may prevent corrosion of buried pipeline in the soil, one must measure the resistivity of the soil. The unit of soil resistivity is ohm-centimeter. According to Parker and Peattie (1999), the resistivity of soil is numerically equal to the resistance of a cube of the soil 1 cm in dimensions, as measured from opposite faces:

$$\rho = \frac{\frac{R}{L}}{A}, \tag{6.46}$$

where: ρ = resistivity in ohm-cm, R = resistance in ohms, L = length in cm, and A = area in cm^2

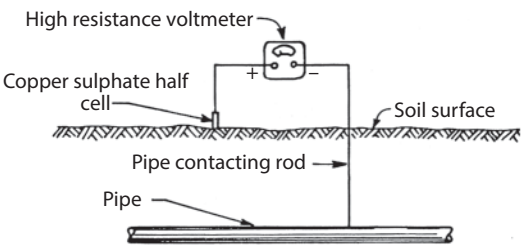

Figure 6.20 Measurement of pipe-to-soil potential on a pipeline. (After Jones, 1988, p. 32, figure 14.4; in: Chilingar *et al.*, 2008, p. 110, figure 5.8.)

Measuring the soil resistivity to prepare for use with a pipe-to-soil survey helps to detect anodic hot spots along the pipelines and to choose locations to place anode beds. The corrositivity of soils is inversely proportional to their resistivities. In other words, low resistivity means high probability of corrosion (see Table 6.6).

The Wenner method (four-terminal method) is commonly used to measure the resistivity at greater depth (Figure 6.21). For details on measuring resistivity, one should consult Parker and Peattie (1999).

An example of soil resistivity profile along a pipeline is shown in Figure 6.22. Point of low resistivity A is probably an anodic hot spot. In the case of bare pipelines, sacrificial anodes are attached at the anodic hot spots. Then the potentials along the line are resurveyed. More anodes are added as needed until a fairly uniform potential profile is obtained (Jones, 1983, p. 36). For a complete protection of a coated pipeline, an anode ground bed with a power supply is installed.

Impressed current systems are preferred over sacrificial anodes when the current requirement exceeds 2–3 amps.

Table 6.5 Common inhibitors. (After Jones, 1988, p. 20; in: Chilingar *et al.*, 2008, table 4.1, p. 84.)

Inhibitor Class	Example:
Organic, anionic	Sodium phosphonates
Organic, cationic	$R \cdot NH_2, R_2 \cdot NH, R_3 \cdot N$ and $[R_4N]^+$
	R = hydrocarbon portion of molecule
Inorganic anions	Sodium chromate $(CrO_4)^=$
	Sodium silicate $(SiO_3)^=$
	Sodium phosphate $(PO_4)^=$
	Sodium molybdate $(MoO_4)^=$
Mixed-charge inhibitors	Zinc cation (Zn^{++})

Table 6.6 Corrosion rate of steel in soil. (After Romanoff, 1957; in: Chilingar *et al.*, 2008, table 5.2, p. 112.)

Area	Corrosion rate, mpy	Type steel	Soil resistivities, Ω-cm
Desert sand, AZ	5	Noncorrosive	Above 10,000
Sandy loam, New England	21	Mildly corrosive	2,000 to 10,000
Clay, CA	137	Very corrosive	Below 500
Tidal marsh	100	Corrosive	500 to 1,000
Average of 44 soils	61	Moderately corrosive	1,000 to 2,000

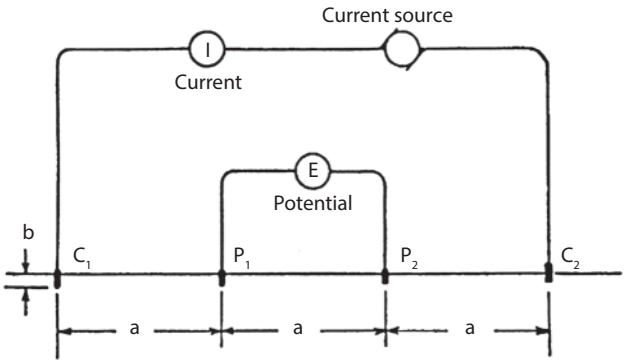

Figure 6.21 Wenner method (four terminal method) of measuring soil resistivity. Distance *"b"* (depth of electrode) is smaller than distance *"a"* (electrode spacing). The resistivity, $\rho = 2\pi\alpha(E/I)$, is averaged to a depth approximately equal to *"a"*. (After Parker and Peattie, p. 4, figure 1.4; in: Chilingar *et al.*, 2008, p. 112, figure 5.9.)

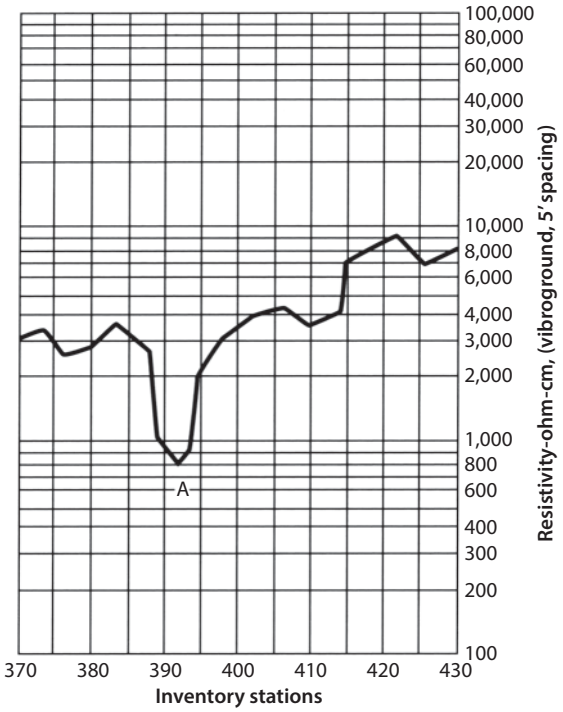

Figure 6.22 Soil profile along a pipeline. Resistivity values are plotted on the ordinate (log scale), whereas distances along pipeline are plotted on the abscissa. A = anodic hot spot. (After Parker and Peattie, 1999, p. 9. figure 1.8; in: Chilingar *et al.*, 2008, p. 113, figure 5.10.)

6.9.12 Interaction between an Old and a New Pipeline

When two pipelines (one old and one new) are interconnected, corrosion leaks will develop more in the new pipeline. The old pipeline being protected by some chemical deposits (scales) will act as cathode, whereas the new pipeline will act as anode (Figure 6.23). Thus, in this case the "old" pipeline is better protected than the "new" one.

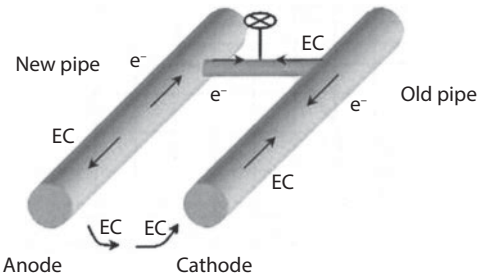

Figure 6.23 Flow of electrons and electric current between the interconected new and old pipelines. After Chilingar *et al.*, 2008, p. 114, figure 5.11.)

6.9.13 Corrosion of Offshore Structures

In the case of offshore structures (see Figure 6.24), Brondel *et al.* (1994) suggests that the simplest solution is to place an insulating barrier over the metal exposed to corrosion. The use of zinc-rich primers can be painted on the exposed portions of the structure to form a barrier against rain, condensation, sea mist and spray. They further point out that the zinc primer not only forms a physical barrier, but also acts as a sacrificial anode should this barrier be breached.

Immersed zone: The immersed zone of platform, which is below the waterline at lowest tide, is subjected to pitting corrosion (as high as 100 mil/yr), as well as general wastage (Cron and Marsh, 1983).

Cathodic protection can prevent pitting, corrosion of welds, and corrosion fatigue.

Sacrificial anodes, which can be made of zinc, magnesium, and aluminium, can weigh 300–800 lb. They can have different shapes (rod, ribbon, cylinder, pencil, and bracelet) and can last for ≈20 years.

Mud zone: The zone below the mud line, where the platform was driven into sea bottom, is called mud zone.

inasmuch as there is no agitation and the presence of a reducing environment, only 1–4 mA/ft^2 current density is required for cathodic protection. Allowance, however, should be made for the cathodic protection of casing, which is in electrical contact with the platform (Cron and Marsh, 1983).

The remaining structure, which is exposed to less severe seawater corrosion, is protected by cathodic protection. There can be other problems, e.g., crustaceans and seaweed attaching to the submerged parts of the offshore structure that can add weight, increasing stress-related corrosion (Brondel *et al.*, 1994). This mechanism can occur when the combined effects of crevice (or pitting) corrosion, and stress propagate cracks in the metal that can lead to structural failure. However, a coating of organisms over the metal keeps the atmosphere from contacting the metal. This restricts the oxygen from reaching the metal and thus reduces corrosion.

Another form of structural stress often incurred in the offshore structures is low-frequency *cyclic stress* resulting from factors such as waves, tides and operating loads (Brondel *et al.*, 1994). Modeling and accounting for these stresses are an extremely important part of corrosion control.

Figure 6.25 illustrates the potential corrosion problems of a jackup rig or a platform that is anchored to the seafloor. The metal supports (legs) at the bottom are sunk into

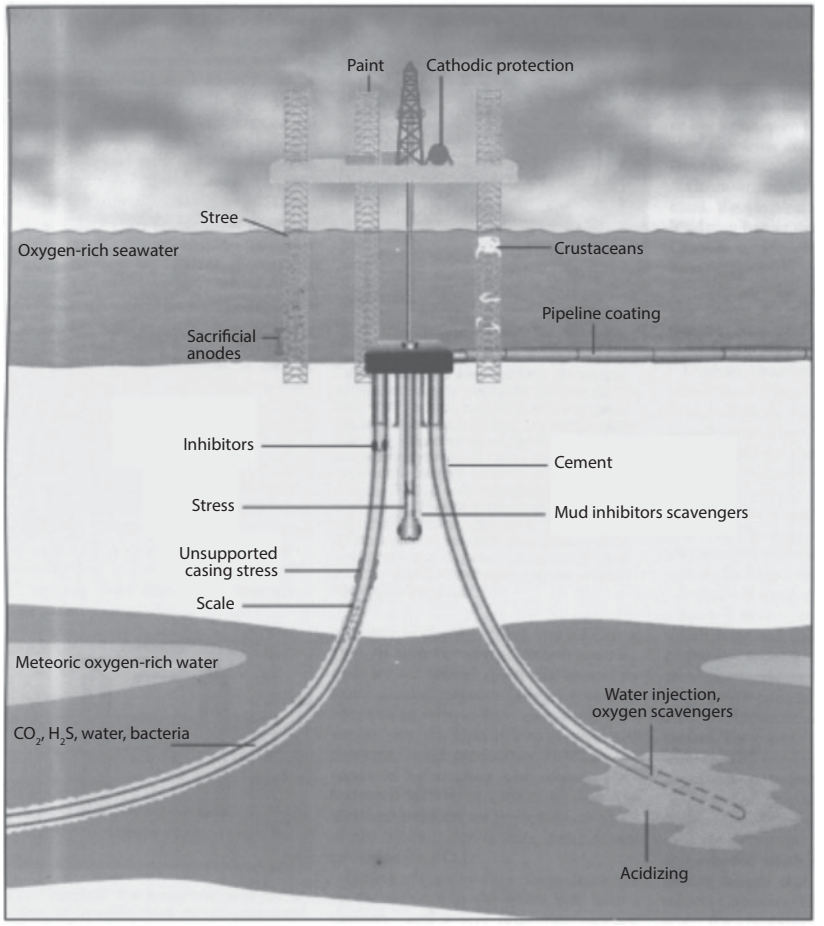

Figure 6.24 Schematic showing various areas of concern pertaining to potential corrosion of an offshore facility. (After Brondel *et al*., 1994.)

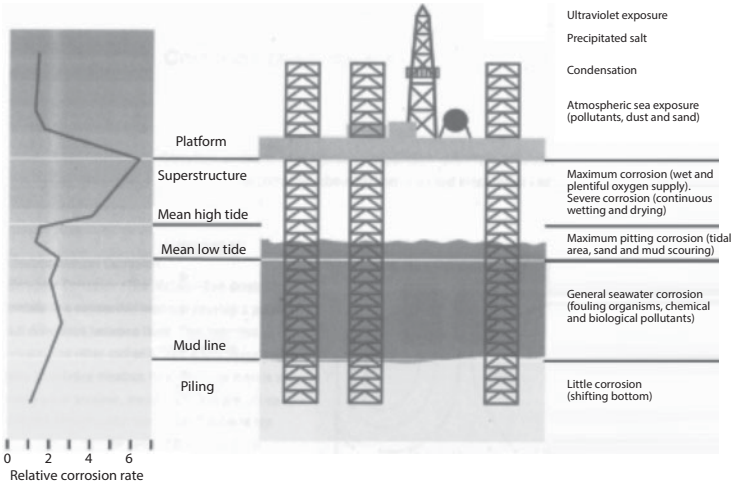

Figure 6.25 Schematic of offshore jackup rig illustrating corrosive environment of the various portions of the rig. (After Brondel *et al*., 1994.)

the seabed and thus may be attacked by H_2S produced by sulfate-reducing bacteria (Maxwell, 1986). Brondel *et al.* (1994) suggest that cathodic protection be used to shield this part of the structure.

6.9.14 Galvanic vs. Imposed Direct Electrical Current

In deciding whether to use the impressed-current or a galvanic cathodic protection system, one has to make an economic study as it is very difficult to put a dollar value on the advantages and disadvantages of each system (see Tables 6.7 and 6.8). In the case of offshore operations, the costs of the two systems are within ≈35% of each other (Cron and Marsh, 1983, p. 1040).

In the case of aluminum sacrificial anodes, the alloying elements are zinc, tin, mercury, and indium, which insure the uniform dissolution of aluminum. According to Cron and Marsh (1983, p. 1039), a 725-lb aluminum anode will generate a current of ≈5.3 amps in the Gulf of Mexico. If galvanic efficiency is 95%, the electrical output of this anode is 1,280 amp-hr/lb with a life of ≈20 years.

Table 6.7 Advantages and disadvantages of galvanic protection. (After Cron and Marsh, 1983; in: Chilingar *et al.*, 2008, table 8.5, p. 219.)

Advantages:	**Disadvantages:**
Permanently activated system, depending on life of anodes	Inflexibility of system once installed.
Maintenance required is minimal.	Many anodes are required.
Not vulnerable to electric failures.	In the case of offshore operations, additional weight to platform
Not vulnerable to mechanical failures.	Distribution of current is difficult to change.
Installation cost per anode is low	In the case of offshore operations, it is costly to replace or repair anodes.
Not vulnerable to storm damage	In the case of offshore operations, it is costly to replace or repair anodes
Instillation cost per anode is low.	
No dependence on external power source.	
In the case of offshore operations, the system is not vulnerable to storms	

Table 6.8 Advantages and disadvantages of impressed-current cathodic protection. (After Chilingar *et al.*, 2008, table 8.6, p. 220.)

Advantages:	**Disadvantages:**
Flexible system, easy to change or repair.	Electric power is required
Replacement costs are low.	Expensive to install each anode.
Testing is required in only a few places.	In the case of offshore operations, the interconnecting cables are vulnerable to damage.
System can be easily deactivated.	
Fewer anodes are used.	System can be deactivated accidently.

In the case of offshore operations, the water depth and vulnerability to storm damage are the deciding factors in choosing a protection system.

6.10 Economics and Preventitive Methods

For each type of corrosion discussed in this chapter, there are different methods of corrosion control. Technological advancement in corrosion control and preventive methods has had a big impact on the economics of corrosion during the past few decades. According to an NBS (National Bureau of Standards) study, there are many preventive steps available:

1. Increase awareness of corrosion costs and potential cost savings.
2. Change the misconception that nothing can be done about corrosion.
3. Change policies, regulations, standards, and management practices to increase corrosion cost savings through sound corrosion management.
4. Improve education and training of staff in the recognition of corrosion type.
5. Implement advanced design practices for better corrosion management.
6. Develop advanced life-prediction and performance-assessment methods.
7. Improve corrosion technology through research.

In corrosion control economics, three factors must be considered in calculations: (1) cost, (2) service life and (3) cost of environmental protection.

Corrosion control offers many alternatives, with different return on investment:

1. Replacing parts and do nothing about corrosion
2. Cathodic protection
3. Inhibitors
4. Coating and painting
5. Water reaeration
6. Dehydration
7. Chemical treatments
8. Different alloys
9. Nonmetallic materials

In their classical paper, Cron and Marsh (1983) gave a good example of corrosion control in an area of uncertainty. They considered an oilfield with some tubing failures. The alternatives were:

1. Install the coated tubing.
2. Inject a corrosion inhibitor.
3. Keep replacing the tubing, with consequent deferred production and risk of losing the well.

First, one has to develop the past history by plotting the log of cumulative leaks versus time. The extrapolated leak curve ("straight line") will give (estimate) the

probable cost of no corrosion control (alternative A; 3 above). Next, the operator will choose an inhibitor (alternative B; 2 above), which can be 70% effective. As a result, corrosion rate will be cut to 30% of its uninhibited rate. The extrapolated leak curve ("line") will show this reduction in corrosion damage. The lowered cost due to decrease in leaks is then compared with the cost of inhibitor. The ROI (return on investment) is equal to the lowered cost per year divided by the investment cost. For a simple comparison of alternatives, A and B, Cron and Marsh (1983, p. 1035) offered the following formula:

$$ROI = \left[\frac{(Op.\ Cost_A + Dep_A) - (Op.\ Cost_B + Dep_B)}{(Inv.\ Cost_B - Inv.\ Cost_A)} \right] \tag{6.47}$$

The depreciation (*Dep*) can be determined using the following formula:

$$Dep = \frac{Inv.\ Cost}{Years\ of\ Life} \tag{6.48}$$

One can evaluate other alternatives similarly. As pointed out by Cron and Marsh (1983), consistent record keeping is necessary to determine the effectiveness of any program.

6.11 Corrosion Rate Measurement Units

The units used in measuring corrosion rate are:

1. Mils penetration per year = *mpy*

   mil = 0.001 inch

   $$mpy = \frac{2{,}831 \times W}{AT}$$

   where W = loss in specimen weight in grams, T = exposure time in days, and A = area of specimen in in^2.

2. Millimeters per year = $\frac{\text{mm}}{\text{yr}} = \frac{mpy}{40}$

3. Micrometers per year = $\frac{\mu\text{m}}{\text{yr}} = mpy \times 25.4.$

4. Milligrams per square decimeter per day = *mdd* = $mpy \times 5.47$.

References and Bibliography

Abdallah, D., Fabim, R., Al-Hendi, K., Al-Muhailan, M., Al-Khalaf, A. A.,Al-Kunit, A. S., Dahtani, H. B., Al-Yateem, K. S., Asrar, N., Aziz, A. A., Kohring, J. J., Benslimani, A., Fituri,

M. F.M., and Sengul, M., 2013 (Autumn). Casing corrosion measurement to extend asset life. *Oilfield Review*, 25(3):18–31.
Allen, G. G., 1977. *Drilling Fluids*. Baroid Petroleum Services, 16 pp.
Allen, T. O. and Roberts, A. P., 1982. *Production Operations: Well Completions, Workover, and Stimulation*. Tulsa, OK: Oil and Gas Consultants Intern., Inc., 250 pp.
American Petroleum Institute, 1977. *Design Calculations for Sucker Rod Pumping Systems*. Dallas, TX: API RP 11L, 24 pp.
American Petroleum Institute, 1983. *API Recommended Practice for Care and Use if Subsurface Pumps*, Dallas, TX: API RP 11 AR, 41 pp.
Annand, R. R., 1981. *Corrosion Characteristics and Control in Deep, Hot Gas Wells*. Southwestern Petroleum Short Course.
Anonymous, 1972. Bacteria have destroyed 10% of the world's crude. *World Oil*, 174(2): 28–29.
ASM Handbook. Reference. 1254–1255.
Atlas, R. M., 1981. Microbial degradation of petroleum hydrocarbons: an environmental perspective. *Microbiol. Rev*., 45: 180–209.
Bailey, N. J. L., Jobson, A. J., and Rogers, M. A., 1973. Bacterial degradation of crude oil: comparison of field and experimental data. *Chem. Geol.,* 11:203–221.
Baneau, G., Booth, G., Magne, E., Morvan, P., Mudge, P., Pisaki, H., Tran, D., Tranter, P. and Williford, F., 1993. New lease on life for the 704. *Oilfield Review*, 5 no. 2/3 (April): 4:14
Battelle Memorial Institute, 1949. *Prevention of the Failure of Metals Under Repeated Stress*. New York, NY: Wiley, 295 pp.
Becker, J. R., 1998. *Corrosion and Scale Handbook*. Penn Well Publ. Co., Tulsa, OK. 324 pp.
Bennett, L. H., 1978. Economic Effects of Metallic Corrosion in the United States. *A Report to Congress by the National Bureau of Standards (National Bureau of Standards*), Gaithersburg, MD), 145 pp.
Bertness, T. A., 1989. Reduction of failures caused by corrosion in pumping wells. *API Drill. Prod. Pract.*, 37: 129–135.
Bertness, T. A., Chilingar, G. V., and Al-Bassam, M., 1989. Corrosion in drilling and producing operations. In: G. V. Chilingar, J. Robertson, and S. Kumar (Editors), *Surface Operations in Petroleum Production, II*, Amsterdam: Elsevier, pp. 283–317.
Blount, F E., 1970. Fundamentals of cathodic protection. In: *Proc. Corrosion Course*, Univ. Oklahoma, OK, Sept. 14–16.
Brondel, D., Edwards, R., Hayman, A., Hill, D., Mehta, and Semerad, T., 1994 (April). Corrosion in the oil industry. *Oilfield Review*, Apr. pp 4–14, https://www.slb.com/~/media/Files/resources/oilfield_review/ors94/0494/p04_18.pdf.
Bryant, R. S., 1986. *Microbial Transformation of Hydrocarbons*. U.S. Dep. Energy Rept. NIPER-213: 19 pp.
Bryant, R. S., Donaldson, E. C., Yen, T. F., and Chilingarian, G. V., 1984. Microbial enhanced oil recovery. In: E. C. Donaldson, G. V. Chilingar, and T. F. Yen, *Enhanced Oil Recovery II, Elsevier Publ*., Amsterdam, p. 423–450.
Bubela, B., 1983. Combined effects of temperature and other environmental stresses on MEOR. In: E. C. Donaldson and J. B. Clark (Editors), Proceedings of 1982 *International Conference on Microbial Enhancement of Oil Recovery*, Afton, OK, May 16–21, pp. 118–123.
Chakrabarty, A. M., 1982. *Biodegradation of Detoxification Environmental Pollutants*. Boca Raton, FL: CRC Press, 160 pp.
Chilingar, G. V. and Beeson, C. M., 1969. *Surface Operations in Petroleum Production*. New York, NY: American Elsevier, 397 pp.
Chilingar, G. V., Mourhatch, R., and Al-Qahtani, G. D., 2008. *The Fundamentals of Corrosion and Scaling for Petroleum and Environmental Engineers*. Gulf Publishing Co., Houston, TX, 276 pp.

Chilingarian, G. V. and Vorabutr, P., 1983. *Drilling and Drilling Fluids*. Amsterdam: Elsevier Science Publishers, 767 pp.

Corrosion Doctors, 2015. *Pipeline Corrosion Problems* (http://www.corrosion-doctors.org/Pipeline/Introduction.htm).

Crawford, P. B., 1983. Possible reservoir damage from MEOR. In: E. C. Donaldson and J. B. Clark (Editors), *Proceedings of 1982 International Conference on Microbial Enhancement of Oil Recovery*, Afton, OK, May 16–21. Springfield, VA: NTIS, pp. 76–79.

Cron, C. J. and Marsh, G. A., 1983. Overview of economics and engineering aspects of corrosion in oil and gas production. *J. Pet. Technol*., June: 1033–1041.

Cryer J., Dennis B., Lewis R., Palmer K, and Watfa M., 1987. Logging techniques for casing corrosion. *The Technical Review*, (35)4: 32–39.

Davies, J. S. and Westlake, D. W. 5., 1979. Crude oil utilization by fungi. Can. J. Microbiol., 25: 146–156.

Davis, J. B., 1967. *Petroleum Microbiology*. Amsterdam: Elsevier, 604 pp.

Dean, H. 1, 1977. Avoiding drilling and completion corrosion. *Pet. Eng*., 10(9): 23–28.

Deming, H. G., 1940. *Fundamental Chemistry*. New York and London: John Wiley and Sons, Inc., 756 pp.

Doig, K. and Wachter, A. P., 1951. Bacterial casing corrosion in the Ventura Field. *Corrosion*, 7: 221–224.

Donaldson, E. C. and Clark, J. B., 1982. Conference focuses on microbial enhancement of oil recovery. *Oil Gas J*., 80(51): 47–52.

Donaldson, E. C., Chilingarian, G. V., and Yen, T. E, 1989b. *Microbial Enhanced Oil Recovery*, Development in Petroleum Science, 22. Amsterdam: Elsevier, 227 pp.

Donaldson, E. C., Chilingarian, G. V., and Yen, T. F, 1989a. *Enhanced Oil Recovery, II, Processes and Operations*. Amsterdam: Elsevier Science, 604 pp.

Fedorak, P. M., Foght, J. M., and Westlake, D. W. S., 1983. Comparative studies on microbial degradation of aromatics and saturates in crude oil. In: J. E. Zajic, D. G. Cooper, T. R. Jack, and N. Kosaric (Editors), *Microbial Enhanced Oil Recovery*, Tulsa, OK: PennWell Books, pp. 162–172.

Fontana, M. G. and Greene, N. D., 1967. *Corrosion Engineering.* New York, NY: McGraw-Hill, 391 pp.

Gates, G. P. L. and Parent, C. F., 1976. Water quality control-presents challenge in giant Wilmington Field. *Oil Gas J*., 74(33): 115–126.

Gatzke, L. K. and Hausler, R. H., 1983. Gas well corrosion inhibition with KP 223/KP 250. *NACE Annual Conf*., April 18–22, Anaheim, CA.

Gaudy, A. E Jr. and Gaudy, E. T, 1980. *Microbiology for Environmental Scientists and Engineers*. New York, NY: McGraw Hill, 736 pp.

Grula, E. A., Russell, H. H., Bryant, D., Kenaga, M., and Hart, M., 1983. Isolation and screening of *Clostridium* for possible use in MEOR. In: E. C. Donaldson and J. B. Clark (Editors), *Proceedings of 1982 International Conference on Microbial Enhancement of Oil Recovery*, Afton, OK, May 16–21. Springfield, VA: NTIS, pp. 43–47.

Grula, M. M. and Sewell, G. W, 1983. Microbial interactions with polyacrylamide polymers. In: E. C. Donaldson and J. B. Clark (Editors), *Proceedings of 1982 International Conference on Microbial Enhancement of Oil Recovery*, Afton, OK, May 16–21. Springfield, VA: NTIS, pp. 129–134.

Guiamet, P. S. and Videla, H. A., 1987. Protective action of *Serratia marcescens* in relation to the corrosion of aluminum and its alloys. In: G. C. Llewellyn and C. E. O'Rear (Editors), *Biodeterioration Research*, New York, NY: Plenum Press, p. 275.

Hackerman, N. and Snavely, E. S., 1971. Fundamentals of inhibitors. In: *NACE Basic Corrosion Course*. NACE, Houston, TX, (9): 1–25.

Heineke, G. W, 1996. Microbiology and epidemiology. In: J. G. Henry and G. W. Heinke (Editors), *Environmental Science and Engineering*, Inc., NJ: Prentice Hall, pp. 254–302.

Heitz, E., Henkhaus, R., Rahmel, A., Waterhouse, R. B., and Rog Holmos, D., 1992. *Corrosion Science: An Experimental Approach*. New York: Ellis Horwood, 225 pp.

Henry, J. G. and Heinke, G. V., 1996. *Environmental Science and Engineering*. NJ: Prentice Hall, 778 pp.

Hilliard, H. M., 1980. Corrosion control in Cotton Valley production. *Soc. Pet. Eng. Cotton Valley Symp., SPE 9062*,Tyler, TX, May 21: 4 pp.

Hitzman, D. O., 1983. Petroleum microbiology and the history of its role in EOR. In: E. C. Donaldson and J. B. Clark (Editors), *Proceedings of 1982 International Conference on Microbial Enhancement of Oil Recovery*, Afton, OK, May 16–21. Springfield, VA: NTIS, pp. 162–218.

Hudgins, C. M., 1969. A review of corrosion problems in the petroleum industry. *Mater. Prot*., 8(1): 41–47.

Hudgins, C. M., McGlasson, R. L., Mehdizadeh, P., and Rosborough, W. M., 1966. Hydrogen sulfide cracking of carbon and alloy steels. *Corrosion*, 22(8): 238–251.

Ironite Products Co., 1979. *Hydrogen Sulfide Control*, 41 pp.

Ivanov, M. V. and Belyaev, S. S., 1983. Microbial activity in water flooded oilfields and its possible regulation. In: E. C. Donaldson and J. B. Clark (Editors), *Proceedings of 1982 International Conference on Microbial Enhancement of Oil Recovery*, Afton, OK, May 16–21. Springfield, VA: NTIS, pp. 48–57.

Jack, T. R. and Thompson, B. G., 1983. Patent employing microbes in oil production. In: J. E. Zajic, D. G. Cooper, T. R. Jack, and N. Kosaric (Editors), *Microbial Enhanced Oil Recovery*. Tulsa, OK: PennWell Books, pp. 14–25.

Jones, L. W, 1988. *Corrosion and Water Technology for Petroleum Producers*. Tulsa, OK: Oil and Gas Consultants International, Inc. (OGCI Publications), 202 pp.

Kane, R. D. and Greer, J. B., 1977. Sulphide stress cracking of high-strength steels in laboratory and oilfield environments. *J. Petrol. Technol.*, 29(11): 1483–1488.

Kirklen, C.A., 1973. *Well Casing Cathodic Protection Effectiveness-An Analysis in Retrospect*. Paper presented at the 48th Annu. Fall Meet., *Soc. Petrol. Engrs., AIME*, Las Vegas, NV, Sept. 30-Oct. 3: 6 pp.

Koch, G. H., Brongers, M. P. H., Thompson, N. G., Virmani, Y. P., and Payer, J. H., 2002. *Corrosion Costs and Preventive Strategies in the United States*. Publication No. FHWA-RD-01-156: 1–11.

Kubit, R. W., 1968. *E log I-Relationship to Polarization. Paper No. 20, Conf. NACE*, Cleveland, OH.

Lazar, I. and Constantinescu, P., 1985. Field trials results of microbial enhanced oil recovery. In: J. E. Zajic and E. C. Donaldson (Editors), *Microbes and Oil Recovery*. El Paso, TX: Bioresources Publications, pp. 122–143.

Levenspiel, 0., 1972. *Chemical Reaction Engineering*. New York, NY: John Wiley and Sons, 578 pp.

Magcobar Services, 1972. *Drilling Fluid Engineering Manual*. Houston TX, 200

Marquis, R. E., 1983. Barobiology of deep oil formations. In: E. C. Donaldson and J. B. Clark (Editors), *Proceedings of 1982 International Conference on Microbial Enhancement of Oil Recovery*, Afton, OK, May 16–21. Springfield, VA: NTIS, pp. 124–128.

Martin, R. L., 1979. Potentiodynamic polarization studies in the field. *Mater. Perform*., 18(3): 41–50.

Martin, R. L., 1980. Inhibition of corrosion fatigue of oilwell sucker rod strings. *Mater. Perform*., 19(6): 20–23.

Martin, R. L., 1982. *Use of electrochemical methods to evaluate corrosion inhibitors under laboratory and field condition*. U.M.I.S.T. Conf. of Electrochemical Techniques, Manchester.

Martin, R. L., 1983. Diagnosis and inhibition of corrosion fatigue and oxygen influenced corrosion. *Mater. Perform*., 32(9): 41–50.

May, P. D., 1978. Hydrogen sulfide control. *Drilling-DCW*, April.

McCoy, W. F. and Costerton, J. W, 1982. Growth of sessile *Sphaerotilus natans* in tubular recycle system. *Appl. Environ. MicrobioL*, 43: 1490–1494.

Meyer, F H., Riggs, O. L., McGlasson, R. L. and Sudbury, J. D. 1958. Corrosion products of mild steel in hydrogen sulfide environments. *Corrosion*, 14(2): 109t–115t.

Moses, V. and Springham, D. G., 1982. *Bacteria and Enhancement of Oil Recovery*. London: Applied Science Publishers, 178 pp.

Moses, V., Robinson, J. P. and Springham, D. G., 1983. Microbial enhancement of oil recovery in North Sea reservoirs: a requirement for anaerobic growth on crude oil. In: E. C. Donaldson and J. B. Clark (Editors), *Proceedings of 1982 International Conference on Microbial Enhancement of Oil Recovery*, Afton, OK, May 16–21. Springfield, VA: NTIS, pp. 154–157.

National Association of Corrosion Engineers, 1979. *Corrosion Control in Petroleum Production*, NACE TPC Publ. No. 5: 101 pp.

Nester, E. W., Roberts, C. E., Pearsall, N. N. and McCarthy, B. J., 1978. Microbiology. New York, NY: Holt, Rinehart and Winston, 769 pp.

NGAA (Natural Gasoline Association of America), 1953. *Condensate Well Corrosion*. Tulsa, OK: N.G.A.A., 203 pp.

Oxford, W. F. Jr. and Foss, R. E., 1958. *Corrosion of Oil- and Gas-Well Equipment*. Dallas, TX: Division of Production, American Petroleum Institute, 87 pp.

Parker, M. E. and Peattie, E. G., 1999. *Pipe Line Corrosion and Cathodic Protection*, 3rd ed. Gulf Professional Publishing, an Imprint of Elsevier, Houston, TX, 166 pp.

PetroWiki, 2015. *Corrosion problems in production*, (http://petrowiki.org/Corrosion_problems_in_production)

Petzel, G. A. and Williams, B., 1986. Operators trim basic EOR research. *Oil Gas J*., 84(6): 41–45pp.

Rahman, S. S. and Chilingarian, G. V., 1995. *Casing Design:Theory and Practice*. Elsevier, Amsterdam, The Netherlands, 373 pp.

Ray, J. D., Randall, B. V., and Parker, J. C., 1978. *Use of Reactive Iron Oxide to Remove H_2S from Drilling Fluid*. 53rd Annu. Fall Tech. Conf. *Soc. Pet. Eng. AIME*, Oct. 1–3, Houston, TX, 4 pp.

Rhodes, F H. and Clark, J. M., 1936. Corrosion of metals by water and carbon dioxide under pressure. *Ind. Eng. Chem*., 28(9): 1078–1079.

Romanoff, M., 1957. *Underground Corrosion*, Circ. 579. National Bureau of Standards.

Ross, T. and Lott, N., 2001. *Billion Dollar U.S. Weather Disasters, 1980–2001*.

Simpson, J. P., 1979. A new approach to oil-base muds for lower-cost drilling. *J. Pet. Technol*., 31(5): 643–650.

Singer, M. E., 1985. Microbial biosurfactants. In: J. E. Zajic and E. C. Donaldson (Editors), *Microbes and Oil Recovery*. El Paso, TX: Bioresources Publications, pp. 19–38.

Singer, M. E., Finnerty, W. R., Bolden, P., and King A. D., 1983. Microbial processes in the recovery of heavy petroleum. In: E. C. Donaldson and J. B. Clark (Editors), *Proceedings of 1982 International Conference on Microbial Enhancement of Oil Recovery*, Afton, OK, May 16–21. Springfield, VA: NTIS, pp. 94–101.

Snavely, E. S., 1971. Chemical removal of oxygen from natural waters. *J. Pet. Technol*., 23(4): 443–446.

Spencer, O. I. and Harding, R. W., 1959. *Secondary Recovery of Oil*, University Park, PA: Pennsylvania State University, 516 pp.
Staehle, R. W., 1978. $70 billion plus or minus $21 billion (editorial). *Corrosion*, 34(6):1–3.
Starkey, R. L., 1958. The general physiology of the sulfate-reducing bacteria in relation to corrosion. *Prod. Mon*., 22(8): 12–30.
Stiff, H. A. and Davis, L. E., 1952. A method for determining the tendency of oilfield water to deposit calcium carbonate. *Trans. AIME, Pet. Div*., 195: 213–216.
Stumm, W. and Morgan, J. J., 1962. Chemical aspects of coagulation. *J. Am. Water Works Assoc.*, 54: 971–974.
Treseder, R. S. and Badrack, B. P., 1997. Effect of cold working on SCC resistance on carbon and low alloy steels – A review. *Corrosion '97*, Paper 41, NACE, Houston, TX.
Udwin, E., 1971. High-rate water filtration. *Plant Eng*., 25(Sept. 30) (Oct. 28): 56–57.
Uhlig, H. H. (Editor), 1948. *The Corrosion Handbook*. New York, NY: Wiley, 1188 pp.
Uhlig, H. H., 1965. *Corrosion and Corrosion Control*, 3rd ed., New York, NY: Wiley, 371 pp.
Unz, M., 1960. Insulating properties of cement mortar coatings. *Corrosion*, 16(7): 343–353.
Videla, H. A., 1996. *Manual of Biocorrosion*. CRC Press, Lewis Publishers, Boca Raton, FL, 273 pp.
Videla, H. A., Guiamet, P. S., doValle, S. M., and Reinoso, E. H., 1988. Effect of fungal and bacterial contaminants of kerosene fuels on the corrosion of storage and distribution systems. In: *Corrosion 88, Paper No. 91*, St. Louis, MO, Houston, TX: NACE.
Von Engelhardt, W. and Tunn, W. L., 1955. *The Flow of Fluids Through Sandstones*. Ill. Geol. Surv. Circ., 194: 16 pp. (translated by P. A. Witherspoon). Also in: *Heidelb. Beitr. Mineral. Petrogr.*, 1954, 4: 12–25.
Watkins, J. W. and Wright, J., 1953. Corrosive action on steel by gases dissolved in water. *Pet. Eng*., 25(12, Nov.): B50–B57.
Watts, R. R., 1982. *Designing for corrosion control in surface production facilities*. SPE paper 9985 presented at SPE International Petroleum Exhibition and Technical Symposium, Beijing, China.
Weeter, R. F, 1965. Desorption of oxygen from water using natural gas for countercurrent stripping. *Petrol. Technol*., 17(5): 51.
Wendt, R. P., 1979. Alkalinity control of H_2S in muds is not always safe. *World Oil*, 188 (2, Aug.): 60–61.
Wendt, R. P., 1979. Control of hydrogen sulfide by alkalinity may be dangerous to your health. *Soc. Mech. Eng., Energy Technol. Conf.*, Houston, TX, Nov. 5–9, 1978, 7 pp.
Wendt, R. P., 1979. The kinetics of Ironite Sponge H_2S reactions. *Pet. Div. Am., Soc Mech. Eng., Energy Tech. Conf.*, Houston, TX. Nov. 5–9, 1978, 17 pp.
Whitman, W., Russell, R., and Altieri, V., 1924. Effect of Hydrogen-Ion Con. *Ind. Eng. Chem*., 16: 665.
Wilhelm, S. M. and Kane, R. D., 1987. Status Report: Corrosion resistant alloys, *Petroleum Engineering International*, March: 36–41.
Wilhelm, S. M. and Kane, R. D., 1987. Status Report: Corrosion resistant concentration on the submerged corrosion of steel. *Ind. Eng. Chem*., 16: 665.
Wright, C. C. and Chilingarian, G. V., 1989. Water quality for subsurface injection. In: G. V. Chilingarian, J. 0. Robertson, Jr., and S. Kumar (Editors), *Surface Operation in Petroleum Production*, II, Developments in Petroleum Science, Amsterdam: Elsevier, pp. 119–171.
Wright, C. C. and Cloninger, D. K., 1963. *The Membrane Filter-a Good Tool for Water Quality Testing*. Western Regional NACE Meet., Anaheim, CA, Sept. 26: 36 pp.

Wright, C. C. and Davies, D. W, 1966. The disposal of oilfield wastewater. *Prod. Mon*., 30(9): 14–17; 22–24.
Wright, C. C., 1963. Rating water quality and corrosion control in waterfloods. *Oil Gas J*., 61(20): 154–157.
Wright, C. C., 1965. Chemical compatibility. *Prod. Mon*., 29(6): 19–21.
Wright, C. C., 1972. Corrosion control in large-volume pumping brine wells. *Mater. Prot. Perform*., 11: 23–26.
Zaba, J., 1962. *Modern Oilwell Pumping*. Tulsa, OK: The Petroleum Publishing Co., 145 pp.

Environmental Aspects of Oil and Gas Production.
John O. Robertson and George V. Chilingar.
© 2017 Scrivener Publishing LLC. Published 2017 by John Wiley & Sons, Inc.

7

Scaling

7.1 Introduction

Most oilfield scale typically consists of a mixture of one or more inorganic deposits, acting as a cementing material, binding available debris, e.g., organic materials, sand, corrosion products, etc., into a solid deposit. Deposition of material occurs as a result of oversaturation of ions in the water. This oversaturation could result from either (1) a pressure or temperature drop or (2) could be the result of the mixing of two or more incompatible waters. Whenever an oil or gas well produces water, or water is injected into the reservoir to enhance oil recovery, there is the possibility that scale will precipitate. Scale that forms downhole about the formation surrounding the wellbore can cause plugging of the reservoir pores, casing perforations, gravel packs, and downhole equipment (valves, chokes pumps, etc.). Suspended particles of scale are capable of plugging and damaging formations, subsurface and surface equipment, e.g., filters, separators, etc. (Mackay, 2008).

Several common minerals found in oilfield scales with a few less common ones are listed in Table 7.1. Crabtree *et al.* (1999) noted that some mineral scales, such as calcium carbonate ($CaCO_3$), can be dissolved with acids, others cannot. The scale is often difficult to treat because tar-like or waxy coatings of hydrocarbons protect the scale from chemical dissolvers. Layers of accumulated impermeable scale are less easily removed that coat the interior of pipelines. In this situation, mechanical techniques or chemical treatments have been traditionally used to cut through the scale. Some hard scales, such as barium sulfate ($BaSO_4$), are extremely resistant to both chemical and mechanical removal. Crabtree *et al.* (1999) pointed out that understanding the conditions that lead to scaling and when and where it occurs helps to understand how to (1) prevent precipitation, (2)

Table 7.1 Common oilfield scales.

Mineral	Formula
Anhydrite	$CaSO_4$
Aragonite	$CaCO_3$
Barite	$BaSO_4$
Calcite	$CaCO_3$
Celestite	$SrSO_4$
Fluorite	CaF_2
Galena	PbS
Gypsum	$CaSO_4$
Mackinawite	FeS
Pyrite	FeS_2
Sphalerite	ZnS

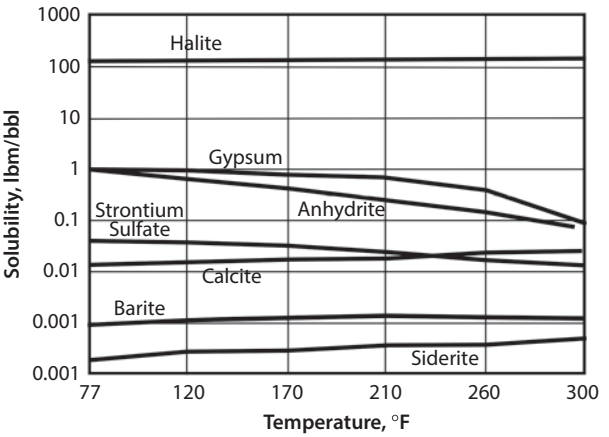

Figure 7.1 Solubilty of frequently found inorganic scales vs. temperature found in oilfield operations. (Modified after Crabtree *et al*., 1999, p. 31.)

possibly dissolve the scale, and (3) design intervention treatments to restore long-term well productivity. The cost of removal of downhole scale from formations and/or equipment replacement is high. It is often less expensive to utilize inhibitors to prevent the scale to form. Inorganic mineral solubility depends on many variables including temperature (Figure 7.1), pressure (Figure 7.2) and salinity (Figure 7.3).

7.2 Sources of Scale

The type and quantity of inorganic ions in the water is of primary importance to the scale-forming properties of that water. Water is a good solvent for most inorganic scales and can carry a large variety and quantity of ions that can form scale.

The formation water in carbonate reservoirs contain an abundance of divalent calcium (Ca^{++}) and magnesium (Mg^{++}) cations. Some formation waters contain barium

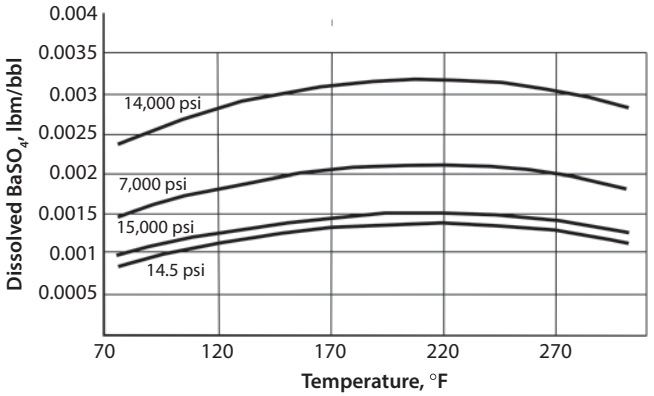

Figure 7.2 The solubility of barium sulfate $BaSO_4$ vs. ressure. Modified after Crabtree *et al*., 1999, p. 31)

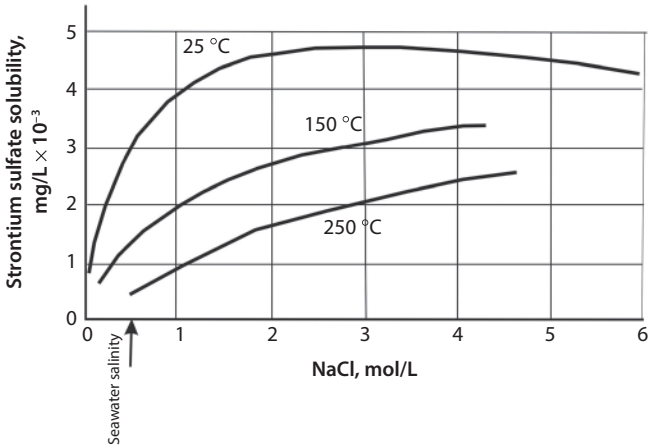

Figure 7.3 Solubility of strontium sulfate vs. salinity at various temperatures. (Modified after Crabtree *et al*., 1999, p. 31.)

(Ba^{++}) and strontium (Sr^{++}) cations. Total dissolved solids in some formations can reach 400,000 mg/l (3.34 ppg). The composition depends on diagenesis and other types of alteration encountered as formation fluids flow and mix over geological time (Crabtree, 1999).

Scale begins to form when the quantity of one or more of the dissolved components exceeds the limit of solubility. As shown in Figure 7.2, the solubility of barium sulfate varies with temperature and pressure. Typically, an increase in temperature increases the solubility. Crabtree *et al*. (1999) noted that more ions are dissolved at higher temperatures and that decreasing pressure decreases solubility. As a rule of thumb, the solubility of most minerals decrease by a factor of two for every 7000-psi (48-MPa) decrease in pressure.

Not all dissolved inorganic minerals conform to the typical trend shown in Figure 7.1, e.g., the solubility of calcium carbonate ($CaCO_3$). The solubility of barium sulfate (Figure 7.2) increases in the temperature range of 70 to 195 °F and then decreases. This trend is influenced by the brine salinity (Crabtree *et al*., 1999).

It should be noted that in general, the solubility of carbonate minerals increases with increasing content of carbon dioxide, (CO_2) and hydrogen sulfide, (H_2S). This trend has a complex nonlinear dependence on brine composition, temperature and the vapor pressure of the gas. With evolution of CO_2, pH increases, adding to the precipitation of calcite (Mackay, 2008).

7.3 Formation of Scale

The precipitation of scale can occur as a result of (1) oversaturation with respect to the inorganic ions and, (2) a drop in pressure of the fluid carrying the inorganic ions, or (3) change in temperature. The types of scale are presented in Table 7.2. Table 7.3 shows the various types of scale that can precipitate due to various oilfield conditions.

The prevention of scale formation is of utmost importance as it is much easier to prevent precipitation than attempt to remove it at a later date. As noted in Table 7.2, some carbonate, hydroxide, oxide, and sulfide scales may be removed by acidizing, whereas many other (e.g., sulfate, phosphate, and ferricyanide) scales are not soluble in acid. These latter are very difficult, if not impossible, to remove by means other than mechanical action.

Solubility of various common scales in distilled water are presented in Table 7.4.

Table 7.2 Oil field scales. Data drawn from handbook of chemistry and physics (1980), Petrowiki (2016) and Mackay (2007).

Name	Formula	Sp. Gr.	Hardness	Cold water solubility, mg/l	Notes
Common oilfield scales					
Anhydrate	$CaSO_4$	2.08	3.5 to 4	2,090	acid soluble
Aragonite	$CaCO_3$	2.94	3.5 to 4		
Barite	$BaSO_4$	4.50	3 to 3.5	2.3	60 mg/l in 3% HCl
Calcite	$CaCO_3$	2.715 to 2.94	3	14	acid soluble
Celestite	$SrSO_4$	3.96	3 to 3.5	113	slightly acid soluble
Gypsum	$CaSO_4 \cdot 2H_2O$	2.39 to 2.37	2	2,410	acid soluble
Halite	NaCl	2.16 to 2.17	2.5	357,000	insoluble in HCl
Other scales					
Fluorite	CaF_2	3.18	4		
Galina	PbS	7.57 to 7.59	2.5 to 2.75		
Iron carbonate hydrate	$FeCO_3$				
Iron oxide	FeO				
Marcasite	FeS	4.887	6 to 6.5		
Pyrite	FeS_2	5.018	6 to 6.5		
Sphalerite	ZnS	3.9 to 4.1	3.5 to 4		
Sand grains					
Quartz	SiO_2	2.65	7	insoluble	HF soluble

Table 7.3 Cause of scale formation. (After Wright and Chilingarian, 1989, p. 326; in: Chilingar *et al.*, 2008, table 6.1, p. 119.)

	Scale formation	
Cause of scale formation	**Chemical name**	**Mineral name**
Loss of dissolved gases	Calcium carbonate	Calcite, aragonite
Solution of gases	Ferric hydroxide	Goethite
	Ferrous sulfide	Amorphous iron sulfide
Commingling of waters	Barium sulfate	Barite
	Strontium sulfate	Celestite
	Calcium sulfate[1]	
	Calcium carbonate	Calcite
Heating without evaporation	Calcium carbonate	Calcite, aragonite
	Calcium sulfate	Gypsum, anhydrite
	Mixed iron oxide	Magnetite
Incompatible chemicals	Calcium phosphate	Hydroxyapatite
	Ferrous ferricyanide	

[1]$CaSO_4 \cdot 2H_2O$ (dihydrate or gypsum). $CaSO_4 \cdot \frac{1}{2} H_2O$ (hemihydrate). $CaSO_4$ (anhydrite).

Table 7.4 Examples of water analysis. (Modified after Jones, 1988, p. 112; in: Chilingar *et al.*, 2088, table 6.4, p. 124.)

	Sample 1 Sea water,		Sample 2 Formation water,		Sample 3 Produced water,	
Ion	**mg/L**	**meq/L**	**mg/L**	**meq/L**	**mg/L**	**meq/L**
Na^+	11.144	484.5	31,602	1,374	28,543	1,241
K^+						
Ca^{++}	464	23.2	18,662	933.1	14,010	700.5
Mg^{++}	1350	111	2,838	232.6	2,470	202.5
Fe^{++}						
Ba^{++}						
Sr^{++}						
Cl^-	19,900	562.4	89,499	2,521.1	75,500	2,126.8
$SO_4^=$	2,600	54.1	410	8.5	432	9
HCO_3^-	149	2.5	617	10.1	502	8.2
CO_3^-	0		0		0	
OH^-	0		0		0	
TDS	35,607		143,559		121,457	
Sp. Gr.	1.026		1.104		1.088	
pH	7.8		6.2		7.4	
O_2	3.8					
H_2S			139		190	

7.4 Hardness and Alkalinity

Water that has a high content of metal ions is often referred to as hard water. This water contains mainly calcium (Ca), magnesium (Mg), and iron (Fe) ions. Total hardness was originally defined as the amount of soap needed to produce foam (Jones, 1988). The total hardness of water (in terms of mg/L of $CaCO_3$), is determined from a water analysis by converting the mg/L of Ca^{++}, Mg^{++}, and Fe^{++} to $CaCO_3$ equivalent in mg/L, whereas the total alkalinity is determined by converting mg/L of HCO_3^-, $CO_3^=$, and OH^- to mg/L of $CaCO_3$, as shown in the following example:

Example 7.1: For a sample of water containing the following ions, calculate the total hardness and the total alkalinity (in terms of $CaCO_3$, mg/L):

Ions	Concentration (mg/L)
$CO_2^=$	0
OH^-	0
HCO_3^-	122
Ca^{++}	105
Mg^{++}	56
Fe^{++}	18

Solution: The concentrations in mg/L are converted to mg/l of equivalent $CaCO_3$ by multiplying the concentration of each ion by the ratio of equivalent weight of $CaCO_3$ (50) to the equivalent weight of the individual ion. Thus, the total hardness (as $CaCO_3$) is equal to:

$$Ca^{++} + Mg^{++} + Fe^{++} = \left(105 \times \frac{50}{20}\right) + \left(56 \times \frac{50}{12.2}\right) + \left(18 \times \frac{50}{27.9}\right)$$
$$= 524.2 \text{ mg/L}$$

Inasmuch as the water in this case does not contain OH^- or $CO_3^=$ ions, the alkalinity is due entirely to HCO_3^- anion. Thus, the total alkalinity = $122 \times 50/61 = 100$ mg/L.

7.5 Common Oilfield Scale Scenarios

7.5.1 Formation of a Scale

Scale in the oilfield occurs as a result of:

1. **Mixing of incompatible formation water waters**
   The mixing of two incompatible waters, e.g., injection and formation water, can exceed the solubility of inorganic ions in the mixed water. In

some areas, seawater is injected into reservoirs during secondary and enhanced-recovery. Seawaters are typically rich in sulfate ($SO_4^{=}$), anions with concentrations often above 2000 mg/l or 0.02 ppg, whereas formation waters contain divalent cations Ca^{++}, Ba^{++} and Sr^{++}. Thus, solubility limits of sulphate scales are exceeded. Calcium sulfate ($CaSO_4$) precipitates in carbonates, whereas barium sulfate ($BaSO_4$) and strontium sulfate ($SrSO_4$) precipitate in sandstone formations. Scales that form downhole are difficult to remove chemically and impossible to remove mechanically. Mixing of incompatible waters can also occur in the surface equipment, producing scales that are more accessible to both chemical and mechanical removal (Crabtree *et al*., 1999).

2. **Self-scaling**
   Self-scaling occurs when either temperature or pressure changes occur as the fluid is produced. As the solubility of the scale is exceeded, it precipitates. Sulfate and carbonate scales can precipitate as a result of pressure changes within the wellbore or at any restriction downhole that results in a pressure drop. Sodium chloride scale (halite) can form where a highly saline brine undergoes a large temperature drop. Water can dissolve 100 lb/bbl (218 kg/m^3) of halite at 2 °C, but only 8 lb/bbl (174 kg/m^3) at surface temperatures. Halite can precipitate at the rate of 2 lb for each barrel of water produced, giving rise to many tons of scale daily (Crabtree *et al*., 1999).

   Reduction in pressure from the wellhead to surface can lead to massive quantities of scale in surface equipment (Mackay, 2008).

3. **Evaporation-induced scale**
   The simultaneous production of a hydrocarbon gas and formation brine (wet gas) can result in scale production. In this case, as the hydrostatic pressure in the tubular equipment decreases, the volume of the hydrocarbon gas expands and the still hot brine phase evaporates. This process can result in the concentration of the inorganic ions, exceeding the mineral solubilities in the remaining water. This is a common cause of halite scaling in high-pressure, high-temperature (HTHP) wells. Other scales may also form this way (Crabtree *et al*., 1999).

4. **CO_2 Flooding**
   Gas flooding a formation with CO_2 gas for secondary recovery can result in scale deposition. In this situation, the water containing CO_2 becomes more acidic and dissolves the calcite of the formation. As fluid is produced, pressure drops within the formation surrounding the producing well and causes the CO_2 to evaporate. This raises the pH of the water and precipitation of carbonate scale in the perforations and formation pores about the wellbore. The precipitation of scale about the wellbore will result in further reduction in pressure and cause additional precipitation. Crabtree *et al*. (1999) reported that this process can completely seal perforations or create an impermeable wall between the borehole and reservoir within a few days, completely shutting down production.

7.5.2 Calcium Carbonate Scale Formation

Calcium carbonate scaling is a function of pH, temperature, ionic strength of the solution, calcium cation and bicarbonate concentrations. The ionic strength of a solution is a function of the cocentration of ions in a solution and is defined as $I = \frac{1}{2}\sum(C_i, Z_i^2)$, where C_i is the molar concentration of the i^{th} ionic species, and Z is the number of net electrical charges associated with the i^{th} species (see Nazaroff and Alvarez-Cohen, 2001, p. 47).

Table 7.5 presents factors for conversion of ion concentration (mg/L or meq/L) to ionic strength. The chemistry of calcium carbonate deposition can be understood by examining the following formulas:

$$CO_2 + H_2O \leftrightarrow H_2CO_3 \tag{7.1}$$

$$H_2CO_3 + H_2O \rightarrow H_3O^+ + HCO_3^- \tag{7.2}$$

$$HCO_3^- + OH^- \rightarrow CO_3^= + H_2O \tag{7.3}$$

$$CO_3^= + Ca^{++} \rightarrow CaCO_3 \downarrow \tag{7.4}$$

As pressure decreases during production, CO_2 is released and $CaCO_3$ precipitates (unstable water):

$$Ca(HCO_3)_2 \rightarrow CO_2 \uparrow + H_2O + CaCO_3 \downarrow \tag{7.5}$$

Deposition of calcium carbonate will occur if the reactions expressed by Eqs. 7.3 and 7.4 are shifted to the right. The following situations may cause the equilibria to shift to the right:

1. A decrease in temperature
2. Decrease in pressure

Table 7.5 Factors for converting ion concentration (mg/L or meq/L) to ionic strength. Concentrations must be multiplied by the factors shown. (After Jones, 1988; in: Chilingar *et al.*, 2008, table 6.3, p. 120.)

Ion	mg/L	meq/L
Sodium, Na^+	2.2×10^{-5}	5×10^{-4}
Calcium, Ca^{++}	5.0×10^{-5}	1×10^{-3}
Magnesium, Mg^{++}	8.2×10^{-5}	1×10^{-3}
Chlorine, Cl^-	1.4×10^{-5}	5×10^{-4}
Sulfate, $SO_4^=$	2.1×10^{-5}	1×10^{-3}
Bicarbonate, HCO_3^-	0.8×10^{-5}	5×10^{-4}

3. A loss of dissolved carbon dioxide
4. An increase in pH

Langelier (1936) developed the scale prediction formula:

$$pH_s = (pK'_2 - pK'_s) + pCa^{++} + pAlk \tag{7.6}$$

where pK'_2 and pK'_s = empirical constants, pCa^{++} = –log[Ca^{++}], and pAlk = –log[alkalinity].

Stiff and Davis (1952) have simplified the work of Langelier (1936) on the scaling index, *SI*, of oilfield waters, i.e., and the tendency to deposit calcium carbonate scale. They defined the stability index as follows:

$$SI = pH_{actual} - pH_s \tag{7.7}$$

or,

$$SI = pH - pCa - pAlk - K \tag{7.8}$$

where, pH_s = pCa + pAlk + K: pCa = –log[Ca^{++}]; pAlk = –log[alkalinity]; and K is a constant, which depends on temperature and total dissolved solids (TDS). If the stability index is positive, the water is oversaturated with $CaCO_3$ and the formation of scale is possible. The stability index predicts the future behavior of water with no estimate of past scaling.

Thus, pH is the commanding factor! If the composition of water is known, one can calculate pH at saturation (pH_s). If the latter is higher than the measured pH, the scale most likely would not form.

Calcium carbonate scale formation may be prevented by anyone of the following techniques.

1. Lowering the pH until the stability index becomes zero or slightly negative.
2. Adding a scale inhibitor
3. Removal of the calcium ion by any of the following means:
   a. Ion exchange, in the case of freshwater.
   b. Precipitation.
   c. Chemical treatment: chelation, sequestration, and peptization.
   d. Dilution to raise the solubility limit.

In studying dispersing agents, Tchillingarian (1952) proved that dispersants such as sodium acid pyrophosphate yield spatially extensive anions which plate the incipient $CaCO_3$ crystals. Thus, on gaining more negative charges, these crystals repulse each other with greater strength. Experimentally, he showed that cataphoretic velocity increases on addition of $Na_2H_2P_2O_7$.

Solubility of $CaCO_3$ at various temperatures is presented in Figure 7.4.

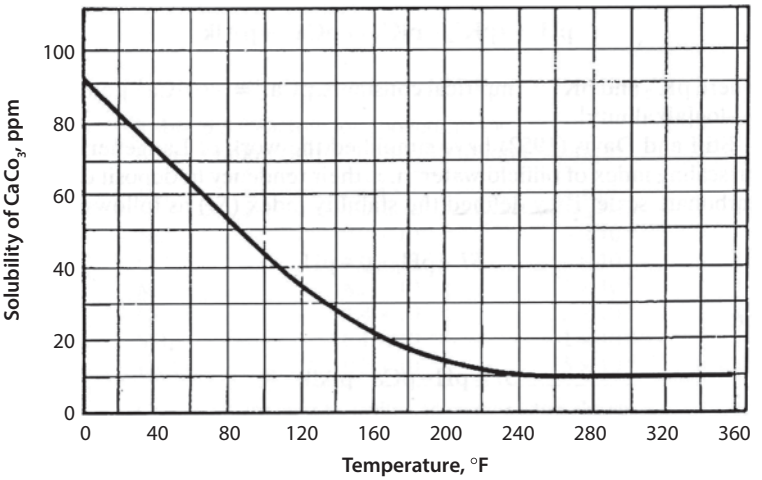

Figure 7.4 Relationship between solubility of $CaCO_3$ and temperature. (After Carlberg *et al*., 1962; in Chilingar *et al*., 2008, p. 122, figure 6.2.)

7.5.3 Sulfate Scale Formation

The sulfate scales commonly occurring in oilfield operations (e.g., waterflooding) are listed in Table 7.1. The most common are:

1. Barium sulfate
2. Calcium sulfate (anhydrite or gypsum)
3. Strontium sulfate

These sulfate types of scale are normally the result of commingling of two different waters, e.g., one water containing sulfate ion and the other water containing barium, strontium, and/or calcium ion. When the mixing of incompatible waters cannot be avoided, the writers suggest one of the following procedures:

1. Allowing precipitation, and then filtering out precipitates,
2. Adding a scale inhibitor
3. Removing the barium, strontium, or calcium ion by ion exchange in the case of freshwater.
4. Sequestering or chelating the barium, strontium, or calcium ion.
5. Diluting the offending ion to below solubility limit.

According to Allen and Roberts (1982), the most common form of calcium sulfate scale deposited downhole is gypsum ($CaSO_4 \cdot 2H_2O$). Figure 7.5 illustrates the relationship between the solubility and temperature, whereas Figure 7.6 shows the solubility of gypsum scale at pressures of 0 and 1,980 psig at 95 °F for various concentrations of sodium chloride. The relationship between the total dissolved solids (TDS) and approximate solubilities of strontium sulfate and barium sulfate in oilfield brines at 60 °C is presented in Figure 7.7.

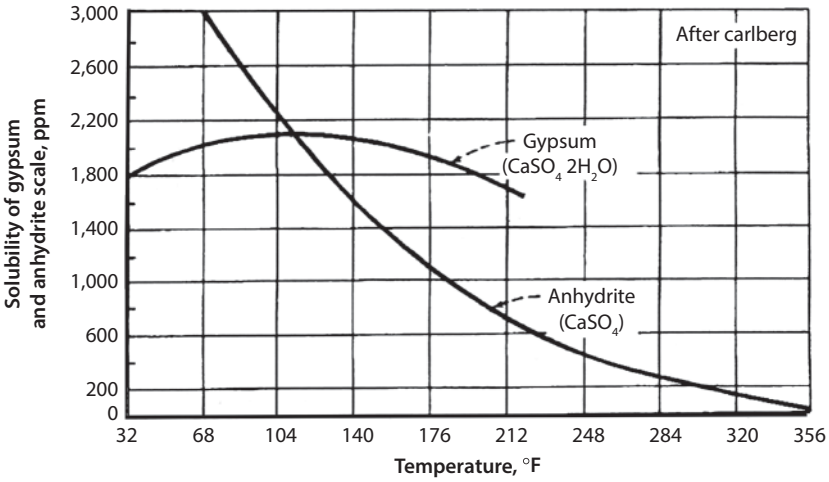

Figure 7.5 Relationship between temperature and solubility of gypsum and anhydrite in fresh water. (After Carlberg *et al*., 1962; in: Chilingar *et al*., 2008, p.120, figure 6.1.)

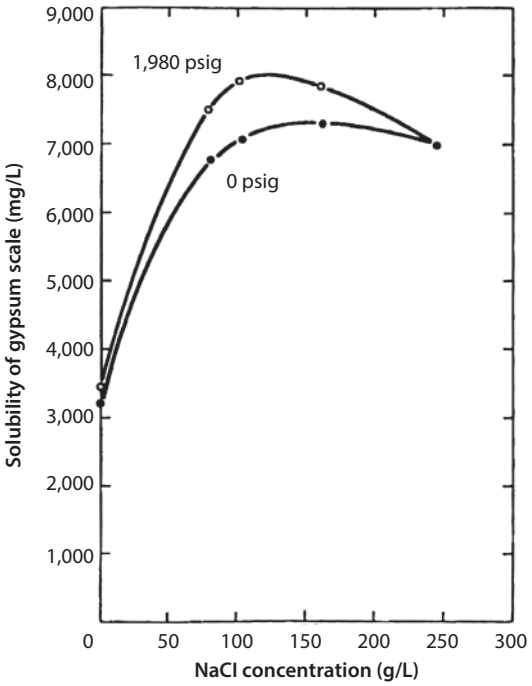

Figure 7.6 Relationship between solubility of NaCl concentration (g/L) and solubility of gypsum scale at 95 °F. (After Fulford, 1968; in: Chilingnar *et al*., 2008, p. 124, figure 6.3 courtesy of SPE)

7.6 Prediction of Scale Formation

Several methods can be used to predict the formation of scale, which depend on the type of precipitant and nature of chemical reactions involved. Becker (1998) used an

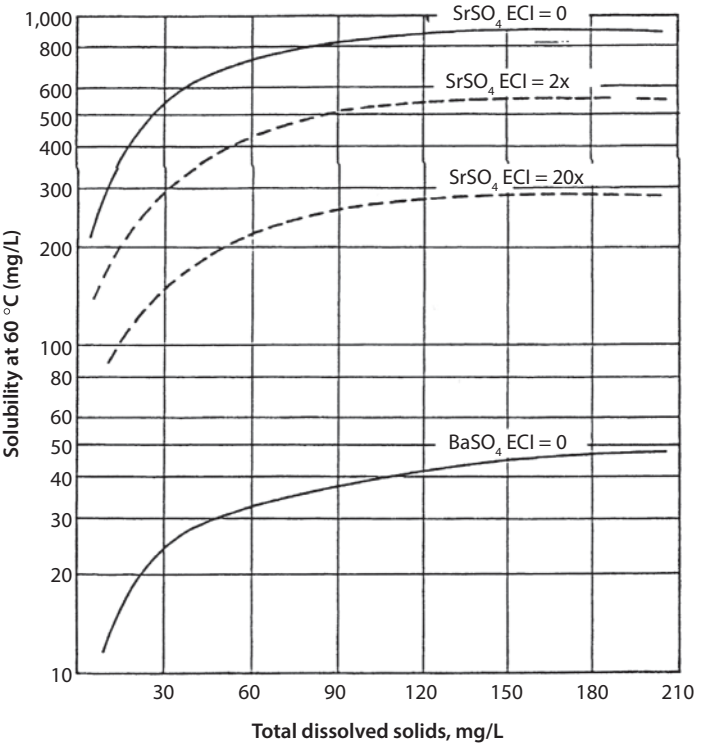

Figure 7.7 Relationship between the total dissolved solids (TDS) and approximate solubilities of strontium sulfate and barium sulfate in oilfield brines at 60 °C. (Modified after Jones, 1988, p. 124, Chilingar *et al*., 2008, p. 132, figure 6.8.)

electromotive force method (emf), which is based on Nernst and Gibb's free energy equation as follows:

$$\in = \in^{0} - \left(\frac{RT}{nF}\right)\ln\left(\frac{a_{red}}{a_{ax}}\right) \tag{7.9}$$

where: $\in$ = actual electrode potential at the given concentration, $\in^{o}$ = standard electrode potential, R = universal gas constant; T = absolute temperature in degrees Kelvin, n = charge number of the electrode reaction; F = Faraday constant (96,500 coulombs); a = chemical activities raised to the power corresponding to stoichiometry of reaction.

The spontaneity of the reaction is then determined by using Gibb's free energy equation:

$$\Delta G = -nF \in \tag{7.10}$$

where the negative value of ΔG shows that reaction will occur spontaneously and scale will form, whereas a positive value of ΔG indicates that scale will not form.

The age and method of collecting the sample may have a bearing on the water analysis value obtained. For example, an aged sample of water may show different values

than a fresh sample for pH, bicarbonate content, and CO_2. The best procedure is to measure water properties immediately after sampling (see Allen and Roberts, 1982).

7.6.1 Prediction of $CaSO_4$ Deposition

Jones (1988) proposed an elegant method which is mostly based on the type of scales and scaling index (see examples below).

On assuming a mixture of 50 vol% seawater and 50 vol% produced water (Table 7.4), determine *SI* for $CaSO_4$ and $CaCO_3$. In the case of $CaCO_3$, assume that water mixture is saturated with a gas containing 5 mol percent CO_2 at 1 bar total pressure.

For $CaSO_4$:

$Na^+ \Rightarrow 0.5 \times (484.5) + 0.5 \times (1.241) = 862.75$ meq/L
$Ca^{++} \Rightarrow 0.5 \times (23.2) + 0.5 \times (700.5) = 361.85$ meq/L
$Mg^{++} \Rightarrow 0.5 \times (111) + 0.5 \times (202.5) = 156.75$ meq/L
$Cl^- \Rightarrow 0.5 \times (562.1) + 0.5 \times (2{,}216.8) = 1{,}344.45$ meq/L
$SO_4^= \Rightarrow 0.5 \times (54.1) + 0.5 \times (9) = 31.55$ meq/L

After converting all concentrations to meq/L, one can follow the following steps (Jones, 1988):

1. The concentration (meq/L) of $CaSO_4$ in water is numerically equal to the lowest value of either Ca^{++} or $SO_4^=$:

$$[CaSO_4] = 31.55 \text{ meq/L}$$

2. The excess common ion (*ECI*) is obtained by subtracting the lowest meq/L of either Ca^{++} or $SO_4^=$ from the other:

$$ECl = 361.25 - 31.55 = 330.3 \text{ meq/L}$$
$$\text{(common ion in excess of } [CaSO_4])$$

3. On adding the concentrations of Na^+ and Mg^{++}, one obtains *NM*:

$$NM = 862.75 + 156.75 = 1{,}019.5 \text{ meq/L}$$

4. Determine the ratio of *NM* to *ECl (R)*:

$$R = \frac{NM}{ECI} = 3.086$$

5. Determine K_s:

$$K_s = [CaSO_4] - R = 28.4$$

If $K_s \leq 6$, water is undersaturated with $CaSO_4$ at 60 °C, step (6) is followed.
If $K_s \geq 9$, the water is oversaturated with $CaSO_4$ at 60 °C, step (7) is followed.
If K_s ranges from 6 to 9, water is near saturation.

If $R < K_s$, step (7) is followed, whereas if $R > K_s$, [$CaSO_4$] is approximately equal to the solubility at 60 °C and *SI* for $CaSO_4$ is near zero.

6. For undersaturated waters ($K_s \leq 6$):

$$S_{60} = [CaSO_4]\left(\frac{936}{NM} + \frac{NM}{2{,}808}\right)$$

where S_{60} is the solubility of $CaSO_4$ (meq/L) in water at 60 °C. Inasmuch as in the example presented $K_s > 9$, step (7) is followed.

7. Determine $M = \dfrac{R}{[CaSO_4]} = 0.0978$

If $M > 0.12$, $S_{60} = 1.2\ K_s$

If $M \leq 0.12$, $S_{60} = 0.68\ K_s$

Inasmuch as *M* in this problem is < 0.12,

$$S_{60} = 0.68(28.4) = 19.3$$

8. Thus, *SI* can be determined:

$$SI = [CaSO_4] - S_{60} = 31.55\text{–}19.3 = 12.25$$

Inasmuch as *SI* is positive, scale will probably form.

An increase in the excess common ion concentration, (*ECI*) value reduces the solubility, whereas an increase in the *NM* value increases the solubility. At a higher temperature, waters, which are undersaturated at 60 °C, may become oversaturated. With increasing common ion concentration (*ECI*), the solubilities of $BaSO_4$ and $SrSO_4$ decrease.

7.6.2 Prediction of $CaCO_3$ Deposition

The following steps are used in predicting $CaCO_3$ formation:

1. Determine the ionic strengths using Table 7.5:

$Na^+ \Rightarrow 0.431$

$Ca^{++} \Rightarrow 0.361$

$Mg^{++} \Rightarrow 0.156$

$Cl^- \Rightarrow 0.6722$

$SO_4^{=} \Rightarrow 0.031$

$HCO_3^- \Rightarrow \dfrac{0.002}{0.163}$

Thus, the total ionic strength (sum of the above) is equal to 1.653

2. Determine *K* from Figure 7.8 $\Rightarrow$ 2.5
   Determine pCa from Figure 7.9 $\Rightarrow$ 0.75
   Determine pAlk from Figure 7.9 $\Rightarrow$ 2.25
3. Thus,

$$pH_s = K + pCa + pAlk = 5.5$$

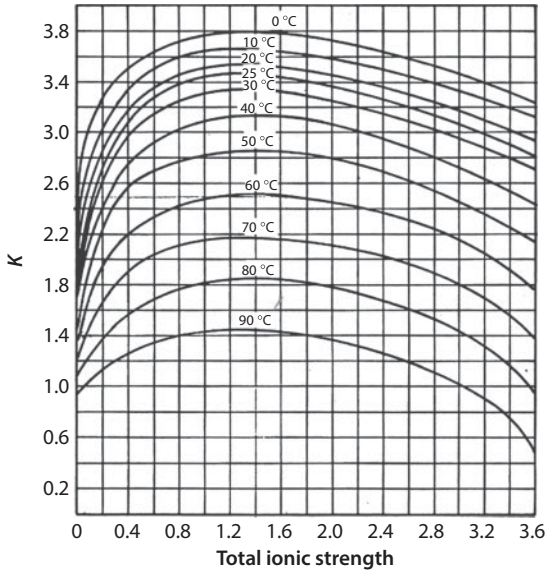

Figure 7.8 Determination of *K* for various ionic strengths. (Modified after Stiff and Davis, 1952; in: Chillingar *et al.*, 2008, p. 128, figure 6.4.)

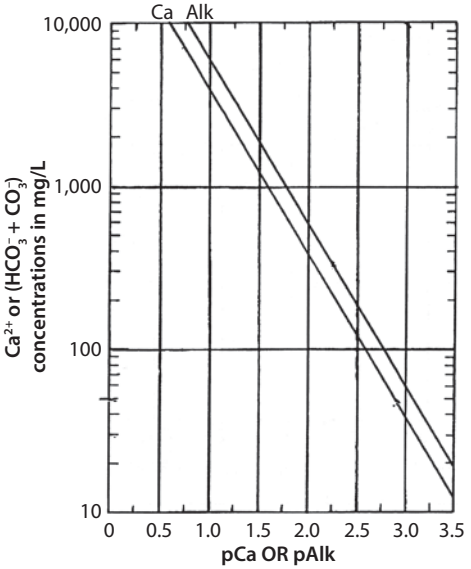

Figure 7.9 Determination of values for pCa and pAlk from concentrations of [HCO_3^-, $CO_3^=$, (After Langelier, 1936; in: Chillingar *et al.*, 2008, p. 129, figure 6.5.)

4. Determine the ratio *R'* (assuming that the gas in contact with water contains 5 mol % CO_2 at a total pressure of 1 bar):

$$R' = \frac{\left(\frac{\text{mg}}{\text{L}}\text{HCO}_3^-\right)\times 0.82}{(\text{mol fraction CO}_2)\times S_f} = \frac{325.5\times 0.82}{0.05\times 40} = 133.4 \quad (7.11)$$

where the mole fraction of CO_2 is determined from gas analysis and S_f is the solubility factor determined from Figure 7.10. At a temperature of 60 °C and a pressure of 1 bar, $S_f = 40$.

5. Determine pH from Figure 7.11 (*R'* versus pH):

$$pH = 9$$

Note: the pH decreases with increasing concentration of CO_2 in water.

6. Determine *SI:*

$$SI = pH_{(actual)} - pH_s$$
$$SI = 9 - 5.5 = 3.5$$

Because the *SI* value is positive, $CaCO_3$ scale will probably form.

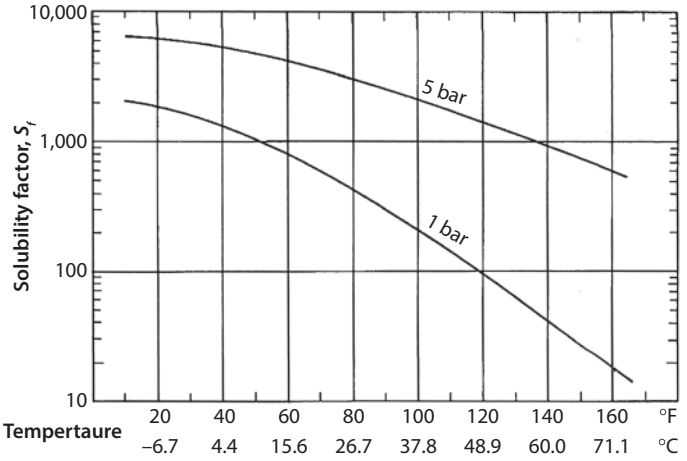

Figure 7.10 Variation of S_f with temperature and pressure. (Modified after Jones, 1988, p. 121; in: Chilingar *et al.*, p. 130, figure 6.6.)

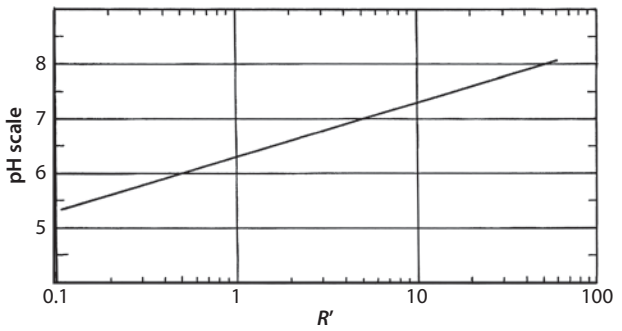

Figure 7.11 Relationship between pH and R′ value. (Modified after Jones, 1988; in: Chilingar *et al.*, 2008, p. 130, figure 6.7.)

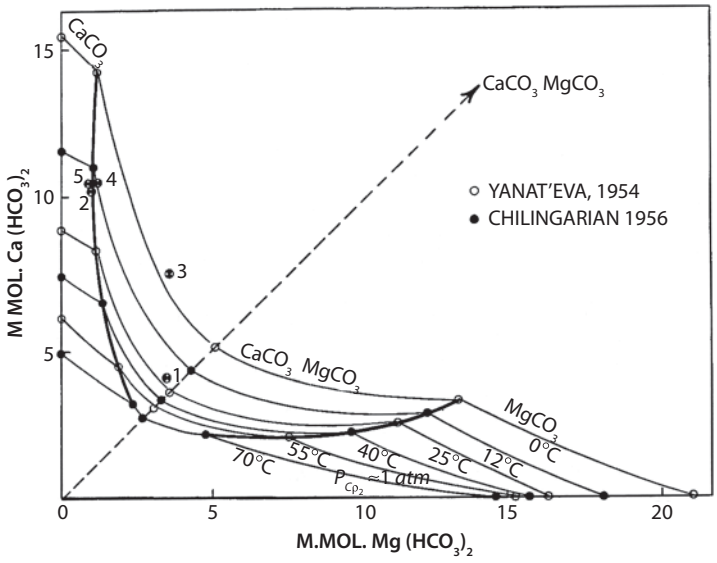

Figure 7.12 Solubility of $CaCO_3$-$MgCO_3$-H_2O system at $P_{CO_2} \approx 1$ atm and temperatures ranging from 0° to 70 °C. Points between ordinate and 45°-line represent solubility of calcite-dolomite mixtures, whereas those between the 45°-line and abscissa represent dolomite-magnesite mixtures. (After Yanat'eva, 1954, p.777; in: Chilingar *et al*., 2008, p. 133, figure 6.9.)

7.7 Solubility of Calcite, Dolomite, Magnesite and Their Mixtures

The solubility of calcite, dolomite, magnesite and mixture of these components in water at $P_{CO_2} \approx 1$ atm and temperatures ranging from 0 to 70 °C are presented in Figure 7.12. The amounts of $Mg(HCO_3)_2$ and $Ca(HC0_3)_2$ (expressed in millimoles per 1,000 g of solution) are plotted on the abscissa and ordinate, respectively. The points of intersection between bisectrix and dolomite saturation curves show the composition of solutions saturated with pure dolomite, whereas the solubilities of pure $CaCO_3$ and $MgCO_3$ are shown on the ordinate and abscissa, respectively. On the other hand, the solubilities of mixtures of dolomite + calcite and dolomite + magnesite (two phase) are shown by the junction (nodal) points. The curve connecting these junction points to the left of bisectrix represents solubility of mixtures of dolomite and calcite, whereas the one at the right of bisectrix represent the mixture of dolomite and magnesite. In all cases, the magnesite had the highest solubility, whereas dolomite was the least soluble.

7.8 Scale Removal

Table 7.6 lists the advantages and disadvantages of several methods of scale removal. The key to any such removal process is not to damage either the formation or equipment. The best scale removal process requires knowledge of the type and quantity of scale and its composition (Crabtree *et al*., 1999). A poor choice could damage the reservoir.

Table 7.6 Comparison of various mechanical , chemical, and jet-blasting scale-removal techniques. (Modified after Crabtree *et al.*, 1999).

Tool	Description	Clean hard bridges	Clean tubular jewelry	Advantages	Disadvantages
Mechanical cleaning					
Impact hammer	Fluid powered percussion hammer. High shock forces shatter of brittle deposits	Yes. Clean rate may be very slow.		Positive surface indication of cleaning. Simple, robust tool.	Large cuttings size makes hole cleaning more difficult. Not compatible with scale dissolvers.
Positive displacement Motor and mill	Fluid-powered 'Moineau' and mill. Mill removed deposits by grinding	Yes. Clean rate may be very slow.		Positive surface indication of cleaning. Small cuttings make hole cleaning easier.	Motor stator and mill are expensive expendables – temperature of 300 °F (150 °C) limit. Not compatable with scale dissolvers. Mill can damage tubulars.
Chemical cleaning					
Fixed wash tool	Fixed tool with many large diametr nozzles. Normally used only with chemical dissolvers.		Yes, if deposit is soluble	Simple, robust tool	Must fluid power is lost to circulating friction. Low nozzle pressure – cannot remove inert deposits.
Indexed jetting tool	Nozzle head rotates – 90° when coiled tubing pressure is cycled. Head has many small-diameter nozzles to improve wellbore coverage.		✓		Abrasives cannot be pumped through turbine. It is a complex tool.
Sonic tools	Used to create high-frequency pressure pulses that remove deposits by shock waves or cavitation.		Yes, if deposit is soluble	Simple	Hydrostatic pressure suppresses cavitation. Tools not effective in removing hard scales in lab tests.
Spinning jetting tool	Rotational torque provided by nozzles offset from tool axis. No speed control.		Yes, if deposit is soluble.	Simple tool. Complete wellbore coverage by rotating jets.	Inefficient jetting due to high rpm (>5000).
Turbine powered jetting tool	Fluid turbine rotates nozzle with two nozzles. Eddy current brake controls, rpm.		✓	Complete wellbore coverage with large cleaning ratios.	Abrasives cannot be pumped through turbine. Complex tool.
Jet Blaster tools					
Bridge Blasting technique	Fluid powered 'Moineau' motor and jet/mill head. Radial jets follow pilot mill.	✓	✓	Positive surface indication of cleaning.	Motor stator is an expensive expendable -- 300 °F temperature limit.
Scale Blasting technique	Nozzle head rotated by two nozzles offset from tool axis. Viscous brake controls rpm.		✓	Complete wellbore with large coverage cleaning radius. Positive surface indication of cleaning.	

In the case of tubular goods and surface equipment, scale strength and texture play significant roles in the choice of removal technique. Strengths and textures can vary from delicate, brittle whiskers or crystals with high microporosity, to dense, low-permeability, low-porosity layers. Scale purity determines its resistance to removal. Scale may occur as a single-mineral phase, but more commonly is a mixture of materials. Pure barium sulfate is normally of low porosity and is extremely impervious to chemical removal, and only slowly removable by most established mechanical techniques. Mixtures of barium sulfate with strontium sulfate, calcium sulfate or calcium carbonate, will frequently yield to a variety of removal methods, both chemical and mechanical (Crabtree *et al*., 1999).

Crabtree *et al*. (1999) stated that chemical removal of scale is often the cheapest; however, most chemical treatments are controlled by how well the reagents can gain access to the scale surface. Consequently, the surface-area-to-volume ratio, is an important parameter. Smaller specific surface areas in thick, nonporous scales are slow to react with any but the strongest chemical reactants. Chemical treatment in tubing is usually too slow to make it a practical scale removal method.

7.9 Scale Inhibition

Scale formation can be avoided by sequestering or chelating the inorganic cation, which can be expensive. Scale inhibitors can prevent the formation of scale without the expense of removing the cations. According to Jones (1988, p. 126), classes of scale inhibition chemicals include:

1. Sodium polyacrylate polymers
2. Amino-phosphates
3. Phosphate esters of amino-alcohols

The scale inhibitor chemical is usually prediluted with water in a concentration of 1–2 vol %. The treating dose ranges from 2 to 10 mg/L.

For an inhibitor to work properly in a reservoir, placement is critical, e.g., in the case where scaling is to be prevented within the reservoir being waterflooded. Mackay (2008) noted that the success of an inhibitor used in reservoirs located in deepwater and other harsh environments often depends upon its proper placement. The question is: "Can we get the inhibitor where it is needed?" He further noted that cost of placement of an inhibitor within such a reservoir is expensive; however, the cost in preventing formation of the scale within the reservoir, resulting in formation damage, is less than the cost of redrilling wells. Looking at costs for these types of projects in 2008, he noted the following:

1. Deepwater wells cost $10 to $100 million.
2. Interval control valves (ICV's) needed to place the inhibitor cost $0.5 to $1 million to install.
3. Hiring a rig for treatment costs from $100,000 to $400,000 a day.

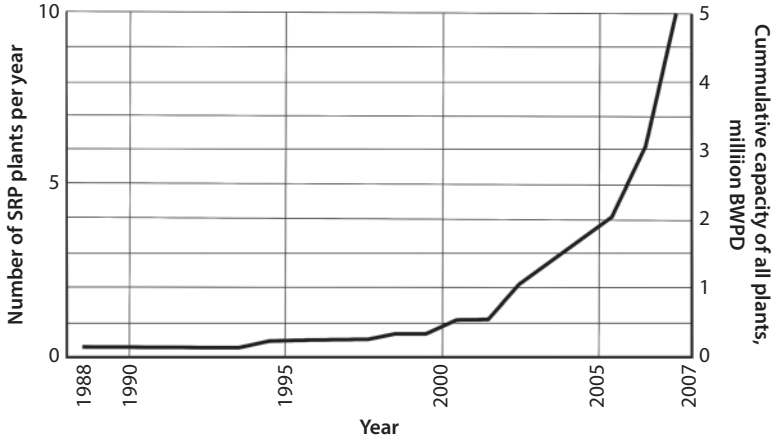

Figure 7.13 Graph showing the growth of the number and total capacity of the sulphate reduction plants (SRP) built in recognition of the formation plugging that can occur when a foreign water is injected into a reservoir. (Modified after Mackey, 2008, slide 17.)

4. A sulphate reduction plant (SRP) installation and operation could cost $20 to $100 million.
5. The success of an SRP depends upon obtaining representative (good quality) brine samples and analysis.

Figure 7.13 demonstrates the growing concern about treatment of injected waters into a reservoir between 1988 and 2007. Although the total cost is significant to treat the water to prevent precipitation, it is less than redrilling the project.

In designing reservoir treatment programs, particularly where intervention may be difficult and expensive, it is important to be aware of the many uncertainties such as:

1. Reservoir description.
2. Injected water and reservoir brine description.
3. Potential future changes to the production schedule, etc.
4. Numerical errors.
5. Continuous monitoring to observe any changes.

7.10 Conclusions

"An ounce of prevention is better than a pound of cure," which in the case of scaling is immense. One has to predict the occurrence of scaling and then take the necessary steps to prevent its occurrence.

References and Bibliography

Allen, T. O. and Roberts, A. P., 1982. *Production Operation, Well Completions, Workover, and Stimulation*. Oil and Gas Consultants International, Inc., Tulsa, OK, 241 pp.

Babalyan, G.A., 1956. *Questions on Mechanism of Oil Recovery, Aznefteizdat,* Baku. 254 pp.
Becker, J. R., 1998. *Corrosion and Scale Handbook.* Tulsa, OK. Penn Well Publishing Company, 329 pp.
Bernard, G. C., 1967. Effect of floodwater salinity on recovery of oil from cores containing clays, *SPE Paper 1725* presented at AIME Meeting in Los Angeles, CA (Oct. 1967)' 8 pp.
Carlberg, B. L., Casad, B. M., Brace, R. L., and Chambers, F. B. Jr, 1962. Stabilize water for high-temperature flooding. *Oil and Gas J*., July 2, pp. 120–122.
Chilingar, G.V., Mourhatch, R. and Al-Qahtani, G. D., 2008. *The Fundamentals of Corrosion and Scaling for Petroleum & Environmental Engineers*, Gulf Publishing, Houston TX, 279 pp.
Chilingar, G. V., 1968. Increase in oil recovery by changing chemistry of water. *Bull. O.N.G.C. (India),* 4(2):25–26.
Chiligarian, G. V., Robertson, J. O. Jr., and Kumar.S, 1989. *Surface Operations in Petroleum Production, II*. Amsterdam: Elsevier Science Publishers B.V., 397 pp.
Chilingarian, G. V., 1956. Solubility of calcite, dolomite, and magnesite, and mixture of these carbonates. *Am. Assoc. Pet. Geol.,* 40(11*)*:2770–2773.
Crabtree, M., Elsinger, D., Flectcher, P., Miller, M., Johnson, A., and King, G., 1999. Fighting Scale – Removal and Prevention. *Oilfield Review*, Aug, pp. 30–45
Fulford, R. S., 1968. Effect of brine concentration and pressure drop on gypsum scaling in oil-wells. *J.Pet. Tech.,* June: 559.
Jones, L. W., 1988. *Corrosion and Water Technology for Petroleum Producers.* Oil and Gas Consultants International, Inc. (OGCI Publications), Tulsa, OK. 202 pp.
Langelier, W G., 1936. The analytical control of anti-corrosion water treatment. *J. Am. Water Works Assoc*., 28:1500.
Langnes, G. L., Robertson, J. O. Jr., and Chilingar, G. V., 1972. *Secondary Recovery and Carbonate Reservoirs.* New York, NY· American Elsevier Publishing Company, Inc., 304 pp.
Lindlof, J. D. and Stoffer, K. G., 1983. A case study of seawater injection incompatibility. *J. Pet. Tech*., July:1256–1262.
Mackay, E. J., 2008. Oilfield Scale. www.spe.org/dl/docs/2008/Mackay.pdf
Nazaroff, W. W. and Alvarez-Cohen, L., 2001. *Environmental Engineering Science.* John Wiley and Sons, lnc., New York, 690 pp.
Patton, C. C., 1977. *Oilfield Water Systems,* 2nd ed. Norman, OK. Campbell Petroleum Series.
Sinnokrot, A. and Chilingar, G. V., 1961. Effect of polarity of oil and presence of carbonate particles on relative permeability of rocks. *The Compass of Sigma Gamma Epsilon,* 38:115–120.
Stiff, H. A. and Davis, L. E., 1952. A method for predicting the tendency of oilfield waters to deposit calcium carbonate. *Petroleum Trans*., AIME*,* 195:213.
Tchillingarian, G., 1952. Study of the dispersing agents. *J. Sed. Pet*., 22(4):229–232.
Templeton, C. C., 1960. Solubility of barium sulfate in sodium chloride solutions from 25 °C to 95 °C. *J. Chemical Data*, 5:514.
Weintritt, D. J. and Cowan, J. C., 1967. Unique characteristics of barium sulfate scale deposition. *J. Petrol. Tech.,* 19:1381.
Wright, C. C. and Chilingarian, G. V., 1989 Water quality for subsurface injection. In: G. V. Chilingarian, J. O. Robertson, and S. Kumar (Editors), *Surface Operations in Petroleum Production,* Amsterdam. Elsevier, pp. 119–171.
Yanat'eva, O. K., 1954. About physical-chemical characteristics of some carbonate rocks. *Dokl. Akad. Nauk. SSSR,* 96(4):777–779.

Environmental Aspects of Oil and Gas Production.
John O. Robertson and George V. Chilingar.
© 2017 Scrivener Publishing LLC. Published 2017 by John Wiley & Sons, Inc.

Appendix A

By Michael D. Holloway

Abbreviations

A

AADE – American Association of Drilling Engineers
AAODC – American Association of Oilwell Drilling Contractors (obsolete; superseded by IADC)
ABAN – Abandonment
ACOU – Acoustic
ACQU – Acquisition Log
ADROC – Advanced Rock Properties Report
ADT – ADT Log
AFE – Authorization for Expenditure, a process of submitting a business proposal to investors.
AHBDF – Along Hole Below Derrick Floor
AIRG – Airgun
AIRRE – Airgun Report
AIT – Array Induction Tool
AL – Appraisal License (United Kingdom), a type of onshore license issued before 1996.
ALC – Vertical Seismic Profile Acoustic Log Calibration Report
ALR – Acoustic Log Report
AMS – Auxiliary Measurement Service Log
ANACO – Analysis of Core Logs Report
ANARE – Analysis Report
AOF – Absolute Open Flow

AOFP – Absolute Open Flow Potential
APD – Application for Permit to Drill
API – American Petroleum Institute: both the organization and measure of oil weight (API gravity) in API.
APPRE – Appraisal Report
APS – Active Pipe Support
ARACL – Array Acoustic Log
ARESV – Analysis of Reservoir
ARI – Azimuthal Resistivity Image
ARRC – Array Acoustic Report
AS – Array Sonic Processing Log
ASI – ASI Log
ASME – American Society of Mechanical Engineers
ASP – Array Sonic Processing Report
ASV – Annular Safety Valve
AV – Annular Velocity or Apparent Viscosity
AVO – Amplitude Versus Offset (geophysics)
AWB – Annulus Wing Block
AWO – Approval for Well Operation

B
B or b – prefix denoting a number in billions
bbl – barrel
Bbl, Barrel – In the oil and gas industry, a barrel is 42 U.S. gallons measured at 60° Fahrenheit.
bcf – billion cubic feet (of natural gas)
BDF – Below Derrick Floor
BDL – Bit Data Log
BGL – Below ground level (used as a datum for depths in a well.)
BGL – Borehole Geometry Log
BGS – British Geological Survey
BGT – Borehole Geometry Tool
BGWP – Base of Group Water Protection
BHA – Bottom Hole Assembly (tool string on coiled tubing or drill pipe.)
BHC – BHC Gamma Ray Log
BHCA – BHC Acoustic Log
BHCS – BHC Sonic Log
BHCT – Bottom Hole Circulating Temperature
BHL – Borehole Log
BHP – Bottom Hole Pressure
BHP, Bottom Hole Pressure – The abbreviation for bottom-hole pressure.
BHPRP – Borehole Pressure Report
BHSRE – Bottom Hole Sampling Report
BHSS – Borehole Seismic Survey
BHTV – Borehole Television Report

BINXQ – Bond Index Quick Look Log
BIOR – Bio-stratigraphic Range Log
BIORE – Biostratigraphy Study Report
BIVDL – BI/DK/WF/Casing Collar Locator/Gamma Ray Log
BO – Back Off Log
boe – barrel(s) of oil equivalent
boed – barrel(s) of oil equivalent per day
boepd – barrel(s) of oil equivalent per day
BOM – Bill of Materials
BOP – Blowout preventer
bopd – barrel(s) of oil per day
BOREH – Borehole Seismic Analysis
BOTHL – Bottom Hole Locator Log
BOTTO – Bottom Hole Pressure/Temperature Report
BP, Blowout Preventer – Casinghead equipment that prevents the uncontrolled flow of oil, gas and mud from the well by closing around the drill pipe or sealing the hole.
bpd – barrels per day
BPFL – Borehole Profile Log
BPLUG – Baker Plug
BPV – Back Pressure Valve (goes on the end of coiled tubing a drill pipe tool strings to prevent fluid flow in the wrong direction)
BQL – B/QL Log
BRPLG – Bridge Plug Log
BRT – Below Rotary Table (used as a datum for depths in a well)
BS&W – Bottom Sediment and Water – Impurities and water contained in the raw fluid produced by an oil well.
BTHL – Bottom Hole Log
BTU, British Thermal Unit – The amount of heat required to raise the temperature of one pound of water one degree Fahrenheit under standard conditions of pressure and temperature.
BUR – Build-Up Rate
bwd – barrels of water per day (often used in reference to oil production)
bwpd – barrels of water per day

C
C&E – Well completion and equipment cost
C&S – Cased and Suspended
C1 – Methane
C2 – Ethane
C3 – Propane
C4 – Butane
C6 – Hexanes
C7+ – Heavy Hydrocarbon Components

CA – Core Analysis Log
CALIL – Caliper Log
CALOG – Circumferential Acoustic Log
CALVE – Calibrated Velocity Log Data
CAPP – Canadian Association of Petroleum Producers
CAS – Casing Log
CB – Core Barrel
CBIL – CBIL Log
CBL – Cement Bond Log (measurement of casing cement integrity)
CBM – Choke Bridge Module – XT Choke
CBM – Conventional Buoy Mooring
CCHT – Core Chart Log
CCL – Casing Collar Locator (in perforation or completion operations, the tool provides depths by correlation of the casing string's magnetic anomaly with known casing features)
CCLP – Casing Collar Locator Perforation
CCLTP – Casing Collar Locator Through Tubing Plug
CD – Core Description
CDATA – Core Data
CDIS – CDI Synthetic Seismic Log
CDP – Common Depth Point (geophysics)
CDP – Comprehensive Drilling Plan
CDRCL – Compensated Dual Resistivity Cal. Log
CDU – Control Distribution Unit
CE – CE Log
CECAN – CEC Analysis
CEME – Cement Evaluation
CERE – Cement Remedial Log
CET – Cement Evaluation Tool
CFD – Computational Fluid Dynamics
CGEL – CG EL Log
CGL – Core Gamma Log
CGPH – Core Graph Log
CGR – Condensate gas ratio
CGTL – Compact Gas to liquids (production equipment small enough to fit on a ship)
CHCNC – CHCNC Gamma Ray Casing Collar Locator
CHDTP – Caliper HDT Playback Log
CHECK – Checkshot and Acoustic Calibration Report
CHKSR – Checkshot Survey Report
CHKSS – Checkshot Survey Log
CHP – Casing Hanger Pressure (pressure in an annulus as measured at the casing hanger)
CHROM – Chromatolog
CILD – Conduction Log
CIMV – Chemical Injection Metering Valve

CITHP – Closed In Tubing Head Pressure (tubing head pressure when the well is shut in)
CIV – Chemical Injection Valve
CL – Core Log
CLG – Core Log and Graph
CM – Choke Module
CMP – Common Midpoint (geophysics)
CMR – CMR Log
CND – Compensated Neutron Density
CNFDP – CNFD True Vertical Depth Playback Log
CNGR – Compensated Neutron Gamma Ray Log
CNL – Compensated Neutron Log
CNLFD – CNL/FDC Log
CNS – Central North Sea
COL – Collar Log
COMAN – Compositional Analysis
COML – Compaction Log
COMP – Composite Log
COMPR – Completion Program Report
COMPU – Computest Report
COMRE – Completion Record Log
CONDE – Condensate Analysis Report
CONDR – Continuous Directional Log
CORAN – Core Analysis Report
CORE – Core Report
CORG – Corgun Log
CORIB – Coriband Log
CORLG – Correlation Log
COROR – Core Orientation Report
COXY – Carbon/Oxygen Log
CPI – CPI Log
CPICB – CPI Coriband Log
CPIRE – CPI Report
CRET – Cement Retainer Setting Log
CsF – Caesium Formate (coincidentally also an acronym of the sole large-scale supplier of caesium formate brine, Cabot Specialty Fluids.)
CSHN – Cased Hole Neutron Log
CSI – CSI Log
CSMT – Core Sampler Tester Log
CSPG – Canadian Society of Petroleum Geologists
CST – CST Log
CSTAK – Core Sample Taken Log
CSTRE – CST Report
CSUG – Canadian Society for Unconventional Gas
CT – Coiled Tubing
CTCO – Coiled Tubing Clean Out

CTD – Coiled Tubing Drilling
CTRAC – Cement Tracer Log
CUT – Cutter Log
CUTTD – Cuttings Description Report
CWA – Clean Water Act
CWOR – Completion Work Over Riser
CYBD – Cyberbond Log
CYBLK – Cyberlook Log
CYDIP – Cyberdip Log
CYDN – Cyberdon Log
CYPRO – Cyberproducts Log

D
D&A – Dry and abandoned. Refers to oil and gas wells.
D&C – Drilling and Completions
DAC – Dipole Acoustic Log
DARCI – Darci Log
DAZD – Dip and Azimuth Display
DC – Drill Collar(s)
DCALI – Dual Caliper Log
DD – Directional Driller or Directional Drilling
DDBHC – DDBHC Waveform Log
DDET – Depth Determination Log
DDM – Derrick Drilling Machine (a.k.a. Top Drive)
DDNL – Dual Det. Neutron Life Log
DDPT – Drill Data Plot Log
DECC – Department for Energy and Climate Change (United Kingdom)
DECT – Decay Time
DEFSU – Definitive Survey Report
DELTA – Delta-T Log
DEN – Density Log
DEPAN – Deposit Analysis Report
DEPC – Depth Control Log
DESFL – Deep Induction SFL Log
DEV – Development Well, Lahee classification
DEVLG – Deviation Log
DEXP – D-Exponent Log
DF – Derrick Floor
DFR – Drilling Factual Report
DH – Drilling History
DHC – Depositional History Curve
DHPTT – Downhole Pressure/Temperature Transducer
DHSV – Downhole Safety Valve
DIBHC – DIS BHC Log
DIEGR – Dielectric Gamma Ray Log
DIL – Dual Induction Log

DILB – Dual Induction BHC Log
DILL – Dual Induction Laterolog
DILLS – Dual Induction Log-LSS
DILSL – Dual Induction Log-SLS
DIM – Directional Inertia Mechanism
DINT – Dip Interpretation
DIP – Dipmeter Log
DIPAR – Dipole Acoustic Report
DIPBH – Dipmeter Borehole Log
DIPFT – Dipmeter Fast Log
DIPLP – Dip Lithology Pressure Log
DIPRE – Dipmeter Report
DIPRM – Dip Removal Log
DIPSA – Dipmeter Soda Log
DIPSK – Dipmeter Stick Log
DIRS – Directional Survey Log
DIRSU – Directional Survey Report
DIS – DIS-SLS Log
DISFL – DISFL DBHC Gamma Ray Log
DISO – Dual Induction Sonic Log
DL – Development License (United Kingdom), a type of onshore license issued before 1996
DLIST – Dip List Log
DLL – Dual Laterolog
DLS – Dog-Leg Severity (directional drilling)
DNHO – Downhole Logging
DOE – Department of Energy, United States
DOWRE – Downhole Report
DP – Drill Pipe
DPDV – Dynamically-Positioned Drilling Vessel
DPL – Dual Propagation Log
DPLD – Differential Pressure Levitated Device (or Vehicle)
DPRES – Dual Propagation Resistivity Log
DPT – Deeper Pool Test, Lahee classification
DQLC – Dipmeter Quality Control Log
DR – Drilling Report
DR – Dummy Run Log
DRI – Drift Log
DRLCT – Drilling Chart
DRLOG – Drilling Log
DRLPR – Drilling Proposal/Prog. Report
DRPG – Drilling Program Report
DRPRS – Drilling Pressure
DRREP – Drilling Report
DRYRE – Drying Report
DS – Deviation Survey

DSCAN – DSC Analysis Report
DSI – Dipole Shear Imager
DSPT – Cross Plots Log
DST – Drill Stem Test
DSTG – DSTG Log
DSTL – Drill Stem Test Log
DSTND – Dual Space Thermal Neutron Density Log
DSTPB – Drill Stem Test True Vertical Depth Playback Log
DSTR – Drill Stem Test Report
DSTRE – Drill Stem Test Report
DSTSM – Drill Stem Test Summary Report
DSTW – Drill Stem Test Job Report/Works
DSV – Diving Support Vessel or Drilling Supervisor
DTI – Department of Trade and Industry (United Kingdom) (obsolete; superseded by dBERR, which was then superseded by DECC)
DTPB – CNT True Vertical Depth Playback Log
DTT – Depth To Time
DWOP – Drilling Well on Paper (a theoretical exercise conducted involving the Service provider managers)
DWQL – Dual Water Quicklook Log
DWSS – Dig Well Seismic Surface Log
DXC – DXC Pressure Pilot Report

E
E&A – Exploration and Appraisal
E&P – Exploration and Production
ECD – Equivalent Circulating Density
ECP – External Casing Packer
ECRD – Electrically Controlled Release Tool
EDP – Emergency Disconnect Package
EDP – Exploration Drilling Program Report
EFR – Engineering Factual Report
EGMBE – Ethylene Glycol Mono-Butyl Ether
EL – Electric Log
ELT – Economic Limit Test
EM – EMOP Log
EMOP – EMOP Well Site Processing Log
EMP – Electromagnetic Propagation Log
EN PI – Enhanced Productivity Index Log
ENGF – Engineer Factual Report
ENGPD – Engineering Porosity Data
ENJ – Enerjet Log
EOFL – End of Field Life
EOR – Enhanced Oil Recovery
EOW – End Of Well Report
EPCU – Electrical Power Conditioning Unit

EPIDORIS – Exploration and Production Integrated Drilling Operations and Reservoir Information System
EPL – EPL Log
EPLG – Epilog
EPT – EPT Log
EPTNG – EPT-NGT Log
ER(D) – Extended Reach (Drilling)
ESD – Emergency Shut-Down
ESP – Electric Submersible Pump
ETAP – Eastern Trough Area Project
ETTD – Electromagnetic Thickness Test
EVARE – Evaluation Report
EWR – End Of Well Report
EZSV – EZSV Log

F
FAC – Factual Report
FACHV – Four Arm Caliper Log
FANAL – Formation Analysis Sheet Log
FC – Float Collar
FCP – Final circulating pressure
FCVE – F Curve Log
FDC – Formation Density Log
FDP – Field Development Plan
FDS – Functional Design Specification
FEED – Front End Engineering and Design
FEWD – Formation Evaluation While Drilling
FFAC – Formation Factor Log
FFM – Full Field Model
FGEOL – Final Geological Report
FH – Full Hole Tool Joint
FID – Final Investment Decision
FIL – FIL Log
FINST – Final Stratigraphic Report
FINTP – Formation Interpretation
FIT – Formation Integrity Test
FIV – Formation Isolation Valve
FL – F Log
FLIV – Flowline Isolation Valve
FLOG – FLOG PHIX RHGX Log
FLOPR – Flow Profile Report
FLOT – Flying Lead Orientation Tool
FLOW – Flow & Buildup Test Report
FLS – Fluid Sample
flt – Fault (geology)
FMECA – Failure Modes, Effects, and Criticality Analysis

FMI – Formation Microimager Log
FMP – Formation Microscan Report
FMS – Formation Multiscan Log
FMTAN – FMT Analysis Report
FOSV – Full Opening Safety Valve
FPIT – Free Point Indicator Tool
FPL – Flow Analysis Log
FPLAN – Field Plan Log
FPSO – Floating Production Storage and Offloading vessel
FPU – Floating Processing Unit
FRA – Fracture Log
FRARE – Fracture Report
FRES – Final Reserve Report
FS – Fail Safe (as in FS valve)
FSO – Floating Storage Offloading vessel
FT – Formation Tester Log
FTRE – Formation Testing Report
FULDI – Full Diameter Study Report
FV – Funnel Viscosity or Float Valve
FWL – Free water level
FWR – Final Well Report
FWV – Flow Wing Valve (also known as Production Wing Valve on a Xmas tree)

G
G/C – Gas Condensate
GAS – Gas Log
GASAN – Gas Analysis Report
GBS – Gravity Based Structure
GBT – Gravity Base Tank
GCLOG – Graphic Core Log
GCT – GCT Log
GDIP – Geodip Log
GE – Condensate gas equivalent
GEOCH – Geochemical Evaluation
GEODY – GEO DYS Log
GEOEV – Geochemical Evaluation Report
GEOFO – Geological & Formation Evaluation Report
GEOL – Geological Surveillance Log
GEOP – Geophone Data Log
GEOPN – Geological Well Prognosis Report
GEOPR – Geological Operations Prog. Report
GEORE – Geological Report
GGRG – Gauge Ring
GIIP – Gas Initially In Place
GIS – Geographic Information System(s)

GL – Gas Lift
GLM – Gas Lift Mandrel (alternative name for Side Pocket Mandrel)
GLR – Gas Liquid Ratio
GLT – GLT Log
GLV – Gas Lift Valve
GOC – Gas Oil Contact
GOM – Gulf of Mexico
GOP – Geological Operations Report
GOR – Gas/Oil Ratio (Number of cubic feet of gas produced per barrel of oil.)
GOSP – Gas/Oil Separation Plant
GPIT – Inclinometry Tool Log
GPLT – Geol Plot Log
GPSL – Geo Pressure Log
GRAD – Gradiometer Log
GRLOG – Grapholog
GRN – Gamma Ray Neutron Log
GRSVY – Gradient Survey Log
GRV – Gross Rock Volume
GST – GST Log
GTL – Gas to liquids
GTW – Gas To Wire
GUN – Gun Set Log
GWPC – Ground Water Protection Council
GWREP – Geo Well Report

H
HAZID – Hazard Identification (meeting)
HC – Hydrocarbons
HCCS – Horizontal Clamp Connection System
HDT – High Resolution Dipmeter Log
HEXT – Hex Diplog
HGS – High (specific-)Gravity Solids
HL – Hook Load
HP – Hydrostatic Pressure
HPGAG – High Pressure Gauge
HPHT – High Pressure High Temperature (same as HTHP)
HPPS – HP Pressure Log
HSE – Health, Safety and Environment or Health & Safety Executive (United Kingdom)
HTHP – High Temperature High Pressure (same as HPHT)
HUD – Hold Up Depth
HVDC – High Voltage Direct Current
HWDP – Heavy Weight Drill Pipe
HWDP – Heavy-Weight Drill Pipe (sometimes spelled Hevi-Wate)
HYPJ – Hyperjet
HYROP – Hydrophone Log

I

I:P – Injector To Producer Ratio
IADC – International Association of Drilling Contractors
IBC – Intermediate Bulk Container
ICoTA – Intervention and Coiled Tubing Association
ICV – Interval Control Valve
ID – Inner or Internal Diameter (of a tubular component such as a casing)
IDC – Intangible Drilling Costs
IDEL – IDEL Log
IEB – Induction Electro BHC Log
IEL – Induction Electrical Log
IF – Internal Flush tool joint
IH – Gamma Ray Log
IJL – Injection Log
IL – Induction Log
ILOGS – Image Logs
IMAG – Image Analysis Report
INCR – Incline Report
INCRE – Incline Report
INDRS – IND RES Sonic Log
INDT – INDT Log
INDWE – Individual Well Record Report
INJEC – Injection Falloff Log
INSUR – Inrun Survey Report
INVES – Investigative Program Report
IOC – International Oil Company
IPAA – Independent Petroleum Association of America
IPC – Installed Production Capacity
IPR – Inflow Performance Relationship
IR – Interpretation Report
IRTJ – IRTJ Gamma Ray Slimhole Log
ISFBG – ISF BHC GR Log
ISFCD – ISF Conductivity Log
ISFGR – ISF GR Casing Collar Locator Log
ISFP – ISF Sonic True Vertical Depth Playback Log
ISFPB – ISF True Vertical Depth Playback Log
ISFSL – ISF SLS MSFL Log
ITS – Influx To Surface
IWCF – International Well Control Federation
IWOCS – Installation / Workover Control System

J

JB – Junk Basket
JT – Joule-Thomson (effect/valve/separator)
JU – Jack-Up drilling rig

K

KB – Kelly Bushing
KOP – Kick Off Plug
KOP – Kick-Off Point (directional drilling)

L

LACT – Lease Automatic Custody Transfer
LACT Unit, Lease Automatic Custody Transfer Unit – A system providing for the automatic measurement, sampling, and transfer of oil from the lease location into a pipeline.
LAT – Lowest Astronomical Tide
LCM – Lost Circulation Material
LCNLG – LDT CNL Gamma Ray Log
LDL – Litho Density Log
LDTEP – LDT EPT Gamma Ray Log
LEAKL – Leak Detection Log
LEPRE – Litho-Elastic Property Report
LGR – Liquid Gas Ratio
LGS – Low (specific-)Gravity Solids
LINCO – Liner and Completion Prog. Report
LIOG – Lithography Log
LITDE – Litho Density Quicklook Log
LITHR – Lithological Description Report
LITRE – Lithostratigraphy Report
LITST – Lithostratigraphic Log
LKO – Lowest Known Oil
LL – Laterolog
LMAP – Location Map
LMRP – Lower Marine Riser Package
LMV – Lower Master Valve (on a Xmas tree)
LNG – Liquefied Natural Gas
LOE – Lease Operating Expenses
LOGRS – Log Restoration Report
LOGSM – Log Sample
LOLER – Lifting Operations and Lifting Equipment Regulations
LOT – Leak-Off Test
LOT – Linear Override Tool
LOT – Lock Open Tool
LP – Low Pressure
LSBGR – Long Spacing BHC GR Log
LSSON – Long Spacing Sonic Log
LT – Linear Time
LUMI – Luminescence Log

LVEL – Linear Velocity Log
LWD – Logging While Drilling

M
M or m – prefix designating a number in thousands (not to be confused with SI prefix M for mega- or m for milli)
MAASP – Maximum Acceptable [or Allowable] Annular Shut-in Pressure
MAC – Multipole Acoustic Log
MACL – Multiarm Caliper Log
MAGST – Magnetostratigraphic Report
MARA – Maralog
MAWP – Maximum Allowable Working Pressure
mbd – thousand barrels per day
mbod – thousand barrels of oil per day
MCM – Manifold Choke Module
MCS – Manifold & Connection System
MCS – Master Control Station
MD – Measured Depth (see also MDSS)
MD – Measurements/Drilling Log
MDL – Methane Drainage License (United Kingdom)
MDSS – Measured Depth Sub-Sea
MDT – Modular formation Dynamic Tester
MEG – Mono Ethylene Glycol
MEPRL – Mechanical Properties Log
MERCR – Mercury Injection Study Report
MERG – Merge FDC/CNL/Gamma Ray/Dual Laterolog/Micro SFL Log
MEST – MEST Log
MF – Marsh Funnel (mud viscosity)
MFCT – Multifinger Caliper Tool
MGL – Magnelog
MIFR – Mini Frac Log
MINL – Minilog
MIPAL – Micropalaeo Log
MIYP – maximum internal yield pressure
mKB – Meters below Kelly Bushing
ML – Microlog
MLL – Microlaterolog
MM or mm – prefix designating a number in millions (not to be confused with SI unit mm for millimetre)
mmbd – million barrels per day
mmbod – million barrels of oil per day
MMBtu – One million British thermal units; a measurement of heating value.
MMcf – One million cubic feet; a measurement of gas volume only.
MMS – Minerals Management Service, (United States)
mmscfd – million standard cubic feet per day
mmstb – million stock barrels

MNP – Merge and Playback Log
MODU – Mobile Offshore Drilling Unit
MOPU – Mobile Offshore Production Unit
MPA – Micropaleo Analysis Report
MPD – Managed Pressure Drilling
MPFM – Multi-Phase Flow Meter
MPK – Merged Playback Log
MPS – Manufacturing Procedure Specification
MQC – Multi Quick Connection Plate
MR – Marine Riser
MRCV – Multi Reverse Circulating Valve
MRIRE – Magnetic Resonance Image Report
MSCT – MSCT Gamma Ray Log
MSFL – Micro SFL Log
MSL – Mean sea level
MSL – Micro Spherical Log
MSS – Magnetic Single Shot
MST – MST EXP Resistivity Log
MTT – MTT Multi-Isotope Trace Tool
MUD – Mud Log
MUDT – Mud Temperature Log
MuSol – Mutual Solvent
MVB – Master Valve Block
MWD – Measurement While Drilling
MWDRE – Measurement While Drilling Report

N
NACE – National Association of Corrosion Engineers
NAPF – Non Aqueous Phase Fluid
NASA – Non Active Side Arm (term used in the North Sea for kill wing valve on a Xmas tree)
NAVIG – Navigational Log
NB – Nominal Bore
NFI – No Further Investment
NFW – New Field Wildcat, Lahee classification
NGDC – National Geoscience Data Centre (United Kingdom)
NGL – Natural Gas Liquids
NGL, Natural Gas Liquids – Gas that is processed through a plant to separate the heavier hydrocarbon liquids from the natural gas stream. These heavier hydrocarbon liquids, NGLs, traditionally have a higher value than the gaseous natural stream.
NGLQT – NGT QL Log
NGR – Natural Gamma Ray
NGRC – National Geological Records Centre (United Kingdom)
NGS – NGS Log

NGSS – NGS Spectro Log
NGT – NGT Log
NGTLD – NGT LDT QL Log
NGTR – NGT Ratio Log
NHDA – National Hydrocarbons Data Archive (United Kingdom)
NHPV – Net Hydrocarbon Pore Volume
NNS – Northern North Sea
NOC – National Oil Company
NOISL – Noise Log
NPD – Norwegian Petroleum Directorate, Norway
NPS – Nominal Pipe Size (sometimes NS)
NPSH – Net Positive Suction Head
NPV – Net Present Value
NPW – New Pool Wildcat, Lahee classification
NRI, Net Revenue Interest – An owner's interest in the revenues of a well.
NRV – Non Return Valve (Chicksan valve that only allows flow in one direction)
NS – North Sea
NTHF – Non-Toxic High Flash
NTU – Nephelometric Turbidity Unit
NUMAR – Magnetic Resonance Image Log

O
O&G – Oil and Gas (referring to the industry or the companies in it)
OBCS – Ocean Bottom Cable System
OBDTL – OBDT Log
OBEVA – OBDT Evaluation Report
OBM – Oil-Based Mud
OCL – Quality Control Log
OCTG – Oil Country Tubular Goods
OD – Outer Diameter (of a tubular component such as casing)
ODT – Oil Down To
OFST – Offset Vertical Seismic Profile
OGML, Oil, Gas, and Mineral Lease – The agreement outlining the basic terms of developing lands or minerals such as royalty to be paid, length of time, description of lands.
OH – Openhole Log
OIM – Offshore Installation Manager
OMRL – OMRL Log
OOE – Offshore Operation Engineer (senior technical authority on an offshore oil platform)
OPEC – Organization of Petroleum Exporting Countries
OPL – Operations Log

OPRES – Overpressure Log
OPS – Operations Report
ORICO – Oriented Core Data Report
OT – Off Tree
OTL – Operations Team Leader
OVCH – Oversize Charts
OWC – Oil Water Contact

P
P&A – plugged and abandoned (of a well)
PAL – Paleo Chart
PALYN – Palynological Analysis Report
PAR – Pre-Assembled Rack
PAU – Pre-Assembled Unit
PBDMS – Playback DMSLS Log
PBR – Polished Bore Receptacle (component of a completion string)
PBTD – Plug Back Total Depth
PBU – Pressure Build Up (applies to integrity testing on valves)
PCCL – Perforation Casing Collar Locator Log
PCDM – Power and Control Distribution Module
PCKR – Packer Log
PCOLL – Perforation and Collar
PDC – Perforation Depth Control
PDC – Polycrystalline Diamond Composite (a type of drilling bit)
PDG – Permanent Downhole Gauge
PDKL – PDK Log
PDKR – PDK 100 Report
PDP – Proved Developed Reserves
PEA – Palaeo Environment Study Report
PENL – Penetration Log
PEP – PEP Log
PERDC – Perforation Depth Control
PERFO – Perforation Log
PERM – Permeability
PERML – Permeability Log
PESBG – Petroleum Exploration Society of Great Britain
PETA – Petrographical Analysis Report
PETD – Petrographic Data Log
PETLG – Petrophysical Evaluation Log
PETPM – Petrography Permeametry Report
PETRP – Petrophysical Evaluation Report
PFC – PFC Log
PFPG – Perforation Plug Log
PFREC – Perforation Record Log
PG – Pressure Gauge (Report)
PGB – Permanent Guide Base

PGOR – Produced Gas Oil Ratio
PH – Phasor Log
PHASE – Phasor Processing Log
PHOL – Photon Log
PHYFM – Physical Formation Log
PI – Productivity Index
PINTL – Production Interpretation
PL – Production License (United Kingdom), a type of onshore license issued before 1996
PLET – Pipeline End Termination
PLG – Plug Log
PLS – Position Location System
PLT – Production Logging Tool
PLTQ – Production Logging Tool Quicklook Log
PLTRE – Production Logging Tool Report
PMV – Production Master Valve
POBM – Pseudo-Oil-Based Mud
PON – Petroleum Operations Notice (United Kingdom)
POOH – Pull Out Of Hole
POR – Density Porosity Log
POSFR – Post Fracture Report
POSTW – Post Well Appraisal Report
POSWE – Post Well Summary Report
PP – DXC Pressure Plot Log
ppcf – Pounds Per Cubic Foot
ppg – Pounds Per Gallon
PPI – Post Pipelay Installation
PPI – Post Production Inspection/Intervention
PPS – Production Packer Setting
pptf – Pounds (per square inch) Per Thousand Feet (of depth)
PRA – Production Reporting & Allocation
PREC – Perforation Record
PRESS – Pressure Report
PROD – Production Log
PROTE – Production Test Report
PROX – Proximity Log
PRSRE – Pressure Gauge Report
PSA – Production Sharing Agreement
PSANA – Pressure Analysis
PSC – Production Sharing Contract
PSD – Planned Shut-Down
PSL – Product Specification Level
PSLOG – Pressure Log
PSP – Pseudostatic Spontaneous Potential
PSPL – PSP Leak Detection Log
PSQ – Plug Squeeze Log

PST – PST Log
PSVAL – Pressure Evaluation Log
PTS – Pipeline Termination Structure
PTSET – Production Test Setter
PTTC – Petroleum Technology Transfer Council, United States
PUD – Proved Undeveloped Reserves
PUN – Puncher Log
PUR – Plant Upset Report
PUWER – Provision and Use of Work Equipment Regulations
PV – Plastic Viscosity
PVT – Pressure Volume Temperature
PVTRE – Pressure Volume Temperature Report
PW – Produced Water
PWB – Production Wing Block
PWRI – Produced Water Re-Injection
PWV – Production Wing Valve (also known as a flow wing valve on a Xmas tree)

Q
QC – Quality control
QCR – Quality Control Report
QL – Quicklook Log

R
RAC – Ratio Curves
RAWS – Raw Stacks VSP Log
RBP – Retrievable Bridge Plug
RCD – Rotating Control Device
RCKST – Rig Checkshot
RCL – Retainer Correlation Log
RCR – Remote Component Replacement (Tool)
REOR – Reorientation Log
RE-PE – Re-Perforation Report
RESAN – Reservoir Analysis
RESEV – Reservoir Evaluation
RESFL – Reservoir Fluid
RESI – Resistivity Log
RESL – Reservoir Log
RESOI – Residual Oil
REZ – Renewable Energy Zone (United Kingdom)
RF – Recovery Factor
RFMTS – Repeat Formation Tester
RFSU – Ready For Start-Up
RFT – Repeat Formation Tester
RFTRE – Repeat Formation Tester Report
RFTS – Repeat Formation Tester Sample
RIGMO – Rig Move

RIH – Run In Hole
RITT – Riser Insertion Tube (Tool) [1]
RKB – Rotary Kelly Bushing (a datum for measuring depth in an oil well)
RLOF – Rock Loadout Facility
RMLC – Request for Mineral Land Clearance
RMS – Ratcheting Mule Shoe
RNT – RNT Log
ROCT – Rotary Coring Tool
ROP – Rate of Penetration
ROV – Remotely Operated Vehicle, used for subsea construction and maintenance
ROWS – Remote Operator Workstation
RPCM – Ring Pair Corrosion Monitoring
RROCK – Routine Rock Properties Report
RSS – Rig Site Survey
RST – RST Log
RTTS – Retrievable Test-Treat-Squeeze (packer)
RWD – RWD Log

S
SAGD – Steam Assisted Gravity Drainage
SALM – Single Anchor Loading Mooring
SAML – Sample Log
SAMTK – Sample Taker Log
SANDA – Sandstone Analysis Log
SAT – SAT Log
SB – SIT-BO Log
SBF – Synthetic Base Fluid
SBM – Synthetic Base Mud
SBT – Segmented Bond Tool
SC – Seismic Calibration
SCAL – Special core analysis
SCAP – Scallops Log
SCDES – Sidewall Core Description
scf – standard cubic feet (of natural gas)
SCHLL – Schlumberger Log also SCHLO, SCHLU
SCM – Subsea Control Module
SCO – Synthetic Crude Oil
SCRS – Sidewall Cores
SCSSSV – Surface Controlled Sub Surface Safety Valve
SD – Sonic Density
SDFN – Shut Down For Night
SDIC – Sonic Dual Induction
SDL – Supplier Document List
SDPBH – SDP Bottom Hole Pressure Report
SDT – Step Draw-down Test (sometimes SDDT)

SDU	–	Subsea Distribution Unit
SEA	–	Strategic Environmental Assessment (United Kingdom)
SECGU	–	Section Gauge Log
SEDHI	–	Sedimentary History
SEDIM	–	Sedimentology
SEDL	–	Sedimentology Log
SEDRE	–	Sedimentology REport
SEM	–	Subsea Electronics Module
Semi (or Semi-Sub)	–	Semi-Submersible Drilling Rig
SEPAR	–	Separator Sampling Report
SEQSU	–	Sequential Survey
SG	–	Static Gradient
SGUN	–	Squeeze Gun
SHA	–	Sensor Harness Assembly
SHDT	–	SHDT Log
SHO	–	Stab and Hinge Over
SHOCK	–	Shcok Log
SHOWL	–	Show Log
SI/TA	–	Shut In/Temporarily Abandoned
SICP	–	Shut-In Casing Pressure
SIDPP	–	Shut-In Drill Pipe Pressure
SIDSM	–	Sidewall Sample
SIP	–	Shut In Pressure
SIPES	–	Society of Independent Professional Earth Scientists, United States
SIT	–	System Integration Test
SITHP	–	Shut In Tubing Hanger Pressure (another term for CITHP)
SITT	–	Single TT Log
SKPLT	–	Stick Plot Log
SL	–	Seismic Lines
SLS	–	SLS GR Log
SLT	–	SLT GR Log
SMLS	–	Seamless Pipe
SNP	–	Sidewall Neutron Porosity
SNS	–	Southern North Sea
SONCB	–	Sonic Calibration Log
SONRE	–	Sonic Calibration Report
SONWR	–	Sonic Waveform Report
SONWV	–	Sonic Waveform Log
SP	–	Spontaneous Potential (Well Log)
SP	–	Shot point (geophysics)
SPCAN	–	Special core analysis
SPEAN	–	Spectral Analysis
SPEL	–	Spectralog
SPFM	–	Single Phase Flow Meter
SPH	–	SPH Log

SPM	–	Side Pocket Mandrel or Strokes Per Minute (of a positive-displacement pump)
SPOP	–	Spontaneous Potential Log
SPP	–	Stand Pipe Pressure
SPROF	–	Seismic Profile
SPT	–	Shallower Pool Test, Lahee classification
SQL	–	Siesmic Quicklook Log
SREC	–	Seismic Record Log
SRT	–	Site Receival Test
SS	–	Subsea, as in a datum of depth, e.g., TVDSS (true vertical depth subsea)
SSG	–	Sidewall Sample Gun
SSMAR	–	Synthetic Seismic Marine Log
SSPLR	–	Subsea Pig Launcher/Receiver
SSSL	–	Supplementary Seismic Survey License (United Kingdom), a type of onshore license
SSSV	–	Sub-Surface Safety Valve
SSTT	–	Subsea Test Tree
SSV	–	Surface Safety Valve
stab	–	Stabilizer
STAGR	–	Static Gradient Survey Report
stb	–	stock tank barrel
STC	–	STC Log
STGL	–	Stratigraphic Log
STIMU	–	Stimulation Report
STKPT	–	Stuck Point
STL	–	STL Gamma Ray Log
STOIIP	–	Stock Tank Oil Initially In Place
STOP	–	Safety Training Observation Program
STRAT	–	Stratigraphy, stratigraphic
STRRE	–	Stratigraphy Report
STSH	–	String Shot
SUML	–	Summarized Log
SUMRE	–	Summary Report
SUMST	–	Geological Summary Sheet
SURFR	–	Surface Sampling Report
SURRE	–	Survey Report
SURVL	–	Survey Chart Log
SUT(A/B)	–	Subsea Umbilical Termination (Assembly/Box)
SV	–	Sleeve Valve
SWD, Salt Water Disposal Well	–	Well used for disposal of saltwater into an underground formation.
SWE	–	Senior Well Engineer
SYNRE	–	Synthetic Seismic Report
SYSEI	–	Synthetic Seismogram Log

T

TAGOGR – Thermally Assisted Gas/Oil Gravity Drainage
TAPLI – Tape Listing
TAPVE – Tape Verification
TAR – True Amplitude Recovery
TB – Tubing Puncher Log
TBT – Through Bore Tree
TCI – Tunsgten Carbide Insert (a type of rollercone drillbit)
TCPD – Tubing-Conveyed Perforating Depth
TD – Target Depth
TD – Total Depth (depth of the end of the well; also a verb, to reach the final depth, used as an acronym in this case)
TDS – Top Drive System
TDT – TDT Log
TDT GR – TDT Gamma Ray Casing Collar Locator Log
TDTCP – TDT CPI Log
TELER – Teledrift Report
TEMP – Temperature Log
TFL – Through Flow Line
TGB – Temporary Guide Base
TGOR – Total Gas Oil Ratio (GOR uncorrected for gas lift gas present in the production fluid)
THERM – Thermometer Log
THP – Tubing Hanger Pressure (pressure in the production tubing as measured at the tubing hanger)
TIE – Tie In Log
TIEBK – Tieback Report
TLOG – Technical Log
TMCM – Tranverse Mercator Central Meridian
TNDT – Thermal Neutron Decay Time
TNDTG – Thermal Neutron Decay Time/Gamma Ray Log
TOC – Top Of Cement
TOC – Total Organic Content
TOL – Top Of Liner
TOOH – Trip Out Of Hole
TORAN – Torque and Drag Analysis
TPERF – Tool Performance
TR – Temporary Refuge
TRA – Tracer Log
TRACL – Tractor Log
TRD – Total Report Data
TREAT – Treatment Report
TREP – Test Report
TRIP – Trip Condition Log
TRSCSSSV – Tubing Retrievable Surface Controlled Sub-Surface Safety Valve
TRSCSSV – Tubing Retrievable Surface Controlled Sub-Surface Valve

TRSV – Tubing Retrievable Safety Valve
TSI – Temporarily Shut In
TT – Transit Time Log
TTRD – Through Tubing Rotary Drilling
TV/BIP – Ratio of Total Volume (ore and overburden) to Bitumen In Place
TVBDF – True Vertical Depth Below Derrick Floor
TVD – True Vertical Depth
TVDPB – True Vertical Depth Playback Log
TVDSS – True Vertical Depth Sub Sea
TVELD – Time and Velocity to Depth
TVRF – True Vertical Depth versus Repeat Formation Tester
TWT – Two-Way Time (seismic)
TWTTL – Two-Way Travel Time Log

U
UBI – Ultrasonic Borehole Imager
UBIRE – Ultrasonic Borehole Imager Report
UFJ – Upper Flex Joint
UGF – Universal Guide Frame
UIC – Underground Injection Control
UKCS – United Kingdom Continental Shelf
UKOOA – United Kingdom Offshore Operators Association
UKOOG – United Kingdom Onshore Operators Group
ULCGR – Uncompressed LDC CNL Gamma Ray Log
UMV – Upper Master Valve (from a Xmas tree)
URT – Universal Running Tool
USGS – United States Geological Survey
UTA – Umbilical Termination Assembly
UTM – Universal Transverse Mercator

V
VDENL – Variation Density Log
VDL – VDL Log
VDU – Vacuum Distillation Unit, used in processing bitumen
VELL – Velocity Log
VERAN – Verticality Analysis
VERIF – Verification List
VERLI – Verification Listing
VERTK – Vertical Thickness
VIR – Value Investment Ratio
VISME – Viscosity Measurement
VIV – Vortex induced Vibration
VLP – Vertical Lift Performance
VO – Variation Order
VOR – Variation Order Request
VRR – Voidage Replacement Ratio

VSP – Vertical Seismic Profile
VSPRO – Vertical Seismic Profile
VTDLL – Vertical Thickness Dual Laterolog
VTFDC – Vertical Thickness FDC CNL Log
VTISF – Vertical Thickness ISF Log
VWL – Velocity Well Log

W
WABAN – Well Abandonment Report
WAG – Water Alternating Gas (describes an injection well which alternates between water and gas injection)
WALKS – Walkaway Seismic Profile
WATAN – Water Analysis
WAVF – Waveform Log
WBM – Water-Based Mud
WC – Watercut
WEG – Wireline Entry Guide
WELDA – Well Data Report
WELP – Well Log Plot
WEQL – Well Equipment Layout
WESTR – Well Status Record
WESUR – Well Summary Report
WFAC – Waveform Acoustic Log
WGEO – Well Geophone Report
WGFM – Wet Gas Flow Meter
WGUNT – Water Gun Test
WH – Well History
WHIG – Whitehouse Gauge
WHM – Wellhead Maintenance
WHP – Wellhead Pressure
WI – Water Injection
WI – Working Interest
WIPSP – WIP Stock Packer
WLC – Wireline Composite Log
WLL – Wireline Logging
WLSUM – Well Summary
WOB – Weight On Bit
WOC – Wait on Cement
WOE – Well Operations Engineer (a key person of Well services)
WOM – Wait on Material
WORKO – Workover
WOW – Wait On Weather
WP – Well Proposal or Working Pressure
WPLAN – Well Course Plan
WPQ – Weld Procedure Qualification
WPR – Well Prognosis Report

WRS – Well Report Sepia
WRSCSSV – Wireline Retrievable Surface Controlled Sub-Surface Valve
WSCL – Well Site Core Log
WSE – Well Seismic Edit
WSERE – Well Seismic Edit Report
WSHT – Well Shoot
WSL – Well Site Log
WSP – Well Seismic Profile
WSR – Well Shoot Report
WSS – Well Services Supervisor (leader of Well services at the wellsite)
WSSAM – Well Site Sample
WSSOF – WSS Offset Profile
WSSUR – Well Seismic Survey Plot
WSSVP – WSS VSP Raw Shots
WSSVS – WSS VSP Stacks
WSTL – Well Site Test Log
WT – Well Test
WTI – West Texas Intermediate benchmark crude
WUT – Water Up To
WVS – Well Velocity Survey

X
XMT or XT – XMas Tree (Christmas Tree, the valve assembly on a production well-head)
XO – Cross-Over

Y
yl – Holdup Factor
YP – Yield Point

Z
Z – Depth, in the geosciences referring to the depth dimension in any x,y,z data.

Source

Holloway M., Nwaoha C., *Dictionary of Industrial Terms*. John Wiley & Sons, Inc., 2013.

Environmental Aspects of Oil and Gas Production.
John O. Robertson and George V. Chilingar.
© 2017 Scrivener Publishing LLC. Published 2017 by John Wiley & Sons, Inc.

About the Authors

John Otis Robertson Jr.

Academician and Doctor of Engineering and Honorary Doctorate of Geology. Owner of Earth Engineering Inc. and formerly Adjunct Professor at ITT-TECH, National City, CA.

State Registered Petroleum Engineer, 50 years' experience in petroleum and environmental engineering and geology. Expert witness in cases of petroleum evaluation, gas storage and gas migration problems.

Author of over 12 textbooks and 75 articles.

George V. Chilingar

Professor Emeritus and academician of Environmental and Petroleum Engineering at the University of Southern California, USA.

Specialist in Geology and Petroleum and Environmental Engineering.

Author of more than 500 publications and 70 monographs and textbooks.

Contributors:

Michael D. Holloway – Fracturing (Chapter 5)

Moayed bin Yousef Al-Bassam, Saudi Arabian Chevrron – Corrosion (Chapter 6)

Environmental Aspects of Oil and Gas Production.
John O. Robertson and George V. Chilingar.
© 2017 Scrivener Publishing LLC. Published 2017 by John Wiley & Sons, Inc.

Author Index

Aadnoy, B. S., 67, 98
Aalmanac, L. A., 98
Abdallah, D., 323
Abdulraheem, A., 175, 179
Abe, H., 114, 179
Abolghasemi, A., 76, 101
Abrams, M. A., 103
Achauer, C. W., 52, 99
Adamson, L. G., 21, 99
Alam, W., 100
Al-Bassam, M., 290, 323
Al-Hendi, K., 323
Al-Khalaf, A. A., 323
Al-Kunit, A. S., 323
Allen, D., 207
Allen, D. R., 109–110, 112, 151, 179
Allen, G. G., 323
Allen, T. O., 323, 338, 341, 348
Allison M. L., 98
Allread, B. M., 62, 98
Al-Muhailan, M., 323
Al-Qahtani, G. D., 272, 274, 275, 277, 281–283, 287, 289, 295–296, 298, 306, 310–318, 320, 324, 333, 336, 338–340, 343–345, 349
Alvarez-Cohen, L., 329, 332, 349
Al-Yateem, K. S., 323
Ambah, S. A., 98
Annand, R. R., 91, 323
Aoyagi, K., 21, 22, 98
Applin, E. R., 179
Applin, P., 179
Archer, D., 191, 194, 195, 207
Armstrong, F. C., 179
Asakawa, T., 21, 22, 98
Aschenbrenner, B. C., 52, 99
Ashayeri, C., 15, 16
Asquith, G., 99
Asrar, N., 323
Atlas, R. M., 323
Aursio, O., 103
Aziz, A. A., 323

Baars, D. L., 179
Babalyan, G. A., 349
Bachinsky, A. U., 198, 207
Bachu, S., 65, 66, 99
Baert, P., 41, 99
Bagheri, R., 76, 101
Bailey, N. J. L., 323
Baldassare, P. G., 48, 99
Baliunas, S. L., 208
Baneau, G., 323
Bannwart, A. C., 103
Bara, J. P., 179
Barbat, W. F., 120, 122, 179
Barboza, T., 2, 16
Baresti, L., 26, 102
Barker, C., 158, 180
Barnoa, J. M., 208
Barrends, F. B. J., 120, 125, 179
Baskov, E. A., 117, 179
Bastasch, M., 190, 194, 207
Becker, J. R., 323, 339, 349
Beckwith, G. H., 128, 179
Beeson, C. M., 98, 297, 324
Beeunas, M. A., 103
Bell, C. W., 104
Bell, J. S., 114, 179
Belyaev, S. S., 303, 325
Bennett, L. H., 269, 323
Bend, 13
Benslimani, A., 323
Benson. L. J., 15
Beresnev, I., 99
Bernard, G. C., 349

Bernd, C., 13, 15
Berner, U., 34, 99
Bertness, T. A., 290, 323
Betler, S., 99
Bezverkhniy, V. A., 202, 208
Biot, M. A., 179
Blanton, T. L. III, 177, 179
Bloom, A. L., 179
Blount, F E., 324
Boade, R. R., 176, 178, 179
Bobrow, D. J., 128, 179
Bockmeulen, H., 160, 179
Bondesan, M., 179
Bonett, A., 72–74, 99
Booth, G., 323
Borgia, G. C., 167–172, 179
Borregales, C., 179
Bosma, M., 103
Bosteels, T., 41, 99
Brace, R. L., 339, 349
Bradley, J., 128, 179
Brandt, 207
Brighenti, G, 166–173, 179
Brill Jr., K. G., 179
Brondel, D., 318, 319, 320–321, 324
Brongers, M. P. H., 326
Brown Jr., R. D., 179
Bryant, D., 301, 325
Bryant, R. S., 300, 311, 312, 324
Bubela, B., 324
Budyko, 187
Buchanan, J. M., 99, 125, 179
Bucher, W. H., 179
Bullard, E., 179
Burst J. F., 21, 99
Buryakovsky, K., 99

California Division of Oil and Gas, 81–83, 85, 87, 90, 92–94, 99
Carbognin, L., 120, 125, 172, 179
Carlberg, B. L., 339, 349
Carovillano, R. I., 71, 87, 102, 103
Casad, B. M., 339, 349
Castle, R. O., 99
Chakrabarty, A. M., 324
Chamberlain, C. K., 179
Chambers Jr., F. B., 339, 349
Chapman, R. E., 4, 15, 99
Chase, C. G., 179
Chesapeake, 245
Chilingar, G. V., 5, 7, 15, 18, 21, 23, 43, 50, 52, 54, 55, 60, 63, 66, 79, 80, 86, 88, 98–104, 109, 110, 134, 137, 139, 179, 188, 199, 200–202, 204, 207, 208, 212, 215, 272, 274, 275, 277, 281–283, 287, 289, 290, 295–298, 306, 310–318, 320, 323, 324, 333, 336, 338–340, 343–345, 349
Chilingarian, G. V., 2, 9, 15, 21, 22, 98, 100, 101, 103, 104, 106–110, 112–116, 120, 123, 125–130, 136, 142–147, 152, 154, 156–160, 162–172, 179, 209, 300, 303, 311, 312, 324, 333, 349
Chin, L. Y., 176, 178, 179
Chipping, D. H., 179
Christiansen, F. W., 179
Clark, J. B., 324
Clark, L. M., 179
Clarke, M. M., 128, 179
Claypool, G. E., 24, 25, 27, 33, 100, 103
Clifton, H. E., 4, 15
Cline, L. M., 179
Cobarrubias, J. W., 100
Colazas, X. C., 121, 142–143, 145–148, 151–152, 179
Coleman, D. D., 6, 15, 33, 100, 103
Colle, J., 179
Coney, P. J., 179
Constantinescu, P., 302, 326
Contaldo, G. J., 179
Cooke Jr., W. F., 179
Cooper, D. G., 303, 324, 325
Copley, T., 100
Cordell, R. J., 21, 100
Corrosion Doctors, 307–309, 324
Costerton, J. W., 302, 326
Cowan, J. C., 349
Crabtree, M., 329–331, 335, 345–347, 349
Craig, B. D., 78, 100
Craig, H., 80, 81, 101, 102
Cramer, H. R., 179
Crawford, P. B., 301–302, 324
Crittenden Jr., M. D., 179
Cron, C. J., 270, 286, 296, 312, 320, 324
Crosby, G. W., 179
Cryer J., 308–309, 324
Currie, J. B., 179
Curwen, T., 2, 3, 8, 15

Dahtani, H. B., 323
Dallenbach, J., 192, 208
Dallmus, K. F., 179
Dana, J. D., 179
Danielsen, J., 174, 179
Davies, J. S., 324
Davis, G. H., 105, 121, 123, 128, 179
Davis, J. B., 287, 324
Davis, L. E., 343, 349
Davis, S. N., 121, 179
de Waal, J. A., 177, 179
Dean, H. I., 324
Deck, B., 192, 202, 207
Delingpole, J., 188, 207
Deming, H. G., 324
Denham, R. L., 179
Dennis B., 308–309, 324
Denton, J. E., 100
Dewey, J. F., 179
Dickey, P. A., 21, 100, 158, 179
Dietz, R. S., 179
Dietzman, W. D., 174, 175, 179
Dillon, R. S., 190, 207
Dixon, T. N., 177, 179
Dobrynin, V. M., 125, 152, 154, 179
Dodson, C. R., 100
Doig, K., 287, 324
Dolan, J., 2, 16
Doligez, B., 4, 15
Donaldson E. C., 100, 106–108, 112–113, 120, 125–128, 130, 142–147, 152, 158–160, 165–172, 175, 179, 300, 302, 311, 312, 324
Dow, W. D., 104
Drake, C. L., 179
Drozd. R. I., 4, 15
Dusseault, M. B., 69–72, 100, 114, 179
Dvali, M. F., 101

Ebbs, D. J., 179
Edwards, R., 318, 319, 320–321, 324
Elmi, C., 167–172, 179
El-Nassir, A., 99
Endres, B. L., 5, 7, 15, 19, 23, 50, 52, 54, 55, 60, 63, 64, 66, 79, 80, 88, 99, 100, 101, 179, 329–331, 335, 345–347, 349
Enever. J. R., 114, 179
Environmental consultants, 100
Enzler, S. M., 187, 189, 207
Erdmn, J. G., 103
Evans, D., 192, 207
Everett, J. E., 179
Ewing, M., 179

Faber, E., 34, 99, 100
Fabim, R., 323
Farouq Ali, S. M., 157–160, 162–165, 179
Fedin, A., 21, 100
Fedin, L., 100
Fedorak, P. M., 303, 324
Ferguson, H. C., 179
Ferronsky, V. I., 179
Fertl, W. H., 15
Finol, A., 157–161, 162–166, 179
Fischer, H., 192, 202, 207
Fituri, M. F. M., 323
Fletcher, P., 329–331, 335, 345–347, 349
Flekkfay, E., 103
Fluckiger, B., 192, 208
Foght, J. M., 303, 324
Fontana, M. G., 324
Fuhlendorf, S. D., 62, 98
Fukuo, Y., 179
Fulford, R. S., 339, 349

Gabrish, R. K., 179, 180
Galloway, D., 179
Gambardella, F., 172, 179
Gambolati, G., 120, 125, 179
Gates, G. P. L., 302, 325
Gatto, P., 171, 179
Gatzke, L. K., 288, 289, 325
Gaudy, A. E Jr., 325
Gaudy, E. T., 325
Geber, M. I., 101
Gee, D. S., 13, 16
Geertsma, J., 101, 126–127
Geografiska A., 191, 207
Gerhard, L. C., 207
Gilluly, J., 150, 179
Glass, T., 26, 102
Gold, T., 24, 101
Gore, A., 207
Gorfunkel, M., 102, 208
Grant, U. S., 150, 179
Greenberg, J., 188, 207
Greene, H. G., 4, 15
Greene, N. D., 324
Greer, J. B., 325
Grignani, D., 179

Groat, C. G., 179
Grula, E. A., 301, 325
Guacci, G., 128, 129, 179, 197
Gurevich, A. E., 50, 52, 54, 60, 66, 101, 113, 114, 123, 124, 129, 179
Guiamet, P. S., 306, 325

Hackerman, N., 325
Hackley, K. C., 100
Haggerty, J. H., 62, 98
Hallenbeck, L. D., 177, 179
Hamilton, D. H., 2, 9, 15, 101, 134, 179
Haneberg, W. C., 128, 179
Hanna, W. F., 179
Harris, F. R., 150, 179
Hart, M., 301, 325
Hausler, R. H., 288, 289, 325
Hawley, J. W., 128, 179
Hayashi, K., 114, 179
Hayman, A., 318–321, 324
Hedberg, H. D., 21, 101
Heineke, G. W,., 15, 307, 325
Heitz, E., 325
Henkhaus, R., 325
Henry, J. G., 325
Hermansen, H., 177, 179
Hetrtick, L. H., 231
Hieb, M., 189, 190, 194, 198, 207
Hill, D. G., 104, 318–321, 324
Hilliard, H. M., 288, 325
Hillis, R. R., 101
Hitzman, D. O., 325
Hodgson, S. F., 4, 15
Holden, J. C., 179
Holmes, A., 179
Holmos, D., 325
Holzer, T. L., 128–130, 179, 190
Hottman, C. E., 179
Howarth, R., W., 207
Howell, 19
Hower, J., 21, 102
Hsu, K. J., 179
Hudgins, C. M., 297, 325
Hudson, F. S., 150, 179
Hunt, M., 51, 101
Hutchinson, P. J., 15

IMC, 101
Indermuhle, A., 192, 208
Ingebritsen, S. E., 179
Ingraffea, A. R., 101, 207
Ito, T., 114, 179
Ivanov, M. V., 303, 325

Jabbari, N., 15, 16
Jachens, R. C., 179
Jack, T. R., 302, 303, 324, 325
Jacquin, C., 179
Jeffery, A. W, A., 33, 102
Jenden, P. D., 15, 30–31, 33, 88, 101, 103
Jewhurst, J., 177, 179
Jobson, A. J., 323
Johnpeer, G. D., 128, 179
Johnson, A. I., 128, 179, 329–331, 335, 345–347, 349
Johnson, D. W., 107, 129, 179
Johnson, H. R., 150, 179
Johnson, P., 99
Johnson, R. K., 179
Jones, D., 179, 193
Jones, L. W., 282, 304, 306, 310–311, 314–316, 325, 336, 340, 344, 347–349
Jones, V. T., 15

Kadkhoday, A., 76, 101
Kamali, M. R., 76, 101
Kane, R. D., 325
Kaplan, I. R., 15, 24, 25–27, 28, 30, 31, 33, 100–102, 104
Kapelysuhnikov, M. A., 101
Karpenko, A. A., 208
Kartsev, A. A., 117, 179
Katz, S. A., 21, 100–102, 179
Kazama, T., 21, 22, 98
Keigwin, I. D., 208
Kenaga, M., 301, 325
Kentie, C. J. O., 165, 179
Keogh, R. A., 6, 15
Khilyuk, L. F., 5, 7, 15, 19, 21, 23, 50, 55, 60, 63, 64, 66, 79, 88, 100, 101, 139, 179, 188, 199–202, 207, 208
Khodakovsky, I. L., 198, 208
Kilburn, K. H., 101, 102
King, G., 329–331, 335, 345–347, 349
Kirklen, C. A., 326
Klausing, R. L., 179
Knight, L., 99
Kobayashi, N., 98
Koch, G. H., 326
Kohring, J. J., 323

Kokin, A. V., 209
Kosaric, N., 303, 324, 325
Kosloff, D., 123, 124, 179
Kotler, P., 62, 102
Kotlyakov, V. M., 208
Kouznetsov, O. L., 102
Kovach, R. L., 123, 179
Kreitler, C. W., 128, 130, 179, 197
Krygowski, D., 99
Kubit, R. W., 326
Kumar, S., 15, 290, 323, 349
Kvendseth, S. S., 127, 179

Lacazette, A., 67–69, 102
Landau, L. D., 208
Landscheidt, T., 208
Langelier, W G., 343, 349
Langnes, G. L., 349
Lazar, I., 302, 326
Lee, J. J., 102
Lee, K. L., 102, 123, 133, 179
Legates, D. R., 208
Levenspiel, O., 326
Leverett, M. C., 47, 102
Lewis R., 308–309, 324
Lifshits, E. M., 208
Lindlof, J. D., 349
Link. W. K., 3, 15
Lister, L. A., 128, 179
Liu, C. L., 6, 15, 21, 100
Liu, M., 100
Llewellyn, G. C., 306, 325
Lofgren, B. E., 179
Loh, W., 103
Louis, C. R., 128, 179
Love, D. W., 128, 179

Mackay, E. J, 14, 15, 329, 332, 349
Magaw, R. I., 75, 102, 103
Magne, E., 323
Magoon, L. B., 104
Mah, R. A., 25, 26, 102, 104
Mannon, R. W., 179
Marabini, M., 171, 179
Marcellus shale coalition, 102
Marlow, R. S., 79, 102
Marov, M. Y., 208
Marquis, R. E., 326
Marris, D. A., 103
Marsden, S. S., 121, 179
Marsh, G. A., 270, 286, 296, 312, 320, 324
Martin, R. L., 326
Mastronianni. D., 192, 202, 207
Mattavelli, L., 179
Matthews, M. Jr., 204, 208
May, P. D., 326
Mayuga, M. N., 109, 110, 112, 151, 179
McAuliffe, C., 21, 102
McCoy, W. F., 302, 326
McGlasson, R. L., 284, 297, 325
McGuirt, J. H., 179
McMillen, S. J., 75, 102, 103
Meehan, R. l., 2, 9, 15, 134, 179
Meents, W. F., 6, 15
Mehdizadeh, P., 297, 325
Mehta, 318, 319, 320–321, 324
Menges, C., 128, 179
Mercusa, G., 172, 179
Merle, H. A., 165, 179
Meshkati, N., 13, 15
Mesini, E., 162–172, 179
Mess, K. W., 114, 179
Meyer, F H., 284, 326
Meyer, R. F., 129, 179
Mikasa, M., 179
Miller, M., 329–331, 335, 345–347, 349
Miroshnikov, A. E., 209
Mokhov, I. I., 202, 208
Monctkon, C., 189, 208
Monin, A. S., 192, 202, 208
Monnin, E. A., 192, 208
Montori, S., 172, 179
Moore, G. W., 4, 13, 15
Morvan, P., 323
Moses, V., 326
Mourhatch, R., 272, 274, 275, 277, 281–283, 287, 289, 295–296, 298, 306, 310–318, 320, 324, 333, 336, 338–340, 343–345, 349
Mudge, P., 323
Mueller, J. E., 179
Muller, B., 103

Naugle, D. E., 62, 98
Naumov, G. V., 198, 208
Nelson, S. A., 106, 179
Newman, G. H., 177, 179
Nikonov, 17, 19
NGSMA, 18, 34, 36, 39, 40, 102

O'Keefe, J. A., 179
O'Rear, C. E., 306, 325
Okumura, T., 179
Oriel, S. S., 179

Pafitis, D., 72–74, 99
Palmer K., 308–309, 324
Pampeyan, E. H., 128, 179
Parent, C. F., 302, 325
Patton, C. C., 349
Payer, J. H., 326
Peck, R. B., 179
Pelphrey, S. R., 100
Penn state extension, 102
Perry Jr., E. A., 21, 102
Petrowiki, 332, 349
Pewe, T. L., 128, 179
Phillips, R. L., 4, 15
Picard, L., 103
Pierson, A. G., 177, 179
Pinta da Cunha, A., 114, 179
Pisaki, H., 323
Pokinwong, P., 100
Poland, J. F., 105, 121, 123, 179
Pope, G. J., 13, 16
Poreda, R. J., 30, 31, 33, 101, 102
Porter, M. E., 13, 16
Poulet, M. J., 179
Powers, M. C., 21, 102
Powley, D. E., 125, 129, 179
Pratt, W. E., 107, 129, 179
Price, L. C., 22, 30, 102
Pride, S., 103
Prokhorov, V. G., 209
Putilov, V. V., 107, 198, 207

Rafidi, N. R., 172, 179
Rahmel, A., 325
Ramos, G., 103
Ratigan, J. L., 114, 179
Ravi, K., 71–72, 103
Raymond, R. H., 128, 179
Raynaud, D., 192, 208
Reedy Jr., F., 179
Reinecker, J., 103
Remers, R. F., 128, 179
Revkin, A., 64, 103
Reynolds, C. B., 101, 128, 179
Reynolds, I. E., 128, 179
Reynolds, S. D., 101
Ricchiuo, T., 167–172, 179
Rice, D. D., 24, 103
Richter, C. F., 125, 179
Riegle, J. R., 103
Rieke III, H. H., 99, 103, 108, 109, 115–116, 136, 177, 179
Riggs, O. L., 284, 326
Rixey, W. G., 75, 103
Roberts, A. P., 323, 338, 341, 348
Roberts, J. E., 111, 179
Robertson Jr., J. O., 5, 7, 15, 19, 23, 50, 52, 54, 55, 60, 63–64, 66, 79, 88, 101, 102, 139, 179, 290, 323, 349
Robinson, A. B., 208
Robinson, N. E., 208
Robinson, Z. W., 208
Roegiers, J. C., 175, 179
Rogers, M. A., 323
Roof, J. G., 103
Rosborough, W. M., 297, 325
Rose, C. S., 128, 179
Ross, T. A., 173, 179
Rossenfoss, S., 206, 208
Running, S. W., 62, 103
Russell, H. H., 301, 325
Rutherford, W. M., 21, 103
Ryzhenko, B. N., 198, 208

Sabinas, F. L., 78, 104
Salazar, A., 179
Sancevic, Z. A., 157–160, 162–165, 179
Sandhu, R. S., 179
Santoro, R. L., 101, 207
Santos, R. G., 103
Sasaki, S., 98
Savidge, J. L., 39, 103
Sawa, T., 98
Sawabini, C. T., 109, 110, 179
Saxena, S. K., 128–130, 179
Schaeffer, F. E., 179
Scheidegger, A. O., 179
Schneider, G. M. C., 165, 179
Schoell, M., 16, 26, 29, 30, 31, 33, 88, 102, 103, 179
Schowalter, T. T., 21, 103
Schumacher, D., 103
Schumann, H. H., 128, 179, 198
Scott, R. F., 123, 124, 179
Scranton, J., 123, 124, 179
Secrest, C. D., 128 179

Sekiguchi, K., 21, 22, 98
Semerad, T., 318, 319, 320–321, 324
Sengul, M., 323
Serebryakov, V. A., 125, 152, 154–156, 179
Serruya, C., 103
Sewell, G. W., 325
Shakun, J., 192, 208
Shin, S., 99
Shonkoff, S. B. C., 101
Shvetsov., M. S., 103
Sidorov, V. I., 102
Siemers, W. T., 176, 178, 179
Simeoni, U., 179
Simkin, E. M., 102
Sinnokrot, A., 349
Slemmons, D. B., 128, 179
Smith, A. G., 179
Smith, I., 192, 202, 207
Smith, J. E., 51, 52, 103
Smith, W. K., 62, 98
Smits, R. M. M., 177, 179
Snavely, E. S., 325
Snyder, R. E., 174, 179
Sonechkin, D. M., 192, 202, 208
Soon, W., 208
Sorgeloos, P., 41, 99
Sorokhtin, N. O., 197, 209
Sorokhtin, O. G., 188, 199–201, 207–209
Soter, S., 24, 101
Springham, D. G., 326
Sproll, W. P., 179
Stahl, W. J., 100
Standing, M. B., 100
Stauffer, T. F., 192, 208
Steedman, R. S., 120, 125, 179
Stevens, R. G., 99
Stiff, H. A., 343, 349
Stocker, D., 192, 208
Stoffer, K. G., 349
Strehle, R. W., 121, 142–143, 145–148, 151–152, 179
Sudbury, J. D., 284, 326
Sulak, R. M., 174, 178, 179
Sundberg, K. R., 20, 103
Sussman, C., 25, 102
Sutton, J., 179
Suvorov, N. P., 197, 198, 207
Sylte, J. E., 177, 179
Taylor, D. W., 179
Tchillingarian, G., 337, 349
Tek, M. R., 8, 16, 79–80, 95–97, 103
Ter-Martirosyan, Z. G., 179
Terry, D., 43, 103
Terzaghi, K., 112, 179
Thackrey, T., 103
Thatcher, W., 128–130, 179
Therwolf, G., 2, 16
Thomas, L. K., 177, 179
Thompson, B. G., 302, 303, 325, 326
Tingay, M., 67, 68, 103
Tissot, B. P., 77, 104
Titus, C. H., 104
Toth, J., 79, 104
Tranter, P., 323
Trevisan, O. V., 103
Trimble, D. E., 179
Twidwell, D., 62, 98

Vagin, S. B., 117, 179
van den Dolder, E. M., 128, 179
Van der Knaap, W., 108, 151, 179
Van der Vlis, 108, 151, 179
van Kooten, J. F. C., 177, 179
van Opstal, G., 165, 179
Van Sickle, V. R., 179
Venus (*Atmosphere, Surface, Internal Structure)*, 200, 209
Vially, R., 100
Videla, H. A., 306, 325
Virmani, Y. P., 326
Vitali, D., 179
Voitkevich, G. V., 209
Vorabutr, P., 324

Wachter, A. P., 287, 324
Wahlen, M., 192, 202, 207
Waiters, L. T., 78, 104
Wallace, E., 195, 209
Walton, R. J., 114, 179
Ward, D. M., 102, 104
Waterhouse, R. B., 325
Watfa M., 308–309, 324
Watson, T., 65, 66, 99
Weatherford laboratories, 33, 104
Weaver, P., 179
Weeks, R. E., 128, 179
Weintritt, D. J., 349
Wells, M. T., 101

Welte, D. H., 26, 77, 104
Wentworth, C. M., 104, 125, 179
Westlake, D. W. S., 303, 324
Whittaker, M. J., 104
Wiborg, R., 177, 179
Williford, F., 323
Wilson, E. L., 179
Wittle, J. K., 104
Woese, C. R., 24, 104
Wold, M. B., 114, 179
Wolf, K. H., 9, 15, 100, 179
Wolfe, R. S., 24, 104
Woodward, L. A., 179
Wright, C. C., 333, 349

Yanat'eva, O. K., 345, 349
Yasamanov, N. A., 205, 209
Yen, T. F., 2, 15, 88, 100, 106–108, 112–113, 120, 125–128, 130, 142–147, 152, 158–160, 162–172, 179
Yerkes, R. F., 99
Yushkevich, G. N., 104

Zajic, J. E., 302, 303, 324–326
Zaks, S. L., 104
Zaman, M. M., 174, 175, 178, 179
Zambon, M., 169, 176–179
Zhuze, T. P., 104
Ziony, J. I., 104, 125, 179

Environmental Aspects of Oil and Gas Production.
John O. Robertson and George V. Chilingar.
© 2017 Scrivener Publishing LLC. Published 2017 by John Wiley & Sons, Inc.

Subject Index

Acidizing, 10
Adiabatic Theory, global temperature, 11, 197
Air emissions, monitoring, 98
Aliso Canyon Oilfield, CA, 2, 8
Antarctic, global temperature, record, 189
Antarctic, ice core, studies, 189–192
Antarctic, ice cores, Dome Concordia, 192
Antarctic, ice cores, Vostok, 190, 192
Antarctic, temperature, vs CO_2 atmosphere, 191–193
Anthropogenic carbon, effect on global temperature, 203–204
Aquifers, cap rock, 105
Aquifers, confined, 105–106
Aquifers, unconfined, 105–106
Aquifers, withdrawal of fluid, 105
Arrhenius, Syante, 187
Atmosphere, carbon content, effect on global temperature, 10–11
Atmosphere, carbon content, historic, 189
Atmosphere, carbon content. anthropogenic, 187
Atmosphere, carbon dioxide, historic record, 191
Atmosphere, CO_2 content, 194
Atmosphere, CO_2 lags temperature increase, 193
Atmosphere, human CO_2 emissions (anthropogenic), 187, 193
Atmosphere, methane, 204–206

Bachaquero Oilfield, Venezuela, 157, 158, 160–163, 165
Baldwin Hills Dam, CA, 1, 2, 9, 80, 131–124
Bolivian Coastal Oilfields, Venezuela, 156–165
Boscan Oilfield, Venezuela, 156–165

Cabimas Oilfield, Venezuela, 158
Carbon content, atmosphere, anthropogenic, 187
Carbon content, atmosphere, effect on global temperature, 10–11
Carbon content, atmosphere, historic, 189
Carbon Cycle, global, 194–195
Carbon dioxide, atmospheric content, 194
Carbon dioxide, atmospheric historic values, 192
Carbon dioxide, historic record, 191
Carbon dioxide, lags temperature increase, 193
Carbon dioxide, molecular stoichiometry, 203–204
Carbon dioxide, solubility in water, 195
Carbon dioxide, sources of, 194
Carbon dioxide, storage in, ocean and vegetation, 195, 203–204
Carbon fingerprinting, 86, 88
Carbon isotope ratios, 25, 27–30, 32
Castaic Hills Oilfield, CA, 91–92, 94
Cement, breakdown – (see Containment),
Cement, breakdown, due to age, 69–74
Cement, breakdown, fractures, 72
Cement, breakdown, gas bubbles, 71
Cement, breakdown, high slurry rate, 70
Cement, breakdown, low density, 71
Cement, breakdown, shrinkage, 70, 71
Cement, breakdown, slurry pressure, 72
Cement, breakdown, stresses about wellbore, 70
Cement, breakdown, vertical driven fractures, 71
Cement, circumferential fractures, 70
Cement, containment, breakdown, 2, 69–74
Cement, effect of low density, 71
Cement, fractures, gas zone, 72

Cement, improper placement, 69, 71–74
Cement, included gas bubbles, 71
Chromatographic analysis, 20
Clean Air Act, 255–257
Compaction, clays, 152
Compaction, decreasing porosity, 111–112
Compaction, effective-stress, 114
Compaction, factors affecting, 150
Compaction, Gulf Coast, USA, 119
Compaction, model, Athy's, 114–115
Compaction, model, Beal's, 118
Compaction, model, Chernov's, 117–118
Compaction, model, Hedberg's, 115–116
Compaction, model, Katz and Ibrahim, 118–119
Compaction, model, spring analogy, 108–109
Compaction, model, Teodorovich, 117–118
Compaction, model, Terzaghi's, 112–114
Compaction, model, theoretical, 108–114
Compaction, model, Weller's, 116–117
Compaction, stress, 108
Compressibility factor, gas, calculation, 35–40
Containment, breakdown, 11–12
Contamination, spills, 242–243
Corrosion, 269–323
Corrosion, alkalinity environment, 286
Corrosion, bacterial, inhibition, 305–306
Corrosion, bacterial, sulfate reducing, 287
Corrosion, blistering, 297
Corrosion, carbonic acid, 290–291
Corrosion, casing leaks, 312
Corrosion, cathode/anode area ratio, 280, 281
Corrosion, cathodic protection, 312–315, 320
Corrosion, cavitation, 294–295
Corrosion, chemical scavengers, 284, 285
Corrosion, chemistry, 274, 282
Corrosion, circuit, 273, 275
Corrosion, classes of, 293–296
Corrosion, conditions for, 274
Corrosion, crevice, 294
Corrosion, damage from, 269
Corrosion, definition, 270–272
Corrosion, definition, corrosion agent, 272
Corrosion, definition, electric charge, 271
Corrosion, definition, electric current, 272
Corrosion, definition, electric potential, 271, 273
Corrosion, definition, electric power, 272
Corrosion, definition, electrical energy, 271
Corrosion, definition, electrochemistry, 270, 275
Corrosion, definition, electrolyte, 273, 275
Corrosion, definition, resistance, 271
Corrosion, drilling, 270
Corrosion, economics, 321–322
Corrosion, electrical chemical, 273, 275
Corrosion, electrical potential, 279–280
Corrosion, electromotive force, 277–279
Corrosion, environment, 269, 273
Corrosion, environment, gas migration, 269
Corrosion, environment, problems, 269
Corrosion, erosion, 295
Corrosion, fatigue, 297
Corrosion, fluid flow variation, 295
Corrosion, galvanic, 294, 320
Corrosion, gas-condensate wells, 288
Corrosion, gaseous, 283–286
Corrosion, gaseous, carbon dioxide, 286
Corrosion, gaseous, oxygen, 283–284
Corrosion, hydrogen sulfide, 284–286, 292–293
Corrosion, inhibitors, 316–317
Corrosion, inhibitors, placement, 288
Corrosion, inspection tools, acoustic, 309–310
Corrosion, inspection tools, potential, 310
Corrosion, intergranular, 294
Corrosion, iron, 280–283
Corrosion, lose containment, 14
Corrosion, measurement units, 322, 323
Corrosion, microbial, 298–302, 305
Corrosion, microbial, bacteria, 298–302
Corrosion, microbial, control, 306–307
Corrosion, microbial, oilfield, 269, 302, 307–321
Corrosion, microorganisms, 303–307
Corrosion, microorganisms, oilfield waters, 304–305
Corrosion, offshore structures, 318–321
Corrosion, old vs new pipe, 317–318
Corrosion, pH environment, 286, 287
Corrosion, pipelines, 307–308
Corrosion, pitting, 294
Corrosion, polarization, 276–277, 280, 282–283
Corrosion, prokaryotes, 303–304
Corrosion, protection, casing, 310
Corrosion, protection, cement, 311
Corrosion, protection, insulation, 311

Corrosion, protection, pipelines, 310
Corrosion, rate of, 274, 275
Corrosion, rate vs. brine production, 289
Corrosion, sacrificial anode, 314
Corrosion, selective leaching, 294
Corrosion, soil resistivity, 314–317
Corrosion, sour, 292–293
Corrosion, stress, 295–296
Corrosion, structural integrity, 269
Corrosion, sweet, 290–291
Corrosion, types of, 289–295
Corrosion, uniform, 293
Corrosion, well casing, 307–308
Corrosion, well casing, inspection tools, 308–310

Denton, TX, 13
Diffusion, gas, 49–52
Diffusion, rate, 50–52
Dissolved gas in fluid, 49–49
Drake oil well, 61
Drilling, bit action, 67
Drilling, fractures, induced, 66–69

Earth Engineering, Inc., 90
East Mesa Geothermal, CA, 120
Ekofisk Oilfield, enhanced recovery, 177
Ekofisk Oilfield, North Sea, 107, 173–178
El Segundo Oilfield, CA, 91
Embrittlement, metal, 292–293, 296–297
Endurance strength, 298
Environmental monitoring program, 3
Evaluation Approach, 3
Explosive limits (LEL), gas, 74–75, 83

Fairfax area, CA, explosion/fire, 2, 8, 79, 87–88
Fairfax area, Gilmore Bank, CA, 9, 88
Fault, activation, 9
Fault, differential pressure across, 4
Fault, leaking, 4
Fault, triggered by seismic activity, 4
Fluid, dissolved gas, 48–49
Fluid, three phase flow, 47
Fracturing, air emissions, 250–254
Fracturing, air emissions, dust, 254–255
Fracturing, *Aperture Rule,* 69
Fracturing, blowouts, subsurface, 219–220
Fracturing, blowouts, surface, 219
Fracturing, *Breakout Rule,* 69
Fracturing, cased wells, 218–219
Fracturing, coal-beds, gas, 214
Fracturing, containment leakage, 13, 219
Fracturing, contamination, 227–230
Fracturing, contamination, groundwater, 220–222
Fracturing, *Continuity Rule,* 69
Fracturing, creation of, 11–12
Fracturing, debate pro/con, 213
Fracturing, federal regulations, 257–264
Fracturing, fluid, makeup report, 249–250
Fracturing, fluids, 230–231
Fracturing, fluids, additives, 227–228, 231–232, 232–235
Fracturing, fluids, direction of flow, 239
Fracturing, fluids, *slickwater,* 238
Fracturing, gas wells, shale, 214–215
Fracturing, groundwater, analysis, 240–242
Fracturing, groundwater, contamination, 211, 239–243
Fracturing, increase oil & gas reserves, 12, 211
Fracturing, increase surface drainage area, 11–12
Fracturing, induced, 66–69
Fracturing, induced, seismic, 246
Fracturing, legal, 12–13
Fracturing, orientation of, 11–13, 69, 217
Fracturing, production, gas, 214–217
Fracturing, production, increase, 215–217
Fracturing, proppants, 235–238
Fracturing, proppants, ceramics, 238
Fracturing, proppants, r esin-coated, 237–238
Fracturing, proppants, silica sand, 236–237
Fracturing, regulatory oversight, 247–249
Fracturing, reservoirs, 11–12, 211–250
Fracturing, reservoirs, conventional, 214
Fracturing, reservoirs, unconventional, 214–217
Fracturing, *Staking Rule,* 68
Fracturing, studies, opposed, 212–213
Fracturing, studies, supporting, 211–212
Fracturing, *Symmetry Rule,* 69
Fracturing, tight porosity, 214
Fracturing, vertical, 216–217
Fracturing, water, additives, 216–217, 219
Fracturing, water, contamination, 246
Fracturing, water, requirement, 244–245
Fracturing, well-design, 222–227
Fracturing, well-design, completion, 225

Fracturing, wells, abandoned, 226–227

Galvanic series, 280
Gas storage project, Aliso Canyon, CA, 2, 8
Gas Storage Project, Huntsman, NE, 93–95
Gas storage project, Hutchinson, KA, 79
Gas Storage Project, Leroy, WY, 80, 95–97
Gas Storage Project, Mont Belvieu, TX, 8, 95
Gas Storage Project, Montebello, CA, 84
Gas Storage Project, Playa del Rey, CA, 84–86
Gas storage project, reservoir
  rate of leakage, 80
Gas, biogenic origin (microbial), 6, 24, 27, 33
Gas, biogenic vs thermogenic, 24
Gas, biogenic, decomposition, 24
Gas, carbon fingerprinting, 86, 88
Gas, carbon isotope ratios, 6, 25, 27–30, 32
Gas, chromatographic analysis, 20
Gas, columns, 56–59
Gas, composition of, 17–19
Gas, compressibility, 35–40, 56–58
Gas, diffusion, rate, 49, 50–52
Gas, dissolved, 48–49
Gas, driving force of, 34–35
Gas, entrapment, 22
Gas, explosion, Hutchinson, KA, 79
Gas, explosive limits (LEL), 74–75, 83
Gas, fermentation, 25–26
Gas, fingerprinting, 6
Gas, gas sampling, surface, 32–33
Gas, geochemical exploration, 20
Gas, hydrocarbon, 6
Gas, hydrogen isotopes (D/H), 6–7
Gas, *Ideal Gas Law,* 34–35
Gas, identification, isotopic composition, 26
Gas, identification, isotopic
  hydrogen(deuterium) ratio, 27–29
Gas, identification, type of, 5–8
Gas, isotopic analyses, 6–7
Gas, isotopic composition, 26
Gas, isotopic hydrogen(deuterium)
  ratio, 27–29
Gas, methane, 17–19, 20
Gas, migration paths, 71, 72, 74
Gas, migration paths, abandoned wells, 64, 66
Gas, migration paths, pipelines, 65
Gas, migration, bubble, 52
Gas, migration, buoyant flow, 54–56, 78
Gas, migration, containment, 78
Gas, migration, continuous phase, 59–61
Gas, migration, diffusion, 49–52
Gas, migration, discontinuous-phase, 52–53
Gas, migration, factors affecting, 41–49
Gas, migration, leaking wells, 79
Gas, migration, minimum
  vertical height, 53–54
Gas, migration, mixtures of, 31–32
Gas, migration, monitoring, 4, 97
Gas, migration, paths, 3–4, 22, 88, 61–75
Gas, migration, paths,
  abandoned wells, 64, 66
Gas, migration, paths, induced
  fractures, 66–69
Gas, migration, paths, man-made, 64–65
Gas, migration, paths, natural, 63
Gas, migration, paths, pipelines, 65
Gas, migration, paths, producing
  wells, 64, 65–66
Gas, migration, paths,
  repressured wells, 65, 66
Gas, migration, secondary, 22
Gas, migration, seeps, 3–4
Gas, migration, stray gas, 23
Gas, migration, types of, 49–61
Gas, migration, velocity, 60
Gas, migration, wellbore, 78
Gas, molecular weight, calculation, 37
Gas, nonhydrocarbon, 30–31
Gas, North San Joaquin Basin, CA, 31
Gas, origin, methane, 17, 20–23, 24
Gas, oxidation of, 29
Gas, PDB (see carbon isotope ratio),
Gas, potential leaks, well, 65
Gas, pressure distribution in column, 61
Gas, primary migration of, 20–23
Gas, quantity leakage calculation, 95
Gas, repressuring reservoirs, 90
Gas, Sacramento Basin, CA, 31
Gas, secondary migration, 22
Gas, seeps, South Salt Lake Oilfield, CA, 89
Gas, SNOW (see hydrogen isotope ratio),
Gas, soil gas sampling, 32–33
Gas, source, 17, 23, 24
Gas, source, methane, 7, 17, 21, 23, 24
Gas, source rock, 21
Gas, storage project, 79–80
Gas, storage project, Aliso Canyon, CA, 2, 8
Gas, storage project, failures, 8
Gas, storage project, hazards of, 2
Gas, storage project, life of, 8

Gas, storage project, Mont Belvieu, TX, 8
Gas, storage project, Montebello, CA, 1
Gas, thermogenic (petrogenic), 6, 24, 26–27, 33–34
Gas, thermogenic origin, 24, 26–27, 33–34
Gas, toxicity, 75–78
Gas, wellbore, depth at which gas can escape, 58
Gas, wells, drilling, 215–217
Gas. migration, minimum vertical height for movement, 53–54
Gas paths, migration, 88
Gas storage reservoir, 7–8
Gasfield, Groningen, Netherlands, 105, 106, 114
Gibbs free energy, scale formation, 342
Global temperature vs. carbon content, 187
Global temperature, 100K cycles, 191
Global temperature, adiabatic, 197–206
Global temperature, adiabatic theory, 188
Global temperature, Antarctic ice cores, 189, 191–193
Global temperature, anthropogenic carbon, 188
Global temperature, atmosphere carbon content, 10–11
Global temperature, Carboniferous Period, 194
Global temperature, climate, 10, 11
Global temperature, deviation of, 189
Global temperature, Earth model, 197–198
Global temperature, historic, 188, 189
Global temperature, historic, recent, 190–191
Global temperature, lower atmosphere, 400,000 years, 190
Global temperature, man's activities (anthropogenic), 188
Global temperature, methane content, 188
Global temperature, Ordovician Period, 194
Global temperature, satellite data, 194
Global temperature, Sun and Earth relationship, 188
Global temperature, UAH satellite data, 190
Global temperature, Venus Model, 198–203
Global warming, 188, 189, 193
Global warming, Syante Arrhenius, 187
Goose Creek Oilfield, TX, 9, 107, 120
Gravity drainage reservoirs, 3, 63
Greenhouse effect, 11, 187, 197–206
Groningen Gasfield, Netherlands, 105, 106, 114
Groundwater contamination, pre-drill, 220–222

Honor Rancho Oilfield, CA, 91, 93, 94
Horizontal drilling, 220
Huntsman Gas Storage Project, NE, 93–95
Hutchinson Oilfield, KA, 79, 91–92
Hutchinson Oilfield, KA, explosion/fire, 91–92
Hydrocarbon migration, 4
Hydrogen sulfide, 77, 78, 302

Ideal Gas Law, 34–35
Inglewood Oilfield, CA, 2, 80–81, 134
Ironite Sponge, 285
Isotopic analysis, 95

La Brea Tar Pits, CA, 140
Lagunillas Oilfield, Venezuela, 158, 159, 160–164
Lake Maracaibo, Venezuela, 9, 112, 113, 120, 157, 158, 160, 162
Land planning, 98
Land use permits, 243–244
Leaking wells, 61–63
Leroy Gas Storage Project, WY, 80, 95–97
Long Beach, CA, 144
Los Angeles Basin Oilfields, 130–152
Los Angeles City Oilfield, CA, 81–83, 134–136
Los Angeles, Belmont High School, CA, 81–83

Marcellus shale, 13
Mene Grande Oilfield, Venezuela, 157–161
Methane, explosive limits, 135
Methane, monitoring emissions, 206
Methane, sources, 7, 17, 23, 24, 205–206
Methane, sources, biogenic (microbial), 6, 24, 27, 33
Methane, sources, thermogenic (petrogenic), 6, 24, 26–27, 33–34
Mimbres Basin, NM, 130
Mont Belvieu, Gas Storage Project, TX, 8, 95
Montebello Gas Storage Project, CA, 84
Montebello Oilfield, CA, 1, 79, 83–84

North San Joaquin basin, CA, 31

Offshore platform, sinking, 177–178
Oil shale, 13–14
Oil, API gravity, 75
Oil, benzene content, 75–78
Oil, BTEX, 77
Oil, composition, 76, 77
Oil, hydrogen sulfide, 77, 78
Oilfield Honor Rancho, CA, 91, 93, 94
Oilfield Tapia, CA, 91, 94
Oilfield, Bachaquero, Venezuela, 157, 158, 160–163, 165
Oilfield, Bolivian, 157–165
Oilfield, Castaic Hills, CA, 91–92, 94
Oilfield, Ekofisk, North Sea, 107, 172–178
Oilfield, El Segundo, CA, 91
Oilfield, Goose Creek, TX, 9, 107, 120
Oilfield, Hutchinson, KA, 79, 91–92
Oilfield, Inglewood, CA, 2, 80–81, 134
Oilfield, Lagunillas, Venezuela, 158–164
Oilfield, Los Angeles City, CA, 81–83, 134–136
Oilfield, Mene Grande, Venezuela, 157–161
Oilfield, North Stavropol, Russia, 152–157
Oilfield, Playa del Rey, CA, 137
Oilfield, Redondo Beach, 138–139
Oilfield, Redondo Beach, CA, 138–139
Oilfield, Salt Lake, CA, 79, 86–89, 139–140
Oilfield, Santa Fe Springs, 140–141
Oilfield, Santa Fe Springs, CA, 89–90, 140–141
Oilfield, South Salt Lake, CA, 89
Oilfield, Stavropol, Russia, 152–157
Oilfield, Tia Juana, Venezuela, 157, 158, 160, 161, 163
Oilfield, Torrance, CA, 138–139
Oilfield, Venezuelan, 157–166
Oilfield, Venice, CA, 84–86, 137
Oilfield, Wilmington, CA, 5, 9, 105, 106, 107, 112, 120, 122, 123–124, 125, 126, 141–152
Oilfield. Cabimas, Venezuela, 158
Oilfields, Aliso Canyon, CA, 2, 8
OK shales, 116

PDB (see carbon isotope ratio),
Permeability, 46–48
Permeability, relative, 47
Petroleum, API gravity, 75
Petroleum, benzene content, 75–78
Petroleum, BTEX, 77
Petroleum, composition, 76, 77
Petroleum, hydrogen sulfide, 77, 78
Pixley Fissure, San Joaquin Valley, CA, 129–130
Playa del Rey Gas Storage Project, CA, 84–86
Playa del Rey Oilfield, CA, 79, 84–86, 136–137
Pore, pressure, reduction, 106
Pore, rock-matrix, collapse, 106
Pore, voids vs. solids, 42–46
Porter Ranch, CA, 2, 5, 8
Po-Veneto Plain, Italy, 166–173
Prokaryotes, 303–304

Rancho La Brea Tar Pits, CA, 23, 89
Redondo Beach Oilfield, CA, 138–139
Rock cycle, carbon storage, 196
Ross dress for less, CA explosion/fire, 87, 88

Sacramento Basin, CA, 31
Sacrificial anode, 314
Salt Lake Oilfield, CA, 79, 86–89, 139–140
San Joaquin Valley, CA, 122, 129–130
San Joaquin Valley, CA, 122, 129
Santa Fe Springs Oilfield, CA, 89–90, 140–141
Scale, alkalinity, 334–335
Scale, barium, 330, 331, 332, 334, 336–338, 339, 342-
Scale, calcium, 345
Scale, CO_2 flooding, 336
Scale, common minerals, 329, 330, 332
Scale, deposition, 329, 332, 337
Scale, deposition, due to temperature change, 336
scale, deposition, incompatible waters, 334–338, 338
Scale, deposition, self-scaling, 335
Scale, dispersing agents, 337
Scale, electrode potential, 340
Scale, equipment, 14
Scale, evaporation-induced, 335
Scale, Gibbs free energy, 342
Scale, hardness, 334–335
Scale, inhibition, 329, 347–348
Scale, inhibitor, sulphate reduction, 348
Scale, ionic strength, 336, 342–343
Scale, iron, 335

Scale, magnesium, 330, 334
Scale, precipitation, 334–339
Scale, ratio "*R*", 343–344
Scale, removal, 345–348
Scale, removal, chemical, 346–347
Scale, removal, mechanical, 346
Scale, solubility, 345
Scale, spontaneity, 341
Scale, stability index, 337
Scale, strontium, 331
Scale, sulfate, 331, 337, 338–339, 341–342
Seeps, oil and gas, 4
SNOW (see hydrogen isotope ratio),
Soil gas, detectors, 5
Soil gas, monitoring, 98
Soil gas, tests, surface, 3
Soil resistivity, 314–317
South Salt Lake Oilfield, CA, gas seeps, 89
Subsidence, Al Afaj, Saudi Arabia, 106
Subsidence, area of, 120
Subsidence, Baldwin Hills Dam, 131–124
Subsidence, Belmont High School, 134–136
Subsidence, Bolivian Oilfields, 157–166
Subsidence, calculation of, 125, 152–156
Subsidence, cap rock, 128
Subsidence, causes of, 106
Subsidence, cities, 106
Subsidence, compaction models, 108–119
Subsidence, differential, 2, 9, 106, 134
Subsidence, East Mesa Geothermal, 120
Subsidence, effect of earthquakes, 122
Subsidence, Ekofisk Oilfield, North Sea, 107
Subsidence, extreme, 125
Subsidence, factors affecting, 128
Subsidence, fissures, 128–129
Subsidence, formation susceptibility, 110
Subsidence, Goose Creek Oilfield, TX, 107, 120
Subsidence, Groningen Gasfield, Netherlands, 105, 106, 114
Subsidence, Inglewood Oilfield, CA, 130–152
Subsidence, Italy, Po Delta, 105, 106, 120
Subsidence, Italy, Po-Veneto Plain, 166
Subsidence, London, England, 106
Subsidence, Long Beach, CA, 120
Subsidence, Los Angeles Basin Oilfields, 122, 125, 127, 130–152
Subsidence, Los Angeles City Oilfield, 134–136
Subsidence, measurement of, 121
Subsidence, Mexico City, Mexico, 107
Subsidence, Mimbres, NM, 130
Subsidence, Niigata, Japan, 120
Subsidence, North Sea, Ekofisk Oilfield, 173–178
Subsidence, North Stavropol, Russia, 152–157
Subsidence, oilfields, causes, 107
Subsidence, Osaka, Japan, 106, 107
Subsidence, Picacho Basin, AZ, 129
Subsidence, Playa del Rey Marina, CA, 137
Subsidence, rate of, 121–122
Subsidence, Redondo Beach Marina, CA, 138–139
Subsidence, reduction of pore water pressure, 111
Subsidence, Salt Lake Oilfield, CA, 139–140
Subsidence, San Joaquin Valley, CA, 122, 129
Subsidence, Santa Fe Springs Oilfield, 140–141
Subsidence, stress & strain, 122–123
Subsidence, surface, 9
Subsidence, Taipei Basin, Taiwan, 122
Subsidence, Tokyo, Japan, 122
Subsidence, Venezuelan Oilfields, 157–166
Subsidence, vertical, 126–127
Subsidence, Wadi al Yatima, Saudi Arabia, 106
Subsidence, water injection, 9
Subsidence, Wilmington Oilfield, CA, 5, 105, 106, 107, 122, 123–124, 125, 126, 142–152
Systems Analysis Approach, 2

Taipei Basin, Taiwan, 122
Tapia Oilfield, CA, 91, 94
Temperature gradient, 58
Tia Juana Oilfield, Venezuela, 157, 158, 160, 161, 163
Tokyo, Japan, 122
Torrance Oilfield, CA, 138–139
Troposphere, greenhouse effect, 197–206

Venezuelan Oilfields, 156–166
Venice Oilfield, CA, 84–86, 137
Venus, atmosphere, 198–203
Volcanism, activity vs CO_2, 191
Volcanism, historic, 195–196

Waste water monitoring, 9
Water injection, monitoring, 9

Water, density calculation, 40–42
Water, oilfield microorganisms, 304–305
Waterflooding, 10, 90
Wells, abandoned, 61–63, 80, 226–227
Wells, casing leaks, 312
Wells, cement, breakdown, 2, 70
Wells, cement, effect of seismic activity, 78–79
Wells, cement, induced fractures, 66–69
Wells, design, fracturing, 222, 225–226
Wilmington Oilfield, CA, 5, 9, 105, 106, 107, 112, 120, 122, 123–124, 125, 126, 141–152

Environmental Aspects of Oil and Gas Production.
John O. Robertson and George V. Chilingar.
© 2017 Scrivener Publishing LLC. Published 2017 by John Wiley & Sons, Inc.

Also of Interest

Check out these other related titles from Scrivener Publishing

By the same authors

The Fundamentals of the Petrophysics of Oil and Gas Reservoirs, By Leonid Buryakovsky, George V. Chilingar, Herman H. Rieke, and Sanghee Shin, ISBN: 9781118344477. Written by some of the world's most renowned petroleum and environmental engineers, this volume is the first book to offer the practicing engineer and engineering student these new cutting-edge techniques for prediction and forecasting in petroleum engineering and environmental management. *NOW AVAILABLE!*

Fracking: ***The Operations and Environmental Consequences of Hydraulic Fracturing***,By Michael D. Holloway and Oliver Rudd, ISBN: 9781118496329. This book explores the history, techniques, and materials used in the practice of induced hydraulic fracturing, one of the hottest and most contested issues of today, for the production of natural gas, while examining the environmental and economic impact. *NOW AVAILABLE!*

Electrokinetics for Petroleum and Environmental Engineers, By George V. Chilingar and Mohammed Haroun, ISBN: 9781118842690. Written by pioneers in electrokinetics, this volume is the first volume ever written that explores the practical uses in petroleum and environmental engineering of this technology. *NOW AVAILABLE!*

Mechanics of Fluid Flow, by Basniev, Dmitriev, and Chilingar, ISBN 9781118385067. A group of some of the best-known petroleum engineers in the world give a thorough understanding of this important discipline, central to the operations of the oil and gas industry. *NOW AVAILABLE!*

Dictionary of Industrial Terms, by Michael Holloway and Chikezie Nwaoha, ISBN 9781118344576. This is the most comprehensive and in-depth dictionary of industrial terms available, a must-have for any engineer, scientist, technician, or operator working in industry. *NOW AVAILABLE!*

Petroleum Accumulation Zones on Continental Margins, by Grigorenko, Chilingar, Sobolev, Andiyeva, and Zhukova. ISBN 9781118385074. Some of the best-known petroleum geologists in the World have come together to produce one of the first comprehensive publications on the detailed (zonal) forecast of offshore petroleum potential, a must-have for any petroleum geologist or geology student. *NOW AVAILABLE!*

Other books by Scrivener Publishing

Zero-Waste Engineering, by Rafiqul Islam, ISBN 9780470626047. In this controversial new volume, the author explores the question of zero-waste engineering and how it can be done, efficiently and profitably. *NOW AVAILABLE!*

Sustainable Energy Pricing, by Gary Zatzman, ISBN 9780470901632. In this controversial new volume, the author explores a new science of energy pricing and how it can be done in a way that is sustainable for the world's economy and environment. *NOW AVAILABLE!*

Flow Assurance, by Boyun Guo and Rafiqul Islam, January 2013, ISBN 9780470626085. Comprehensive and state-of-the-art guide to flow assurance in the petroleum industry.

An Introduction to Petroleum Technology, Economics, and Politics, by James Speight, ISBN 9781118012994. The perfect primer for anyone wishing to learn about the petroleum industry, for the layperson or the engineer. *NOW AVAILABLE!*

Ethics in Engineering, by James Speight and Russell Foote, ISBN 9780470626023. Covers the most thought-provoking ethical questions in engineering. *NOW AVAILABLE!*

Formulas and Calculations for Drilling Engineers, by Robello Samuel, ISBN 9780470625996. The most comprehensive coverage of solutions for daily drilling problems ever published. *NOW AVAILABLE!*

Emergency Response Management for Offshore Oil Spills, by Nicholas P. Cheremisinoff, PhD, and Anton Davletshin, ISBN 9780470927120. The first book to examine the Deepwater Horizon disaster and offer processes for safety and environmental protection. *NOW AVAILABLE!*

Advanced Petroleum Reservoir Simulation, by M.R. Islam, S.H. Mousavizadegan, Shabbir Mustafiz, and Jamal H. Abou-Kassem, ISBN 9780470625811. The state of the art in petroleum reservoir simulation. *NOW AVAILABLE!*

Energy Storage: A New Approach, by Ralph Zito, ISBN 9780470625910. Exploring the potential of reversible concentrations cells, the author of this groundbreaking volume reveals new technologies to solve the global crisis of energy storage. *NOW AVAILABLE!*